Reclaimed Calcined Clay for Low Carbon Cements (Re-C3)

Appendices

A report part-funded by an ISCF TFI: large collaborative R&D projects
ISCF TFI: large collaborative R&D projects: 10001906

Authors:
Mineral Products Association
Heidelberg Materials UK
Tarmac Cement
Imerys Minerals
Forterra
University College London
University of Dundee

August 2024

Contents

(Click links below to go to desired appendix)

Developing Industrial Symbiosis using UK Waste Clay Resources for New Generation Building Materials (Re-C3)

Appendix 1 –

Technical Dossier

Authors:
Colum McCague (MPA)
Yubin Cao (UCL)

Date: January 2024

Executive Summary

Cement is a powder blend of cementitious materials or components, with reactive components typically being clinker (e.g., Portland cement clinker), alkali activators (e.g., waterglass), or a combination of these. The remaining components are known as supplementary cementitious materials (SCMs), which include common materials in the UK such as ground granulated blast furnace slag (GGBS), fly ash, and limestone powder. Small quantities of other materials, like gypsum, may be added to enhance performance, such as regulating the setting time. When mixed with water, cement forms a paste that solidifies through reactions with water or other processes.

Currently, fly ash and GGBS are by-products from declining industrial processes in the UK—coal-fired power generation and blast furnace steel production, respectively. This trend may extend globally, and while these materials are effective in reducing embodied carbon in the short to medium term, their dominance is expected to diminish in the future. Consequently, research into alternative materials is ongoing.

Calcined clay materials have emerged as a promising alternative. When heated, certain clays become pozzolanic, meaning they can react with lime and water to produce a hardened cement. Metakaolin, derived from high-grade kaolin clay, is the most recognized type of calcined clay used in cement. It typically substitutes around 10-15% of clinker due to economic and workability constraints and is currently used in the UK primarily for specialist applications. Most metakaolin is imported from Europe, Asia, or the Americas, while local kaolin is predominantly used in paint, ceramics, and paper industries. Lower-grade clays are abundant but remain untested or trialed in the UK.

In the UK, the use of calcined clay cements is governed by specific standards. BS 8500 provides guidelines for concrete production and composition, including the integration of alternative materials like calcined clay. BS 8615 focuses specifically on natural calcined pozzolana, including calcined clay, setting out requirements for its properties to ensure effective use in cement. These standards are evolving in response to new research and testing, which may lead to updated guidelines as the use of calcined clay becomes more prevalent. This ongoing refinement will help ensure that calcined clays are used effectively, enhancing the sustainability of cement production in the UK.

Contents

1. Raw materials

1.1. Classification of clays

Kaolinitic clay based pozzolans are available from a variety of sources, either natural minerals or industrial by-products (secondary clays). In terms of the industrial by-products, they can be further subdivided into two categories (as shown in Fig. 1): i) waste clays (WCs), which require activation treatment before application, e.g., by-products from mineral extraction, paper industries sludge and dam sediments, etc. [30-32], ii) clay wastes (CWs), including broken tile, brick fragments, or ceramic wastes, etc., which have already suffered different levels of thermal treatment and possessed a certain degree of pozzolanic reactivity [33, 34]. By reviewing previous work [35-37], these kaolinitic clays could be used as SCMs in blended cement. Nevertheless, in terms of CWs, even though they possess a certain degree of pozzolanic reactivity, the properties are hard to control and have greater inconsistency, owing to different thermally treatment parameters. When CWs are utilized as SCMs, they need further mechanical and thermal treatments [38-40].

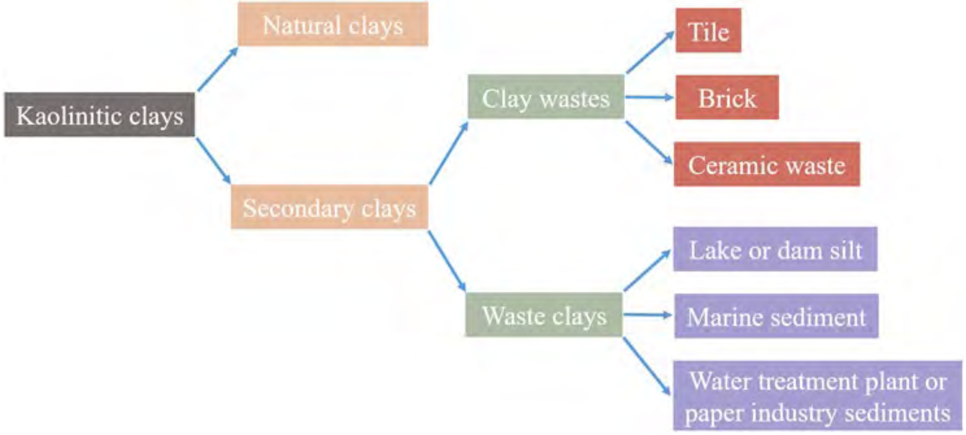

Fig. 1. Classification of clays.

1.2. Activation methods and process

1.2.1. Thermal activation

"Potential reactivity" of calcined clay refers to two aspects, i) pozzolanic reactivity (chemically reactive ability): the ability to react with a range of alkalis such as CH, in the presence of water [47]; ii) the ability of improving the microstructure of the hydrated cement [48], especially for clays containing superfine-quartz. Calcination converts the crystalline kaolinite to amorphous meta kaolin (MK), thereby increasing the chemical reactivity of waste derived clays [49, 50].

By thermally treating kaolinite in the range of 500-900 °C, the obtained MK is a metastable state clay, possessing high activity, which is substantially an anhydrous aluminosilicate. Three types of heating technologies are commonly employed for clay calcination, i.e., the rotary kiln, a fluidised bed process and flash calcination. In general, a chains section is normally applied that can dry and shred the original clayey material in advance, thus avoiding the use of extra pre-processing facilities. In the rotary kiln method, the material has a residence time of around 1-2 hours in the firing chamber to ensure good reactivity of MK [49]. The application of a fluidised bed process reduces the calcining time from hours to minutes [51]. Flash calcination takes place in special flash calciner consisting of rapid heating, calcining and cooling processes, which is able to reduce the calcining time to seconds (0.5-12 s). In this method, the original clayey material should be dried and ground to powder in advance, and then fed to a stream of hot gas at temperatures of between 800-1000 °C [52, 53]. The flash calcination method enables implementation of several heat recovery cycles, hence it has relatively high energy utilization efficiency. The authors also showed that compared with other calcination methods, MK with higher pozzolanic reactivity can be obtained by this method.

The kaolinitic clay after thermal treatment, emerged different degrees of structural collapse: the Si-O network remains essentially intact, while the Al-O network structure is reorganized due to dehydroxylation [17], which can be verified by the XRD test, FTIR test, or NMR technique, etc. [54-56]. The dehydroxylation rate (from kaolinite to metakaolin) is a major factor affecting the chemical pozzolanic activity of clays, as shown in Fig. 5. The optimum calcination temperature for the kaolin producing MK, is still not consistent in different studies. The reason may partially be due to the different mineral structure of kaolin. The kaolinitic clay mineral is the weathering products of feldspars. Due to the different geographical conditions and weathering conditions, the weathered products possess different crystallinity, presenting various mineral structures [57]. The difference in crystallinity of kaolin is mainly reflected in the hydroxyl group, which affects the optimum dehydroxylation temperature [44]. In addition, the calcination temperature, calcination duration, heating rate, calcination method and cooling method also play a significant role [4, 58, 59]. Table 3 summarizes some important parameters related to clay calcination. Researchers reported different results on the optimum calcination temperature and heating time of clay activation.

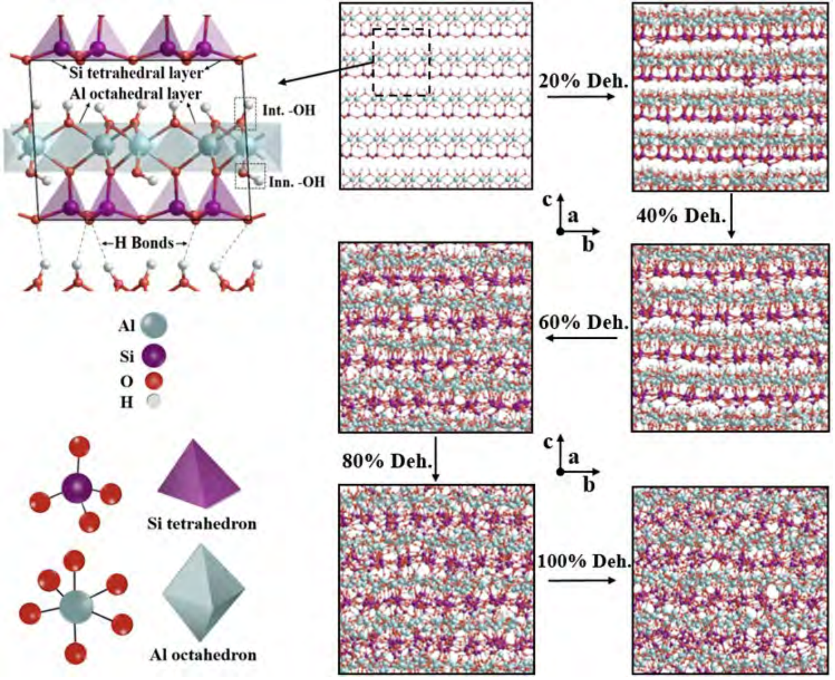

Fig. 2. Diagrammatic sketching model of molecular structure and dehydroxylation process of kaolinite updated from Sperinck et al. [60].

Table 1 Comparation of different clay calcination parameters.

Sources of clays	Calcination method	Calcination temperature	Calcination duration	Heating rate	Cooling condition	Dehydroxylation rate (%)	Ref.
Kaolin clay	Laboratory furnace	650 °C	1.5 h	-	AC[b]	97	[50]
Dam sludge	Furnace	600, 700, 800 °C	5 h	10 °C/min	-	-	[64]
Kaolin sands	Electric muffle furnace	650 °C	1 h	-	FC[a]	-	[65]
Ground kaolinite	Electric furnace	500, 550, 600, 650 °C	1 h	25 °C/min	FC[a]	11, 76, 88, 91	[66]
Greek kaolin	Laboratory furnace	650 °C	3 h	10 °C/min	-	-	[44]
Paper sludge	Electrical laboratory furnace	700 °C	2 h	20 °C/min	AC[b]	100	[67]
De-inking sludge	Electrical fixed-bed furnace	700, 750 °C	2 h	250 °C/h	FC[a]	100	
Water-treatment sludge			>5 h			100	
Natural clay mineral	Gas suspension calciner	700 - 1000 °C	1.5 s	-	AC[b]	-	[14]
	Flash calciner		1.2 s	-			

[a] Where, FC is furnace condition, which means the calcined material is maintained in the furnace, slow cooling, until the furnace temperature reached ambient;

[b] AC is ambient condition, which means the calcined material is quenched to ambient condition, rapidly lowering to the room temperature.

Generally, the clay undergoes the following processes during the calcination process, as show in Fig. 5, and the corresponding phase transition reactions are also presented below:

1. Dehydration process: the mass change from ambient temperature to 200°C is the loss of evaporative free water and organics combustion.

$$H_2O(L) \xrightarrow{\sim 200℃} H_2O(g)$$

2. Decomposition process: the gibbsite decomposition contributes to the mass loss from 200 to around 400°C;

$$2Al(OH)_3 \xrightarrow{200\sim 400℃} Al_2O_3(s) + 3H_2O(g)$$

3. Dehydroxylation process: from 500°C to 900°C, and the mass change is the loss of dehydroxylation of kaolinite;

$$Al_2O_3 \cdot 2SiO_2 \cdot 2H_2O \xrightarrow{500°C\sim 900°C} Al_2O_3 \cdot 2SiO_2(S) + 2H_2O(g)$$

Fig. 3 shows the different stages in the calcination process of kaolinitic clay. The best calcination temperature range for kaolinitic clay is V stage, from around 750 to 900 °C to possess a high activity. This calcination temperature range can ensure that the kaolinite is completely dehydroxylated and the active component does not recrystallize. Considering the activation rate and energy consumption, calcination temperature of around 700-850 °C is normally applied [63].

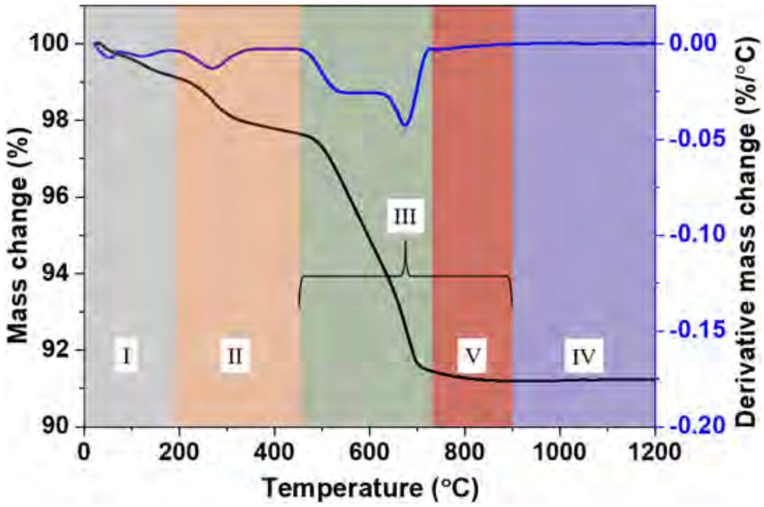

Fig. 3. Typical TGA-DTG curves of a kaolinitic clay from sandstone manufacturing.

1.2.2. Mechanical activation

In addition to thermal activation, mechanical ball milling is another activation method for kaolinitic clay. Ball milling can achieve partial dehydroxylation and activation of kaolin. Simultaneously, it can also achieve the granularity refinement of impurities (such as quartz) in clay to improve the physical filling ability of impurities [35, 59]. Souri et al. [42] studied the differences in physico-chemical properties and chemical activity of kaolin obtained by mechanical activation and thermal activation. The study found that the material obtained by ball milling exhibited a certain pozzolanic activity. However, compared with the material obtained by thermal activation, it has a large difference in particle morphology and specific surface area. They also pointed out that thermal activation caused the coordination of Al to shift from Ⅵ to Ⅴ and Ⅳ, while mechanical activation had very limited effect on Al transformation.

1.2.3. Pozzolanic Reactivity

It is well known that clay mineral is a mixture of kaolinite (phyllosilicate) and other passive phase crystals such as quartz, carbonates and metal oxides (e.g., iron oxide). Structurally, kaolinite is composed of one tetrahedral layer of $(Si_2O_5)^{2-}$ and one octahedral layer of $(Al_2(OH)_4)^{2+}$, and each layer constituting the faces of the sheet [16, 41]. Kaolinite is extremely stable at ambient environment [42]. When it is subjected to proper thermal treatment, the mineral loses its crystallinity owing to the process of dehydroxylation and releases of active silica and alumina [43]. The product metakaolin (MK) is a kind of transition phase, which reserves the lamellar structure of kaolinite, while the sheet and tubular dimensions are reduced [44].

In order to control the quality of clay as SCM, some important parameters are controlled. According to the standard of ASTM C-618 [46], calcined clays for class N have to fulfil both the chemical and physical requirements as shown in Table 2. Chemically, the content of silicon dioxide (SiO_2), aluminium oxide (Al_2O_3) and iron oxide (Fe_2O_3) should exceed 70% of the total components to ensure sufficient active components for the pozzolanic reaction. Physically, the strength activity index of calcined clay blended cement should reach the reference sample (OPC) 75%.

Table 2 Chemical and physical requirements for class N artificial pozzolanic materials.

ASTM C 618 Required content	Required indexes
Silicon dioxide (SiO_2) plus aluminium oxide (Al_2O_3) plus iron oxide (Fe_2O_3), min, %	70
Sulfur trioxide (SO_3), max, %	4
Moisture content, max, %	3
Loss on ignition, max, %	10
Amount retained when wet-sieved on 45 µm (No. 325) sieve, max, %	34
Strength activity index: with PC, at 7 days, min (percent of control)	75*
Strength activity index: with PC, at 28 days, min (percent of control)	75*

* Meeting the 7-days or 28-days strength activity index will indicate specification compliance.

1.3. UK clay sources

According to the literature, most of the clay samples, obtained in the United Kingdom, contain kaolinite, illite and montmorillonite and some of them has a small amount of chlorite (Gasparre, 2005; Kemp and Wagner, 2006; Zhou, 2016). Other minerals like vermiculite and muscovite can also be found in the United Kingdom but normally only in small quantities (refer to Table 3).

Kaolinite, a 1:1 clay, is recognized as a highly effective pozzolanic material after calcination. However, kaolinitic clay deposits are relatively scarce in the United Kingdom (UK). Instead, the UK has a significant abundance of 2:1 clays, such as illite and smectite. According to studies by Ridgway (1982) in Common Clays and Shales and Ball Clays (Minerals Dossier Nos. 22 and 11, respectively), the genesis and composition of UK clay deposits are closely related to their depositional environments, with many forming in marine or freshwater settings. These works remain some of the most comprehensive reviews of industrial mineral deposits in the UK. Further supporting this, the Engineering Geology Special Publication No. 21 by the Geological Society of London (Reeves, Sims, and Cripps, 2006) provides a succinct overview of UK geology, particularly focusing on clay-rich strata. This publication highlights that, in the UK, superficial clay deposits are typically dominated by illite or the mica group, with smectite being more prevalent in certain regions, particularly those with northern influences such as parts of Norway, Sweden, Finland, and the north-west of Russia.

Thus, it is not uncommon for clay samples from UK superficial deposits to be dominated by illite, smectite, or the mica group, rather than kaolinite, aligning with the broader distribution patterns observed in the northern hemisphere.

A superficial deposit is a thin layer of gravel, sand, silt and clay sitting on bedrock. Such a thin layer will be depleted in a short amount of time and only make up a small portion of the soil in that region. Hence, it is even more crucial to look at the clay minerals of the bedrocks rather than the superficial deposit. Some information regarding the clay minerals in some of the bedrock in the UK are summarised in Table 3 and the distribution of the bedrocks is shown in Fig 4. Most of the clay samples from the marked area have illite and/or smectite as the dominant group. Other clay minerals such chlorite, calcite, vermiculite, and kaolinite are normally not the dominant group in most UK clay samples, except for Dunnottar and Arbuthnott group which has chlorite and vermiculite as its dominant group. It can be noted that vermiculite appears in southern and northern England, while other places did not report the presence of vermiculite. This aligns with the data presented by Ito and Wagai (2017). Other than this, some calcite and quartz can be found in Bath Fuller's Earth, which might affect the rheology of the cement paste or fresh concrete if used as SCM. It is also notable that in most of the samples, mixed-layered clay minerals are present, which up till now the effect of it on rheology is still unclear.

It is important to clarify that the information presented here offers only a preliminary insight into the clay minerals found in the UK. The distribution of clay minerals can vary significantly, even within samples from the same area. While the study by Kemp and Wagner (2006) provides valuable data, it specifically focuses on the London Clay Formation in southern England. This formation is not representative of the more extensive clay deposits across the UK, as it contains an unusually high montmorillonite (smectite/bentonite) content, leading to issues with ground swelling and instability.

Therefore, while illite and smectite are indeed dominant in some regions, it should be recognized that kaolinite, smectite, illite (including illite-smectite mixed layers), and chlorite are among the most common clay minerals found throughout the UK. However, this conclusion primarily reflects the geological bedrocks of these areas, rather than superficial deposits.

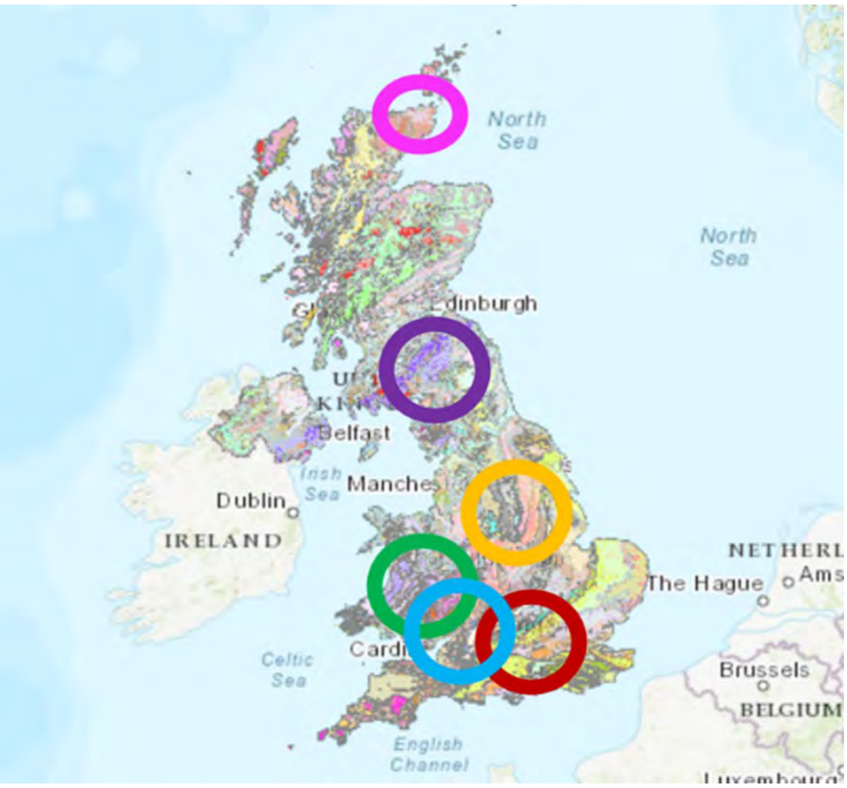

Figure 4: The location of clay listed in Table 3 (The colour of circles corresponds to the colour of the location in the table)

Table 3: Information of United Kingdom clay group (Hawkins, A. B., et al., 1986; Jones and Sellwood, 1989; A Forster, et al., 1995; Hillier et al., 2006; Hobbs et al., 2012; Kemp et al, 2012)

Location	Group	Source
Southern England	Inferior Oolite Group (K, I, S, C, K/S, I/S)	(Jones and Sellwood, 1989)
Mid-West England to Eastern Wales	Downtown Group (K, I, S, C, I/S)	(Hillier et al., 2006)
Welsh Borderland	Ditton Group (K, I, S, C, I/S)	
Taff Fawr	Brecon Group (I, S, C, I/S)	
Southern to Mid-England	Lias Group (K, I, S, C, I/S)	(Hobbs et al., 2012)
Southern England	Wealden Group (K, S, I, V, C, I/S)	(Kemp et al, 2012)
Southern England	Gault Clay (K, S, I, V, C)	(A Forster, et al., 1995)
Bath	Bath Fuller's Earth (K, I, S, Ca, Q)	(Hawkins et al., 1986)
Border of England and Scotland	Stonehaven Group (K, I, S, V, C, I/S, C/V)	(Hillier et al., 2006)
	Dunnottar and Arbuthnott Group (C, V, C/V)	
	Garvock Group (S)	
	Strathmore Group (S, C, S/C)	
	Upper Old Red Sandstone (K, I, S, I/S)	
Orcadian Basin	Old Red Sandstone (K, I, S, C, I/S, S/C)	(Hillier et al., 2006)

Where K= Kaolinite, I= Illite, V= Vermiculite, C= Chlorite, S= Smectite, Ca= Calcite, Q= Quartz
Note: K/I means kaolinite and illite mixed layer

2. Reactivity testing

The definition of pozzolans is interpreted in ASTM C125-15b: *a siliceous or aluminosilicate material which, by itself, possesses little or no cementitious value, but in finely divided form and in the presence of water, will chemically react with calcium hydroxide (CH) at ambient temperatures to generate compounds possessing cementitious properties* [68]. According to the definition, pozzolanic reactivity assessment methods are mainly divided into two categories, direct method and indirect method. The direct method is to evaluate the consumption capacity of calcium hydroxide from pozzolanic material. The indirect method is to evaluate the macroscopical property, e.g., strength activity index (SAI), of materials containing pozzolanic material.

2.1. Indirect methods

Indirect methods, also known as mechanical methods, evaluate the pozzolanic reactivity of SCMs by measuring the mechanical performance. The commonly utilized method is strength activity index (SAI), blending 20%-30% pozzolans to substitute Portland cement (as shown in Eq. 6). In the formulation of the mixture, the binder to sand ratio (b/s) and water to binder ratio (w/b) are 1:3 and 1:2, respectively [4].

$SAI_{(d)} = (ST_{(d)}/SC_{(d)}) \times 100\%$	Eq. 1

where, $SAI_{(d)}$ is the compressive strength activity index at 7, 28 days; $ST_{(d)}$ is the compressive strength of the test sample at same curing days; $SC_{(d)}$ is the compressive strength of the control sample at the same curing days. The materials will be identified as pozzolanic materials with the strength activity index reached 75% [46]. What should be noted that the SAI results are also affected by the w/c ratio; the increase of water demand for pozzolans inevitably leads to an excess of water, which may lead to an increase in the porosity of the cement matrix and a decrease in strength.

Avet et al. [70] introduced a novel rapid, relevant and reliable (R^3) method to assess the pozzolanic reactivity of thermally treated kaolinitic clay, by testing the heat release and bound water content of the simulated system (activated clay, $CaCO_3$, limestone, gypsum and alkali) of LC^3-50. The PPC30 system (30% calcined clay and 5% gypsum of clinker) was also studied as the control system. They found a good correlation between the compressive strength and R^3 results. An improved correlation coefficient was found in both calcined clay blended system at later curing age. The pozzolanic reactivity of calcined clay in blended cement can also be measured by the electrical conductivity test [13] and heat evolution by using conduction calorimetry [71, 72]

2.2. Direct methods

Direct methods are based on the chemical reactivity by assessing the content of reactive components or the calcium hydroxide consumption-ability in activated clay. The amount of calcium hydroxide (CH) can be easily determined according to EN 196-2 standard. The most employed methods are Frattini test [73], Chapelle test [74-76] and Saturated lime (SL) test [77], as summarized in Table 4. The source of calcium hydroxide in Frattini test comes from cement hydration, which is different from Chapelle test and Saturated lime test, in which calcium hydroxide is added directly. The experimental temperature in these three methods is different. Saturated lime test and Frattini test are conducted at 40°C, while Chapelle test is conducted in boiling water. Some researchers also use TGA-DTG to determine the remaining amount of calcium hydroxide in calcium hydroxide mixed calcined clay system to evaluate the pozzolanic reactivity [47, 78].

Studies have shown that there is a superior correlation between the tests of Frattini and SAI [77]. Since Portland cement produces calcium hydroxide around one-fourth of its initial weight when it is fully hydrated, the author attributed the correlation of the test results to the mass ratio of calcium hydroxide and pozzolanic material of 1:1. However, there is no good correlation between these tests and the SL test results. The author pointed out that this is mainly due to the different proportions of calcium hydroxide and pozzolan (0.15:1) in the experiment, as shown in Table 4.

Table 4 Comparison between tests of: SL, Chapelle, Frattini and SAI [77].

	SL Test	Chapelle test	Frattini Test	SAI test
Curing time	Not specified	16 h	8, 28 and 90 d	7 and 28d
Test temperature	40 °C	100 °C	40 °C	20±2 °C
Source of CH	Saturated lime solution	Calcium hydroxide	Cement hydration	Cement hydration
CH: Pozzolan	0.15:1	1:1	1:1	1:1
Involved activity	CA	CA	CA	C-PA

CA: chemical activity; C-PA: chemical and physical activity.

2.3. Other methods

From recent studies [47, 54, 79-81], a range of other methods are also applied to evaluate the pozzolanic reactivity of calcined clay such as thermogravimetry analysis-differential thermal analysis (TGA-DTA), X-ray diffraction (XRD), Fourier transformed infrared (FTIR) spectroscopy, Atomic absorption spectroscopy (AAS) and Nuclear Magnetic Resonance (NMR) spectroscopy. These advanced techniques can help to determine the phases, molecular bonds and coordination changes in materials. Fig. 5 presents the results tested by NMR. As the calcination temperature increases, the Al signal changes from the dominant 6-coordinated to the dominant 4-coordinated, which further increases the pozzolanic activity of the calcined clay by adding chemical binding sites [62].

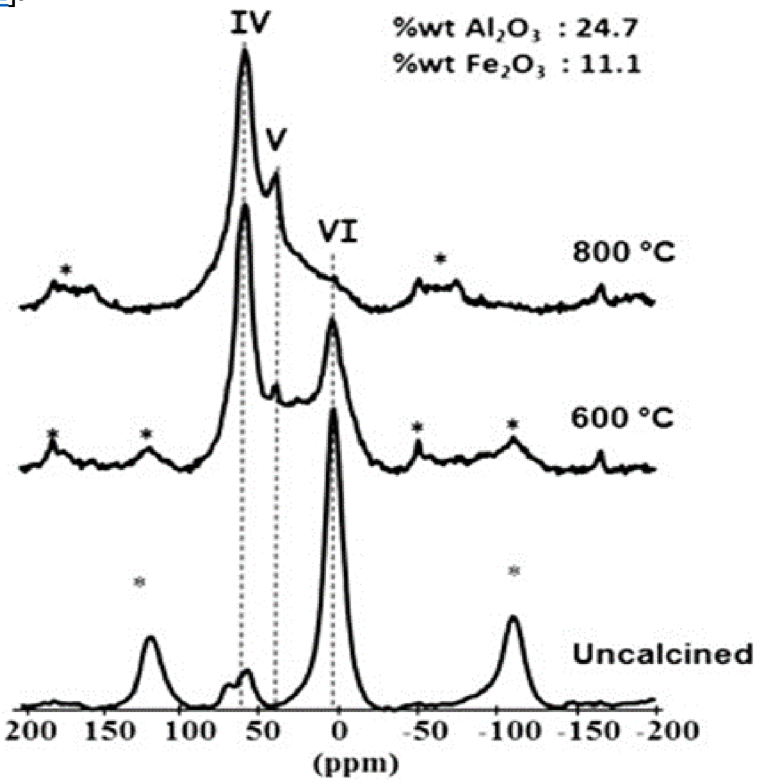

Fig. 5. ^{27}Al MAS NMR spectra of uncalcined clay and calcination products [62].

3. Rheology

Rheology is a study that investigates the correlation between stress applied and deformation observed under a certain loading condition and environment. It can be widely agreed that Portland cement-based system is normally a thixotropic material, which indicates lower viscosity once start flowing and gradually recover after stops flowing. In practical applications, rheology is an important aspect that must be taken into consideration as it will affect the pumpability and flowability or workability of the concrete. Rheology not only governs the workability of fresh concrete, but it also has a significant impact on the hardened properties, such as compressive strength and durability. This is especially true because, with lower workability, concrete can become exceedingly difficult to compact, which may result in honeycombs (durability issues) or, more severely, not being able to perform as designed (unable to bear load). Therefore, understanding the rheological behaviour of cement paste is important not only to ensure easier placement but also better hardened concrete quality.

Currently, most of the studies on rheology of fresh cements and concretes have been conducted on systems containing Portland cement. The rheological effects of SCMs such as fly ash and GBFS have also been studied extensively. In recent years, more researchers have been increasingly investigating the rheological effects of calcined clays (Akhlaghi et al., 2017; Ez-Zaki et al., 2021; Ferreiro et al., 2017; Mishra et al., 2019; Muzenda et al., 2020; Nair et al., 2020; Parashar and Bishnoi, 2021; Zaribaf et al., 2015). However, these systems are designed for when metakaolin (or at least calcined kaolinitic clay) is the SCM (Scrivener et al., 2018).

While it can be agreed that a smaller particle size will have a larger water demand due to the increase in specific surface area, there are also other factors that affect the rheological behaviour of cement paste, especially when SCM is added to increase the hardened performance. Particles size distribution is one of the many factors and is particularly important in this project as calcined clay is involved. Other than this, the shape of the particles also plays a vital role. For example, it is agreed that fly ash can improve the rheology of the concrete due to its spherical shape, which provides a ball-bearing effect (Marinković and Dragaš, 2018). Therefore, the shape of particles in the cement paste plays a significant role in rheological behaviour.

In cement and concrete systems, it is generally accepted that the water to cement ratio is one of the most influential factors affecting rheological behaviour. A high water to cement ratio can give excellent workability. However, the higher the water to cement ratio, the lower the strength of the hardened cement paste, mortar or concrete. Therefore, to achieve good workability with low water to cement ratios, a high range water reducer or superplasticiser is used. There are 3 types of superplasticisers: lignosulfonate (1st generation), naphthalene (2nd generation), and polycarboxylate ether (3rd generation). Currently, most of the superplasticisers used are polycarboxylate ether-based due to their high-cost efficiency and their effectiveness in fluidising cement paste, mortar or concrete. Most polycarboxylate ether-based superplasticisers can be divided into 2 parts: the backbone monomer and the side chain monomer. The main purpose of the backbone monomer is to provide electrostatic attraction or repulsion to the whole polymer, allowing the superplasticiser to adsorb onto the surface of a particle. On the other hand, the side chain monomer is for steric hindrance, which means physically repelling the incoming particles.

As previously mentioned, particle size and the shape of the particles will affect the rheological behaviour. This is especially true when there is clay contamination, especially montmorillonite, in the fine or coarse aggregate. Montmorillonite, unlike illite and kaolinite, has an expansive interlayer, which can trap the side chain of polycarboxylate ether. To solve this problem, some researchers have developed some variation of polycarboxylate ether to enhance the clay tolerance, shown in Table 5. Researchers that use a sacrificial agent with polycarboxylate ether is also shown in the same table.

Table 5 Literature about montmorillonite in cement paste and proposed solutions

Literature	**Clay**		**Solution proposed**	**Result**
Liu, X., et al. (2020), He, D., et al. (2021) Utilise electrostatic force (+ charge)	Raw clay, 1-6% of kaolinite, mica and montmorillonite		Introduce a chemical compound to occupy the interlayer known as CRA, so that the EO side chain will not enter the occupied interlayer	The CRA worked as theory suggested, the workability slightly improved with longer retention.
Tan, H., et al. (2017). Utilise hydrogen bond	Raw clay, 1.5% montmorillonite		Since EO side chain in the main thing that intercalate with the interlayer of Mmt clay, therefore, PEG (EO chains) Is introduced to occupy the interlayer	Adding PEG chain and PCE SP into clay cement present a mixture with higher fluidity.
Lei, L. and J. Plank (2014) Use non-PEG type	Raw clay, 1% montmorillonite, 3% kaolin, 12% muscovite		Modify the side-chain into vinyl ether based as PEG side chain has natural affinity for the interlayer of montmorillonite.	The adsorption into the interlayer decreased. The SP with MPEG has a very high adsorption.
Chen, G., et al. (2018).	Raw clay, 0% to 3% of montmorillonite		Modify the end of PCE side chain into carboxylic acid which can provide negative charge	The adsorption onto clay decreases but will adversely affect the fluidity retention if anionic density too high.
Xu, L. et al. (2015) Large pendant	Raw clay, 0%-2% of montmorillonite		Use a side chain with a large enough head to avoid intercalation	Effective, the slump obtained is way higher than the one without superplasticizer.

The overall results show that the modification on the polycarboxylate ether has increased the clay tolerance when examined by XRD peak, with no increase in 001 peaks when used modified carboxylate ether or a small increase when a sacrificial agent is used. Although these clay-tolerance-enhanced superplasticisers have been proven effective with raw clay (e.g., montmorillonite) present in concrete, little to no researchers have used them when calcined clays are present (Table 6). It is also understood that following calcination, montmorillonite collapses and adopts an Illite structure therefore the rheological issues found with raw clays in concrete may not be relevant for calcined clays.

Table 6: Superplasticisers used with calcined clay.

Literature	**Clay**	**Type of SP used**	**Result**
Sposito, R., et al. (2021)	20% Metakaolin, 20% meta-illite, 20% meta-muscovite, 20% Amaltheen Clay	HPEG, amphMPEG (amphoteric)	HPEG > amphMPEG, attribute to the shorter side chain and higher anion density of HPEG
Schmid, M. and J. Plank (2020) *This experiment contains 20% quartz	22% Kaolinite, 31.8% illite-smectite, 20% Quartz, 10.3% Muscovite+Chlorite (10% to 50% replacement)	HPEG, long and short side chain MPEG (with different anionic density) and IPEG with long and short side chain	HPEG > MPEG > IPEG. Longer side chain with higher anionic density seems to always perform better than its short chain counterparts
Li, R., et al. (2021)	51% Kaolinitie, 19.7% illite-smectite, 18.1% muscovite, 10.3% Quartz (20% to 40% replacement)	HPEG, MPEG with different length of side chain, MPEG with 114 side chain and cation	AGAIN, HPEG > zwitterionic MPEG > MPEG (longer side chain is better)
Sposito, R., et al. (2021).	20% for natural clay, 20% for clay minerals	HPEG and IPEG	Calcined clay has smaller –ve zeta potential. Mk affect zeta potential. Water demand, Kaolinite %, Phyllosilicate % and SSA affect the rheology of cement paste.
Schmid, M. and J. Plank (2021)	Metakaolin, meta-illite and meta-montmorillonte	HPEG and MPEG	Meta-illite in this paper has huge SSA which affect the fluidity

4. Reaction mechanism of calcined clay cements

It is well known that the major chemical reactions in calcined clay blended cement system, are the hydration of tricalcium silicate (C_3S) and dicalcium silicate (C_2S) to generate calcium silicate hydrate (CSH) gel and calcium hydroxide (CH), as shown in Eq. 7 - 8. The hydration product of CSH gel, accounting for 2/3 of all the hydration products, is the main strength provider of the cement matrix [85]. When the OPC paste reacts and hydrates thoroughly, the amount of CH makes up over 20 wt.% [86]. The presence of CH effectively improves the resistance of carbonization and acid corrosion of cement products by maintaining a high alkalinity in the cementitious system. However, the enrichment of CH would react with active composition e.g., active silica, silicate and carbonate from fine or coarse aggregate, and cause Alkali Silica Reaction (ASR) or Alkali Carbonate Reaction (ACR), leading to cracking and degradation [87].

$$3CaO \cdot SiO_2 + nH_2O \rightarrow xCaO \cdot SiO_2 \cdot (n-3+x)H_2O + (3-x)Ca(OH)_2 \qquad \text{Eq. 7}$$

$$2CaO \cdot SiO_2 + nH_2O \rightarrow xCaO \cdot SiO_2 \cdot (n-2+x)H_2O + (2-x)Ca(OH)_2 \qquad \text{Eq. 8}$$

$$Al_2O_3 \cdot SiO_2(calcined\ clay) + Ca(OH)_2(OPC\ hydration) + H_2O \rightarrow CSH + CASH \qquad \text{Eq. 9}$$

When calcined clay is utilized as a partial substitute of clinker, the pozzolanic components of siliceous and aluminous can react with CH to mitigate the expansive effect of ASR and ACR. In addition, the reaction produces additional supplementary cementitious compounds (SCCs), such as CSH, CAH and CASH, as shown in Eq. 9. Previous studies demonstrated that the SCCs possess cognate properties similar to products that generated during hydration process of Portland cement. The properties of SCCs generations depend basically on the MK/CH ratio [4, 88, 89]. Externally, curing temperature will also affect the rate and type of SCCs [90]. The SCCs is able to refine the microstructure of concrete, particularly in the pores and the interfacial transition zone (ITZ) where CH is enriched. The refinement of pores and densification of ITZ can further enhance the mechanical strength and durability of concretes, and reduce capillary water absorption as well [91].

5. Calcined clay with limestone powder

The benefits of combining calcined clay and limestone power in a cement system with Portland cement clinker has been highlighted by many researchers. In these cements, the hydration of clinker is still the dominant chemical reaction. The reactive component in calcined clay reacts with CH to generate aluminate hydrates and gels of CSH and calcium (alumino) silicate hydrate C(A)SH. In addition, there are also some synergetic reactions between clinker, calcined clay, limestone and gypsum.

Limestone powder has been widely adopted in cements as a SCM [122]. The presence of limestone powder in cements is conducive to the generation of hemi-carboaluminate ($C_4A\bar{C}_{0.5}H_{12}$, Hc) and mono-carboaluminate ($C_4A\bar{C}H_{11}$, Mc) and the stabilization of ettringite [130, 131]. When combined with calcined clay in cements, limestone powder can react with the aluminate phases (from clinker or calcined clay) and CH to generate hemi- and mono-carboaluminate (as shown in Eq. 10, so as to improve the physical and chemical properties of cement and concrete products [122, 132]). The addition of limestone powder also minimizes the transformation of ettringite ($C_6A\bar{S}_3H_{32}$) to monosulfoaluminate ($C_4A\bar{S}H_{12}$) (Eq. 11). This is because calcium mono-carboaluminate and ettringite are more stable than calcium carbonate and monosulfoaluminate [133]. Fig. 6 shows the different hydration products of the clinker-calcined clay-limestone cement system at 1 day, 28 days and 90 days [45]. As one can see from the XRD results, a similar amount of ettringite was observed for the reference Portland cement and the 50% clinker calcined clay cement (LC^3-50), after 1 day, 28 days and 90 days of hydration. Compared with 1 day of hydration, Hc and Mc products appeared in the 50% clinker system at 28 and 90 days of hydration. However, in the reference Portland cement samples, no Hc and Mc products were found.

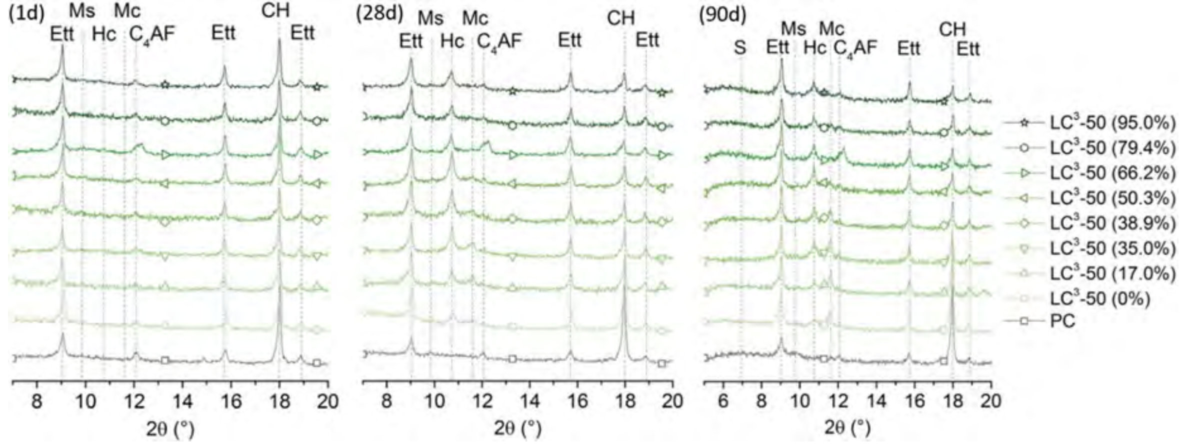

Fig. 6. XRD patterns of hydration for control OPC and LC^3 samples at 1, 28 and 90 days [45].

The stoichiometric formation of calcium mono-carboaluminate is considered: in the presence of excess calcium ions in pore aqueous solution, one mole of metakaolin can react with one mole of CH to generate one mole calcium mono-carboaluminate. Hence, the widely accepted blending ratio of calcined clay and limestone by weight is 2: 1 (considering 50% of metakaolin in calcined clay) [134].

$$\bar{A}_{(from\ MK\ or\ clinker)} + C\bar{C} + 3CH \rightarrow C_3\bar{A}C\bar{C}H_{11} \qquad \text{Eq. 10}$$

$$3C_4A\bar{S}H_{12} + 2C\bar{C} + H_{18} \rightarrow C_6A\bar{S}_3H_{32} + 2C_4A\bar{C}H_{11} \qquad \text{Eq. 11}$$

Cement chemistry notation, $\bar{A}$=aluminates, $A=Al_2O_3$, $C=CaO$, $\bar{C}=CO_2$, $CH=Ca(OH)_2$, $H=H_2O$, $S=SiO_2$, $\bar{S}=SO_3$.

6. Mechanical properties

The reaction products in calcined clay cements can lead to a refinement in microstructure compared to traditional composite cements, which in turn improves the mechanical properties (e.g. strength and modulus of elasticity). It is generally accepted that the mechanical properties of calcined clay cements are linked to the kaolinite content of the raw clays [98].

Li et al. [99] reported that utilizing up to 20% of ceramic polishing waste paste by volume as SCM to replace 33% Portland cement in mortar, the compressive strength at 7 and 28 days revealed a significant improvement, both of which were increased by more than 85%. However with brick powder, Aliabdo et al. [69] found that the compressive strength reduced at 28 days compared with the reference cement.

Duan et al. [100] applied microhardness to study the effect of SCMs (with 10 wt.% replacement ratio) on the ITZ of blended cement concrete. The study found that with the extension of the curing age, the addition of SCMs compacted the ITZ and refined the pore structure, especially for the calcined clay cement (MK-28) (in Fig. 7).

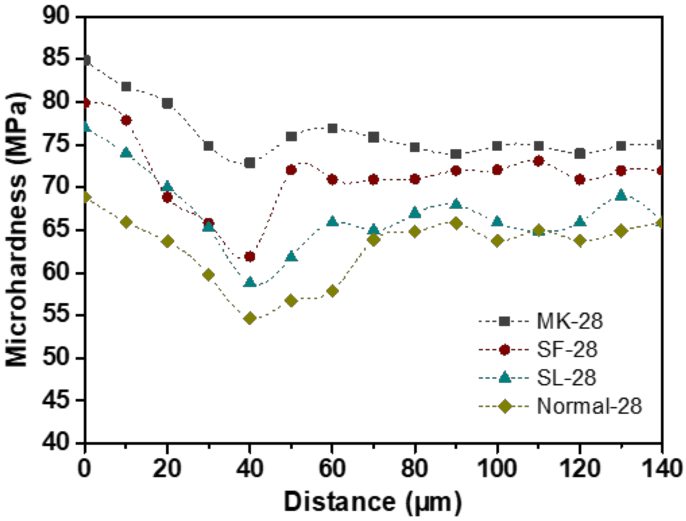

Fig. 7. Effect of SCMs on microhardness of ITZs in blended cement concretes [100].

The use of limestone and calcined clay can supply extra calcium carbonate and alumina in cements. This not only leads to accelerated cement hydration, but also more hydration products such as CSH gel, CASH compounds and carbo-aluminate hydrates [142].

Maraghechi et al. [143] found that the kaolinite content in raw clay is the dominant factor governing the compressive strength of mortars or concretes based on clinker-calcined clay-limestone cements. As shown in Fig. 8(a), the compressive strength of the clinker-calcined clay-limestone cements were significantly lower than that of the Portland cement reference cement. At later curing ages, the compressive strength at 7 days was comparable to that of the reference. In addition, the PPC-30 cement (30% clinker replaced by calcined clay) mortar showed comparable compressive strength with the 50% clinker cement at 7 days, and somewhat higher strengths at 28 and 90 days. Avet investigated the influence of various types of clays on the compressive strength of the 50% clinker cement system (LC^3-50) [70]. It was reported that the compressive strength was largely dependent on the kaolin content in the raw clay. As shown in Fig. 9, clay with higher content of kaolin exhibited higher compressive strength at all ages. The similar results was also pointed out by Scrivener in [20].

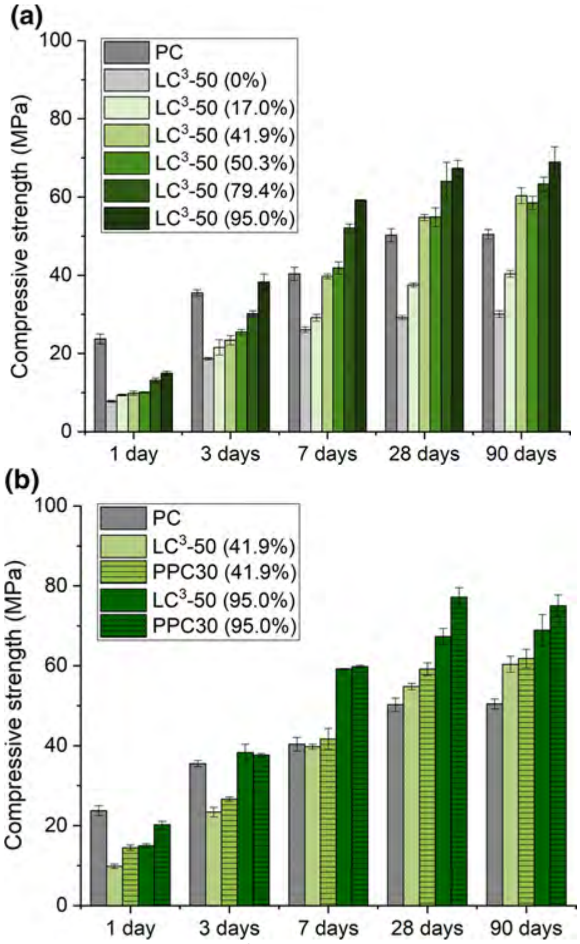

Fig. 8. (a) Compressive strength of LC^3-50 mortars as a function of kaolinite content and age; (b) Comparison of PPC-30 vs LC^3-50 mortars prepared using the same clay [143].

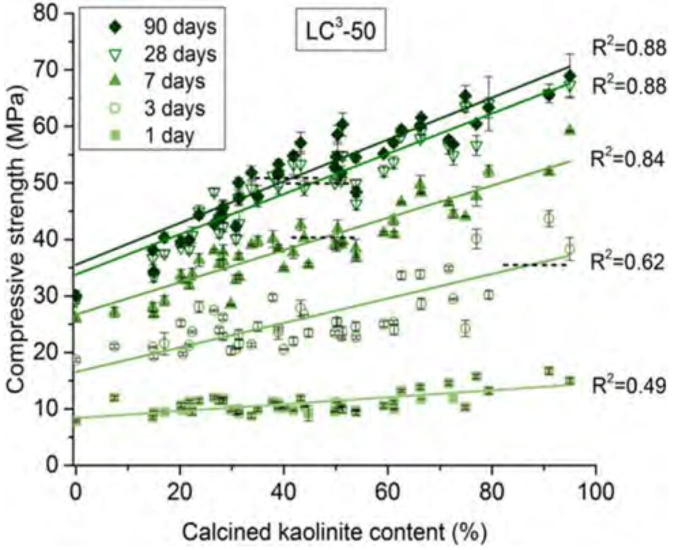

Fig. 9. Correlation between kaolin content in the raw clay and compressive strength [70].

7. Durability of mortar and concrete

Calcined clay cements are known to have a high resistance to alkali-silica reactions and attacks from chlorides or sulfates [101].

7.1. Sulfate Resistance

It has been reported that the use of calcined clays as SCMs can remarkably improve the sulfate resistance of concretes [106-108]. One reason is that the substitution of Portland cement by calcined clay reduces the quantity of tricalcium aluminate hydrates (C_3A). Another reason is attributed to the pozzolanic reaction of calcined clays, generating additional gel phases, filling pores and cracks in the cement matrix. In addition, the removal of CH generated from cement hydration lowers the quantity of ettringite formation, and effectively minimize the damage caused by sulfate attack.
The coupling of limestone and calcined clay in cements allows for higher substitution of clinker and further reduces the tricalcium aluminate (C_3A) content. Less soluble alumina in the system reduces the potential for expansive ettringite to form.

Shi et al. [149] studied the sulfate resistance of cement containing calcined clay and limestone immersed in 0.11 M Na_2SO_4 solution at 5 ℃ and 20 ℃. The results showed that the specimens containing calcined clay illustrated excellent sulfate resistance (in Fig. 10). It is regarded that the pozzolanic reaction of calcined clay consumed CH, resulting in a reduction of available calcium ions concentration to form gypsum and ettringite. Apsa and Rao [150] investigated the sulfate resistance of cements containing calcined clay and limestone. The study found that with an increase in calcined clay content, the sulfate resistance was significantly improved compared to the reference cement. Partial substitution of clinker by limestone and calcined clay can reduce the expansion rate and dynamic modulus loss of mortar after suffering the sulfate attack [151]. The authors also noted that although Mc and Hc can chemically react with sulfate to generate ettringite, the improved permeability essentially guaranteed good sulfate resistance.

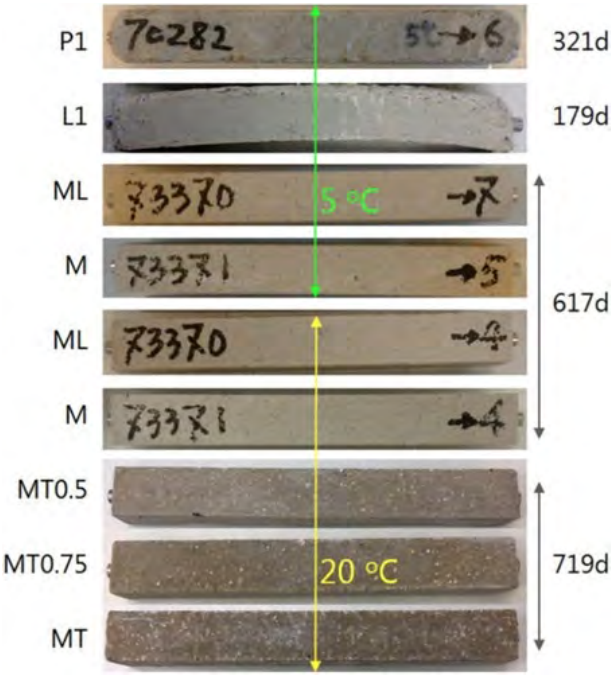

Fig. 10. Visual inspection of the Specimens surface (P: Portland cement; L: limestone; ML: metakaolin and limestone; MT: calcined montmorillonite) [149].

7.2. Carbonation resistance

Carbonation is a slow process from surface to inside, owing to its low CO_2 concentration in the atmosphere. The CH will react with CO_2 during the carbonation process, which will lead to reduced pH in pore solution from 12.5-13.5 down to 8.5-9.0, and accelerate the corrosion of reinforced concrete [152]. In calcined clay cements, the CH content is relatively low compared to that in traditional cements which can lead to higher carbonation rates. The significance of this is not currently known as there are no known studies which have investigated carbonation vs. traditional cements in detail, particularly in concretes.
Chloride resistance

Guo et al. [112] reported that the use of 16% calcined clay (MK) and silica fume (SF) as SCMs, the chemical binding capacity of chloride ion of MK-blended cement paste was 6 times compared to that of SF-blended cement paste and 2 times compared to that of Portland cement paste. This is mainly attributed to the increased content of Al^{3+} from MK.

As one can see from the XRD results as shown in Fig. 11, the hydration products of mono-carboaluminate can completely convert into the stable Friedel's salt after immersion in NaCl solution. Gbozee et al. [113] found that, considering the exposure conditions, the mono-carboaluminate did not contribute much to the chemical bonding compared to the mono-sulfoaluminate. When the calcined clay cement was exposed to NaCl at room temperature, the mono-sulfoaluminate converted to Friedel's salt and this played a significant role in chemically binding the chloride ions. Marangu et al. [114] found that the chloride ion concentration in the calcined clay cement decreased sharply in the depth of 10-20 mm, which may be due to the physical or chemical binding of the cement matrix slowing down the chloride ions penetration rate [115]. Compared to the Portland cement control sample, PPC35 (35% calcined clay) presented relative lower chloride penetration, due to the increased amount of CSH and calcium aluminate hydrate (CAH) gel generated from the pozzolanic reaction [116].

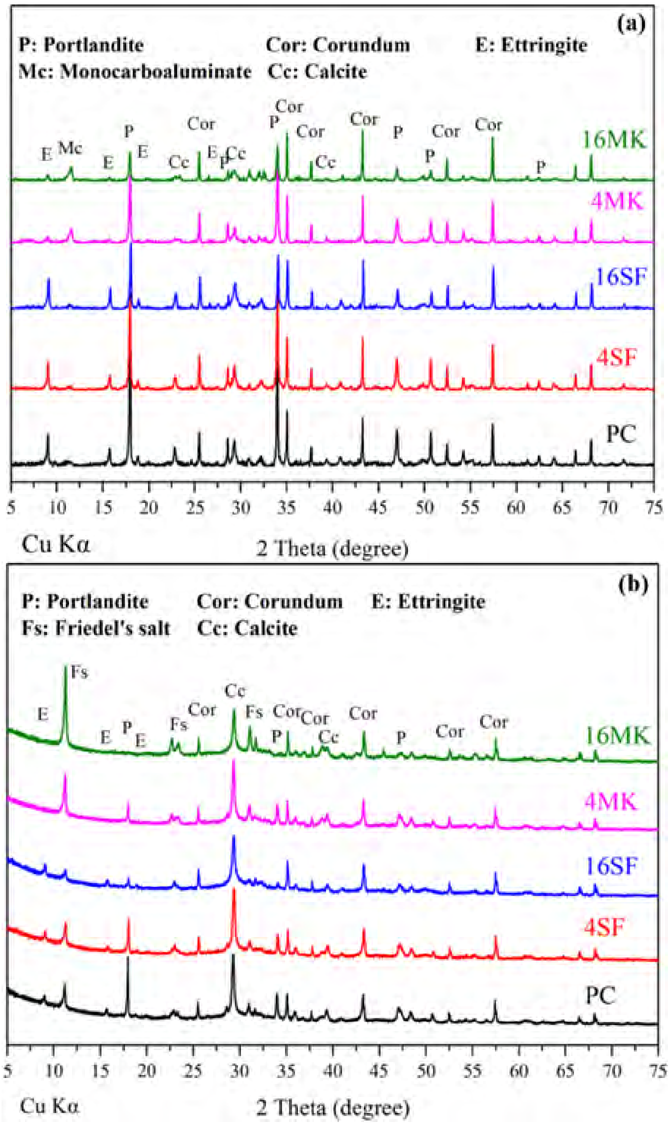

Fig. 11. (a) XRD patterns of MK or SF blended Portland cement pastes; (b) XRD patterns of cement pastes after equilibrium binding in 3 mol/L NaCl solution [112].

It is found that a combination of clinker, calcined clay and limestone in cements could refine the pore structure of the matrix compared with other, traditional cements [45]. The total porosity was notably reduced when the initial kaolinite content was higher than 38.9%. With the curing age increased from 3 days to 28 days, the pore refinement was further improved. The same phenomena also were reported in [146]. Antoni investigated the erosion depth of chloride ions with different kaolin content in raw clay, after soaking in 3 wt.% NaCl solution for 1 and 2 years [143]. They found that the erosion depth of clinker-calcined clay-limestone cements using clays with 50% or above kaolin content was less than 10 mm. However, the chloride erosion depth for the reference Portland cement had already run through the mortar cube samples, as shown in the Fig. 12. As a result of the study in [145], the clinker-calcined clay-limestone system also showed similar promising resistance to chlorides. Antoni et al. illustrated that the excellent chloride resistance of the clinker-calcined clay-limestone system was related to its finer pore size distribution, while the total porosity of the clinker-calcined clay-limestone system was actually higher than that of Portland cement [142].

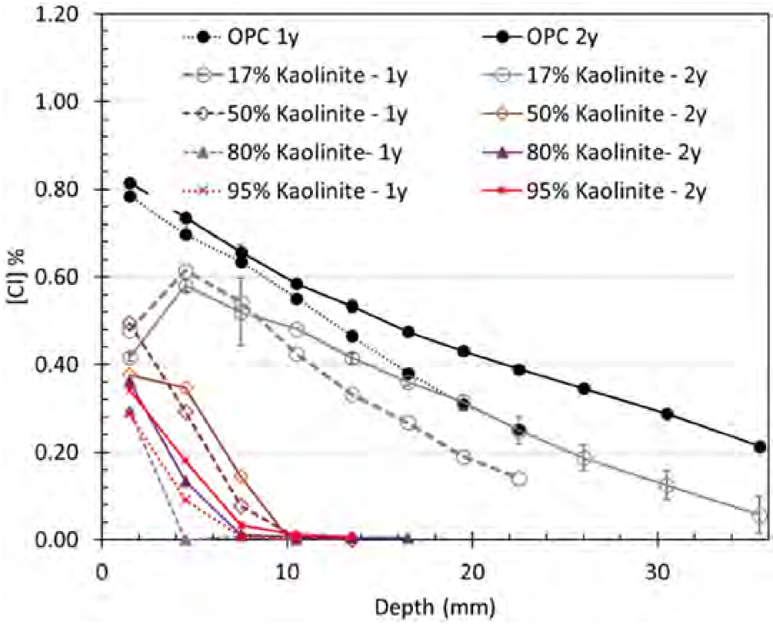

Fig. 12. Chloride erosion depth of OPC and LC^3-50 (with different kaolinite content in raw clays) [143].

Reports have noted that the capability of chloride binding in the clinker-calcined clay-limestone system is better than that of Portland cement. It is widely accepted that the binding of chloride ions in cement matrix are related to the Friedel's salt or physically absorption in the diffusion layer of CSH hydrates. In the clinker-calcined clay-limestone system, the incorporation of limestone and calcined clay increases the calcium and aluminium contents, which therefore helps to increase the volume of hydration products and improve the chloride binding capacity. Shi et al. [147] indicated that the use of MK-limestone increased the quantity of mono-carboaluminate generation during cement hydration. Sui et al. [148] found that the clinker-calcined clay-limestone system possessed superiority in resistance to chloride diffusion compared with other traditional cements. They also suggested that at least three factors (i.e. pore structure, binding capacity and pore solution) are important to the diffusion of chloride ions.

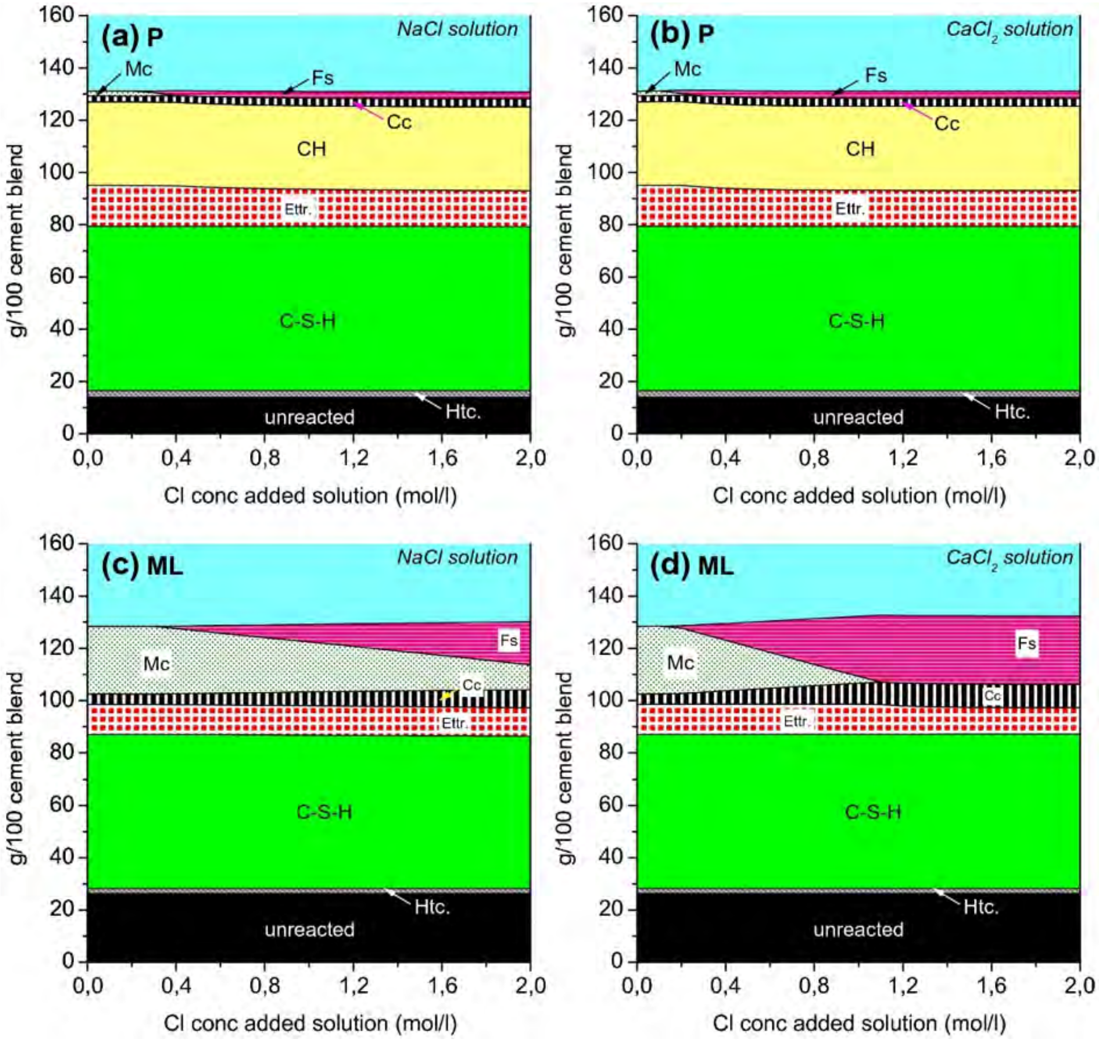

Fig. 13. Phase assemblages' prediction of the Portland cement (P) and MK-limestone blended cement (ML) pastes exposed to different Cl solutions (NaCl and $CaCl_2$). Ettr: ettringite; Mc: mono-carboaluminate; Fs: Friedel's salt; Htc: Hydrotalcite [147].

8. Environmental and economic benefits

Table 5 compares different parameters of different cement systems. It is obvious that the calcination temperature for kaolinitic clay is much lower (~800 °C) than that for clinker (1450°C), which means lower energy consumption. The advantage of calcined clay is that lower grade fuels (such as petroleum coke and even biomass) can be used to reach a relative low calcination temperature [158]. Compared with the production of Portland cement, clinker-calcined clay cement and clinker-calcined clay-limestone cements save 650 and 730 MJ/tonne of fuels, respectively. Joseph et al. [159] pointed out that the energy consumption of clay calcination was around 50% of clinker production, with the same fuel in India. In addition, for clinker-calcined clay cement and clinker-calcined clay-limestone cement, CO_2 emissions is significantly reduced by 26% and 33%, respectively. According to the mineral commodity summaries (2020), the total world cement production in 2019 is around 4.1 billion tons, especially high in the developing countries (e.g., China, 2.2 billion, India, 0.32 billion) [160]. If clinker-calcined clay cements and clinker-calcined clay-limestone cements are used instead

of Portland cement, CO_2 emissions can be reduced by 1.066 billion and 1.353 billion each year.
For commercial calcined clays, existing Portland cement clinker kilns can be retrofitted into clay calciners. The chain section can be applied to dry and break the raw kaolinitic clay materials, therefore it could avoid the requirement for additional pre-treatment equipment [141]. By utilizing refurbished rotary kilns, the energy demand is reported as approximately 2734 MJ/tonne. Compared with refurbished rotary kilns, the energy consumption of flash calcination is reduced by a further 12%, and the CO_2 emissions could decrease by a further 21%.

Table 5 Parameters for clay and different cements.

Category	Clinker content	Calcination temperature(°C)	CO_2 emissions, kg CO_2 eq./tonne of clay or cement	Energy demand, in MJ/tonne of clay or cement	Ref.
Clay	-	Refurbished kiln	249	3088	[161, 162]
	-	Flash calciner	196	2734	
Clinker-calcined clay-limestone	50%	$\sim800^{a}$, 1450^{b}	550	3990	[141, 157]
	85%	$\sim800^{a}$, 1450^{b}	610	4070	
PC	90%	1450^{b}	820	4720	

The lower temperature requirement for clay calcination, effectively saves the cost of energy consumption. Table 6 compares the products cost and commercial price of different cements. It can be seen that clinker-calcined clay-limestone (rotary) and clinker-calcined clay-limestone (flash) exhibit an obvious price advantage compared with Portland cement. Díaz et al. and Scrivener et al. analysed the commercial feasibility of utilizing old clinker kiln to retrofit clay calciner or adopting flash calciner to calcine clay. They found that both scenarios revealed better return on investment (ROI) [18, 141]. Joseph et al. indicated that clinker-calcined clay-limestone cements possessed comparable competitiveness with existing pozzolanic cements in India [159].

By investigating the potential mechanical/durability benefits of calcined clay cements, Pillai et al. evaluated the service life and life cycle of clinker-calcined clay-limestone cements compared with Portland cement and pulverised clinker-fly ash cement (FA + PC) [163]. They proposed that the service life of concrete based on the clinker-calcined clay-limestone system and the clinker-fly ash cement can be noticeably longer than that of structures using PC only.

Table 6 Commercial unit price and products cost. Data from: [141, 164]

Materials type	Products cost (USD/t)	Price (USD/t)
clinker-calcined clay-limestone (rotary)	61.42	108.33
clinker-calcined clay-limestone (flash)	56.41	108.33
PC	72.02	116.05

9. UK standards

In the UK, the use of calcined clay cements in concrete is guided by two key standards: BS 8500 and BS 8615. BS 8500 specifies the complementary guidelines to BS EN 206, which covers the production and composition of concrete. This standard outlines the criteria for different types of concrete mixes, including those incorporating calcined clays. Calcined clay cements were first included in this standard in 2019.

BS 8615 specifically addresses “natural calcined pozzolana”, a class of SCMs that includes calcined clay. This standard sets out the requirements for the chemical and physical properties of natural calcined pozzolana, ensuring that when these materials are used in concrete, they contribute positively to the strength, durability, and overall performance of the structure. BS 8615 provides a clear framework for the safe and effective use of calcined clay in cement, ensuring that it meets the necessary standards for construction.

In 2020, the Mineral Products Association (MPA) identified that very little calcined clay concrete was being produced in the UK which was due to a lack of (1) clay calcination plants in the UK and (2) experience/understanding of cements/concretes containing calcined clays, particularly using clays from UK sources. To address these issues the MPA along with project partners applied for funding from UK Research and Innovation (UKRI) to investigate the potential of calcined clays from UK-sourced materials, with a particular focus on using reclaimed materials. A key focus of this work will be to address the main gaps in the standards and guidance.

In summary, while BS 8500 and BS 8615 already provide a solid foundation for the use of calcined clay cements, further testing and research are likely to refine these standards. This will help to ensure that calcined clay cements are used effectively and safely, contributing to the development of more sustainable construction practices across the UK.

10. Summary

UK-sourced waste derived clays are potentially suited as supplementary cementitious materials for use as components of cements. However, before considering these materials as SCMs, it is necessary to i) characterise the raw clay materials, ii) optimise their heating, iii) test their reactivity in cements and iv) optimise admixtures and dosages. The “R3” method has been identified as the most suitable method for reactivity testing of prospective calcined clays as SCMs. Comparted with traditional cements, calcined clay cements are potentially lower in carbon while without compromising on performance. Performance is verified by carrying out a standard suite of tests to characterise and verify performance for concrete applications.

11. References

[1] Liu YJ, Xu YM, Geng CL. Sulfoaluminate cement: An alternative to Portland cement. in Advanced Materials Research. 2012. Trans Tech Publ.

[2] Shoubi MV, Barough AS, Amirsoleimani O. Assessment of the roles of various cement replacements in achieving the sustainable and high performance concrete. International Journal of Advances in Engineering & Technology, 2013. 6(1): p. 68.

[3] Rashad AM. A comprehensive overview about the influence of different additives on the properties of alkali-activated slag–A guide for Civil Engineer. Construction and building materials, 2013. 47: p. 29-55.

[4] Mohammed S. Processing, effect and reactivity assessment of artificial pozzolans obtained from clays and clay wastes: A review. Construction and Building Materials, 2017. 140: p. 10-19.

[5] Mikulčić H, Vujanović M, Duić N. Reducing the CO2 emissions in Croatian cement industry. Applied Energy, 2013. 101: p. 41-48.

[6] Teklay A, Yin C, Rosendahl L, Køhler LL. Experimental and modeling study of flash calcination of kaolinite rich clay particles in a gas suspension calciner. Applied Clay Science, 2015. 103: p. 10-19.

[7] Wee J-H. A review on carbon dioxide capture and storage technology using coal fly ash. Applied Energy, 2013. 106: p. 143-151.

[8] Suresh D, Nagaraju K. Ground granulated blast slag (GGBS) in concrete–a review. IOSR journal of mechanical and civil engineering, 2015. 12(4): p. 76-82.

[9] Khan MI, Siddique R. Utilization of silica fume in concrete: Review of durability properties. Resources, Conservation and Recycling, 2011. 57: p. 30-35.

[10] Wang Y, Cao Y, Zhang P. Effective Utilization of Waste Glass as Cementitious Powder and Construction Sand in Mortar. Materials, 2020. 13(3): p. 707.

[11] Nehdi M. Clay in cement-based materials: Critical overview of state-of-the-art. Construction and Building Materials, 2014. 51: p. 372-382.

[12] Brigatti MF, Galan E, Theng B. Structure and mineralogy of clay minerals, in Developments in clay science. 2013, Elsevier. p. 21-81.

[13] Tironi A, Trezza MA, Scian AN, Irassar EF. Assessment of pozzolanic activity of different calcined clays. Cement and Concrete Composites, 2013. 37: p. 319-327.

[14] Ferreiro S, Canut M, Lund J, Herfort D. Influence of fineness of raw clay and

calcination temperature on the performance of calcined clay-limestone blended cements. Applied Clay Science, 2019. 169: p. 81-90.

[15] Kenne Diffo B, Elimbi A, Cyr M, Dika Manga J, Tchakoute Kouamo H. Effect of the rate of calcination of kaolin on the properties of metakaolin-based geopolymers. Journal of Asian Ceramic Societies, 2015. 3(1): p. 130-138.

[16] Ghorbel H, Samet B. Effect of iron on pozzolanic activity of kaolin. Construction and Building Materials, 2013. 44: p. 185-191.

[17] Rashad AM. Metakaolin as cementitious material: History, scours, production and composition–A comprehensive overview. Construction and building materials, 2013. 41: p. 303-318.

[18] Scrivener K, Martirena F, Bishnoi S, Maity S. Calcined clay limestone cements (LC3). Cement and Concrete Research, 2018. 114: p. 49-56.

[19] Zhang Z, Zhu H, Zhou C, Wang H. Geopolymer from kaolin in China: an overview. Applied Clay Science, 2016. 119: p. 31-41.

[20] Scrivener KL. Options for the future of cement. Indian Concr. J, 2014. 88(7): p. 11-21.

[21] Zunino F, Scrivener KL. Processing of Calcined Clays for Applications in Cementitious Materials: The Use of Grinding Aids and Particle Classification After Grinding. in Proceedings of the International Conference of Sustainable Production and Use of Cement and Concrete. 2020. Springer.

[22] Scrivener K. Future cements: Research needs for sustainability and potential of LC3 Technology. in Book of Abstracts. 2016.

[23] Tuyan M, Andiç-Çakir Ö, Ramyar K. Effect of alkali activator concentration and curing condition on strength and microstructure of waste clay brick powder-based geopolymer. Composites Part B: Engineering, 2018. 135: p. 242-252.

[24] Longhi MA, Rodríguez ED, Walkley B, Zhang Z, Kirchheim AP. Metakaolin-based geopolymers: Relation between formulation, physicochemical properties and efflorescence formation. Composites Part B: Engineering, 2020. 182: p. 107671.

[25] Panda B, Ruan S, Unluer C, Tan MJ. Investigation of the properties of alkali-activated slag mixes involving the use of nanoclay and nucleation seeds for 3D printing. Composites Part B: Engineering, 2020. 186: p. 107826.

[26] Paiva H, Velosa A, Cachim P, Ferreira VM. Effect of metakaolin dispersion on the fresh and hardened state properties of concrete. Cement and Concrete Research, 2012. 42(4): p. 607-612.

[27] Schulze SE, Rickert J. Suitability of natural calcined clays as supplementary cementitious material. Cement and Concrete Composites, 2019. 95: p. 92-97.

[28] Scrivener K, Avet F, Maraghechi H, Zunino F, Ston J, Hanpongpun W, Favier A. Impacting factors and properties of limestone calcined clay cements (LC3). Green Materials, 2018. 7(1): p. 3-14.

[29] Rong Z, Jiang G, Sun W. Effects of metakaolin on mechanical and microstructural properties of ultra-high performance cement-based composites. Journal of Sustainable Cement-Based Materials, 2018. 7(5): p. 296-310.

[30] Ahmad S, Malik MI, Wani MB, Ahmad R. Study of concrete involving use of waste paper sludge ash as partial replacement of cement. IOSR Journal of Engineering (IOSRJEN), 2013. 3(11): p. 6-15.

[31] Schankoski RA, Pilar R, Prudêncio Jr LR, Ferron RD. Evaluation of fresh cement pastes containing quarry by-product powders. Construction and Building Materials, 2017. 133: p. 234-242.

[32] Belas N, Belaribi O, Aggoun S, Bendani K, Bouhamou N-E, Mebrouki A. Enhancing value of dam Dredged sediments as a component of a self-compacting concrete. Intenational Jornal of Geotechnical and Geological Engineering, 2014. 14(12): p. 110-116.

[33] Gagarin A, Thankappan AK, Antony J. Strength and Durability of Mortar Incorporating Roof Tile Powder as Partial Cement Replacement Material. 2017, Department of Civil Engineering Federal Institute of Science Ande Technology ….

[34] Pereira-de-Oliveira LA, Castro-Gomes JP, Santos PM. The potential pozzolanic activity of glass and red-clay ceramic waste as cement mortars components. Construction and Building Materials, 2012. 31: p. 197-203.

[35] Aglietti E, Lopez JP, Pereira E. Mechanochemical effects in kaolinite grinding. II. Structural aspects. International journal of mineral processing, 1986. 16(1-2): p. 135-146.

[36] Singh M, Srivastava A, Bhunia D. An investigation on effect of partial replacement of cement by waste marble slurry. Construction and Building Materials, 2017. 134: p. 471-488.

[37] Horpibulsuk S, Phojan W, Suddeepong A, Chinkulkijniwat A, Liu MD. Strength development in blended cement admixed saline clay. Applied clay science, 2012. 55: p. 44-52.

[38] Awoyera P, Dawson A, Thom N, Akinmusuru J. Suitability of mortars produced using laterite and ceramic wastes: Mechanical and microscale analysis. Construction and Building Materials, 2017. 148: p. 195-203.

[39] Prahara E. Compressive strength and water absorption of pervious concrete that using the fragments of ceramics and roof tiles. in EPJ Web of Conferences. 2014. EDP Sciences.

[40] Toker Derdiyok M, Ergin H. The Use of Fired Ceramic Tile Wastes in the Production of Blended Cement. in 2015-Sustainable Industrial Processing Summit. 2015. Flogen Star Outreach.

[41] Zhou CH, Keeling J. Fundamental and applied research on clay minerals: From climate and environment to nanotechnology. Applied Clay Science, 2013. 74: p. 3-9.

[42] Souri A, Kazemi-Kamyab H, Snellings R, Naghizadeh R, Golestani-Fard F, Scrivener K. Pozzolanic activity of mechanochemically and thermally activated kaolins in cement. Cement and Concrete Research, 2015. 77: p. 47-59.

[43] Tironi A, Trezza M, Irassar E, Scian A. Thermal treatment of kaolin: effect on the pozzolanic activity. Procedia Materials Science, 2012. 1: p. 343-350.

[44] Fitos M, Badogiannis EG, Tsivilis SG, Perraki M. Pozzolanic activity of thermally and mechanically treated kaolins of hydrothermal origin. Applied Clay Science, 2015. 116: p. 182-192.

[45] Avet F, Scrivener K. Investigation of the calcined kaolinite content on the hydration of Limestone Calcined Clay Cement (LC3). Cement and Concrete Research, 2018. 107: p. 124-135.

[46] ASTM C. 618-03. Coal Fly Ash and Raw or Calcined Natural Pozzolan for Use in Concrete. Philadelphia (PA): American Society for Testing and Materials, 2003.

[47] Hollanders S, Adriaens R, Skibsted J, Cizer Ö, Elsen J. Pozzolanic reactivity of pure calcined clays. Applied Clay Science, 2016. 132-133: p. 552-560.

[48] Walker R, Pavía S. Physical properties and reactivity of pozzolans, and their influence on the properties of lime–pozzolan pastes. Materials and structures, 2011. 44(6): p. 1139-1150.

[49] Almenares RS, Vizcaíno LM, Damas S, Mathieu A, Alujas A, Martirena F. Industrial calcination of kaolinitic clays to make reactive pozzolans. Case studies in construction materials, 2017. 6: p. 225-232.

[50] Ilić BR, Mitrović AA, Miličić LR. Thermal treatment of kaolin clay to obtain metakaolin. Hemijska industrija, 2010. 64(4): p. 351-356.

[51] Hanpongpun W. Investigation of the use of Limestone Calcined Clay Cement (LC3) applied to Thailand. 2019, EPFL.

[52] San Nicolas R, Cyr M, Escadeillas G. Characteristics and applications of flash metakaolins. Applied Clay Science, 2013. 83: p. 253-262.

[53] Snellings R, Horckmans L, Van Bunderen C, Vandewalle L, Cizer Ö. Flash-calcined dredging sediment blended cements: effect on cement hydration and properties. Materials and Structures, 2017. 50(6): p. 241.

[54] Garg N, Skibsted J. Pozzolanic reactivity of a calcined interstratified illite/smectite (70/30) clay. Cement and Concrete Research, 2016. 79: p. 101-111.

[55] Fabbri B, Gualtieri S, Leonardi C. Modifications induced by the thermal treatment of kaolin and determination of reactivity of metakaolin. Applied Clay Science, 2013. 73: p. 2-10.

[56] Uchima JS, Restrepo OJ, Tobón JI. Pozzolanicity of the material obtained in the simultaneous calcination of biomass and kaolinitic clay. Construction and Building Materials, 2015. 95: p. 414-420.

[57] Al-Ani T, Sarapää O. Clay and clay mineralogy. Physical-chemical Properties and Industrial Uses, 2008.

[58] Zhang Z, Yao X, Zhu H, Hua S, Chen Y. Activating process of geopolymer source material: Kaolinite. Journal of Wuhan University of Technology-Mater. Sci. Ed., 2009. 24(1): p. 132-136.

[59] Vizcayno C, De Gutierrez R, Castello R, Rodriguez E, Guerrero C. Pozzolan obtained by mechanochemical and thermal treatments of kaolin. Applied Clay Science, 2010. 49(4): p. 405-413.

[60] Sperinck S, Raiteri P, Marks N, Wright K. Dehydroxylation of kaolinite to metakaolin—a molecular dynamics study. Journal of Materials Chemistry, 2011. 21(7): p. 2118-2125.

[61] Brindley G, Nakahira M. A new concept of the transformation sequence of kaolinite to mullite. Nature, 1958. 181(4619): p. 1333.

[62] Alujas A, Fernández R, Quintana R, Scrivener KL, Martirena F. Pozzolanic reactivity of low grade kaolinitic clays: Influence of calcination temperature and impact of calcination products on OPC hydration. Applied Clay Science, 2015. 108: p. 94-101.

[63] Rashad AM. Metakaolin as cementitious material: History, scours, production and composition – A comprehensive overview. Construction and Building Materials, 2013. 41: p. 303-318.

[64] Chikouche MA, Ghorbel E, Bibi M. The possibility of using dredging sludge in manufacturing cements: Optimization of heat treatment cycle and ratio replacement. Construction and Building Materials, 2016. 106: p. 330-341.

[65] Janotka I, Puertas F, Palacios M, Kuliffayová M, Varga C. Metakaolin sand–blended-cement pastes: Rheology, hydration process and mechanical properties. Construction and Building Materials, 2010. 24(5): p. 791-802.

[66] Taylor-Lange SC, Riding KA, Juenger MC. Increasing the reactivity of metakaolin-cement blends using zinc oxide. Cement and Concrete Composites, 2012. 34(7): p. 835-847.

[67] Giménez RG, Vegas I, de la Villa RV, Frías M. Ion mobilisation and transport through cement mortars blended with thermally activated paper sludge in natural climatic conditions. Water, air, and soil pollution, 2009. 203(1-4): p. 39-52.

[68] ASTM C. C125 - 15b (2016) Standard terminology relating to concrete and concrete aggregates. ASTM International, West Conshohocken, Pennsylvania.

[69] Aliabdo AA, Abd-Elmoaty A-EM, Hassan HH. Utilization of crushed clay brick in concrete industry. Alexandria Engineering Journal, 2014. 53(1): p. 151-168.

[70] Avet F, Snellings R, Alujas Diaz A, Ben Haha M, Scrivener K. Development of a new rapid, relevant and reliable (R3) test method to evaluate the pozzolanic reactivity of calcined kaolinitic clays. Cement and Concrete Research, 2016. 85: p. 1-11.

[71] Marchetti G, Pokorny J, Tironi A, Trezza MA, Rahhal VF, Pavlík Z, Černý R, Irassar EF. Blended Cements with Calcined Illitic Clay: Workability and Hydration, in Calcined Clays for Sustainable Concrete. 2018, Springer. p. 310-317.

[72] Frankeová D, Slížková Z. Determination of the pozzolanic activity of mortar's components by thermal analysis. Journal of Thermal Analysis and Calorimetry, 2016. 125(3): p. 1115-1123.

[73] ASTM C. Standard test methods for sampling and testing fly ash or natural pozzolans for use in portland-cement concrete. 2013.

[74] Ferraz E. Pozzolanic activity of metakaolins by the French standard of the modified Chapelle test: A direct methology. Acta Geodynamica et Geomaterialia, 2015: p. 289-298.

[75] Asbridge A, Walters G, Jones T. Ternary blended concretes-OPC/GGBFS/metakaolin. Denmark: Concrete Across Borders, 1994: p. 547-557.

[76] Quarcioni V, Chotoli F, Coelho A, Cincotto M. Indirect and direct Chapelle's methods for the determination of lime consumption in pozzolanic materials. Revista Ibracon de Estruturas e Materiais, 2015. 8(1): p. 1-7.

[77] Donatello S, Tyrer M, Cheeseman C. Comparison of test methods to assess pozzolanic activity. Cement and Concrete Composites, 2010. 32(2): p. 121-127.

[78] Suraneni P, Weiss J. Examining the pozzolanicity of supplementary cementitious materials using isothermal calorimetry and thermogravimetric analysis. Cement and Concrete Composites, 2017. 83: p. 273-278.

[79] Danner T, Norden G, Justnes H. Characterisation of calcined raw clays suitable as supplementary cementitious materials. Applied Clay Science, 2018. 162: p. 391-402.

[80] Abo-El-Enein SA, Amin MS, El-Hosiny FI, Hanafi S, ElSokkary TM, Hazem MM. Pozzolanic and hydraulic activity of nano-metakaolin. HBRC Journal, 2019. 10(1): p. 64-72.

[81] Elimbi A, Tchakoute H, Njopwouo D. Effects of calcination temperature of kaolinite clays on the properties of geopolymer cements. Construction and Building Materials, 2011. 25(6): p. 2805-2812.

[82] Mardani-Aghabaglou A, Sezer Gİ, Ramyar K. Comparison of fly ash, silica fume and metakaolin from mechanical properties and durability performance of mortar mixtures view point. Construction and Building Materials, 2014. 70: p. 17-25.

[83] Tironi A, Trezza MA, Scian AN, Irassar EF. Kaolinitic calcined clays: Factors affecting its performance as pozzolans. Construction and Building Materials, 2012. 28(1): p. 276-281.

[84] Mardani-Aghabaglou A, İnan Sezer G, Ramyar K. Comparison of fly ash, silica fume and metakaolin from mechanical properties and durability performance of mortar mixtures view point. Construction and Building Materials, 2014. 70: p. 17-25.

[85] Foley EM, Kim JJ, Taha MR. Synthesis and nano-mechanical characterization of calcium-silicate-hydrate (CSH) made with 1.5 CaO/SiO2 mixture. Cement and concrete research, 2012. 42(9): p. 1225-1232.

[86] Zeng Q, Li K, Fen-chong T, Dangla P. Determination of cement hydration and pozzolanic reaction extents for fly-ash cement pastes. Construction and Building Materials, 2012. 27(1): p. 560-569.

[87] Shi Z, Lothenbach B. The role of calcium on the formation of alkali-silica reaction products. Cement and Concrete Research, 2019. 126: p. 105898.

[88] Murat M. Hydration reaction and hardening of calcined clays and related minerals. Cement and Concrete Research, 1983. 13(2): p. 259-266.

[89] Bredy P, Chabannet M, Pera J. Microstructure and porosity of metakaolin blended cements. MRS Online Proceedings Library Archive, 1988. 136.

[90] Rojas MFa, de Rojas MS. The effect of high curing temperature on the reaction kinetics in MK/lime and MK-blended cement matrices at 60 C. Cement and Concrete Research, 2003. 33(5): p. 643-649.

[91] Lagier F, Kurtis KE. Influence of Portland cement composition on early age reactions with metakaolin. Cement and Concrete Research, 2007. 37(10): p. 1411-1417.

[92] Cassagnabere F, Diederich P, Mouret M, Escadeillas G, Lachemi M. Impact of metakaolin characteristics on the rheological properties of mortar in the fresh state. Cement and Concrete Composites, 2013. 37: p. 95-107.

[93] Zhou D, Wang R, Tyrer M, Wong H, Cheeseman C. Sustainable infrastructure development through use of calcined excavated waste clay as a supplementary cementitious material. Journal of Cleaner Production, 2017. 168: p. 1180-1192.

[94] Jiang G, Jie L, Sun W. Effects of metakaolin on properties of high performance mortar.

Journal of Southeast University (Natural Science Edition), 2015. 45(1): p. 121-125.

[95] Kawashima S, Kim JH, Corr DJ, Shah SP. Study of the mechanisms underlying the fresh-state response of cementitious materials modified with nanoclays. Construction and Building Materials, 2012. 36: p. 749-757.

[96] Pierkes R, Schulze SE, Rickert J. Durability of concretes made with calcined clay composite cements, in Calcined Clays for Sustainable Concrete. 2018, Springer. p. 366-371.

[97] Huenger K-J, Sander I, Zuckow N. On the Workability of Mortar and Concrete Mixtures containing Calcined Clay Blends. 2019.

[98] Jin X, Li Z. Effects of mineral admixture on properties of young concrete. Journal of materials in civil engineering, 2003. 15(5): p. 435-442.

[99] Li L, Zhuo Z, Zhu J, Chen J, Kwan A. Reutilizing ceramic polishing waste as powder filler in mortar to reduce cement content by 33% and increase strength by 85%. Powder Technology, 2019.

[100] Duan P, Shui Z, Chen W, Shen C. Efficiency of mineral admixtures in concrete: Microstructure, compressive strength and stability of hydrate phases. Applied Clay Science, 2013. 83: p. 115-121.

[101] Hossain M, Karim M, Hasan M, Hossain M, Zain MFM. Durability of mortar and concrete made up of pozzolans as a partial replacement of cement: A review. Construction and Building Materials, 2016. 116: p. 128-140.

[102] Wang Y, Cao Y, Zhang P, Ma Y, Zhao T, Wang H, Zhang Z. Water absorption and chloride diffusivity of concrete under the coupling effect of uniaxial compressive load and freeze–thaw cycles. Construction and Building Materials, 2019. 209: p. 566-576.

[103] Bao J, Li S, Zhang P, Ding X, Xue S, Cui Y, Zhao T. Influence of the incorporation of recycled coarse aggregate on water absorption and chloride penetration into concrete. Construction and Building Materials, 2020. 239: p. 117845.

[104] Mindess S, Young F, Darwin D. Concrete 2nd Editio. Technical Documents, 2003.

[105] Güneyisi E, Gesoğlu M, Mermerdaş K. Strength deterioration of plain and metakaolin concretes in aggressive sulfate environments. Journal of Materials in Civil Engineering, 2010. 22(4): p. 403-407.

[106] Aiswarya S, Prince Arulraj G, Dilip C. A review on use of metakaolin in concrete. IRACST–Engineering Science and Technology: An International Journal (ESTIJ), 2013. 3(3): p. 592-597.

[107] Kirsanova A, Kramar L. Application features of additives based on metakaolin in concrete. in IOP Conference Series: Materials Science and Engineering. 2015. IOP Publishing.

[108] Zhang M, Chen J, Lv Y, Wang D, Ye J. Study on the expansion of concrete under attack of sulfate and sulfate–chloride ions. Construction and Building Materials, 2013. 39: p. 26-32.

[109] de Lucas EA, Medina C, Frías M, de Rojas MIS. Clay-based construction and demolition waste as a pozzolanic addition in blended cements. Effect on sulfate resistance. Construction and Building Materials, 2016. 127: p. 950-958.

[110] Kavitha O, Shanthi V, Arulraj GP, Sivakumar V. Microstructural studies on eco-friendly and durable self-compacting concrete blended with metakaolin. Applied Clay Science, 2016. 124: p. 143-149.

[111] Zhang P, Wittmann FH, Vogel M, Müller HS, Zhao T. Influence of freeze-thaw cycles on capillary absorption and chloride penetration into concrete. Cement and Concrete Research, 2017. 100: p. 60-67.

[112] Guo Y, Zhang T, Tian W, Wei J, Yu Q. Physically and chemically bound chlorides in hydrated cement pastes: A comparison study of the effects of silica fume and metakaolin. Journal of materials science, 2019. 54(3): p. 2152-2169.

[113] Gbozee M, Zheng K, He F, Zeng X. The influence of aluminum from metakaolin on chemical binding of chloride ions in hydrated cement pastes. Applied Clay Science, 2018. 158: p. 186-194.

[114] Marangu JM, Thiong'o JK, Wachira JM. Chloride ingress in chemically activated calcined clay-based cement. Journal of Chemistry, 2018. 2018.

[115] Dousti A, Beaudoin JJ, Shekarchi M. Chloride binding in hydrated MK, SF and natural zeolite-lime mixtures. Construction and Building Materials, 2017. 154: p. 1035-1047.

[116] Arya C, Buenfeld N, Newman J. Factors influencing chloride-binding in concrete. Cement and Concrete research, 1990. 20(2): p. 291-300.

[117] Machner A, Zajac M, Haha MB, Kjellsen KO, Geiker MR, De Weerdt K. Stability of the hydrate phase assemblage in Portland composite cements containing dolomite and metakaolin after leaching, carbonation, and chloride exposure. Cement and Concrete Composites, 2018. 89: p. 89-106.

[118] Machner A, Zajac M, Haha MB, Kjellsen KO, Geiker MR, De Weerdt K. Chloride-binding capacity of hydrotalcite in cement pastes containing dolomite and metakaolin. Cement and Concrete Research, 2018. 107: p. 163-181.

[119] Ye H, Jin X, Chen W, Fu C, Jin N. Prediction of chloride binding isotherms for blended cements. Comput. Concr., 2016. 17(5): p. 655-672.

[120] Fan Y, Zhang S, Kawashima S, Shah SP. Influence of kaolinite clay on the chloride diffusion property of cement-based materials. Cement and Concrete Composites, 2014. 45: p. 117-124.

[121] Ramezanianpour A, Jovein HB. Influence of metakaolin as supplementary cementing material on strength and durability of concretes. Construction and Building materials, 2012. 30: p. 470-479.

[122] Wang D, Shi C, Farzadnia N, Shi Z, Jia H, Ou Z. A review on use of limestone powder in cement-based materials: Mechanism, hydration and microstructures. Construction and Building Materials, 2018. 181: p. 659-672.

[123] Bederina M, Makhloufi Z, Bouziani T. Effect of limestone fillers the physic-mechanical properties of limestone concrete. Physics Procedia, 2011. 21: p. 28-34.

[124] Zhang M-h, Li H. Pore structure and chloride permeability of concrete containing nano-particles for pavement. Construction and Building Materials, 2011. 25(2): p. 608-616.

[125] Aqel M, Panesar D. Hydration kinetics and compressive strength of steam-cured cement pastes and mortars containing limestone filler. Construction and Building Materials, 2016. 113: p. 359-368.

[126] Soroka I, Stern N. Calcareous fillers and the compressive strength of Portland cement. Cement and Concrete Research, 1976. 6(3): p. 367-376.

[127] Craeye B, De Schutter G, Desmet B, Vantomme J, Heirman G, Vandewalle L, Cizer Ö, Aggoun S, Kadri E. Effect of mineral filler type on autogenous shrinkage of self-compacting concrete. Cement and Concrete Research, 2010. 40(6): p. 908-913.

[128] Tironi A, Scian AN, Irassar EF. Blended cements with limestone filler and kaolinitic calcined clay: Filler and pozzolanic effects. Journal of Materials in Civil Engineering, 2017. 29(9): p. 04017116.

[129] Tennis P, Thomas M, Weiss W. State-of-the-Art Report on Use of Limestone in Cements at Levels of up to 15%. Illinois, accessed November, 2011. 9: p. 2015.

[130] De Weerdt K, Haha MB, Le Saout G, Kjellsen KO, Justnes H, Lothenbach B. Hydration mechanisms of ternary Portland cements containing limestone powder and fly ash. Cement and Concrete Research, 2011. 41(3): p. 279-291.

[131] Bizzozero J, Scrivener KL. Limestone reaction in calcium aluminate cement–calcium sulfate systems. Cement and Concrete Research, 2015. 76: p. 159-169.

[132] Wang D, Shi C, Farzadnia N, Shi Z, Jia H. A review on effects of limestone powder on the properties of concrete. Construction and building materials, 2018. 192: p. 153-166.

[133] Krishnan S, Bishnoi S. Understanding the hydration of dolomite in cementitious systems with reactive aluminosilicates such as calcined clay. Cement and Concrete Research, 2018. 108: p. 116-128.

[134] Antoni M. Investigation of cement substitution by blends of calcined clays and limestone. 2013, EPFL.

[135] Vance K, Aguayo M, Oey T, Sant G, Neithalath N. Hydration and strength development in ternary portland cement blends containing limestone and fly ash or metakaolin. Cement and Concrete Composites, 2013. 39: p. 93-103.

[136] Muzenda TR, Hou P, Kawashima S, Sui T, Cheng X. The role of limestone and calcined clay on the rheological properties of LC3. Cement and Concrete Composites, 2020: p. 103516.

[137] Vance K, Kumar A, Sant G, Neithalath N. The rheological properties of ternary binders containing Portland cement, limestone, and metakaolin or fly ash. Cement and Concrete Research, 2013. 52: p. 196-207.

[138] Zaribaf BH, Uzal B, Kurtis K. Compatibility of superplasticizers with limestone-metakaolin blended cementitious system, in Calcined Clays for Sustainable Concrete. 2015, Springer. p. 427-434.

[139] Santos FN, de Sousa SRG, Bombard AJF, Vieira SL. Rheological study of cement paste with metakaolin and/or limestone filler using Mixture Design of Experiments. Construction and building materials, 2017. 143: p. 92-103.

[140] Nair N, Haneefa KM, Santhanam M, Gettu R. A study on fresh properties of limestone calcined clay blended cementitious systems. Construction and Building Materials, 2020. 254: p. 119326.

[141] Cancio Díaz Y, Sánchez Berriel S, Heierli U, Favier AR, Sánchez Machado IR, Scrivener KL, Martirena Hernández JF, Habert G. Limestone calcined clay cement as a low-carbon solution to meet expanding cement demand in emerging economies. Development Engineering, 2017. 2: p. 82-91.

[142] Antoni M, Rossen J, Martirena F, Scrivener K. Cement substitution by a combination of metakaolin and limestone. Cement and Concrete Research, 2012. 42(12): p. 1579-1589.

[143] Maraghechi H, Avet F, Wong H, Kamyab H, Scrivener K. Performance of Limestone Calcined Clay Cement (LC3) with various kaolinite contents with respect to chloride transport. Materials and Structures, 2018. 51(5).

[144] Dhandapani Y, Santhanam M. Assessment of pore structure evolution in the limestone calcined clay cementitious system and its implications for performance. Cement and Concrete Composites, 2017. 84: p. 36-47.

[145] Dhandapani Y, Sakthivel T, Santhanam M, Gettu R, Pillai RG. Mechanical properties and durability performance of concretes with Limestone Calcined Clay Cement (LC3). Cement and Concrete Research, 2018. 107: p. 136-151.

[146] Avet F, Scrivener K. Hydration study of limestone calcined clay cement (LC 3) using various grades of calcined kaolinitic clays, in Calcined Clays for Sustainable Concrete. 2018, Springer. p. 35-40.

[147] Shi Z, Geiker MR, De Weerdt K, Østnor TA, Lothenbach B, Winnefeld F, Skibsted J. Role of calcium on chloride binding in hydrated Portland cement–metakaolin–limestone blends. Cement and Concrete Research, 2017. 95: p. 205-216.

[148] Sui S, Georget F, Maraghechi H, Sun W, Scrivener K. Towards a generic approach to durability: Factors affecting chloride transport in binary and ternary cementitious materials. Cement and Concrete Research, 2019. 124: p. 105783.

[149] Shi Z, Ferreiro S, Lothenbach B, Geiker MR, Kunther W, Kaufmann J, Herfort D, Skibsted J. Sulfate resistance of calcined clay – Limestone – Portland cements. Cement and Concrete Research, 2019. 116: p. 238-251.

[150] Apsa VRR. Performance of Limestone Calcined Clay Cement (LC^3) International Journal of Recent Technology and Engineering 2019. 7(6C2): p. 260-265.

[151] Yu C, Yuan P, Yu X, Liu J. Degradation of Calcined Clay-Limestone Cementitious Composites Under Sulfate Attack, in Calcined Clays for Sustainable Concrete. 2018, Springer. p. 110-116.

[152] Marciniak A, Grymin W, Margiewicz T, Koniorczyk M. Influence of freezing-induced damage on the carbonation rate of concrete. European Journal of Environmental and Civil Engineering, 2017. 21(10): p. 1285-1300.

[153] Díaz E, González R, Rocha D, Alujas A, Martirena F. Carbonation of concrete with low carbon cement LC3 exposed to different environmental conditions, in Calcined Clays for Sustainable Concrete. 2018, Springer. p. 141-146.

[154] Khan M, Nguyen Q, Castel A. Carbonation of limestone calcined clay cement concrete, in Calcined Clays for Sustainable Concrete. 2018, Springer. p. 238-243.

[155] Repacholi M. Clay mineralogy: spectroscopic and chemical determinative methods. 2012: Springer Science & Business Media.

[156] Tironi A, Trezza MA, Scian AN, Irassar EF. Potential use of Argentine kaolinitic clays as pozzolanic material. Applied Clay Science, 2014. 101: p. 468-476.

[157] Gettu R, Patel A, Rathi V, Prakasan S, Basavaraj A, Palaniappan S, Maity S. Influence of supplementary cementitious materials on the sustainability parameters of cements and concretes in the Indian context. Materials and Structures, 2019. 52(1): p. 10.

[158] Naqi A, Jang JG. Recent progress in green cement technology utilizing low-carbon emission fuels and raw materials: A review. Sustainability, 2019. 11(2): p. 537.

[159] Joseph S, Bishnoi S, Maity S. An economic analysis of the production of limestone calcined clay cement in India. Indian Concr. J, 2016. 90(11): p. 22-27.

[160] Interior USDot, Survey UG. Mineral Commodity Summaries, 2020. 2020: Government Printing Office.

[161] Habert G, Billard C, Rossi P, Chen C, Roussel N. Cement production technology improvement compared to factor 4 objectives. Cement and Concrete Research, 2010. 40(5): p. 820-826.

[162] Habert G, De Lacaillerie JDE, Roussel N. An environmental evaluation of geopolymer based concrete production: reviewing current research trends. Journal of cleaner production, 2011. 19(11): p. 1229-1238.

[163] Pillai RG, Gettu R, Santhanam M, Rengaraju S, Dhandapani Y, Rathnarajan S, Basavaraj AS. Service life and life cycle assessment of reinforced concrete systems with limestone calcined clay cement (LC3). Cement and Concrete Research, 2019. 118: p. 111-119.

[164] Li J, Tharakan P, Macdonald D, Liang X. Technological, economic and financial prospects of carbon dioxide capture in the cement industry. Energy Policy, 2013. 61: p. 1377-1387.

Re-C3: Reclaimed Calcined Clay Cements

Appendix 2 -

Characterization of raw and lab calcined clays

Authors
Imerys:
Barbara Benevenuti
Deeba Ansari
Tony Newton
Serge Ghilardi
Philippe Thouilleux

23/01/2024

Contents

Table of Figures

Table of Tables

1. Introduction

In the context of the Re-C3 project, Imerys was in charge of preparing and characterizing samples of raw and laboratory calcined clays (activated clays).
For that, Imerys selected 5 samples of raw clays from its own operations and received 5 samples from its cement producing partners.

The 10 selected raw clay samples were characterized following different methods, and then crushed and calcined to obtain samples of laboratory calcined clays that were also analysed. Part of each raw and calcined sample was sent to the University College of London (UCL), to be evaluated by them in the Workpackage E.

In this report will be presented the tests performed and the results obtained with these samples, which should help in the selection of the candidates retained for the further steps of the project.

2. Experimental procedure

2.1. Materials

The ten raw clays samples and their suppliers are presented in Table 1.

Supplier	Re-C3 ID
Imerys	RC1
Imerys	RC2
Imerys	RC3
Imerys	RC4
Imerys	RC5
Heidelberg	RC6
Heidelberg	RC7
Tarmac	RC8
Tarmac	RC9
Aggregates Industry	RC10

Table 1: Raw clay samples tested in the project

After the clays were activated by calcination, the obtained samples were identified by codes indicating the maximum temperature in their calcination cycle and the time of calcination. For example, CC1-800-3 indicates the laboratory calcined clay obtained from the raw clay 1, after 3 hours of calcination at the maximum temperature of 800°C.

Samples	Re-C3 ID
RC1 calcined at 800°C for 3h	CC1-800-3
RC2 calcined at 800°C for 3h	CC2-800-3
RC3 calcined at 800°C for 3h	CC3-800-3
RC4 calcined at 800°C for 3h	CC4-800-3
RC5 calcined at 800°C for 3h	CC5-800-3
RC6 calcined at 850°C for 3h	CC6-850-3
RC7 calcined at 850°C for 3h	CC7-850-3
RC8 calcined at 850°C for 3h	CC8-850-3
RC9 calcined at 850°C for 3h	CC9-850-3
RC10 calcined at 850°C for 3h	CC10-850-3

Table 2: Calcined clay samples tested in the project

2.2. Methods

2.2.1. Preparation of the raw clay samples

The raw clays were received in the Imerys Technology Center (ITC) in Lyon in different forms: some were fine powders, other pebbles, some were dry and others had residual humidity.

All the samples requiring drying were kept for 24 hours in an oven at 110°C.
All samples were milled to a dMAX<63µm prior to their characterization in the raw state. Prior to calcination, the samples in pebble form were crushed to a d_{MAX}<5mm.

2.2.2. Preparation of the laboratory calcined clay samples

In order to obtain a homogeneous and representative sample, at least 10kg of coarse raw clay were ground to obtain a 0-5mm material, from which a 1kg sample was taken by quartering.

For the fine clays, the 1kg sample was directly obtained from the larger received sample by quartering. The 1kg clay samples were then divided in two crucibles, containing around 500g of clay each that were placed in a laboratory static oven and they were submitted to a calcination cycle.

In the first round of tests the Imerys' clays were prepared at 800°C, temperature which is considered by Imerys as ideal for kaolinitic clays, while the cement producers' clays were calcined at 850°C, temperature indicated by Heidelberg as the optimal one for their material.
The temperature profile used in the calcination was as follows:

- Room temperature to 300°C, heating speed of 600°C/hour, for 30min
- 300°C to 600°C, heating speed of 200°C/hour, for 1h30
- 600°C to 800/850°C, heating speed of 100°C/hour, for 2h or 2h30
- 800/850°C to room temperature, cooling speed not controlled.

The calcined clays were left to cool down, and then milled in a ball mill, until they reached a d_{50} around 5µm, which is Imerys' commercial calcined clays usual fineness. Depending on the hardness of the clays, more or fewer milling cycles were required to reach the targeted fineness.

Figure 1 shows the main steps of preparation of the calcined clays and the pieces of equipment used.

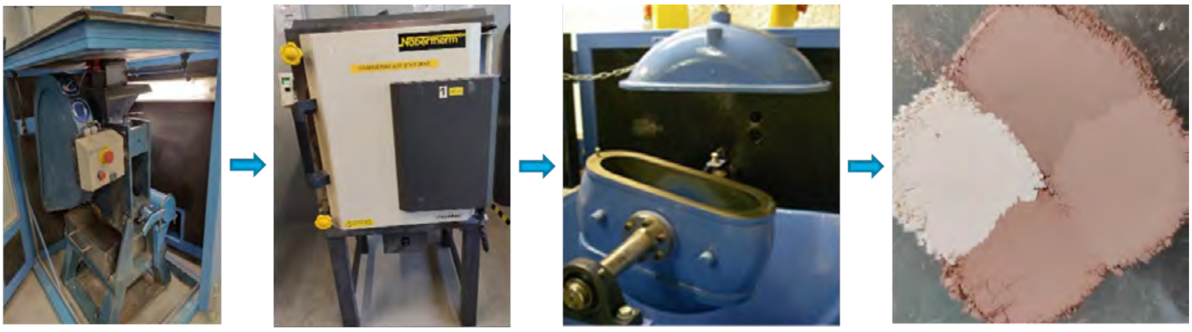

Grinding in jaw crusher Calcination in lab static oven Milling in ball mill Milled calcined clays

Figure 1: Steps of preparation of the calcined clay samples.

2.2.3. Characterization of the raw clay samples

The milled raw clays were characterized by:

- **X-ray fluorescence**, using a Panalytical Zetium and the SuperQ 6.3 software, with glass disc samples, to quantify their chemical composition.
- **X-ray diffraction**, using a Panalytical X'Pert Pro and the Highscore software, to semi-quantify their mineralogical composition.
- **Thermogravimetric analysis and differential scanning calorimetry**, using an ATG/DSC NETZSCH STA449F3, to quantify their mass loss and identify the dehydroxylation and other reactions taking place when the clays are exposed to high temperatures. The samples are heated at 10°C/min up to 1000°C.
- **Colorimetry**, using a X-Rite Ci4200, to evaluate their colour.

2.2.4. Characterization of the laboratory calcined clay samples

The calcined clays were characterized by the same methods as the raw clays, and also by **dry laser granulometry**, using a Malvern Mastersizer 3000 and a 3-bar pressure, in order to measure their grain size distribution after milling.

3. Results

In the coming paragraphs are presented the characteristics of the raw and laboratory calcined clays, obtained through the testing methods described above. The main parameter we look to assess is the kaolin content on the raw clay, which is directly correlated to the metakaolin content in the calcined clays, having therefore a significant influence on the reactivity of the final product.

The direct quantification of this phase is not simple, thus different methods were used and their results were compared. It is important to notice that all of these methods have some limitations, and it is not unexpected that they provide different estimations of the amount of kaolinite in the raw clay.

3.1. Chemical composition by X-ray Fluorescence (XRF)

3.1.1. Raw clays

Table 3 below shows the chemical composition of the raw clays, expressed in the form of oxides, considering the loss on ignition (LOI, at 1000°C).

Samples	LOI	Al_2O_3	SiO_2	K_2O	Fe_2O_3	TiO_2	CaO	MgO	Na_2O	P_2O_5
RC1	2.5	16.0	73.3	5.3	1.6	0.1	0.1	0.3	0.6	0.13
RC2	8.7	31.9	52.7	4.2	1.5	0.1	0.1	0.4	0.3	0.10
RC3	10.5	34.5	50.0	3.0	1.2	0.0	0.1	0.4	0.2	0.13
RC4	10.9	35.1	49.4	2.9	1.0	0.1	0.1	0.4	0.2	0.11
RC5	54.7	18.3	23.6	0.8	1.4	0.4	0.4	0.2	0.1	0.03
RC6	14.2	11.6	47.8	2.6	5.0	0.7	15.3	2.4	0.3	0.12
RC7	10.9	21.7	52.5	2.8	7.3	1.0	1.3	1.8	0.3	0.31
RC8	10.0	20.9	55.3	2.4	6.7	1.2	1.7	1.3	0.3	0.20
RC9	9.2	23.9	53.5	1.2	8.0	1.1	1.7	1.1	0.3	0.08
RC10	11.9	22.1	48.9	1.7	7.8	0.9	4.0	1.9	0.4	0.26

Table 3: XRF results for the raw clays

The LOI for most samples is close to 10%, except for the RC1, which has a significantly lower LOI, and for the RC5, which has a much higher one.

Pure kaolin has an LOI close to 15%. Lower LOI are an indication of the presence of low amounts of kaolinite, or other clays that undergo dehydroxylation.

The very high LOI of RC5 comes from the fact that this clay contains about 50% of organic matter, in a form similar to lignite, which burns at high temperatures.

The alumina content ranges from 11.6%, for RC6, to 35.1%, for RC4. From the alumina content the theoretical maximal kaolinite content can be calculated, the results are shown in *Table 4*. In reality, part of the alumina is present in the form of other minerals, as it will be observed in the XRD results.

Maximum kaolinite content (calculated) (%)	**RC1**	**RC2**	**RC3**	**RC4**	**RC5**	**RC6**	**RC7**	**RC8**	**RC9**	**RC10**
	40.4	80.7	87.1	88.9	46.3	29.3	55.0	52.9	60.5	56.0

Table 4: Maximum kaolinite content calculated from the Al2O3 content measured by XRF

The silica amount of the samples is also variable. Part of the silica may be in the form of reactive materials such as kaolinite and other clays, and part in the form of inert minerals, like quartz.

The K_2O, and to a lesser extent the Na_2O, indicate the presence of clays other than kaolinite, such as muscovite.

The iron content is mainly related to the presence of iron oxides which affect mostly the colour of the clays. High amounts of iron are usually correlated to a reddish or brown colour, but have no impact on the reactivity of the clay.

The CaO (and MgO to a lesser extent) is usually associated with calcium (or magnesium) carbonate presence, which may generate lime (or magnesia) after calcination. The presence of lime in the calcined clay will have a significant impact on its hydration in cementitious systems.

TiO_2 is commonly found in association with clays, with no impact on their reactivity.

3.1.2. Laboratory calcined clays

Table 5 presents the chemical composition of the calcined clays.

It is interesting to note that even after 3 hours of calcination at 800°C or 850°C, the clays still present some LOI at 1000°C, indicating that some phases decompose at temperatures higher than those used in the calcinations. As expected, the chemical composition was not affected by the calcination, so the XRF results are very close to that of the raw clays, when deducting the LOI (which corresponds mostly to the bound water).

Samples	LOI	Al_2O_3	SiO_2	K_2O	Fe_2O_3	TiO_2	CaO	MgO	Na_2O	P_2O_5
CC1-800-3	0.7	16.7	73.5	5.3	2.4	0.1	0.2	0.3	0.7	0.13
CC2-800-3	1.0	34.8	56.9	4.4	1.8	0.1	0.1	0.4	0.3	0.11
CC3-800-3	0.9	38.7	54.9	3.3	1.3	0.0	0.1	0.5	0.2	0.13
CC4-800-3	0.8	39.1	55.0	3.1	1.2	0.1	0.1	0.4	0.2	0.12
CC5-800-3	1.9	39.2	52.0	1.6	2.8	0.7	1.0	0.5	0.2	0.08
CC6-850-3	6.1	12.7	51.7	2.9	5.8	0.7	16.9	2.7	0.4	0.13
CC7-850-3	2.9	23.9	57.3	3.2	7.8	1.1	1.3	1.9	0.3	0.32
CC8-850-3	3.2	22.8	59.4	2.6	7.2	1.3	1.7	1.4	0.3	0.19
CC9-850-3	1.2	26.0	57.9	1.3	9.2	1.2	1.8	1.2	0.3	0.09
CC10-850-3	1.7	24.5	54.5	2.1	8.9	1.0	4.6	2.1	0.5	0.28

Table 5: XRF results for the calcined clays

3.2. Mineralogical composition by X-ray Diffraction (XRD)

3.2.1. Raw clays

Table 6 presents the mineralogical composition by XRD of the raw clays.

The measured amounts of kaolinite are coherent with the Al_2O_3 contents as measured by the XRF, the RC1 and the RC6 clay having the lower kaolinite contents. The RC5, once discounting the organic matter, which is “invisible” to the XRD, has the higher kaolinite content, together with the RC9.

All the samples also contain other clay phases (here regrouped under the “mica” designation) and quartz, and the Imerys and Heidelberg clays contain some feldspar. These two last phases can be considered as inert, suffering no modification during the calcination. These four phases account for more than 90% of the mineralogical composition of the clays, the rest being composed of calcite, iron and titanium containing phases.

It is important to keep in mind that XRD analysis may be affected by the presence of amorphous or badly crystalized phases, and that some diffraction peaks may interfere with others, making the quantification of the phases less precise. Moreover, some different phases may generate peaks at similar angles and may be confused with each other. The values given here should be regarded as indications of the composition of the clays, but not as precise figures.

Samples	**Kaolinite**	Mica	Quartz	Feldspar	Sum major phases	Albite	Schorl (Tourmaline)	Calcite	Pyrite & Hematite	Halloysite	Chlorite	Anatase & Rutile
RC1	**8**	19	33	33	93	QT	7					
RC2	**58**	19	7	12	96	QT	4					
RC3	**71**	16	4	6	97	QT	QT					
RC4	**78**	10	3	7	98	QT			QT			
RC5	**89**	9	2		100							
RC6	**42**	44	11	3	100	QT		DETECTED	DETECTED	QUERY		
RC7	**60**	26	11	3	100				DETECTED		QUERY	QUERY
RC8	**66**	24	10	QT	100	QT			DETECTED	QUERY	QT	QUERY
RC9	**89**	QT	11	QT	100				DETECTED		QUERY	QUERY
RC10	**78**	13	9	QT	100	QUERY		DETECTED	DETECTED		QUERY	QUERY

Table 6: XRD results for the raw clays

QT = Query Trace. This is a very small bump in the background of the scan that could be nothing, but could also be a minute quantity of that mineral
QUERY= There is a peak, but it is not possible to determine with confidence what this is due to significant peak overlaps/interferences.
DETECTED= There is a clear peak, but it is from a mineral that we are not able to quantify.
ND = not detected.

3.2.2. Laboratory calcined clays

The mineralogical composition of the calcined clays is given in *Table 7.*

Samples	**Kaolinite**	Mica	Quartz	Feldspar	Albite	Schorl (Tourmaline)	Calcite	Pyrite & Hematite	Halloysite	Anatase & Rutile	Amorphous phase
CC1-800-3	ND	DETECTED	31	32	QUERY	6					YES
CC2-800-3	ND	DECTECTED	8	14	QT	QT				QUERY	YES
CC3-800-3	ND	DECTECTED	3	9	QT			QT		QT	YES
CC4-800-3	ND	DECTECTED	3	8	QT			QT		DETECTED	
CC5-800-3	ND	DECTECTED	3	QT	-	QT	ND				
CC6-850-3	ND	DECTECTED	12	5	QT		DETECTED	DETECTED		QT	YES
CC7-850-3	ND	DECTECTED	12	6	QT			DETECTED		DECTECTED	YES
CC8-850-3	ND	DETECTED	12	5	QT			DETECTED			
CC9-850-3	ND	DETECTED	12	ND	QT					DECTECTED	
CC10-850-3	ND	DECTECTED	8	5	QT		DETECTED	DETECTED	DETECTED	DECTECTED	YES

Table 7: XRD results for the calcined clays

As after calcination the kaolinite and some other clays undergo an amorphization process due to the dehydroxylation, the XRD of calcined clays is less precise than that of the raw clays. Only the quartz and the feldspar can be quantified in a relatively precise way, and their amounts are similar to those observed in the raw clays, confirming that they weren't affected by the calcination.

Kaolinite is not detected after calcination, suggesting all of it was converted to metakaolin, which appears as an amorphous phase in the table. The other clays (mica) mostly disappear from the XRD spectrum, but some traces of it can still be detected, suggesting that their dehydroxylation may not be complete in the calcination conditions used here.

Other minor phases, such as hematite and anatase are also detected. As discussed above, the presence of iron containing oxides will give a darker colour to the clays. The presence of crystalline titania has no impact on the reactivity of the clay, but it may constitute a health hazard, as breathable titania is suspected to be carcinogenic. The amount of titania in the finer portion of the clay should stay below 1% for the clay to be considered as safe for manipulation, as it seems to be the case here.

3.3. Thermogravimetric Analysis (TGA) and Differential Scanning Calorimetry (DSC)

The TGA/DSC of raw clays helps to quantify kaolinite and other clay phases, in addition to the XRD method. The loss of the clay bound water is detected by the TGA, and the endothermic peak linked to dehydroxylation of kaolinite (~550°C) and other clays (various temperatures) can be detected by DSC.

The stabilization of the TGA signal indicates that there is no further loss of water from the clays, which could be considered as the end of the "useful" calcination. Any further heating may change the mineralogy of the phases, usually in the sense of reducing the reactivity (as, for example, the conversion of reactive metakaolin to inert mullite at 1150°C). This recrystallization of the amorphous clay phases (metakaolin and other "meta-clays") can be observed as it generated an exothermic peak in the DSC.

By analysing TGA and DSC results we can determine the minimal calcination temperature and time, to make sure all the clay is dehydroxylated, and have an indication about the maximal calcination temperature, to avoid recrystallization. It doesn't allow, however, to find the temperature for optimal reactivity, which will depend on the reactivity of each individual phase, which doesn't evolve in the same way in regard to the temperature. The optimal temperature will, in consequence, vary as a function of the composition of the clay.

The TGA/DSC of calcined clays allows to verify if there is residual kaolinite (and other raw clays), which can be detected as they generate some mass loss, due to the dehydroxylation, and an endothermic peak.

3.3.1. RC1 and CC1-800-3

The TGA and DSC curves for the RC1 before and after calcination are presented in Figure 2 and Figure 3, respectively.

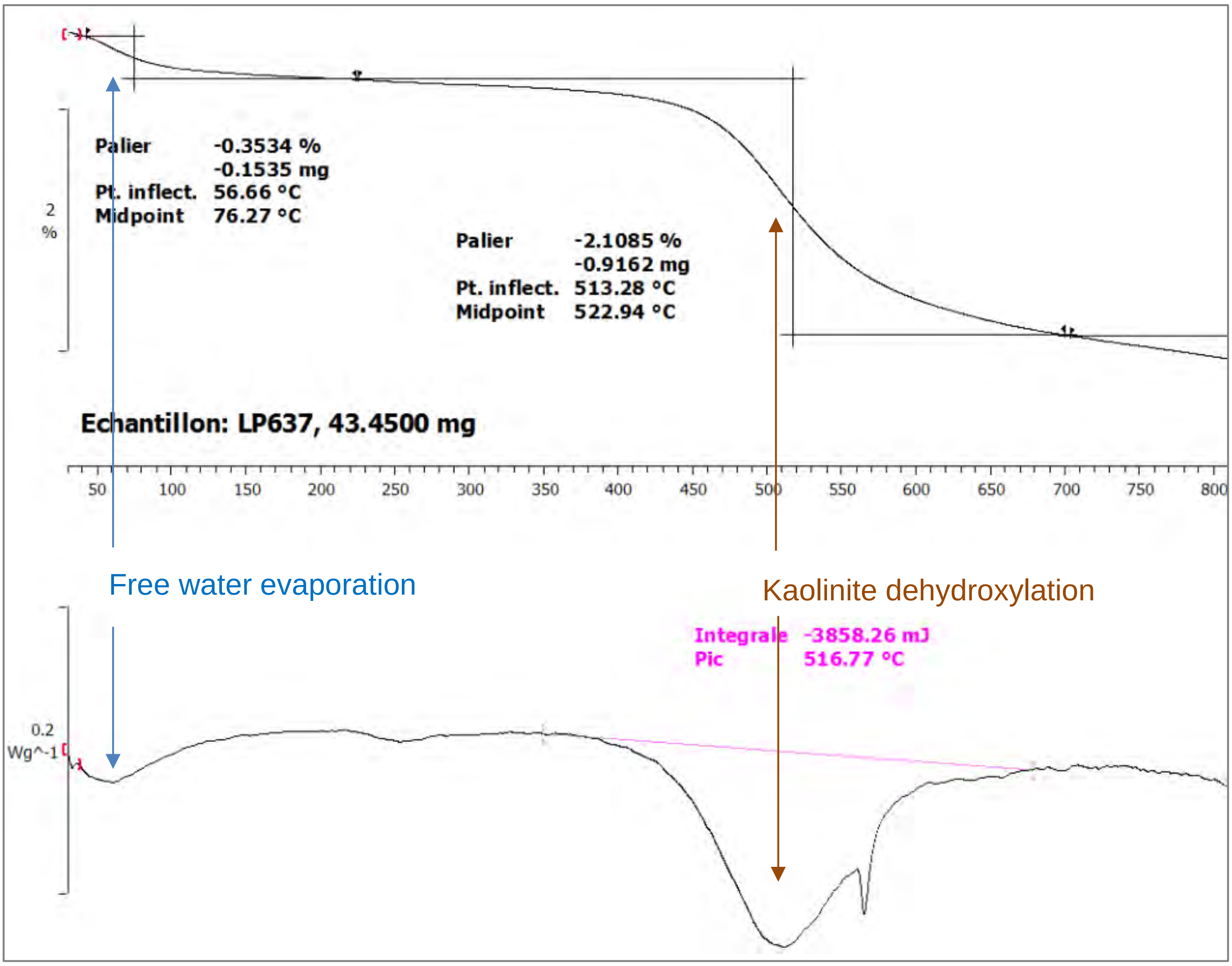

Figure 2: TGA (top) and DSC (bottom) of RC1

A small mass loss in the TGA and an endothermic peak in the DSC are observed at 100°C, which can be attributed to the evaporation of the free water in the sample. This peak is observed with each one of the clays.

Close to 300°C a gradual mass loss starts, which accelerates around 500°C. This corresponds to an endothermic peak centred at 517°C, which can be attributed to the dehydroxylation of the kaolinite. A smaller peak can be observed at 570°C, due to an unknown phase transformation. The mass loss related to the dehydroxylation is of 2.1%. This value can be used to estimate the amount of kaolinite present in the raw clay. At the end of this chapter all the TGA masses losses will be presented together with the calculated kaolinite for all the clays. After 700°C it seems to be no further DSC phenomenon, but the mass loss continues (not clear if it is due to a variation in the baseline, or to an actual phenomenon).

After calcination (Figure 3), the sample presents a very small (<1%) but continuous mass loss since the beginning of the heating in the TGA, which cannot be easily explained. In the DSC no significant phenomenon can be observed, except for a small peak at 550°C. Is it the same endothermic phenomenon observed with the raw clay?
In any case, the dehydroxylation of the kaolinite seems to be (nearly) completed, as the large endothermic peak related to it disappeared.

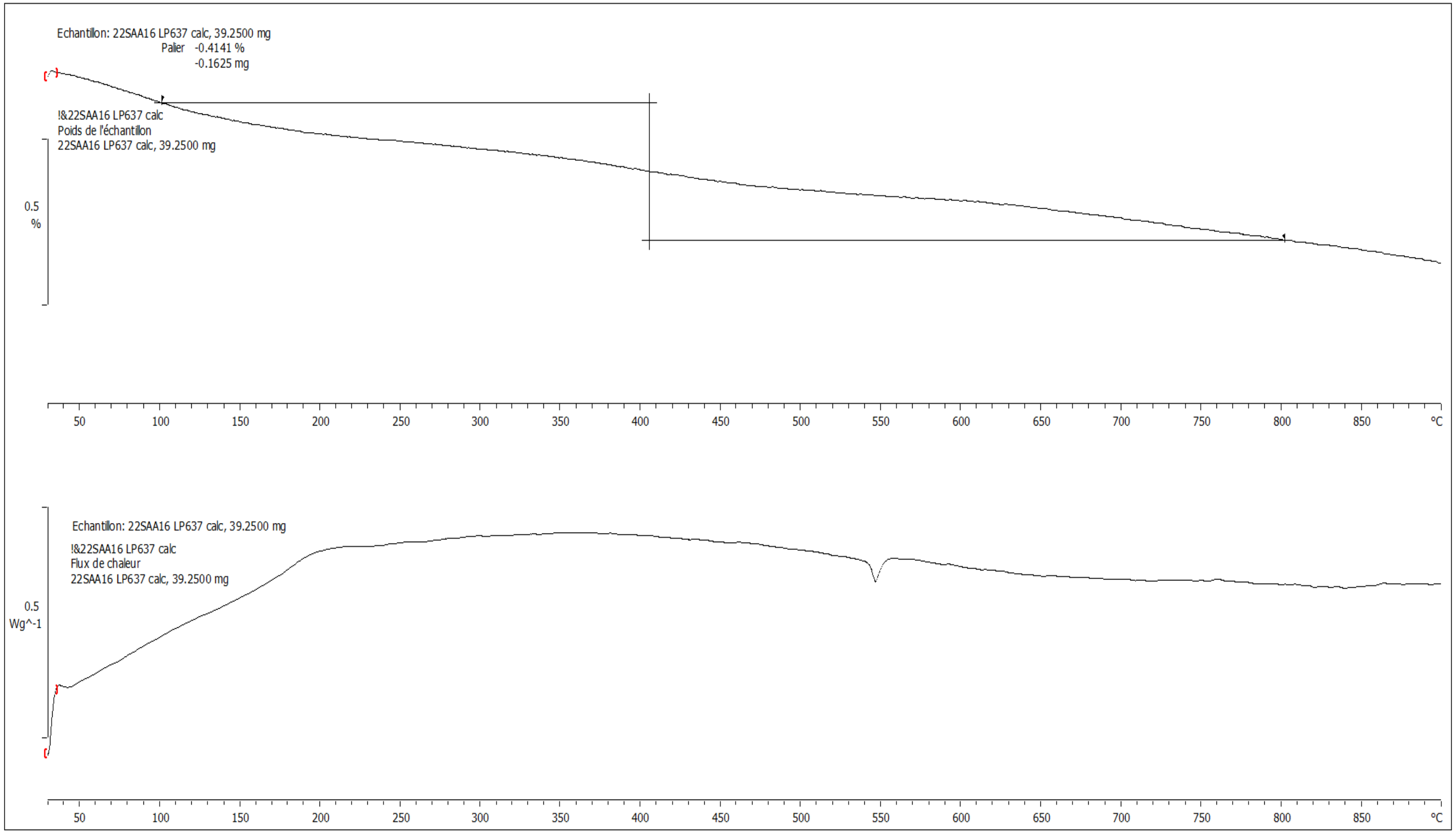

Figure 3: TGA (top) and DSC (bottom) of CC1-800-3

3.3.2. RC2 and CC2-800-3

The TGA and DSC of RC2 (Figure 4) also reveal the presence of a small amount of free water. A small endothermic peak is observed at about 240°C, without any corresponding mass loss, and cannot be explained. The peak correlated to the kaolinite dehydroxylation is seen at 524°C, and accompanied of a strong mass loss, indicating the presence of a high amount of kaolinite.

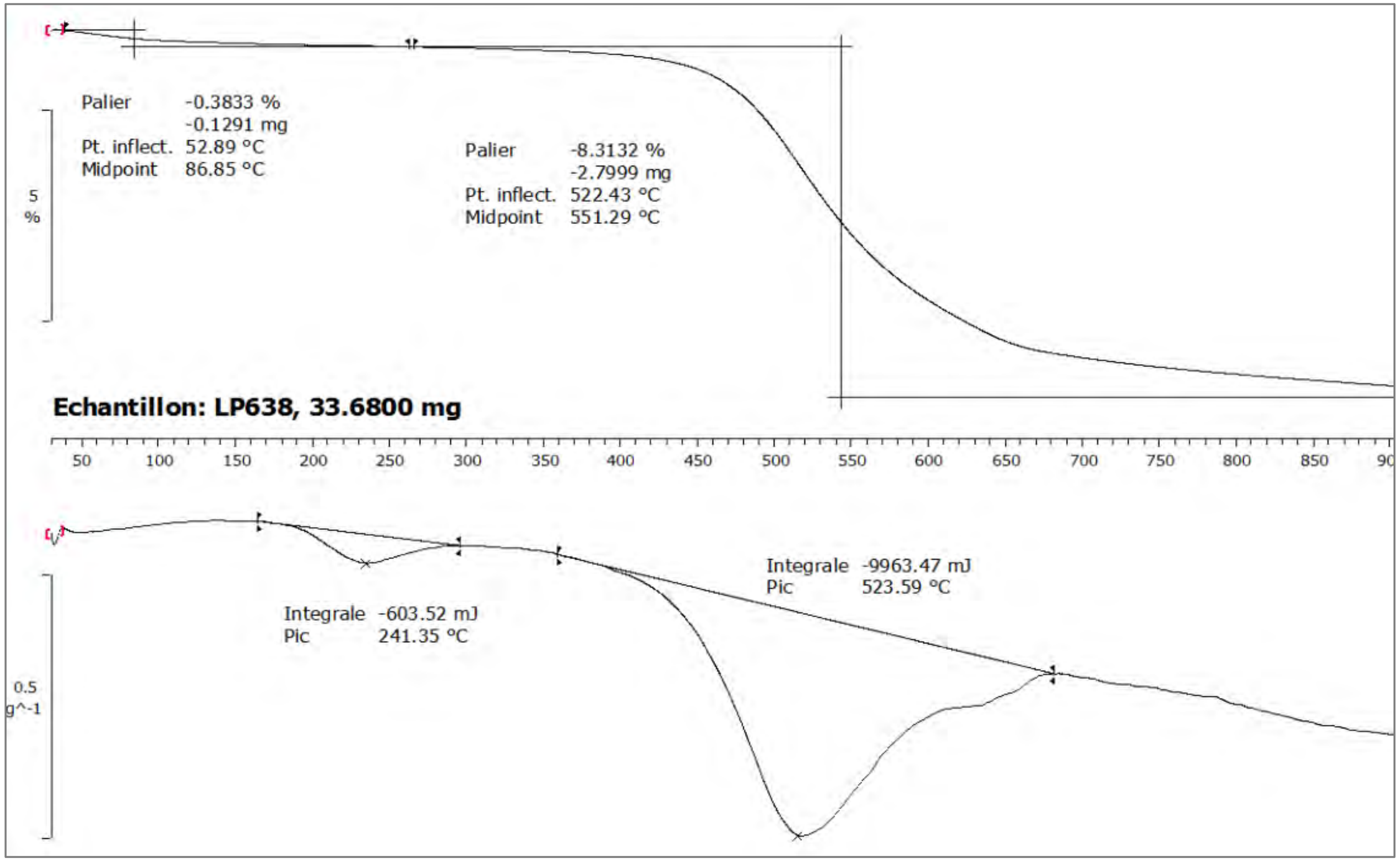

Figure 4: TGA (top) and DSC (bottom) of the RC2

The TGA and DSC of CC2 (Figure 5) shows no significant phenomenon, suggesting that there is no residual raw clay. The small mass loss (<1%) is however still observed.

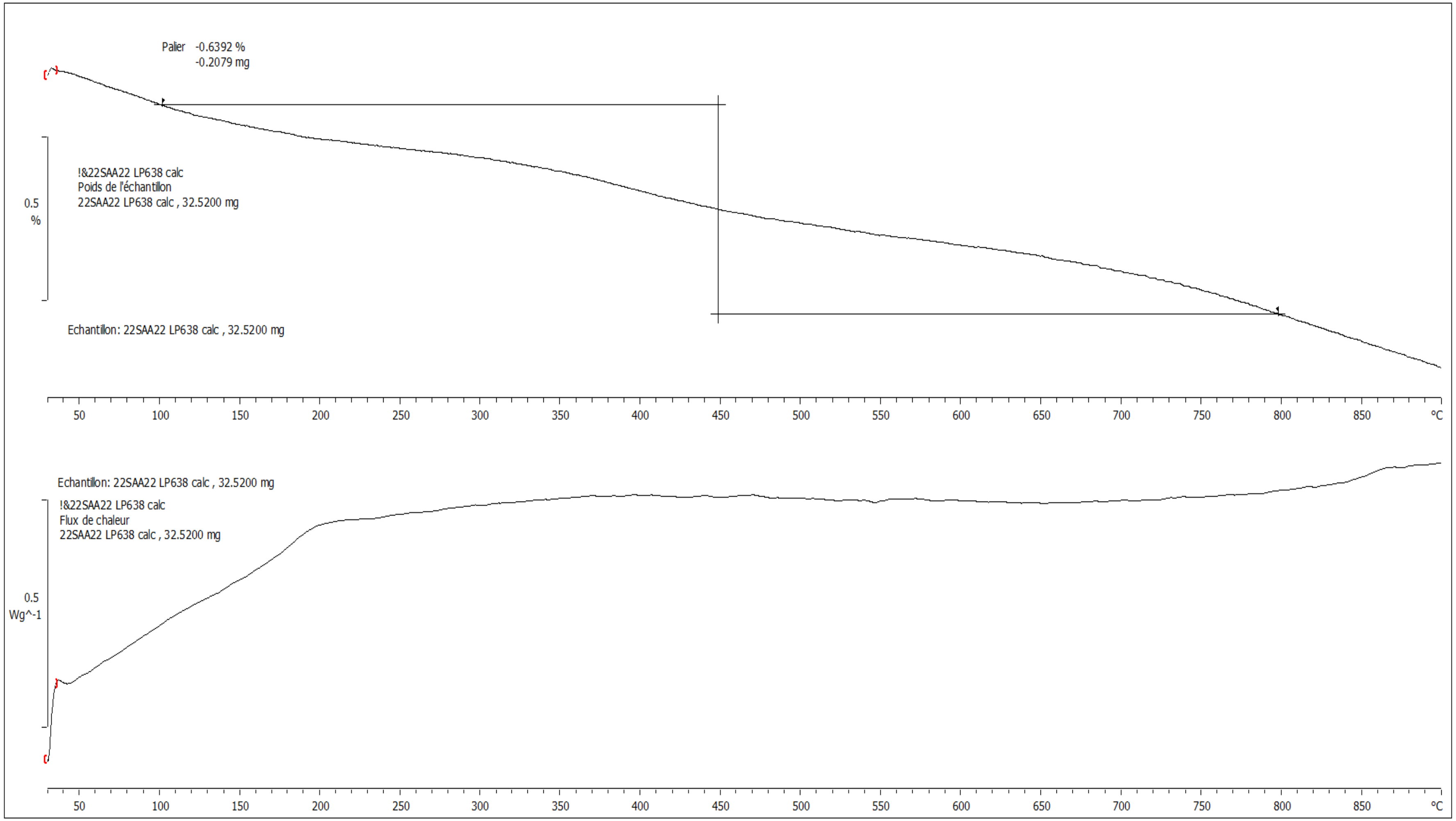

Figure 5: TGA (top) and DSC (bottom) of the calcined CC2-800-3

3.3.3. RC3 and CC3-800-3

The TGA and DSC of the RC3 indicate the presence of a small amount of free water, and a high amount of kaolinite.

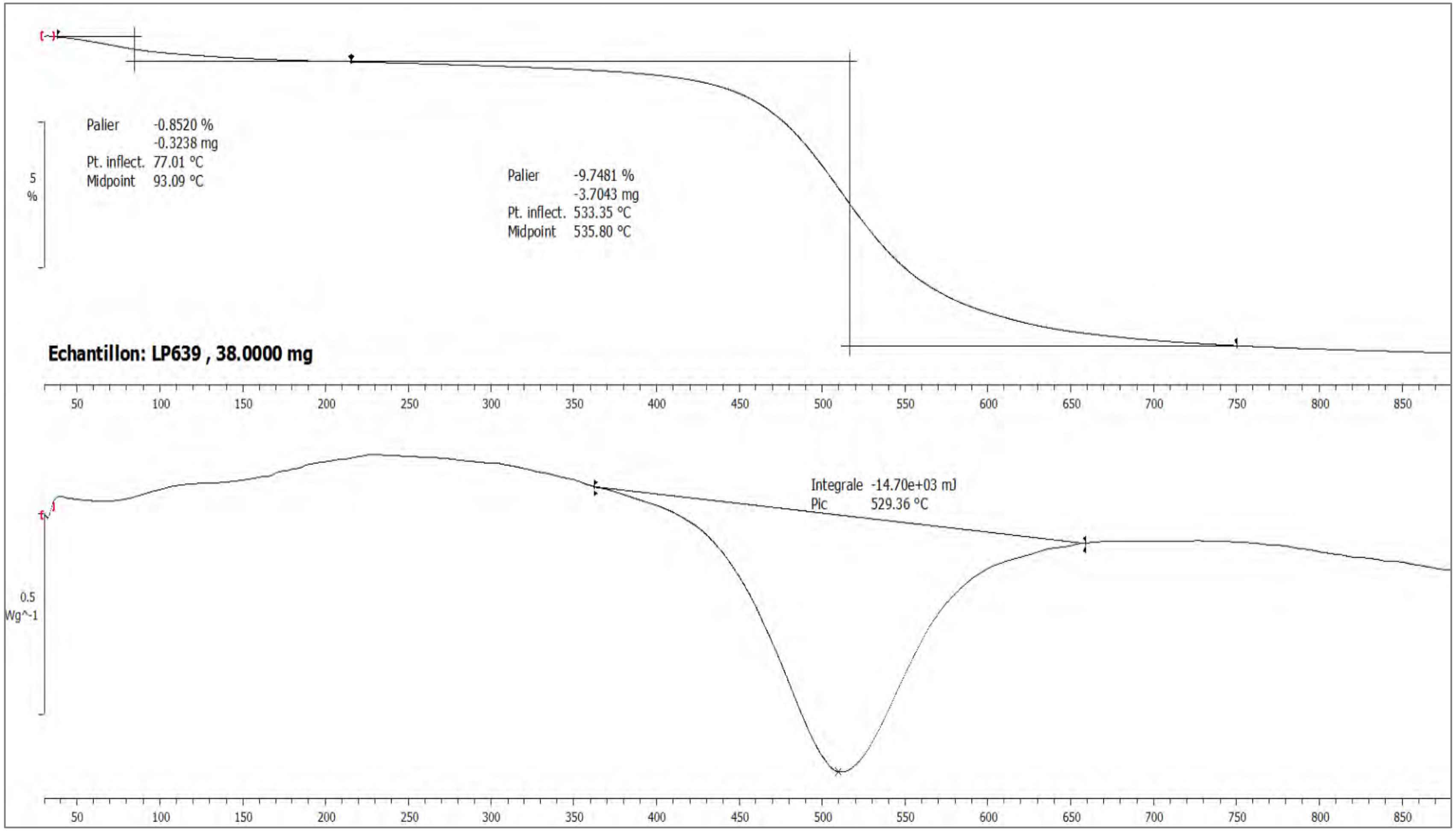

Figure 6: TGA (top) and DSC (bottom) of RC3

After calcination no residual kaolinite is detected. A small and continuous mass loss is observed in the TGA, with no obvious explanation.

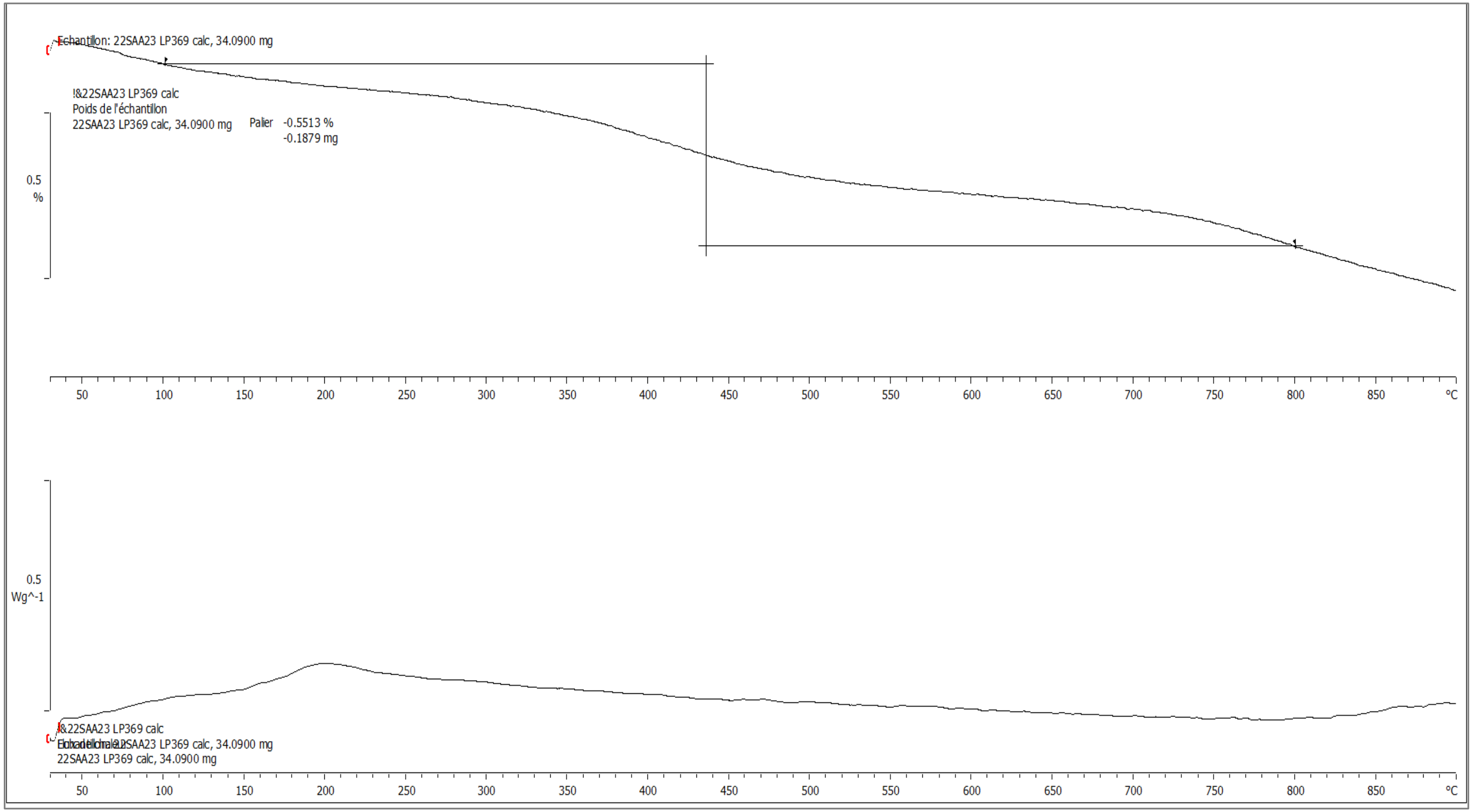

Figure 7: TGA (top) and DSC (bottom) of CC3-800-3

3.3.4. RC4 and CC4-800-3

The TGA/DSC profiles of the RC4 are very similar to those of the RC3, except for a small exothermic peak at 240°C, which is not correlated to a mass loss and that cannot be easily explained.

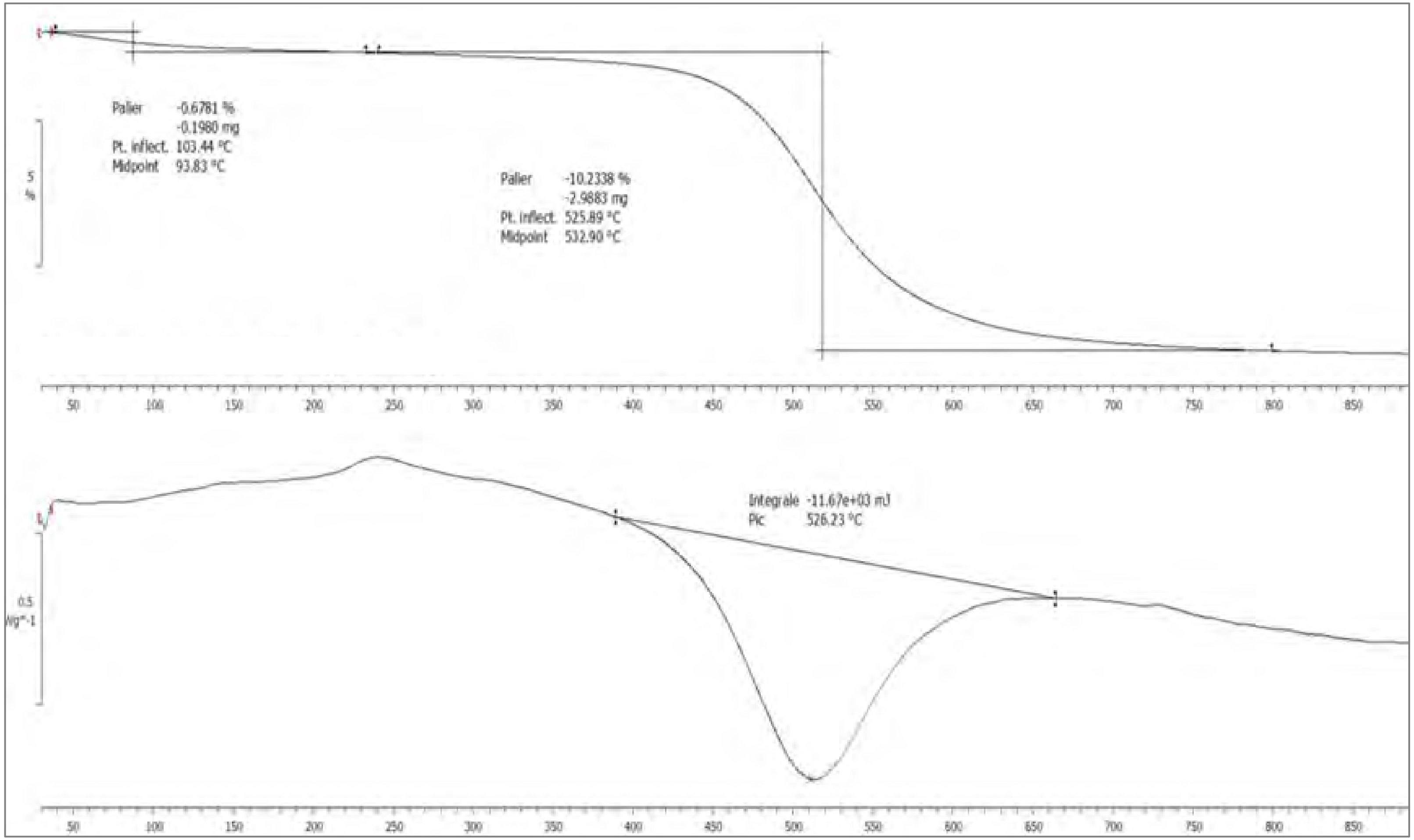

Figure 8: TGA (top) and DSC (bottom) of RC4

The exothermic peak around 240°C is still visible after calcination (Figure 9), which is counterintuitive (the sample being already exposed to high temperatures, why would a transformation take place at this temperature?).
Once again there is no residual kaolinite in the sample, indicating its complete calcination.

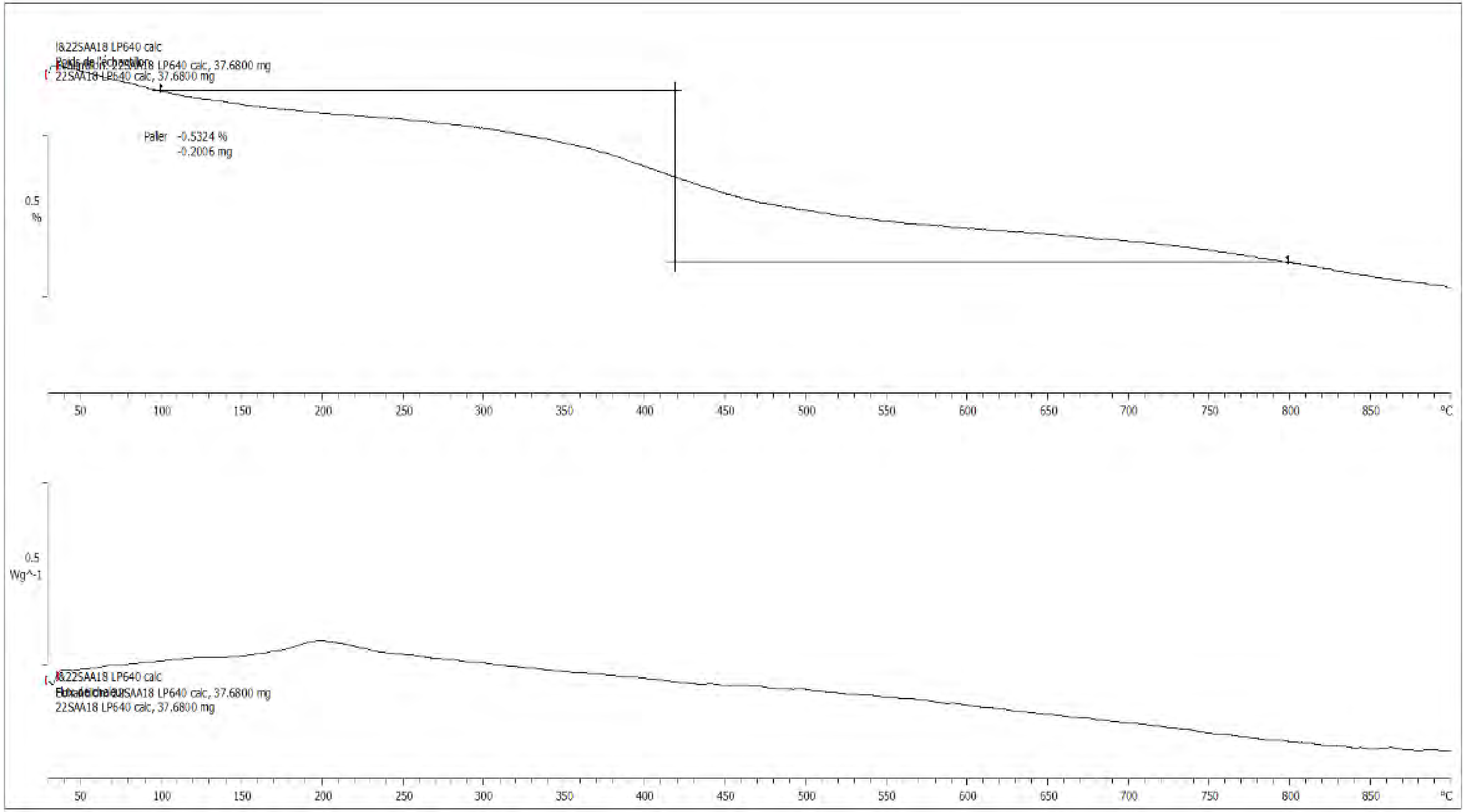

Figure 9: TGA (top) and DSC (bottom) of CC4-800-3

3.3.5. RC5 and CC5-800-3

The RC5 was not analysed by DSC, but only by TGA and DTG (differential thermogravimetry). It presents a 10% mass loss before 100°C, due to the evaporation of its free water. It then has a strong mass loss starting at 200°C and lasting until 600°C. From the DTG signal the mass loss seems to come from two different phenomena. The first and most intense one should be the combustion of the organic matter, releasing CO_2 and water. The second one should be the dehydroxylation of the kaolinite.

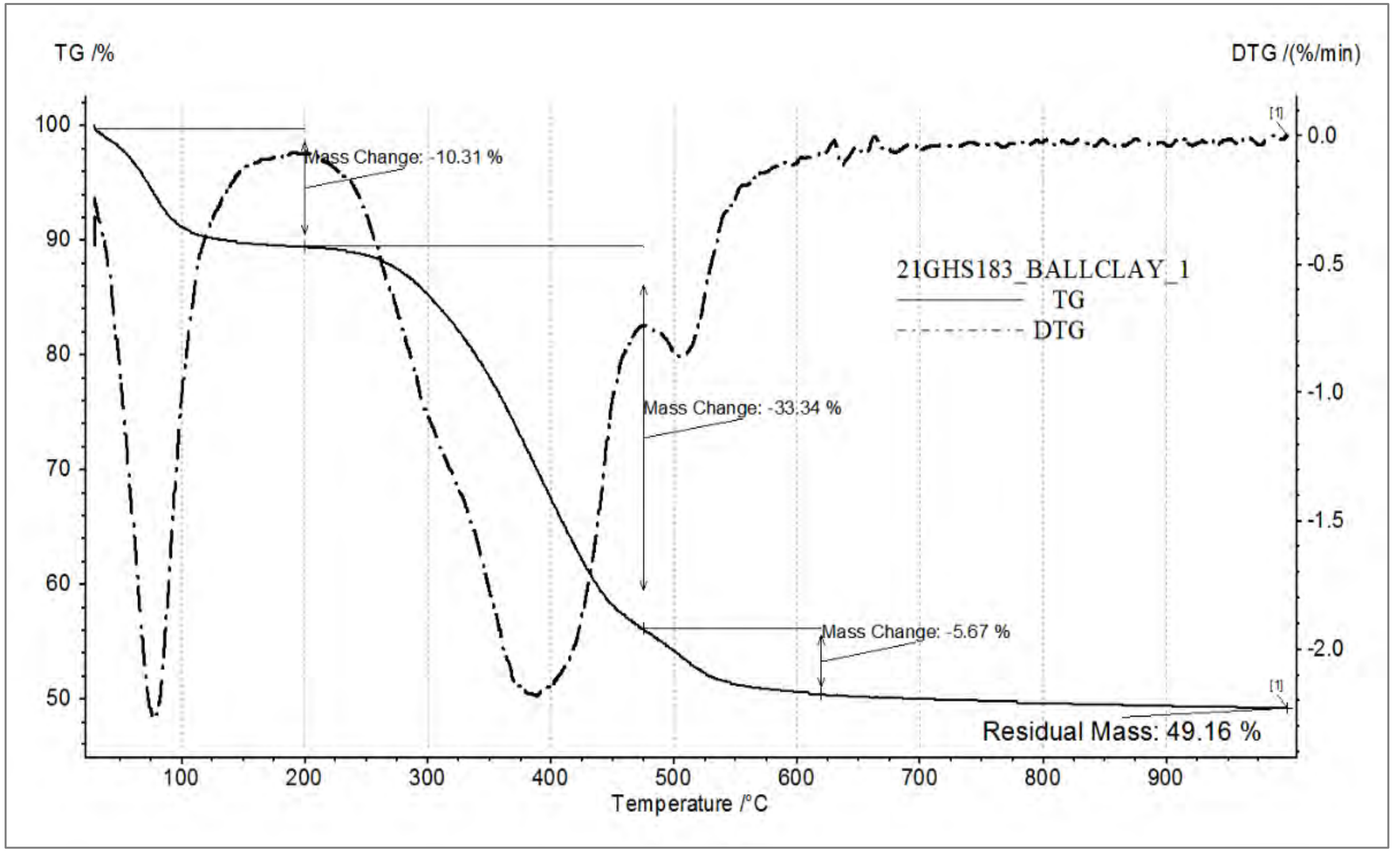

Figure 10: TGA and DTG of RC5

After calcination (Figure 11) the peak around 240°C is observed once more, while no residual kaolinite is detected.

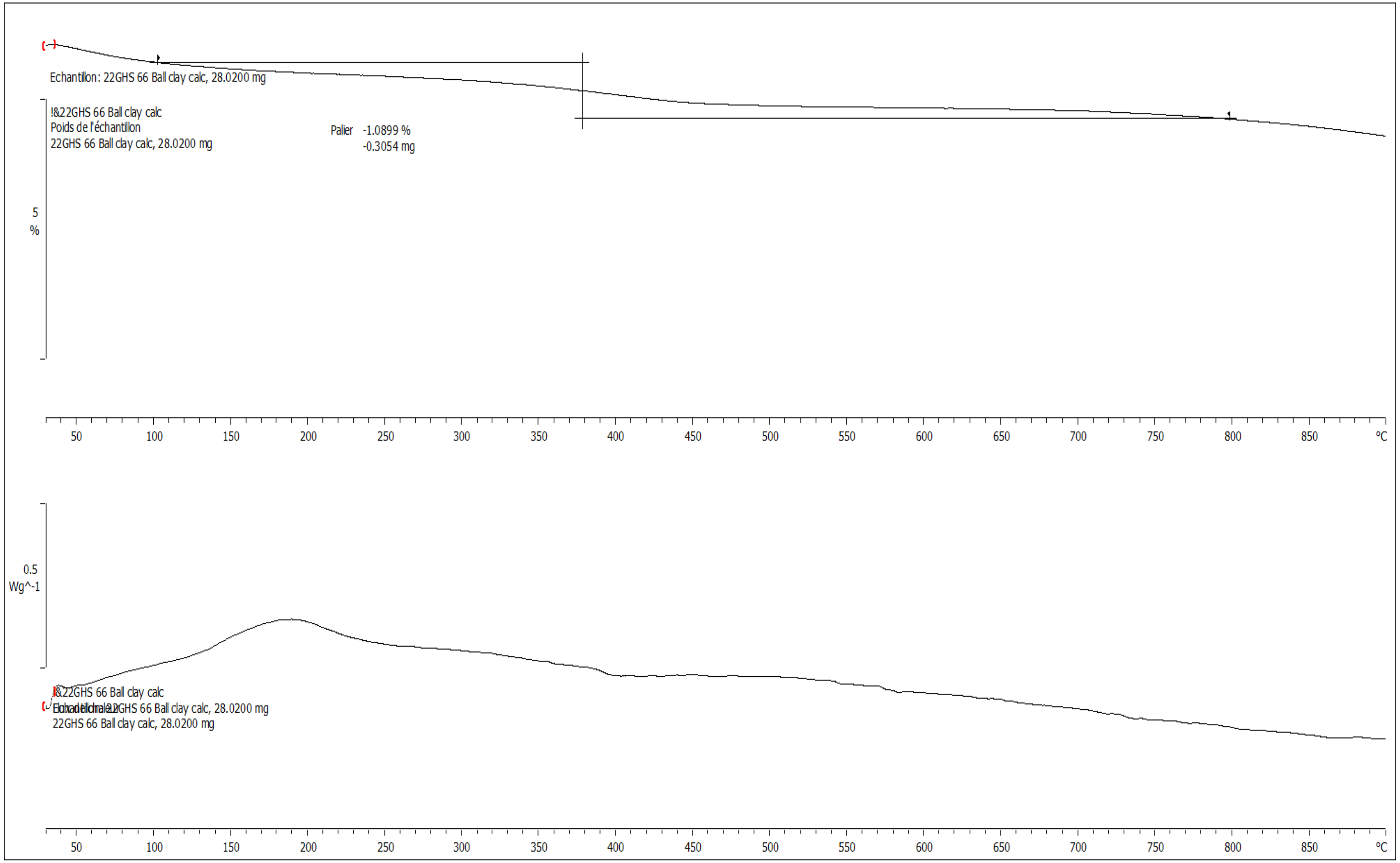

Figure 11: TGA (top) and DSC (bottom) of CC5-800-3

3.3.6. RC6 and CC6-850-3

The DSC profile of this sample is much more complex than the previous ones, showing many exothermic and endothermic phenomena, the most visible one being around 770°C.

The TGA indicate the presence of free water (peak before 100°C), some mass loss at 480°C and around 770°C. The first could be related to the dehydroxylation of clays minerals other than kaolinite, but it is also possible that the sample contain kaolinite in a slightly more disorganized form that dehydroxylates at lower temperatures.

The later peak could be attributed to the decarbonation of the calcium carbonate, as this sample presents a high amount of calcium. From the XRF results, it contains 15.3% of CaO. If we consider the calcium is in the form of carbonate, the sample should contain about 28% of calcium carbonate, which upon heating would release 13% of CO_2, a value close to the 11% of mass loss observed in the TGA.

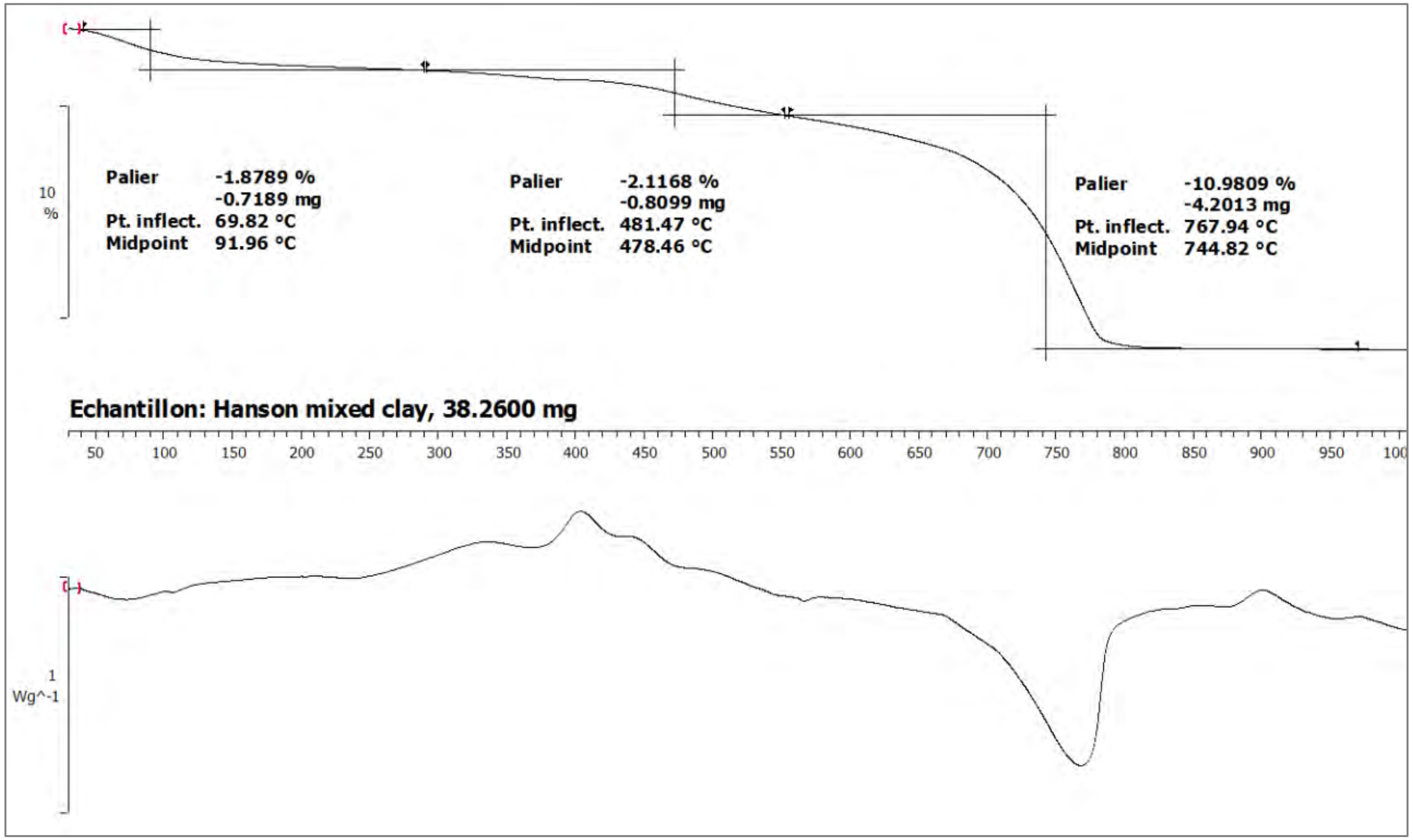

Figure 12: TGA (top) and DSC (bottom) of RC6

Interestingly, even after calcination at 850°C, the CC6 still presents a significant mass loss, close to 5%, in the TGA. Some endothermic peaks are also observed in the DSC, suggesting that the calcination (and thus the phases' modifications) were not complete in the calcination cycle. A higher temperature, and perhaps a longer calcination time, should be used in the preparation of this calcined clay, except if it is confirmed that the reaction taking place is the decarbonation of the calcium carbonate. In this case, it would be better to conduct the calcination at lower temperatures for two reasons: limiting the CO_2 emissions, which would increase the CO_2 footprint of the clay, and avoid wasting energy in a reaction that produces an unwanted phase. Indeed, the presence of free lime is usually avoided in cementitious systems.

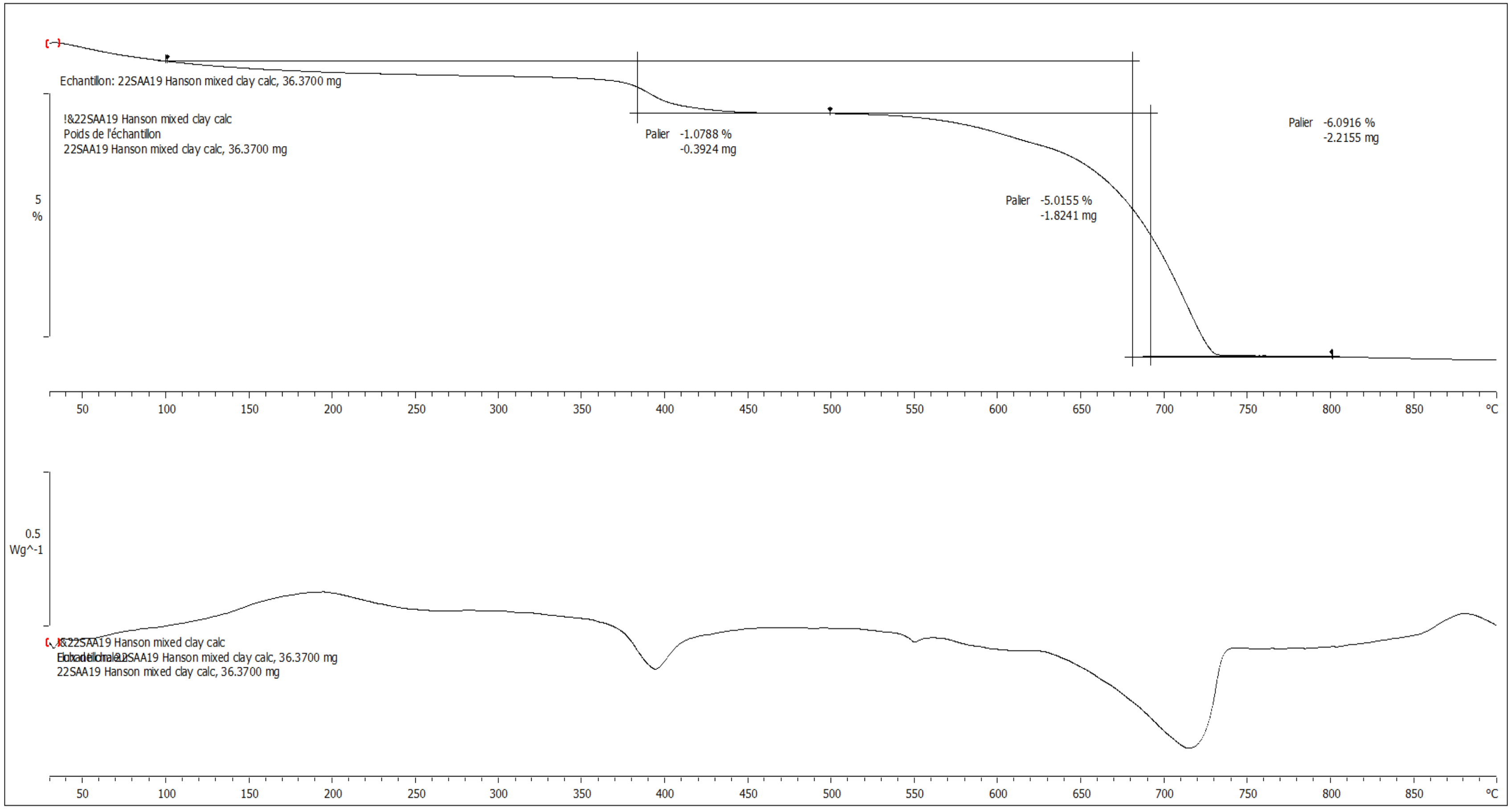

Figure 13: TGA (top) and DSC (bottom) of CC6-850-3

3.3.7. RC7 and CC7-850-3

RC7 also presents a very complex DSC profile, with a large exothermic peak that cannot be easily explained by the identified phases. Simultaneously to it, some smaller endothermic peaks are observed, including one taking place a little before 500°C, accompanied by some mass loss. Once again it could be a more disorganized form of kaolinite, or another clay mineral. No mass loss is observed at higher temperatures, as it was the case for the RC6.

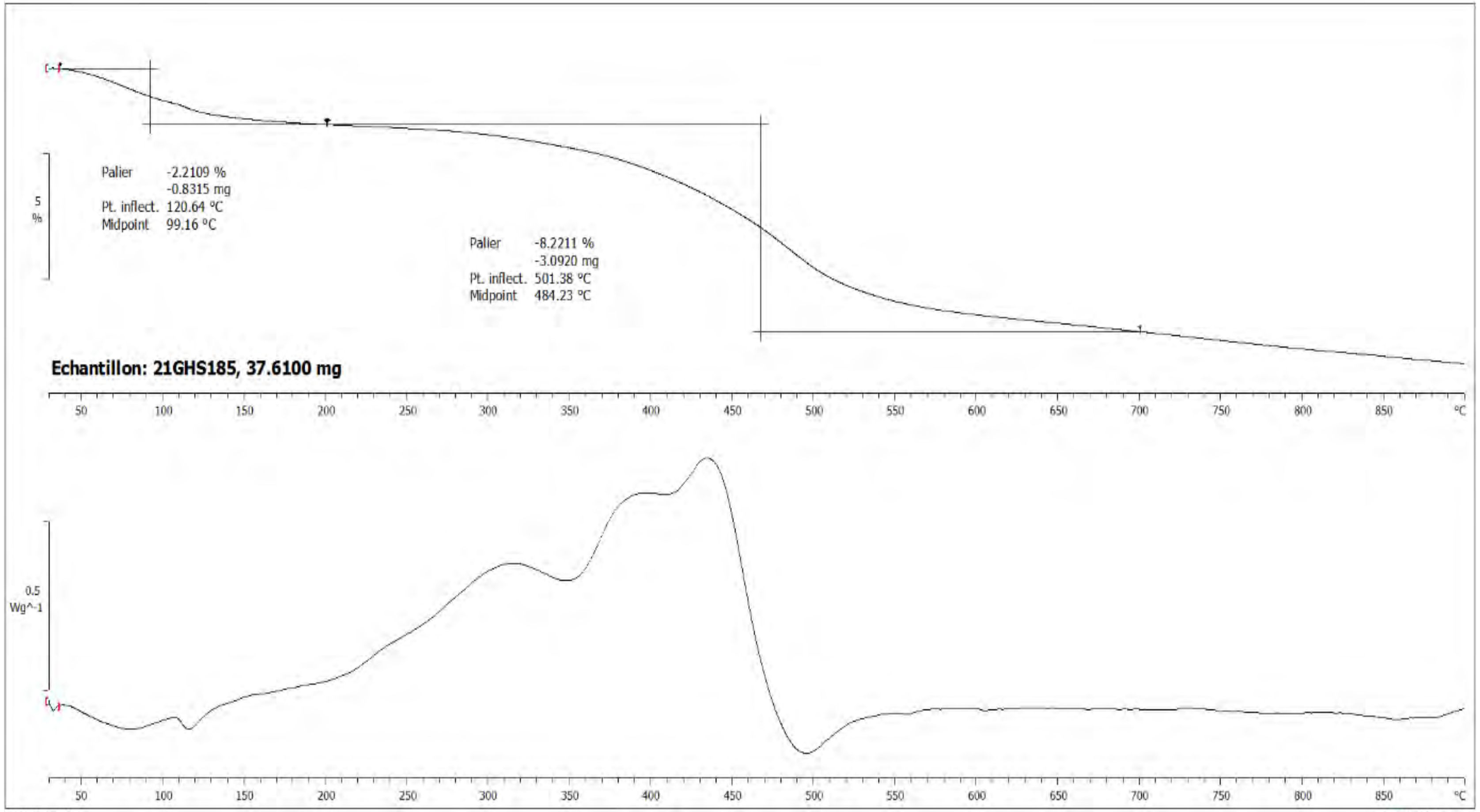

Figure 14: TGA (top) and DSC (bottom) of RC7

After calcination the mass loss is lower than that of CC6, but it is still higher than that observed with the Imerys clays. Are there still some unreacted phases?

The SCM peaks, however, are very small, suggesting that the present clay minerals were dehydroxylated.

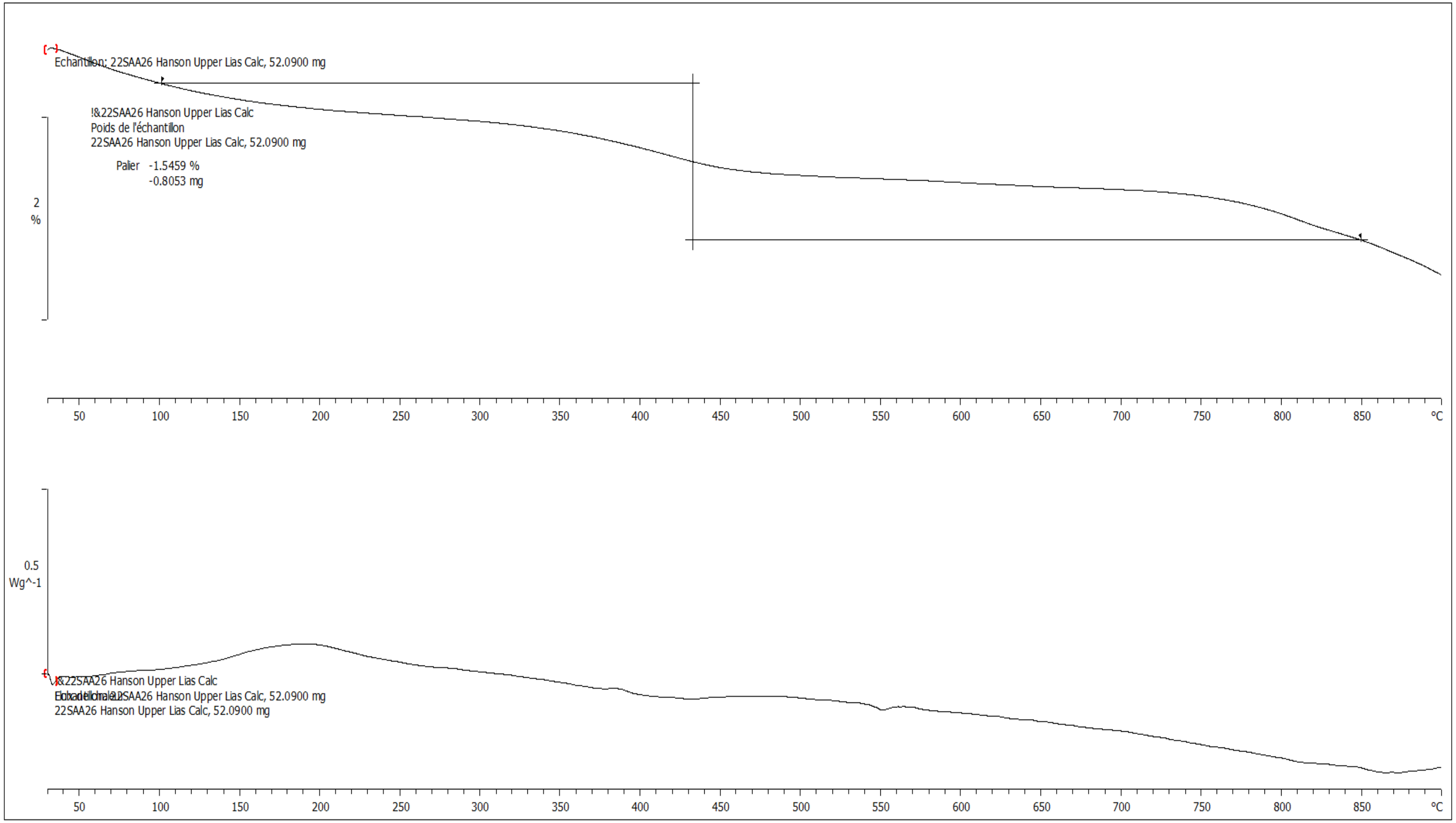

Figure 15: TGA (top) and DSC (bottom) of CC7-850-3

3.3.8. RC8 and CC8-850-3

This clay has different DSC phenomena taking place between 250°C and 550°C, including exothermic reactions. Again, a significant mass loss around 497°C, which should be related to the dehydroxylation of the kaolinite.

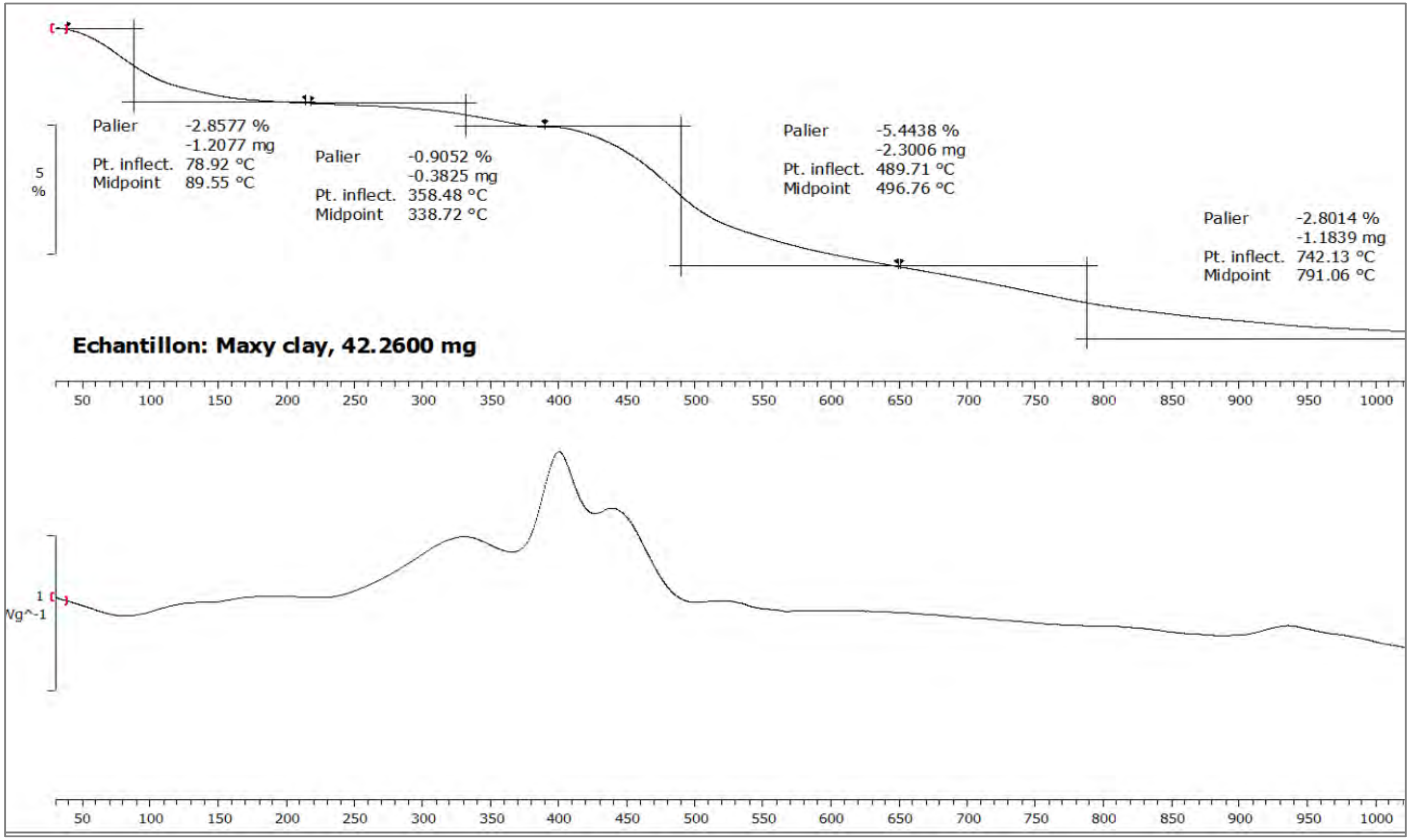

Figure 16: TGA (top) and DSC (bottom) of RC8

After calcination there is again some unexplained mass loss, but very small endothermic peaks in the DSC profile, suggesting that the dehydroxylation of the clay minerals present in the sample was nearly complete.

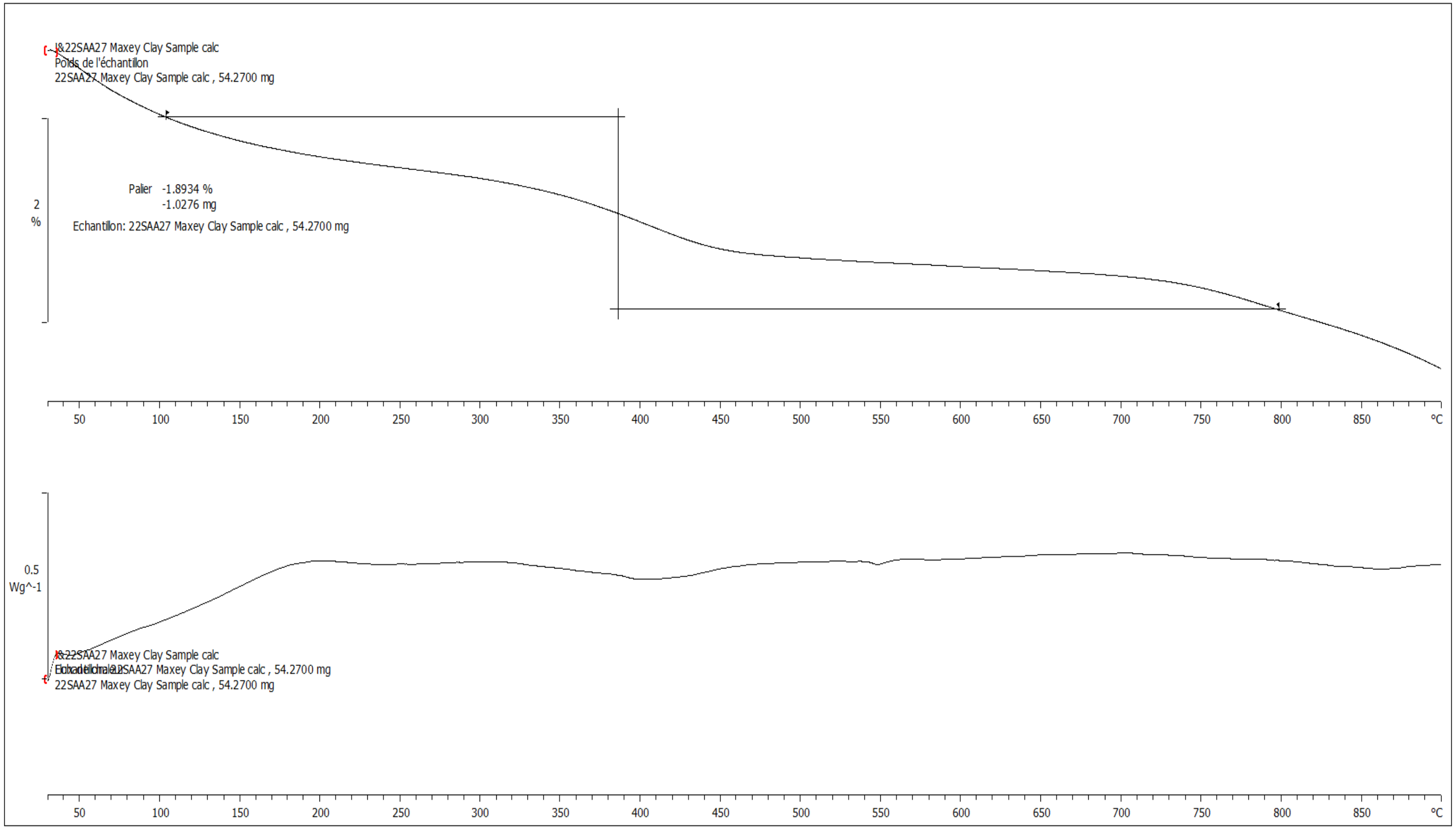

Figure 17: TGA (top) and DSC (bottom) of CC8-850-3

3.3.9. RC9 and CC9-850-3

The DSC profile of this sample is closer to that of the Imerys samples, with a clear endothermic peak around 513°C related to the kaolinite. Some other small endothermic peaks are observed at higher and lower temperatures, and are accompanied by small mass losses, which could be attributed to other clay minerals.

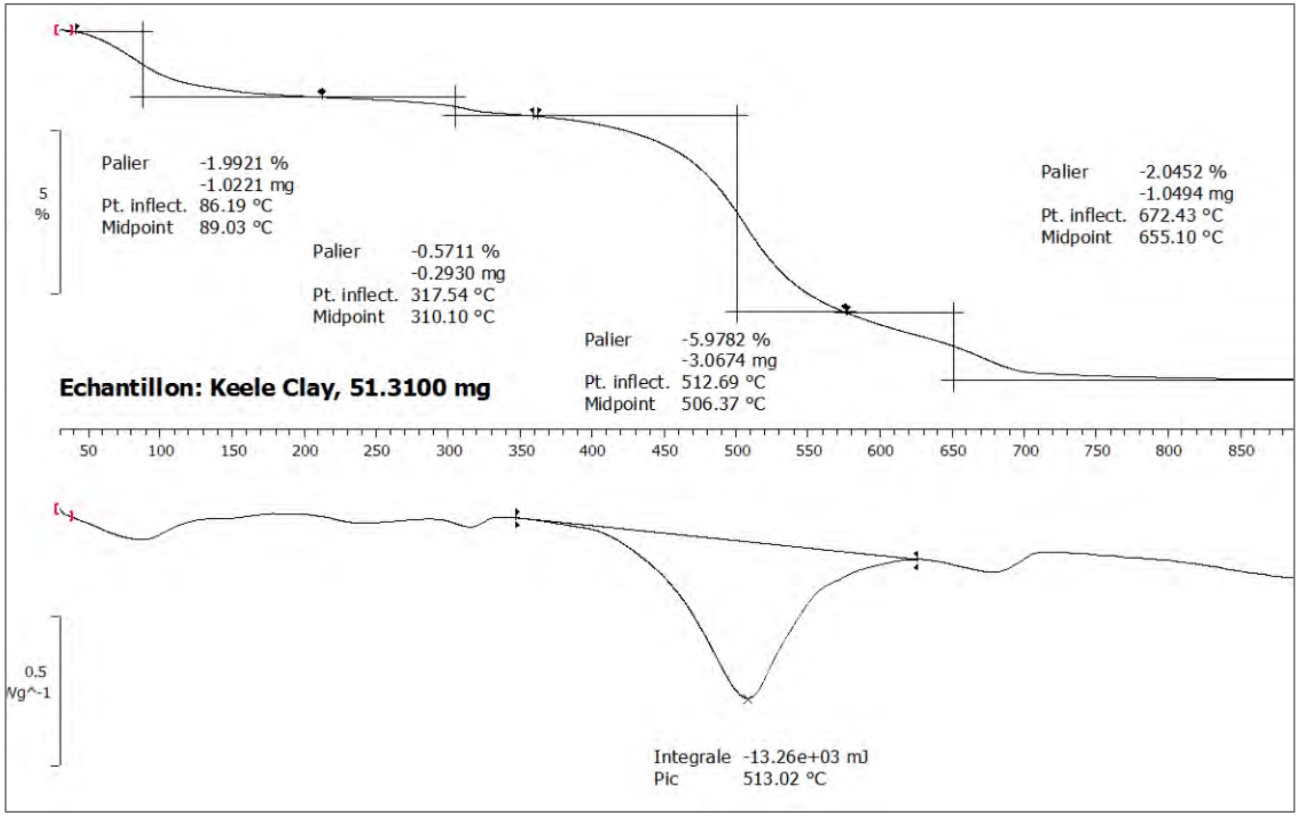

Figure 18: TGA (top) and DSC (bottom) of RC9

After calcination there is still some small mass loss and residual DSC peaks, indicating that the calcination was nearly completed.

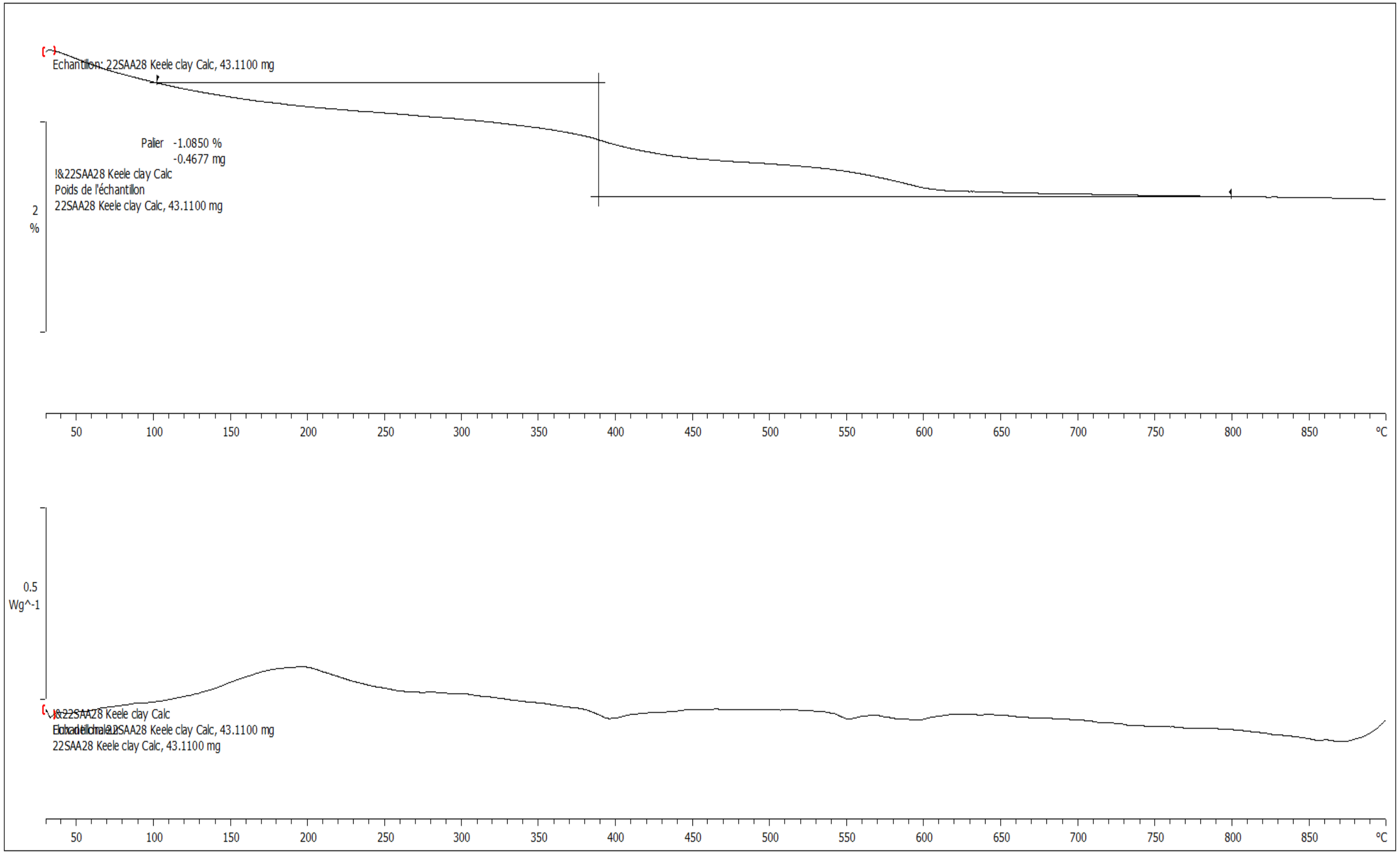

Figure 19: TGA (top) and DSC (bottom) of CC9-850-3

3.3.10. RC10 and CC10-850-3

The DSC profile is yet again very complex, suggesting the presence of diverse minerals, even if some mass loss is observed around 500°C, as expected from the presence of kaolinite.

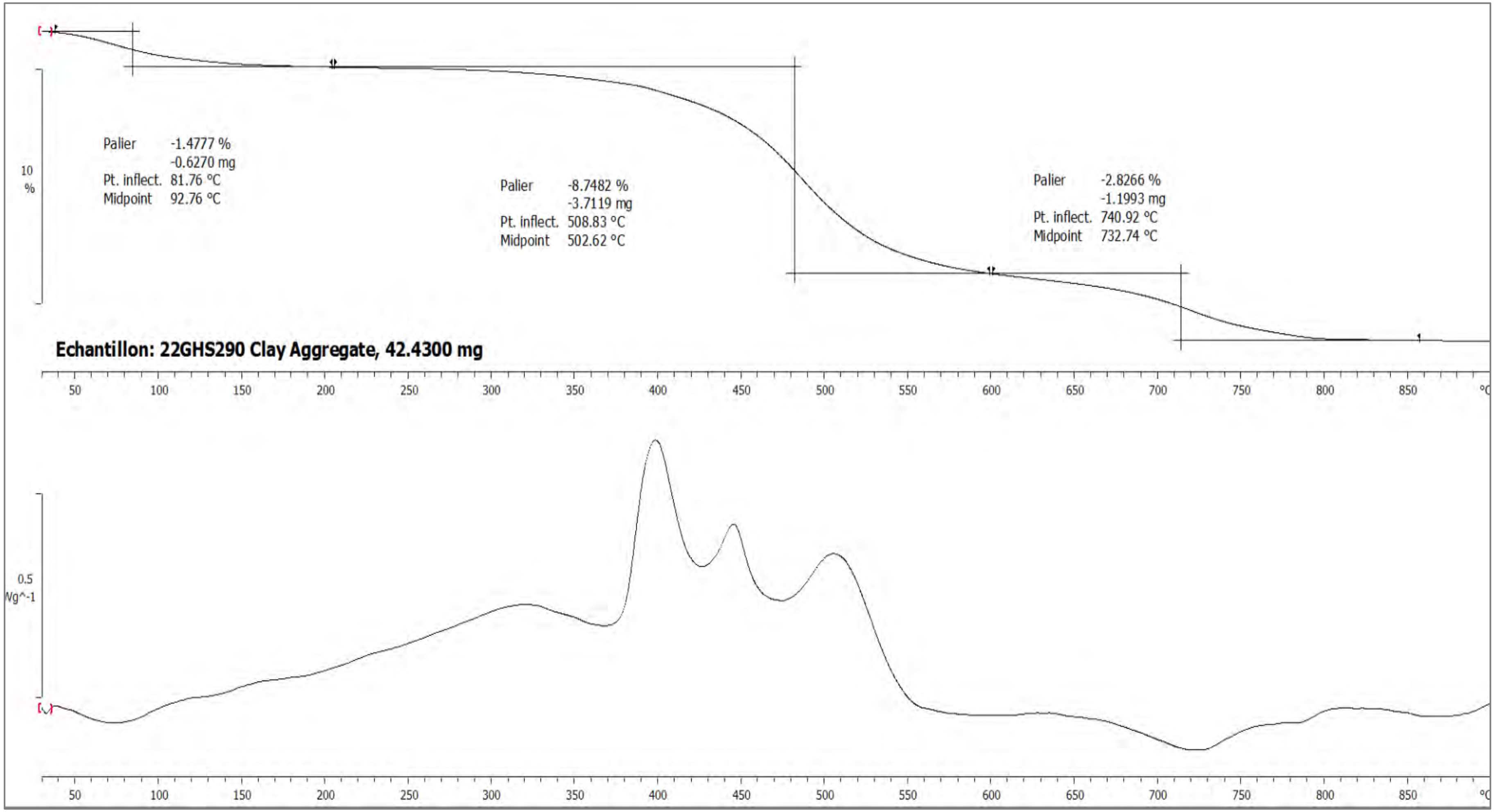

Figure 20: TGA (top) and DSC (bottom) of RC10

As for the previous clay, after calcination this sample still generates some small mass loss and endothermic peaks, indicating that the dehydroxylation of the clay phases was almost, but not completely, finished.

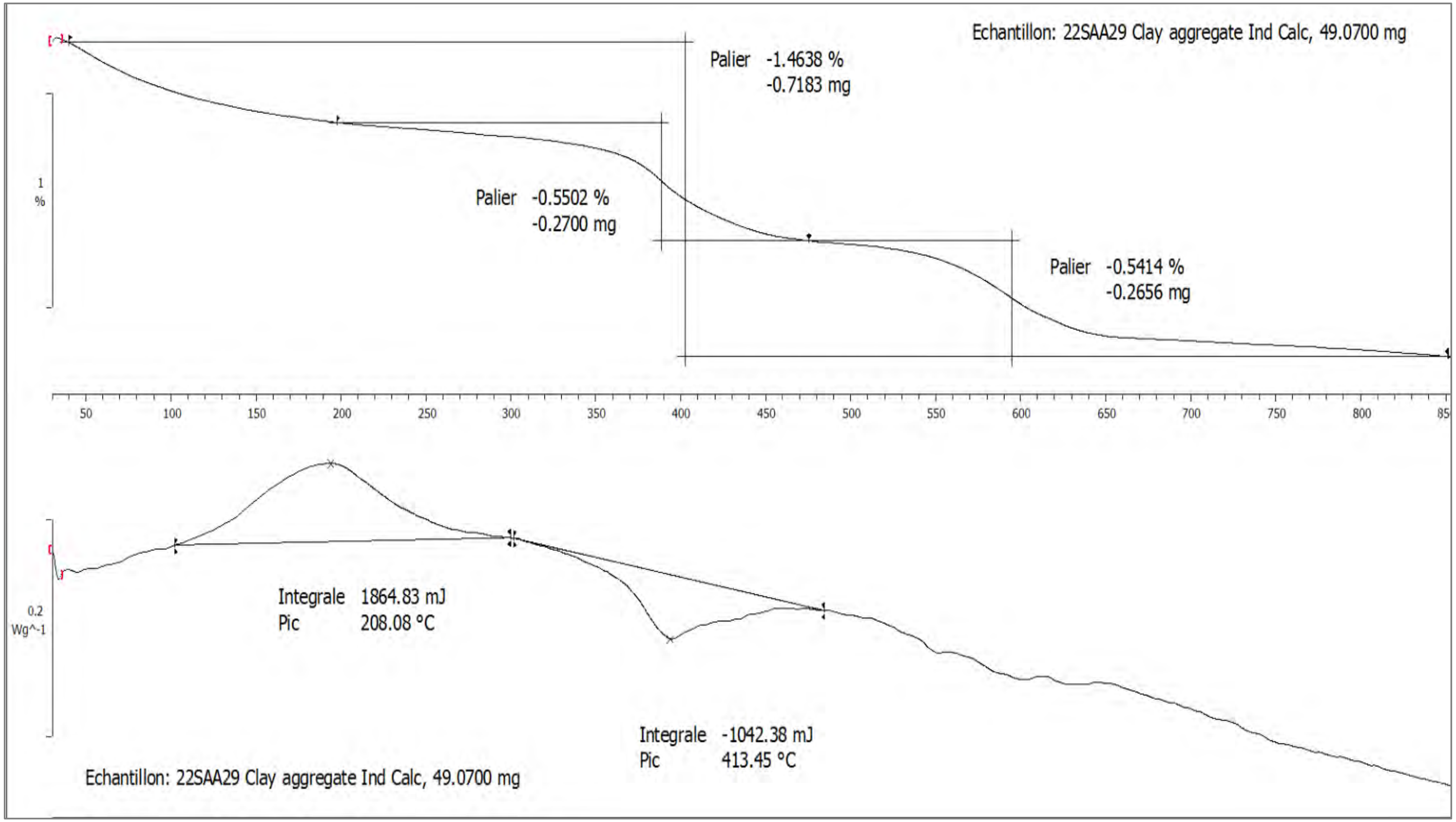

Figure 21: TGA (top) and DSC (bottom) of CC10- 850-3

The kaolinite content of the raw clays can be estimated from their mass loss in the temperature range in which the kaolinite dehydroxylates. The exact temperature of dehydroxylation depends on the degree of crystalline organisation, which is not known for the clays tested here. Therefore, a relatively large range was considered, from 400°C to 700°C.

The choice of considering such a large range can lead, however, to an overestimation of the kaolinite content, as other phases can also generate mass losses at these temperatures.

The mass loss in the range 400°C-700°C and the calculated kaolinite amount in the clays are presented in Table 8.

Samples	Mass loss 400-700°C (%)	Calculated kaolinite (%)
RC1	2.1	**15.0**
RC2	8.3	**59.3**
RC3	9.7	**69.3**
RC4	10.2	**72.9**
RC5*	5.7	**40.7**
RC6	3.6	**25.7**
RC7	6	**42.8**
RC8	6	**42.8**
RC9	7.9	**56.4**
RC10	8.2	**58,6**

Table 8: Calculation of the kaolinite content of raw clays from the TGA

**For RC5, only the mass loss in the range 475°C to 700°C is taken into account, to avoid considering the mass loss due to the organic matter combustion.*

3.4. Colour of raw and calcined clays

The L*a*b* colour coordinates for the raw and calcined clays are presented in Table 10 together with the representation of their colours.

As expected, the colour of the clays is correlated to their iron contents measured by XRF. The Imerys clays, which have Fe_2O_3 contents below 2%, have lighter colours, while those from the cement producers are more brown or reddish.

It is interesting to observe that the clays get redder (indicated by the increasing a* values) and more yellowish (indicated by the increasing b* values) after calcination. This can be due to the oxidation of the iron during the calcination, going from the magnetite (black) to the hematite (red) form.

The exception is the RC5 clay, which is black before calcination due to the carbon in the form of organic matter it contains. After all the carbon is consumed by the combustion, the obtained clay has a beige shade.

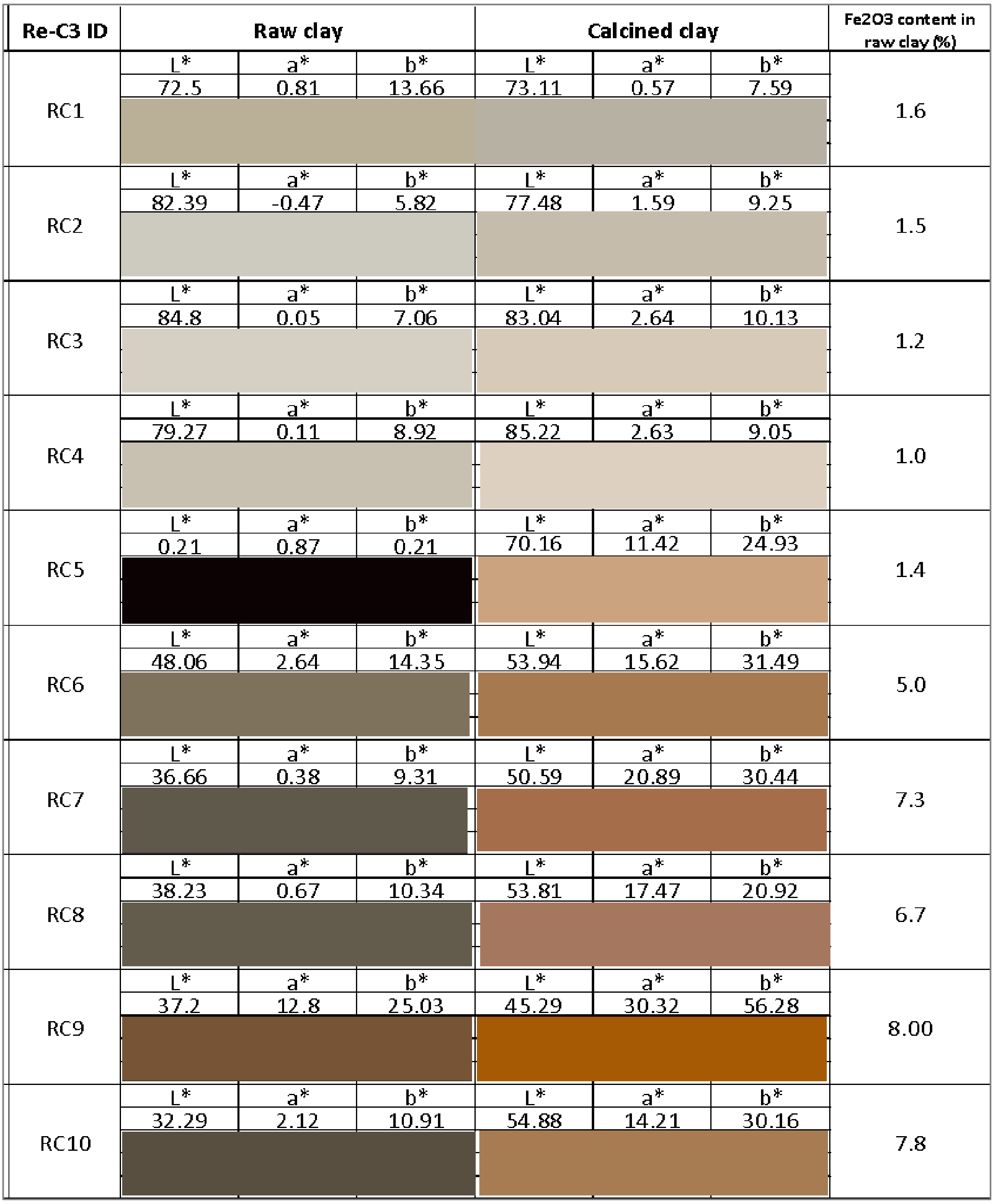

Re-C3 ID	Raw clay			Calcined clay			Fe2O3 content in raw clay (%)
	L*	a*	b*	L*	a*	b*	
RC1	72.5	0.81	13.66	73.11	0.57	7.59	1.6
RC2	82.39	-0.47	5.82	77.48	1.59	9.25	1.5
RC3	84.8	0.05	7.06	83.04	2.64	10.13	1.2
RC4	79.27	0.11	8.92	85.22	2.63	9.05	1.0
RC5	0.21	0.87	0.21	70.16	11.42	24.93	1.4
RC6	48.06	2.64	14.35	53.94	15.62	31.49	5.0
RC7	36.66	0.38	9.31	50.59	20.89	30.44	7.3
RC8	38.23	0.67	10.34	53.81	17.47	20.92	6.7
RC9	37.2	12.8	25.03	45.29	30.32	56.28	8.00
RC10	32.29	2.12	10.91	54.88	14.21	30.16	7.8

Table 9: Colour of the raw and calcined clays

3.5. Particle Size Distribution (PSD) of calcined clays

The granulometry of the calcined and milled clays, as well as the number of turns they were submitted to, are presented in Table 10.

Samples	**Turns**	Dx (10)	Dx (20)	**Dx (50)**	Dx (80)	Dx (90)	Quartz in raw clay
CC1-800-3	**7000**	0.63	1.17	**5.14**	24.6	42.2	33
CC2-800-3	**5000**	0.79	1.43	**5.61**	19.6	29.8	7
CC3-800-3	**500**	0.90	1.57	**4.61**	13.2	20.8	4
CC4-800-3	**500**	1.08	1.94	**4.88**	9.81	13.5	3
CC5-800-3	**500**	0.85	1.50	**4.4**	12.5	26	2
CC6-850-3	**2250**	0.68	1.28	**5.43**	26.8	47.9	11
CC7-850-3	**4000**	0.78	1.45	**5.93**	29.7	58.7	11
CC8-850-3	**6500**	0.70	1.28	**5.84**	34.9	62.5	10
CC9-850-3	**7000**	0.62	1.18	**5.42**	35.4	57.1	11
CC10-850-3	**2000**	0.80	1.5	**5.82**	23.5	42.8	9

Table 10: PSD by laser granulometry of the calcined clays

The d50 of all the clays are close to the target of 5µm, but, in order to get to this fineness, the clays needed to undergo variable numbers of turns in the ball mill. CC3, CC4 and CC5 are the softest ones, and needed only 500 turns to reach d_{50} below 5µm.
CC1, CC8 and CC9, on the other hand, needed the highest number of turns to reach the targeted fineness.
The number of turns required to mill the calcined clays is directly related to their harnesses, which depends on the hardness of the minerals they contain. Metakaolin and other clays phases are expected to be soft and easily ground, but the quartz should be much harder to ground. The clays with higher amounts of quartz, shown in the last column of the table, tend to be the hardest to mill, indeed.

4. Discussion

One of the key properties of a clay to be valorised in the composition of a cement is its reactivity, i.e. its ability to react with water and produce hydrates generating strength. The reactivity of a clay is related to the amount it contains of phases that can undergo these hydration reactions, in opposition to inert phases, such as quartz and feldspar.
The most important active phase present in clays is kaolinite, even if phases such as illite and montmorillonite also contribute to its reactivity.

Besides preparing the calcined clay samples for further analysis by UCL, a goal of the present work was to quantify the kaolinite present in the 10 evaluated samples, in order to help selecting the 4 most promising ones to the next stage of the project. Moreover, we looked for a first indication of the optimal calcination temperature for these clays.

Considering the results of the three relevant methods presented in chapter 3, calculations of kaolinite contents in the 10 raw clays were made and are shown in Table 11.

Samples	Maximum kaolinite content (calculated from the Al_2O_3 amount from XRF)	Kaolinite content calculated from water loss in the range 400-700°C in TGA	Kaolinite content from XRD
RC1	40	15	8
RC2	81	59	58
RC3	87	69	71
RC4	89	73	78
RC5	46	41	49*
RC6	29	26	42
RC7	55	43	60
RC8	53	43	66
RC9	61	56	89
RC10	56	59	78

Table 11: Calculation of the kaolinite content in the raw clay through different methods

** The XRD measures 89% of kaolinite in the RC5, but it doesn't consider the 54.7% of organic matter in the material. When taking it into account, the kaolinite content corresponds to 49%.*

The XRF is a very precise method, the total Al_2O_3 indicated by it can be considered as accurate and reliable. However, as it doesn't indicate in which phase the alumina is present, it allows only to determine the maximum possible amount of kaolinite in the sample, from the stoichiometry. Even if a partial substitution of the aluminium by other elements in the structure of the kaolinite is possible, **the maximum kaolinite content for each clay should be in the range indicated in the first column of Table 11.**

In the case of the calculation from the TGA, **the estimated kaolinite amounts for the clays 1 to 5 and 9 (in blue) should be close to the real values**, as the mass loss between 400°C and 700°C seems to be correlated to a single DSC endothermic peak, centred around 500-550°C, which should correspond to the dehydroxylation of the kaolinite. No other reaction seems to take place, and the values are below the maximum calculated from the XRF, therefore the estimation can be considered reasonably accurate.
For the other clays, however, the characteristic DSC endothermic peak of the kaolinite doesn't appear clearly, and there are other ones present, indicating that the mass loss observed by TGA is probably caused by more than one reaction. The kaolinite content is probably overestimated in these cases.

Considering the XRD, the kaolinite contents measured exceed the maximum possible for most clays (in red), probably because it confounds other phases with it. Only for the four first clays the values seem to be coherent with the two other methods, probably because these samples contain low amounts of other clay phases.

Considering these results, the clays tested in this study can be classified in two groups: the kaolinitic clays, which contain kaolinite as only, or nearly only, clay mineral undergoing dehydroxylation when heated, and the mixed clays, which contains more than one clay mineral that dehydroxylate during calcination. It doesn't mean that one group will behave necessarily better than the other in cementitious systems, but only that the last are composed of multiple active minerals, being therefore more complex to analyse.

In the kaolinitic clays group are found the five Imerys clays and Tarmac's RC9. All these clays have a clear DSC endothermic peak around 500°C, and a significant mass loss at this temperature related to the dehydroxylation of the kaolinite. Their optimal calcination temperature should be easier to define, as there is only one clay mineral to be considered. Once the kaolinite is converted into metakaolin, there is no need or advantage on going towards higher temperatures. The minimal temperature to assure complete dehydroxylation is to be sought.

The mixed clay group, on the other hand, presents diverse phenomena visible in the DSC and TGA profiles, which are different for each clay, indicating they contain diverse phases. The XRD didn't bring any information on the composition of these phases, as they all appeared as mica.
A deeper analysis is required to identify the additional phases present in the mixed clays, and to determine the reactions observed in the TGA/DSC: Dehydroxylation of other clay minerals? Recrystallization? Decarbonation of limestone?
Some of these reactions can be beneficial to the reactivity of the obtained calcined clay, others could be detrimental to it. Finding the temperature providing the best compromise between all these reactions will need a more complex analysis.
Otherwise, a more pragmatic approach may be taken, where optimal calcination conditions giving the highest reactivity are found in an empirical way, without trying to investigate the individual contribution of each mineral in the clays.

One could expect that the clays from the kaolinitic group present better reactivity than the ones from the mixed group, but it is necessary to evaluate if the other clays phases present in these samples also contribute to the reactivity, which may be the case.
Reactivity tests, such as the R3 developed by the RILEM, and/or direct strength measurements of mortars prepared with these clays are the most straightforward way to establish a ranking of the clays in terms of performance, and to select the candidates for the next stage of the study.

The composition will also affect the ease of grinding the material, those richer in quartz seeming to be harder to grind. The optimal fineness of each clay must be investigated, as there is no advantage in reducing the grain size of the quartz particles.

Regarding the colour of the clays, there seems to exist a good correlation between the iron amount and the "redness" of the sample. The clays get even redder after calcination, because of the formation of hematite due to the oxidation of the iron containing phases. The companies developing kilns to calcine clays are well aware of this effect of the iron oxidation, and have developed processes to avoid it, if the redness of the clay is seen as an issue.

5. Conclusion and next steps

The 10 candidate clays tested in this part of the study have different compositions, some containing mainly kaolinite as clay mineral (Imerys clays and Tarmac’s RC9), the remaining containing various clay minerals that undergo transformations upon calcination.

The association of XRF, XRD and TGA/DSC analyses was needed to get an estimation of the composition of the clays, which will be used to select the 4 most promising ones.

Determining the composition of the clays is also important to define the optimal calcination temperature for each sample, as a good balance must be found between the temperature of dehydroxylation and of recrystallization of the different clay phases, and the energy consumption. Some extra investigation is needed to set the optimal temperature for each clay, which should be carried out in another workpackage.

The composition will also impact the optimal particle size distribution. Once again, a compromise must be found between obtaining fine and thus reactive clay phases, and not spending too much energy on grinding inert phases, such as quartz.

Reactivity tests, such as the R3 test, should be carried out to confirm the optimal parameters of preparation of the calcined clays, to be retained for the next steps of the project.

Finally, because of the presence of iron, most of the clays present a reddish colour. According to the literature it has no impact on the pozzolanic activity of the clay, but it may be not well perceived in the construction industry, which is not yet used to it.
It will be up to the group to define if some colour correction process should be used in the production of the pilot calcined clays, in the next step of the project.

Re-C3: Reclaimed Calcined Clay Cements

Appendix 3 -

Activation of waste fired bricks

Evaluation of the potential use of waste fired bricks as a source of calcined clay.

Authors

Forterra:

Dr Andrew Smith

Lisa Wachter

Date: February 2024

Executive Summary

Waste bricks generated as part of the clay brick manufacturing process are a waste arising that has the potential to be utilised as a Supplementary Cementitious Material (SCM) however it is known that the firing temperature of most modern brick plants, far exceeds the published “optimal” calcination temperature of clays in order to maximise reactivity.

Research undertaken by this author in the late 1990’s but not published, along with the PhD thesis Dr Martin O’Farrell (1999), identified one of Forterra’s clay types, and subsequent brick wastes showed significant pozzolanic properties, and as such was a potential candidate material for this project. Brick waste from the same location, and brick type has been used in this project, Kings Dyke Brick Powder (KDBP) made from the milling down of Fletton brick production waste.

In order to get a comparison with a high temperature brick made from a very different clay type, fireclay raw materials that are used to manufacture the Measham Buff (MBB) range of bricks was identified.

Analysis of these fired brick types showed that they have very different fired mineralogy’s, along with different chemistries, stemming from the very different raw clays, and production process, namely firing temperature. It should be stressed that unlike the other calcined clays in this project, these clays are fired at a temperature which destroys the clay minerals completely, so there is no residual Metakaolin (thought to be the primary active pozzolanic mineral phase in calcined clays).

Testing shows that the KDBP made from the Fletton bricks, is more reactive than the fireclay based MBB. Both however are significantly less reactive than the other calcined clays produced as part of this project, however the KDBP that was selected as one of the calcined clays in the Demonstration Project, Work Package L, has been shown to be only marginally less reactive in concrete trials.

1. Contents

2. Introduction

In addition to the raw clays identified and provided by the Project Partners in this programme of work, Forterra proposed the potential of using waste fired clay brick as an alternative source of “calcined clay”.

Unlike the work undertaken on the raw clays, the firing conditions, (calcination) for the bricks is dictated by the desired properties of the bricks in service, therefore typically fired up to temperatures that fall between 950°C and 1150°C, depending upon the brick type and the raw materials used.

As part of this project, Forterra proposed looking at 2 very different waste brick materials, a “London Brick Fletton” brick waste from Forterra’s Kings Dyke brickworks and a “Stock” buff soft mud brick from Measham brickworks. Both have very different primary raw materials, manufacturing process and ultimately different firing temperatures, indicative of potentially very different “calcined clay properties”.

Waste brick arisings typically come from the sorting process, prior to packaging, and can be as a result of mechanical damage to the bricks, breakages, cracking or chipping, irregular or out of specification colour and texture, along with bricks that are underfired as a result of issues in the firing process. Such arisings are typically processed on the respective brickworks, where they are put through a primary crusher and potentially screened to give coarse aggregate and 0-4mm dust/sand.

Normally the coarse crushed brick is used to maintain haul roads within the clay quarry, and the dust/sand is used as a “grogging” agent, added back into the raw clay mix at the start of the manufacturing process, where it helps open up the clay body of the brick, allowing for faster more efficient drying.

Use of the part processed crushed brick waste as a calcined clay type Supplementary Cementitious Material (SCM), offers a “higher value” alternative use for these arisings, and ultimately provides an indication that finely milled clay brick construction and demolition waste could be utilised as a source of SCM.

The chemistry and mineralogy of the fired brick waste is presented in this report along with details of the assessment of reactive silica content and the ball milling process and specification of the final milled brick waste powder for each brick type.

3. Materials

There are 2 clay brick waste materials being evaluated in this report. Firstly the "KD Grog" and secondly the "Measham Buff Brick". Throughout this report they will be referred to as KDBP and MBB for simplicity.

3.1. Kings Dyke Brick Powder (KDBP)

The starting raw material for the brick waste is known internally as KD "grog". This essentially is crushed and screened waste brick produced at Forterra's Kings Dyke brickworks, which is located between Whittlesey and Peterborough.

The clay raw material used for brick manufacturing is Lower Oxford Clay (sometimes referred to as Fletton Knots in the old literature). "Fletton Bricks" is the generic name given to bricks produced by Forterra and sold under the "London Brick" brand name. London Brick Company (LBC) being the original manufacturer, which dates back to the 1920's.

The bricks are manufactured using what is known as a "semi-dry pressing" process, where the clay is won from the quarry, transported on conveyor, passes through hammer mills initially and then through a dry pan grinding process (no added water) and the resulting granulate feed (nominally 2mm to dust) is fed into a holding hopper and then discharged into the mould boxes as required before being mechanically pressed using a 4 stroke pressing process. This is a "hand to mouth" process so there is little or no storage of the clay (except over night or over the weekends when the quarry isn't operating) so the clay is used in an as received state, with approximately 6-8% moisture content at the time of pressing.

3.2. Measham Buff Brick (MBB)

The starting raw material for this brick waste stream is an imported "Fireclay" that is used to produce buff and yellow "stock" bricks. Measham brickworks lies on the outskirts of Measham in the very western side of North-West Leicestershire. The fireclay is not indigenous to Measham but is imported a short distance from the Swadlincote, where the clay itself is a by-product of the historic open cast coal mining activity in the region.

Fireclays are a unique clay type in the UK that formed directly below the coal seams as a result of the leaching of certain elements, especially iron compounds over time, resulting in a clay that is high in silica and alumina and low in iron, therefore has a tendency to fire to a buff, cream or white colour during the brick firing process, and in an oxidising kiln environment.

These bricks are produced using the "soft mud" process that replicates the aesthetics of a hand thrown clay brick, which has a sanded and creased surface texture. Clay preparation involves the grinding of the raw clay to <2mm before being mixed with water to form a "soft mud" consistency containing in the region of 24-28% water in the clay mix.

This wet clay is then fed via a delivery system to the brick making process, where the clay is discharged into a pre sanded mould before a rocker presses and compacts the clay into the mould. The mould is then inverted to release the brick, and the pressed brick is taken off to the drying chambers in order to remove the water, before it can be fired in the kiln.

4. Brick Powder Production

The two brick waste materials being investigated are waste streams (bricks that are defective; broken chipped etc and rejected by the quality control system in place) arising from the brick manufacturing process at two of Forterra's brick production facilities, Kinds Dyke and Measham. As previously described the two brick types are very different both in raw material composition, and in the nature of the manufacturing process, including the ultimate firing temperature.

As brick waste arising from a site ranges in size from the standard brick (215 x 102.5 x 65mm) through to fragments of broken bricks, the first process is a mobile plant jaw crusher on site which reduces the bricks down to 0-20mm.

Whilst this can be used as a feed stock into a ball mill, the actual ball milling efficiency is increased by screening and ball milling the 0-2mm fraction. Currently the 2-20mm fraction is already utilised internally as an aggregate for Forterra's Fenlite range of concrete blocks, and the 0-2mm fraction (Figure 1.) is used as a facing material and applied to the surface of certain clay bricks within the range.

Figure 1. Crushed and screened KDG (0-2mm fraction) prior to ball milling.

4.1. Ball Milling

Ball milling of the waste brick materials was undertaken in Forterra's laboratory ball mill (Figure 2). The mill has a capacity to mill c. 70kg of material using a charge of 192kg of steel balls with 4 different diameters, 15mm, 20mm, 25mm, 30mm in roughly equal proportions (by mass).

The mill has a maximum design rotational speed of 52rpm which means that the midpoint within the "optimal" rotation speed to achieve optimum grinding is 33rpm. All brick waste materials have been ground at this rotational speed with only the duration being changed to achieve the desired Particle Size Distribution (PSD) and corresponding target Specific Surface Area (SSA).

Initial discussions within the project partners identified that the optimal Dx50 (µm) (average particle size) should be c. 15µm, which became the standard target size.

The brick waste was dried at 105°C for 48 hours before being allowed to cool and then loaded into the ball mill. Each milling process used approximately 70kg ± 4kg and was milled for 180 minutes (KDBP) or 210 minutes (MBB), producing the particle size distributions as presented in Table 1.

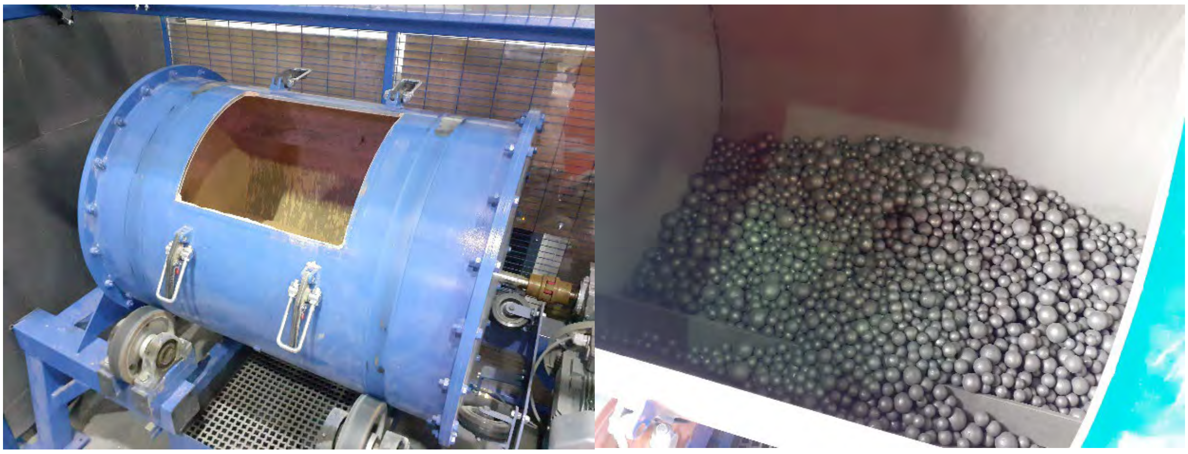

Figure 2. Laboratory scale ball mill with a capacity to mill c. 70kg of material at a time.

Both resulting brick waste "powders" were analyses using a Malvern Mastersizer 3000 using the Hydro EV delivery system (a wet measurement method rather than as a dry powder). The results are the average values from 15 analyses from 3 independent samples for each brick type.

Table 1. Resulting particle size distribution and specific surface area for the brick waste materials ball milled at 33rpm for 180 minutes.

	KDBP	MBB	Target
Milling Time @ 33rpm (minutes)	180	210	
Dx90 (μm)	95.7	87.7	< 115
Dx50 (μm)	14.7	13.8	< 15
Dx10 (μm)	1.49	1.42	< 1.5
Specific Surface Area (SSA) m^2/kg	1402	1484	> 1400

Through previous internal work at Forterra, the specification, “target”, for the milled brick waste was set at the values shown in Table 1. The difference in milling times, of the 2 brick materials, to achieve a similar PSD and SSA probably reflect the difference in the firing temperatures of the bricks, and the resulting “hardness”. MBB is also known to contain a significantly higher quartz content, as well as an increase glassy matrix which has probably contributed to the higher resistance to grinding.

5. Brick Powder Characterisation

Initial characterisation of the waste brick materials selected for this project were undertaken to establish the chemistry and mineralogy using conventional assessment analytical methods, namely X-ray fluorescence (XRF) for chemistry and X-ray diffraction (XRD) for mineralogy. In addition, for the analysis of the raw clays only, both Sulphur and Carbon were determined using a LECO high temperature decomposition in pure oxygen method. In addition, the reactive SiO_2 content was determined by the method defined in EN 196-2 based on SiO_2 solubility in boiling potassium hydroxide.

5.1. Chemistry

Table 2. shows the chemistry of both clay brick waste materials as well as the raw clay from which they are made. Analysis was undertaken using X-ray fluorescence spectroscopy (XRF) by a UKAS accredited test house, on fusion bead samples.

Table 2. Major element oxide percentages for the 2 brick clays: Lower Oxford Clay – LOC for the KDG brick waste and Carboniferous Fireclay for the MBB bricks, as determined by X-ray Fluorescence.

	Raw Clay		Brick Waste	
	Lower Oxford Clay	Fireclay	KDBP	MBB
LOI @ 1000°C	18.14	11.53	2.93	0.32
Na_2O	0.49	0.05	0.52	0.15
MgO	1.46	0.80	1.71	0.69
Al_2O_3	16.14	23.97	18.09	22.10
SiO_2	47.80	55.35	55.56	69.50
P_2O_5	0.17	0.06	0.19	0.05
K_2O	2.63	1.95	3.14	2.08
CaO	7.67	0.31	11.12	0.26
TiO_2	0.84	1.09	0.96	1.01
Mn_3O_4	0.05	0.07	0.05	0.05
Fe_2O_3	4.61	4.81	5.72	3.79
C	6.29	1.41	<0.05	<0.05
S	1.732	0.209	0.951	<0.05
($SO_{3\text{ equiv}}$)	4.32	0.52	2.37	0.01

The chemistry of both the raw clays and the fired brick materials reflects the fundamental composition of the original raw material and the loss of volatiles during the high temperature firing process the bricks go through.

The key differences between the 2 clay types, in terms of chemistry, are the SiO_2 and Al_2O_3 content, and the CaO content, in terms of the oxides and the carbon and sulphur content. The fireclay is by far the simplest in terms of chemistry, which is subsequently reflected in the raw clay mineralogy discussed later. The fireclay is dominated by Al_2O_3 and SiO_2, with relatively high alumina:silica ratio. This is indicative of clay rich raw materials, which is borne out by the typical fireclay mineralogy being dominated by kaolinite and illite, along with quartz.

The Lower Oxford Clay (LOC) is a more complex raw material, higher CaO content, higher MgO content, total alkalis are higher (Na_2O, K_2O, MgO and CaO), as are the carbon and sulphur content and associated LOI. The LOC contains a number of minerals and organic carbon that decompose during the firing process and thus are lost in the fired brick. The CaO relates to fossiliferous and finely disseminated calcite and dolomite within the clay. The high carbon content relates to carbon in both organic and inorganic phases, the inorganic being in the form of carbonate (calcite and dolomite) and finely disseminated organic carbon throughout the deposit. The high sulphur content relates to pyritic iron sulphide and traces of gypsum within the clay body.

5.2. Mineralogy

Figure 3. shows the corresponding qualitative XRD traces for KDBP and MBB, from which the mineralogy can be determined. Analysis was undertaken using a “random oriented” powder mount, using CuKα x-ray radiation and a scan between 15°-55° 2θ, 0.02° 2θ step size and scan speed of 1 degree per minute.

The XRD shows the fired mineralogy to be very different, reflecting the very different mineralogical composition of the raw clays. Fireclays in the raw state are relatively simple clay deposits, predominantly (>90%) made up of kaolinite, illite and fine-grained quartz.

The Lower Oxford Clay on the other hand is minerals a more complex mix of illite, kaolinite and chlorite clay minerals with variable amounts of quartz, calcite, gypsum pyrite and feldspars, reflecting the very anoxic deposition conditions during the Upper Jurassic Period. In addition, the clay also contains approximately 6-7% organic carbon.

In terms of the fired brick mineralogy, the complexity of the raw material is reflected in the complexity of the mineralogy of the fired brick material. The MBB material has a relatively simple mineralogical composition, quartz, mullite and potassium feldspar, in addition to the amorphous ceramic glass which is not readily detectable using XRD. This results from the predominantly alumina and silica rich raw material and the relatively higher firing temperature, typically 1080°C. The majority of the alkalis are found in the ceramic glass rather than forming new crystalline phases, however small amounts of potassium feldspar are formed during the firing process.

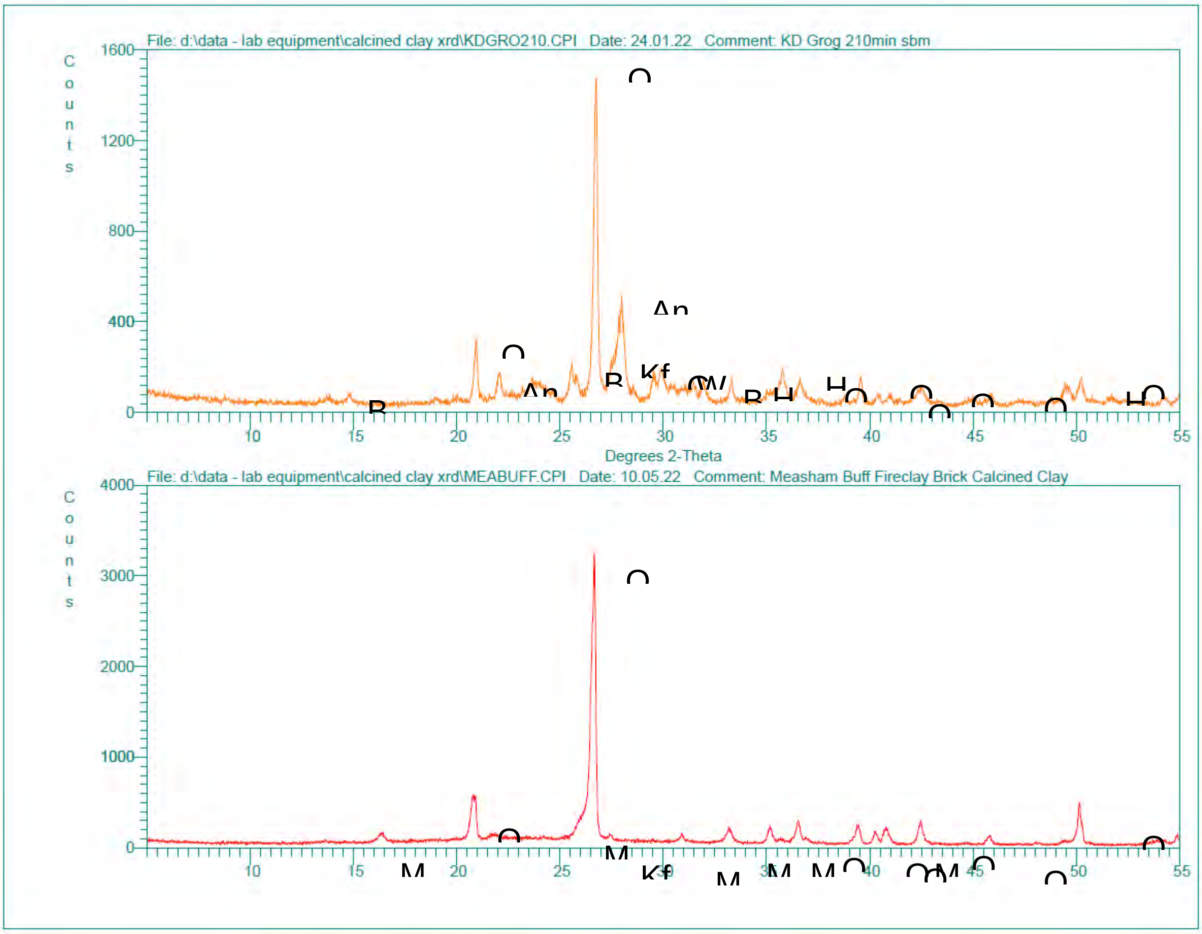

Figure 3. X-ray diffraction traces and associated mineralogical interpretation of the principal peak positions for the KDG (upper trace) and MBB (lower trace).

Q- quartz, M- mullite, Kf – potassium feldspar (microcline), An – anorthite, C – calcite, W – wollastonite, B – bassanite, H- hematite.

The KDBP mineralogy is considerably more diverse, not only due to the complexity of the raw clay, but also as a result of the lower firing temperature, typically 960°C to 980°C. One of the key differences between the 2 brick types is the relatively high CaO content of the Lower Oxford Clay. This along with the silica in the form of quartz, and that released as a result of the thermal breakdown of the clay minerals, coupled with extended periods of time are high temperatures, often results in wollastonite (calcium silicate) being formed in small amounts, as well as spinel (calcium magnesium alumino silicate), although none was identified in the KDG, but has been in the past.

5.3. Reactive Silica

Determination of the “reactive silica” content was undertaken using the method referenced in BS EN 450 and EN 197-1, namely EN 196-2 which measures the silicon dioxide soluble after treatment with hydrochloric acid and with boiling potassium hydroxide solution.

For continuity and direct comparison UCL (University College London) have undertaken a Modified ICC “reactivity” testing on both brick powders to enable direct comparison against the bespoke calcined clay products produced during this research programme. The results are p[resented in Figure 4

Table 3. Reactive SiO_2 content of the 2 brick waste powders

	KDG	MBB
Total SiO_2 (by XRF)	54.16%	71.40%
Reactive SiO_2 (by EN 196-2)	39.74%	43.23%
% Reactive	73.4%	60.5%

Although the SiO_2 content is higher in the MBB brick powder, proportionally only a little over 60% of it is available and “reactive”, whereas a little over 73% of the total SiO_2 is “reactive” in the KDBP brick powder.

Based on the reported mineralogy of the fired bricks, this would suggest that the more complex silicate mineralogy of the KDBP material and any ceramic glassy phase present, will still liberate SiO_2 in highly alkaline environments, however the predominantly quartz and mullite rich MBB brick powder, despite having a higher total SiO_2 content, has a lower proportional “reactive” SiO_2 suggesting that the SiO_2 in the form of quartz is more soluble than that bound into the crystal structure of mullite, in the fired brick.

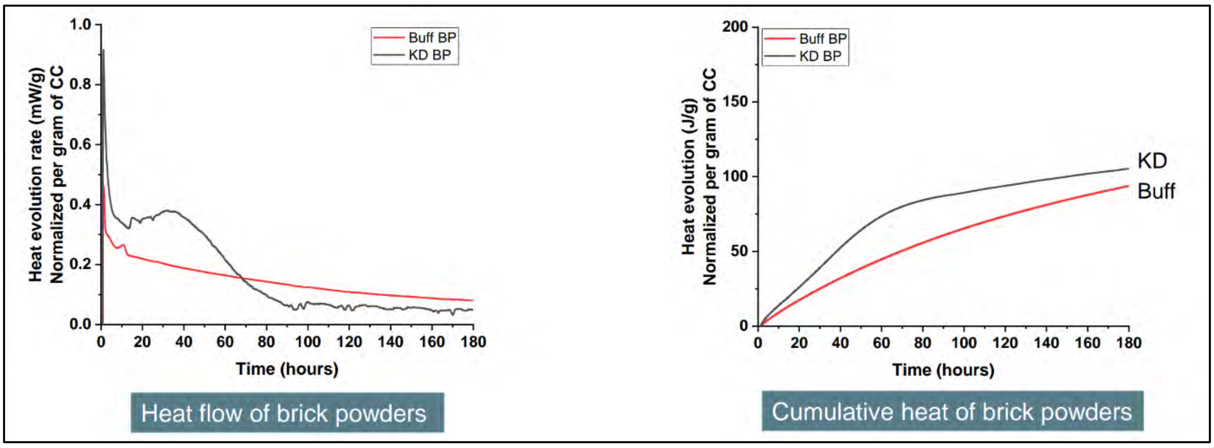

Figure 4 Brick powder results of the Modified ICC test method (a pozzolanic reactivity test based on released heat over time) carried out by UCL

Figure 4 shows the results of the work undertaken by UCL into the reactivity of the brick powders using the modified ICC heat evolution technique. The results confirm the Reactive Silica (EN 196-2) results shown in Table 3, in so much as the KDBP releases a greater amount of heat indicating a more reactive material. It should be noted however that the overall "cumulative heat" release after 180 hrs, at about 110 J/kg, is significantly lower than the results from the other laboratory calcined clays, which typically fall between 250-600 J/kg. (See Work Package E Report for further details on this test method and results).

6. Brick Waste as a Supplementary Cementitious Material

One of the key objectives of the project is to establish the different performance characteristics of the different "calcined clay" sources as cement replacements. Outside of the scope of this work package, but of wider interest to the project as a whole, Forterra have undertaken some standard concrete cube strength trials replacing the CEM I with the brick waste powders created for this project, based on our standard laboratory Self Compacting Concrete (SCC) base design (C60/70). The initial results are presented here.

6.1. KDBP & MBB Brick Powders

Forterra's concrete laboratory is based at the Somercotes precast concrete plant in Derbyshire. Investigations into new raw materials, cements and admixtures are carried out on a Standard Lab Concrete (SLC) to maintain continuity in all assessments. This SLC is based on a "Concrete Wall Panel" mix design.

Of particular interest to Forterra is the impact calcined clay cements has on the early stage strength development of concrete, especially when using a SCC which designed to achieve at least 15N/mm^2 compressive strength at 15 hours to enable safe demoulding and lifting of concrete units cast the previous day. The mix design is therefore over designed to achieve the production requirements, i.e. demoulding at 15hrs, rather than the product/unit requirements.

Table 4. Concrete cube mix design and compressive strength results when using a Forterra standard laboratory mix design for a SCC mix (C60/70).

		Control	KDBP 10%	KDBP 30%	KDBP 50%	MBB 30%
Ketton CEM I (PC1)	% of dry constituents	23	21	16	11.5	16
Brick Powder		n/a	2	7	11.5	7
0/4mm Sand		39	39	39	39	39
4/10mm Lst		38	38	38	38	38
Superplasticiser SP4	% based on binder content	1.36	1.36	1.36	1.36	1.36
W:B Ratio		0.31	0.31	0.31	0.31	0.31
Cube Strength 24hr	MPa (N/mm^2)	51.6	46.2	38.7	26.5	33.1
Cube Strength 28d		96.8	81.7	90.6	81.2	64.6
Δ% v Control (24hr)	%	n/a	89.5	75.0	51.3	64.1
Δ% v Control (28d)		n/a	84.0	93.6	83.9	66.7

Table 4 and Figure 5 show the results of the initial lab trials with Forterra's standard lab mix. In terms of performance, all comply with the concrete requirements for a C60/70 SCC. The KDBP replacements up to 50% despite having a significant reduction in 24hr strength, still achieved the 28d strength for the concrete design, though the 24hr strengths were roughly half that of the Control cubes.

Overall the 30% replacement by MBB has not achieved similar strengths to the equivalent KDBP cubes, indicating that the MBB brick powder is less reactive, and potentially reflects a parity in the corresponding strength, equivalent to the cement reduction of approximately 1/3rd. This indicates that the MBB brick powder may only be acting as a filler rather than an active secondary cementitious material.

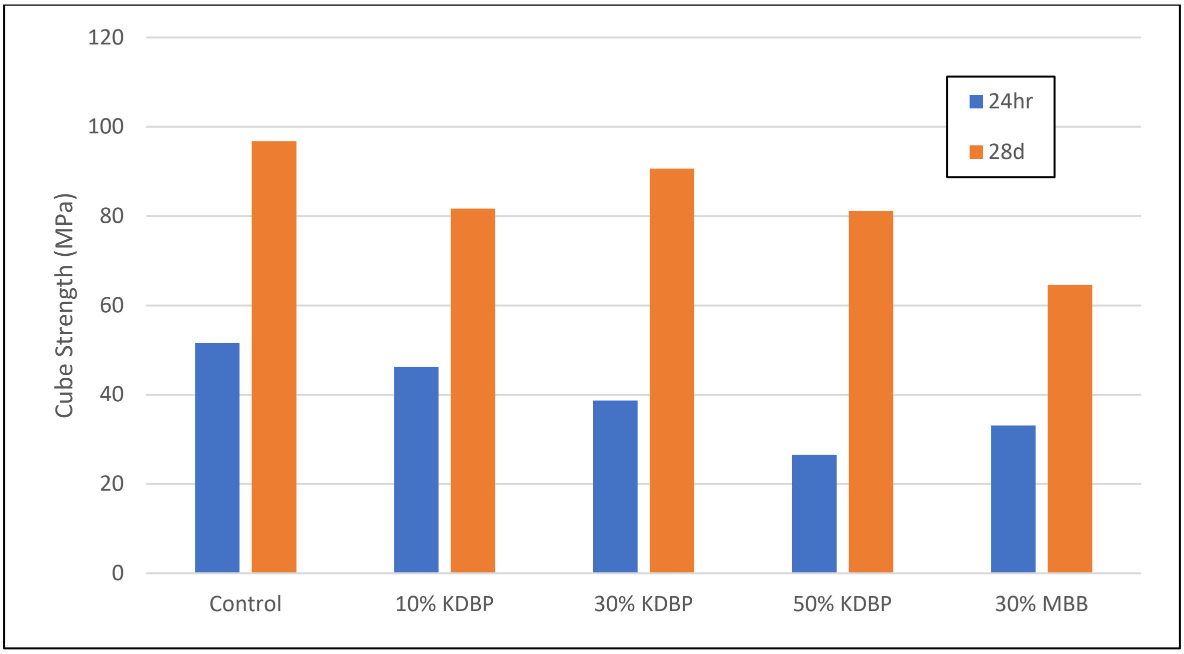

Figure 5. 24hr and 28d compressive strengths for the standard laboratory SCC C60/70 mix design.

7. Conclusions

Based on the results to date, it appears that the KDBP brick powder is acting as a SCM even at replacement levels of CEM I up to 50%. Whilst 24hr strength are significantly compromised, the 28days strengths are approximately 80% of the Control sample concrete, indicating that the KDBP is acting during the latter stages of strength development rather than during the early strength gain period.

Based on the one result so far, the MBB appears to be providing little or no SCM properties to the concrete as the 30% replacement cube strength is approximately 30% of the Control sample, although this is based on one set of test cubes and will be repeated to confirm the results, along with the 10% and 50% replacement cube sets.

8. References

O'Farrell M (1999) THE DURABILITY OF MORTAR WITH GROUND CLAY BRICK AS PARTIAL CEMENT REPLACEMENT. University of Glamorgan PhD Thesis.

(1999). BS EN 1015-3: Methods of test for mortar for masonry. Determination of consistence of fresh mortar (by flow table). BSI.

(2019). BS EN 12350-8: Testing fresh concrete - Self-compacting concrete. Slump-flow test. BSI.

(2009-2021). BS EN 12390 Part 1-4: Testing of hardened concrete. BSI.

(2016). BS EN 196-1: Methods of testing cement - Determination of strength. BSI.

(2011). BS EN 197-1: Cement. Composition, specifications and conformity criteria for common cements. BSI.

British Standards Institution (2012) BS EN 450-1 Fly ash for concrete Part 1 Definitions, specifications and conformity criteria

University College London

Re-C3: Reclaimed Calcined Clay Cements

Appendix 4 -

Characterisation, calcination temperature optimization and pozzolanic reactivity evaluation of UK reclaimed clays

Authors:
UCL:
Yubin Cao
Shi Shi
Tongbo Sui
Yun Bai

Date: December 2023

Contents

1. Introduction

Ten UK clays sourced from different origins were investigated in Re-C3 project. The raw clays were firstly ground and characterised by thermogravimetric analysis (TG). Based on the TG results, in particular derivative thermogravimetry analysis (DTG), several calcination temperatures were identified for the subsequent calcination in a laboratory-scale furnace. The calcined clays obtained from the laboratory-scale furnace under these temperatures were then analysed using TG, XRD, FTIR, G3-morphology characterisation and SEM. In addition, the pozzolanic reactivity of each calcined clay was also evaluated by a modified R3 method.

Based on the results obtained, the following deliverables are reported in this report:

(1) The recommended optimal calcination temperature for each raw clay.

(2) Ranking of the pozzolanic reactivity of 10 calcined clays.

(3) Recommendation of a rapid pozzolanic reactivity evaluation method for low-grade calcined clays.

2. Experimental Procedure

2.1 Materials

The ten clays were provided by different industry partners and the details are shown in **Table 1**. Chemical reagent, Calcium hydroxide powders (CH), potassium hydroxide pellet (KOH) and potassium sulfate (K_2SO_4), were used to simulate the cement pore solution as per R3 test to evaluate the pozzolanic reactivity of calcined clays.

Table 1 Raw clays tested in this project.

ID of Raw Clay	Source
RC1	LP637 Imerys
RC2	LP638 Imerys
RC3	LP639 Imerys
RC4	LP640 Imerys
RC5	LP641 Imerys
RC6	21 GHS 284 Hanson Mixed Clay
RC7	21 GHS 285 Hanson Upper Lias Clay
RC8	21 GHS 286 Maxey Clay Sample Tarmac
RC9	21 GHS 287 Keele Clay Sample Tarmac
RC10	21 GHS 290 Clay Aggregate Industry

2.2 Method

The experimental process adopted is shown in Figure 1.

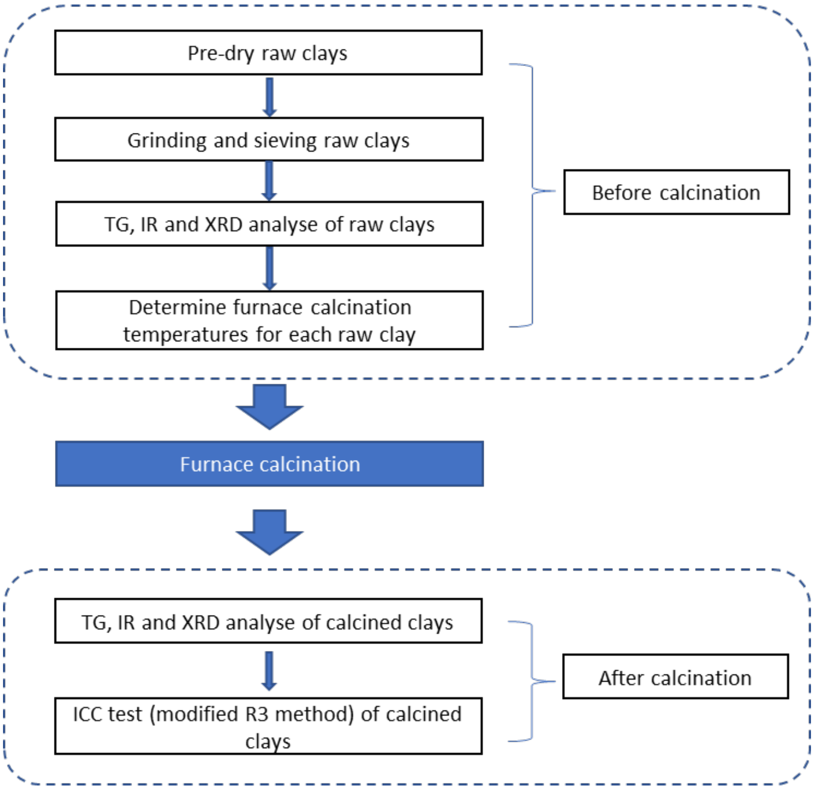

Figure 1 Experimental process.

2.2.1 *Pre-dry, grinding* and *sieve of the raw clays*

The raw clays were firstly pre-dried at 60 °C in an oven for 24 hours to facilitate grinding and sieving. The pre-dried clays were then ground by hand with a pair of mortar and pestle to reduce the influence of large particles on the calcination. All particles were passed the 150 microns sieve and then used in the following tests.

2.2.2 TG, FTIR and XRD tests for raw clays

The ground and sieved raw clays were characterized with X-ray Diffraction (XRD), TG-DTG, and Fourier-transform infrared spectroscopy (FTIR) tests.

- XRD analysis – The XRD data were carried out with a Siemens D5000 X-ray diffractometer (as shown in **Figure 2**) using Cu-Kα radiation ($\lambda = 1.5418$ Å, i.e. 15.415 nm) over the 2θ range 5–70° with a step size of 0.02° and a count time of 10 s.
- FTIR – The FTIR patterns were collected by a Bruker-ALPHA FT-IR spectrometer (**Figure 3**).
- TG – The TG/DTG analysis were carried out with a NETZSCH TG 209 F1Libra (as shown in **Figure 2**). Around 25-30 mg of samples were placed in an aluminum pan and heated up to 1000°C at a rate of 10°C/min under nitrogen purge (20 ml/min).

Figure 2 X-ray Diffraction (XRD) Analyzer (left) and Thermal Gravimetric (TG) Analyzer (right).

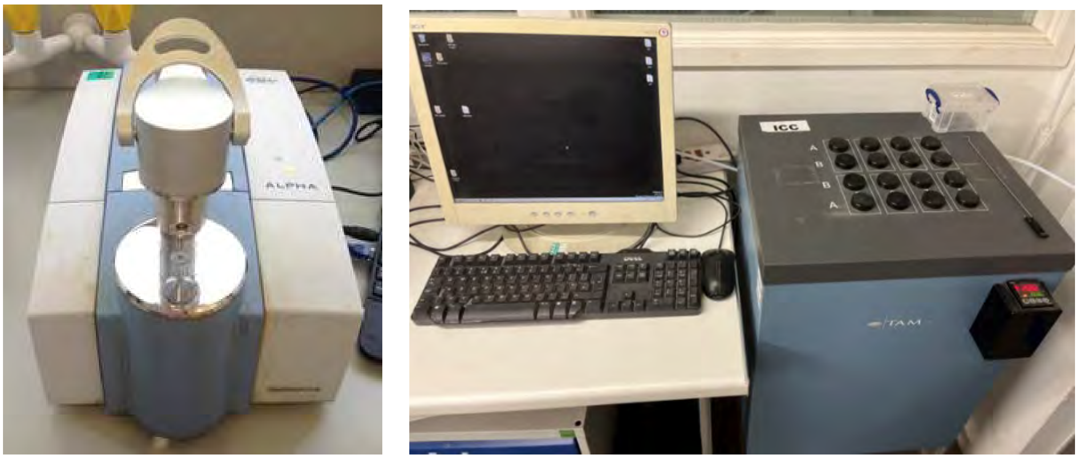

Figure 3 FTIR analyzer (left) and ICC instrument (right).

According to the obtained TG-DTG curve of each raw clay, the furnace calcination temperature can be determined and is shown in Table 2. For example, **Figure 7** shows out the TG-DTG curve of the RC7. The calcination temperatures for RC7 as determined by the following considerations:

- T_1 – The peak temperature of main dehydration peak
- T_2 – The end temperature of the main dehydration peak
- T_3 – The peak temperature of the second dehydration peak
- T_4 – The end temperature of the second dehydration peak
- T_5 – From literature review, the source of pozzolanic reactivity is not only from the dehydration of aluminosilicate, but also from the bond breakdown of Si-O-Al/Si bonds, which needs higher temperature (> 900 °C). This temperature is also suggested by industry, which calcined clay blended cement shows a higher performance.

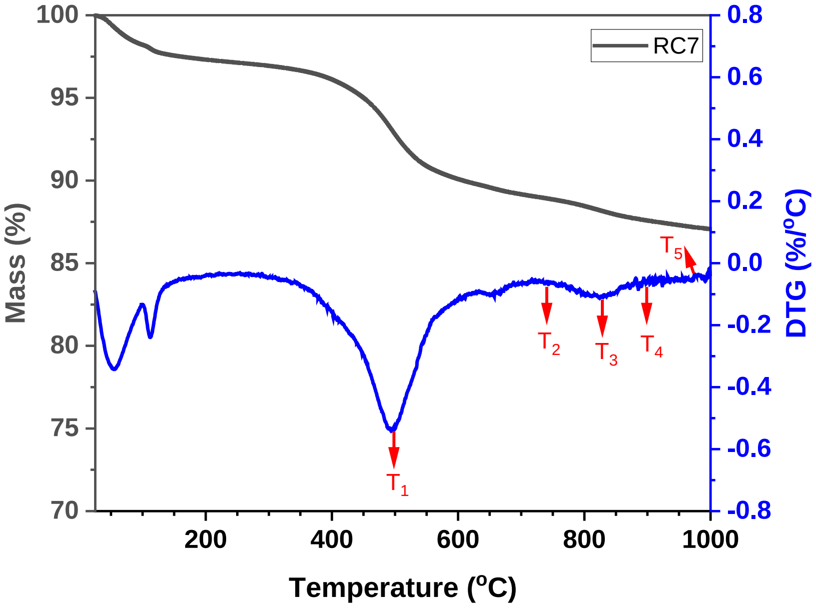

Figure 4: The TG-DTG curve of RC7

2.2.3 Furnace calcination

Around 30g raw clay was placed in a crucible, which was then placed in a laboratory furnace. The heating programme for each calcination temperature (as shown in **Table 2**) was set as follows:

1) Heating process: from ambient to the targeted temperatures

2) Heating rate: 20 °C/min

3) Heating time to the targeted temperature: 35-45 min

4) Resident time at the targeted temperature: 3 hours

The calcined clays were left in the furnace for an overnight cooling to the room temperature and were then stored in a sealed bag.

Figure 5 Laboratory furnace used in this project.

Table 2 Summary of the calcination temperatures investigated for each raw clay.

Industry	Raw clay ID	Calcination temperatures
Imerys	RC1	850/800/525 ^{o}C
	RC2	850/800/525 ^{o}C
	RC3	850/800/525 ^{o}C
	RC4	850/800/525 ^{o}C
	RC5	900/850/525 ^{o}C
Hanson	RC6	940/850/800/750 ^{o}C
	RC7	940/900/850/750/500 ^{o}C
Tarmac	RC8	850/800/500 ^{o}C
	RC9	940/900/850/750/500 ^{o}C
Clay Aggregate Industry	RC10	940/900/850/750/500 ^{o}C

2.2.4 Characterisation of calcined clays

In the following discussion, the calcined clay was named as CC with the same raw clay ID and calcination temperature. For example, CC1-525 refers to the Calcined RC1 which was calcined at 525 ^{o}C for 3 hours. Each calcined clay was characterized with TG, FTIR and XRD.

2.2.5 Pozzolanic reactivity evaluation of calcined clays

R3 method was commonly used to evaluate the pozzolanic reactivity of calcined clays. The basis of the R3 test is to use a simplified system to isolate the reaction of the calcined clay from that of the clinker. To simulate the environment where the reaction of calcined clay in blended cement happens, the solutions were prepared by dissolving potassium hydroxide and potassium sulfate in deionized water. All systems had a water-to-solid ratio of 1.2 to supply hydration processes with excessive water and generate a homogenous paste. This project modified the ratio of calcined clay to calcium hydroxide from 1:3 to 1:1 due to a relatively lower kaolinite content existing in the UK clays. In this way, it is anticipated that the results obtained could be sensitive enough to differentiate the reactivity difference between the calcined low-grade clays investigated in this project.

The pozzolanic reactivity of the calcined clays were evaluated with a modified R3 method using isothermal conduction calorimetry (ICC). An 8-channel TAM-Air calorimeter by TA Instruments US (**Figure 3**) was used in this project. In this work, all data were normalized to the weight of calcined clays. The test was carried at 40 °C to shorten test time. The mixture design for the ICC test is shown in **Table 3**.

Table 3 The mixture design for the pozzolanic reactivity evaluation.

System	CC	Portlandite	K_2SO_4	KOH	H_2O
Modified PPC system	15	15	0.882	0.192	36

The experimental procedure is presented as follows:

1. The potassium hydroxide and potassium sulfate were dissolved in distilled water and stored at 40 °C in an oven for 24 hours before the test.

2. The calcined clay and calcium hydroxide were mixed together and also stored at 40 °C in an oven for 24 hours before the test. The ampoules and lids were also stored in the same oven for 24 hours.

3. On the testing day, the mixed solid materials were mixed with the prepared solutions for 2 minutes, and then around 15g fresh paste was transferred into the ampoule and then loaded in the testing channels.

4It should be noted that, the time between the start of mixing and the start of recording the exotherm was 5 minutes for each sample.

3. Results

3.1 RC1 (Imerys)

3.1.1 TG/DTG analysis

During TG test, the samples were heated at TG furnace (N_2 was used as protective air) from 25 °C to 1000 °C. The TG curves show the mass loss (dehydration, dehydroxylation and decomposition) of samples during the thermal heat. The TG-DTG result of raw clays could help to determine the proper calcination temperatures for large-scale calcination and the chemical compositions in addition to the XRD test. The TG-DTG curves could also help to roughly estimated the kaolinite content in raw clays.

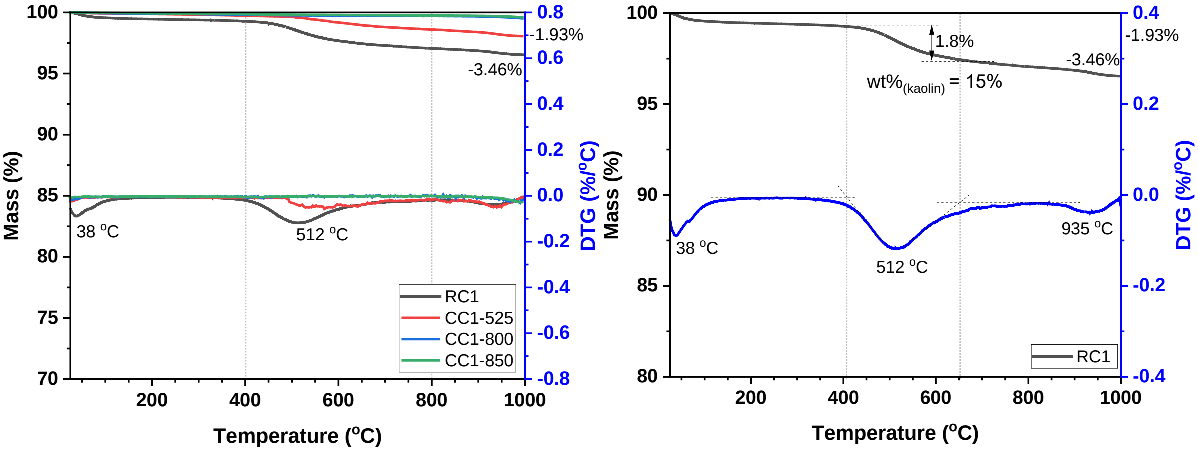

Figure 6 The TG-DTG curves of RC1 before and after calcination at different temperatures.

Figure 6 shows the TG -DTG curves of RC1 and calcined RC1 at different temperatures, while RC1 shows a total mass loss of around 3.46%. The mass loss happened before 100 °C in the TG curve of RC1 was attributed to the loss of absorbed water (dehydration) in the raw material. The main mass loss which happened in the range of 400 °C to 800 °C was attributed to the dehydroxylation of kaolin minerals.

The kaolin content in raw clay could be calculated based on the Equation 1. The mass loss happened between 460 °C to 720 °C was attributed to the dehydroxylation of kaolin. Calculated kaolin content based on the molar mass of each component in RC1 is around 15%.

Kaolin: $Al_2O_3 \cdot 2SiO_2 \cdot H_2O \xrightarrow{400-800\ ℃} Al_2O_3 \cdot 2SiO_2(s) + 2H_2O\ (g)$ (Equation 1)

3.1.2 XRD analysis

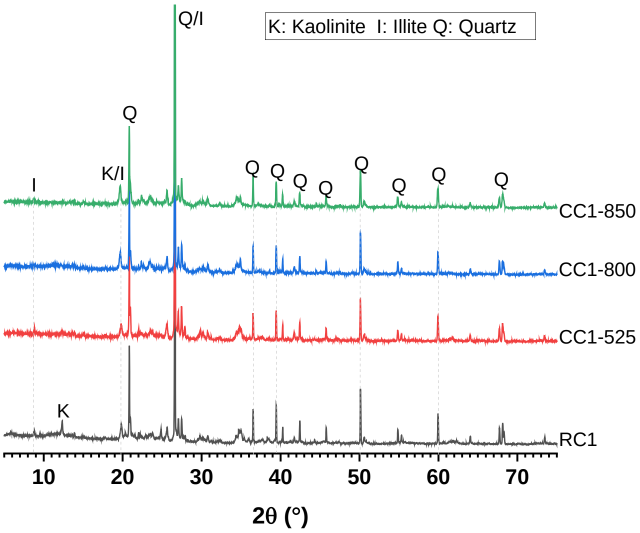

Figure 7 The XRD patterns of RC1 and calcined RC1 at different temperatures.

Figure 7 shows the XRD patterns of RC1 and calcined RC1. At 525 °C, the peaks corresponding to kaolinite disappeared, indicating a significant loss of crystallinity. Calcination at 850 °C does not produce additional changes to the decomposed structure. The small peaks assigned to illite at around 9° 2θ disappeared. From the results, for RC1, we could see that calcination at 525 °C could destroy the crystalline structure of kaolinite.

3.1.3 FTIR analysis

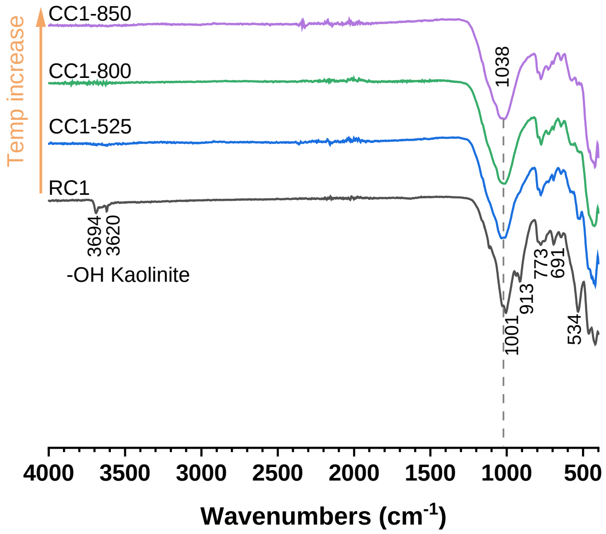

Figure 8 The FTIR patterns of RC1 and calcined RC1 at different temperatures.

Figure 8 shows the FTIR patterns of RC1 and calcined RC1 at different temperatures. The small peaks of RC1 at 3624 and 3694 cm^{-1} were due to the stretching vibrations of hydroxyl (-OH) groups in kaolinite. And the band at 3624 cm^{-1} indicates the inner-hydroxyl group which was located at the interface between the Si tetrahedral and the

Al octahedral layers, while band near 3694 cm^{-1} was the inter-hydroxyl groups originate from the internal Al octahedral surface hydroxyl groups.

The main peak located at 1001 cm-1 was assigned to the stretching vibration of Si-O-T (T = Si or Al) bonds. The existence of small peak at 913 cm^{-1} is defined as Al-OH bending vibration bands, which could also be assigned to the proof of the ordered structure of kaolinite. So, during the thermal treatment, the dehydroxylation of kaolinite is the hydroxyl of the above two parts.

After exposed to 525 °C, the vibration peaks assign to -OH groups in kaolinite disappeared. This indicated the dehydroxylation of kaolinite, which was transferred from an ordered crystal structure into an amorphous structure. Meantime, the small peaks assigned to the Al–OH bending vibration was also disappeared. The FTIR results was consistent with the XRD.

3.1.4 Pozzolanic reactivity analysis

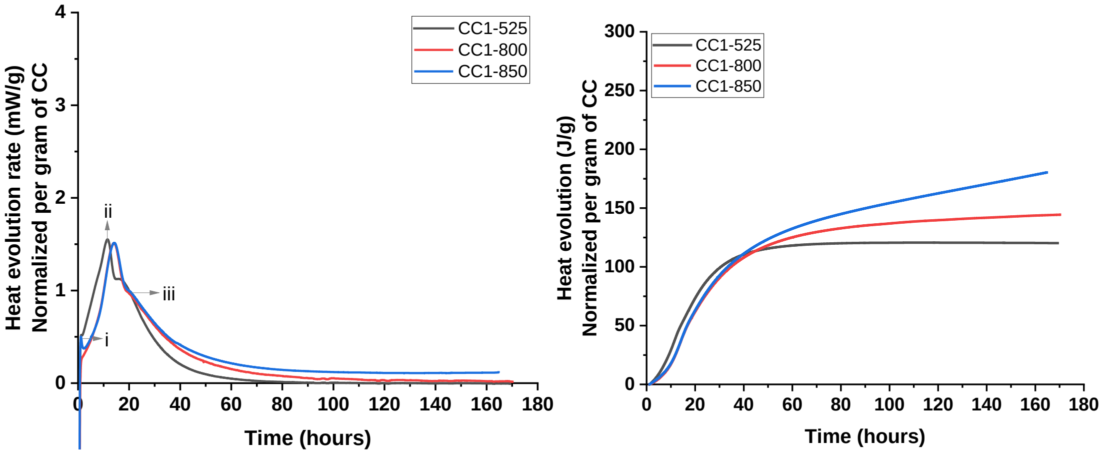

Figure 9 The heat evolution rate (left) and cumulative released heat (right) of calcined RC1 at different temperatures.

The R3 test using isothermal calorimetry gives a rapid indication of calcined clay reactivity.

Figure 9 shows the heat release rate and cumulative heat release of calcined RC1. There are three exothermal peaks appeared for all calcined clays. The first exothermic peak i is related to the initial wetting and dissolution of raw materials. The exothermic peak ii is corresponded to the formation of calcium (aluminum) silicate hydrate (C-(A)-S-H) gel and AFt, while peak iii was due to the transformation of AFt to AFm.

The cumulative heat of CC1-850 is the highest among three samples, which indicates that RC1 calcined at 850 °C showing the highest pozzolanic reactivity.

3.2 RC2 (Imerys)

3.2.1 TG/DTG analysis

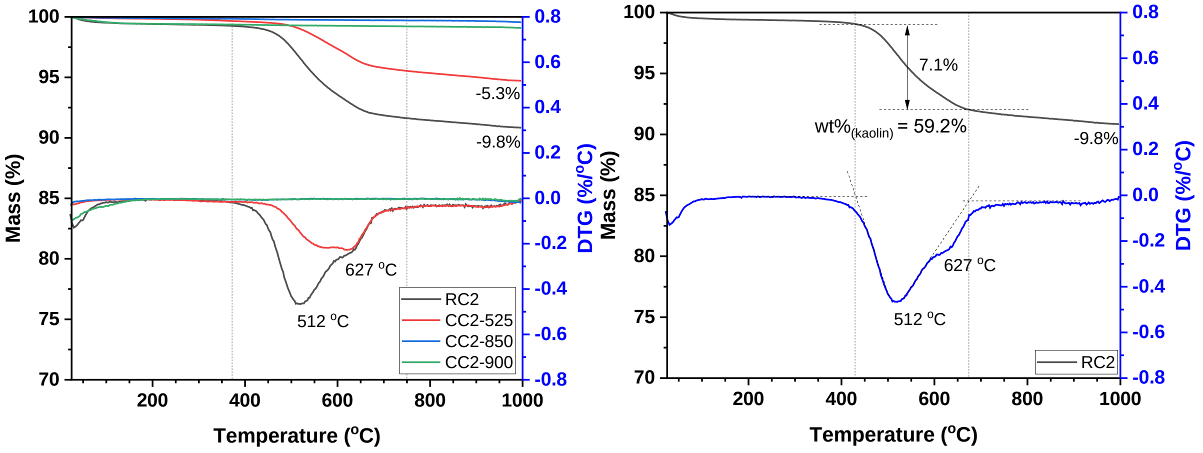

Figure 10 The TG-DTG curves of RC2 before and after calcination at different temperatures

As shown in **Figure 10**, the mass loss of RC2 is around 9.8%. And the calculated kaolin content in RC2 is around 65.8%. For RC2, the dehydroxylation peak (the dehydroxylation rate reaches the highest) is at around 512 °C. However, after calcined at 525 °C for 3 hours in laboratory furnace, the total mass loss of CC2-525 is 5.3%, and there is an overlap peak in the DTG curve. This indicates that kaolin in RC2 could not be fully activated if it was calcined at 525 °C furnace. Increased the calcination temperature to 850 °C and 900 °C, it could see that the kaolin in raw clays was fully dehydroxylated, indicating that it was fully activated.

3.2.2 XRD analysis

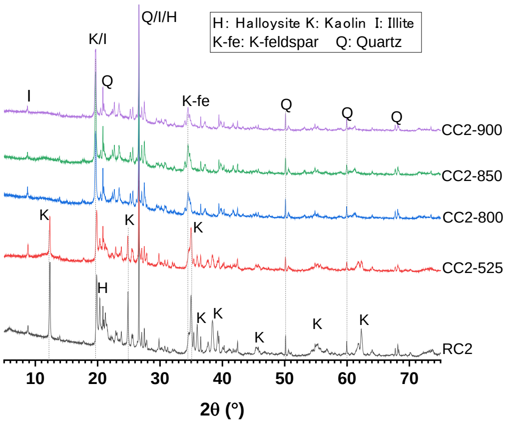

Figure 11 The XRD patterns of RC2 and calcined RC2 at different temperatures.

The XRD pattern (**Figure 11**) of RC2 shows a group of intensive peaks at 12°, 25° and 35° 2θ, which could be assigned to the crystalline kaolinite. The disappear of above crystalline peaks means the destruction of crystal structure of kaolinite. After calcined at 525 °C for 3 hours, there is still remaining crystalline kaolinite. This confirmed that calcination at 525 °C is not sufficient to fully activated the RC2, which is consistent with the TG results. With the increasing calcination temperatures, the ordered crystalline structure of kaolinite was fully deconstructed.

3.2.3 FTIR analysis

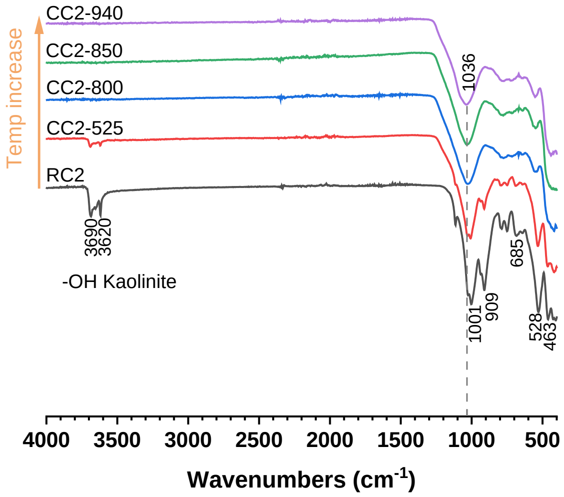

Figure 12 The FTIR patterns of RC2 and calcined RC2 at different temperatures.

As shown in **Figure 12**, the peaks located at 3690 and 3520 cm^{-1} which were assigned to the stretching vibrations of hydroxyl (-OH) groups in kaolinite was still remain in CC2-525. Similar to RC1, the existence of Al-OH bending vibration bands (small peak at 909 cm^{-1}) in RC2 means the ordered structure of kaolinite. The main peak located at 1001 cm^{-1} was assigned to the asymmetric stretching vibration of Si-O-T (T could be Al or Si) bonds. The shifting of this band to a higher wavenumbers 1036 cm^{-1} was due to the breakdown of Si-O-Al.

3.2.4 Pozzolanic reactivity analysis

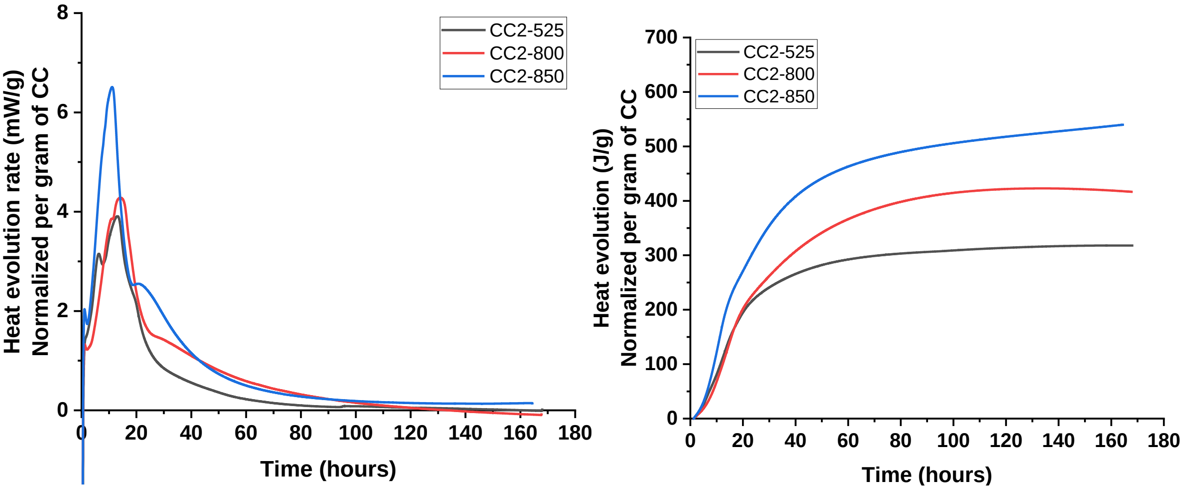

Figure 13 The heat evolution rate (left) and cumulative released heat (right) of calcined RC2 at different temperatures.

As shown in **Figure 13**, the cumulative heat of CC2-850 is the highest which indicates that CC2-850 showing the highest pozzolanic reactivity.

3.3 RC3 (Imerys)

3.3.1 TG/DTG analysis

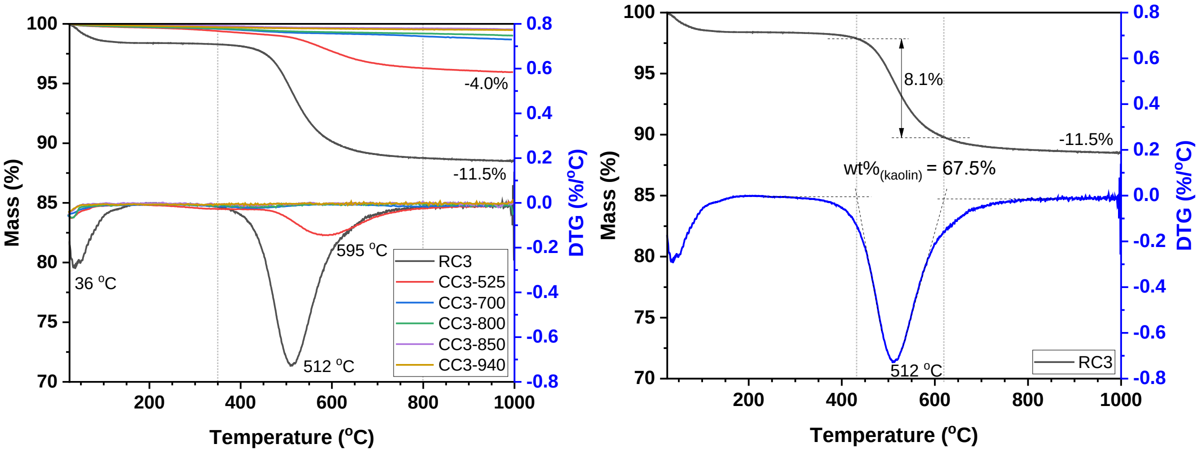

Figure 14 The TG-DTG curves of RC3 before and after calcination at different temperatures.

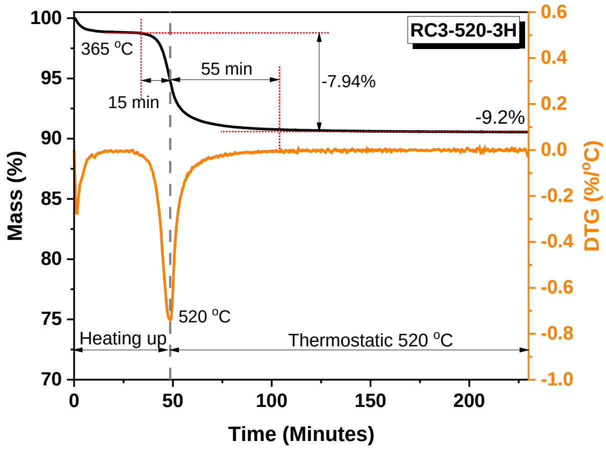

Figure 15 The TG-DTG of RC3 during the process from 25 °C to 520 °C and then constant at 520 °C for 3 hours.

The mass loss of RC3 is around 11.5%, so the calculated kaolin content in RC3 reaches 79.8%. Similar to RC1 and RC2, the dehydroxylation is also located at 512 °C. As shown in **Figure 15**, after calcined at 525 °C in TG machine for 55 minutes, there is no mass loss, which means the kaolinite in RC3 is fully dehydrated.

However, after calcined at 525 °C furnace for 3 hours, the total mass loss of CC3-525 reduces to 4%. The dehydration process at laboratory furnace is not thorough as at TG machine. As Increased the calcination temperature to 700 °C, it could see that the mass loss of CC3-700 is minor, indicating that it was fully dehydroxylated. Continue to increase the calcination temperature to until 940 °C, there is minor changes in the mass loss.

3.3.2 XRD analysis

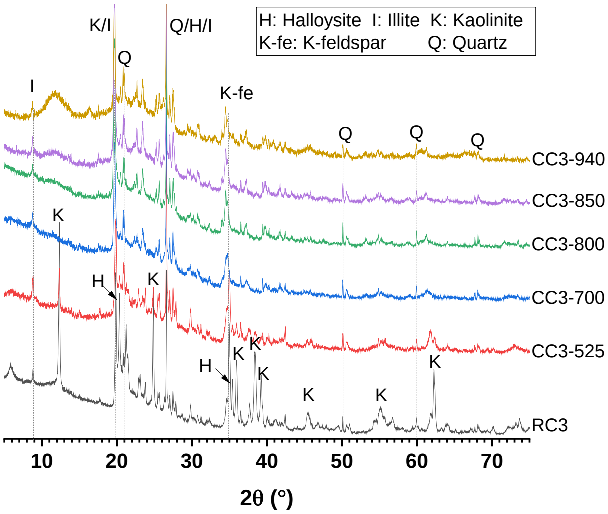

Figure 16 The XRD patterns of RC3 and calcined RC3 at different temperatures.

From **Figure 16**, RC3 shows similar patterns to RC2, with a group of intensive peaks at 12°, 25° and 35° 2θ that are assigned to the crystalline kaolinite. After calcined at 700 °C, the crystalline structure of kaolinite in CC3-700 disappeared. High temperature treatment converted kaolinite to amorphous metakaolin. After calcined at 850 and 940 °C, there is a hump centred at around 12° 2θ. This might due to the recrystallisation of metakaolin at higher temperatures (over 850 °C), while the product showing a poorly ordered structure.

3.3.3 FTIR analysis

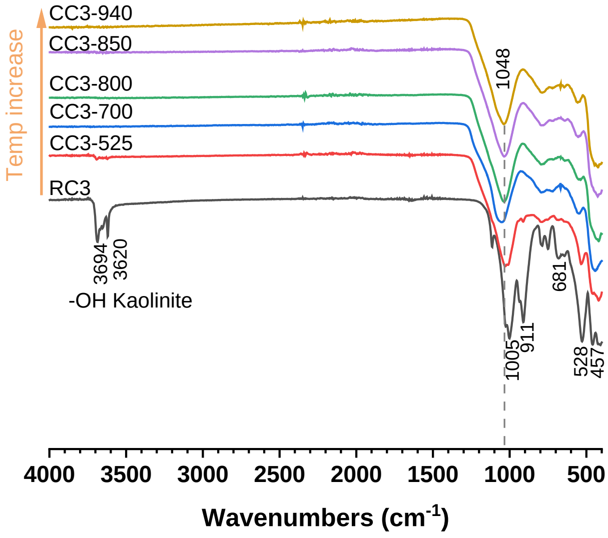

Figure 17 The FTIR patterns of RC3 and calcined RC3 at different temperatures.

From **Figure 17**, the stretching vibrations of hydroxyl (-OH) groups in kaolinite (peaks located at 3694 and 3520 cm^{-1}) disappeared in CC3-525. And the Al-OH bending vibration bands also disappeared. This means that RC3 could be fully dehydroxylated after calcination at 525 °C for 3 hours.

3.3.4 Pozzolanic reactivity analysis

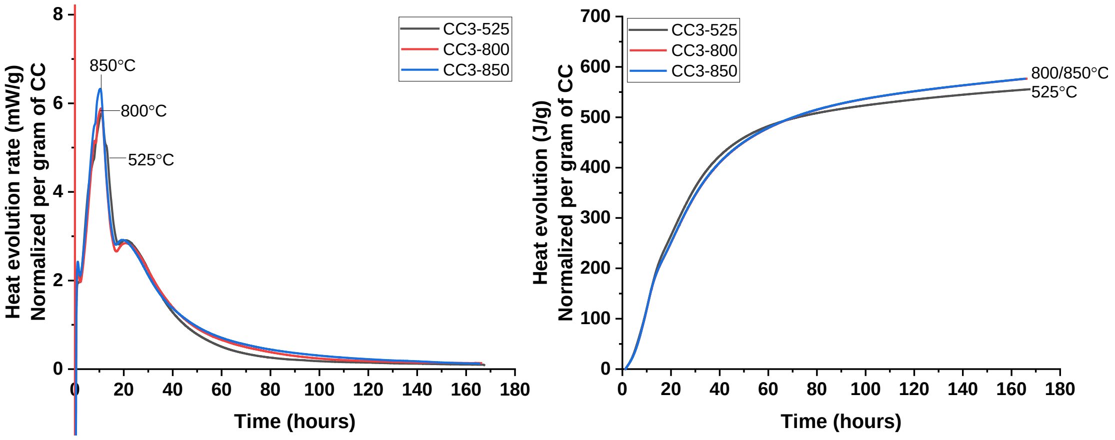

Figure 18 The heat evolution rate (left) and cumulative released heat (right) of calcined RC3 at different temperatures.

The ICC results (as shown in **Figure 18**) confirmed the conclusion that the calcined clays calcined at 525, 800 and 850 °C showing the similar cumulative heat. This indicates that the calcined clays exhibiting similar pozzolanic reactivity.

3.4 RC4 (Imerys)

3.4.1 TG/DTG analysis

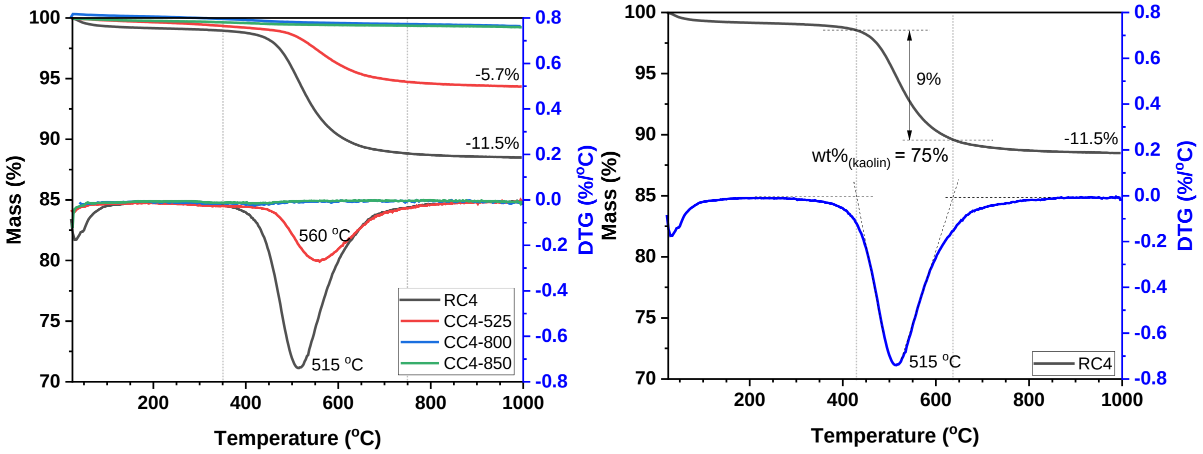

Figure 19 The TG-DTG curves of RC4 before and after calcination at different temperatures.

From **Figure 19**, the mass loss of RC4 is around 11.5%, and the calculated kaolin content in RC4 reaches 86.2%. The dehydroxylation peak is located at 515 °C. After calcined at 525 °C for 3 hours, the total mass loss of CC4-525 reduces to 5.7% and the dehydroxylation peak located at 560 °C. Increased the calcination temperature to 800 °C, it could see that the kaolin in raw clays was fully dehydroxylated, indicating that it was fully activated. Continue to increase the calcination temperature to until 850 °C, there is minor changes in the mass loss.

3.4.2 XRD analysis

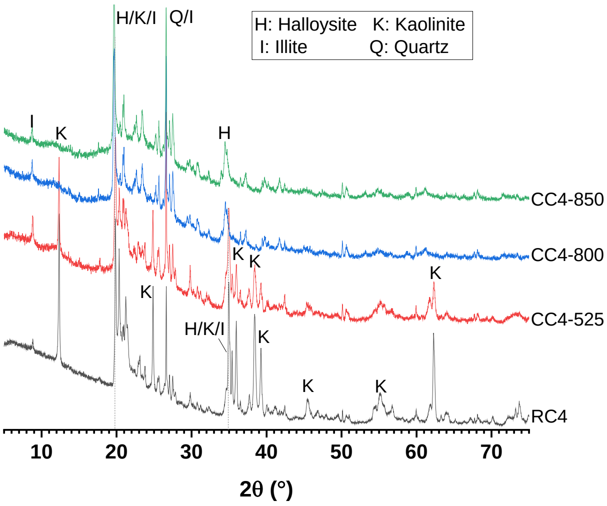

Figure 20 The XRD patterns of RC4 and calcined RC4 at different temperatures.

From **Figure 20**, RC4 shows similar patterns to RC3, with a group of intensive peaks at 12°, 25° and 35° 2θ that are assigned to the crystalline kaolinite. After calcined at 700 °C, the crystalline structure of kaolinite in CC3-700 disappeared. High temperature treatment converted kaolinite to amorphous metakaolin. After calcined at 850 and 940 °C, there is a hump centred at around 12° 2θ. This might due to the recrystallisation of metakaolin at higher temperatures (over 850 °C), while the product showing a poorly ordered structure.

3.4.3 FTIR analysis

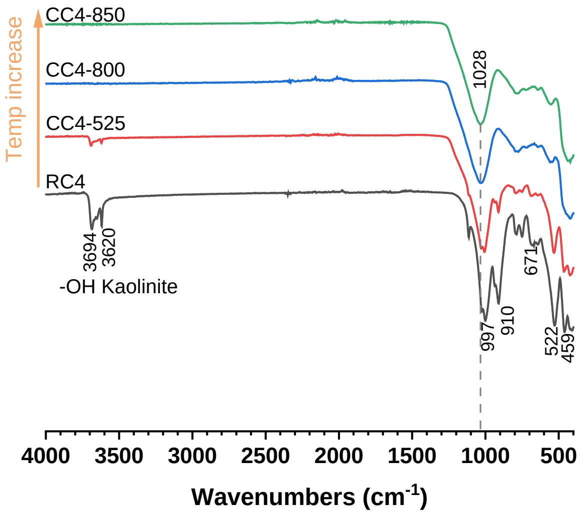

Figure 21 The FTIR patterns of RC4 and calcined RC4 at different temperatures.

From **Figure 21**, after calcined at 525 °C for 3 hours, the intensity of stretching vibrations of hydroxyl (-OH) groups in kaolinite (peaks located at 3694 and 3620 cm^{-1}) reduced. And the Al-OH bending vibration bands could be also detected. This means that RC4 could not be fully dehydroxylated after calcination at 525 °C for 3 hours. Increasing the calcination temperature to 800 °C, the stretching vibration bands of hydroxyl (-OH) groups and bending vibration bands of Al-OH were both disappeared. This indicates the kaolinite in RC4 was fully activated.

3.4.4 Pozzolanic reactivity analysis

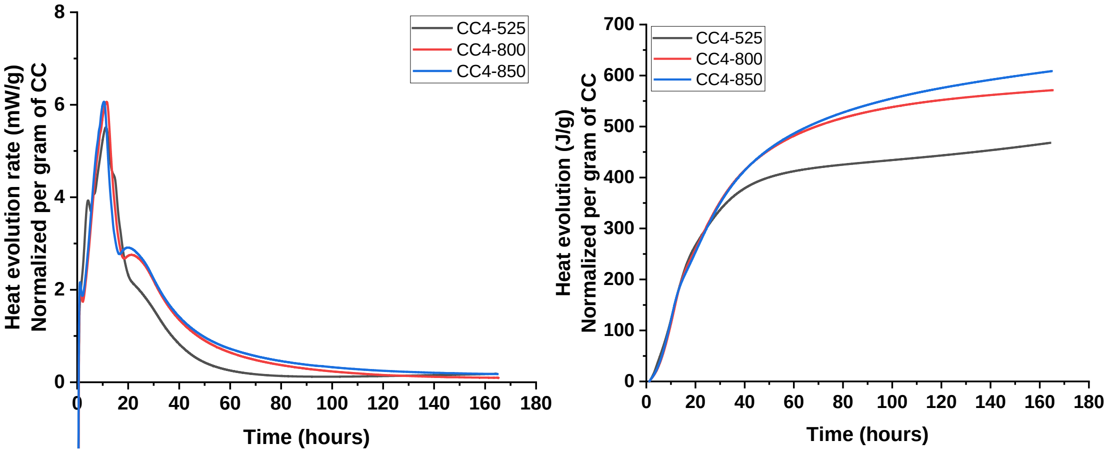

Figure 22 The heat evolution rate (left) and cumulative released heat (right) of calcined RC4 at different temperatures.

From the ICC results (**Figure 22**), we could see that CC4-850 and CC4-800 showing similar cumulative heat value. The CC4-525 shows the lowest cumulative heat value. The CC4-850 shows the highest pozzolanic reactivity, followed by CC4-800 and CC4-525.

3.5 RC5 (Imerys)

3.5.1 TG/DTG analysis

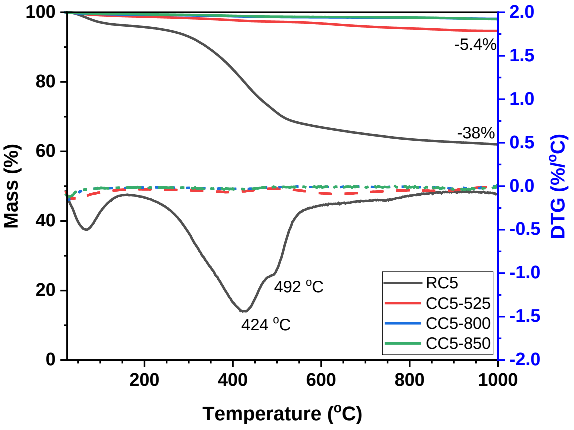

Figure 23 The TG-DTG curves of RC5 before and after calcination at different temperatures.

As shown in **Figure 23**, the mass loss of RC5 reaches around 38%. And the main mass loss peak starts from 150 °C until to around 600 °C. The high mass loss of RC5 is mainly due to the existence of organics. So, it is not possible to calculate the kaolinite content by Tangent method. After calcined at 525 °C for 3 hours, the mass loss of RC5 reduces to 5.4%. Increasing the calcination temperatures to 800 and 850 °C, the mass loss is negligible.

3.5.2 XRD analysis

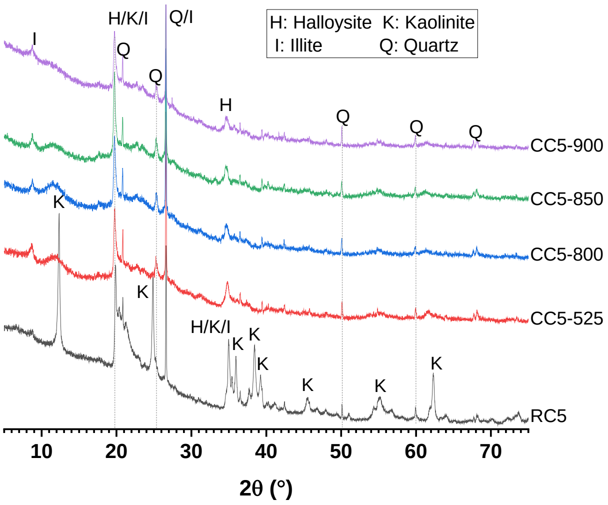

Figure 24 The XRD patterns of RC5 and calcined RC5 at different temperatures.

As shown in **Figure 24**, the XRD pattern of RC5 is similar to RC2, RC3 and RC4, with a group of intensive peaks that are assigned to the crystalline kaolinite. The existence of organics could not be detected by XRD. After calcined at 525 °C for 3 hours, the crystalline peak in CC5-525 disappeared, which is different to RC2, RC3 and RC4. This may be due to the finer particle size of RC5.

3.5.3 FTIR analysis

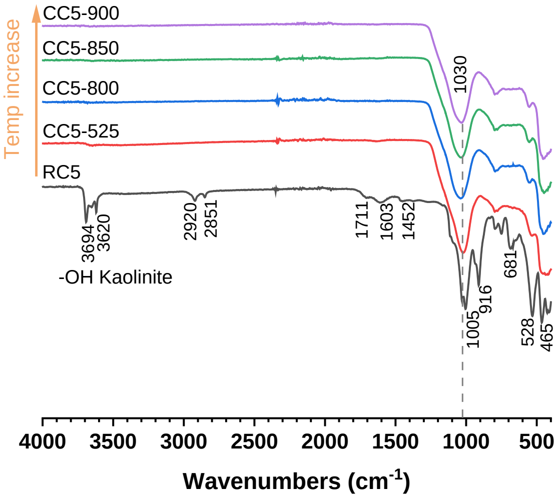

Figure 25 The FTIR patterns of RC5 and calcined RC5 at different temperatures.

From **Figure 25**, the existence of organics (small peaks at 2920/2851 cm^{-1} and ~1600 cm^{-1}) in RC5 could be detected from FTIR pattern. The peaks assigned to the stretching vibrations of hydroxyl (-OH) groups in kaolinite could not longer be detected in CC5-525. This is consistent with the aforementioned XRD data.

3.5.4 Pozzolanic reactivity analysis

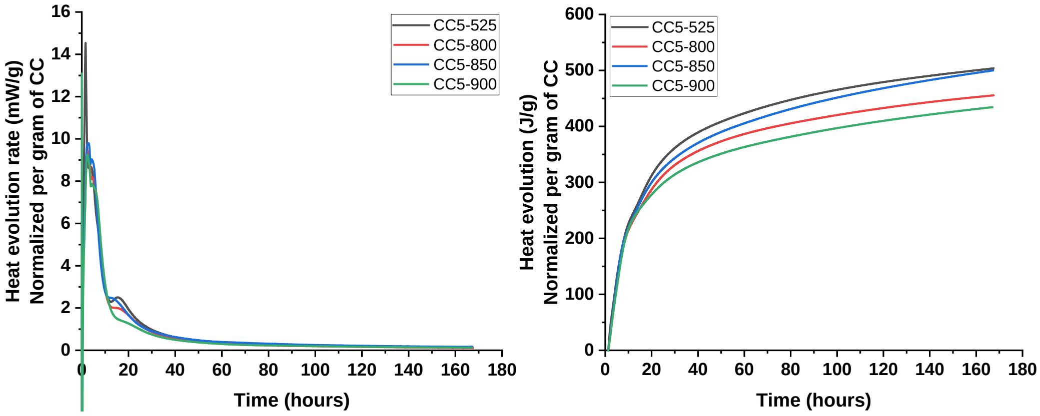

Figure 26 The heat evolution rate (left) and cumulative released heat (right) of calcined RC5 at different temperatures.

As shown in **Figure 26**, CC5-525 shows the highest cumulative heat. CC5-850 shows similar cumulative heat to CC5-525, followed by CC5-800. The CC5-900 shows the lowest cumulative heat. The ICC results of calcined RC5 indicates that CC5-525 showing the highest pozzolanic reactivity, while the CC5-900 showing the lowest pozzolanic reactivity.

3.6 RC6 (Hanson)

3.6.1 TG/DTG analysis

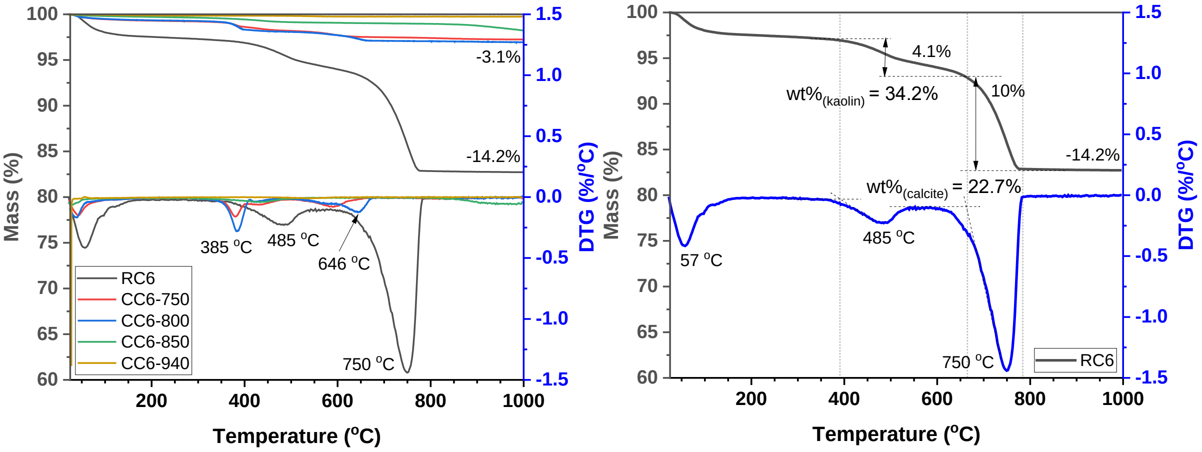

Figure 27 The TG-DTG curves of RC6 before and after calcination at different temperatures.

From **Figure 27**, The mass loss of RC6 is around 14.2%. And there are two main peaks in the DTG curve of RC6. The first small peak is located at around 485 °C and the second peak is located at around 750 °C. According to the Tangent method, the kaolinite content based on the first peak is around 25.8%, while the calcite content based on the second peak is 25.2%. After calcined at 750 and 800 °C, the mass loss is 3.1%. The mass loss peaks locate at 385 and 646 °C. The calcination at high temperature destroyed the crystalline structure of kaolinite and calcite. So, the mass loss peaks in the calcined clays shift to lower temperature.

3.6.2 XRD analysis

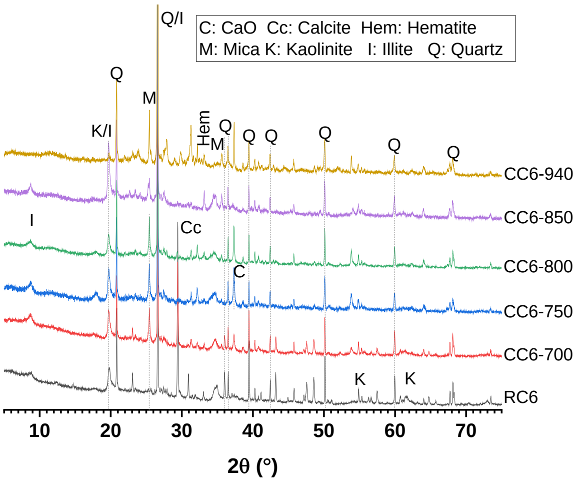

Figure 28 The XRD patterns of RC6 and calcined RC6 at different temperatures.

From the XRD pattern of RC6 (**Figure 28**), we could see that there are fewer crystal peaks of kaolinite. However, there is a significant peak at 29° 2θ which could be assigned to the crystalline calcite. After calcined at 700 °C and 750 °C, the crystalline peak of calcite could still be detected. When the calcination temperature increases to 800 °C and above, the calcite is no longer detected.

3.6.3 FTIR analysis

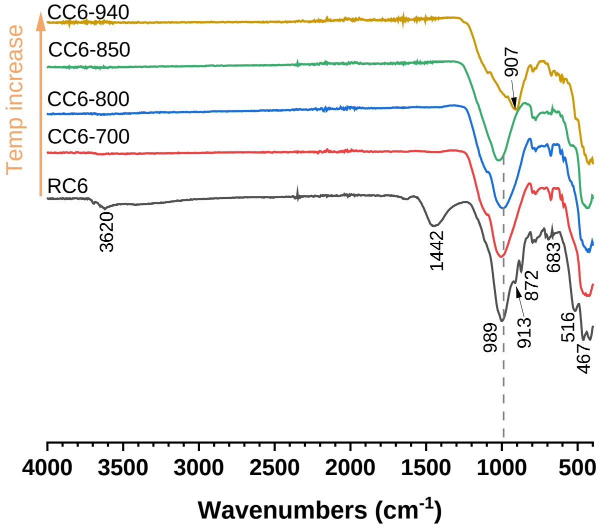

Figure 29 The FTIR patterns of RC6 and calcined RC6 at different temperatures.

The FTIR spectrum of RC6 (**Figure 29**) show a hump at around 3620 cm^{-1}, which could be assigned to the stretching vibrations of hydroxyl (-OH) groups in kaolinite. But the crystal structure of kaolin in the material is too poor to present characteristic peaks. The hump at around 1442 cm^{-1} is due to the C-O stretching vibration in calcite. The calcination caused the shifting of the main peak at 989 cm^{-1} to a higher wavenumber. This is due to the fracture of Si-O-Al bonds. But after calcined at 940 °C, the main peak shifts to 907 cm^{-1}. This is due to the agglomeration between silicon chains. As per the reference, this agglomeration would reduce the pozzolanic reactivity of calcined clay.

3.6.4 Pozzolanic reactivity analysis

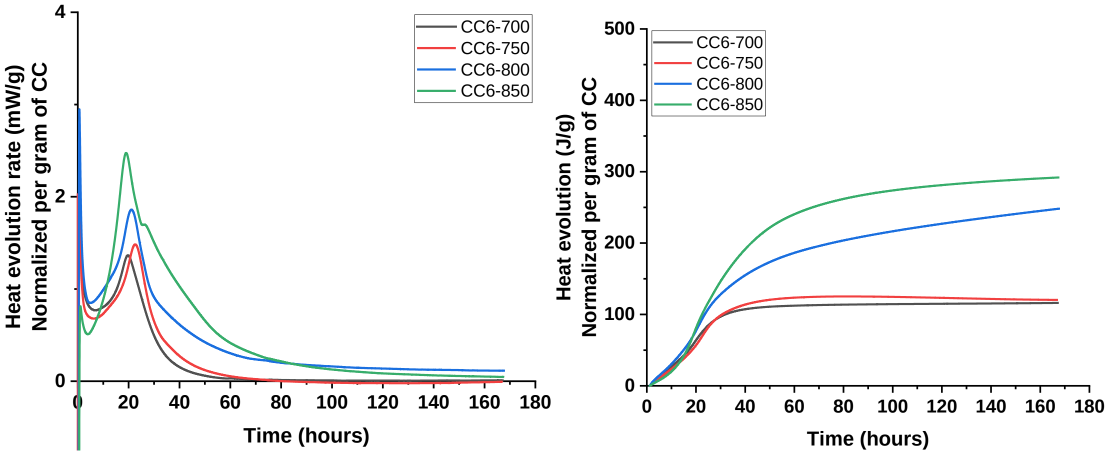

Figure 30 The heat evolution rate (left) and cumulative released heat (right) of calcined RC6 at different temperatures.

The ICC results of calcined RC6 (**Figure 30**) show that CC6-850 has the highest cumulative heat, followed by CC6-800. This indicates that CC6-800 has the highest pozzolanic reactivity. The CC6-700 and CC6-750 show similar cumulative heat and pozzolanic reactivity. But it should be noted that, the decomposition of calcite also influences the cumulative heat of calcined clay.

3.7 RC7 (Hanson)

3.7.1 TG/DTG analysis

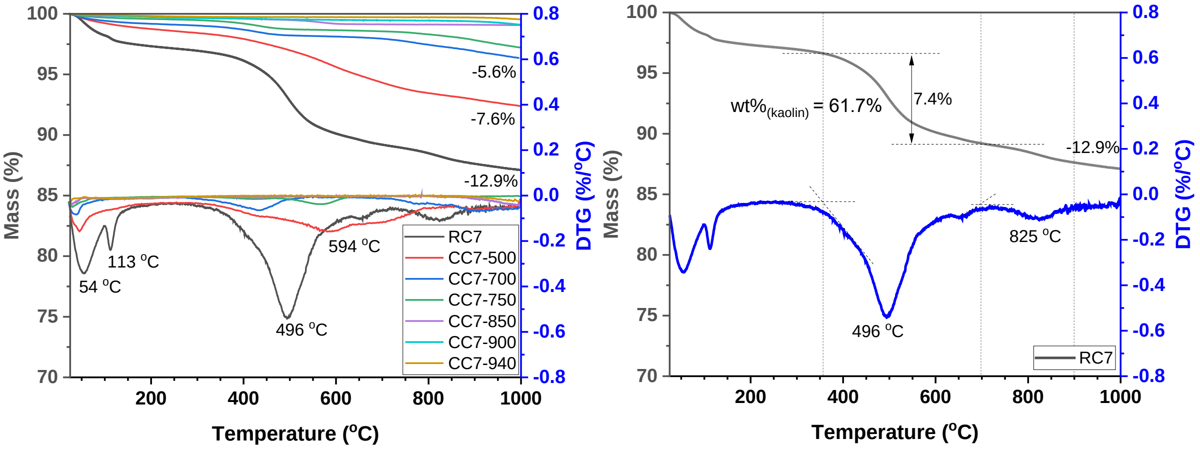

Figure 31 The TG-DTG curves of RC7 before and after calcination at different temperatures.

The TG -DTG curves (**Figure 31**) of RC7 and calcined RC7 at different temperatures is shown in **Figure 31**, while RC7 shows a total mass loss of around 12.9%. After calcined at 500 °C for 3 hours, there still a mass loss of 7.6%. Until increasing the calcination temperature to 850 °C and above, there is minor mass loss. The mass loss of RC7 is attributed to the dehydration happening before 200 °C, dehydroxylation happened in the range of 300 °C to 700 °C and the decomposition of other clay minerals, i.e., calcite. Based on the dehydroxylation rate, the calculated kaolin content in RC7 is around 61.7%.

3.7.2 XRD analysis

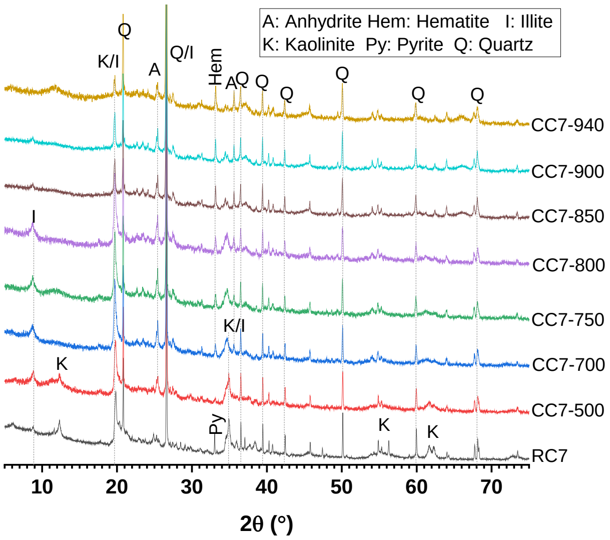

Figure 32 The XRD patterns of RC7 and calcined RC7 at different temperatures.

As shown in **Figure 32**, there is small peak at around 12° 2θ which could be assigned to the crystalline kaolinite. But the intensity of this peak is not strong like RC2 and

RC3. This is because that the crystalline structure of kaolinite in RC7 is poor. The pyrite in RC7 could be the reason for its reddish color after calcination.

3.7.3 FTIR analysis

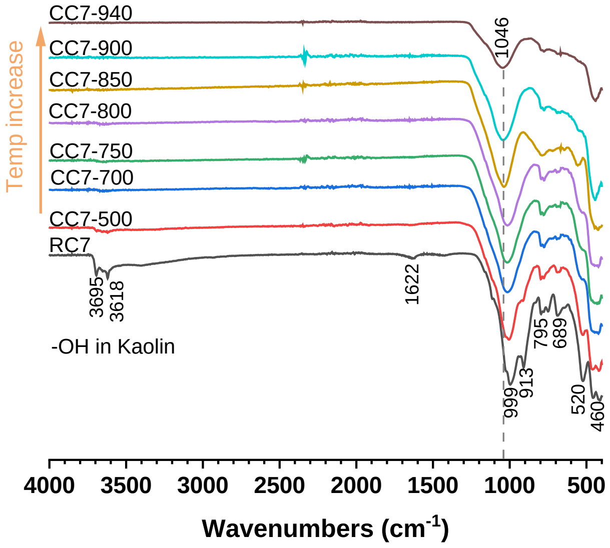

Figure 33 The FTIR patterns of RC7 and calcined RC7 at different temperatures.

The FTIR patterns (**Figure 33**) of RC7 and calcined RC7 is shown in **Figure 33**. The raw clay RC7 shows a group of peaks located at 3695 and 3618 cm^{-1}, which could be assigned to the stretching vibrations of hydroxyl (-OH) groups in kaolinite. A small hump at 1622 cm^{-1} is due to the stretching vibration of C-O bonds in carbonates. The peaks at 913 and 689 cm^{-1} are due to the Al-OH bending vibration. After calcined at 500 °C for 3 hours, the peak intensity reduces. This means that RC7 could not be fully dehydroxylated. Increasing the calcination temperature to 700 °C, the stretching vibration bands of hydroxyl (-OH) groups and bending vibration bands of Al-OH were both disappeared. This indicates the kaolinite in RC7 was fully activated.

3.7.4 Pozzolanic reactivity analysis

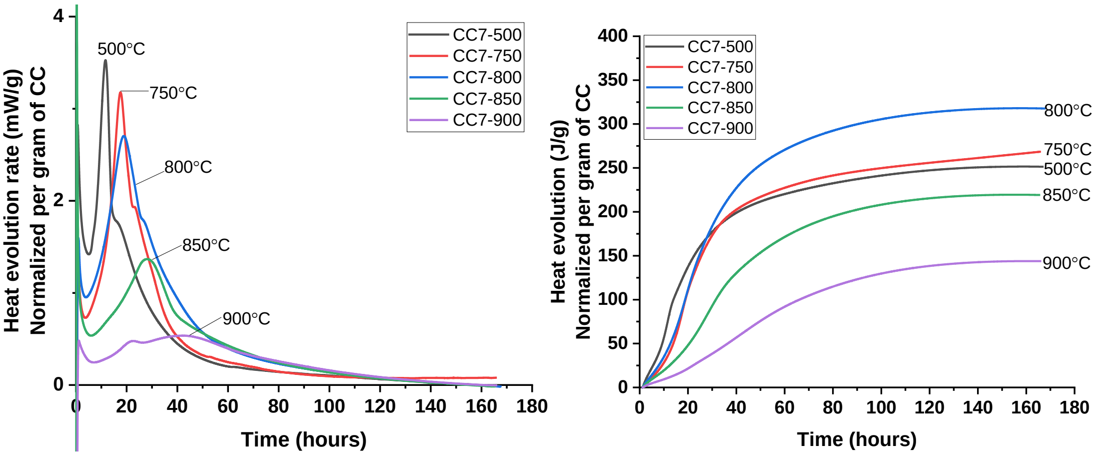

Figure 34 The heat evolution rate (left) and cumulative released heat (right) of calcined RC7 at different temperatures.

As shown in **Figure 34**, the pozzolanic reactivity of calcined RC7 increases with the calcination temperatures from 500 °C to 800 °C, and the CC7-800 shows the highest cumulative heat and pozzolanic reactivity. When the calcination temperature increases to 850 °C and 900 °C, the pozzolanic reactivity of calcined RC7 decreases. The decreased cumulative heat and pozzolanic reactivity might attributed to the recrystallization of amorphous kaolinite.

3.8 RC8 (Tarmac)

3.8.1 TG/DTG analysis

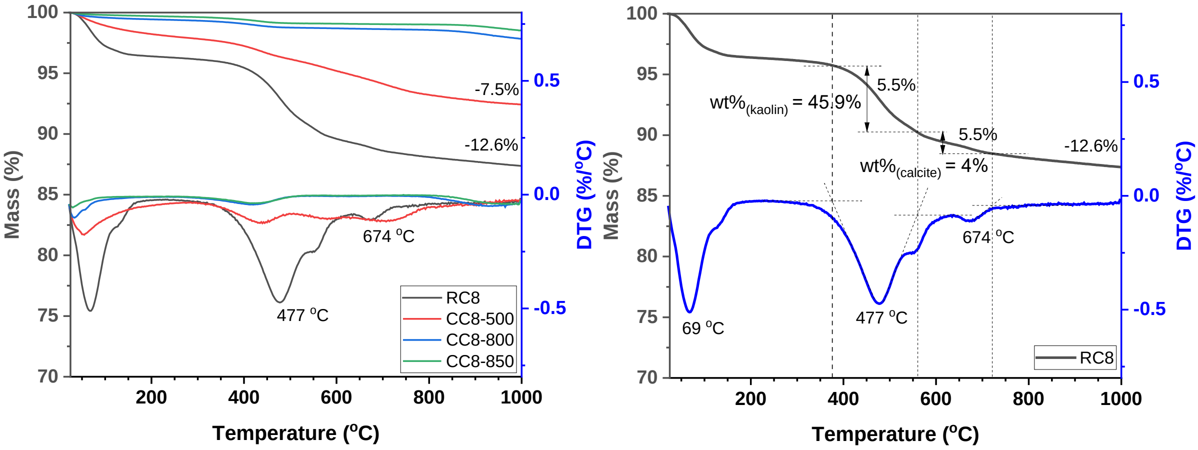

Figure 35 The TG-DTG curves of RC8 before and after calcination at different temperatures.

As shown in **Figure 35**, the mass loss of RC8 is around 12.6%. And there are two main peaks in the DTG curve of RC8. The first small peak is located at around 477 °C and the second peak is located at around 674 °C. According to the Tangent method, the kaolinite content based on the first peak is around 45.9%, while the calcite content based on the second peak is 4%.

3.8.2 XRD analysis

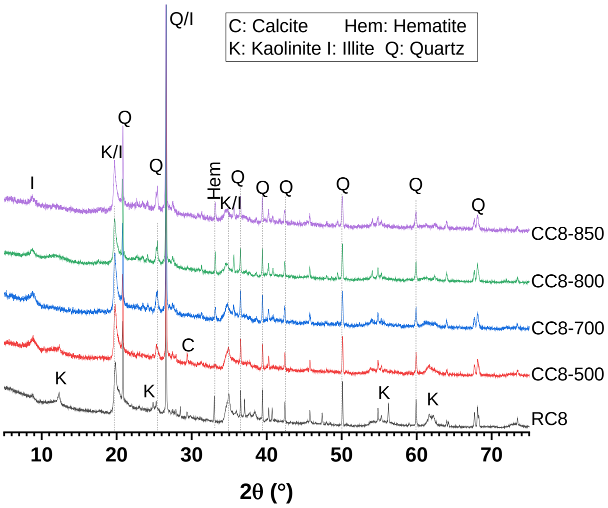

Figure 36 The XRD patterns of RC8 and calcined RC8 at different temperatures.

From the XRD pattern (**Figure 36**) of RC8, we could see that there are fewer crystal peaks of kaolinite (at 12° 2θ) and calcite (at 29° 2θ). After calcined at 700 °C and above, the crystalline peak of kaolinite and calcite could not be detected.

3.8.3 FTIR analysis

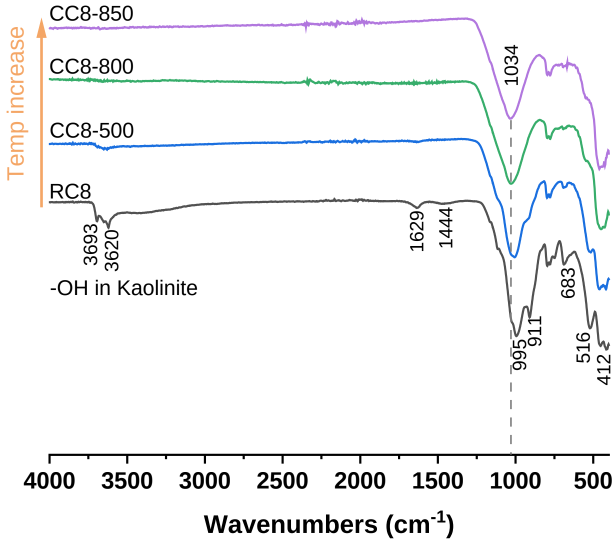

Figure 37 The FTIR patterns of RC8 and calcined RC8 at different temperatures.

From **Figure 37**, the stretching vibrations of hydroxyl (-OH) groups in kaolinite could be detected as a hump is shown at around 3620 cm^{-1}. But the crystal structure of kaolin in the material is too poor to present characteristic peaks. The hump at around 1629 cm^{-1} is due to the C-O stretching vibration in calcite. The calcination caused the shifting of the main peak at 995 cm^{-1} to a higher wavenumber. This is due to the fracture of Si-O-Al bonds.

3.8.4 Pozzolanic reactivity analysis

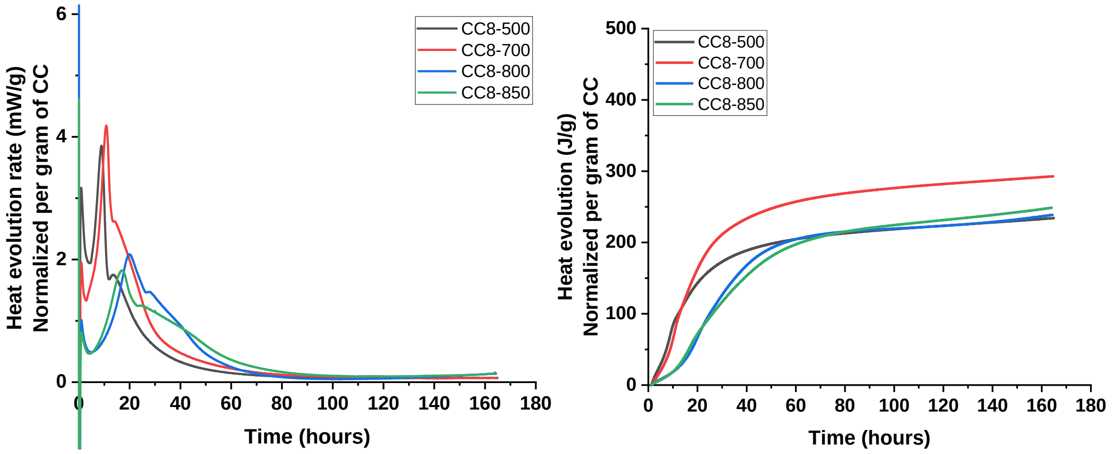

Figure 38 The heat evolution rate (left) and cumulative released heat (right) of calcined RC8 at different temperatures.

From the ICC results (**Figure 38**), it is clear to see that the calcined clays CC8-700 showing the highest cumulative heat value, indicating the highest pozzolanic reactivity. The other three calcined clays show similar pozzolanic reactivity.

3.9 RC9 (Tarmac)

3.9.1 TG/DTG analysis

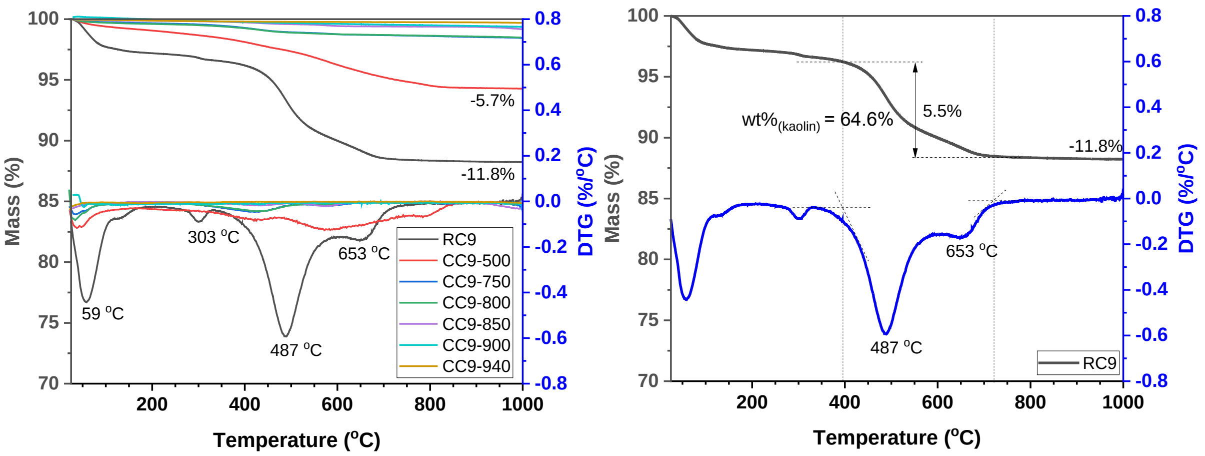

Figure 39 The TG-DTG curves of RC9 before and after calcination at different temperatures.

The RC9 shows a total mass loss of around 11.8% in **Figure 39**. After calcined at 500 °C for 3 hours, there still a mass loss of 5.7%. Until increasing the calcination temperature to 850 °C and above, there is minor mass loss. The mass loss of RC9 is attributed to the dehydration happening before 200 °C, dehydroxylation happened in the range of 300 °C to 700 °C and the decomposition of other clay minerals, i.e., calcite.

There is one peak in the DTG curve of RC9, which could be due to the dehydroxylation of kaolinite and decomposition of calcite. If we assign it to the dehydroxylation, the calculated kaolin content in RC9 is around 64.6%.

3.9.2 XRD analysis

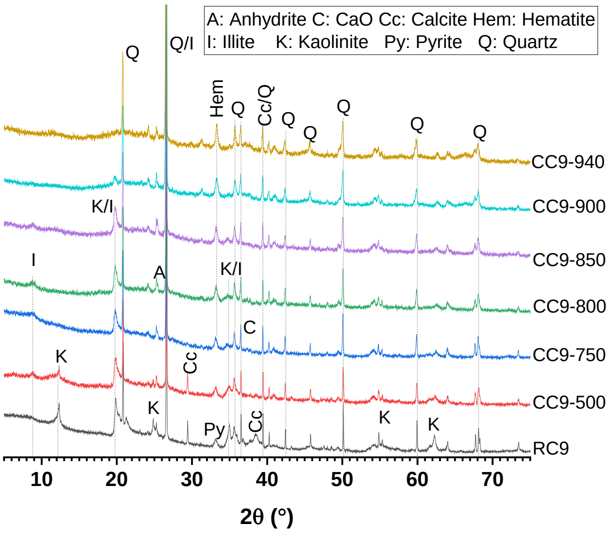

Figure 40 The XRD patterns of RC9 and calcined RC9 at different temperatures.

From the XRD pattern of RC9 (**Figure 40**), it is clear to see the crystalline peaks of kaolinite (at 12° 2θ) and calcite (at 29° 2θ). After calcined at 750 °C and above, the crystalline peak of kaolinite and calcite could not be detected. The pyrite in RC9 could be the reason for its reddish color after calcination.

3.9.3 FTIR analysis

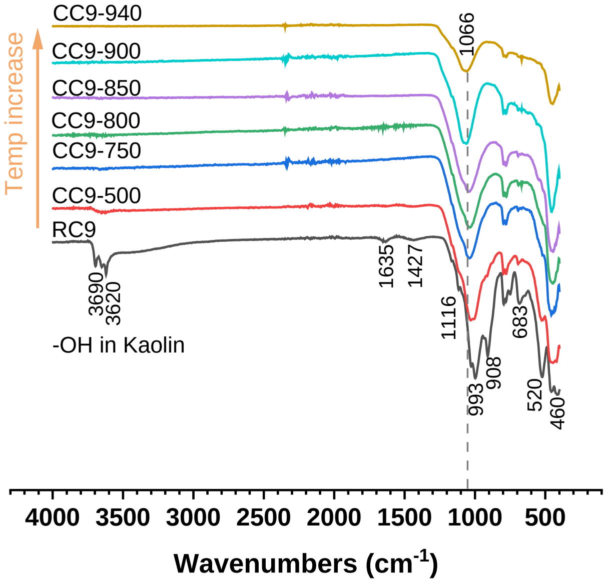

Figure 41 The FTIR patterns of RC9 and calcined RC9 at different temperatures.

As shown in **Figure 41**, the raw clay RC9 shows a group of peaks located at 3690 and 3620 cm^{-1}, which could be assigned to the stretching vibrations of hydroxyl (-OH) groups in kaolinite. The small humps at 1635 and 1427 cm^{-1} are due to the stretching vibration of C-O bonds in carbonates. After calcined at 500 °C for 3 hours, the intensity of peaks at 908 and 683 cm^{-1} attributed to Al-OH bending vibration reduced but could be also detected. This means that RC9 could not be fully dehydroxylated after calcination at 500 °C for 3 hours. Increasing the calcination temperature to 800 °C, the stretching vibration bands of hydroxyl (-OH) groups and bending vibration bands of Al-OH were both disappeared. This indicates the kaolinite in RC9 was fully activated.

3.9.4 Pozzolanic reactivity analysis

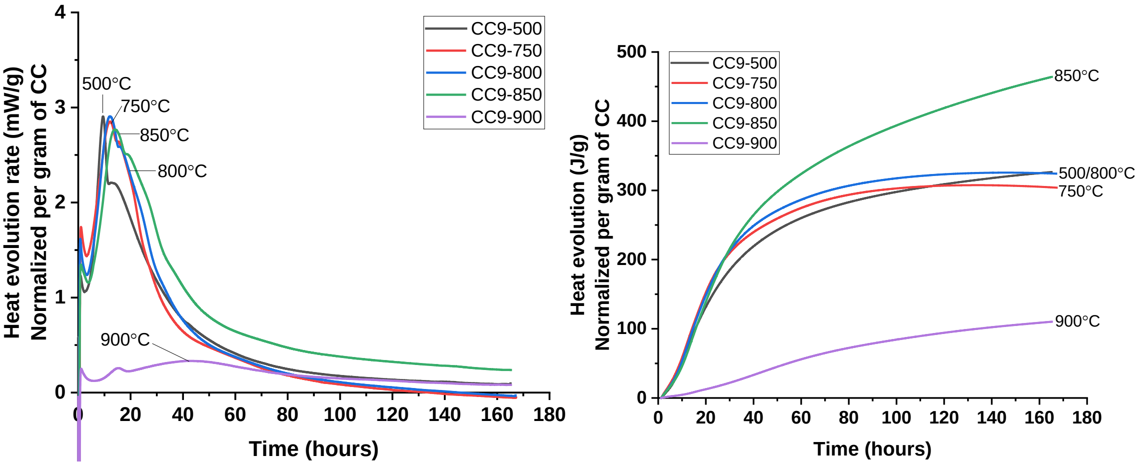

Figure 42 The heat evolution rate (left) and cumulative released heat (right) of calcined RC9 at different temperatures.

As shown in **Figure 42**, the pozzolanic reactivity of calcined RC9 increases with the calcination temperatures from 500 °C to 850 °C, and the CC9-850 shows the highest cumulative heat and pozzolanic reactivity. When the calcination temperature increases to 900 °C, the pozzolanic reactivity decreases. The decreased cumulative heat and pozzolanic reactivity might attributed to the recrystallization of amorphous kaolinite.

3.10 RC10 (Clay aggregate industry)

3.10.1 TG/DTG analysis

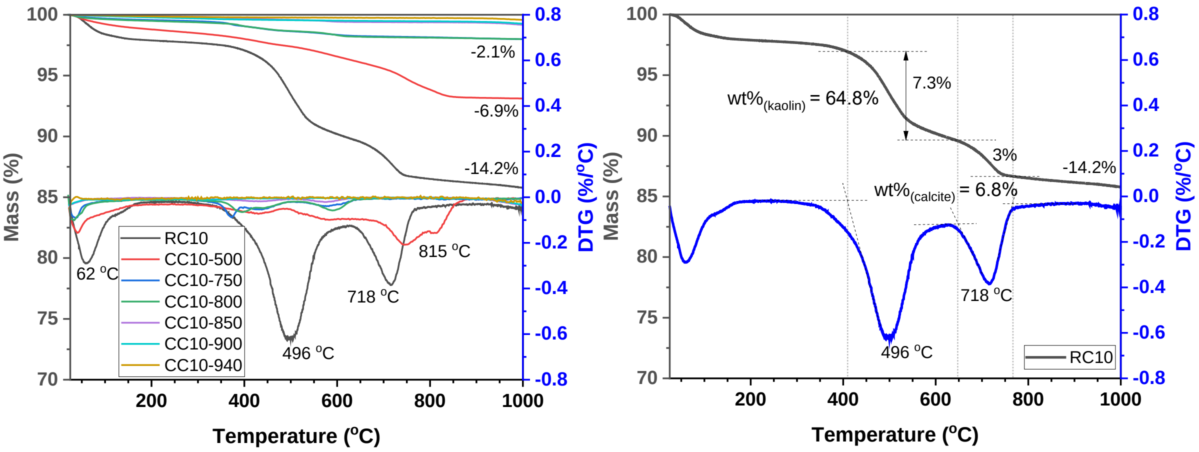

Figure 43 The TG-DTG curves of RC10 before and after calcination at different temperatures.

As shown in **Figure 43**, the mass loss of RC10 is around 14.2%. And there are two main peaks in the DTG curve of RC10. The first peak is located at around 496 °C and the second peak is located at around 718 °C. According to the Tangent method, the kaolinite content based on the first peak is around 64.8%, while the calcite content based on the second peak is 6.8%. After calcined at 750 and 800 °C, the mass loss is 2.1%. The calcination at high temperature destroyed the crystalline structure of kaolinite and calcite.

3.10.2 XRD analysis

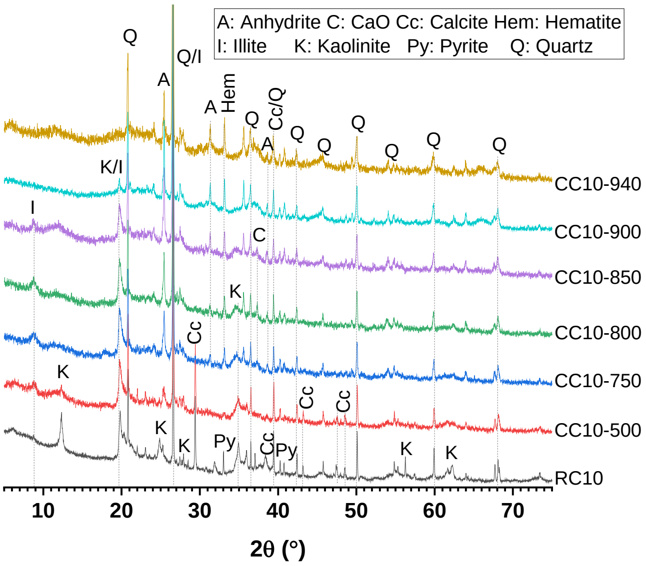

Figure 44 The XRD patterns of RC10 and calcined RC10 at different temperatures.

From the XRD pattern of RC10 (**Figure 44**), we could see that there are crystalline peaks of kaolinite. However, there is a significant peak at 29° 2θ which could be assigned to the crystalline calcite. After calcined at 700 °C and above, the crystalline peak of calcite could not be detected.

3.10.3 FTIR analysis

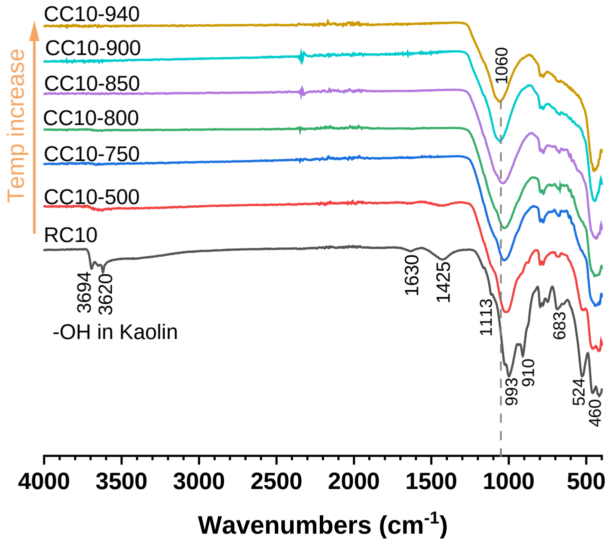

Figure 45 The FTIR patterns of RC10 and calcined RC10 at different temperatures.

As shown in **Figure 45**, the stretching vibrations of hydroxyl (-OH) groups in kaolinite could be detected as the peaks shown at around 3694 and 3620 cm^{-1}. But the crystal structure of kaolin in the material is too poor to present significant characteristic peaks. The humps at around 1630 and 1425 cm^{-1} are due to the C-O stretching vibration in calcite. The calcination caused the shifting of the main peak at 995 cm^{-1} to a higher wavenumber. This is due to the fracture of Si-O-Al bonds. The peaks at 910 and 683 cm^{-1} are due to the Al-OH bending vibration. After calcined at 500 °C for 3 hours, the peak intensity reduces. This means that RC10 could not be fully dehydroxylated at 500 °C. Increasing the calcination temperature to 700 °C, the stretching vibration bands of hydroxyl (-OH) groups and bending vibration bands of Al-OH were both disappeared. This indicates the kaolinite in RC10 was fully activated.

3.10.4 Pozzolanic reactivity analysis

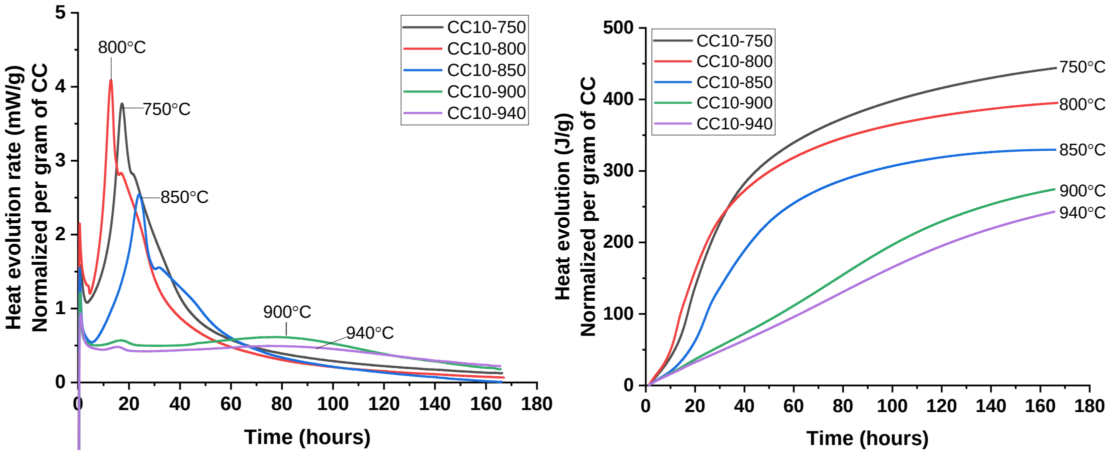

Figure 46 The heat evolution rate (left) and cumulative released heat (right) of calcined RC10 at different temperatures.

From **Figure 46**, the cumulative heat of CC10-750 reaches the highest indicating the highest pozzolanic reactivity among calcined clay. With the calcination temperatures increases from 750 °C to 940 °C, the calcined clays show gradually decreasing pozzolanic reactivity. The decreased cumulative heat and pozzolanic reactivity might attributed to the recrystallization of amorphous kaolinite.

4. Conclusions

The following conclusions could be drawn from the above results and discussion.

(1) The kaolinite content of nine clays (excluding RC5) can be sorted as RC4 > RC3 > RC10 > RC9 > RC2 > RC7 > RC8 > RC6 > RC1 (as shown in Table 4). However, there are more OH groups in the kaolinite than the other clay minerals. However, the tested UK clays are not pure with different proportions of companion minerals such as quartz and carbonates. Therefore, the kaolinite contents in raw clays calculated based on TG-DTG results could only for general comparison, not precise.

Table 4 Calculated kaolinite content in each raw clay based on the TG-DTG results.

Clay ID	Kaolinite content (wt.%) based on the TG-DTG results
RC1	15
RC2	59.2
RC3	67.5
RC4	75
RC5	n/a
RC6	34.2
RC7	50.4
RC8	45.9
RC9	64.6
RC10	64.8

(2) The pozzolanic reactivity of raw clays are: RC4 > RC3 > RC2 > RC5 > RC9 > RC10 > RC7 > RC8 = RC6 > RC1. The calcined clays at different temperatures show different cumulative heat and pozzolanic reactivity. The pozzolanic reactivity of each clay are the highest cumulative heat value as shown in Table 5.

(3) The optimal calcination temperature for each clay also could be determined by the highest cumulative heat as shown in Table 5. This can provide advice for enterprises to choose the optimal factory calcination temperature. It should be noted that, the activity of calcinated IMERYS clays (RC2, RC3 and RC4) at 800 °C and 850 °C is similar.

Table 5 The highest cumulative heat of each clay at different temperatures.

Clay ID	Temperature (°C) (Highest cumulative heat)	Cumulative heat (J/g)
RC1	850	178.8
RC2	850	538.1
RC3	800=850	574.1
RC4	850	606.1
RC5	850	506.1
RC6	850	290.8
RC7	800	318.0
RC8	700	290.9
RC9	850	460.5
RC10	750	441.5

(4) There is a positive correlation between the kaolinite content and the cumulative heat. To analyse the relationship between the kaolinite content and the cumulative heat, we take the calculated kaolinite content as the x-axis and the maximum heat as y-axis. The result is shown in the **Figure 47**. The data show a liner (y = a+ bx) relationship with R-Square of 0.818.

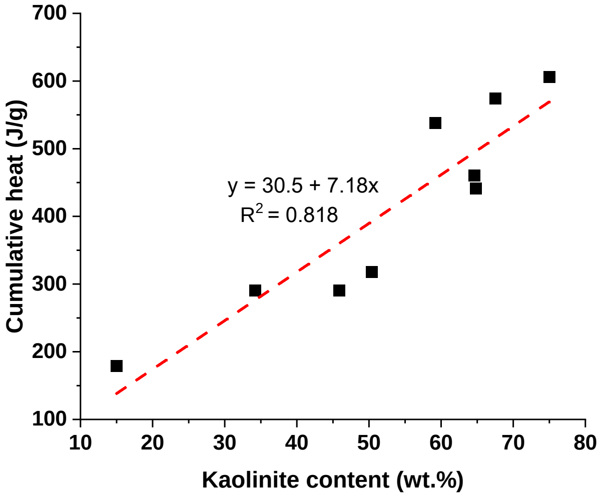

Figure 47 The fitting relationship between the kaolinite content and the cumulative heat.

University College London

Re-C3: Reclaimed Calcined Clay Cements

Appendix 5 -

Calcined clay blended binary and ternary cement study without admixtures

Authors:

UCL:
Yubin Cao
Shi Shi
Tongbo Sui
Yun Bai

November 2022

Contents

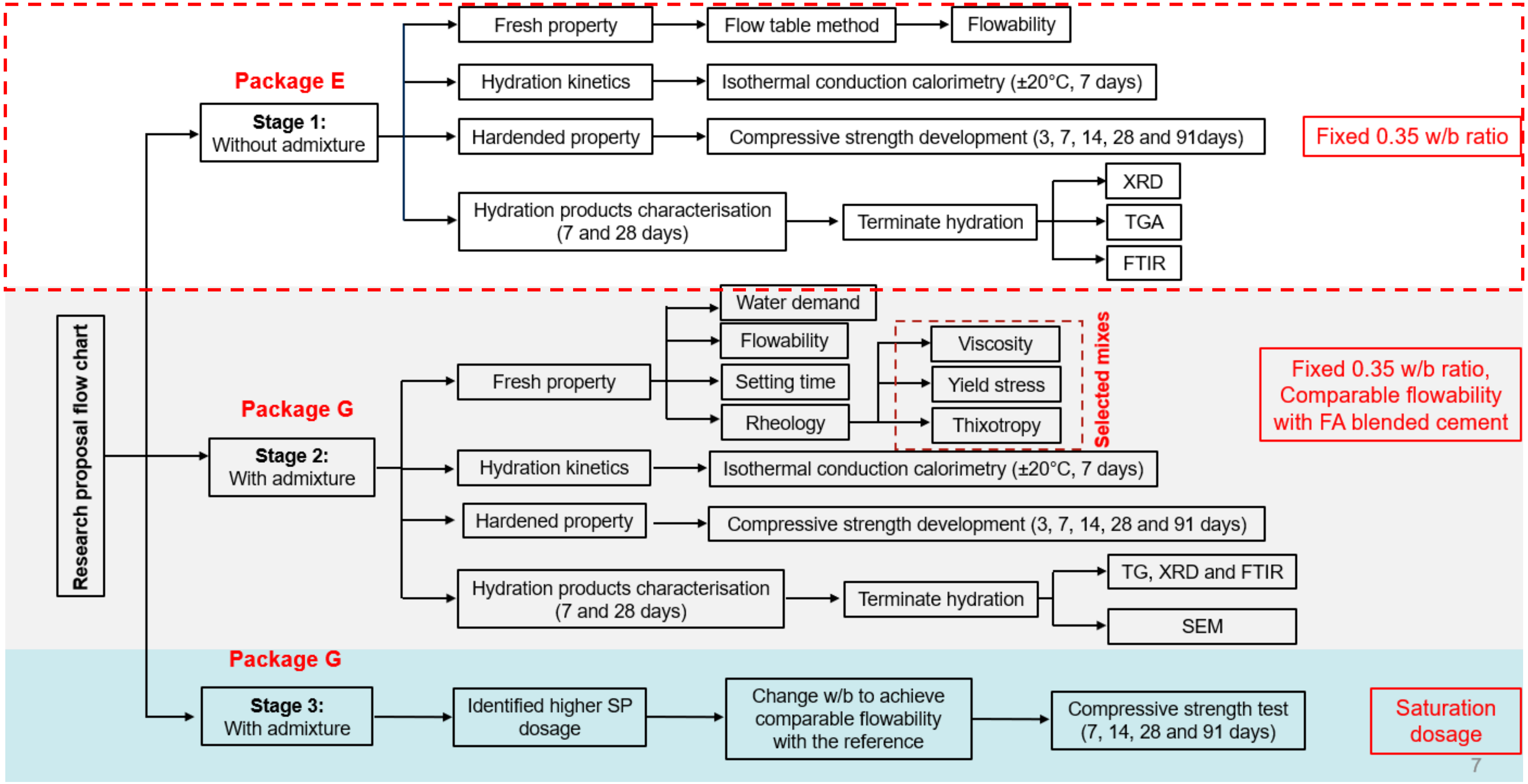

Figure 1 *Flow chart of the work packages.*

1 Action E1: Characterisation of received clays/bricks

1.1 Aim

The aim of Action E1 is to characterise raw clays and calcined clays from different sources to identify the clay minerals and the type of impurities, and thereby providing fundamental information for lab scale calcination of the raw clays.

1.2 Received materials

10 raw clays and two brick powders were supplied by Imerys, Hanson, Tarmac and Forterra, as shown in table 1. Besides brick powder, the received raw clays were firstly grinded and sieved (as shown in figure 2), and then the ground raw clays were characterised by TGA and XRD. Part of the results (TG and FTIR results) are reported in **section report: calcination temperature optimization and pozzolanic reactivity evaluation**. Different raw clays show different colours because of the present of different type and content of iron minerals.

NO.	Samples	Re-C3 ID (Raw Clay/brick powder)	Re-C3 ID (Calcined Clay)
1	LP638	RC2	CC2
2	LP639	RC3	CC3
3	LP640	RC4	CC4
4	LP641	RC5	CC5
5	Hanson Mixed Clay	RC6	CC6
6	Hanson Upper Lias	RC7	CC7
7	Maxey clay sample	RC8	CC8
8	Keele Clay Sample	RC9	CC9
9	Aggregates Industry	RC10	CC10
10	Kings Dyke Grog Brick	KD-BP	-
11	Measham Buff Brick	BU-BP	-

Table 1 *Raw materials and the abbreviations of raw clays, calcined clays and brick powders.*

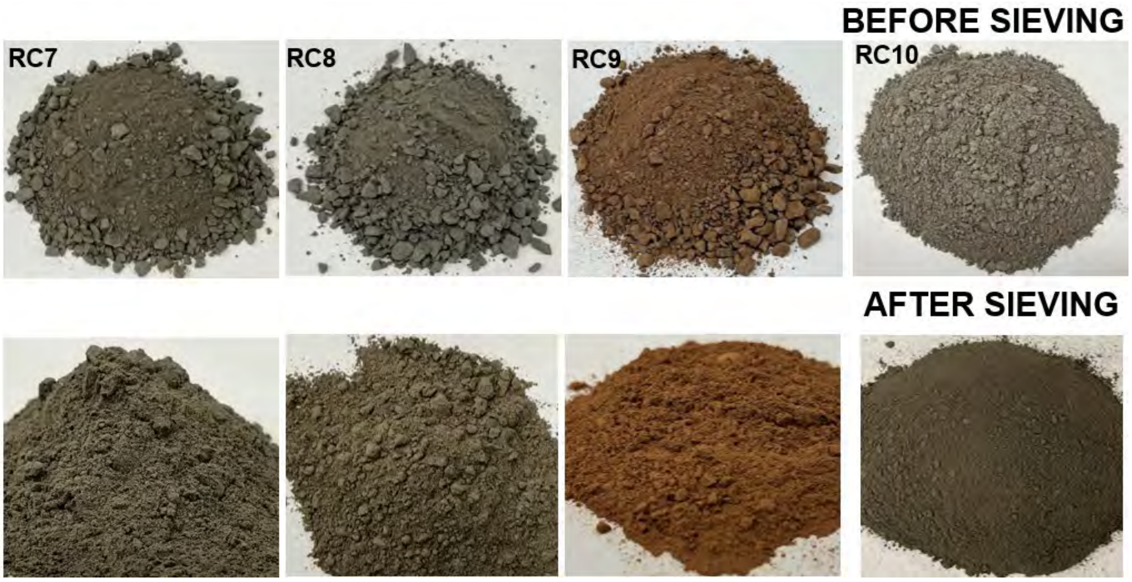

__Figure 2__ photos of Raw clays and ground raw clays.

Figure 2 shows the XRD results of the ground raw clays. The dominant clay mineral in the raw clays is kaolinite, as shown in Figure 3. Besides kaolinite, Illite, muscovite and montmorillonite also can be found from the XRD results. Besides RC2 and RC3, large amounts of impurities can also be detected, including quartz, calcite and Iron oxides. In addition, the clay mineral content was quantitatively analyzed by TG test and this part was reported in **section report: calcination temperature optimization and pozzolanic reactivity evaluation**.

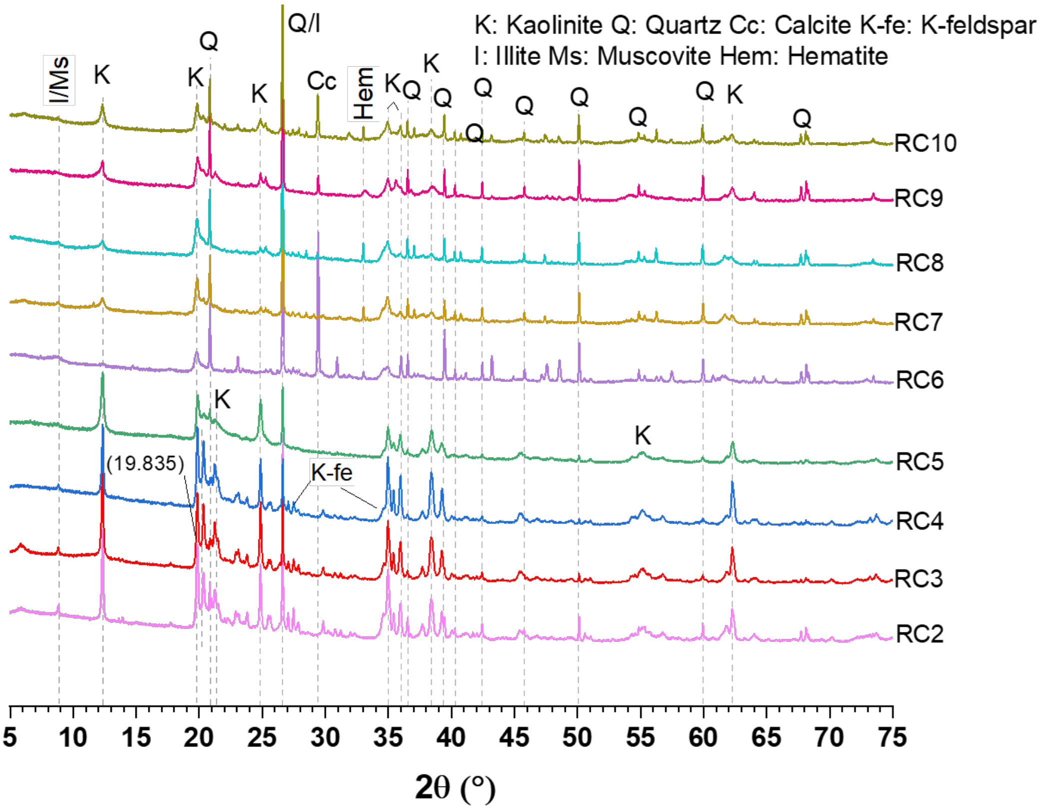

__Figure 3__ XRD results of ground raw clays.

2 Action E2: Reactivity test of calcined clay/brick powders

2.1 Aim

The aim of the Action E2 is to evaluate the pozzolanic reactivity of different grade calcined clays and brick powders provided by Imerys and Forterra.

2.2 Pozzolanic reactivity test

The pozzolanic reactivity results of calcined clays calcined with different temperatures and brick powders are reported in **section report: calcination temperature optimization and pozzolanic reactivity evaluation.**

3 Action E3: Fresh properties and water demand

3.1 Aim

The aim of this action is to investigate the effect of the replacement of calcined clays/brick powders on the fresh properties of calcined clay blended binary and ternary cement pastes, and thereby providing the information for the addition of superplasticiser.

3.2 Materials, mix design and test methods

The materials used in this study including CC2, CC3, CC7, CC9, KD-BP and BU-BP. The cement (Ketton Portland Cement CEM I 52.5N) and CC7 used in this project was supplied by Hanson. The commercial MK, CC2 and CC3 were supplied by Imerys, while the Limestone (LS), CC9, ground granulated blast-furnace slag (GGBS) and siliceous fly ash (FA) were supplied by Tarmac. Forterra provided two types of brick powder, KD and BU-BP.

There are two cement systems, binary and ternary cements. The replacement ratio of calcined clay in both cement systems was 30%, and in ternary cement 15% LS was used to additionally replace cement. To achieve testable flowability, the water to binder ratio used in this study was 0.35.

The preparation of cement paste involves two steps. The first step was to add water to the proportionately prepared powder and mixed at low speed for 90 seconds, followed by a pause. The second step was to remove the paste from the walls and the bottom of the bowl with a rubber scrape during the pause and then mixed at high speed for 90 seconds to get the cement paste. The workability performance was tested by flow table method to determine the flowability of blended cement paste as per GB/T 28627-2012. The water to binder ratio was also adjusted to achieve comparable flowability to determine the water demand properties of calcined clay blended binary and ternary cement pastes.

Group	EN 197 designation	ID	CEM I 52,5 N	Limestone	Calcined clay/Brick powder		GGBS	Fly ash
			%	%	Source	%	%	%
II/B	CEM II/B-Q	1	70	-	CC2	30	-	-
	CEM II/B-Q	2	70	-	CC3	30	-	-
	CEM II/B-Q	4	70	-	CC7	30		
	CEM II/B-Q	6	70	-	CC9	30		
	CEM II/B-Q	8	70	-	Buff-BP	30	-	-
	CEM II/B-Q	9	70	-	KD-BP	30	-	-
II/C	CEM II/C-M (Q-L)	10	55	15	CC2	30	-	-
	CEM II/C-M (Q-L)	11	55	15	CC3	30		
	CEM II/C-M (Q-L)	13	55	15	CC7	30		
	CEM II/C-M (Q-L)	15	55	15	CC9	30	-	-
	CEM II/C-M (Q-L)	17	55	15	BU-BP	30	-	-
	CEM II/C-M (Q-L)	18	55	15	KD-BP	30	-	-
Refs	CEM I 52,5 N	19	100	-	-	-	-	-
	CEM II/A-L	20	85	15	-	-	-	-
	CEM II/B-V	21	70	-	-	-	-	30
	CEM II/B-S	22	70	-	-	-	30	-
	CEM III/A	23	55	15	-	-	30	-
	CEM IV/B(V)	24	55	15	-	-	-	30

Table 2 *Experimental mix design for calcined clay blended binary and ternary cements.*

3.3 fresh properties and water demand

3.3.1 Flowability of cement paste at 0.35 water to binder ratio

The flowability results of calcined clays/brick powders blended binary and ternary cement pastes are shown in Figure 4. In binary cement system, 30% replacement of CEM I by GGBS or fly ash show comparable flow diameter with CEM I. However, besides buff brick powder, the remaining calcined clays or brick powder show lower flowability than the reference (30% fly ash blended binary cement). Among the calcined clays and brick powders, CC3 shows the lowest flowability which is 100 mm. CC2 and CC7 show comparable flow diameter, which are 125 and 123 mm respectively. It should be noticed that calcined clays show lower flow diameter than brick powders, which indicates that calcined clays possess higher water adsorption property. In both binary and ternary systems, the same calcined clay/brick powder blended cements show a comparable workability, which indicates the effect of 15% limestone replacement in ternary cement system shows little effect on the workability. It also can be seen that the flow diameter of 15% limestone blended cement is 165 mm, which is similar with CEM I under the same w/b ratio.

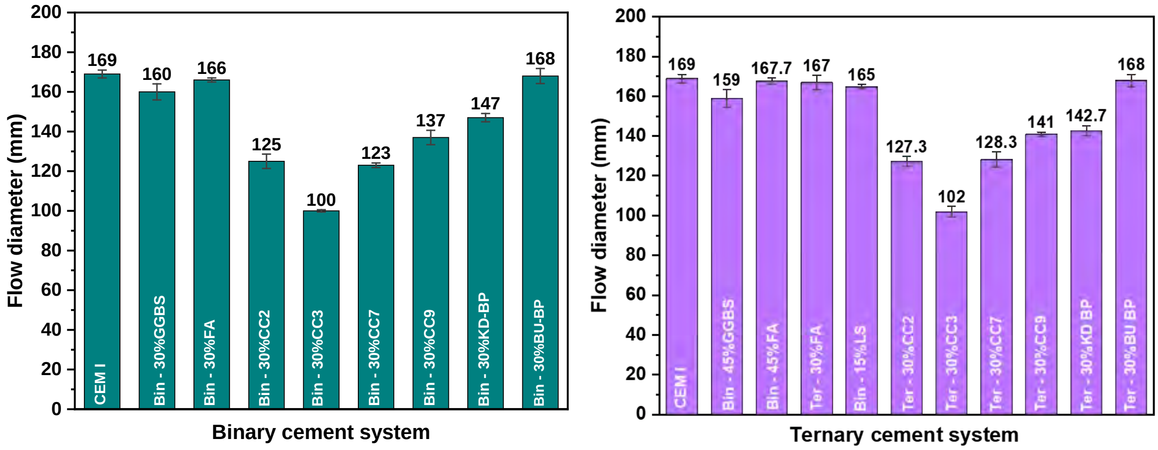

Figure 4 *Flowability of calcined clay blended binary and ternary cement pastes.*

3.3.2 Water demand performance of calcined clay blended binary cement pastes

To achieve comparable flowability with the reference sample (166±10 mm), different water to binder ratios needs to be adjusted for different calcined clay blended binary cement paste, as shown in Figure 5. It shows same trend with the flow diameter results, which CC3 blended cement needs the highest water to binder ratio to achieve comparable workability. Compared with calcined clays, brick powders need lower water to binder ratio.

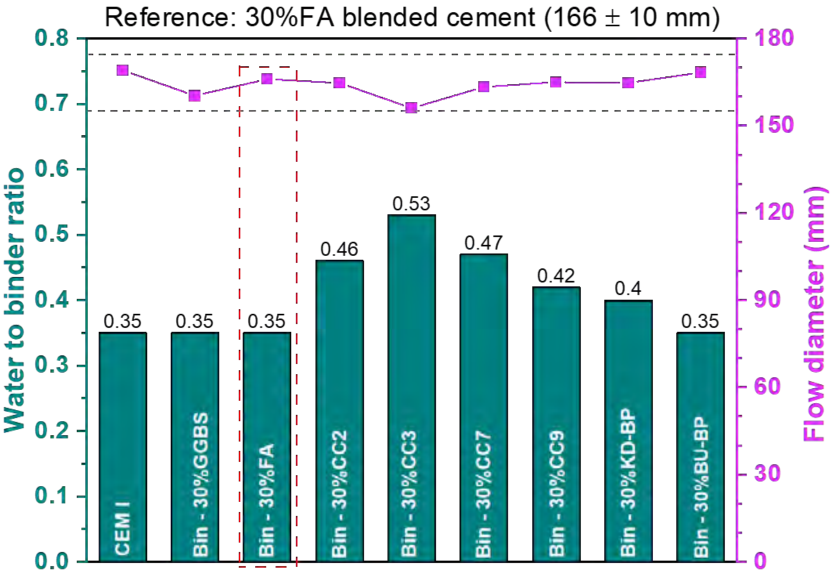

***Figure 5** Water demand performance of calcined clay blended binary cement paste.*

4 Action E4: hydration kinetics, strength development of cement pastes

4.1 Aim

The aim of Action E4 is to investigate the effect of the replacement of CEM I by different grade calcined clays on the hydration kinetics and compressive strength development without adding admixtures.

4.2 Sample preparation and test methods

The heat evolution of different pastes was measured with a TAM Air isothermal calorimeter at 20 °C. Before adding water, the dry powders were homogenised for one minute in a zip bags. After adding the water (0.35 w/b) and mixing the paste manually for two minutes, 10 g of the paste was poured into the ampoule. The duration between the beginning of mixing and the placement of the substance in the calorimeter was five minutes. Distilled water was used as a reference. The heat flow and cumulative heat of the paste were normalised to 1 g of the paste.

The cement pastes (0.35 w/b) were cast into a 25×25×25 mm mould. The moulds were covered with cling film and wrapped in a moist towel during the curing process and samples were demoulded after curing for 24 hours at 20 °C. Then the samples were wrapped with a wet hessian cloth and stored in a sealed bag at 20 °C until the age of test. The compressive strength of samples was tested at 3, 7, 14, and 28 days. Three samples were tested for each age.

4.3 Hydration kinetics and compressive strength

4.3.1 Hydration kinetics

Figure 6 shows the hydration kinetics of the binary cement paste. Figure 6 (a) shows that all blended binary cements reach the acceleration period earlier than CEM I. This may be due to the impurities (quartz or calcium carbonate) provide more nucleation sites for hydration process, which speeds up the hydration of cement. During the acceleration period, the silicate exothermic peaks reduce in all blended cement due to the substitution of CEM I by calcined clays/brick powders. In addition, an aluminate exothermic peak can be clearly observed in the calcined clay or brick powder blended binary cement. This is attributed to be the 1:1 silicon to aluminium ratio in metakaolin providing additional aluminate, which causes the shortage of gypsum in the system. Due to the shortage of sulfate, the peak at around 35 hours which belonging to the conversion of AFt to AFm also disappears, instead of a broad peak from 40 to 70 hours. Due to the delayed conversion of AFt to AFm caused by the lack of sulphate, this peak appears later in all mixes than in CEM I and fly ash blended cement.

Figure 6 (b) shows that the replacement of CEM I by calcined clays/ brick powders significantly reduce the cumulative heat. CC3 blended binary cement paste shows the highest heat release, followed by CC2 and fly ash. CC7 and CC9 blended cement show comparable cumulative heat and lower than that of fly ash. Both KD and BU brick powders show lower cumulative heat than calcined clays, and buff brick powder blended cement paste shows the lowest heat release.

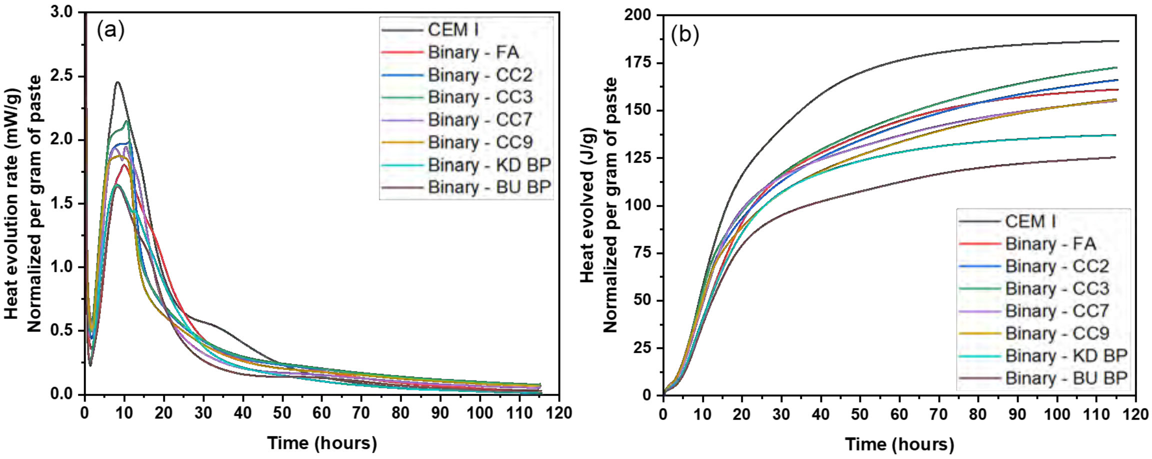

Figure 6 *Hydration kinetics of binary cement paste, (a) heat flow and (b) cumulative heat.*

Figure 7 shows the hydration kinetics of calcined clay/brick powder blended ternary cement pastes. Because of the larger substitution ratio of the cement, the ternary system contains less clinker, which reduces the silicate exothermic peak compared with binary cement and CEM I. Simultaneously, a significant increase in the exothermic peak of the aluminate can also be found between 10-15 hours, which is due to the lack of gypsum. After the aluminate exothermic peak, CC2, CC3, and CC9 blended ternary cements exhibit a quick drop in heat flow curves due to the rapid and intense hydration of the aluminates. These findings are consistent with previous studies. Figure 7 (b) shows the cumulative heat. CC2 and CC3 blended ternary cements show the highest value among the samples. CC9 shows comparable heat with fly ash blended ternary cement. Both KD and buff brick powders also show lower cumulative heat than calcined clays and fly ash, which indicates brick powers possess lower pozzolanic reactivity than calcined clays.

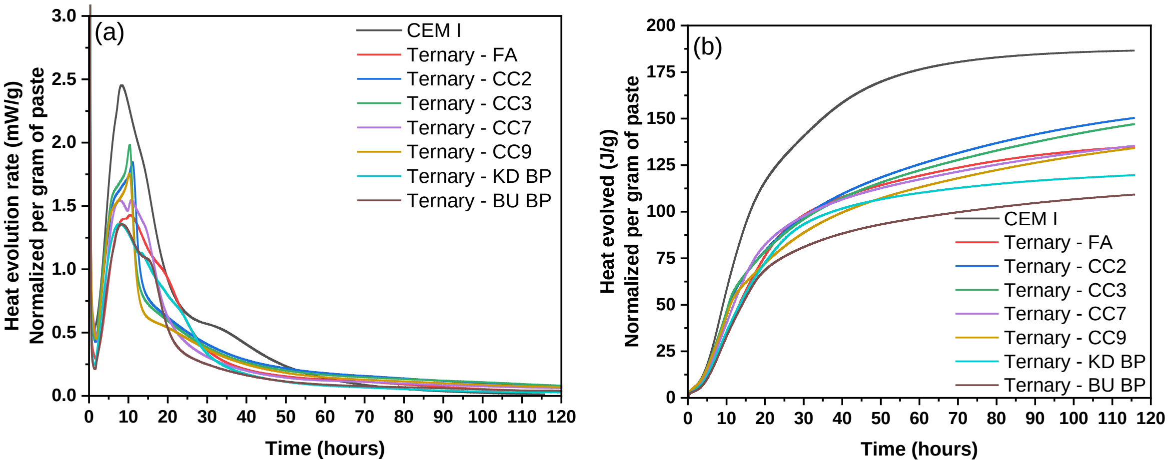

Figure 7 *Hydration kinetics of ternary cement paste, (a) heat flow and (b) cumulative heat.*

4.3.2 Compressive strength development

Figure 8 shows the compressive strength results of blended binary and ternary cement pastes without adding admixtures from 3 to 91 days. As shown in Figure 8 (a), all samples containing calcined clays or brick powders show lower compressive strength than CEM I at 3 days. The lower early age strength is primarily attributable to dilution effects, caused by the addition of SCMs. Besides BU brick powder blended cement, all calcined clays and KD brick powder blended cement show higher strength than that of fly ash blended cement at 7 days. From 7 days to 14 days, calcined clays (CC2, CC3 and CC9) blended binary cements show higher increase rate than the reference and brick powder blended cements. At 28 days, the compressive strength of the samples shows higher than that of the reference. Although the cumulative heat of CC9 is lower than CC2 and CC3, CC9 blended cement shows the highest compressive strength at 28 days, which indicates besides the pozzolanic reactivity, the presence of impurities may also contribute to the compressive strength development. Especially for CC2 and CC9 blended binary cement, they show comparable results with CEM I at 28 days. Overall, all calcined clays or brick powders blended binary cements show better performance than the reference, while the buff brick powder blended cement performs similarly to the reference.

In ternary cement system, the compressive strength of calcined clay/brick powder blended cement pastes is comparable or higher than that of fly ash blended binary/ ternary cement, as shown in Figure 8 (b). However, it is lower than 45% GGBS blended binary cement system and calcined clay/brick powder blended binary cement pastes. Among the calcined clays and brick powders, CC2, CC3, CC7 and CC9 show comparable compressive strength from 3 to 28 days. CC2 blended ternary cement shows the highest compressive strength at 91 days.

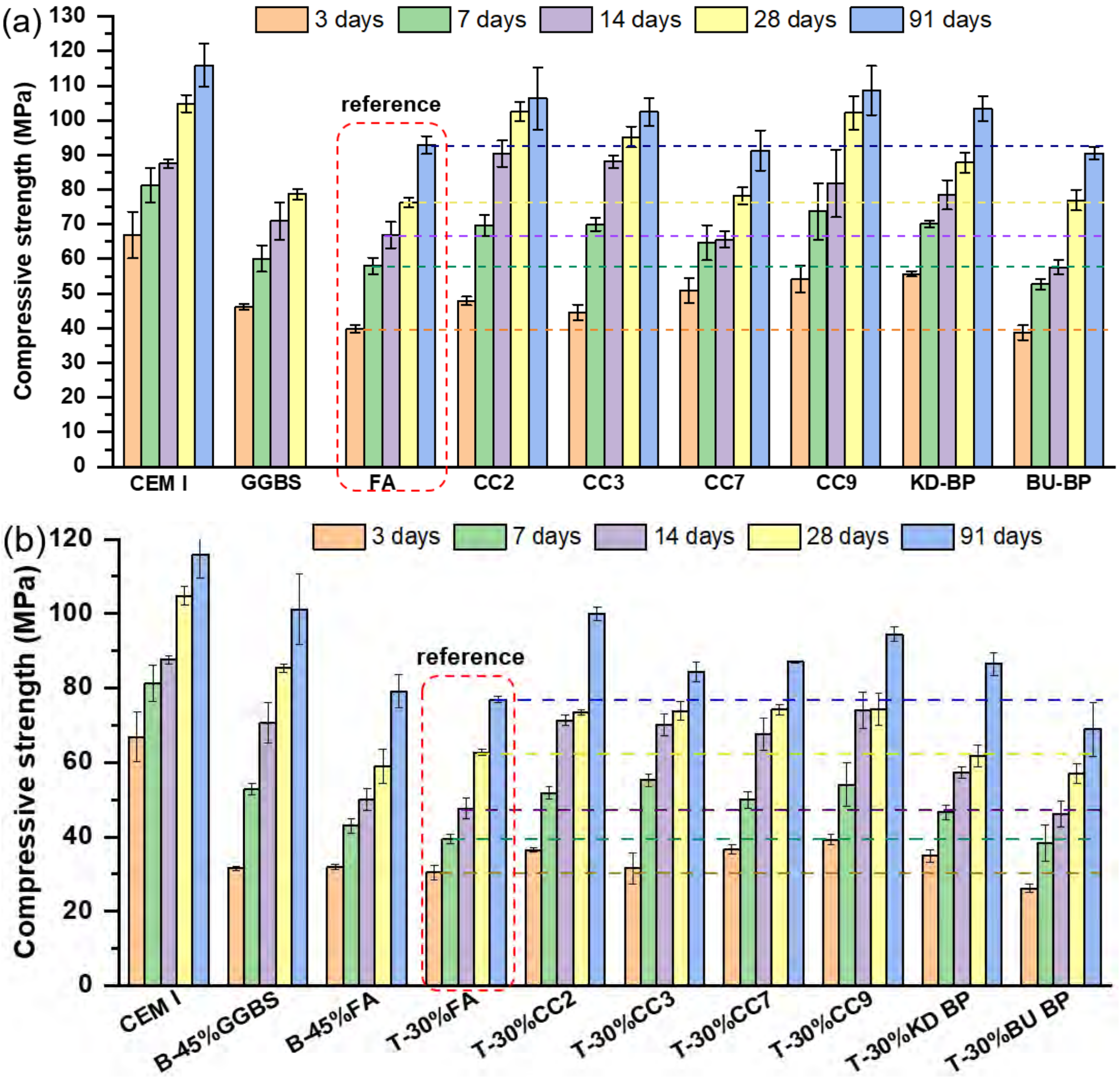

Figure 8 *Compressive strength of binary and ternary cement pastes: (a) binary and (b) ternary.*

5 Action E5: Characterisation of hydration products

5.1 Aim

The aim of this action is to investigate the effect of calcined clays on the hydration products of blended binary/ternary cements, and thereby providing information to help understand the effect of the addition of calcined clays on the Hydration kinetics and compressive strength.

5.2 Powder sample preparation and test methods

Small pieces from the cubic centre were collected after being crushed from the compressive strength test at the age of 7 and 28 days. These small pieces were then immersed in isopropyl alcohol for seven days to terminate the hydration. After seven days, the samples were dried in a vacuum desiccator for three days at ambient temperature. The samples were then ground to powder for hydration products characterisation.

The Stoe STADI-P machine was used for XRD analysis using Cu K1 radiation (Wavelength = 1.54060 Å) applying 40 kV and 30 mA. The sample was measured from 5° to 60° (2θ) with a step size of 0.495° and a counting rate of 10s/step. XRD analysis was utilized to identify crystalline phases in hardened cement paste, including CH, AFm, AFt and calcium carbonate. Bruker ALPHA II FTIR Spectrometers was used for the FTIR test. The instrument was configured for 32 background scans with a resolution of 4 cm-1 from 4000 cm-1 to 400 cm-1. A background scan was performed on the instrument before the powder sample was placed for scanning. Thermogravimetric analysis (TGA) was conducted using Netzsch, TG209 F1. About 30 mg powder samples were tested at a heating rate of 10°C/min under nitrogen conditions ranging from 25°C to 1000°C. The flow rate of nitrogen is 20 cm^3/min.

5.3 Characterisation of hydration products

5.3.1 XRD analysis

The XRD results of the calcined clays or brick powders blended binary cements at 7 and 28 days are shown in Figure 9. It can be observed that the primary crystal phases of the blended cements are calcite, alite, belite, ettringite and portlandite as well as hemicarboaluminate (Hc) and monocarboaluminate (Mc). Both Hc and Mc show lower crystallinity. As shown in Figure 9 (a), we can clearly detect the existing of Hc and Mc in CC2, CC3 and CC9 blended binary cements at 7 days. Combined with the compressive strength results, these calcined clays and brick powders blended binary cements also show better performance. However, there is no obvious Hc and Mc peaks in GGBS, FA and BU BP blended binary cements. Previous study suggested that the formation of Hc and Mc is contributed to the microstructure improvement and compressive strength development. It is noticed that there is no presence of calcite in the mixture. So, the calcium carbonate for the formation of Hc and Mc comes from CEM I.

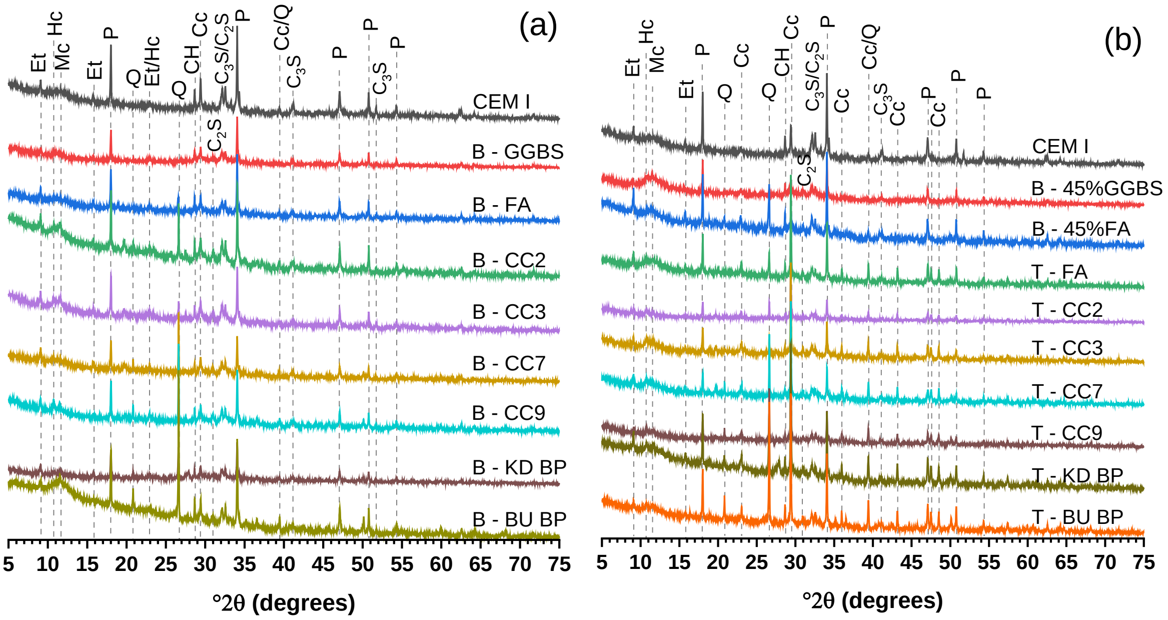

Figure 9 *XRD results of blended binary cement systems at (a) 7 days and (b) 28 days. (Et-ettringite, Hc-hemicarboaluminate, Mc-monocarboaluminate, P-portlandite, Q-quartz, Cc-calcite, C3S-alite, C2S-belite).*

Figure 10 shows the XRD results of calcined clays or brick powders blended ternary cements at 7 and 28 days. Figure 10 demonstrates that ternary cement contains alite, belite, calcite, quartz, and various hydration products, including ettringite, portlandite, Hc, and Mc. Due to the addition of LS in ternary cement systems, the calcite peaks became predominate in the system. LS reacts with the aluminate phase from clinker or calcined clay and generates more AFm phase, resulting in the enhancement of Hc and Mc peaks. At 28 days, clinker components, alite and belite, can still be found, which indicates that clinker hydration still has not finished. The intensity of portlandite in CC2, CC3, CC7, CC9 and KD brick powder show weaker than that in fly ash blended cement, which means calcined clays ad KD brick powder possess higher pozzolanic reactivity than fly ash to consum portlandite to generate more hydration products.

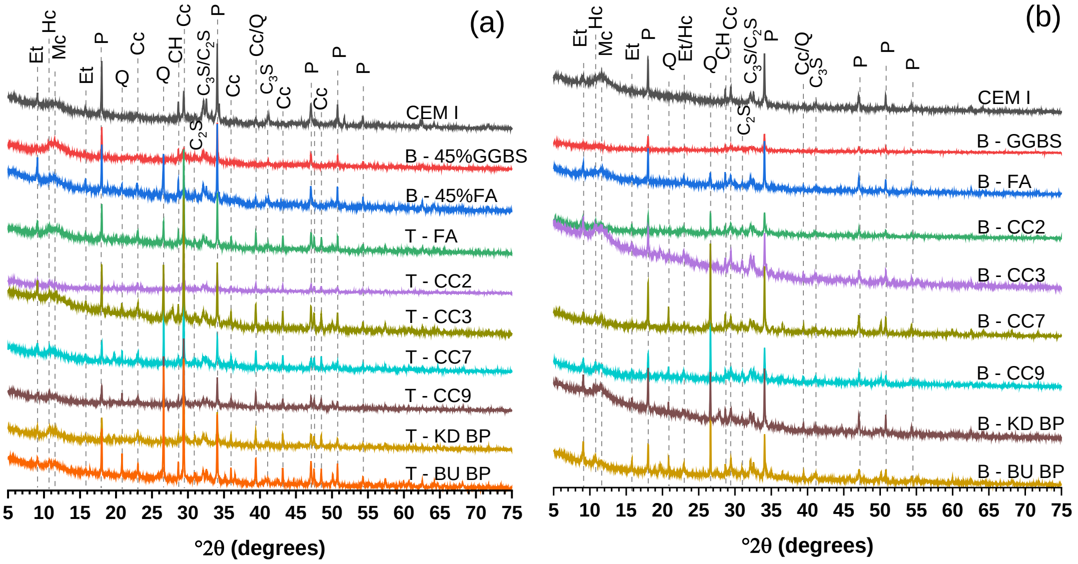

Figure 10 *XRD results of blended ternary cement systems at (a) 7 days and (b) 28 days. (Et-ettringite, Hc-hemicarboaluminate, Mc-monocarboaluminate, P-portlandite, Q-quartz, Cc-calcite, C3S-alite, C2S-belite).*

5.3.2 TG-DTG analysis

Figure 11 shows the TG-DTG results of the hydration products of calcined clays and brick powders blended binary and ternary cements at 28 days of curing. The peaks that occur up to around 100 °C correspond to the dehydration of C(A)SH and AFt. The shoulder peak at about 150 °C is recorded as the dehydration of AFm phases, such as mono-sulphate, Hc and Mc. The second stage is the decomposition of portlandite occurs between 400 to 500 °C. The last peak which occurs between 550 and 900 °C, is the decomposition of calcium carbonates. The presence of carbonates in binary cement is due to the addition of limestone in CEM I.

Compared to the fly ash blended reference sample, the shoulder peaks at 140°C is significantly enhanced in calcined clay/ brick powder blended binary cements, as shown in Figure 11 (a). this may be due to the addition of calcined clay/brick dust providing more reactive aluminate to the cement system, and generate more Hc and Mc, which is consistent with the findings in XRD results. It is also discovered that the peaks corresponding to CH decomposes at around 430 °C. For calcined clay and KD brick powder blended cements are weaker than those of the fly ash reference group, which indicates they possess higher pozzolanic reactivity and generate more hydration products at 28 days. Due to their low reactivity found from ICC results, BU brick powder blended cement consumes less CH than calcined clays.

In ternary cement system, since the CEM I content is only 55%, the dehydration peaks at around 100 °C for C(A)SH and AFt are significantly weaker compared to CEM I, as shown in Figure 11 (d). The dehydration peak corresponding to the AFm phase at around 140 °C is more significance in calcined clay/brick powder blended cements than in the reference group and binary system. Due to the residual LS in the ternary system, the decarbonisation peak at around 550-950 °C is especially significant, consistent with the results in XRD and FTIR.

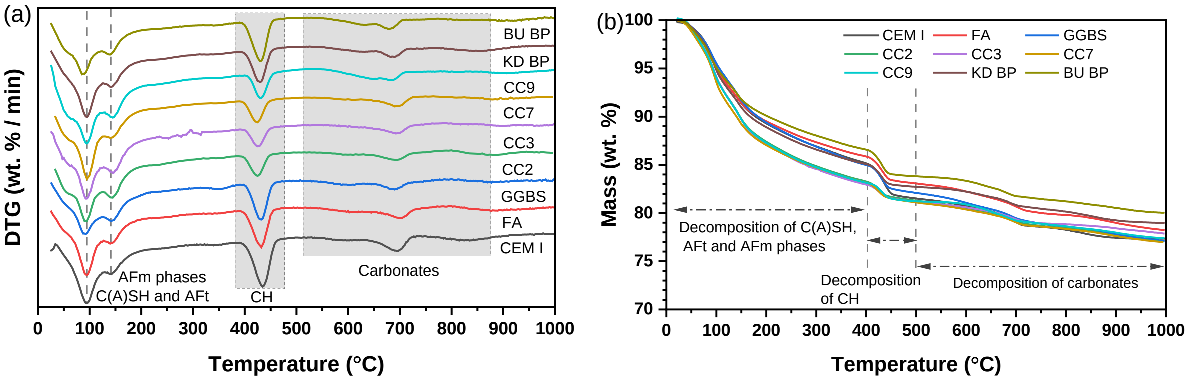

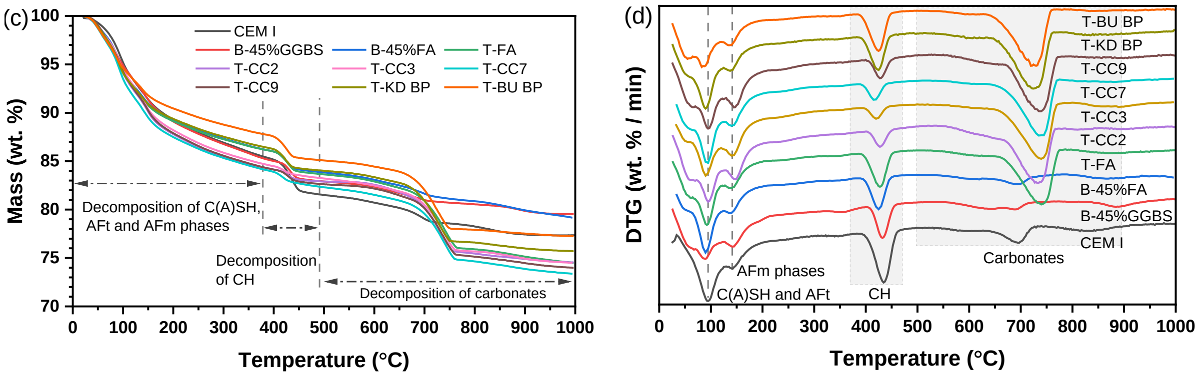

Figure 11 *TG-DTG results of blended cement systems at 28 days (a and b) binary cement, (c and d) ternary cement.*

5.3.3 FTIR analysis

FTIR spectroscopy can identify hydration products by analysing their unique infrared bands. Figures 12 show the FTIR spectroscopy of the binary and ternary system at 28 days. At around 3636 cm^{-1}, an absorption band corresponds to the vibrations of the O-H bond in CH. It can be observed that the calcined clay blended cement does not behave significantly in this absorption band compared to the reference group, which may be due to the reduced CH production and the depletion of CH by pozzolanic reactivity. The O-H bond in water vibrations causes the wide absorption band that emerges at about 3400 cm^{-1}. Even though the samples are dehydrated by soaking in IPA and vacuumed dry, there is still a minor quantity of free water present in the samples. The absorption band at 1413 cm^{-1} corresponds to the asymmetries stretching of the C-O bond. Calcined clays blended cements exhibit a little shift to the right at this absorption band compared to the reference group, which may cause by the calcium carbonate in the cement combining with the aluminium phase to generate Hc and Mc. This also causes the altering the carbon-calcium ratio and lowering the C-O asymmetric stretching vibration, which confirms the presence of Hc and Mc in the XRD results. In addition, an absorption peak at 873 cm-1 indicates an out-of-plane bending vibration of C-O. The absorption in these two C-O bands is due to the presence of LS in CEM I. At 1099 or 1105 cm^{-1}, the absorption peak corresponds to the S-O vibration in SO_4^{2-}. All samples possess a broader S-O absorption band than the reference group. This is presumably due to the reaction between the LS existing in the cement and the extra aluminate phase of the calcined clay, which produces Hc and Mc. This is consistent with the above XRD results. Due to the capacity of Hc and Mc to stabilise ettringite, the S-O absorption band is widened. In addition, there is an absorption peak at 950 cm^{-1}, corresponding to the asymmetric stretching vibration of the Si-O-Si (Al) bond in C(A)SH. This absorption band is displaced to varying degrees in various SCMs mixes due to varying calcium to silicon ratios. This is because the calcium-to-silicon ratio affects the chain length of C(A)SH, particularly the length of the silicon chain, and hence causes a peak shift.

In ternary cement system, two C-O bond absorption peaks (1415 cm^{-1} and 875 cm^{-1}) are identified, and both are more prominent than in the binary system, which is caused by the addition of more LS. There is a shift in the C-O bond absorption band at 1415 cm^{-1} in the binary system, and the shift also presents in the ternary system, which is due to the calcium carbonate reacting with the aluminium phase to produce Hc and Mc, the modification of carbon-calcium ratio influenced the C-O asymmetric stretching vibration. The behaviour of the S-O absorption peak (1099 cm^{-1}) is comparable to that of the binary system.

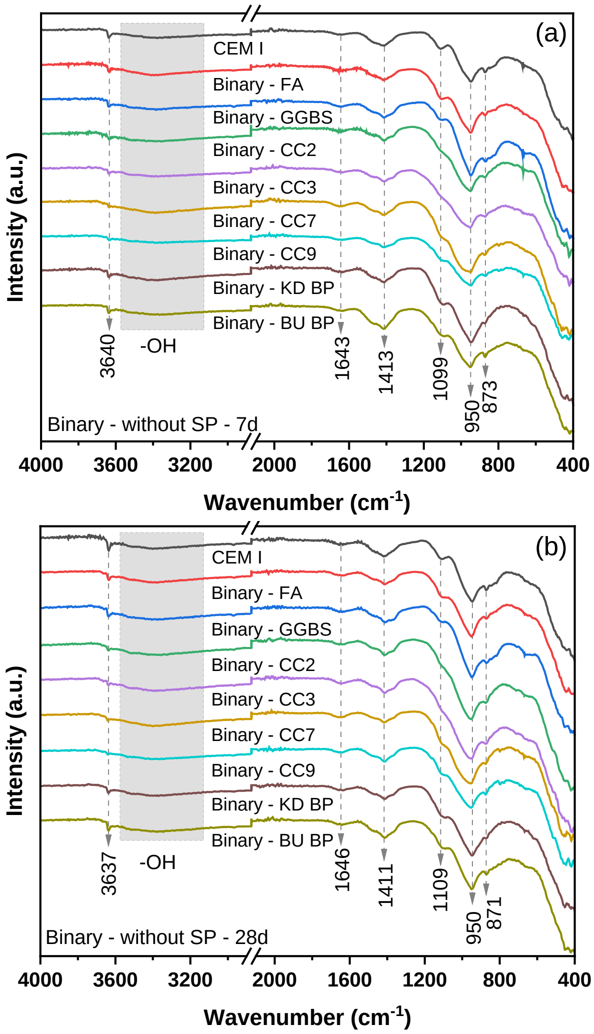

***Figure 12** FTIR results of binary cement at fixed 0.35 w/b ratio (a) 7 days and (b) 28 days.*

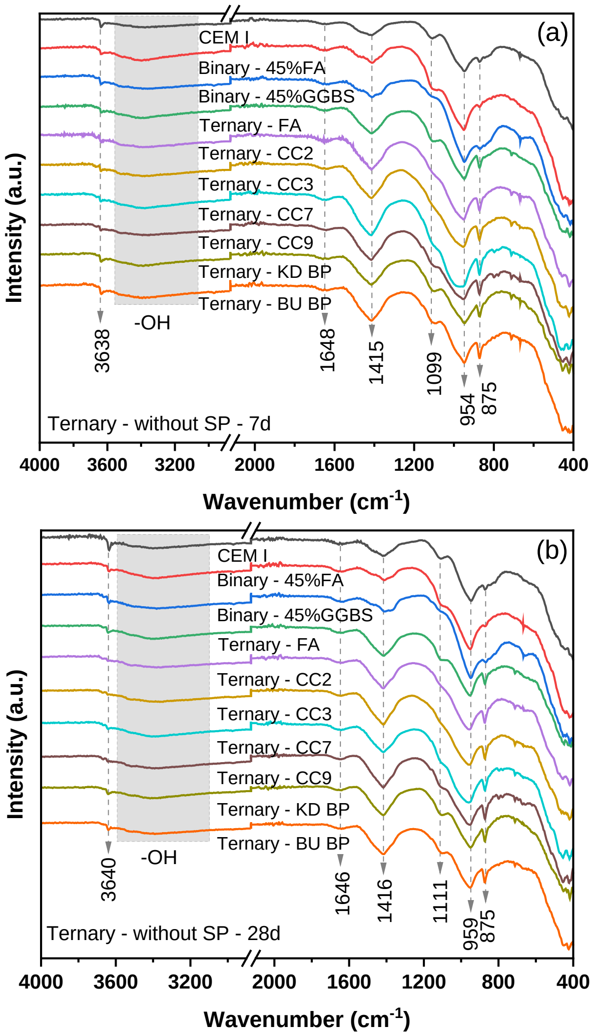

Figure 13 *FTIR results of ternary cement at fixed 0.35 w/b ratio (a) 7 days and (b) 28 days.*

6 Action 6: Conclusions

Work package E investigated the fresh properties, hydration kinetics, compressive strength and hydration products of different calcined clays and brick powders in binary and ternary systems without adding admixtures. The following conclusions could be drawn based on the results.

1. Besides RC2 and RC3, CC7, CC9 and two brick powders contain a proportion of impurities, including calcite, quartz and ferrite.
2. In binary and ternary cement systems, the water demand of calcined clay blended cement is generally higher than that of fly ash blended cement, which significantly reduces the flowability of blended cement paste.
3. In the binary and ternary systems, the compressive strength of calcined clay blended cement in early ages is comparable to that of FA blended cement, but the calcined clay blended cement has better compressive strength than that of FA blended cement after 28 days. The compressive strength of Buff brick powder blended cement is comparable to that of FA blended cement, while KD brick powder blended cement is better than FA blended cement.
4. Based on the XRD patterns, Hc and Mc were detected in both binary and ternary systems. TG and FTIR analysis can help confirm the existence of these hydration products.
5. According to the TG-DTG analysis, the peak with the highest mass loss in the binary system corresponds to the decomposition of CH, while the peak with the highest mass loss in the ternary system corresponds to the decomposition of LS, indicating that there is still a significant amount of LS in the LC3 system which is not involved in the reaction. The chemical and physical effect of LS is insufficient to compensate for the reduced compressive strength resulting from the decreased cement content.
6. This study shows that the use of UK calcined clay and brick powder to replace FA in binary and ternary systems is technically feasible and has great potential. The low-grade clays are more suitable for binary system, while the high-grade clays are more suitable for ternary system.

University College London

Re-C3: Reclaimed Calcined Clay Cements

Appendix 6 -

Calcined clay blended binary and ternary cement study with admixtures

Authors:

UCL:
Yubin Cao
Shi Shi
Tongbo Sui
Yun Bai

November 2022

Contents

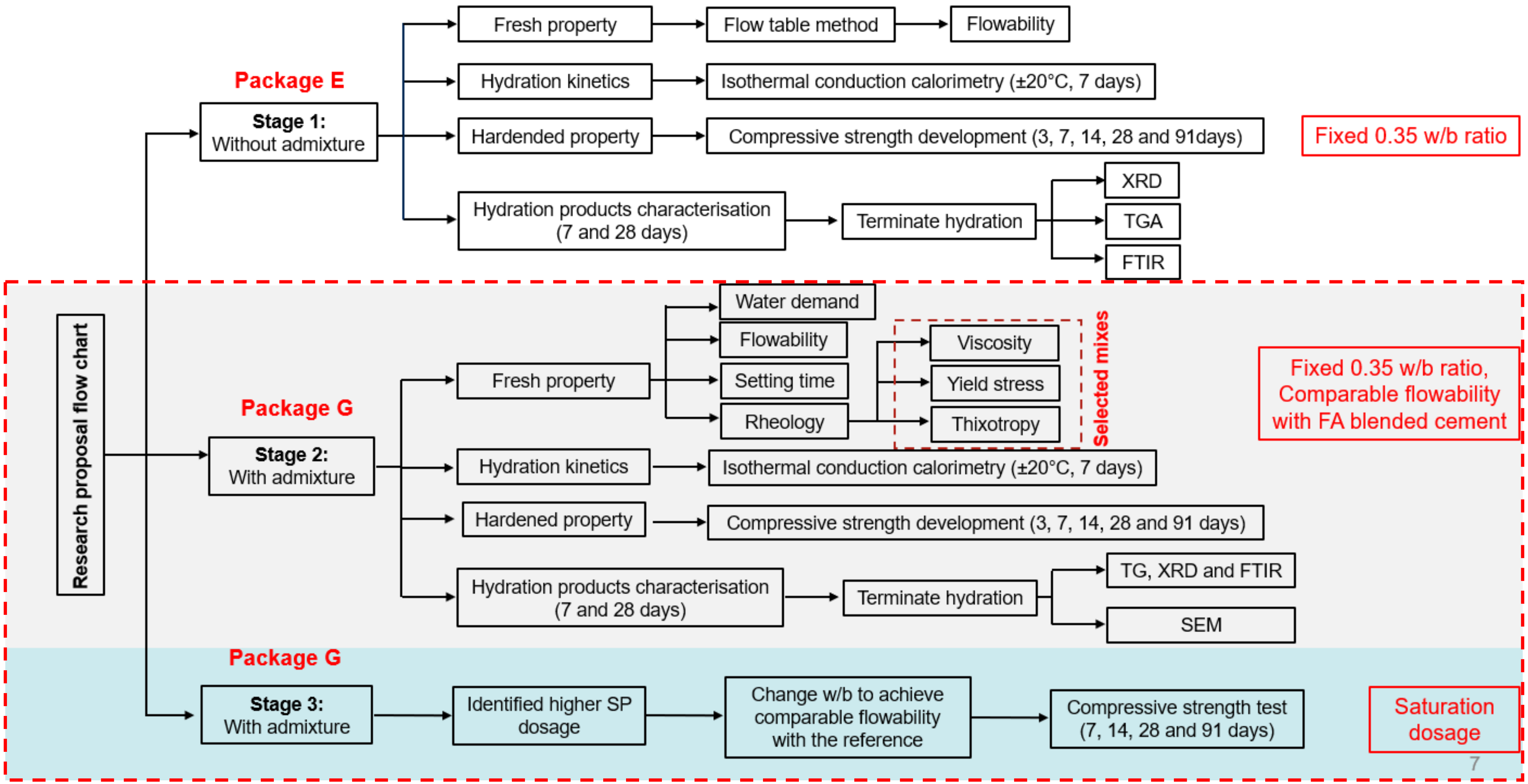

Figure 1 Flow chart of the work packages.

1 Action G1: Fresh properties and rheology of cement pastes + surface charge

1.1 Aim

The aim of Action G1 is to investigate the improvement of the addition of superplasticiser on the fresh properties and rheology of calcined clay blended binary and ternary cements, and thereby providing the guidance for industries to effectively produce calcined clay blended cement products.

1.2 Materials, mix design and test methods

The raw clays and brick powders were supplied by Imerys, Hanson, Tarmac and Forterra, as shown in table 1. The materials used in this study including CC2, CC3, CC7, CC9, KD-BP and BU-BP. The cement (Ketton Portland Cement CEM I 52.5N - PC) and CC7 used in this project was supplied by Hanson. The commercial MK, CC2 and CC3 were supplied by Imerys, while the Limestone (LS), CC9, ground granulated blast-furnace slag (GGBS) and siliceous fly ash (FA) were supplied by Tarmac. Forterra provided two types of brick powder, KD and BU-BP. The superplasticiser used in this section was provided by Sika.

There are two cement systems, binary and ternary cements. The replacement ratio of calcined clay in both cement systems was 30%, and in ternary cement 15% LS was used to additionally replace cement (15%LS, 30%CC and 55%PC). To achieve testable flowability, the water to binder ratio used in this study was 0.35.

The preparation of cement paste involves two steps. The first step was to add 70 % water to the proportioned powder and blend at a low speed for 30 seconds, then added 30 % water with the SP and continued with low speed stirring for 60 seconds before the pause. The second step was to remove the paste from the walls and the bottom of the bowl with a rubber scrape during the pause and then mix at high speed for 90 seconds to get the cement paste. The workability performance was tested by flow table method to determine the flowability of blended cement paste as per GB/T 28627-2012. A Vicat Needle Test (VNT) was used to test the initial setting time (IST) of the blended cement paste with comparable flowability (BS EN 196-3, 2016).

Table 1 *Raw materials and the abbreviations of raw clays, calcined clays and brick powders.*

NO.	Samples	Re-C3 ID (Raw Clay/brick powder)	Re-C3 ID (Calcined Clay)
1	LP638	RC2	CC2
2	LP639	RC3	CC3
3	LP640	RC4	CC4
4	LP641	RC5	CC5
5	Hanson Mixed Clay	RC6	CC6
6	Hanson Upper Lias	RC7	CC7
7	Maxey clay sample	RC8	CC8
8	Keele Clay Sample	RC9	CC9
9	Aggregates Industry	RC10	CC10

10	Kings Dyke Grog Brick	KD-BP	-
11	Measham Buff Brick	BU-BP	-

1.3 Fresh properties and rheology of cement pastes + surface charge

1.3.1 *flowability modification*

As mentioned in Section report E, calcined clay shows higher water demand performance due to the presence of layered structure, clay minerals. Hence, the flowability of calcined clay blended cement paste was adjusted by changing water to binder ratio and adding SP, and the reference group is 30%FA blnded cement paste (±10 mm), as shown in Figure 2. The layered structure of clay mineral increases the specific sureface area (SSA), and thereby significantly increases the water demand to achieve comparable flowability performance. Different calcined clays show diffferent water demand performance, as shown in Figure 2(a). CC3 blended binary cement shows the highest water to binder ratio to achieve comparable flowability. Compared with brick powders, calcined clays show higher water demand performance, which maybe due to higher terperature of brick production (around 1000 °C) changes the morphology of clay mineral and reduces the SSA.

Figure 2(b) shows the results of superplasticiser dosage of calcined clay blended binary and ternary cements with comparable flowability. Different with w/b adjustement, CC7 blended binary and ternary cements show comparable or higher SP dosage, which is around 0.6% of total binder. 15%LS replacement shows little effect on the superplasticier dosage. Overall, it can be seen from the reults that both mentods can effectively modify the flowability of calcined clay blended cements, and the quality of calcined clay shows different water demand and needs different SP dosage to achieve comparable flowability.

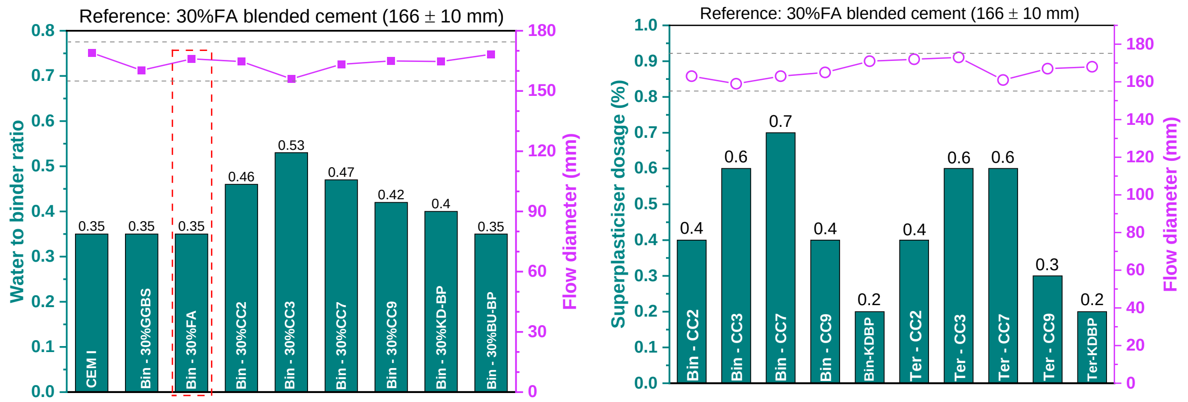

(a) (b)

Figure 2 *Flowability of blended cement after w/b adjustment (a) and SP addition (b).*

1.3.2 *Setting time*

Figure 3 shows the initial setting time of calcined clay blended binary cement with comparable flowability modified by the addition of SP. GGBS blended cement paste shows comparable initial setting time with CEM I. Compared with GGBS, the replacement of PC by calcined clay/brick powder prolongs the initial setting time, which indicates the initial chemical reaction (pozzolanic reactivity) of fly ash/calcined clay/brick powder is weaker than GGBS (pozzolanic reactivity and hydraulic reactivity). And the weaker chemical reaction of calcined clay/brick powder blended cement may attribute to lower strength development at early stage.

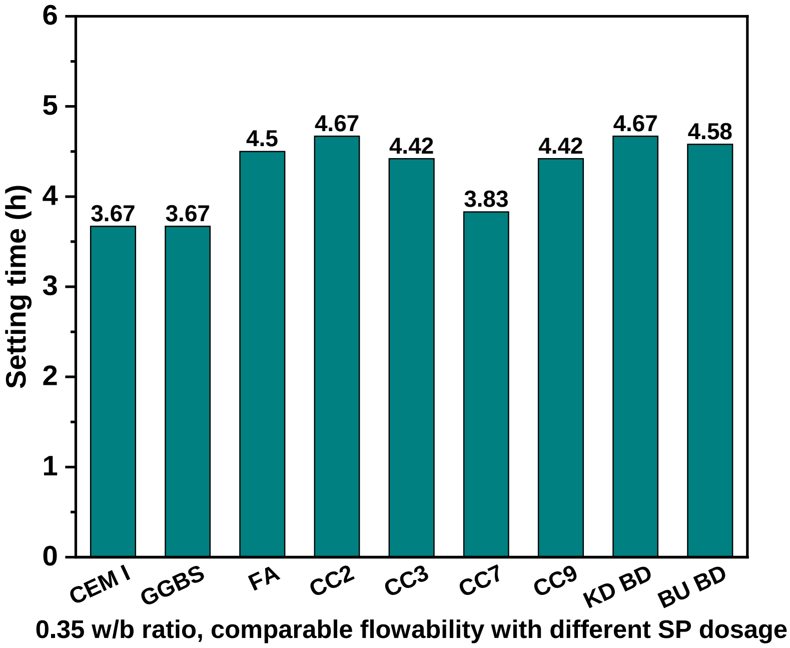

Figure 3 *setting time of calcined clay blended binary cements with comparable flowability.*

1.3.3 Rheology of cement pastes + surface charge

For fresh properties of cement paste, besides flowability and setting time, the rheological properties and surface charge (zeta potential) are also included. These results will be presented in **Section report: characterisation and performance of flash and rotary calcined clays**.

2 Action G2: Hydration kinetics, strength development of cement pastes

2.1 Aim

The aim of the Action G2 is to evaluate the effect of SP addition on hydration kinetics and strength development of calcined clay/brick powder blended binary and ternary cements.

2.2 Sample preparation and test methods

The heat evolution of different pastes was measured with a TAM Air isothermal calorimeter at 20 °C. Before adding water, the dry powders were homogenised for one minute in a zip bags. After adding the water (0.35 w/b) and mixing the paste manually for two minutes, 10 g of the paste was poured into the ampoule. The duration between the beginning of mixing and the placement of the substance in the calorimeter was five minutes. Distilled water was used as a reference. The heat flow and cumulative heat of the paste were normalised to 1 g of the paste.

The cement pastes (0.35 w/b) were cast into a 25×25×25 mm mould. The moulds were covered with cling film and wrapped in a moist towel during the curing process and samples were demoulded after curing for 24 hours at 20 °C. Then the samples were wrapped with a wet hessian cloth and stored in a sealed bag at 20 °C until the age of test. The compressive strength of samples was tested at 3, 7, 14, 28 and 91 days. Three samples were tested for each age.

2.3 Hydration kinetics

Figures 4 and 5 show the heat evolution and cumulative heat of calcined clay/brick powder blended cements with comparable workability adjusted by the addition of SP. Figures 4 and 5 (a) demonstrates that the addition of SP extends the induction period of calcined clay/brick powder blended cement paste than that of without adding SP, which is consistent with the findings of previous studies (Avet and Scrivener, 2018). As the initial setting time (IST) is often believed to mark the beginning of the acceleration period, the binary and ternary systems have a longer IST than the CEM I, which is consistent with the setting time results. In addition, the presence of SP significantly reduces the exothermic peak of the aluminate since the SP retards the hydration of the cement.

The cumulative heat release of the mixture can be seen in Figures 4 and 5 (b). Under comparable flowability, ternary cement shows lower cumulative heat than binary cement. Compared with the cumulative heat without SP addition, although the addition of SP reduces the heat release at early stage due to its dispersion effect, it shows little effect on the long-term heat release (at 110 hours). Combined the results of heat evolution and cumulative heat, it can be concluded that the addition of SP will slow down the early-stage reaction, but it will not influence the long-term chemical reaction.

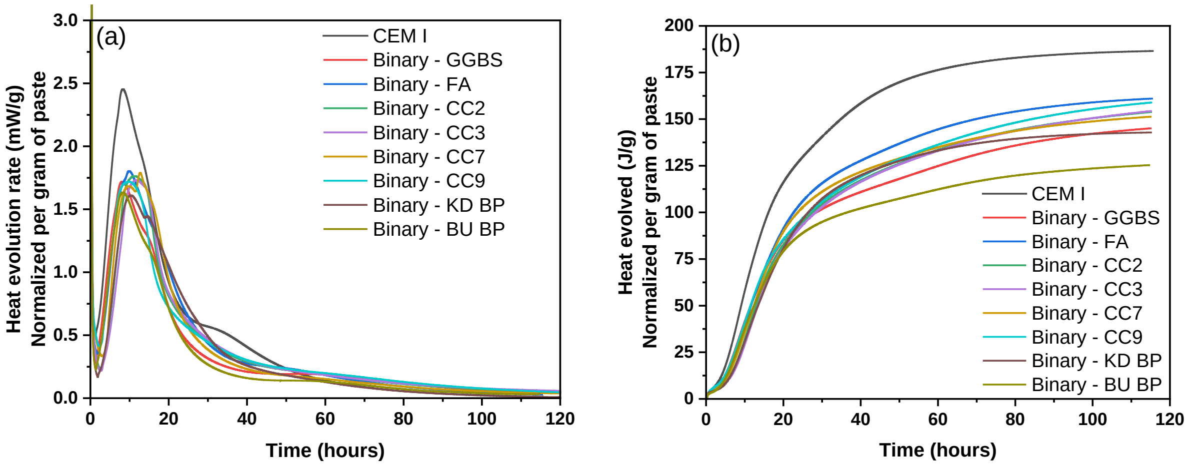

Figure 4 *Hydration kinetics of binary cement at fixed 0.35 w/b ratio with the addition of SP.*

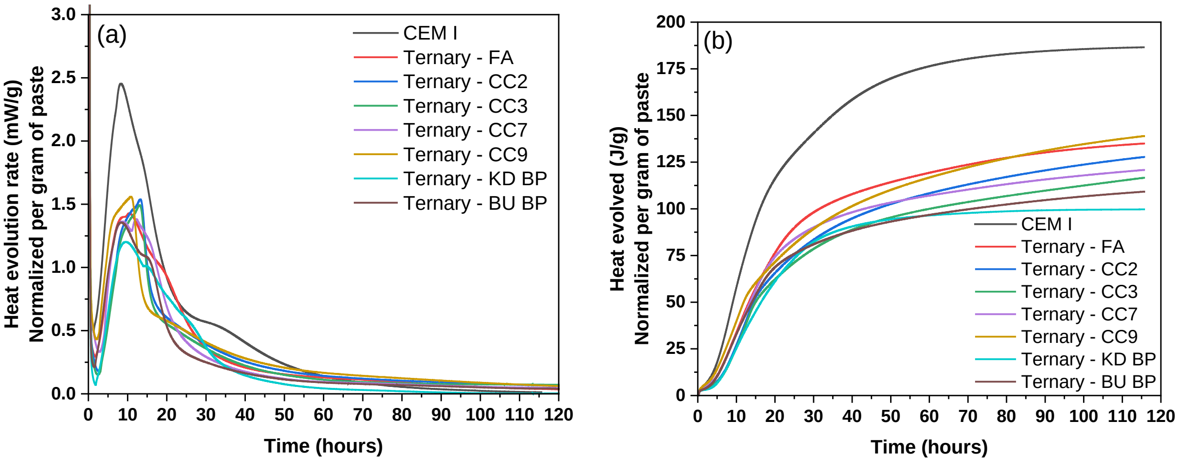

Figure 5 *Hydration kinetics of ternary cement at fixed 0.35 w/b ratio with the addition of SP.*

2.4 Compressive strength development

Figures 6 and 7 shows the compressive strength of calcined clay and brick powder blended binary and ternary cement paste from 3 days to 91 days. For both binary and ternary cements, the compressive strength with comparable flowability shows comparable or even higher performance than the refence sample. CC2 and CC3 (higher grade clay) blended binary cements shows comparable compressive strength in both binary system and ternary system, which means 15% LS replacement shows little effect on the compressive strength. However, for the lower grade calcined clays, the compressive strength of binary cement is significantly lower than the ternary cement, which indicates that low grade calcined clay cannot provide sufficient active aluminate or silicate to generate hydration products to contribute to the compressive strength development. Hence, which level of clay mineral content is suitable for ternary cement and which level of clay mineral content is suitable to produce binary cement should be further investigated. KD brick powder shows good performance in both binary and ternary cement system, and BU brick powder shows lower compressive strength than KD and calcined clays. Hence, the production temperature of brick will influence the performance of brick powder when it is used as supplementary cementitious materials.

As mentioned in Section 2.3, due to the addition of SP delays early hydration, it could be seen that the strength of each mixture shows lower development than that of the samples without adding SP in 7 days. From 14 days, the addition of SP shows little effect on compressive strength development.

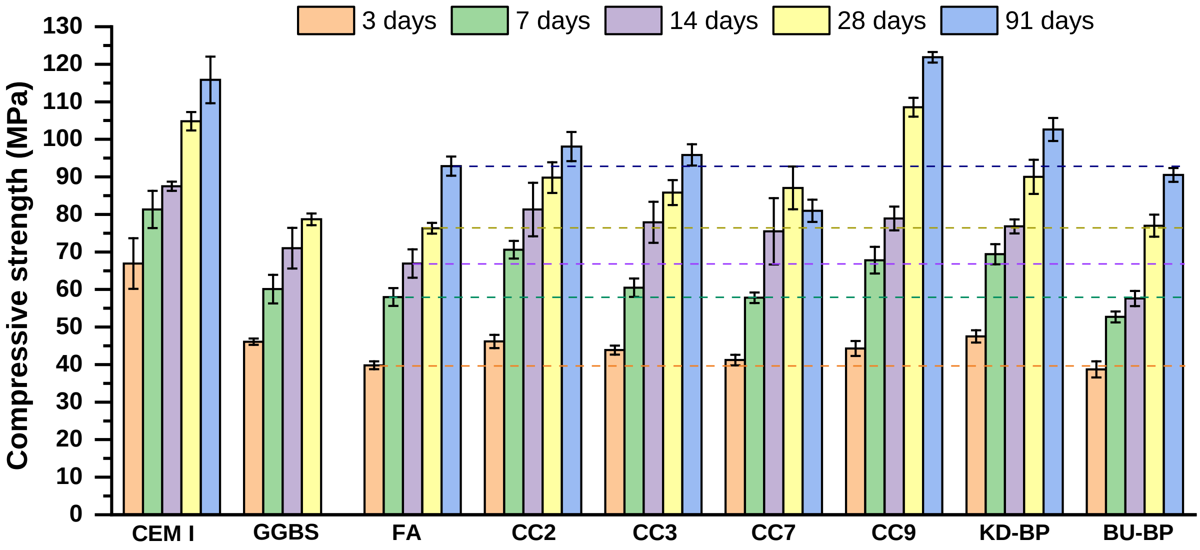

Figure 6 Compressive strength of binary cement pastes at fixed 0.35 w/b ratio with the addition of SP.

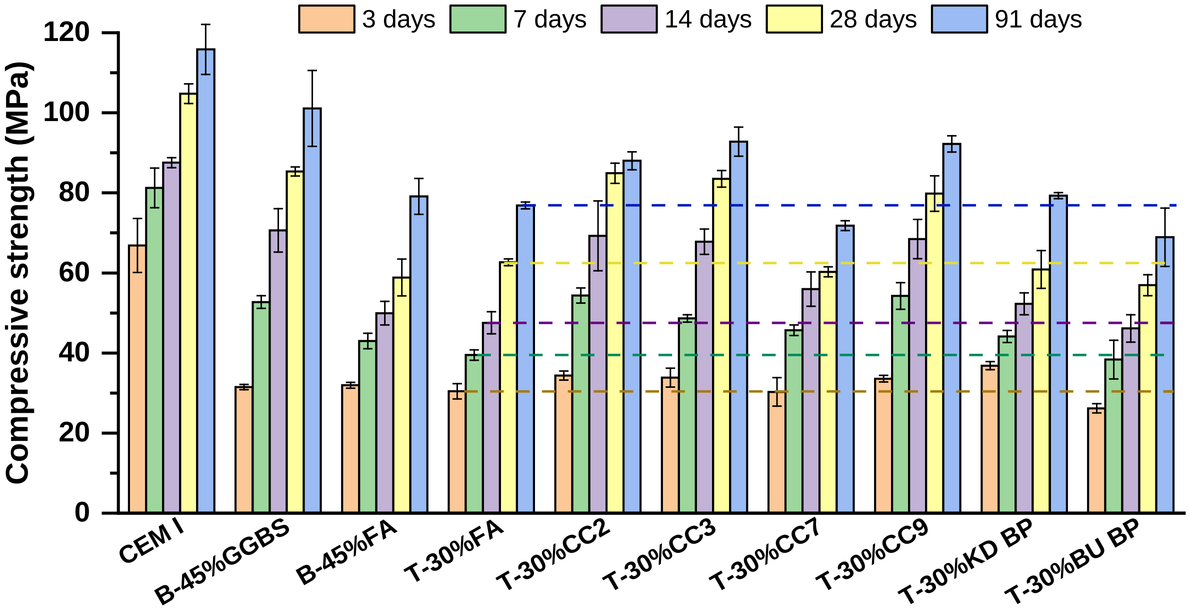

Figure 7 Compressive strength of ternary cement pastes at fixed 0.35 w/b ratio with the addition of SP.

3 Action G3: Characterisation of hydration products

3.1 Aim

The aim of this action is to investigate the effect of superplasticiser on calcined clay/brick powder blended binary and ternary cement pastes, and thereby providing the information for the usage of superplasticiser.

3.2 Powder sample preparation and test methods

Small pieces from the cubic centre were collected after being crushed from the compressive strength test at the age of 7 and 28 days. These small pieces were then immersed in isopropyl alcohol for seven days to terminate the hydration. After seven days, the samples were dried in a vacuum desiccator for three days at ambient temperature. The samples were then ground to powder for hydration products characterisation.

The Stoe STADI-P machine was used for XRD analysis using Cu K1 radiation (Wavelength = 1.54060 Å) applying 40 kV and 30 mA. The sample was measured from 5° to 60° (2θ) with a step size of 0.495° and a counting rate of 10s/step. XRD analysis was utilized to identify crystalline phases in hardened cement paste, including CH, AFm, AFt and calcium carbonate. Bruker ALPHA II FTIR Spectrometers was used for the FTIR test. The instrument was configured for 32 background scans with a resolution of 4 cm-1 from 4000 cm-1 to 400 cm-1. A background scan was performed on the instrument before the powder sample was placed for scanning. Thermogravimetric analysis (TGA) was conducted using Netzsch, TG209 F1. About 30 mg powder samples were tested at a heating rate of 10°C/min under nitrogen conditions ranging from 25°C to 1000°C. The flow rate of nitrogen is 20 cm^3/min.

3.3 Characterisation of hydration products

3.3.1 XRD analysis

The XRD results of the calcined clays or brick powders blended binary cements with the addition of SP at 7 and 28 days are shown in Figure 8. It can be observed that the primary crystal phases in hardened cement paste are still calcite, alite, belite, ettringite and portlandite as well as hemicarboaluminate (Hc) and monocarboaluminate (Mc), which is same with the results of binary cements without adding SP.

As shown in Figure 8 (a), we can clearly find the existing of Hc and Mc in CC2, CC3, CC7 and CC9 blended binary cements at 7 days and 28 days. Combined with the compressive strength results, these calcined clays and brick powders blended binary cements also show better performance. However, both Hc and Mc show lower crystallinity in CEM I, fly ash and GGBS blended cements and there is no obvious Hc and Mc peaks in BU BP blended binary cements. It should be noticed that the peak of ettringite in CC2, CC3, CC7 and CC9 blended cements is clearer than that in GGBS and fly ash blended cement. Previous studies also showed that the generation of Hc and Mc is contributed to the stability of ettringite. Overall, the addition of SP shows little effect on the hydration products.

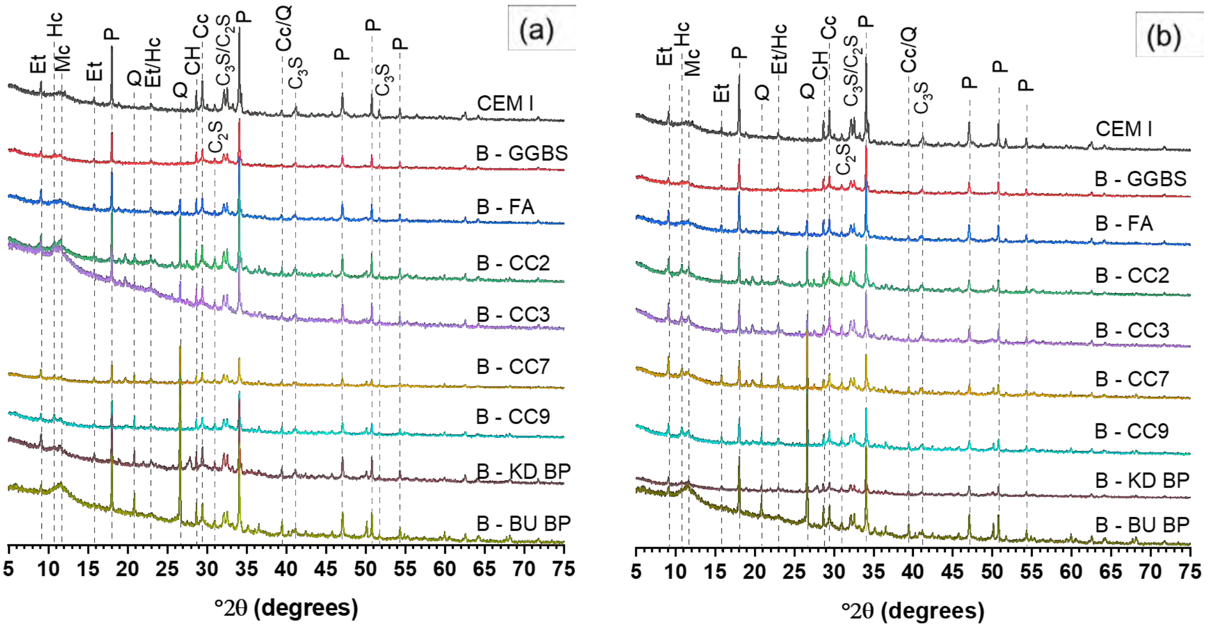

Figure 8 *XRD results of blended binary cement systems with SP addition at (a) 7 days and (b) 28 days. (Et-ettringite, Hc-hemicarboaluminate, Mc-monocarboaluminate, P-portlandite, Q-quartz, Cc-calcite, C3S-alite, C2S-belite).*

3.3.2 TG-DTG analysis

Figure 9 shows the TG-DTG results of the hydration products of calcined clays and brick powders blended binary cements at 7 and 28 days of curing. The peaks that occur up to around 100 °C correspond to the dehydration of C(A)SH and AFt. The shoulder peak at about 150 °C is recorded as the dehydration of AFm phases, such as mono-sulphate, Hc and Mc. The second stage is the decomposition of portlandite occurs between 400 to 500 °C. The last peak which occurs between 550 and 900 °C, is the decomposition of calcium carbonates. The presence of carbonates in binary cement is due to the addition of limestone in CEM I.

Compared to the fly ash blended reference sample, the shoulder peaks at 140°C is significantly enhanced in calcined clay/BU brick powder blended binary cements, as shown in Figure 9 (a and c). This may be due to the addition of calcined clay/brick powder providing more reactive aluminate to the cement system, and generate more Hc and Mc, which is consistent with the findings in XRD results. However, the shoulder is relative weaker in KD brick powder blended binary cement. The peaks of the 28-day curve are identical to that of the 7-day peaks. This is owing to the continuous hydration process producing additional C(A)SH, AFt, and AFm. It is also discovered that the peaks corresponding to CH decomposes at around 430 °C. For calcined clay and KD brick powder blended cements are weaker than those of the fly ash reference group, which indicates they possess higher pozzolanic reactivity and generate more hydration products at 28 days, as shown in Figure 9 (c).

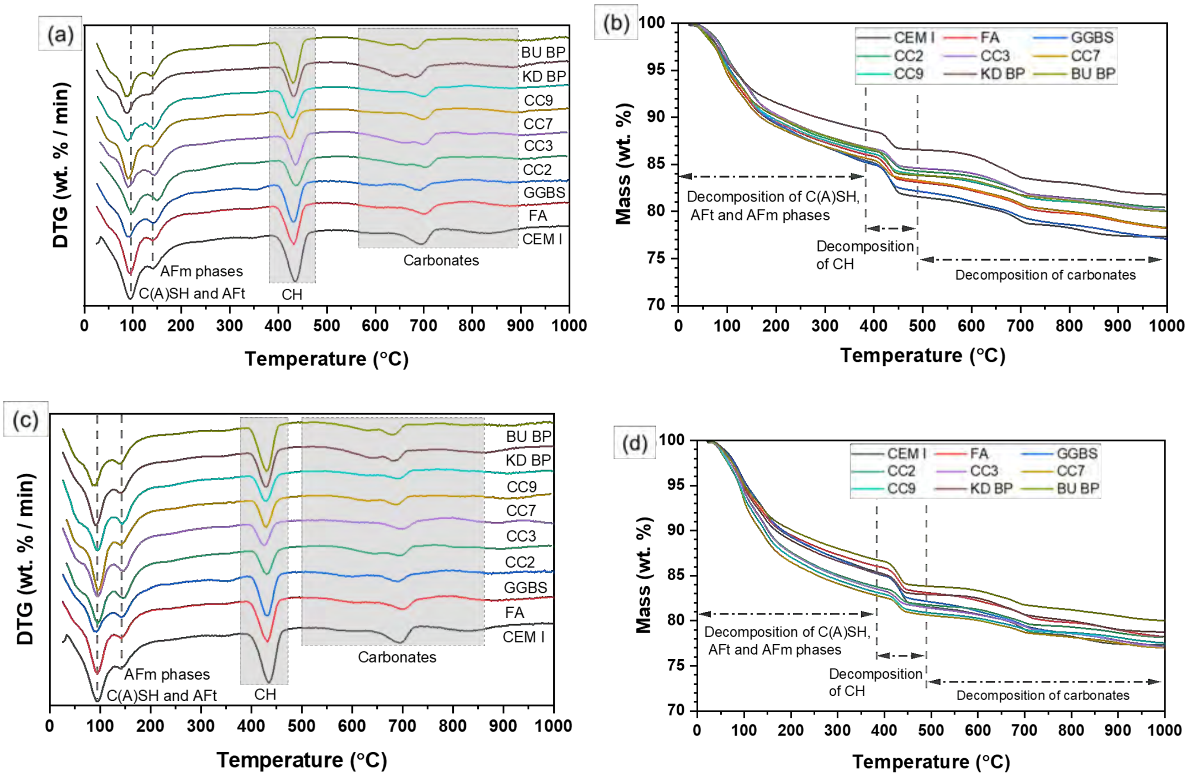

Figure 9 *TG-DTG results of calcined clay blended binary cement at 7 days (a) and 28 days (b).*

3.3.3 FTIR analysis

FTIR spectroscopy can identify hydration products by analysing their unique infrared bands. Figures 10 shows the FTIR spectroscopy of the binary cement with comparable flowability modified by adding SP at 28 days. At around 3636 cm^{-1}, an absorption band corresponds to the vibrations of the O-H bond in CH. It can be observed that the calcined clay blended cement does not behave significantly in this absorption band compared to the reference group, which may be due to the reduced CH production and the depletion of CH by pozzolanic reactivity. The O-H bond in water vibrations causes the wide absorption band that emerges at about 3400 cm^{-1}. Even though the samples are dehydrated by soaking in IPA and vacuumed dry, there is still a minor quantity of free water present in the samples. The absorption band at 1413 cm^{-1} corresponds to the asymmetries stretching of the C-O bond. Calcined clays blended cements exhibit a little shift to the right at this absorption band compared to the reference group, which may cause by the calcium carbonate in the cement combining with the aluminium phase to generate Hc and Mc. This also causes the altering the carbon-calcium ratio and lowering the C-O asymmetric stretching vibration, which confirms the presence of Hc and Mc in the XRD results. In addition, an absorption peak at 873 cm-1 indicates an out-of-plane bending vibration of C-O. The absorption in these two C-O bands is due to the presence of LS in CEM I. At 1099 or 1105 cm^{-1}, the absorption peak corresponds to the S-O vibration in SO_4^{2-}. All samples possess a broader S-O absorption band than the reference group. This is presumably due to the reaction between the LS existing in the cement and the extra aluminate phase of the calcined clay, which produces Hc and Mc. This is consistent with the above XRD results. Due to the capacity of Hc and Mc to stabilise ettringite, the S-O absorption band is widened. In addition, there is an absorption peak at 950 cm^{-1}, corresponding to the asymmetric stretching vibration of the Si-O-Si (Al) bond in C(A)SH. This absorption band is displaced to varying degrees in various SCMs mixes due to varying calcium to silicon ratios. This is because the calcium-to-silicon ratio affects the chain length of C(A)SH, particularly the length of the silicon chain, and hence causes a peak shift.

Compared with the FTIR results of calcined clay blended cement without SP addition, the addition of SP shows little effect on FTIR results.

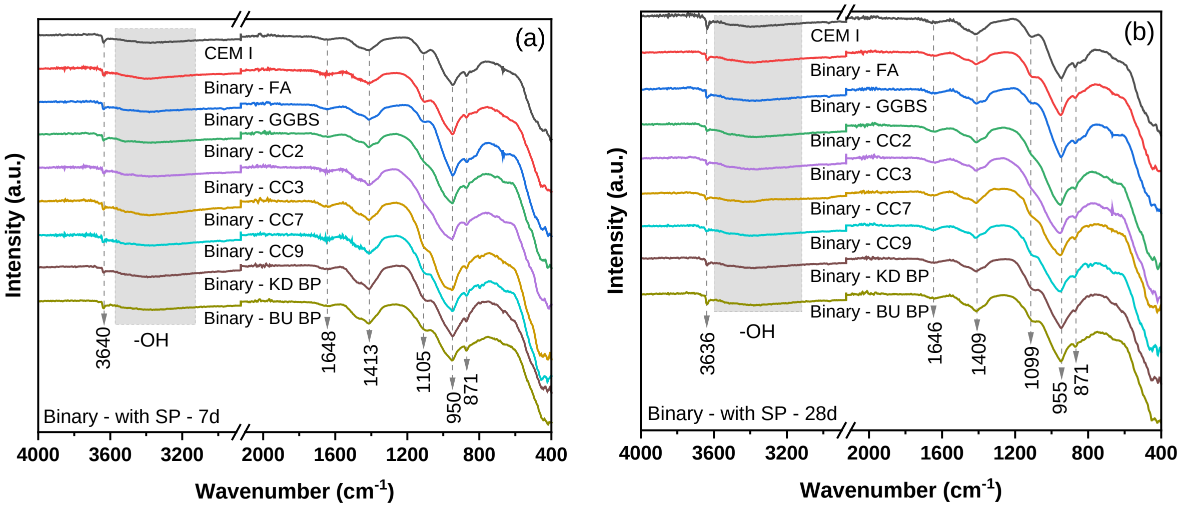

***Figure 10** FTIR results of binary cement with comparable workability (a) 7 days and (b) 28 days.*

4 Conclusions

Work package G investigated the addition of superplasticiser on fresh properties, hydration kinetics, compressive strength and hydration products of different calcined clays and brick powders blended binary and ternary cement. The following conclusions could be drawn based on the results.

1. The addition of superplasticiser could significantly improve the workability of calcined clay/brick powder blended binary and ternary cement. Different grades of calcined clay need different dosage of superplasticiser to achieve comparable flowability.
2. The usage of superplasticiser will delay the compressive strength development of early stage, but show little effect on long term compressive strength, which also could be proved from ICC results.
3. The addition of superplasticiser shows little effect on the hydration products.

University College London

Re-C3: Reclaimed Calcined Clay Cements

Appendix 7 -

The effect of sulphates on the performance of low-carbon cement formulated with different calcined clays

Authors:

UCL:
Yubin Cao
Shi Shi
Tongbo Sui
Yun Bai

Date: March 2024

Contents

1. Introduction

This project investigated the effect of sulphate percentage on the fresh and mechanical performance of calcined clays (different grades and different calcination methods) blended low-carbon cement, thereby optimizing the sulphate content for different calcined clay blended cements.

The hydration kinetics of different calcined clay blended cement systems were investigated by Isothermal conduction calorimetry, and the hydration products were analysed by X-ray diffraction and Thermogravimetric analysis. In addition, the workability and compressive strength of the different sulphate contents cement systems were tested to verify the optimal sulphate content.

2. Experimental programme

2.1. Materials

The clinker used in the project is from Hanson Company, and its composition is shown in **Table 1**. Five different calcined clays from different suppliers were used in this project and are shown in **Table 2**. In addition, gypsum and alkaline sulphate used as sources of SO_3 and other materials in the project are also recorded in **Table 2**.

Table 1. Compositions of Hanson clinker.

SiO_2	Al_2O_3	Fe_2O_3	CaO	MgO	SO_3	Na2O	K_2O
22.61	5.27	3.15	66.65	1.14	0.78	0.29	0.62

Table 2. Raw materials for this project.

Clinker	Calcined clay	Gypsum	Alkaline Sulphate	Alkali
Hanson	CC2-F (Flash	37.9% SO_3 content	99% pure Na_2SO_4	KOH
	CC7-F			
	CC9-F			
	CC9-R (Rotary			
	Brick powder			

As shown in **Table 3**, the kaolinite content of different clays is different. Based on the Imerys XRF data results, RC2 has the highest kaolinite content, accounting for 54%. RC9 kaolinite content is close behind with 49%. RC7 has the least kaolinite content, accounting for only 12%.

Table 3. Kaolinite composition of clays.

ID	Materials	Kaolinite composition (%)
RC2	Raw Clay 2 from Imerys	54
RC7	Raw Clay 7 from Hanson	12
RC9	Raw Clay 9 from Tarmac	49

2.2.Mixture design

This experiment used two water-binder ratios for different experiments. Testing the ion dissolution performance of different types of calcined clays imitated the R^3 method, with a water-binder ratio of 1.2 (50g calcined clay + 60g deionized water). To simulate the environment of the cement pore solution, deionized water (DI water) was used to adjust the pH value of the solution to 13 using 4g KOH. **Table 4** shows the control group of other experiments, consisting of pure clinker with varying levels of SO_3 (in the form of gypsum).

Table 4. Composition of the control group.

	ID	Clinker	Clay	Gypsum	SO3 contents
Control Group	1	100	0	0	0
	2	98.67	0	1.33	0.5
	3	97.37	0	2.63	1
	4	96.03	0	3.97	1.5
	5	94.73	0	5.27	2
	6	93.40	0	6.60	2.5
	7	92.10	0	7.90	3
	8	90.77	0	9.23	3.5

The samples in the remaining experiments are calcined clay blended cement systems. The calcined clay accounts for 30% of the overall powder, and the water-binder ratio is 0.5. The mixed system is divided into two groups according to the SO_3 content and source. The source of SO_3 for Group_1 is gypsum, and the composition is shown in **Table 5**.

Table 5. Mixture design of Group_1.

ID	Clinker (%)	Clay (%)	Gypsum (%)	SO3 content (%)
1	70.00	30	0	0
2	68.67	30	1.33	0.5
3	67.37	30	2.63	1
4	66.03	30	3.97	1.5
5	64.73	30	5.27	2
6	63.40	30	6.60	2.5
7	62.10	30	7.90	3
8	60.77	30	9.23	3.5

For Group_2, the source of SO_3 is gypsum and sodium sulphate. For different calcined clay mixed cement systems, the optimized sulphate content is different. Taking the optimized sulphate parameters in the experiment as the substituted sample, sodium sulphate was used to replace gypsum, with substitution rates of 15%, 30%, 50% and 100%. **Table 6** shows the components of the mixed system with different alkaline sulphate substitution rates, taking the SO_3 content of 2.5 wt.% as an example.

Table 6. Mixture design of Group_2 (2.5 wt.% SO_3 content).

NO.	Clinker (%)	Clay (%)	Gypsum (%)	Na_2SO_4 (%)	Substitution (%)
1	63.73	30	5.6	0.67	15
2	64.03	30	4.63	1.33	30
3	64.47	30	3.3	2.23	50
4	65.53	30	0	4.47	100

2.3.Calculation methods

The calculation process and specific components of other sulphate content systems are shown in following contents. The specific gram weight is shown under the condition the components percentage of each group is kept constant.

Example of 2.5% SO3 substituted by sodium sulphate

- SO_3 relative atomic mass is 80
- Na_2SO_4 relative atomic mass is 142

1. Complete substitution

Assume that the amount of sodium sulphate added is x grams.

$$2.5\% \times 30 = x \times 99\% \times \frac{80}{142}$$
$$x = 1.34g$$

Verify a calculation:

$$SO_3\ content = (1.34 \times 99\% \times \frac{80}{142}) \div 30 = 2.5\%$$

Content: 19.66g Clinker + 1.34g sodium sulphate + 9g Calcined clay

2. Partial substitution

Assume that the amount of sodium sulphate added is x grams.

$$2.5\% \times 50\% \times 30 = x \times 99\% \times \frac{80}{142}$$
$$x = 0.67g$$

Verify a calculation:

$$SO_3\ content = (0.67 \times 99\% \times \frac{80}{142} + 0.99 \times 37.9\%) \div 30 = 2.5\%$$

Content: 19.34g Clinker + 0.67g sodium sulphate + 0.99g Gypsum + 9g Calcined clay

2. Partial substitution

Assume that the amount of sodium sulphate added is x grams.

$$2.5\% \times 30\% \times 30 = x \times 99\% \times \frac{80}{142}$$
$$x = 0.4g$$

Verify a calculation:

$$SO_3\ content = (0.4 \times 99\% \times \frac{80}{142} + 1.39 \times 37.9\%) \div 30 = 2.5\%$$

Content: 19.21g Clinker + 0.4g sodium sulphate + 1.39g Gypsum + 9g Calcined clay

2. Partial substitution

Assume that the amount of sodium sulphate added is x grams.

$$2.5\% \times 15\% \times 30 = x \times 99\% \times \frac{80}{142}$$
$$x = 0.2g$$

Verify a calculation:

$$SO_3\ content = (0.2 \times 99\% \times \frac{80}{142} + 1.68 \times 37.9\%) \div 30 = 2.5\%$$

Content: 19.12g Clinker + 0.2g sodium sulphate + 1.68g Gypsum + 9g Calcined clay

3. Results and Discussion

3.1.Characterization of Calcined clay

Different types of calcined clays have different specific surface areas (SSA), particle size distributions (PSD) and metakaolin contents. In addition, while the calcined clay obtained by different calcination methods of the same source clay demonstrates minimal impact on its mineral composition, it does, however, induce alterations in both the SSA and PSD. These factors might affect the ion dissolution performance and pozzolanic reactivity of the calcined clay, thereby affecting the potential of the calcined clay as SCM.

3.1.1. Physical properties

As shown in **Figure 1**, the PSD of calcined clays 9 obtained by flash calcination (CC9-F) is similar to that of CC7-F. The fineness of calcined clays 9 obtained by the rotary calcination method (CC9-R) is smaller, which is reflected in the fact that its distribution curve is further to the left. The diameter of CC2-F particles is mainly in the range of 10-100 μm, and particles of 1-100 μm constitute the main body of brick powder (BP). According to Figure 23b, CC9-R has the largest SSA of 1.29 m^2/g, followed by BP with an SSA of 0.549 m^2/g. CC7-F and CC9-F have similar specific surface areas of 0.313 and 0.345 m^2/g respectively. The specific surface area of CC2-F is 0.187 m^2/g, which is the smallest among the five calcined clays. As mentioned above, CC7-F and CC9-F have the same trend of particle size distribution curves and therefore have similar SSA. However, the fineness of CC9-R is finer, but the value of SSA is the largest.

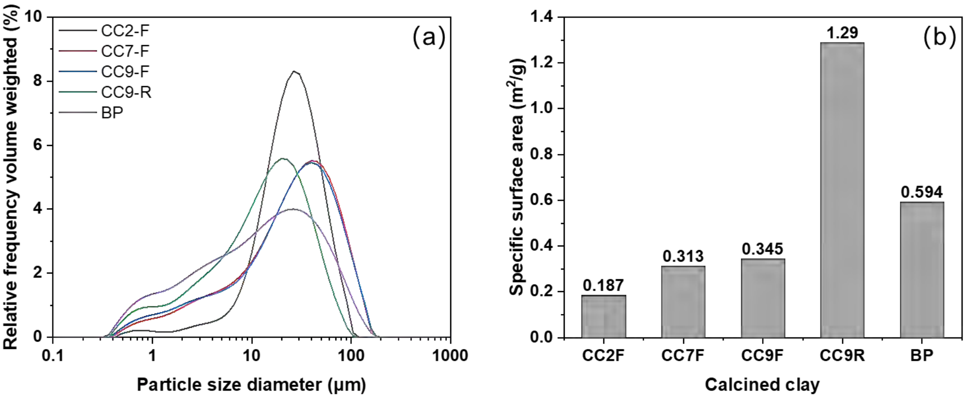

Figure 1. Physical properties of different types of calcined clay, (a) PSD and (b) SSA.

Table 7 shows the sulphate ion dissolution performance of these five calcined clays (per gram) at 4, 24, and 48 hours. At 48 hours, the value includes the sulphate depletion point of all cement systems in the project, so the sulphate dissolved from the calcined clay measured before 48 hour is the effective sulphate ion that participates in the early hydration of cement. According to the table, the highest sulphate ions (17.22 mg) per gram of BP were dissolved at 48 hours, followed by CC7-F, which dissolved 7.95 mg of SO_4^{2-}. CC9-R, CC9-F, and CC2-F dissolved fewer sulphate ions, which were 0.48 mg, 0.13 mg, and 0.06 mg respectively at 48 hours.

Table 7. Sulphate ion dissolution performance per gram of calcined clays. (Note: The unit of time is hours and the unit of SO_4^{2-} is milligrams).

Time	CC2-F	CC7-F	CC9-F	CC9-R	BP
	SO_4^{2-}	SO_4^{2-}	SO_4^{2-}	SO_4^{2-}	SO_4^{2-}
48h	0.06	7.95	0.13	0.48	17.22
24h	0.05	8	0.12	0.42	9.44
4h	0.05	4.27	0.1	0.28	11.65

3.1.2. Pozzolanic reactivity

As shown in Figure 2(b), in the first 72 hours, the cumulative heat release of CC2-F is the highest, and the main peak of heat flow is significantly higher than other calcined clays tested (Figure 2a). Therefore, among the four tested clays, CC2-F has the highest pozzolanic reactivity. The cumulative heat release of CC9-R is second, followed by CC9-F. The results indicate that different calcination methods affect the pozzolanic reactivity of calcined clay. CC9-R has a larger SSA, which increases the silica solubility and pozzolanic reactivity of calcined clay. The section with the lowest pozzolanic reactivity is pictured as CC7-F. In addition, comparing the same calcination methods, the order of pozzolanic reactivity is CC2-F > CC9-F > CC7-F, which also echoes the kaolinite content of the three raw clays.

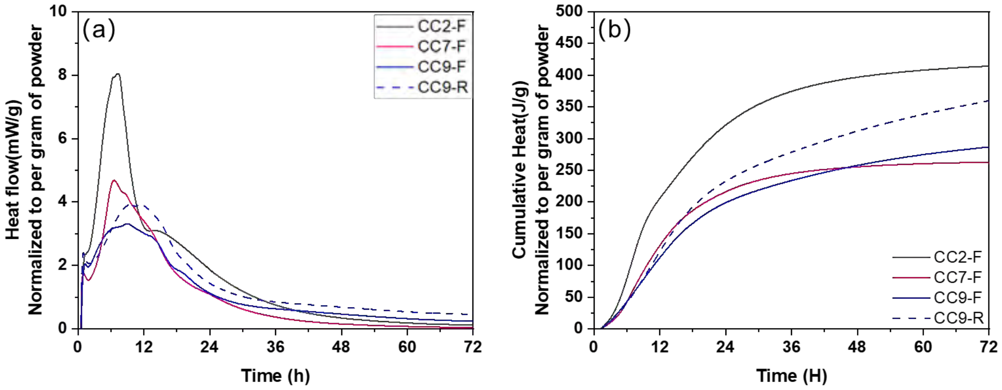

Figure 2. ICC results of four different calcined clay, (a) Heat flow and (b) Cumulative heat.

3.2.Effect of different levels of calcium sulphate dosage

3.2.1. Hydration kinetics of different grades and different calcination methods calcined clay blended cement

The early hydration kinetics of blended cement with different calcined clays and controls are monitored by isothermal calorimetry. In this project, the hydration kinetics of different cement systems are mainly observed in the first 72 hours. According to ASTM C563 (2018), the optimum sulphate dosage for each cement system is obtained by calculating the cumulative heat release over 24 and 72 hours as a function of the system's SO_3 content (Parabola). Because of the low reproducibility of the initial peak, heat observed before the completion of the induction period is ignored. The tested blended cement systems are renamed according to the different sulphate dosage, respectively CC2-F-NO SO_3 to CC2-F-3.5% SO_3; CC7-F-NO SO_3 to CC7-F-3.5% SO_3; CC9-F -NO SO_3 to CC9-F-3.5% SO_3; CC9-R-NO SO_3 to CC9-R-3.5% SO_3 and control group Clinker-NO SO_3 to Clinker-3.5% SO_3.

The heat flow and cumulative heat release of CC2-F blended cement for 72 hours are shown in **Figure 3**. According to **Figure 3**a, the height of the main peak of CC2-F without additional SO_3 is lower than that of other systems with added SO_3. In addition, CC2-F-0.5% SO_3 shows a lack of sulphate, because the width and height of its main peak are lower than those of cement systems with high sulphate content. Cumulative heat release can also reflect the impact of sulphate deficiency on early hydration. As shown in **Figure 3**c, the cumulative heat release of CC2-F-NO SO_3 and CC2-F-0.5% SO_3 is lower than other cement systems with higher sulphate content. In addition, as shown in **Figure 3**b, the duration of the induction period of the cement system with insufficient sulphate is longer than that of other cement systems.

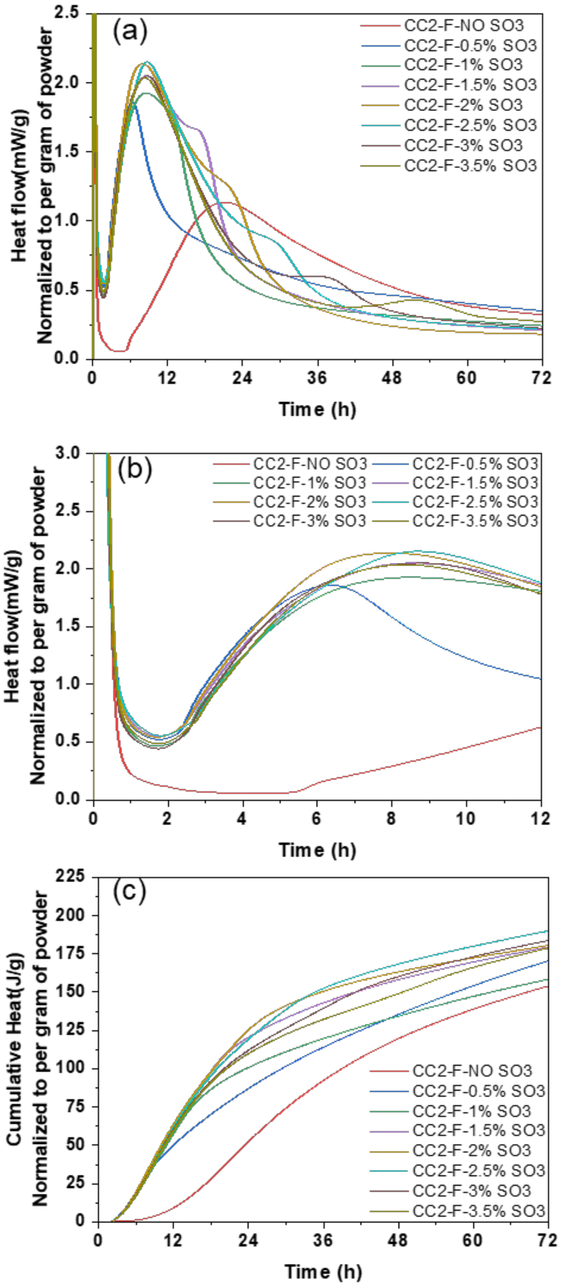

Figure 3. Calorimetry measurements on CC2-F blended cement pastes, (a) Heat flow for 72 hours, (b) Heat flow for 12 hours and (c) Cumulative heat for 72 hours.

The introduction of the sulphate depletion point (SD) can more intuitively express the impact of the sulphate dosage in the cement system on cement hydration. When the heat flow curve reaches the sulphate depletion point, the sulphate ion concentration in the pore solution decreases to unable to delay the reaction of the aluminium phase, the sulphate ions adsorbed by C-S-H are released, causing C_3A to redissolve and rapidly form new ettringite. As shown in **Figure 4**a, SD cannot be observed for CC2-F-NO SO_3 and CC2-F-0.5% SO_3, indicating that the lower sulphate content cannot effectively delay the hydration of C_3A after the main peak. This is the same point as described in ASTM C563 (2018), where the sulphate depletion point is usually only seen in cement near and above the optimal SO_3 content. Additionally, the proper SD is situated between the primary hydration peak and the point at which the heat flow declines to a third of its greatest value. According to **Figure 4**c, when the SO_3 content in the cement system is greater than 3%, the system is supersuphated. Therefore, the optimal SO_3 content of the CC2-F blended cement system is between 1% and 3%.

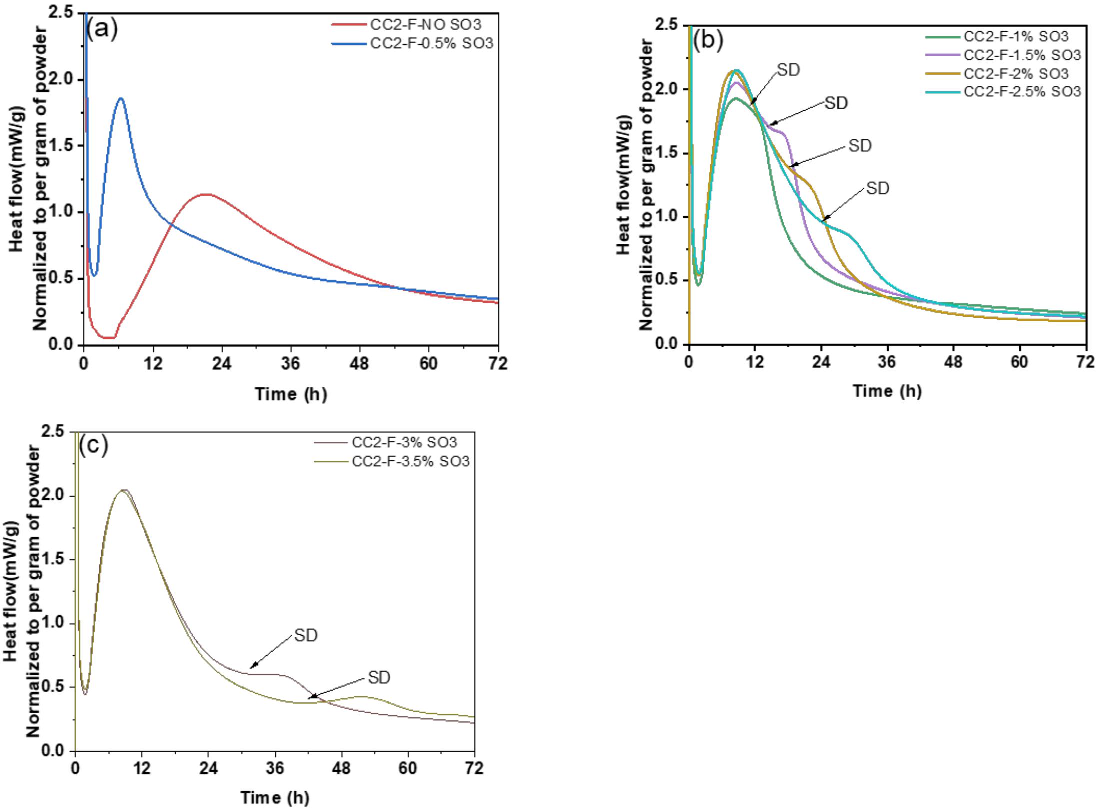

Figure 4. Heat flow curves of CC2-F blended cement. SD is the sulphate depletion point.

In compliance with the requirements of ASTM C563 (2018), a system with SO_3 contents from 1% to 3.5% are selected, and the parabolic relationship of the cumulative heat release at 24 hours and 72 hours is drawn. As shown in **Figure 5**, the parabolic equation is $y = A + B^{*}x + C^{*}x^{\wedge}2$, and the optimal sulphate content is $(-B) \div 2A$. After calculation, the optimal sulphate content of the CC2-F mixed cement system at 24h is 2.29%, and the optimal sulphate content at 72h is 2.56%. The optimal sulphate content may change with hydration age. Therefore, the optimal SO_3 content should be a compromise between different ages. The optimal dosage of the CC2-F blended cement system is 2.5%.

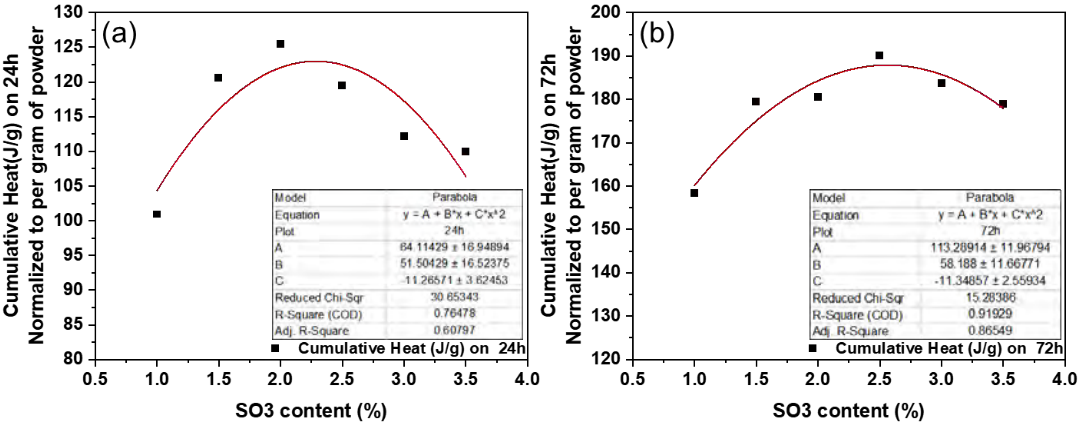

Figure 5. Polt of cumulative heat versus SO_3 level in CC2-F blended cement. (a) 24 hours and (b) 72 hours.

The SO_3 content in the clinker is 0.78%, and the SO_3 effectively dissolved per gram of CC2-F is 0.06mg * 96 (SO_4^{2-} relative atomic mass) / 80 (SO_3 relative atomic mass), the calculated result is 0.05mg. The cement system with 2.5% SO_3 content for ICC contains 19.02g of clinker and 9g of CC2-F. After calculation, the optimal total SO_3 content of the calcined clay blended cement system with 30% CC2-F is 3%.

Figure 6 shows the ICC results of CC7-F blended cement. CC7-F-NO SO_3 and CC7-F-0.5% SO_3 show insufficient sulphate, which is like the results of CC2-F blended cement. In addition, CC7-F-3% SO_3 and CC7-F-3.5% SO_3 sulphate content are supersulphated. According to the fitted parabola in **Figure 7**, the optimal sulphate content of the CC7-F blended cement system is 2.2% at 24h and 2.5% at 72h. However, when the SO_3 content is 2%, the cumulative heat release is greater than the parabolic fitting results. Comprehensive consideration, the optimal SO_3 content of CC7-F blended cement is 2%. After the same calculation steps as CC2-F blended cement, the total SO_3 content of CC7-F blended cement is 2.7%.

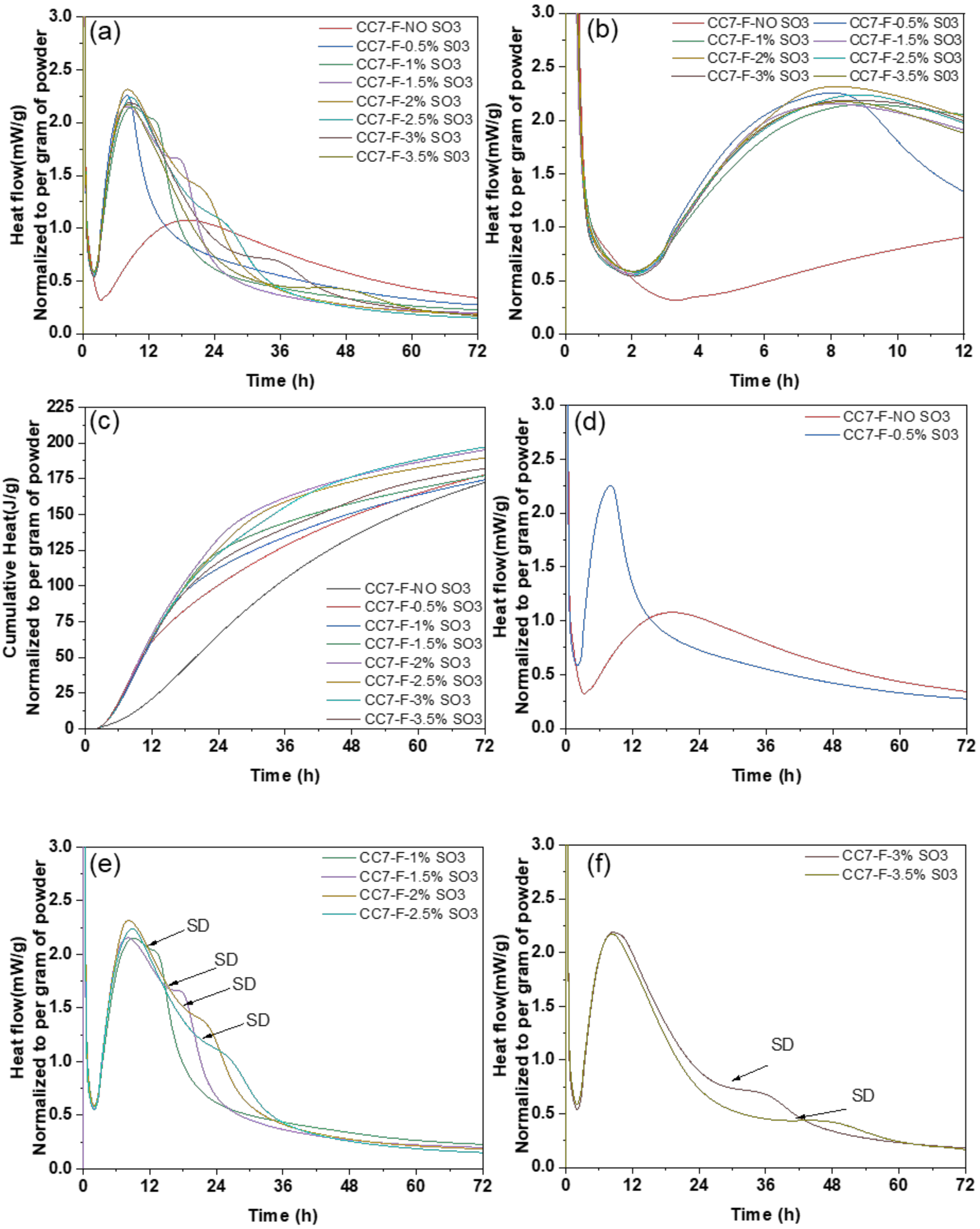

Figure 6. Calorimetry measurements on CC7-F blended cement pastes, (a) Heat flow for 72 hours, (b) Heat flow for 12 hours, (c) Cumulative heat for 72 hours, (d) Heat flow curves of CC7-F-undersulphated systems, (e) Heat flow

curves of CC7-F-property sulphated systems and (f) Heat flow curves of CC7-F-supersulphated systems.

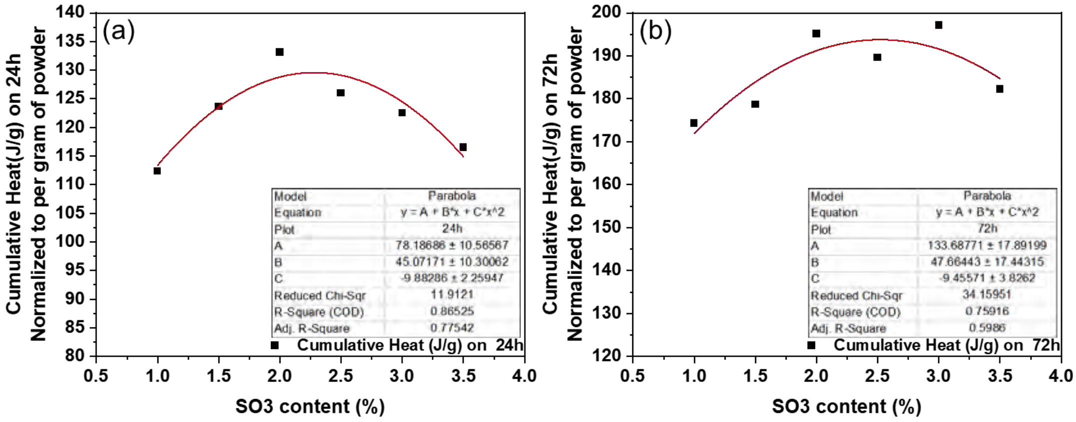

Figure 7. Polt of cumulative heat versus SO_3 level in CC7-F blended cement. (a) 24 hours and (b) 72 hours.

The heat flow curve and cumulative heat release of CC9-F blended cement are shown in **Figure 8**. CC9-F-NO SO_3 and CC9-F-0.5% SO_3 are sulphate-deficient systems. However, different from the above results, the low sulphate content of 0.5% SO_3 is more obvious, which is manifested in the obvious delay of the main hydration peak (**Figure 8**a), the extension of the induction period (**Figure 8**b) and the unclear SD (**Figure 8**d). This phenomenon is also shown in CC9-R blended cement (**Figure 9**). For this case, a hypothesis is proposed that compared with CC2-F and CC7-F, the raw clay of clay 9 is rich in aluminium, so with the same amount of SO_3, both CC9-F and CC9-R blended cement show more obvious undersulphated performance. Aluminate is not consumed by sufficient SO_3, and excess aluminate inhibits the hydration of C_3S. In addition, the optimal SO_3 parameters of CC9-F and CC9-R blended cement range from 1% to 2.5%. When the SO_3 addition amount of the two cement systems is 2.5%, the cumulative heat release is the highest.

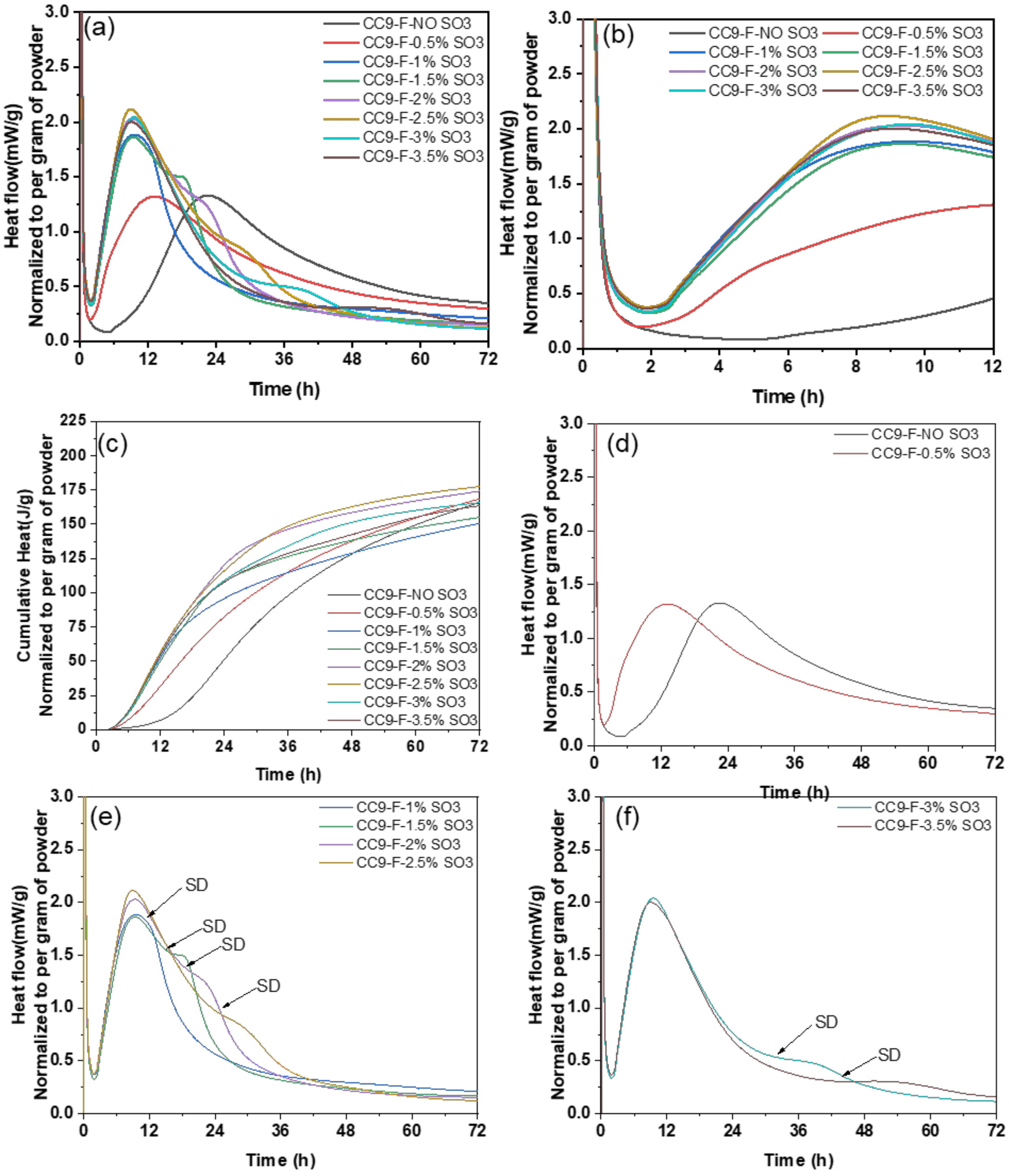

Figure 8. Calorimetry measurements on CC9-F blended cement pastes, (a) Heat flow for 72 hours, (b) Heat flow for 12 hours, (c) Cumulative heat for 72 hours, (d) Heat flow curves of CC9-F-undersulphated systems, (e) Heat flow curves of CC9-F-property sulphated systems and (f) Heat flow curves of CC9-F-supersulphated systems.

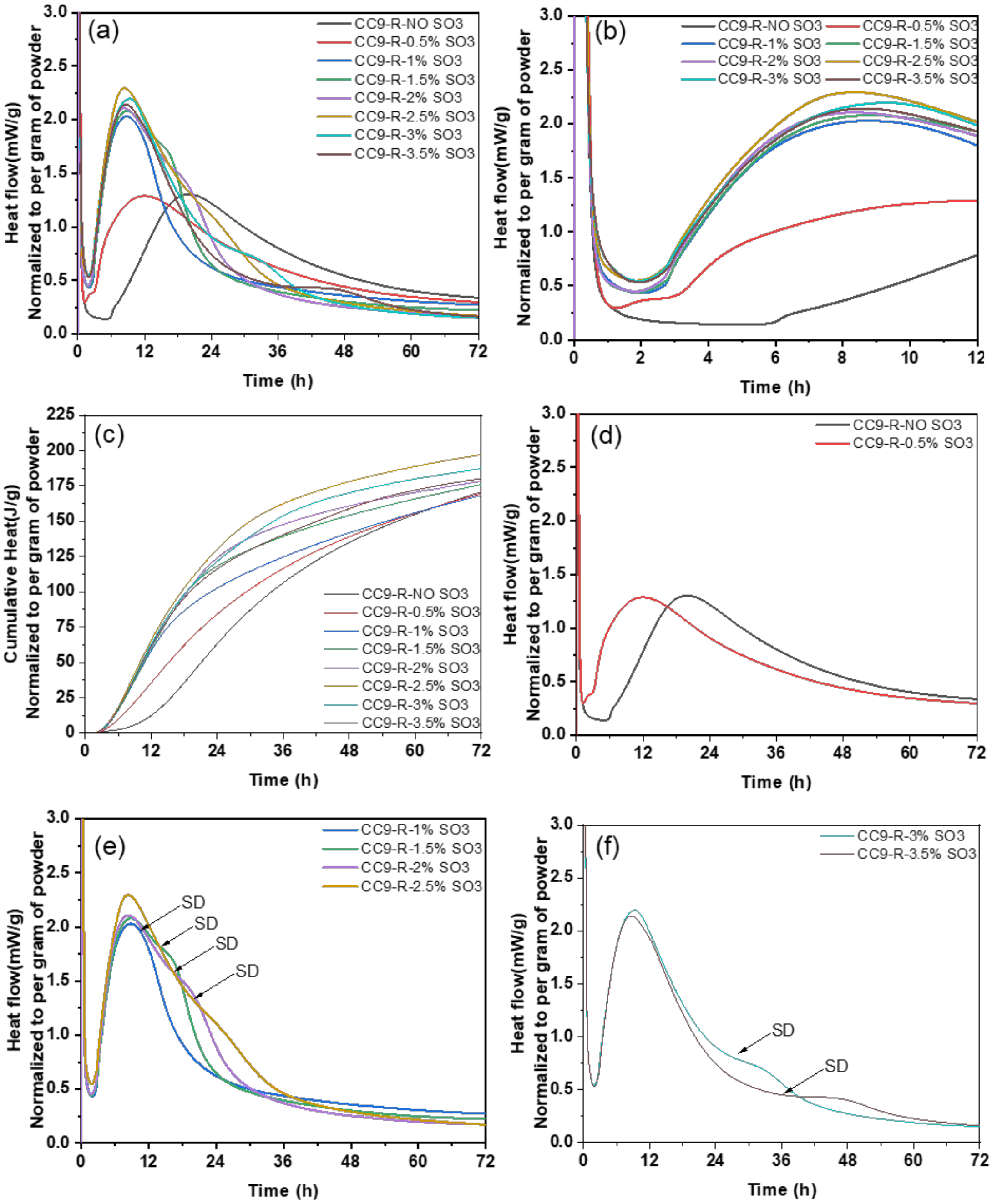

Figure 9. Calorimetry measurements on CC9-R blended cement pastes, (a) Heat flow for 72 hours, (b) Heat flow for 12 hours, (c) Cumulative heat for 72 hours, (d) Heat flow curves of CC9-R-undersulphated systems, (e) Heat flow curves of CC9-R-property sulphated systems and (f) Heat flow curves of CC9-R-supersulphated systems.

According to the fitted parabolas shown in **Figure 10** and **Figure 11**, the optimal SO_3 addition amount of the CC9-F blended cement system at 24h and 72h is 2.5%. The total SO_3 content of CC9-F blended cement is 3%. The optimal SO_3 addition amount of CC9-R blended cement system at 24h is 2.5%, and that at 72H is 2.6%. However, the cumulative heat release of CC9-R at 2.5% SO_3 content is higher than the fitting results. Comprehensive consideration, the optimal SO_3 addition content of CC9-R is 2.5%, and the total SO3 content is 3%.

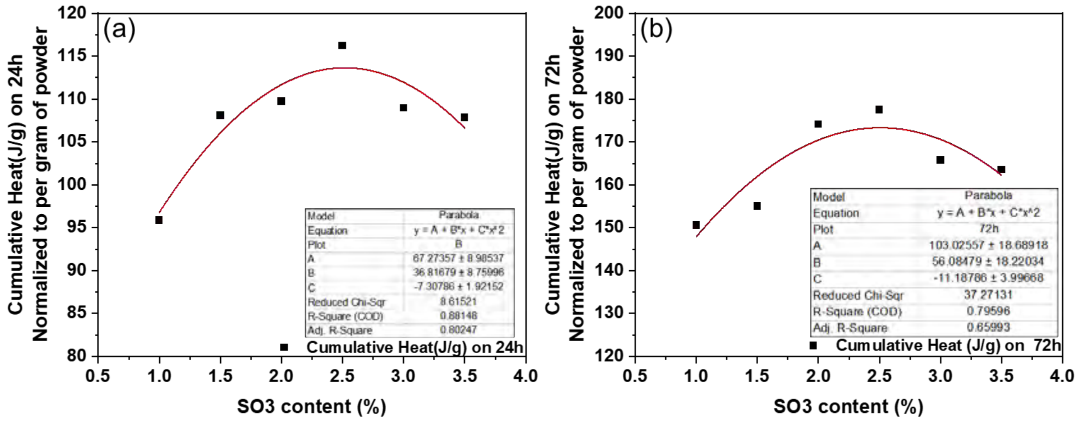

Figure 10. Polt of cumulative heat versus SO_3 level in CC9-F blended cement, (a) 24 hours and (b) 72 hours.

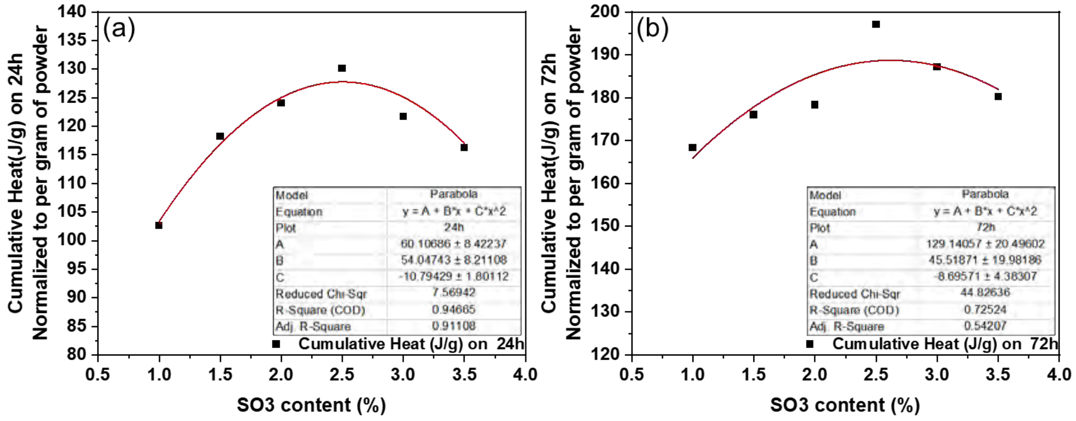

Figure 11. Polt of cumulative heat versus SO_3 level in CC9-R blended cement, (a) 24 hours and (b) 72 hours.

A cement system consisting solely of clinker and gypsum is the control group. The increase in clinker content is the primary cause of the cumulative heat release being higher than that of the calcined clay blended cement systems, as seen in **Figure 12**. The optimal SO_3 addition amount for this system at 24 hours is 2.9%, and at 72 hours it is 3%, according to the parabola fitted in **Figure 12**.

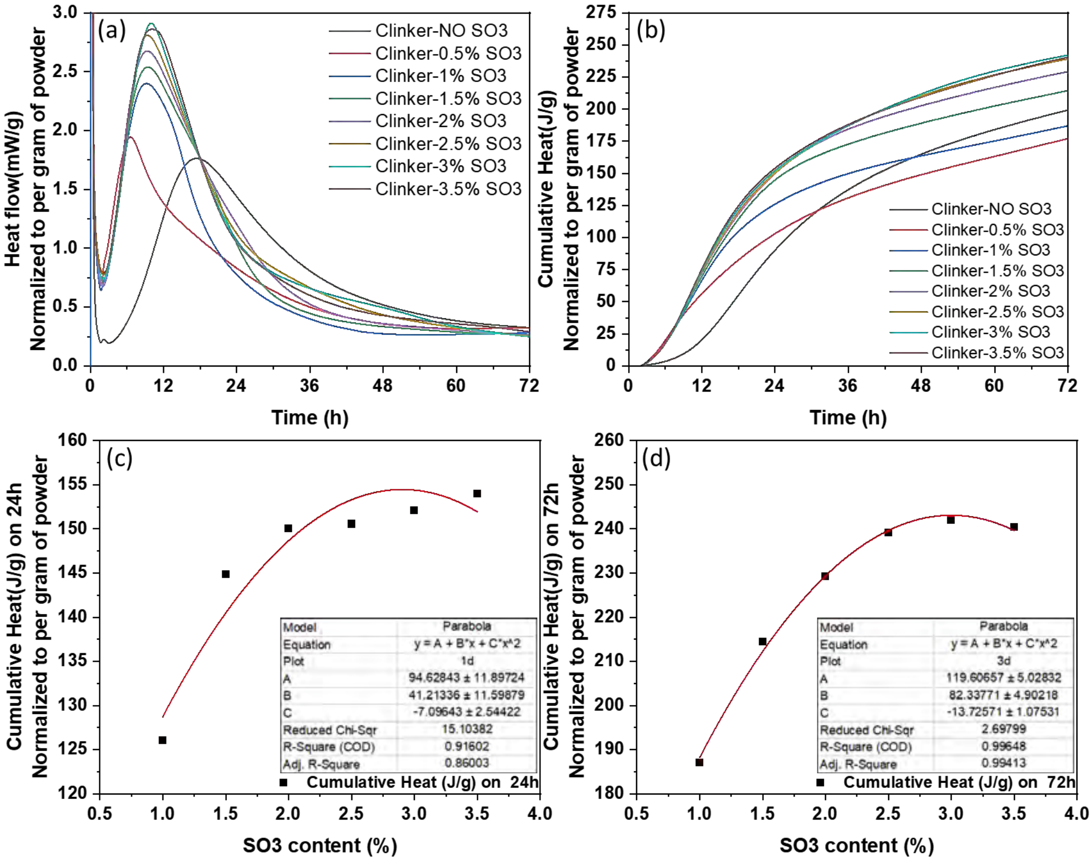

Model	Parabola
Equation	y = A + B*x + C*x^2
Plot	1d
A	94.62843 ± 11.89724
B	41.21336 ± 11.59879
C	-7.09643 ± 2.54422
Reduced Chi-Sqr	15.10382
R-Square (COD)	0.91602
Adj. R-Square	0.86003

Model	Parabola
Equation	y = A + B*x + C*x^2
Plot	3d
A	119.60657 ± 5.02832
B	82.33771 ± 4.90218
C	-13.72571 ± 1.07531
Reduced Chi-Sqr	2.69799
R-Square (COD)	0.99648
Adj. R-Square	0.99413

Figure 12. Calorimetry measurements on clinker cement pastes, (a) Heat flow for 72 hours, (b) Cumulative heat for 72 hours, (c) Polt of cumulative heat versus SO_3 level for 24 hours and (d) Polt of cumulative heat versus SO_3 level for 72 hours.

3.2.2. Hydration products of different grades calcined blended cement

XRD analysis

As shown in **Figure 13**, after seven days of curing, monosulphate is produced in all cement systems. Additionally, three calcined clay blended cement systems produced ettringite after adding sulphate. The hydration products determined by XRD and ICC results are the same. In a cement system with insufficient sulphate, the aluminium phase reacts to form monosulphate. At a suitable sulphate content, the aluminium phase first reacts with sulphate to form ettringite. When the sulphate is exhausted, ettringite is converted to form AFm. The hydration products of the CC9-F and CC9-R blended cement systems are the same under 1 day and 7 days curing periods. This confirms that flash calcination and rotary calcination methods do not change the mineral composition of the calcined clay. In addition, no monocarboaluminate and hemicarboaluminate are not found in the XRD results, indicating that sealing work is qualified during the experiment and the samples are not carbonized.

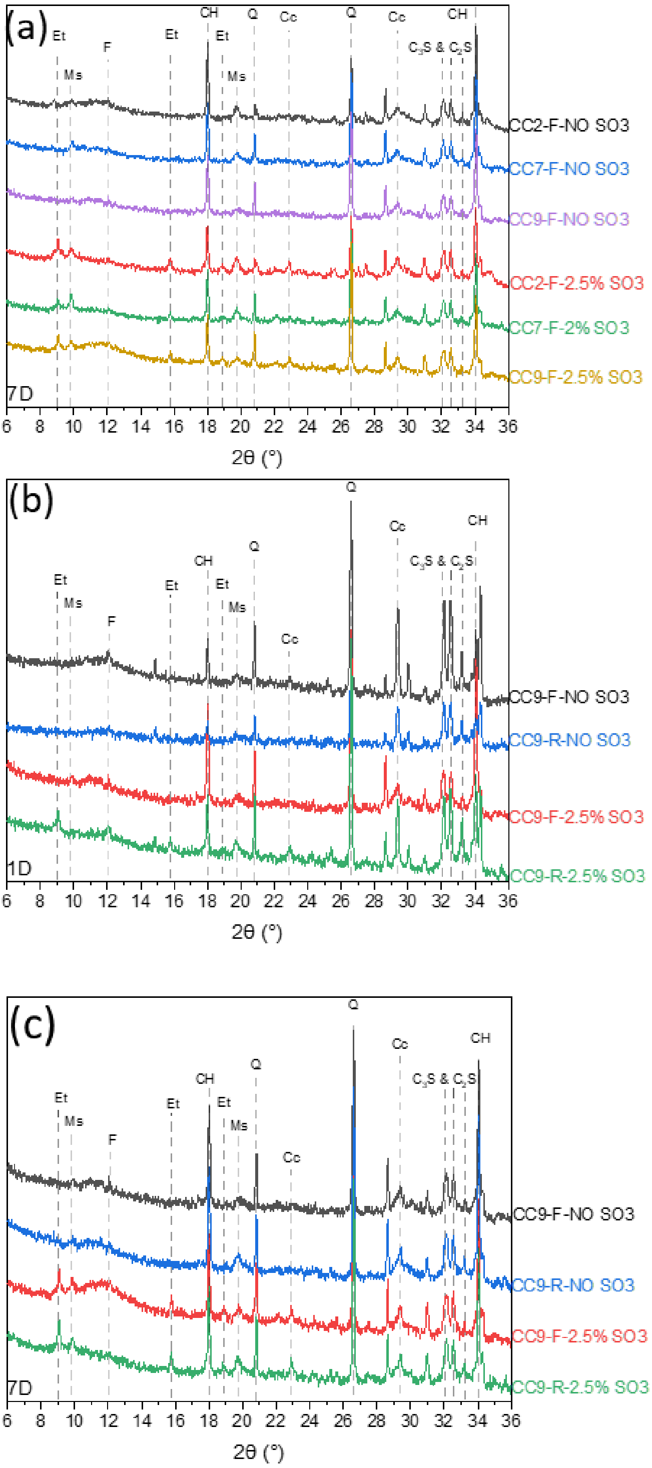

Et: Ettringite Ms: Monosulphate F: Ferrite

CH: Portlandite Q: Quartz Cc: Calcite

Figure 13. XRD patterns of different types of calcined clay blended cement systems under different curing periods, (a) 7 days curing period, (b) 1 day curing period and (c) 7 days curing period.

TG analysis

Figure 14 shows the results of TGA and DTG for different grades of calcined clay cement systems after SO_3 optimization. Compared with the blended cement system, when the curing period is one day, the mass loss of CC2-F blended cement is the largest, followed by CC9-F, and finally CC2-F. The clay with high pozzolanic reactivity promotes the hydration of cement and produces more hydration products. As shown in **Figure 14**b, the DTG peak at about 90 °C corresponds to the dehydration of AFt. The CC2-F and CC9-F blended cement systems have larger peaks. **Figure 15** shows the results of TGA and DTG with a 7-day curing period. Same as the one-day curing samples, the order of hydration products from more to less is CC2-F, CC9-F, CC7-F, corresponding to the strong to weak pozzolanic reactivity. The difference is that the sample cured for 7 days has a peak near 160°C, which may correspond to the dehydration of AFm.

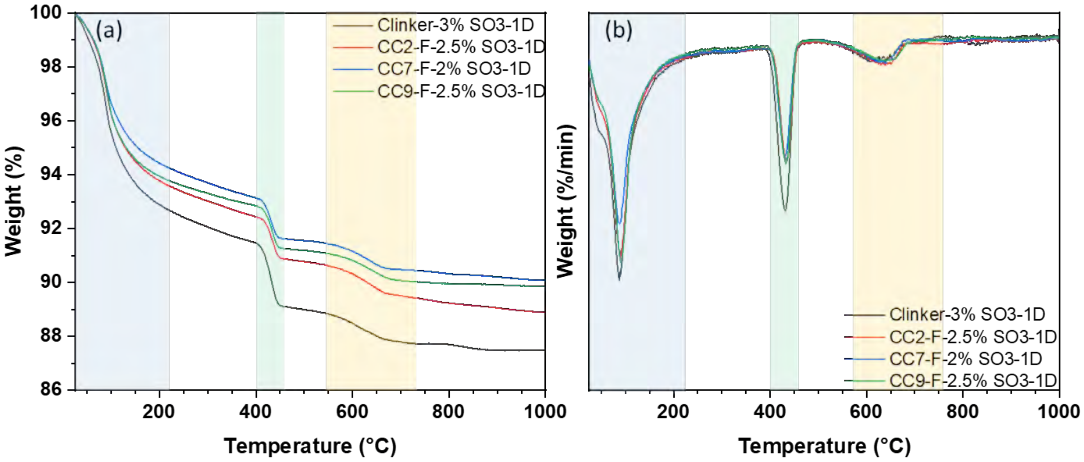

Figure 14. TG results of 1 day curing of different grades calcined clay blended cement systems, (a) TGA curves (b) DTG curves.

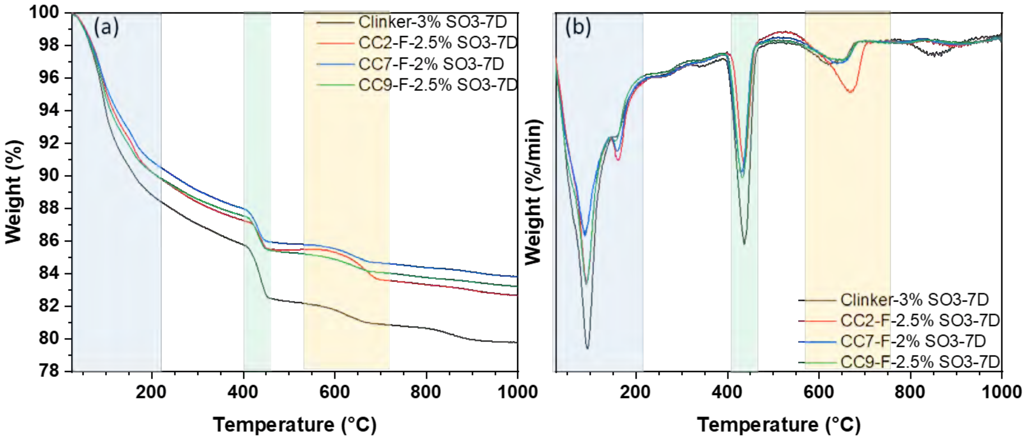

Figure 15. TG results of 7 days curing of different grades calcined clay blended cement systems, (a) TGA curves (b) DTG curves.

Figure 16 shows the TGA and DTG results of CC9-F blended cement with different SO_3 additions for a one-day curing cycle. The amount of SO_3 added increases, the hydration products also increase. This may be related to the formation of a large amount of AFt due to excessive sulphate concentration. As the addition of SO_3 increases, the peak value of AFt becomes larger and the AFt content becomes higher. The cement sample results of the 7-day curing period show that the cement system with 2.5% SO_3 addition and the cement system with 3.5% SO_3 addition have the largest hydration products (**Figure 17**a). However, **Figure 17**b shows CC9-F-3.5% SO_3 has more AFt. Combined with CC9-F-3.5% SO_3, which is supersulphated, 2.5% SO3 is the optimal SO_3 addition amount, which is the same as the ICC result.

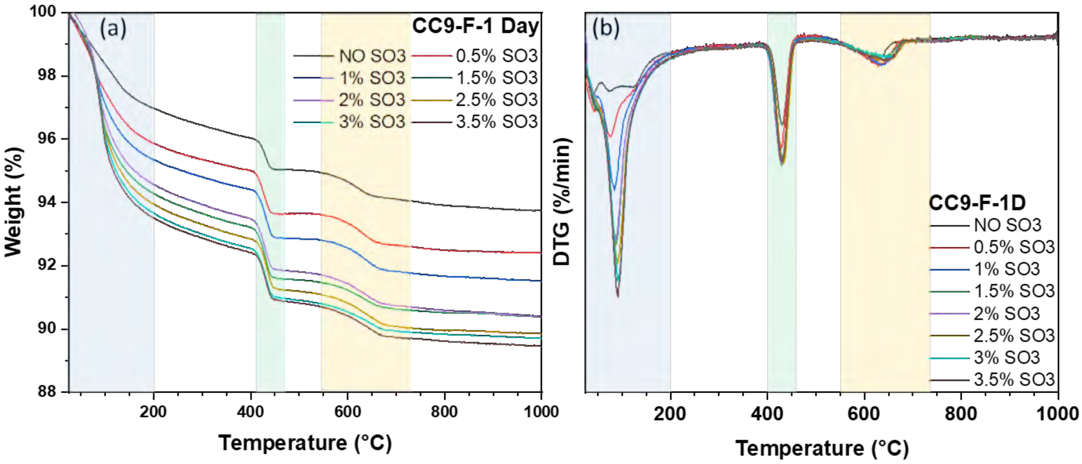

Figure 16. TG results of 1 day curing CC9-F blended cement systems with different levels of SO_3, (a) TGA curves (b) DTG curves.

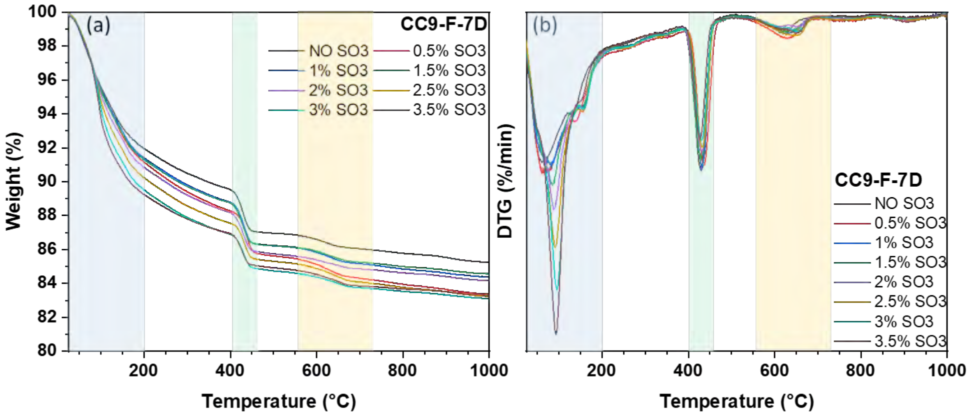

Figure 17. TG results of 1 day curing CC9-F blended cement systems with different levels of SO3, (a) TGA curves (b) DTG curves.

3.2.3. Workability

In cement systems, yield stress quantifies fluidity. The Bingham model, which is frequently used to determine yield stress, explains nonlinear flow behaviour. The equation is $y = y0 + B^*x + C^*x^\wedge 2$, where y0 is the yield stress. In this project, the down curve of the rheometer is used to fit the model. In the experiment, only 30% CC9-F blended cement is used to explore the effect of sulphate content on paste fluidity. **Figure 18**a shows the Bingham model of the cement system under different SO_3 parameters for 7 minutes, also depicted in **Figure 18**b is the change in yield stress following fitting. The yield stress of the pastes increases at the seventh minute as the gypsum is added.

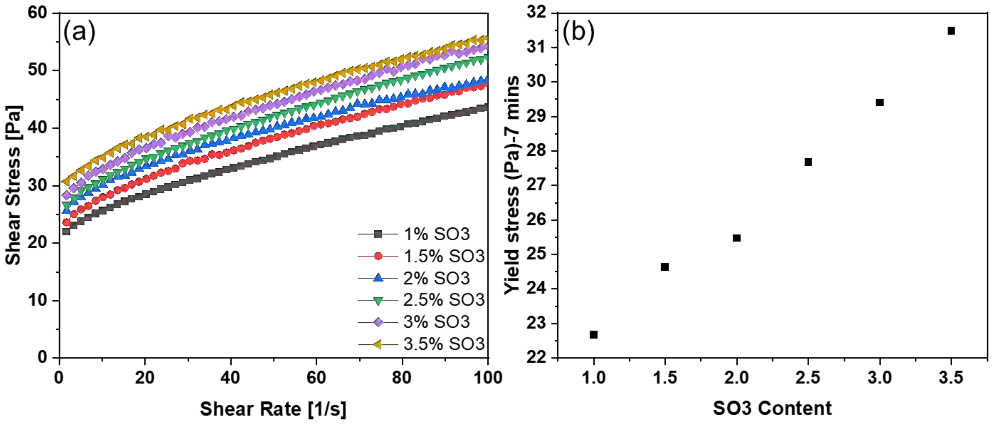

Figure 18. Rheological properties of cement pastes with different SO_3 dosages for 7 minutes, (a)Typical flow curves and (b) yield stress.

The yield stress of the cement paste tends first to reduce and then increase at the 30th minute as the addition of SO_3 increases, as illustrated in **Figure 19**. When the SO_3 content increases again, the excessive sulphate content will form more ettringite, and change the shape of ettringite from spherical to elongated, increasing the specific surface area, and then increasing the yield stress of cement paste. According to the parabola fitted by the yield stress of different SO_3 additions (**Figure 19**b), when the SO_3 addition is 2.2%, the rheological properties of cement paste are optimal.

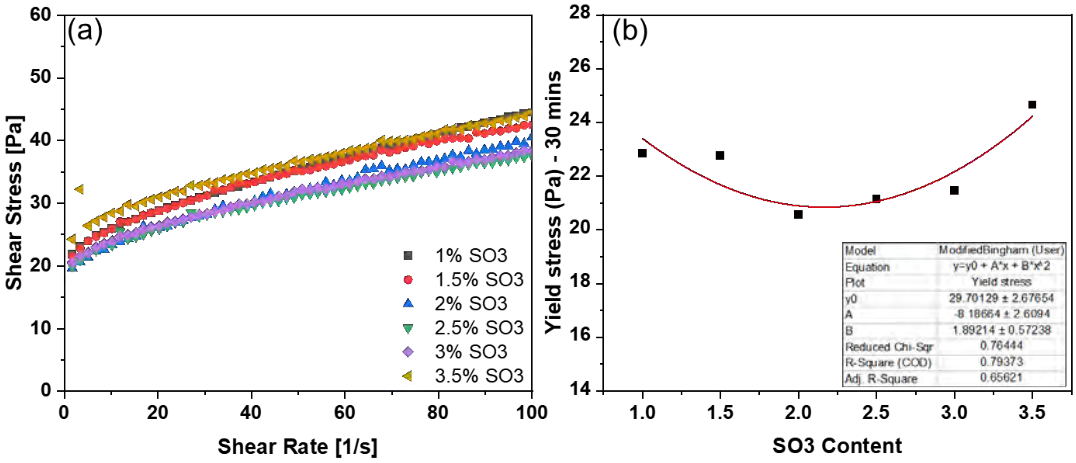

Model	ModifiedBingham (User)
Equation	y=y0 + A*x + B*x^2
Plot	Yield stress
y0	29.70129 ± 2.67654
A	-8.18664 ± 2.6094
B	1.89214 ± 0.57238
Reduced Chi-Sqr	0.76444
R-Square (COD)	0.79373
Adj. R-Square	0.65621

Figure 19. Rheological properties of cement pastes with different SO_3 dosages for 30 minutes, (a)Typical flow curves and (b) yield stress

When the time reaches 60 minutes, the yield stress test findings may not be consistent because of the phase separation, due to the segregation of the sediment-containing layer and the supernatant that contains a lot of water and finer cement particles, as shown in **Figure 20**.

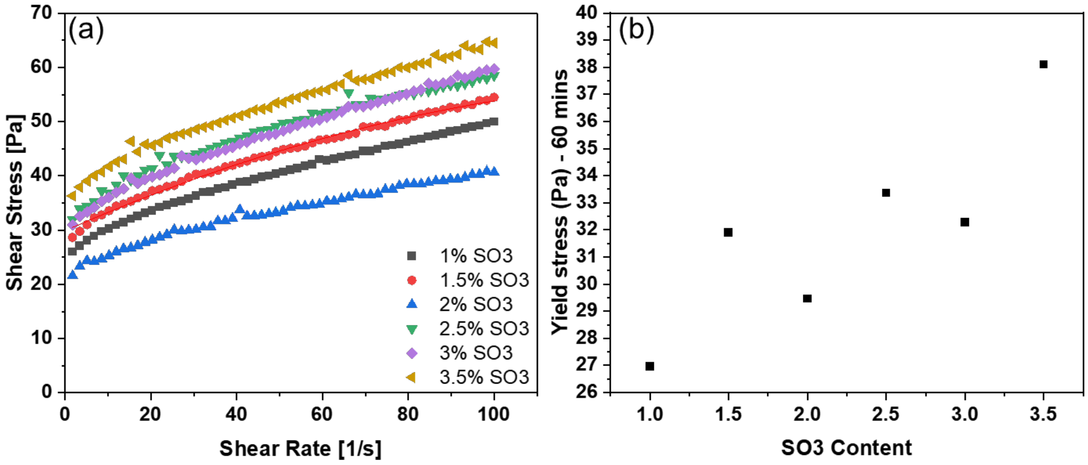

Figure 20. Rheological properties of cement pastes with different SO_3 dosages for 60 minutes, (a)Typical flow curves and (b) yield stress.

3.2.4. Compressive strength

According to ASTM C563 (2018), the 1-day and 7-day compressive strength of CC9-F blended cement are tested in this project, as shown in **Figure 21**. As the SO_3 addition amount increases, the 1-day and the 7-day compressive strength show a trend of first increasing and then decreasing, which corresponds to the above ICC results. In the undersulphated system, the increase of sulphate content will generate more ettringite and less AFm. Compared with the later, the former has a larger volume, so the porosity of the cement will be reduced, and the compressive strength will be high. Therefore, the fitted parabola will first show an upward trend. After reaching the optimal SO_3 addition amount, continuing to increase the SO_3 content leads to a decrease in compressive strength.

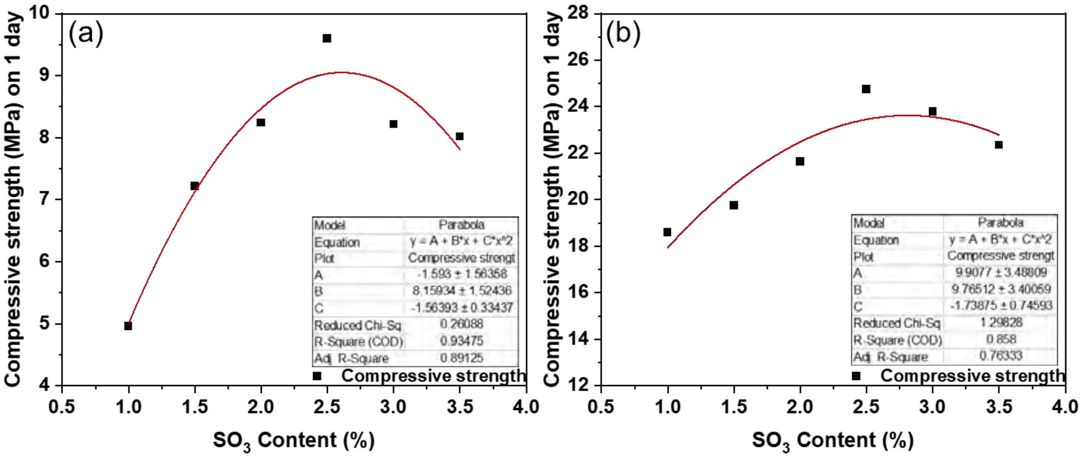

Figure 21. Compressive strength versus SO3 level in CC9-F blended cement, (a) 1-day and (b) 7-day.

3.3. Effect of alkaline sulphate substitution

3.3.1. Hydration kinetics

As shown in **Figure 22**, different levels of alkaline sulphate are used to replace gypsum as a new source of SO_3 in the CC9 -F blended cement system, which will increase early cumulative heat release. It is intuitively observed that with the increase of the alkaline sulphate substitution rate, the cumulative heat release shows a trend of first increasing and then decreasing. The increase in cumulative heat release is due to the advance of the main peak and the increase in area, and there is a period of higher heat flow after SD than the cement system with only gypsum added, as shown in **Figure 23**. The early appearance of the main peak is due to the shortening of the induction period.

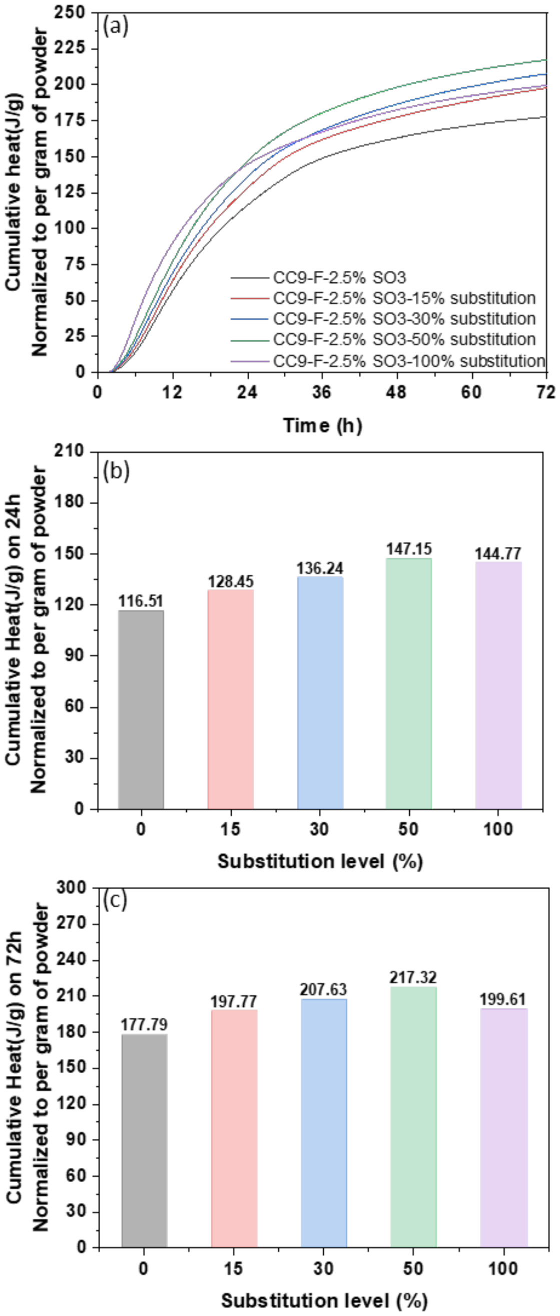

Figure 22. Cumulative heat of Na_2SO_4 CC9-F pastes, (a) Cumulative heat for 72 hours, (b) Polt of cumulative heat versus SO3 substitution level for 24 hours and (c) Polt of cumulative heat versus SO3 substitution level for 72 hours.

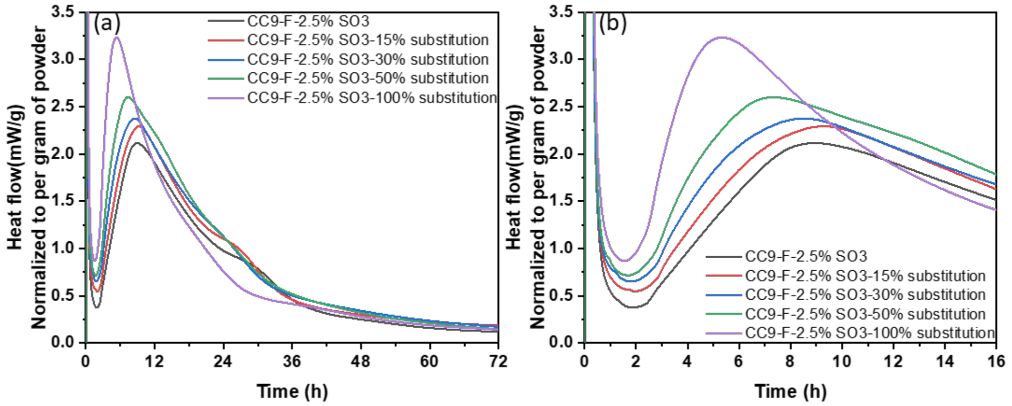

Figure 23. Calorimetry measurements on Na_2SO_4 CC9-F pastes, (a) Heat flow for 72 hours, (b) Heat flow for 16h.

In other calcined clay blended cement systems and clinker systems, replacing gypsum with alkaline sulphate shows the same trend in the heat flow curves and cumulative heat release (**Figure 24**, **Figure 25** and **Figure 26**). The experiment shows that the addition of alkaline sulphate strengthens the early hydration of cement.

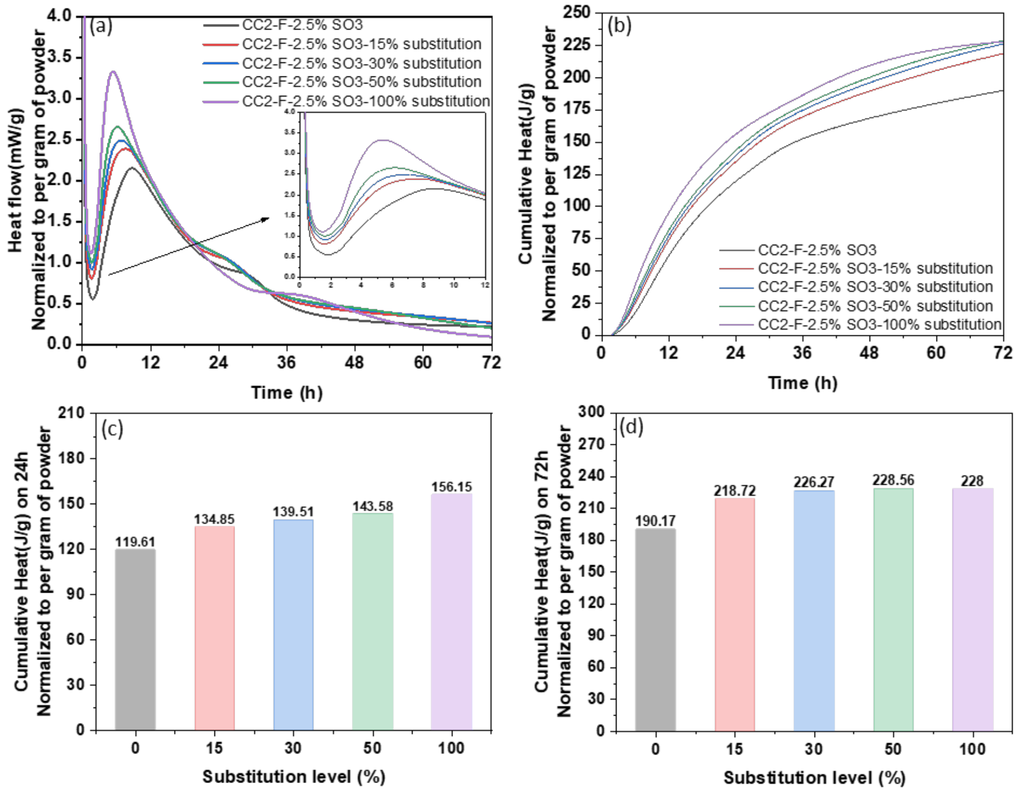

Figure 24. Calorimetry measurements on Na_2SO_4 CC2-F pastes, (a) Heat flow for 72 hours, (b) Cumulative heat for 72 hours, (c) Polt of cumulative heat versus

SO$_3$ substitution level for 24 hours and (d) Polt of cumulative heat versus SO3 substitution level for 72 hours

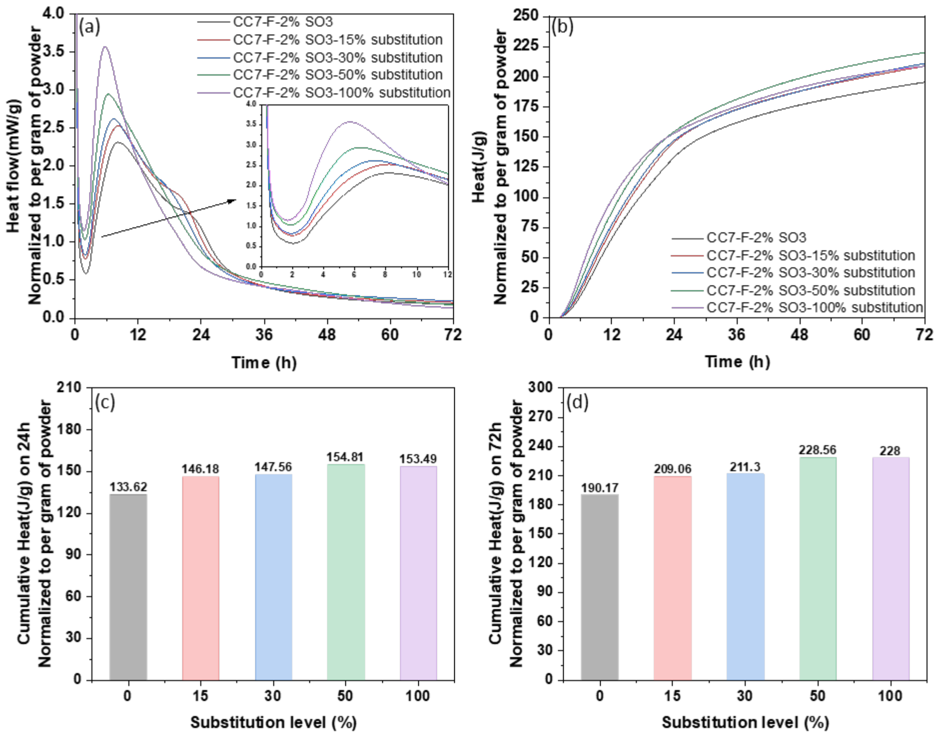

Figure 25. Calorimetry measurements on Na$_2$SO$_4$ CC7-F pastes, (a) Heat flow for 72 hours, (b) Cumulative heat for 72 hours, (c) Polt of cumulative heat versus SO$_3$ substitution level for 24 hours and (d) Polt of cumulative heat versus SO3 substitution level for 72 hours

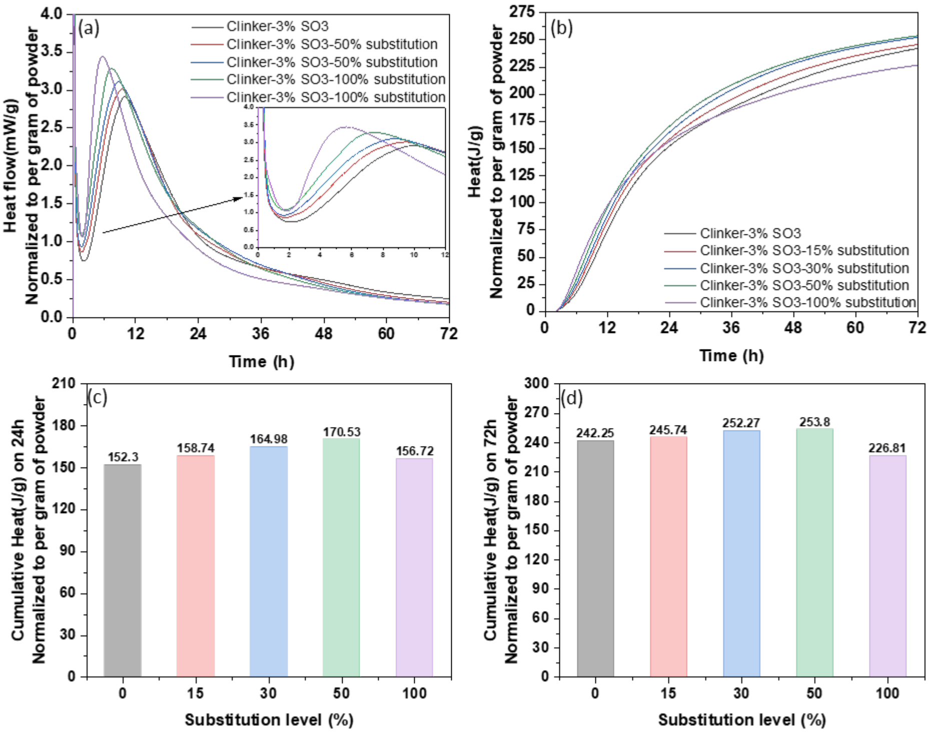

Figure 26. Calorimetry measurements on Na_2SO_4 clinker pastes, (a) Heat flow for 72 hours, (b) Cumulative heat for 72 hours, (c) Polt of cumulative heat versus SO_3 substitution level for 24 hours and (d) Polt of cumulative heat versus SO3 substitution level for 72 hours

3.3.2. Hydration products

Figure 27 shows the TG results for CC9-F blended cement systems using Na_2SO_4 as a source of SO_3. The use of alkaline sulphate produced more hydration products and promoted early hydration of cement, which is the same as the result of ICC. The dehydration peak of AFm was not observed in the DTG curves of the sample with a 1-day curing, but the peak appeared under the 7-day curing. Furthermore, 50% Na_2SO_4 replaces gypsum cement system generates AFt after one-day curing is less than the other three systems because its DTG peak near 90°C is smaller (**Figure 27**b). In addition, a small increase in mass occurred in the CC9-F-50% substitution system at 550°C. CC9-F-30% substitution and CC9-F-100% substitution systems also show a mass increase near 900°C (**Figure 27**c). Subtracting the increased mass of this part, the remaining mass of the CC9-F-50% substitution system is approximately 82%, and the mass loss is greater than other systems.

Therefore, the 50% substitution rate is the one that promotes hydration the most in the experimental groups and has the same trend as the ICC results.

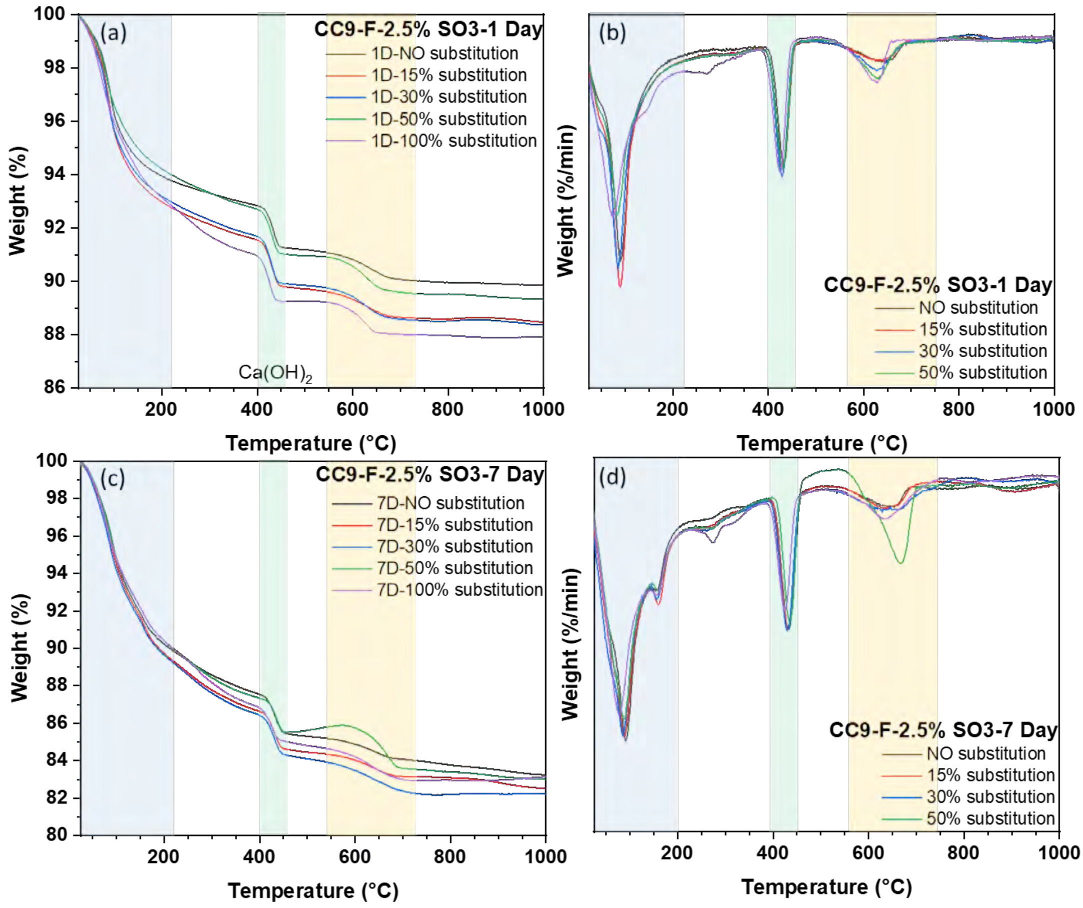

Figure 27. TG results of CC9-F blended cement systems with different levels of Na2SO4 substituted, (a) TGA curves for 1 day curing period, (b) DTG curves for 1 day curing period, (c) TGA curves for 7 day curing period and (d) DTG curves for 7 day curing period.

4. Conclusions

This project explores the sulphate optimization of blended cement systems with calcined clays of different grades and calcination methods. Different techniques were used to explore the effects of different calcined clays on cement hydration kinetics and hydration products in sulphate-optimized cement systems. In addition, the workability and compressive strength of the cement systems with different sulphate substitutions were analysed, which verified the authenticity of the optimal sulphate dosage. Finally, sodium sulphate was used to replace calcium sulphate as the SO_3 source in these cement systems, and the influence of alkaline sulphate on the early hydration kinetics and hydration products of the cement system was further analysed. The main conclusions are as follows:

- Different clay mineral compositions and calcination methods will affect the ion dissolution performance of calcined clay. Compared with flash calcination, the calcined clay obtained by the rotary calcination method shows better ion dissolution performance.
- Different grades of calcined clay have different pozzolanic reactivities. The higher kaolinite content in the raw clay shows the higher pozzolanic reactivity and the stronger promotion effect on cement hydration at the early stage.
- Different calcination methods will affect the pozzolanic reactivity and specific surface area of calcined clay. For same raw clay, compared with flash calcination, the calcined clays produced by rotary calcination have higher specific surface areas and pozzolanic reactivity.
- Different types of calcined clay blended cement systems have different optimal sulphate contents. The addition of alkaline sulphate promotes early hydration of the cement system.

Re-C3: Reclaimed Calcined Clay Cements

Appendix 8 -
Characterization of the Pilot Calcined Clays

Authors
Imerys:
Barbara Benevenuti
Deeba Ansari
Tony Newton
Serge Ghilardi
Philippe Thouilleux

29/01/2024

Contents

Table of Figures

Table of Tables

1. Introduction

The work presented in this report was done in addition to the initially planned workpackages C and I, which were under the responsibility of Imerys.
The extra work conducted by Imerys consisted in characterizing the clays calcined at pilot scale, with the goal of contributing to the interpretation of the results obtained in the other workpackages, where the performance of the calcined clays was evaluated in mortars and concretes.
The results presented here will be compared and combined to the data generated by the other partners, in order to get the most complete and accurate set of properties for each of the pilot calcined clays.

2. Experimental procedure

2.1. Materials

The six pilot calcined clays and their respective description are presented in Table 1. In addition, the dry clay added to the RC2 and RC3, in order to obtain an acceptable humidity degree prior to their calcination in the rotary kiln, was also characterized.

Table 1: Pilot calcined clay and raw clay samples

Samples	Description
CC2-F	Imerys’ RC2 calcined in a flash kiln
CC2-R	Imerys’ RC2 calcined in a rotary kiln
CC3-R	Imerys’ RC3 calcined in a rotary kiln
CC7-F	Heidelberg’s RC7 calcined in a flash kiln
CC9-F	Tarmac’s RC9 calcined in a flash kiln
CC9-R	Tarmac’s RC9 calcined in a rotary kiln
Polwhite	Raw clay added to RC2 and RC3 prior to rotary calcination

More details about the preparation of the calcined clays can be found in the reports dedicated to the pilot trials.

2.2. Methods

The pilot calcined and milled clays were received at the Imerys laboratory, and analysed as such, except for the XDR analysis, for which the samples were milled under 100µm.

The samples were characterized by:

- **Loss on ignition (LOI)**, by heating the samples at 950°C for 60 minutes.
- **X-ray fluorescence**, using a Panalytical Zetium, with glass disc samples, to quantify their chemical composition.
- **X-ray diffraction**, using a Bruker D8 Advance diffractometer and the TOPAS V6 software, to quantify their mineralogical composition. The internal standard method was used to quantify the amorphous phases.
- **Dry laser granulometry**, using a Malvern Mastersizer 3000 and a 3-bar pressure, in order to measure their grain size distribution.
- **Specific surface area by BET**, using a Belsorp Max X device.
- **Colorimetry**, using a X-Rite Ci4200, to evaluate their colour.

Besides the intrinsic characterization of the clays, an applicative test was also carried out. The calcined clays were combined to Portland cement and limestone to compose LC3-type binders, which were then tested in mortars, having their strengths measured following the EN 196-1.
The binder and mortar compositions are presented in Table 2 and Table 3, respectively.

Table 2: LC3-type binder composition

	(%)
CEM I 52.5N	30
Limestone	60
Calcined clay	10

Table 3: EN 196-1 mortar composition

	(%)
LC3-type binder	25
Standard sand	75
water/binder	0.5

3. Results and discussion

3.1. Chemical composition by X-ray Fluorescence (XRF)

The LOI and the chemical composition of the pilot calcined clays are presented in Table 4.

Table 4: LOI and chemical composition by XRF

%	LOI	SiO_2	Al_2O_3	Fe_2O_3	CaO	MgO	K_2O	Na_2O	P_2O_5	SO_3	MnO	TiO_2	Sum (w/o LOI)
CC2F	2,1	57,2	33,0	2,6	0,2	0,4	4,8	0,3	0,1	0,0	0,0	0,2	99,0
CC2R	0,8	55,9	36,2	1,7	0,1	0,4	4,3	0,3	0,1	0,0	0,0	0,1	99,1
CC3R	0,8	55,1	38,3	1,2	0,2	0,3	3,5	0,2	0,1	0,0	0,0	0,1	99,1
CC7F	0,8	59,6	22,1	7,6	2,5	1,7	3,0	0,3	0,3	1,2	0,5	1,1	99,9
CC9F	1,3	63,4	21,6	8,8	2,0	0,9	1,2	0,2	0,1	0,1	0,0	1,2	99,4
CC9R	1,1	61,9	22,5	8,6	2,2	1,1	1,5	0,2	0,1	0,2	0,1	1,2	99,6

Despite the calcination they went through, all the clays still present some loss on ignition (at 1000°C). It can be due to some residual uncalcined clays phases, to phases that decompose at temperatures higher than those of the calcination process (around

800-850°C), or simply to the humidity captured by the clays after calcination.
The results on the chemistry of the pilot calcined clays are in line with the previous analysis made on the raw and laboratory calcined samples, carried out in the workpackage C.
CC2 and CC3 have higher alumina contents, while CC7 and CC9 have more iron and calcium. All the clays, with the exception of CC9, have relatively high potassium contents, which is related to the presence of clays phases.

A gap of 3% in the alumina content is observed between the CC2F and the CC2R. This can be explained by the addition of Polwhite in the rotary kiln feed used to produce the CC2R. Indeed, in order to reach the maximal humidity level acceptable in the rotary kiln, RC2 and R3 needed to be mixed with around 20% of the dry raw clay Polwhite. This product consists in a kaolinitic clay with relatively high alumina contents, which led to the slightly superior alumina in the rotary calcined clays.
The RC9 had a good level of humidity and could be calcined in the rotary kiln without the addition of Polwhite. The small difference in chemistry between CC9F and CC9R can be attributed to the chemistry variations within the batch of raw clay, and to the uncertainty of the XRF method.
The flash calciner imposes no limit on the humidity, so no additions had to be made to the flash clays.

3.2. Mineralogical composition by X-ray diffraction (XRD)

The mineralogy of the calcined clays is presented in Table 5. The amorphous phases were quantified by the internal standard method, and include the metakaolin and eventually other amorphous or badly crystallised minerals.

Table 5: Mineralogical composition by XRD

%	**CC2F**	**CC2R**	**CC3R**	**CC7F**	**CC9F**	**CC9R**
Amorphous phases	46	46	70	47	50	46
Muscovite	26	31	13	14	12	13
Quartz	11	8	3	26	35	34
Feldspar	14	14	13	9	0	1
Anatase + Rutile	0	0	0	1	1	2
Hematite	1	1	0	2	1	4
Magnetite	0	<0.1	<0.1	1	1	0
Mullite	2	nd	nd	nd	nd	nd
Anhydrite-II	nd	nd	nd	1	nd	nd

Because of the difficulties of quantifying amorphous phases in the XRD, the precision of the results is smaller than that usually obtained for completely crystalline materials. Nevertheless, the XRD gives an indication of the amount of potentially reactive phases and of the impurities present in the clays.

With the exception of CC3R, all the samples have similar amounts of amorphous phases. As the alumina content of CC2 is superior to that of CC7 and CC9, it is expected that the first clay contains more metakaolin, the two last probably containing other meta-clays and perhaps other amorphous minerals.

CC2F and R have high amounts of muscovite, a clay phase that can increase the water demand of the material.

CC7 and CC9 have high amounts of quartz, a hard mineral that can impact on the grindability of these clays, and thus to their particle size distribution after milling. The feldspar, present in most of the samples, can have a similar effect on the grindability.

As seen with the XRF, all the clays contain some iron, which is observed by XRD in the form of hematite (red) and magnetite (black). The two clays that underwent the colour control process in the flash calcination, CC7F and CC9F, have the higher magnetite contents. This observation is coherent with the working principle of the colour control method, which consists in controlling the cooling atmosphere to prevent the conversion of magnetite to hematite, ensuring the clay has a more greyish tone.

Nevertheless, during the preparation of the samples, it was observed that the flash calcined clays presented some large particles (above 100µm) which are likely composed of hematite (dark red colour).

In CC2F, some mullite was detected, indicating a slight overcalcination (mullite being formed when metakaolin is heated above 1100°C). No traces of raw clays were detected, indicating that the calcination was completed for all the samples.

3.3. Colourimetry

The L*a*b* colour coordinates of the pilot calcined samples are shown in Table 6.

Table 6: Colour in L*a*b* coordinates

	CC2F	**CC2R**	**CC3R**	**CC7F**	**CC9F**	**CC9R**
L* (brightness)	72,4	78,4	83,6	43,7	38,8	42,6
a* (green to red)	1,8	2,0	1,8	4,1	5,9	27,4
b* (blue to yellow)	7,5	8,2	8,2	8,3	18,8	45,4

All the samples tend to reddish (positive a* values) and yellowish (positive b* values) tones, CC2F, CC2R and CC3R being the lighter ones (higher L* values). This result is certainly related to their lower iron content.

The effect of the colour treatment in the flash calcination can be observed when comparing CC9F and CC9R. The flash clay has lower a* and b* values, having a colour much closer to dark grey, which is clearly visible in Figure 1.

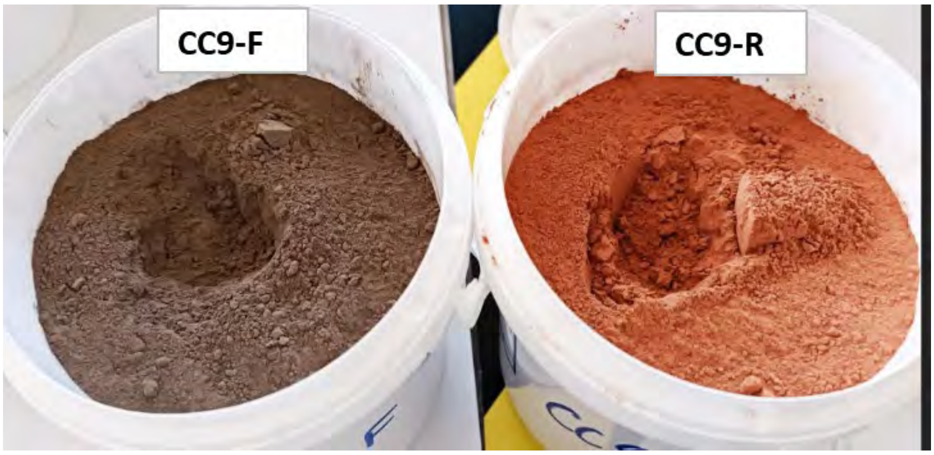

Figure 1: Colour of flash calcined (left) and rotary calcined (right) CC9

3.4. Particle size distribution by laser granulometry

The characteristic percentile values of the granulometry of the pilot calcined clays are presented in Table 7, and the PSD in Figure 2.

Table 7: d(10), d(50) and d(90) by dry laser granulometry

Samples	d(10)	d(50)	d(90)
CC2-F	3,88	20	74
CC2-R	1,34	7,6	30
CC3-R	0,89	4,4	16
CC7-F	1,26	16	73
CC9-F	1,29	17	75
CC9-R	1,33	9,4	40

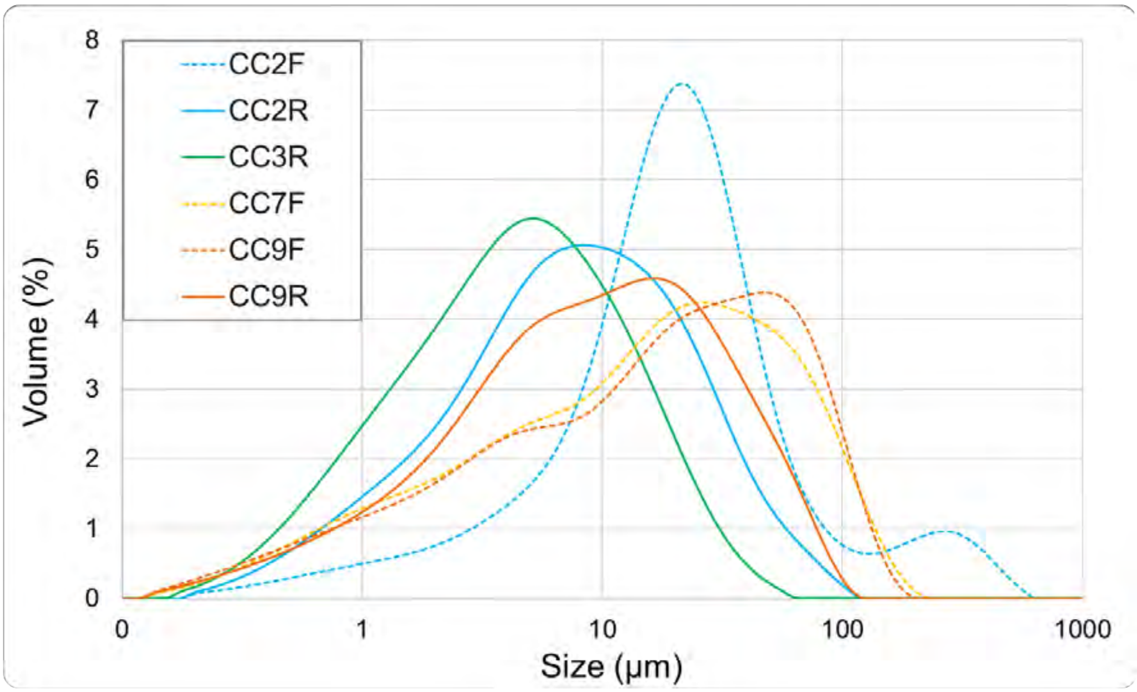

Figure 2: Particle size distribution by dry laser granulometry

The rotary calcined clays, which were milled at Imerys' facility in Lixhe, are finer than the flash calcined ones, milled by FLSmidth. It can be observed both when comparing the d(X) values and in the PSD in the chart above, where the rotary clays are represented in continuous lines and the flash one in dashed lines.

This finer granulometry could result in higher reactivity of the clays but also higher water demands and more difficulty to disperse the particles in mortars and concretes. These characteristics are to be evaluated in the work carried out by the partners.

CC2F is a particular case, as this sample didn't need any milling. It was considered as already fine enough at the exit of the flash calciner, but, as it can be observed by its d(10) and the PSD, it contains a little less of fines and a little more of coarse particles than the two other flash clays, which underwent a milling step and present a very similar PSD.

The clays milled in Lixhe have a monomodal but quite dispersed PSD, with an overall fineness that differs for each sample, CC3R being the finer material, and CC9R being the coarser. This could be related to the softness of the clays which depends on the impurities present.

3.5. Specific surface by BET

The specific surface of the samples measured using the BET method are given in Table 8.

Table 8: Specific surface by BET

	CC2F	CC2R	CC3R	CC7F	CC9F	CC9R
SS BET (m2/g)	6,9	6,0	7,0	17,7	11,8	17,7

The specific surface of the pilot calcined clays seems to depend more on the nature of the clay than on the process of calcination. The CC2F, CC2R and CC3R have relatively low surfaces, the remaining clays have higher ones.

In the case of CC2, the flash calcined material has a slightly higher surface than the rotary calcined one, despite its lower fineness. The dilution of the RC2 with Polwhite to produce CC2R could explain this observation, as Polwhite may present a lower specific surface.

For the CC9, the rotary material has a significantly larger surface than the flash one. It could be related to the higher fineness of the CC9R, but also to the phases formed during the calcination, which are not exactly the same, as observed by XRD.

As for the PSD, the specific surface can affect the reactivity and the water demand of the clays. It remains to be evaluated in the mortar and concrete tests.

3.6. Strengths in low carbon mortar

The 6 pilot calcined samples were used in a limestone calcined clay cement (LC3) configuration, combining 30% Portland cement, 10% calcined clay and 60% limestone, in order to obtain very low carbon binders.

The binders were then tested in standard mortars according to EN 196-1, with the goal of evaluating their compressive strength development.

This test comes in complement to the much larger work carried out by our partners both in mortar and concrete formulations, where binary and ternary binders composed with the calcined clays were tested. The binders evaluated in the other workpackages had all much higher Portland cement and calcined clays contents, complying with the existing CEM classes. Here we seek a first indication on how the calcined clays would behave in systems with lower “active binder” amounts.

The compressive strength results for the mortars formulated with each of the pilot calcined clays are presented in Figure 3.

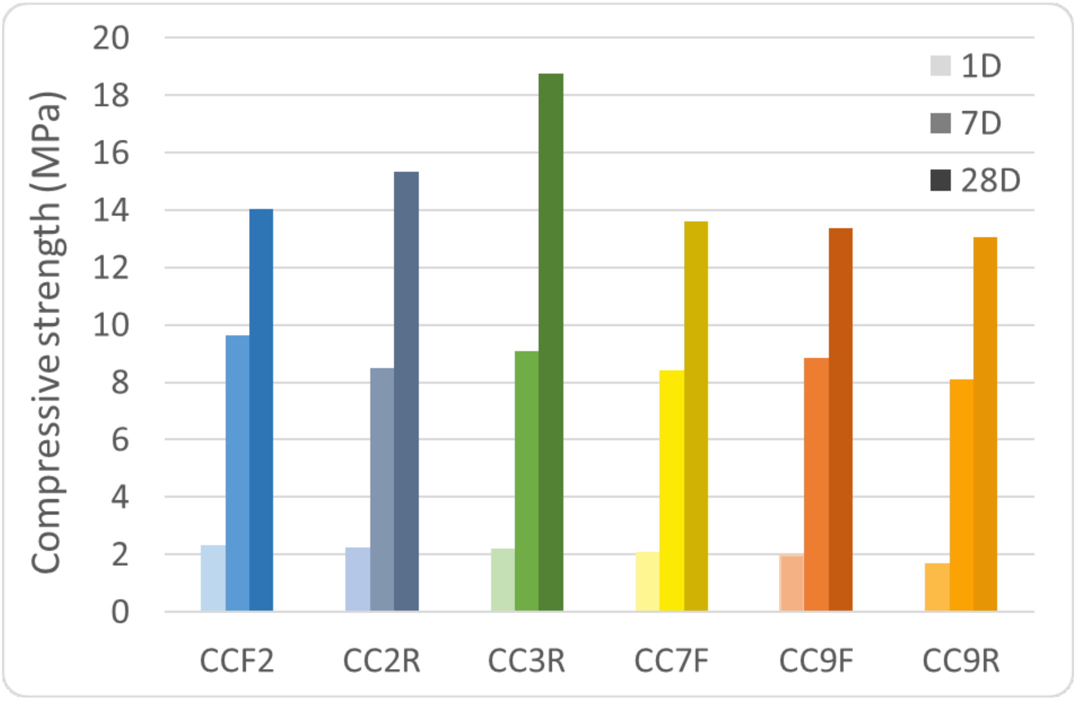

Figure 3: Compressive strengths in low carbon mortars

The overall strengths are relatively low, compared to CEM I and more conventional binders, which is expected given the reduced amounts of active materials in the binder composition (which contains 60% of relatively inert limestone). Low carbon binders such the one tested here are intended to be used in different configurations, including lower water/binder than the one imposed by the EN 196-1, of 0.5.

The results obtained here remain interesting, however, allowing the performance of the different calcined clays to be compared.

The 1-day strengths are similar to all the mortars, as at this age the clays are not expected to react to a significant degree. After 7 days some differences start to be seen, and become more visible at 28 days. The mortar containing CC3R reaches the higher strengths, followed by CC2R and the remaining clays.

There are certainly many characteristics of the clays which influence their reactivity and resulting obtained strengths. One frequently mentioned in the literature is the alumina content in the clay.

Figure 4 shows the strengths in function of the alumina contents measured by XRF. When considering CC2F, CC2R and CC3R, there seems to exist a relatively linear correlation between the two parameters, but the three other clays fall out of the trend, generating more strengths than what could be expected from their lower alumina content.

This observation must be compared to the results obtained with the binders tested by our partners, to verify if a similar behaviour is observed when higher amounts of clay are present.

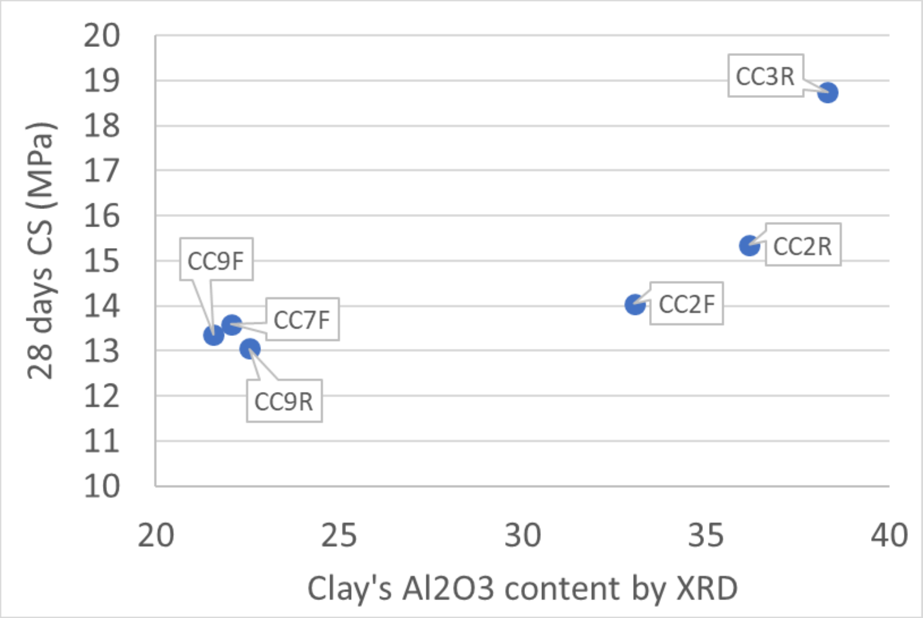

Figure 4: 28d strengths x Al_2O_3 content

4. Conclusion

The calcined clays prepared in the pilot trials have properties according to the expectations. Their calcination level seems to be adequate, with no residual raw clay and no or very little overcalcined clays being detected on the samples.

The milling of the flash calcined samples resulted in a consistent fineness, CC7R and CC9R having very similar PSD. The rotary milled samples have a slightly more dispersed granulometry, and are a little bit finer than the flash ones. The fineness of the clays may affect their reactivity and water demand, so the results obtained here must be cross-referenced with the results obtained with the mortar and concrete tests. The same observation can be made related to the specific surface as measured by BET, which showed significant differences between the clays that cannot be explained by the PSD.

The colourimetry results indicate that the clays with lower iron content have lighter colours, but also that the colour control process, used in the flash calcination, can convert the reddish colour of iron rich clays into a more habitual grey tone.

Finally, the applicative tests in very low carbon mortars showed that the clays with higher alumina content led to slightly higher strengths. These results are also to be compared to the ones obtained with the binders containing more Portland cement and calcined clays, tested in the other workpackages.

The properties of the pilot calcined clays determined in the present study are in line with the ones of the laboratory calcined clays prepared by Imerys in the workpackage C, indicating that a screening study at laboratory scale is pertinent to assess clay samples potential.

FORTERRA

Re-C3: Reclaimed Calcined Clay Cements

Appendix 9 -
Determination of Kaolinite Content of Raw Clays

Analytical methodology to determine the kaolinite content, along with other clay species in the raw clays.

Authors
Dr Andrew Smith (Forterra)

Date: March 2024

Executive Summary

Many researchers working in the field of calcined clays typically use a measured kaolinite content in the raw clay to determine whether or not the material is suitable or not. The Bureau of Indian Standards have recently published a Calcined Clay raw materials standard that clearly states a minimum threshold of 40% kaolinite, and a methodology for measuring the kaolinite content of the raw clay. (Bureau of Indian Standards, 2023).

The purpose of this report is firstly to critically assess the commonly used techniques used to measure, or more accurately, estimate, the kaolinite content, and highlight how it is possible to misinterpret analytical results when used in isolation, especially the interpretation of Thermogravimetric Analysis (TGA) weight loss curves, without taking into account the complex nature of many mixed clay materials, and the fact that other clay and none clay minerals also loose weight within the temperature range associated with dehydroxylation of kaolinite. A simple use of the weight loss within the 400-650°C, or 300-750°C, may therefore overestimate the kaolinite content.

The use of techniques such as X-ray Diffraction and X-ray Fluorescence in combination, it is possible to generate a Normative Mineralogy, which is an approximation to quantitative X-ray Diffraction. It uses the chemistry as building blocks of chemical elements to logically build the known minerals present. The result of that process is presented within this report and has been successfully deployed to make sense of complex mixed clay mineral assemblages.

As a sense check, the results from the TGA have been used to correlate the measured weight losses between 400-650°C and the Normative Mineralogy. The results show that within a range of ±10% weight loss it is possible to get a reliable value for the clay mineral contents of the raw clays, and thus validates the values for clay mineral content, especially kaolinite, used in this project.

This then highlights that fact that, with the exception of RC1-5, the kaolinite contents of the clays by TGA alone, is unreliable. It also highlights that the overall reactivity of the calcined clays, even those with <40% kaolinite, have shown significant pozzolanic reactivity, and thus setting a threshold that:

a) kaolinite is the only reactive “meta” clay mineral, and
b) may not truly reflect the kaolinite content of a sample,

may not be valid. This therefore suggests that a more pragmatic and potentially more accurate measure of the reactivity of raw clays, once calcined, is to use a performance-based testing approach, rather than prescriptive (kaolinite >40%), as is presented in the Indian Standards (2023).

Contents

1. Introduction

One of the primary objectives of the Re-C3 project has been to investigate potential clay resources and arisings that are either lower grade by-products of the production of high purity kaolinitic China and Ball Clays (Imerys), mixed clays from sites that are currently not utilised, such as interburden, and materials derived from the processing of fired waste brick production.

Previous work on calcined clays and associated reactivity has identified that kaolinitic clays are the most reactive, and that illitic and montmorillonitic clays are less so, Fernandez *et al* (2011) and Hollanders *et al* (2016). He *et al* (1985) and Ambrose *et al* (1985) have proposed that the reactivity of kaolinite is heightened due to the way that they dehydroxylate during the conversion from kaolinite to metakaolin. The crystal structure, and specifically the coordination number of Al from Al^{VI} to Al^{IV} and Al^{V}, generated structural disorder. When compared to illite and montmorillonite structures, the hydroxyl and aluminate groups are at the surface of the kaolinite structure, resulting in the Al^{V} groups being directly exposed to the conditions adjacent to the metakaolin and thus can easily react. It is thought that this is why kaolinite, in the form of metakaolin, has the higher pozzolanic potential amongst the clay mineral species.
Much of the more recent work by researchers, specifically that investigating the Limestone-Calcined Clay Cements (LC3), has therefore focussed on kaolinitic rich clay deposits, and in some cases, National Standards, such as the Bureau of Indian Standards, IS 18189 (2023), now define raw clays suitable for conversion into calcined clays as *“A clay with at least 40 percent kaolinite content activated through thermal calcination.”.*

Whilst kaolinitic rich clays do show high levels of reactivity, once calcined to form metakaolin, it has long been thought that other clay deposits, not classed a kaolinite rich, also have potential as pozzolanically active calcined clays, when used as Supplementary Cementitious Materials (SCM’s) in the replacement of clinker in cements.

If there is a perceived requirement to link calcined clay pozzolanic reactivity to raw clay type, there is a need to accurately identify the mineralogy of the raw clay resource, not only to specifically be able to quantify the clay mineral content (total clay content), but also to be able to speciate the clay mineral content into one or more of the 4 main clay mineral groups; kaolinite, illite, montmorillonite and chlorite.
This report explains some of the common analytical techniques used to determine kaolinite content used by researchers in this field, as well as the general mineralogy and chemistry for raw clays, and highlights some of the potential difficulties in accurately quantitatively determining the kaolinite and other clay mineral content.

2. Analytical Techniques for Determining the Mineralogy of Clay Raw Materials.

There are three principal techniques widely used to identify the mineralogy of clay deposits, X-ray Diffraction (XRD), X-ray Fluorescence (XRF), and Thermogravimetric Analysis. The use of all three combined provides the most reliable determination, especially of the clay mineral species.

2.1. X-ray Diffraction (XRD)

X-ray diffraction (XRD) is a versatile non-destructive analytical technique used to analyse physical properties such as phase composition, crystal structure and orientation of powder, solid and liquid samples.

Minerals, such as those found in clay deposits are made up of tiny crystallites. The chemical composition and structural type of these crystals defined the type of mineral 'phases' present. Mineral deposits are rarely single-phase, often containing 2 or more minerals (multiphase mixtures) and may contain crystalline and non-crystalline components. In the case of calcined clay, the mineral kaolinite found in the raw clay is crystalline, whilst the metakaolin produced by calcination is “amorphous” and has no crystalline structure.

In an X-ray diffractometer, different crystalline phases give different diffraction patterns, similar to a unique fingerprint. Mineral phase identification can be performed by comparing X-ray diffraction patterns obtained from unknown samples to patterns in reference databases. The most comprehensive database being the ICDD (International Center of Diffraction Data).

The relative strengths of the patterns from different mineral phases in a multiphase mixture are used to determine the full composition of a sample, either qualitatively (what phases are present) or quantitatively (by using internal standards or by using algorithms such as the Rietveld technique).

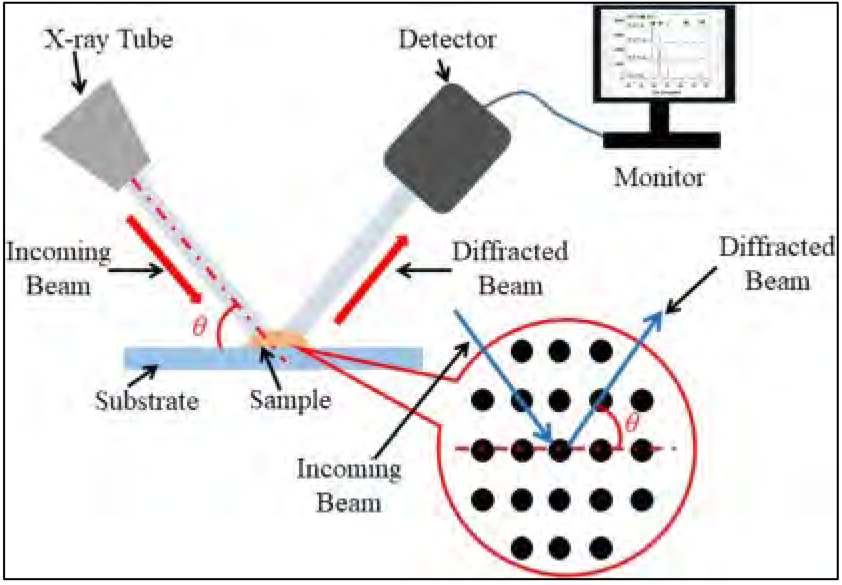

Figure 1. X-ray diffraction schematic showing the relationship between the X-ray source (tube) and the detector, giving the 2θ angle which is used to identify the crystal

structure and thus the mineral phase present.

The X-rays produced by the source (typically CuKα), illuminate the sample, similar to a beam of light, as shown in Figure 1.. It is then diffracted by the sample phase and enters the detector. By moving the source or sample and detector to change the diffraction angle (2θ, the angle between the incident and diffracted beams), the intensity of the diffraction is measured, and recorded. The position (2θ angle) and intensity (peak height), when plotted as a trace, indicates the position of crystal structures in the sample, as “peaks”. As each mineral is made up of a number of peaks at specific angles, these can be used to identify the mineral phases present.

2.2. X-ray Fluorescence (XRF)

“XRF (X-ray fluorescence) is a non-destructive analytical technique used to determine the elemental composition of materials. Similar to XRD, XRF analysis determines the chemistry of a sample by measuring the fluorescent (or secondary) X-rays emitted from a sample when it is excited by a primary X-ray source. Each of the elements present in a sample produces a set of characteristic fluorescent X-rays (“a fingerprint”) that is unique for that specific element, which is why XRF spectroscopy is an excellent technology for qualitative and quantitative analysis of material composition.

When a solid (powder or fusion bead) sample is irradiated with high energy X-rays from a controlled X-ray tube, and an atom in the sample is struck with an X-ray of sufficient energy (greater than the atom’s K or L shell binding energy), an electron from one of the atom’s inner orbital shells is dislodged.

The atom regains stability, filling the vacancy left in the inner orbital shell with an electron from one of the atom’s higher energy orbital shells. The electron drops to the lower energy state by releasing a fluorescent X-ray. The energy of this X-ray is equal to the specific difference in energy between two quantum states of the electron. The measurement of this energy is the basis of XRF analysis.

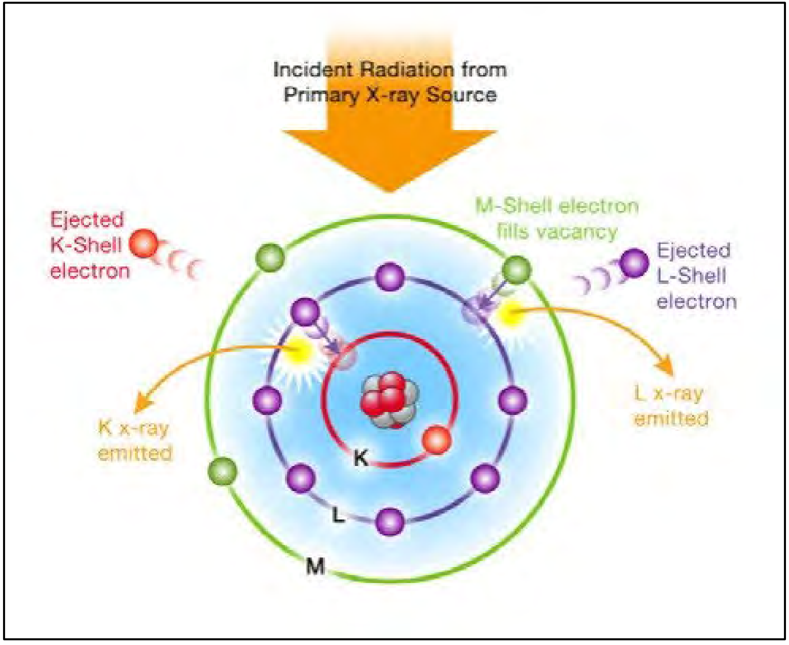

Figure 2. Diagrammatic representation of the generation of secondary (fluorescent) X-rays as a result of bombardment with X-rays from a primary source. (Diagram taken from *ThermoFisher Scientific* web page).

Most atoms have several electron orbitals (K shell, L shell, M shell, for example). When X-ray energy causes electrons to transfer in and out of these shell levels, XRF peaks with varying intensities are created and will be present in the spectrum, a graphical representation of X-ray intensity peaks as a function of energy peaks. The peak energy identifies the element, and the peak height/intensity is generally indicative of its concentration.” (Adapted from ThermoFisher Scientific web page https://www.thermofisher.com/blog/ask-a-scientist/what-is-xrf-x-ray-fluorescence-and-how-does-it-work/#:~:text=composition%20of%20materials.-,XRF%20(X-ray%20flu last accessed 26/02/24)

2.3. Thermogravimetric Analysis (TGA)

Thermogravimetric Analysis (TGA) is a technique in which the mass of a substance is monitored as a function of temperature or time as the sample specimen is subjected to a controlled temperature program in a controlled atmosphere.

A TGA consists of a sample pan/holder that is supported by a precision balance. That pan resides in a furnace and is heated or cooled during the experiment. The mass of the sample is monitored during the experiment. A sample purge gas controls the sample environment. This gas may be inert (eg Nitrogen) or a reactive gas (air or oxygen) that flows over the sample and exits through an exhaust.

These instruments can quantify loss of weight through the heating cycle typically resulting in the loss of water, pyrolysis, oxidation, and mineral decomposition. All these quantifiable applications are usually done upon heating through a specific temperature range, for minerals in high temperature applications this can be from ambient to 1200°C.

The output from a TGA apparatus is normally a graphical plot showing weight loss over temperature, as shown in Figure 3. The abscissa (X-axis) can be displayed as time or temperature and the ordinate (Y-axis) can be displayed as weight (mg) or weight percent (%).

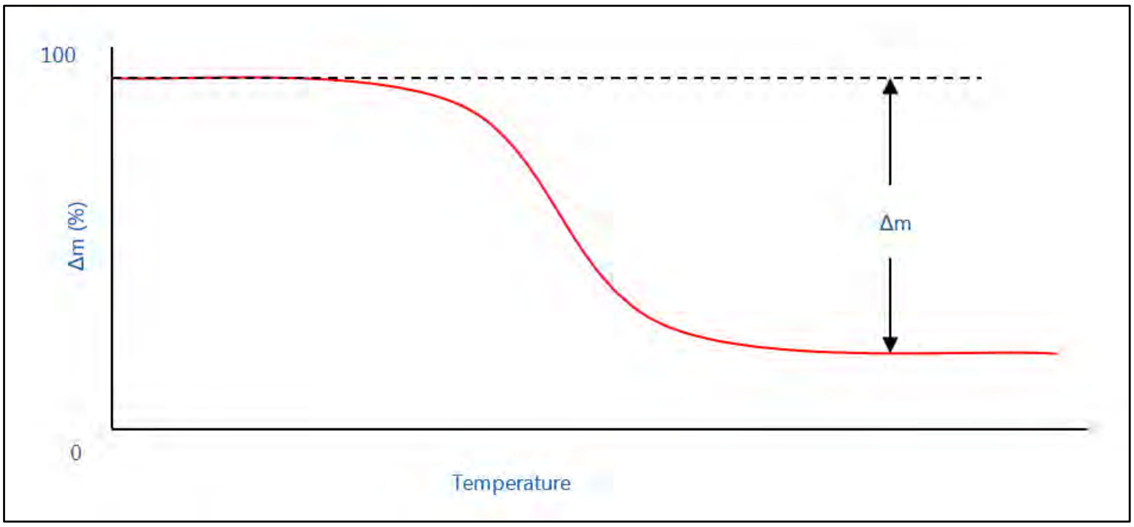

Figure 3. Typical thermogravimetric result curve (taken from Linseis.com web pages)

With the majority of minerals the weight loss is over a specific defined temperature range, the peak activity, or greatest rate of weight loss is indicated by the steepness of the curve, however the use of another thermal analysis technique, such as Differential Thermal Analysis (DTA) or Differential Scanning Calorimetry (DSC) run at the same time, or on the same sample, can identify the "peak activity", which similar to XRD and XRF provides traces that are like fingerprints, and help the analyst identify what minerals are reacting at any given time.

3. Assessment of the Re-C3 Project Raw Clays

At the start of the project 10 clay based potential raw materials were put forward by the project's industry partners, along with a fired clay brick waste from Forterra. The 10 clays are identified in Table 1, coded RC 1-10, RC standing for Raw Clay (as opposed to CC for Calcined Clay).

The clays vary from China Clays from the Southwest of England dominated by the kaolinite rich deposits associated with the in-situ weathering of the Cornubian Batholith Granites, and the sedimentary kaolinitic Ball Clay deposits in the Newton Abbot region of Devon, to more mixed clays associated with both the Jurassic clays of the East of England and the Carboniferous Shales from the Midlands and Northern Ireland.

Table 1. Raw clays selected for the Re-C3 Project

ID of Raw Clay	Source	Geological Setting
RC1	Imerys	China Clay
RC2	Imerys	China Clay
RC3	Imerys	China Clay
RC4	Imerys	China Clay
RC5	Imerys	Ball Clay (Lignitic)
RC6	Heidelberg UK Clay	Jurassic Clay
RC7	Heidelberg UK Clay	Jurassic Clay (Upper Lias)
RC8	Tarmac Clay	Jurassic Clay (Kellaway)
RC9	Tarmac Clay	Carboniferous Marl
RC10	Aggregates Industry Clay	Carboniferous Shale
KDRC	Forterra Clay	Jurassic (Lower Oxford Clay)

In order to understand the mineralogy of each of these raw clays, analysis was undertaken by a number of parties, including UCL, Imerys and Forterra, and reported separately in associated Reports and Appendices for this project. However, due to the variances with the interpretation of the results of the XRD and TGA, it was agreed that a summary report, (this report) should be produced in order to explain the specific challenges that this brings.

3.1. X-ray Diffraction Results

As part of the project both UCL and Imerys undertook qualitative x-ray diffraction

(XRD) analysis of dried powdered samples of the 10 raw clays under investigation (Table 2). In addition, Imerys undertook quantitative analysis using Rietveld modelling (Table 3).

Table 2. Qualitative X-ray Diffraction mineral content (Major (M), Minor (m), Trace (t))

Samples	Kaolinite	Illite	Montmorillonite	Chlorite	Quartz	Feldspar	Calcite	Pyrite	Hematite	Muscovite	Schorl (Tourmaline)
RC1	M				M	M				M	t
RC2	M				M	M				M	t
RC3	M				m	M					t
RC4	M				m	M		t			
RC5	M	M			m			t	t		
RC6	M	M			M	m	t	t	t		
RC7	M	M		m	M	m			t		
RC8	M	M		m	M	M			t		
RC9	M	M		m	M	M			t		
RC10	M	M		m	M	M	t		t		

Note: As a guide, the terms Major >5%, Minor 2-5%, Trace 0-2% apply.

Table 3. Quantitative XRD results provided by Imerys using Reitveld Modelling.

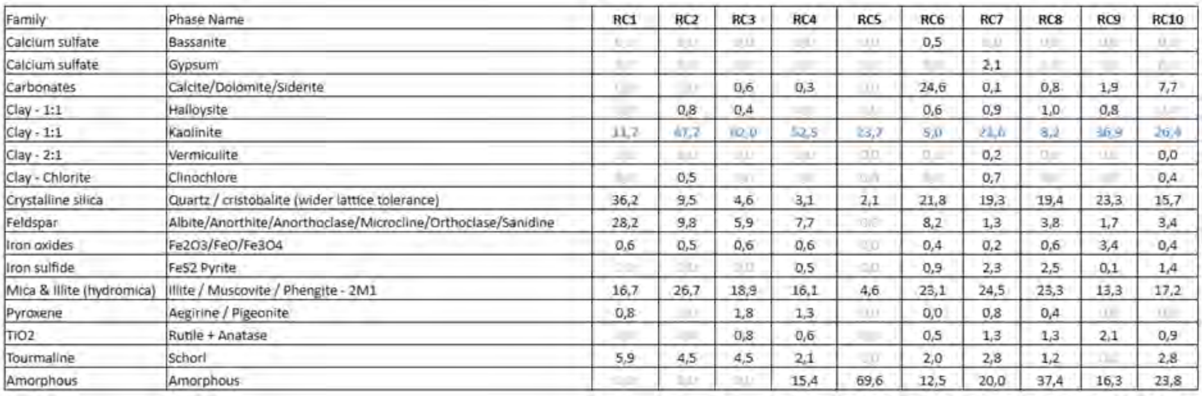

Family	Phase Name	RC1	RC2	RC3	RC4	RC5	RC6	RC7	RC8	RC9	RC10
Calcium sulfate	Bassanite						0,5				
Calcium sulfate	Gypsum							2,1			
Carbonates	Calcite/Dolomite/Siderite			0,6	0,3		24,6	0,1	0,8	1,9	7,7
Clay - 1:1	Halloysite		0,8	0,4			0,6	0,9	1,0	0,8	
Clay - 1:1	Kaolinite	11,7	47,2	60,0	52,5	23,7	5,0	21,6	8,2	36,9	26,4
Clay - 2:1	Vermiculite							0,2			0,0
Clay - Chlorite	Clinochlore		0,5					0,7			0,4
Crystalline silica	Quartz / cristobalite (wider lattice tolerance)	36,2	9,5	4,6	3,1	2,1	21,8	19,3	19,4	23,3	15,7
Feldspar	Albite/Anorthite/Anorthoclase/Microcline/Orthoclase/Sanidine	28,2	9,8	5,9	7,7		8,2	1,3	3,8	1,7	3,4
Iron oxides	Fe2O3/FeO/Fe3O4	0,6	0,5	0,6	0,6		0,4	0,2	0,6	3,4	0,4
Iron sulfide	FeS2 Pyrite				0,5		0,9	2,3	2,5	0,1	1,4
Mica & illite (hydromica)	Illite / Muscovite / Phengite - 2M1	16,7	26,7	18,9	16,1	4,6	23,1	24,5	23,3	13,3	17,2
Pyroxene	Aegirine / Pigeonite	0,8		1,8	1,3		0,0	0,8	0,4		
TiO2	Rutile + Anatase			0,8	0,6		0,5	1,3	1,3	2,1	0,9
Tourmaline	Schorl	5,9	4,5	4,5	2,1		2,0	2,8	1,2		2,8
Amorphous	Amorphous				15,4	69,6	12,5	20,0	37,4	16,3	23,8

The qualitative results are shown in Table 2 and demonstrate that there is a clear distinction between the Imerys clays RC1-5 and the 5 other clays supplied by Heidelberg, Tarmac and Aggregate Industries. The key difference being that the Imerys clays are all derived from their operations in SW England, “China Clay” operations in Devon/Cornwall (RC1-4) or from their Ball Clay operations in Devon (RC5). These clays are dominated by kaolinite and relic minerals that have not weathered from the host granites, namely, quartz, feldspars muscovite mica and shorl (tourmaline).

The 5 other clays are of mixed ages, RC6-8 are Jurassic in age and come from deposits in the East of England, whilst RC9-10 are of carboniferous age and are from the Midlands and Northern Ireland. These show classic mineralogy's associated with these clay deposits, typically mixed clays with kaolinite, illite montmorillonite and chlorite in varying amounts, again associated with none clay minerals such as quartz, feldspars, carbonates and iron bearing minerals, typically hematite, but occasionally pyrite.

There results show some anomalies with what would typically be expected with specific mineral assemblages for these different clay deposits. The Imerys clays are very accurate and reflect the typical materials that pass through the Imerys lab, however the clays RC6-10 are of lower precision due to the complexity of the mineral assemblages present, and probably the lack of experience of the Imerys XRD operators with these mixed clay deposits. Minerals such as Tourmaline are not found in the Jurassic and Carboniferous clays, and differentiating between illite and the mica muscovite is difficult as they have a very similar dominant platy crystalline structure. There is therefore a significant reliance placed on the experience and knowledge of the XRD operator/interpreter in order that a viable and accurate mineral assemblage is reported.

3.2. X-ray Fluorescence Results

Unlike XRD which can be “subjective”, and the results open to interpretation, XRF provides an absolute, in analytical terms. XRF analysis was undertaken by Imerys, and the results reported in Table 4. The major element oxide chemistry of the raw clays, as is to be expected, is dominated by alumina and silica, reflecting the dominant alumino-silicate minerals present in the materials. The primary alkali is predominantly potassium, which is typically associated with illite, muscovite mica and potassic feldspars. RC6, RC10 and KDRC all have elevated levels of calcium which is commonly associated with calcite and dolomite (carbonates) as well as present in some feldspars and in calcium montmorillonite.

The only other major elemental oxide is that of iron, and although low in the RC1-5 samples, ranges from 4.5% to 8% in the other materials. Iron is present in many mixed clay deposits, typically as iron oxides or hydroxides, but can also be present in chlorite clay minerals, as well as in pyrite, and iron sulphide, especially in “black anoxic” type clay deposits such as RC6-8 and KDRC.

Table 4. X-ray Fluorescence Major Element Oxide Chemistry of the Raw Clays (Courtesy of Imerys)

Samples	LOI	Al_2O_3	SiO_2	K_2O	Fe_2O_3	TiO_2	CaO	MgO	Na_2O	P_2O_5
RC1	2.50	16.00	73.30	5.30	1.60	0.10	0.10	0.30	0.60	0.13
RC2	8.70	31.90	52.70	4.20	1.50	0.10	0.10	0.40	0.30	0.10
RC3	10.50	34.50	50.00	3.00	1.20	0.00	0.10	0.40	0.20	0.13
RC4	10.90	35.10	49.40	2.90	1.00	0.10	0.10	0.40	0.20	0.11
RC5	54.70	18.30	23.60	0.80	1.40	0.40	0.40	0.20	0.10	0.03
RC6	14.20	11.60	47.80	2.60	5.00	0.70	15.30	2.40	0.30	0.12
RC7	10.90	21.70	52.50	2.80	7.30	1.00	1.30	1.80	0.30	0.31
RC8	10.00	20.90	55.30	2.40	6.70	1.20	1.70	1.30	0.30	0.20
RC9	9.20	23.90	53.50	1.20	8.00	1.10	1.70	1.10	0.30	0.08
RC10	11.90	22.10	48.90	1.70	7.80	0.90	4.00	1.90	0.40	0.26
KDRC	18.14	16.14	47.80	2.63	4.61	0.84	7.67	1.46	0.49	0.17

In addition to the elemental oxides, the other key feature of the XRF data sets are the values for LOI, (Loss on Ignition). This value is the weight loss measured when a sample is dried at 105°C to give a dry weight. This is done to remove all the absorbed water content. The sample is then heated in a kiln to typically 950°C or 1000°C in order to drive off all the volatiles, which include CO_2 from the organic carbon, CO_2 from carbonates, H_2O, OH, and F from clay minerals, and SO_2 from pyrite. The resulting weight loss can therefore be used in the same way as the major elemental oxides, to understand what the likely mineral assemblages are present in the materials being tested.

In the absence of accurate quantitative XRD, there is another way to model the mineral assemblage of a given sample, based on the XRD and XRF data. The combined use of XRD and XRF results for each raw clay can be used to calculate a “Normative Mineralogy” based on a simple principle, minerals generally have a reasonably well-defined chemistry, each element is present in roughly defined quantities. By identifying what minerals are present by qualitative XRD, you can use the XRF data as building blocks to create these mineral assemblages. This has been undertaken as part of this project and presented here in Section 4 of this report.

3.3. Thermogravimetric Analysis Results

Thermogravimetric Analysis (TGA) is another “absolute” determinator test method. The technique, as discussed in Section 2.3 of this report, measures the weight loss as a result of a sample achieving a certain temperature during a controlled ramp firing. The weight loss at any given temperature is an aggregate of all mineral transformations taking place at that time/temperature, which could include reactions such as, combustion of organic carbon, dehydroxylation (loss of OH as water vapour), or the degassing of calcite, releasing CO_2.

During the raw material investigations undertaken by Imerys, and reported as Work Package C in this report, each of the raw clays were assessed using TGA, in order to help quantify the kaolinite content of each of the clays. As previously explained, it is difficult to use just one analytical technique to determine kaolinite content, and in this case the working assumption that all weight loss between 400°C and 650°C is attributable to kaolinite dehydroxylation, whilst true for pure kaolinitic clays, is complicated for mixed clays, as other clay species also dehydroxylate in the same temperature range. Therefore, the technique is not “fool proof”, and the interpretation of the results needs to be treated with care.

Imerys’ results are reproduced and tabulated here in Table 5. Using the chemistry of known standard mineral compositions it is possible to identify the “expected weight loss” from a “pure” clay mineral, as well as some other minerals that are known to be present, giving the following relationships that relate to weight loss between 400-650°C, as shown in Table 5. Many of these are based on complete breakdown and release of the volatiles, however there are some overlaps with reactions that start before 400°C and continue beyond 650°C, as explained in the table.

Many academic papers present kaolinite contents based on this technique, especially in relation to work on calcined clay, and use the weight loss between 400-650°C as a measure of the kaolinite content. These have been reproduced here for the RC1-10 clays in Table 6. The results for the RC1-4 clays are as would be expected, these are predominantly single clay species clays with little or no other minerals present that contain volatiles. The results are therefore plausible and in the “right ball park”, especially as these are results that match the values reported by Imerys. As this is part and parcel of Imerys’ core business and analytically this is something that they do on a day to day basis, the validity of these results and interpretations, logically is high.

Table 5 Theoretical weight loss due to thermal transformations within the 400-650°C temperature range.

Mineral (Pure)	% Weight loss 400-650°C	Weight loss resulting from:	Comments
Kaolinite	14%	OH	Typically, >95% of weight loss associated with dehydroxylation of kaolinite occurs between 400-650°C Metakaolin is formed at temperatures above 650°C and is stable up to circa. 800°C
Illite	12%	OH	Typically, >95% of weight loss associated with dehydroxylation of illite occurs between 400-650°C. Meta-illite is formed above 700°C and is stable up to circa 900-920°C
Montmorillonite	36%	OH	Most of the weight loss for Ca-Montmorillonite occurs between 150°C and 400°C, with approximately 5% weight loss occurring between 400-650°C
Chlorite	12%	OH	Typically 6% of weight loss occurs up to 650°C, the remaining 6% is lost at temperatures 700-900°C
Muscovite	4%	OH	Typically a poorly defined weight loss peak between 500-750°C
Calcite	44%	CO_2	Only partial as the breakdown of carbonates typically ranges from 600-900°C
Dolomite	48%	CO_2	Dolomite has a complex decomposition TGA curve, with 2 discrete periods of weight loss. The first at about 550-600°C associated with the calcium carbonate component (54%) and then further weight loss as the magnesium carbonate (46%) decomposes at about 650-750°C
Pyrite	33%	S as SO_2	Typically in oxidizing environments fine grained pyrite oxidises to Fe_2O_3 releasing SO_2 between 450-650°C
Organic carbon	Up to 100%	CO_2 or CO	Depending on the type (rank) of the organic carbon, combustion/oxidation occurs between 450-650°C

The results for RC5 is somewhat problematic, as the weight loss from the TGA results in Imerys' report in the temperature range is higher than physically/chemically possible for kaolinite. We know from the very high LOI value from the XRF results that a significant proportion of the weight loss is associated with the "combustion" of organic carbon, which takes place at a similar temperature. This therefore complicates the interpretation.

RC6-8, the Jurassic clays, have high kaolinite contents, comparable with those from the China Clay deposits in Cornwall, however, based on published work by Ridgway (1982), and as an expert in clay mineralogy, this value is highly unlikely. The Jurassic and Carboniferous clays are mixed clay species assemblages, containing more than one type of clay mineral, as well as a number of other none clay minerals that have weight losses within the 400-650°C range, mainly carbonates and organics.

Table 6. Calculated kaolinite contents based on TGA weight loss values between 400-650°C

Sample	Weight Loss (400-650°C)	Kaolinite Content Calculation (%)
RC1	2.1%	15
RC2	8.3%	59
RC3	9.7%	69
RC4	10.2%	73
RC5	16.0%*	114
RC6	11.0%	79
RC7	8.2%	59
RC8	5.4%	39
RC9	8.0%	57
RC10	8.7%	62

The Jurassic clays, RC6-8, are predominantly associated with deposition in a marine environment, and therefore the dominant clay mineral is often illite or mixed layer illite/montmorillonite, although kaolinite is also present, but generally as the second most abundant clay mineral (Ridgway 1982).

RC9-10 both show elevated kaolinite contents based on the weight loss, accounting for over half of the sample, however the vast majority of Carboniferous clays and shales are known to be dominated by equal proportions of kaolinite and illite (Ridgeway 1982). As both kaolinite and illite dehydroxylate in roughly the same temperature range, and that they contain similar amounts of crystalline water in the form of OH (14% and 12% respectively), it is highly likely that these results are spurious, and inaccurate.

4. Normative Mineralogy

As previously discussed, most mineralogists and geologists have traditionally used a combination of the XRD and XRF results to establish a credible “Normative Mineralogy” before the advent of the Rietveld Models for quantitative XRD analysis. Whilst it has its flaws, typically as a result of the “chemistry” of the mineral standards used, it does provide a standardised approach and a relatively good approximation of the mineral assemblage of the samples being analysed.
Using these principles, Table 7, shows the calculated “Normative Mineralogy” of the 10 raw clays in the study, plus the raw clay used to manufacture the fired clay bricks used to create the brick powder (KDBP).

Whilst the Normative Mineralogy results shown in Table 7 are the best fit, based on mineralogy and chemistry, it is worth considering a “sense check” to see how these relate to the TGA weight losses measured. By converting the expected weight loss from the mineral assemblages calculated in the Normative Mineralogy exercise, again using standard mineral compositions, it is possible to back calculate the expected weight loss from each mineral based on the percentage in the sample. The results of this exercise are presented in Table 8.

Table 7. Normative Mineralogy based on modelling the chemistry (XRF data) with the mineralogy (XRD data).

Samples	Kaolinite	Illite	Montmorillonite	Chlorite	Quartz	Feldspar	Carbonates (Calcite/Dolomite	Fe Compounds (Hematite &	Muscovite	Schorl (Tourmaline)
RC1	4				46	20		2	28	
RC2	54				8	16			17	5
RC3	69				4	13			10	4
RC4	75				1	17		1	3	3
RC5[2]	38	10			1			1		
RC6	6	24[1]			29	7	29	4		
RC7	12	31[1]	9	9	20	10		4		
RC8	16	24[1]	24	1	19	5	1	10		
RC9	49	13		2	19	7		7		
RC10	28	21		13	20	3	7	3		
KDRC	7	29		9	23	8	10	6		

Note:
1 Mixed layer illite/montmorillonite is common in these clay types so the absolute values stated are likely to be aggregated.
2 Low total due to high organic carbon (lignite) content contributing to the LOI

Table 8. Calculated weight loss based on the Normative Mineralogy mineral % contents in Table 7

Sample	TGA Weight Loss (400-650°C) (%)	Normative Mineralogy Calculated Total Weight Loss (%)	Calculated % Weight loss based on Normative Mineralogy						
			Kaolinite	Illite	Montmorillonite	Chlorite	Calcite	Muscovite	Organic[1]
RC1	2.1	1.7	0.56					1.12	
RC2	8.3	8.5	7.86					0.68	
RC3	9.7	10.0	9.66					0.40	
RC4	10.2	10.6	10.50					0.12	
RC5	16.0[2]	17.3	5.32	1.20					10.80
RC6	11.0	16.4	0.84	2.88			12.70		
RC7	8.2	9.8	1.68	3.72	3.29	1.08			
RC8	5.4	5.7	2.28	2.88	0.12		0.40		
RC9	8.0	8.7	6.86	1.56		0.24			
RC10	8.7	9.1	0.98	3.48		1.56	3.08		
KDRC	16.2	17.6	0.98	3.43		1.08	4.40		7.70

Notes

[1] These are estimates as organic carbon thermal decomposition takes place over a wide temperature range.

[2] Uncertainty of actual temperature range weight loss due to very high organic carbon content. Value is the best estimate from the TGA curve.

On the whole the total weight loss based on the Normative Mineralogy values for the clay and none clay minerals in each sample, are reasonably close, within ±10% variance. There are 3 samples with high weight losses within the 400-650°C temperature range, RC5, RC6 and KDRC, that fall within the 10% variance value, but none the less are at the upper level of this. This is most likely due to the high levels of none clay mineral content that are also highly likely to be thermally decomposing within the target temperature range, RC5 and KDRC due to high organic carbon contents, and RC6 due to a very high calcite (carbonate) content.

The resulting calculated weight loss for each of the clay sources can therefore be regarded as being representative of the actual mineralogical assemblages and provides confidence that the values are as close as possible to reality and fall within the variability of the analytical accuracy of the techniques utilised in this project.

5 Conclusions

This investigation into the true mineralogy of the raw clays used in this project to manufacture calcined clay products, shows that the commonly used techniques for determination of the kaolinite content, and thus suitability of the clay resource as a viable raw material for the production of reactive calcined clays is at best unreliable and ultimately inaccurate.

The project on the whole, based on the clays that were taken forward for full assessment, shows that clay resources with less than the commonly reported 40% minimum kaolinite content, can be successfully converted into reactive calcined clays. Whilst kaolinite is known to have reactive properties when converted to metakaolin, little work has been undertaken on the mixed clay deposits where kaolinite and illite, and in some cases montmorillonites and chlorites as secondary clay minerals, perform well as calcined clay replacements for Portland Cement.

These results suggest that when it comes to standards for assessment of clay resources as potential calcined clay feedstock, the criteria used shouldn't be prescriptive in terms of the minimum level of kaolinite present in the deposit, or for that matter a limit on the total clay content. The assessment criteria should use a performance-based assessment technique, that measures reactivity, either in test concrete mortar prisms, or in concrete cube tests. By doing this, there is a much wider scope for the utilisation of currently under-utilised raw material sources, and therefore a much wider opportunity to capitalise on the use of clays to create calcined clays for cement replacement.

References

J. Ambroise, M. Murat, J. Péra, (1985) Hydration reaction and hardening of calcined clays and related minerals. V. Extension of the research and general conclusions, Cement and Concrete Research, 15 (1985) 261-268.

Bureau of Indian Standards (2023) IS 18189 : 2023 Portland Calcined Clay Limestone Cement – Specification.

R. Fernandez, F. Martirena, K.L. Scrivener, (2011) The origin of the pozzolanic activity of calcined clay minerals: A comparison between kaolinite, illite and montmorillonite, Cement and Concrete Research, 41 (2011) 113-122.

C. He, B. Osbaeck, E. Makovicky, (1985) Pozzolanic reactions of six principal clay minerals: Activation, reactivity assessments and technological effects, Cement and Concrete Research, 25 (1995) 1691-1702.

S. Hollanders, R. Adriaens, J. Skibsted, Ö. Cizer, J. Elsen, (2016) Pozzolanic reactivity of pure calcined clays, Applied Clay Science, 132 (2016) 552-560

J.M. Ridgway. (1982) Common Clay and Shale, Mineral Dossier 22, Mineral Resources Consultative Committee, Institute of Geological Sciences (Now the British Geological Survey).

Re-C3: Reclaimed Calcined Clay Cements

Appendix 10 -
Determination of Kaolinite Content of Raw Clays

Authors
Nina Cardinal (Heidelberg Materials UK)
Simon Chudley (Tarmac Cement)

Date: January 2024

Executive Summary

‘Developing Industrial Symbiosis using UK Waste Clay Resources for New Generation Building Materials (Re-C3)’ is a multi-partner, UKRI-funded project led by the Minerals Products Association which brought together industrial (Heidelberg Materials UK, Tarmac Cement, Imerys, Forterra) and academic (University College London, Dundee University) partners, also involving the Concrete Admixture Association. It was concerned with the development of waste- and by-product derived clays for calcination for use as supplementary cementitious materials (SCM), including an extensive concrete durability testing programme.

Work package J of the project, carried out by Heidelberg Materials UK and Tarmac Cement, assessed the characteristics of the four calcined clays and the one brick powder selected for this stage of the project in various compositions of EN 197-1 and EN 197-5 composite cements, CEM II/B-Q and CEM II/C-M. To assess the effect of processing technologies, two of the selected calcined clays were produced by using both FLSmidth's flash calciner in Denmark, and IBU-tec's rotary kiln in Germany. The assessment programme consisted of testing against the British standard for calcined clays, BS 8615-1, (Bristish Standards Institution, 2019) and against the requirements of EN 197-1, the European standard for cements (British Standards Institution, 2011). The main conclusions drawn from work package J are as follows:

- All clays, except for the high kaolinitic clay after flash calcination, required grinding after calcination to optimise the clay fineness and reactivity.
- There was no discernible effect of flash versus rotary calcination on compressive strength nor fresh mortar properties.
- While SO_3 additions increased the early strength of the calcined clay cements, they reduced the 28-day strength and beyond.
- All clays produced respectable strength results, most cements with up to 40% calcined clay content meeting the 42,5N strength class. Also, the clays with lower kaolinite contents demonstrated good reactivity. Most of the calcined clay cements without limestone additions outperformed the 25% and 40% fly ash reference cements in terms of strength development.
- The clays met the requirements of BS 8615-1 except for the water requirement in some cases and the 90-day activity index when tested with a high strength reference cement.
- The calcined clay cements with and without limestone additions have a higher water demand and exhibit a lower mortar flow than any of the reference cements and the water demand is highest and the flow lowest in the higher kaolinitic clays.
- The early strength of the CEM II/B-Q cements is comparable to that of the 25% fly ash reference cements, whereas that of the CEM II/C-M cements is closer to that of the 40% fly ash reference cement.
- An increase in clay content from 25 to 35% does generally lead to a small reduction in early and later strength.

Based on the work carried out in work package J, the following additional work is recommended.

- Guidelines should be developed on how to determine the mineralogical phases of clays consistently.
- The water requirement limit in BS 8615-1 should be reviewed.
- The effect of different clinker sources on the strength development of calcined clay cements warrants further investigation.

Contents

1. Introduction

This report deals with work package J of the UKRI funded project ‘Developing industrial symbiosis using UK waste clay resources for new generation building materials’, known as Re-C3. Work package J is concerned with the characterisation of clays calcined at a pilot scale and with the performance of binary and ternary blended cements made with these calcined clays. The testing in work package J has been carried out at the cement testing laboratories of Heidelberg Materials UK and Tarmac Cement.

Following the initial assessment of ten waste clay sources by Imerys and UCL, four clays of different origins were selected for pilot scale calcination via the rotary kiln and flash calcination process. Two of the four clays were calcined via both routes to allow a comparison of the clay properties resulting from the two different processes.

This report deals with the assessment of these four clays and a waste brick powder supplied by Forterra against the requirements of the British Standard for pozzolanic materials for use with Portland cement, BS 8615-1 (Bristish Standards Institution, 2019). It also covers an extensive cement characterisation programme in which the calcined clays were blended with different CEM I cements and limestone powders by the laboratories to make various compositions of the EN 197-1 & EN 197-5 composite cements and compared against a range of reference cements. Selected combinations are also being assessed in a concrete durability testing programme at Dundee University in work package K of the project.

2. Materials and Nomenclature

The four clays and one brick powder taken to the pilot phase are listed Table 1 below. The brick powder (BP1) provided by Forterra is waste product from the brick manufacturing process, ground to a fine powder. The Imerys calcined clays (CC2 and CC3) are produced from two different waste slurries arising during the production of ultrapure kaolinite. And both, the Heidelberg Materials UK and Tarmac Cement calcined clays (CC9 and CC7), are produced with raw clay from quarries where the clays have limited end uses. CC2 and CC9 were calcined by the two different calcination processes, rotary kiln and flash calciner. The material designations listed in the second column of the table will be used throughout this report.

Table 1: Material Designations

Clay Designation		**Clay Provider**	**Calcination Process**
Raw	**Calcined**		
RC2	CC2R	Imerys	Rotary
RC2	CC2F	Imerys	Flash
RC3	CC3R	Imerys	Rotary
RC9	CC9F	Tarmac	Flash
RC9	CC9R	Tarmac	Rotary
RC7	CC7F	Heidelberg Materials UK	Flash
BP1	BP1	Forterra	Not applicable

In work package C of the project, Imerys characterised the raw clays by X-ray Fluorescence (XRF) and X-ray Diffraction (XRD) analysis, as did FLSmidth ahead of the calcination at their pilot plant in Denmark. Forterra used the XRF data from Imerys and FLSmidth to estimate the mineralogical composition of the clays using normative mineralogy. Furthermore, the RC7 clay was characterised by Heidelberg Materials' global R&D laboratory using Quantitative X-ray Diffraction (QXRD) and Fourier-transform infrared spectroscopy (FTIR), the latter for the determination of the kaolinite content only. The mineralogical compositions resulting from these different methods are shown in Table 2 below for RC7.

Table 2: Mineralogical composition estimate for RC7

Cay Mineral	**Method**				
	Normative mineralogy using		**QXRD**		**QXRD/FTIR**
	Imerys XRF	**FLSmidth XRF**	**Imerys**	**FLS**	**HM Global**
Quartz	20	14	11	18	20
Feldspar	10		3		12*
Calcite		5		4	
Fe Oxides	4	4			0.2
Kaolinite	12	24	60	42	25/25
Illite	31	37	26	17	24
Chlorite	9	7		7	
Smectite	9	7		7	
Vermiculite					1
Anatase					2
Pyrite					3
Amorphous					13

*sum of Andesine, Albite and Microcline

The results in Table 2 highlight significant differences in the estimates in clay mineral composition. Particularly noteworthy in the context of calcined clays for secondary cementitious materials (SCM) are the high values obtained for kaolinite by QXRD by Imerys and FLSmidth. It is believed that these are overestimations of the actual values. The Rietveld model, often used to obtain quantitative estimates of mineralogical compositions from XRD, tends to be reliable for generally known materials. The Imerys analysis may therefore be accurate for high kaolinitic china clays but not for the more 2:1 dominant RC7 clay. The comparison of results from the normative mineralogy approach and QXRD carried out by Imerys on RC2 and RC3, not presented in the table above, are very close, confirming the assumption that the Rietveld model used by Imerys is calibrated for the high kaolinite clays of Imerys.

As a guide for the mineralogical composition of the four clays investigated in work package J, Table 3 uses the results from the normative mineralogy approach for RC7 and RC9, the Heidelberg Materials UK and Tarmac Cement clays, and Imerys' QXRD results for RC2 and RC3. It highlights RC2 and RC3 to be high in kaolinite, RC7 to be low in kaolinite and RC9 representing an intermediate kaolinite content.

Table 3: Mineralogical composition estimate of clays in pilot phase

	RC2	**RC3**	**RC7**	**RC9**
Quartz	7	4	20	19
Feldspar	12	6	10	7
Calcite				
Fe Oxides			4	7
Kaolinite	58	71	12	49
Illite	19*	16*	31	13
Chlorite			9	2
Smectite			9	0

*In respect of the Imerys clays, which are a by-product of the China clay process, the Illite content identified is more likely to be Mica. Both Mica and Illite have similar crystalline structures and are therefore difficult to speciate without knowing the geological setting of the deposit. In the case of the kaolinitic rich China clays, these are weathered and thermally altered granites in which Mica is an abundant minor mineral.

The reference cements and constituents and the limestone for blending with the clays are listed in Table 4 below.

Table 4: Reference cement and cement constituents nomenclature

Material	**Designation**
CEM I - 52,5N	PC1
	PC2
	PC3
Limestone Powder	L1
	L2
	L3
CEM II/A-LL – 52,5N	N/A
GGBS	GGBS
Fly Ash	FA

The naming convention used through this report for the blended calcined clay cements is illustrated in Table 5 below.

Table 5: Illustration of cement nomenclature used throughout report

Cement Group	**Cement Detail**	**Designation**
CEM II/B-Q	75% Source 1 PC + 25% Imerys Source 2 clay flash calcined	75:25 PC1:CC2F
	70% Source 2 PC + 30% Forterra Brick Powder	70:30 PC2:BP1
CEM II/C-M	55% Source 1 PC + 30% Hanson clay flash calcined + 15% Source 2 limestone	55:30:15 PC1:CC7F:L2
	50% Source 1 PC + 40% Tarmac clay rotary calcined + 10% Source 1 Limestone	50:40:10 PC1:CC9:L1

3. Test Programme

Table 6 below lists the cements that were blended, mixed and tested as part of cement validation programme. They fall into three groups, CEM II/B-Q, CEM II/C-M and reference cements. A total of 30 cements were tested. All CEM II/B-Q cements were prepared and tested by Tarmac Cement's National Laboratory, the CEM II/C-M cements were prepared and tested by Heidelberg Materials UK and the reference cements were tested at both Heidelberg Materials UK and Tarmac Cement's laboratories. The testing of the reference cements at both laboratories was carried out to establish comparability of results between the two laboratories.

Table 6: Cement matrix

Cement Name	% CEM I	% Calcined Clay	% Limestone	% GGBS	% Fly Ash
CEM II/B-Q Cements					
75:25 PC1:BP1	75	25	-	-	-
70:30 PC1:BP1	70	30	-	-	-
65:35 PC1:BP1	65	35	-	-	-
70:30 PC2:BP1	70	30	-	-	-
75:25 PC1:CC2R	75	25	-	-	-
75:25 PC1:CC9F	75	25	-	-	-
70:30 PC1:CC2F	70	30	-	-	-
70:30 PC1:CC9R	70	30	-	-	-
70:30 PC1:CC2R	70	30	-	-	-
70:30 PC1:CC3R	70	30	-	-	-
70:30 PC1:CC9F	70	30	-	-	-
70:30 PC1:CC7F	70	30	-	-	-
65:35 PC1:CC2R	65	35	-	-	-
65:35 PC1:CC9F	65	35	-	-	-
70:30 PC2:CC2R	70	30	-	-	-
70:30 PC3:CC2R	70	30	-	-	-
CEM II/C-M					
55:30:15 PC1:BP1:L1	55	30	15	-	-
50:40:10 PC1:BP1:L1	50	40	10	-	-
55:30:15 PC2:BP1:L1	55	30	15	-	-
55:30:15 PC1:CC2F:L1	55	30	15	-	-
55:30:15 PC1:CC9R:L1	55	30	15	-	-
55:30:15 PC1:CC2R:L1	55	30	15	-	-
55:30:15 PC1:CC3R:L1	55	30	15	-	-
55:30:15 PC1:CC9F:L1	55	30	15	-	-
55:30:15 PC1:CC7F:L1	55	30	15	-	-
50:40:10 PC1:CC2R:L1	50	40	10	-	-
50:40:10 PC1:CC9F:L1	50	40	10	-	-
55:30:15 PC2:CC9F:L1	55	30	15	-	-
55:30:15 PC3:CC9F:L1	55	30	15	-	-
55:30:15 PC1:CC9F:L2	55	30	15	-	-
55:30:15 PC1:CC9F:L3	55	30	15	-	-

Reference Cements					
CEM I Ref (PC1)	100	-	-	-	-
CEM I Ref (PC2)	100	-	-	-	-
CEM I Ref (PC3)	100	-	-	-	-
CEM II/A-LL Ref (11% L)	100 CEM II	-	-	-	-
CEM II/B-V Ref (25% FA)	75	-	-	-	25
CEM II/B-V Ref (40% FA)	60	-	-	-	40
CEM III/A Ref (36%GGBS)	64	-	-	36	-
CEM III/A Ref (45% GGBS)	55	-	-	45	-

Within the CEM II/B-Q group the main cement was a 70:30 blend of CEM I and calcined clay, in the CEM II/C-M group it was a 55:30:15 blend of CEM I, calcined clay and limestone, where the limestone content accounts for the limestone of the minor additional constituent (MAC) content of the CEM I. All four calcined clays and the brick powder were tested in these two combinations. Factors such as different clay and limestone levels, the influence of different CEM I and limestone sources, and the influence of the calcination process were studied on CC2 and CC9 as well as the brick powder.

4. Results

4.1Reference Cements and Comparison of Laboratories

The reference cements were tested against the requirements of BS EN 197-1. The testing was performed at both laboratories to establish comparability of results between the two laboratories.

The graph below shows the difference in compressive strength between the two laboratories. The results demonstrate good reproducibility between the two laboratories. When referring in later sections of this report to the reference cement strengths, this has been calculated as the average of the values obtained by both laboratories.

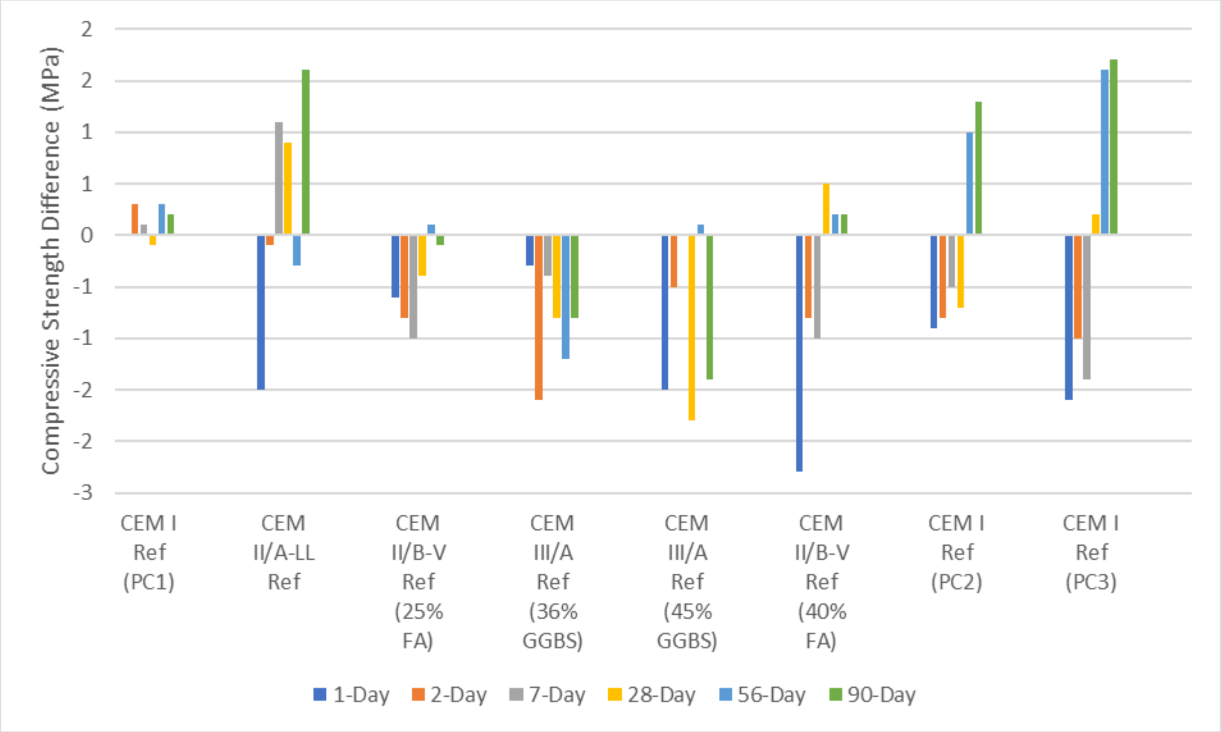

Figure 1: Comparison of compressive strength results between Heidelberg Materials UK and Tarmac Cement laboratories

The absolute compressive strength of the reference cements is shown in Figure 2 below. The CEM I and CEM II/A-LL reference cements all meet the requirement of the BS EN 197-1 52,5 N strength class with PC2 exhibiting the highest strength. All fly ash and blast furnace cements meet the requirement of the BS EN 197-1 42,5 N strength class.

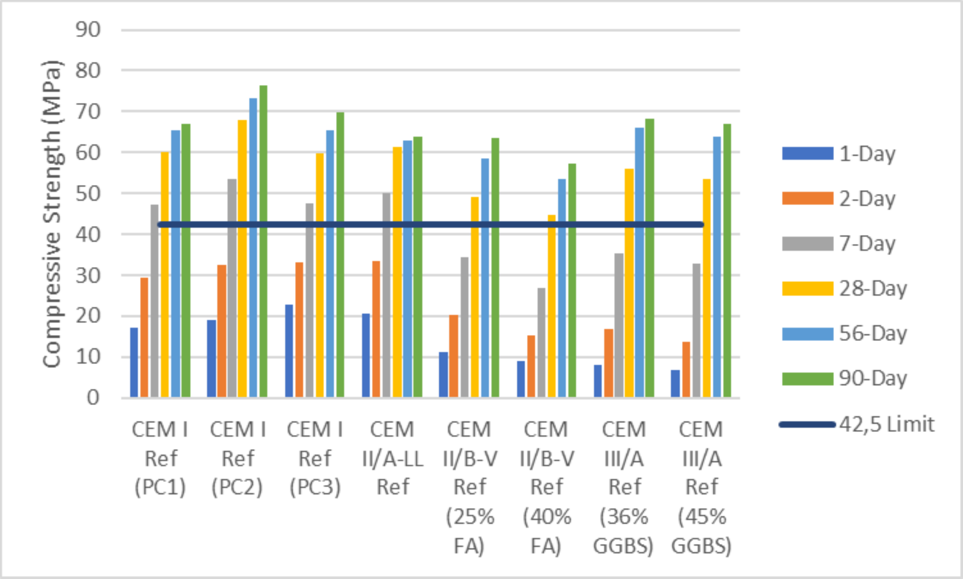

Figure 2: Compressive strength of reference cements

The percentage differences between the two laboratories for the other important cement physical characteristics are shown in Figure 3 below.

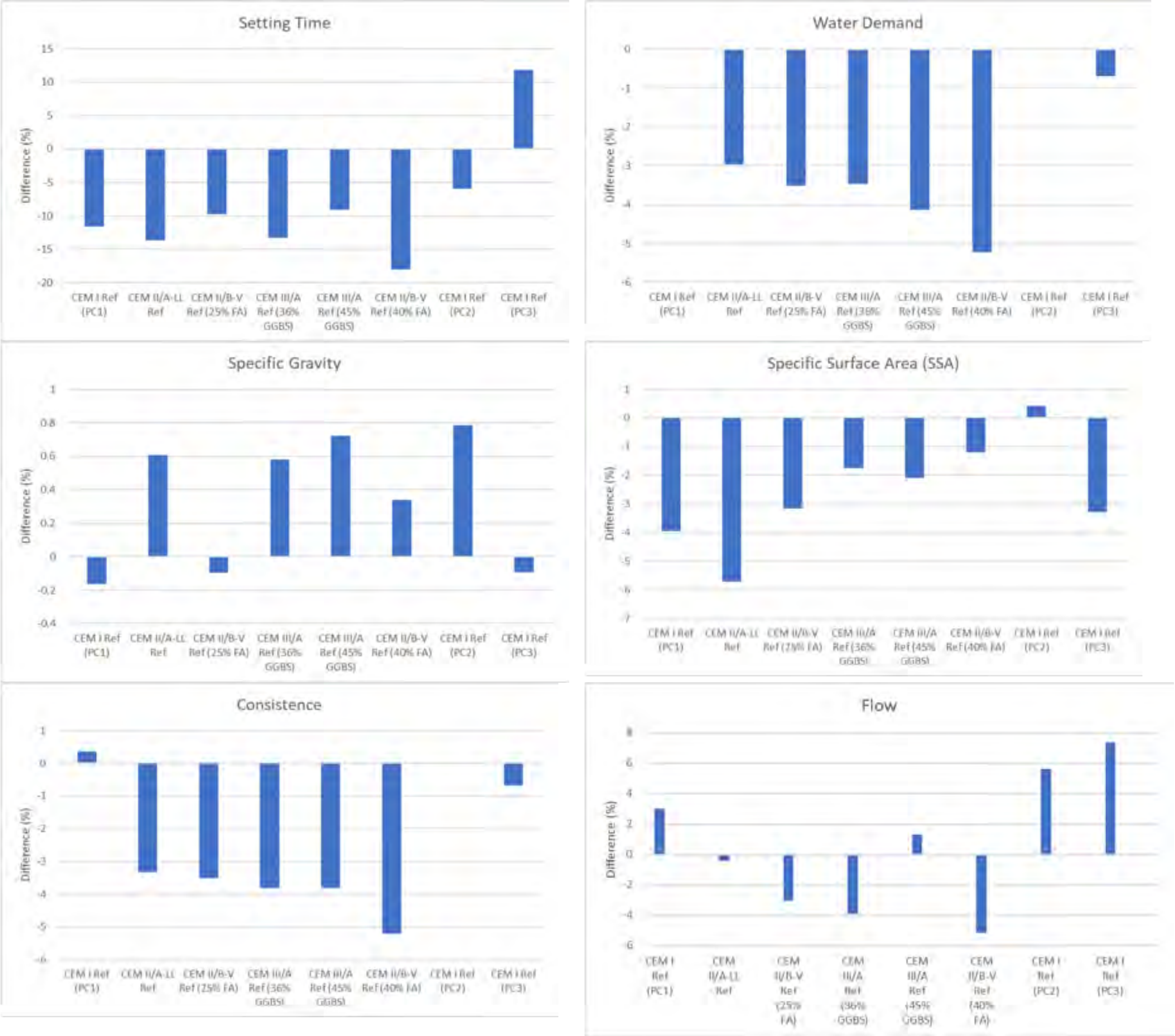

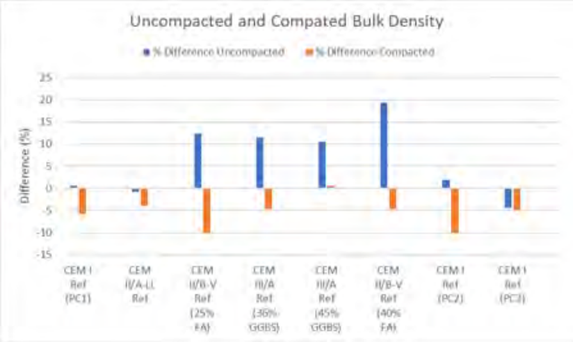

Figure 3: Comparison between Tarmac and Hanson laboratory for various cement characteristics

With the exception of setting time and bulk density, there is good agreement between the two laboratories, in general not exceeding 5% difference. While there is a larger difference for setting time, it is not a concern for the assessment as also for the calcined clay cements, as will be shown later, the setting time results are all well above the minimum requirement for the cement type in BS EN 197-1. The larger difference in bulk density, not a requirement of BS EN 197-1, is due to the nature of the test method which is difficult to standardise. As bulk density does not affect the performance of a cement, it is not a concern.

XRF and Particle Size Distribution (PSD) analyses were also performed by both laboratories on the reference cements. The percentage difference for each of the analysed oxides is shown in Figure 4 below. There is generally good agreement. The large percentage differences relate to manganese oxide (MnO) and sodium oxide (Na_2O), both of which have low concentrations in cement, MnO ranged from 0.05 to 0.15% and Na_2O from 0.05 to 0.64 across all reference cements. A lower accuracy of the XRF method at these low concentrations may explain the differences observed for these two oxides. The XRF analyses of the reference cements are tabulated in the Appendix.

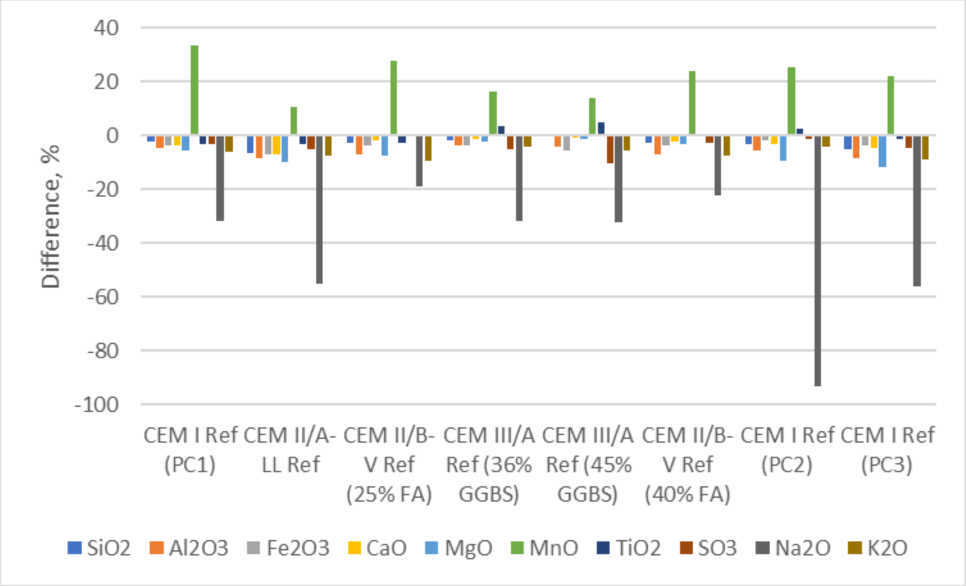

Figure 4: Comparison between Tarmac and Hanson laboratory for XRF analysis

The PSD of all reference cements were also carried out at both laboratories. A comparison of the results between the two laboratories is provided in Figure 5 for two of the reference cements, one of the limestones, and one of the calcined clays. This comparison provides confidence that results obtained at the two labs exhibit good comparability.

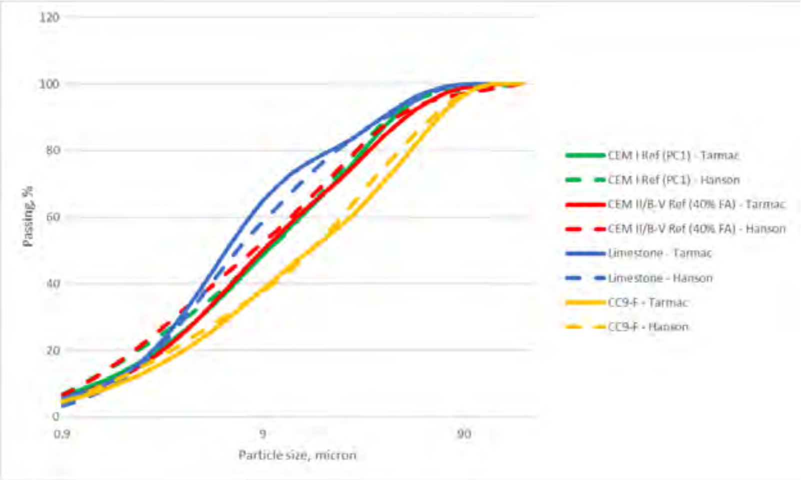

Figure 5: Comparison between Tarmac and Hanson laboratory for XRF analysis

A comparison of the PSD of the three limestone sources and the three CEM I sources used in the programme is shown in Figure 6 below. They have all very similar PSDs, only the L3 limestone fines are slightly finer.

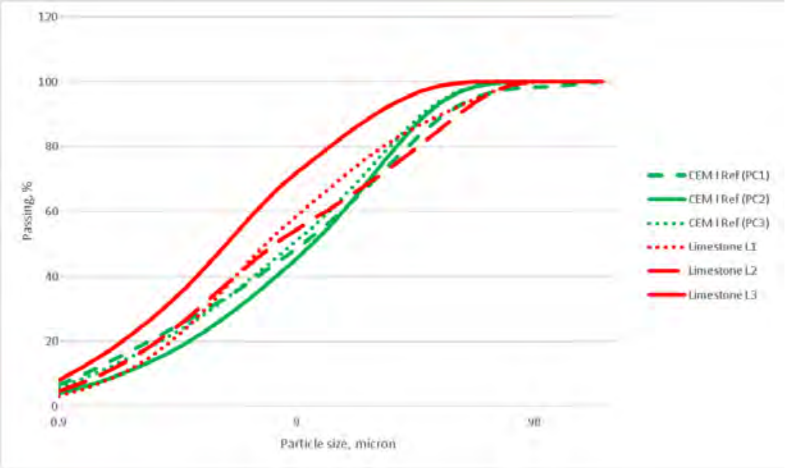

Figure 6: PSD of limestone fines and CEM I cements

4.2Calcined Clay Properties

4.2.1 Chemical Composition and Particle Size Distributions

The chemical composition of the calcined clays, obtained by XRF analysis, is shown in Table 7 below.

Table 7: Chemical composition of the clays

Clay	SiO_2	Al_2O_3	Fe_2O_3	CaO	MgO	MnO	TiO_2	SO_3	Na2O	K_2O	Na2Oeq	Sum
CC9F	63.17	21.38	8.93	2.08	0.85	0.11	1.23	0.12	0.06	1.11	0.79	99.83
CC9R	61.25	22.14	8.43	2.28	1.08	0.13	1.18	0.22	0.14	1.47	1.11	99.43
CC7F	59.90	22.67	7.80	2.29	1.74	0.02	1.19	1.22	0.27	3.14	2.34	100.24
CC2F	56.58	33.02	2.27	0.17	0.41	0.03	0.18	0.03	0.26	4.83	3.44	101.22
CC2R	55.87	35.96	1.71	0.12	0.39	0.02	0.12	0.02	0.18	4.17	2.92	101.48
CC3R	54.75	38.98	1.27	0.02	0.29	0.01	0.07	0.00	0.11	3.53	2.43	99.01
BP1	53.95	18.88	6.16	10.55	1.82	0.03	1.10	2.46	0.46	3.16	2.54	98.55

Comparing CC9F with CC9R and CC2F with CC2R, there is little difference in chemical composition when processed via the flash and rotary calcination processes. CC9F/R and CC7F having surprisingly similar analyses, the only notable difference being the sulphur trioxide (SO_3) and sodium equivalent ($Na_2Oeq.$). Compared to CC9 and CC7, CC2 and CC3 stand out for their much higher aluminium trioxide (Al_2O_3) content, offset by the lower iron trioxide (Fe_2O_3), calcium oxide (CaO), magnesium oxide (MgO), and titanium dioxide (TiO_2) contents. CC2 and CC3 are also very low in SO_3. The brick powder, BP1, stands out for the higher CaO content and relatively high SO_3 content.

The d50 values of the particle size distributions of the calcined clays are listed in Table 8 below and the full distributions are shown in Figure 7. The following observations can be made from these results:

- CC9F and CC7F have almost identical PSDs owing to the fact that they were ground to the same target following calcination.
- CC2F was deemed fine enough following flash calcination and was not ground. This has resulted in a slightly coarser material with a different shape to the distribution.
- The three rotary calcined clays were all ground post calcination, resulting in very similarly shaped distributions, all three slightly finer than the ground flash calcined clays, with CC3R being the finest.
- The brick powder stands out for being the finest materials.

Table 8: d50 values of calcined clay particle size distributions

Clay	d50 (micron)
CC9F	16
CC7F	16
CC2F	21
CC9R	11
CC2R	8
CC3R	5
BP1	3

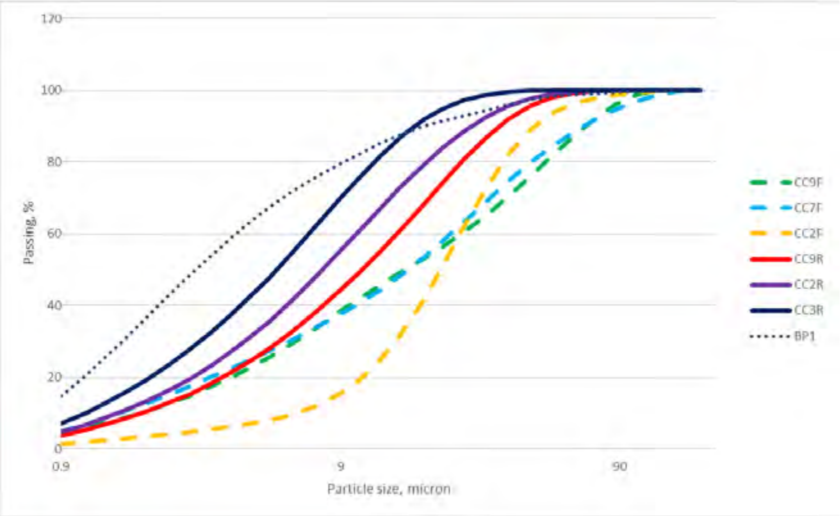

Figure 7: Particle size distribution of the calcined clays

4.2.2 Calcined Clay Properties to BS 8615-1

There are European standards for GGBS (British Standards Institution, 2006) and fly ash (British Standards Institution, 2012) but not yet for calcined clays. The UK, however, has its own standard for pozzolanic materials which comes in two parts, BS 8615 Part 1 and Part 2 (British Standards Institution, 2019). Part 1 deals with natural pozzolana and natural calcined pozzolana and Part 2 with high reactivity natural calcined pozzolana. The calcined clays in this project were assessed against the requirements of Part 1. The results of this assessment are presented in the following sections and tables.

Table 9 below shows the results against the chemical requirements of BS 8615-1. DTS stands for ‘deemed to satisfy’ as BS 8615 states that if the CaO content is below 10%, then the requirement for reactive CaO is satisfied. The results in the table demonstrate that all clays meet the requirements of the standard with the exception of BP1 being just above the upper limit for CaO.

Table 9: Chemical properties of calcined clays against the requirements of BS 8615-1

		BP1	**CC2F**	**CC2R**	**CC3R**	**CC7F**	**CC9F**	**CC9R**	**BS 8615-1**
LOI	EN 196-2	2.9	1.1	0.6	1.0	1.6	0.3	0.8	≤ 7.0%
Chloride	EN 196-2	0.07	0.00	0.00	0.00	0.00	0.00	0.00	≤ 0.1%
SO_3	EN 196-2	2.83	0.00	0.00	0.08	0.84	0.09	0.19	≤ 3.0%
Free CaO	EN 451-1	0.1	0.1	0.0	0.0	0.2	0.7	0.7	≤ 1.5%
CaO	EN 196-2	**10.6**	0.2	0.1	0.0	2.3	2.1	2.3	≤ 10.0%
Reactive CaO	EN 196-2	**10.4**	DTS	DTS	DTS	DTS	DTS	DTS	≤ 10.0%
Reactive SiO_2	EN 196-2	48.0	43.4	37.5	52.0	57.6	51.3	56.7	≥ 25.0%
$SiO_2 + Al_2O_3 + Fe_2O_3$	EN 196-2	79.0	91.9	93.5	95.0	90.4	93.4	91.8	≥ 70.0%
Na_2Oeq	EN 196-2	2.5	3.4	2.9	2.4	2.3	0.8	1.1	≤ 5.0%
MgO	EN 196-2	1.8	0.4	0.4	0.3	1.7	0.9	1.1	≤ 4.0%
P_2O_5	ISO 29581-2	0.001	0.003	0.001	0.001	0.002	0.003	0.003	≤ 5.0%
Clay Content	EN 933-9	0.1	0.2	0.3	0.5	0.4	0.2	0.5	≤ 1.5g / 100g
TOC	EN 13639	0.1	0.0	0.0	0.0	0.2	0.1	0.0	≤ 0.5%

The physical properties are shown in Table 10 below. All clays meet the requirements for the 28-day and 90-day activity index of BS 8615-1 with the exceptions of BP1, CC2F, CC2R and CC9R at 90days with the highest strength reference cement, PC2. All clays also comfortably satisfy the initial setting time requirement but the water requirement of CC2F, CC2R, CC3R and CC7F is higher than BS 8615-1 allows.

Table 10: Physical properties of calcined clays against the requirements of BS 8615-1

		Reference Cement	**BP1**	**CC2F**	**CC2R**	**CC3R**	**CC7F**	**CC9F**	**CC9R**	**BS 8615-1**
45micron residue (%)	EN 933-10	-	8.3	8.5	0.9	0.1	17.5	23.5	4.5	≤ 40.0%
43micron residue (%)	PSD	-	9.7	12.6	4.3	1.2	20.2	24.0	7.6	-
28d AI (75:25%)	EN 196-1	PC1	82	94	111	111	99	94	95	≥ 75%
		PC2	75	85	89	89	90	88	86	
90d AI (75:25%)		PC1	89	89	97	108	98	96	91	≥ 85%
		PC2	**82**	**79**	**84**	88	92	88	**84**	
Soundness (70:30%)	EN 196-3	PC1	0	0	0	0	0	0	1	≤ 10mm
		PC2	0	1	0	0	0.5	0	0	
Initial Set (75:25%)	EN 196-3	PC1	1.4	1.4	1.3	1.5	1.2	1.4	1.3	≤ 2x TC
		PC2	1.3	1.3	1.2	1.4	1.3	1.4	1.3	
Water requirement (%)	EN 450-1	PC1	109	**122**	**118**	**127**	**118**	107	111	≤ 115%

The fact that the activity indices are different depending on the reference cement used is purely a reflection of the strength of the reference cement, PC2 being higher strength than PC1. A higher strength reference cement results in a lower activity index. The activity index is determined as a ratio of the compressive strength of the reference cement and the compressive strength of a blend where 25% of the reference cement have been replaced by the calcined clay. Any value >75% therefore indicates that the calcined clay contributes to the strength development rather than being an inert filler or even having an adverse effect on strength. The results show that BP1 makes a moderate contribution to the 28-day strength development which increases at 90-days. All other clays have very high activity index at 28-days, in the case of CC2R and CC3R, the clay cement exceeding the strength of the reference cement. The fact that the 90-day activity index is lower in several cases than the 28-day activity index indicates that between 28- and 90-days the reference cement gains proportionally more strength than the calcined clay cement. The fact that the activity index of CC2R is higher than of CC2F may be related to potentially two facts: CC2R was ground after calcination whereas CC2F was not, and in order to achieve a satisfactory consistency for rotary calcination additional, dry kaolinitic clay was added to the raw waste clay for CC2R.

4.2.3 Calcined Clay Colour

When measuring the colour of cement, the Hunter Scale is used. It is expressed in three values, L, a, and b, where L represents the brightness black/white coordinate, a the red/green coordinate and b the yellow/blue coordinate. The L-a-b values for the calcined clays and brick powder are shown in Table 11 below.

Table 11: Colour comparison of calcined clays

	L	a	b
CC9F - ground	52.93	2.09	9.61
CC9F - filter dust	55.82	11.46	17.87
CC7F - ground	60.15	3.49	4.46
CC7F- filter dust	62.3	4.46	6.98
CC9R	56.80	15.10	20.58
CC2F	77.03	1.00	7.05
CC2R	82.49	1.04	7.62
CC3R	69.9	3.03	3.1
BP1	63.17	6.26	8.32

The difference in colour between the ground calcined clay and the filter dust in case of flash calcined CC7F and CC9F clays is noticeable. The reducing atmosphere used by FLSmidth to control the colour of the clay does not apply to the filter dust. In fact, the filter dust colour of CC9F is quite close to that of the rotary calcined CC9R clay where no colour control was applied and the oxidation of iron containing minerals leads to a red hue of the clay. The higher brightness of CC2F, CC2R and CC3R compared to CC7F, CC9F, CC9R and BP1 is noticeable. A visual comparison of the reference materials, calcined clays and cements blended with the calcined clays is provided in Figure 8 below.

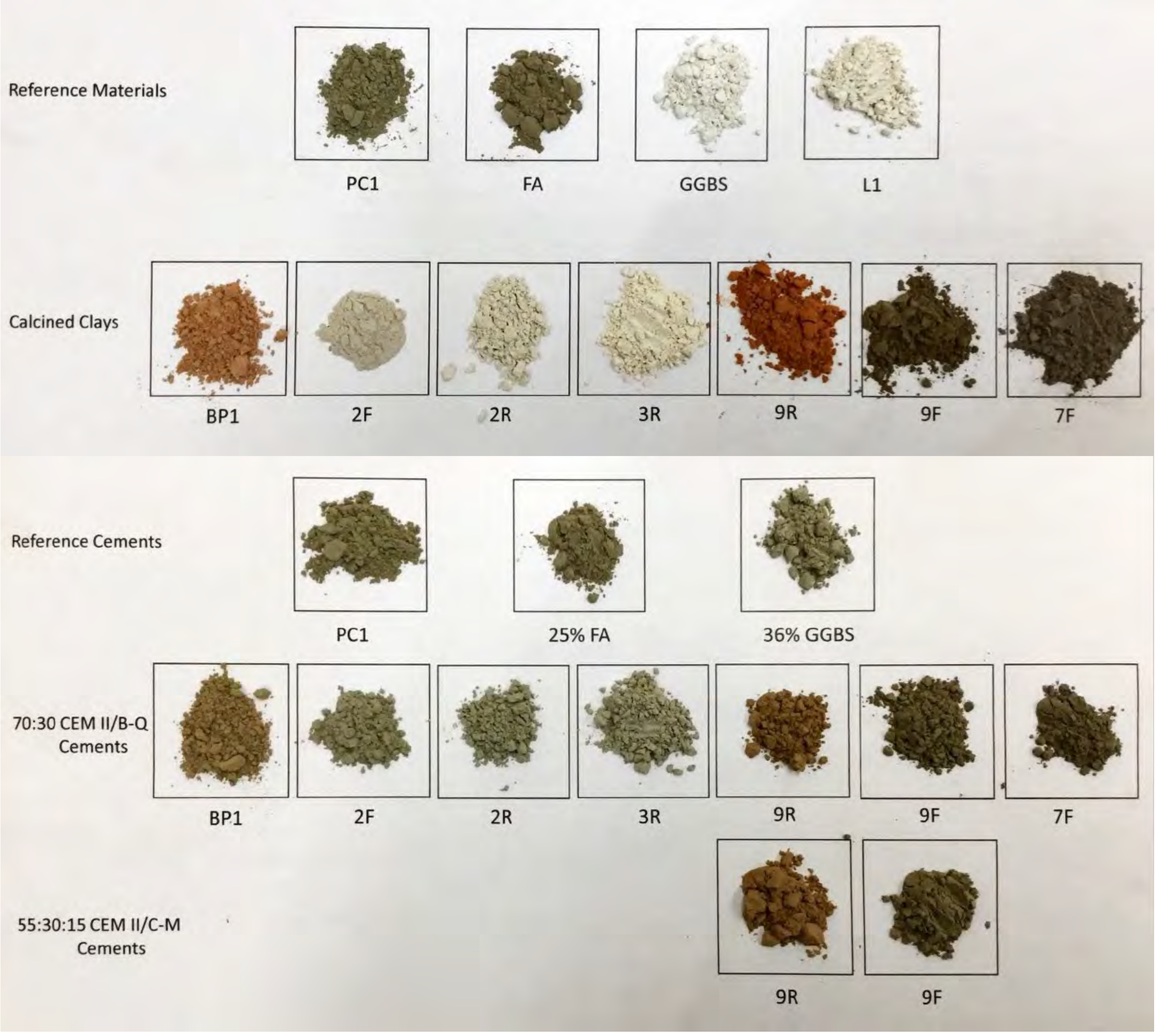

Figure 8: Visual comparison of reference materials, calcined clays and blended cements

4.3Calcined Clay Cement Properties to BS EN 197-1

4.3.1 Chemical Composition and Particle Size Distributions

The chemical compositions of the blended cements determined by XRF and the PSD data are provided in the appendix. As they are purely a function of the calcined clay, reference cement and limestone analyses and PSDs, they are not further discussed here.

4.3.2 Fresh Mortar Properties

The initial setting time results of the calcined clay cements are compared with the reference cements in Figure 9 below. The CEM II/B-Q cements and corresponding reference cements were tested in Tarmac Cement's National Laboratory, and the CEM II/C-M cements and corresponding reference cements were tested in Heidelberg Materials' National Laboratory. The same applies to the standard consistence results presented later in this paragraph.

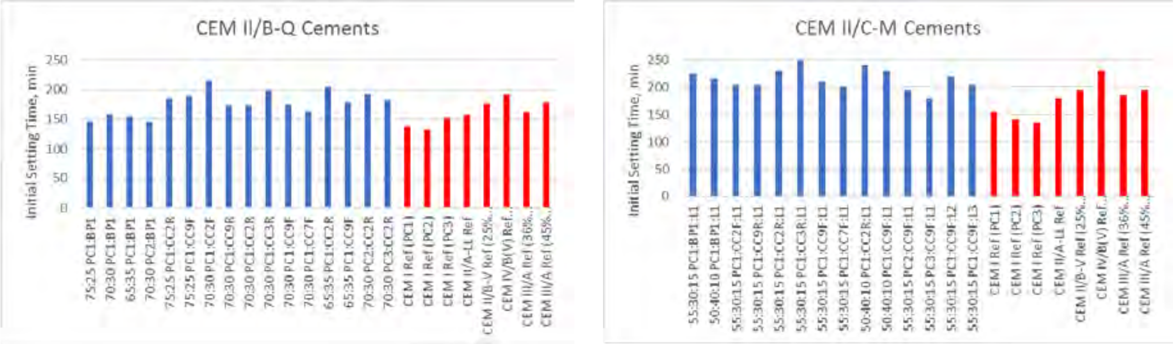

Figure 9: Initial setting time of calcined clay and reference

For both, the CEM II/B-Q and CEM II/C-M cements, the setting times are higher than those of the CEM I reference cements and closest to the setting time of the fly ash reference cements. They are all significantly higher than the minimum setting time requirement of EN 197-1 for 42,5 N cements of 60 minutes.

The water demand results in Figure 10 below highlight that most of the calcined clay cements have a higher water demand than any of the reference cements and that the CC2R, CC2F and CC3R clays, which have a higher kaolinite content, result in higher water demand than the BP1, CC7F, CC9R and CC9F clays. In addition to the higher kaolinite content, higher fineness may also play a role, as CC2R and CC3R also exhibit higher fineness.

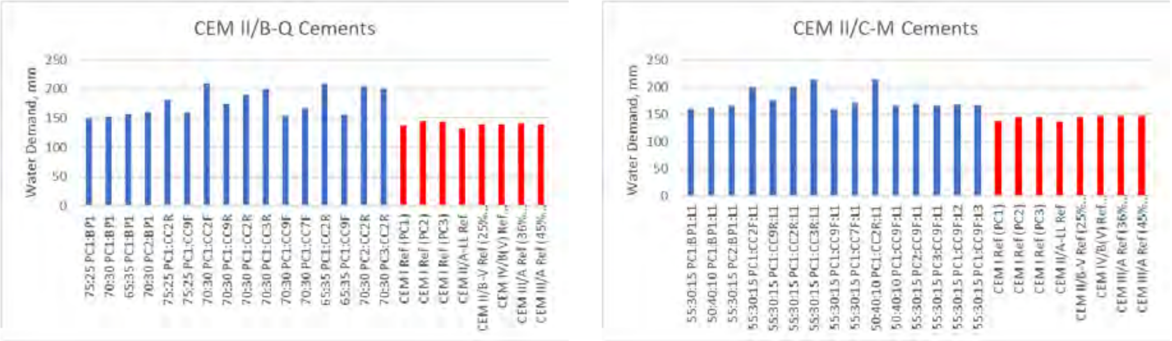

Figure 10: Water demand of calcined clay and reference cements

Congruent with the water demand results, the flow, determined using the flow table method to BS EN 1013-3 (British Standards Institution, 1999), of all calcined clay cements is lower than that of the reference cements, Figure 11, and the higher kaolinite clays, CC2F, CC2R and CC3R result in the lowest flow. Again, higher fineness may also play a role as all calcined clay blended cements have a higher fineness than the reference cements.

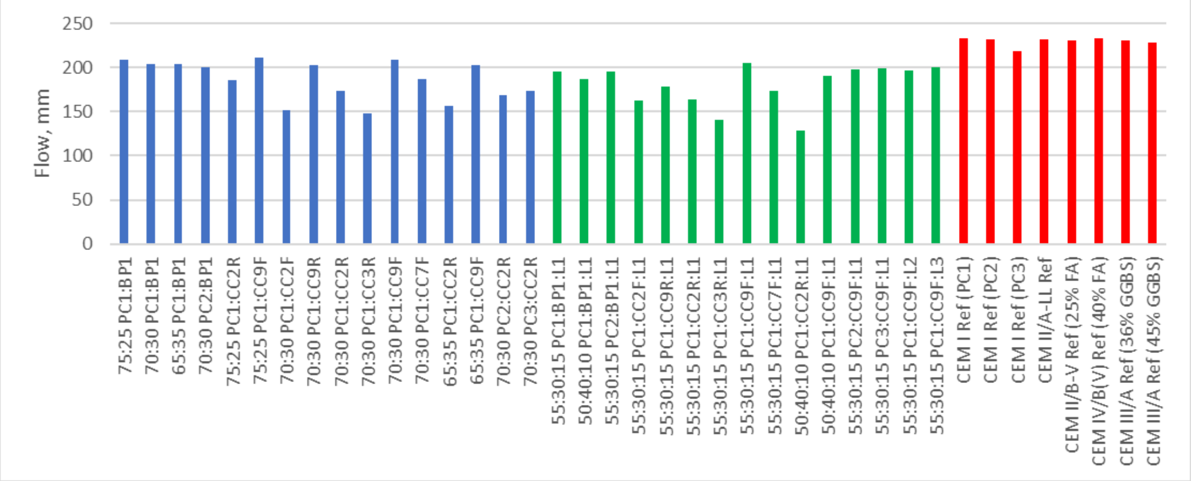

Figure 11: Flow of calcined clay and reference cements

Table 12 and Table 13 below compare the flow results for BP1, CC9F and CC2R at different clay replacement levels. They show that the effect of increasing calcined clay content on flow is most pronounced for the higher kaolinite CC2R clay and that increasing the calcined clay content by 10% from 30% to 40% in the CEM II/C-M cements results in a higher loss of flow than the increase by 10% from 25% to 35% in the CEM II/B-Q cements. Comparing the 70:30% and 55:30:15% cements shows that the difference in flow at the same calcined clay level is small between the two groups of cements, the CEM II/C-M cements giving only slightly lower flow results than the CEM II/B-Q cements.

Table 12: Effect of increasing calcined clay content on flow in CEM II/B-Q cements

	Flow, mm		
CEM I:Calcined Clay Ratio	**75:25**	**70:30**	**65:35**
BP1	209	204	204
CC9F	211	209	203
CC2R	185	173	156

Table 13: Effect of increasing calcined clay content on flow in CEM II/C-M cements

	Flow, mm	
CEM I:Calcined Clay:LSF Ratio	**55:30:15**	**50:40:10**
BP1	195	187
CC9F	205	190
CC2R	165	129

Table 14 below compares the flow and water demand for flash calcined and rotatory calcined clays. While the water demand and flow results complement one another, i.e. a higher water demand results in a lower flow, there is no consistent difference between rotary and flash calcined clays. Cements with the CC9 clay exhibit a slightly lower flow with rotary calcination, whereas cements with CC2 clays show no difference in the CEM II/C-M cement but a decrease in flow for the flash calcined materials in the CEM II/B-Q cement.

Table 14: Effect of calcination process on flow and water demand

	Flow, mm		**Water Demand, ml**	
	70:30	**55:30:15**	**70:30**	**55:30:15**
CC2F	151	163	210	200
CC2R	173	164	191	200
CC9F	209	205	155	160
CC9R	202	178	175	175

The expansion results, a measure of soundness, of all calcined clay cements were mostly 0 mm and a maximum of 2 mm, meeting comfortably the requirement of ≤10 mm of EN 197-1.

4.3.3 Compressive Strength

Compressive strength testing was carried out at 1, 2, 7, 28, 56 and 90 days for all CEM II/B-Q and CEM II/C-M cements. The results are tabulated in the appendix, where the results of the reference cements are the average values of the results obtained at the Heidelberg Materials UK and Tarmac Cement laboratories. The following sections explore the influence of clinker replacement level, clay fineness, calcination process, source of cement constituents, and SO_3 content on cement strength development.

4.3.3.1 Effect of clinker replacement level

This section focusses on the effect of calcined clay content and clinker replacement level on the strength of the CEM II/B-Q and CEM II/C-M cements respectively when compared with PC1 and fly ash reference cements.

Figure 12 below shows the strength development up to 90 days for all CEM II/B-Q cements made with the PC1 reference cement.

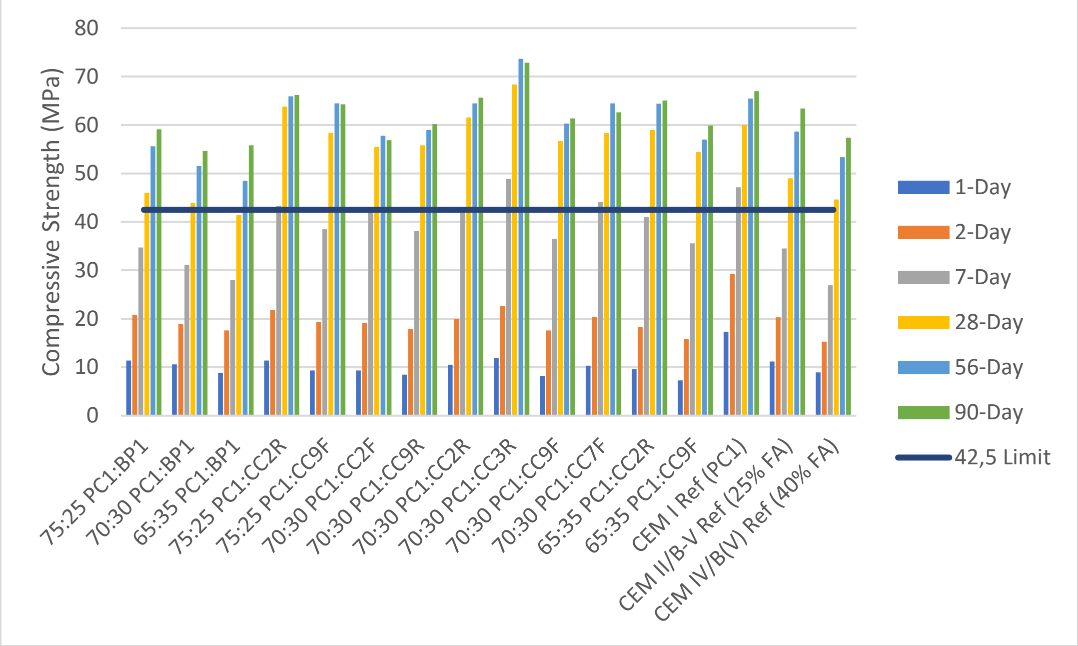

Figure 12: Strength development of CEM II/B-Q cements with PC1 reference cement

While the 1- and 2-day strengths are lower than that of the PC1 reference cements they are generally comparable to the CEM IV/B-V cement with 25% fly ash and higher than the fly ash cement with 40% fly ash. All cements meet the 2-day 10 MPa 42,5 N strength minimum requirement of EN 197-1 comfortably. At 28-days, all CEM II/B-Q cements exhibit significantly higher strength levels than both fly ash reference cements and exceed the EN 197-1 42,5 N limit by a significant margin with the exception of the cements with the BP1 clay. In fact, all cements, except the BP1 cements, would meet the BS EN 197-1 52,5 L strength requirement. The highest strength is exhibited by the cements made containing CC2R and CC3R, the higher kaolinitic clays, whereas CC2F exhibits strength levels similar to those of CC7F and CC9F. In this context it must be remembered that a kaolinite addition was made to CC2R and CC3R prior to rotary calcination as the clays were too wet for the process. This addition was not made to CC2F. Furthermore, CC2R and CC3R were ground after calcination whereas CC2F was not, resulting in CC2F being coarser, see Figure 7.

The graphs in Figure 13 below show the strength development for BP1, CC2R and CC9F at the three different clinker replacement levels of 25%, 30% and 35%. In all cases there is a small reduction in early and later strength with increasing clay content, the only exception being the 56- and 90-day strength of the cements containing CC2R. The strength loss with increasing calcined clay content for CC2R is surprising given that it had a 28-day activity index >100%.

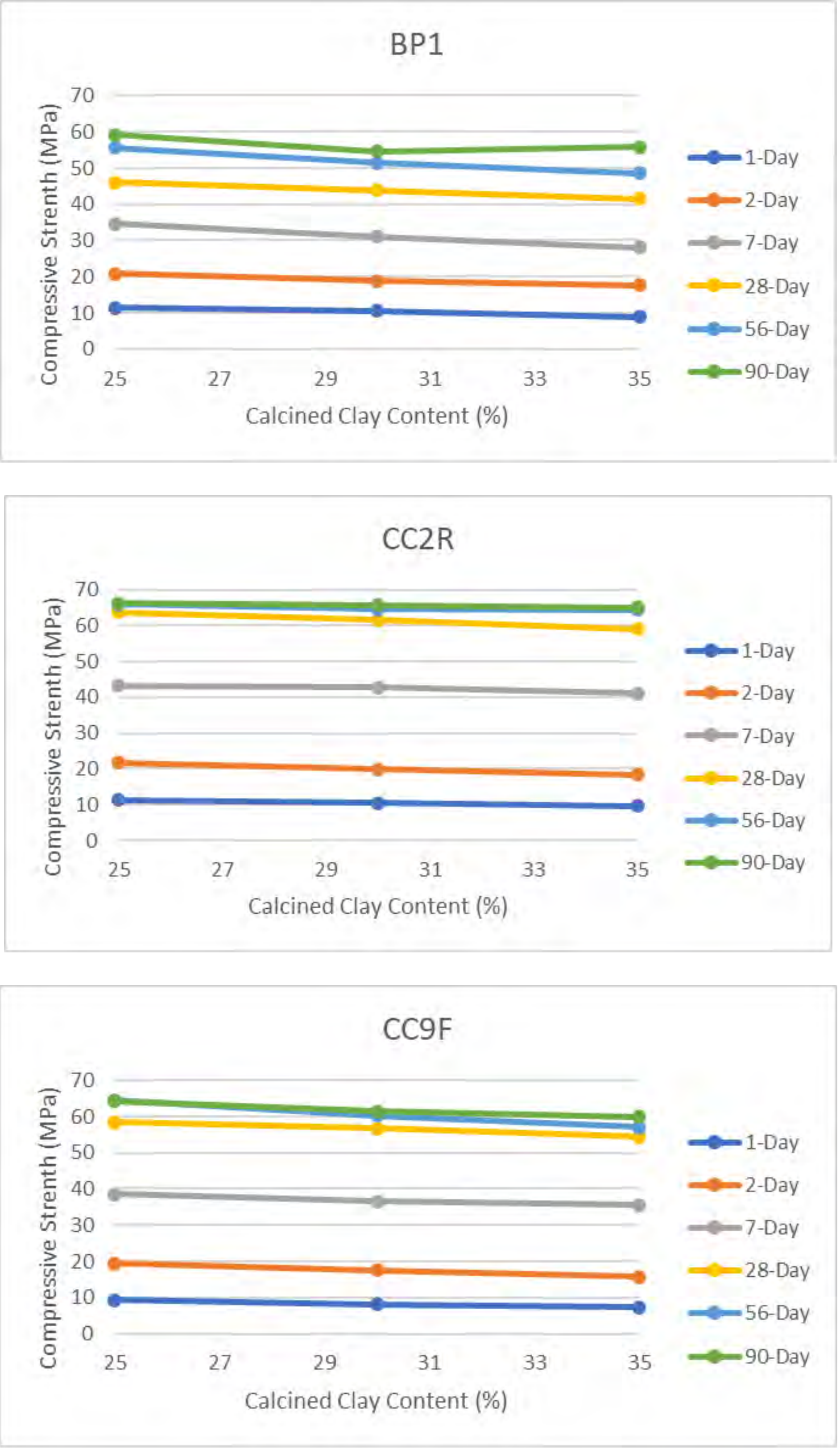

Figure 13: Strength development of CEM II/B-Q cements at different clinker replacement levels

Figure 14 shows the strength development up to 90 days for all CEM II/C-M cements made with the PC1 reference cement and source L1 limestone fines.

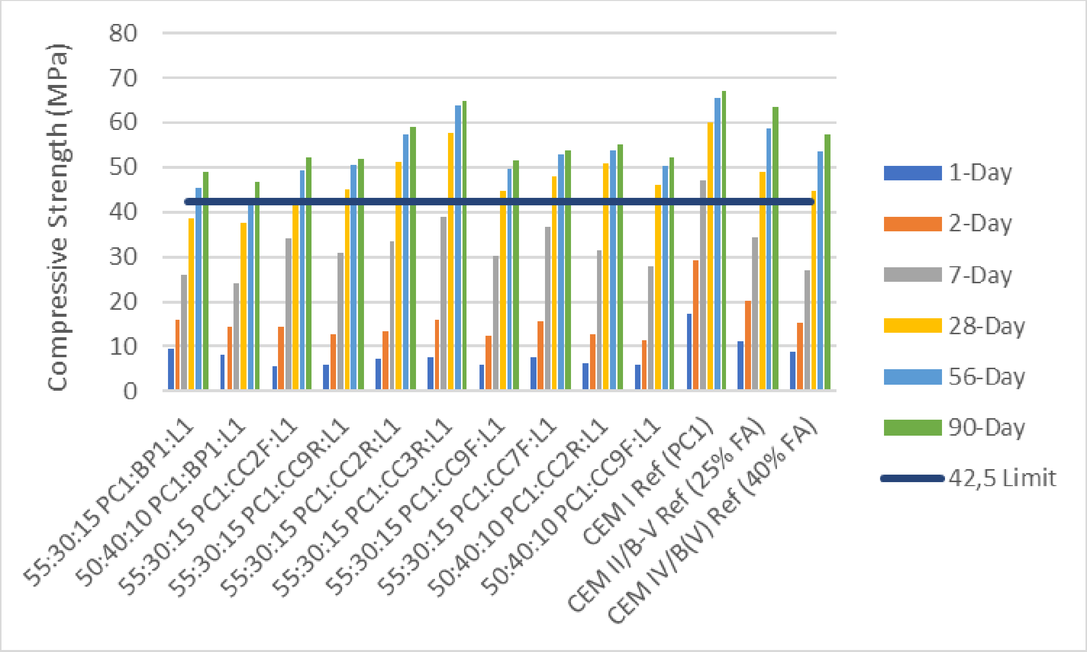

Figure 14: Strength development of CEM II/C-M cements with PC1 reference cement and L1

In the case of the CEM II/C-M cements the 1-day strengths are mostly lower not only than the PC1 reference cement strength but also compared to the two fly ash reference cements. At 2-days the strengths are comparable to the 40% fly ash reference cements. While meeting the 2-day 10 MPa 42,5 N strength minimum requirement of EN 197-1, it is borderline in many of the cases. At 28-days, with the exception of the BP1 cements, all CEM II/C-M cements exhibit either similar or higher strength levels than both fly ash reference cements. They also meet the 42,5 N limit albeit borderline except for the CC2R, CC3R and CC7F cements. As for the CEM II/B-Q cements, the highest strength is exhibited by the cements made with the CC2R and CC3R clays, the higher kaolinitic clays. Only the 55:30:15% cement made with CC3R closely matches the 28-day strength of the reference PC1, but exbibits lower 1-day, 2-day and 7-day strength than PC1.

Table 15 below compares the 28-day strength of the CEM II/B-Q cements with 30% calcined clay and the CEM II/C-M cements with 30% calcined clay and 15% limestone fines. A significant reduction in strength is found when comparing the 70:30% with the 55:30:15% cements, ranging from 12 to 24% and 18% on average. This indicates that there is no synergetic effect of the limestone fines with the calcined clay, in fact, in all but one cases the percentage reduction in strength is higher than the 15% limestone fine addition.

Table 15: 28-day strength comparison of 70:30 CEM II/B-Q and 55:30:15 CEM II/C-M cements

	28-day Strength, MPa		Reduction, %
	70:30	55:30:15	
BP1	43.9	38.7	12
CC2F	55.5	42.0	24
CC9R	55.8	45.0	19
CC2R	61.6	51.4	17
CC3R	68.4	57.7	16
CC9F	56.7	44.7	21
CC7F	58.3	48.1	17

The graphs in Figure 15 below show the strength development for BP1, CC2R and CC9F for the two different replacement levels, i.e. 55:30:15% vs 50:40:10%, and Table 16 below gives the percentage difference in strength between the 55:30:15% and 50:40:10% cements. For the cements with BP1 and CC2R calcined clays, the 55:30:15% cements, the strengths are slightly higher, typically by approximately 5%, than the 50:40:10% cements; at 1-day the strength difference is more pronounced percentage wise. For the CC9F, there is no clear picture.

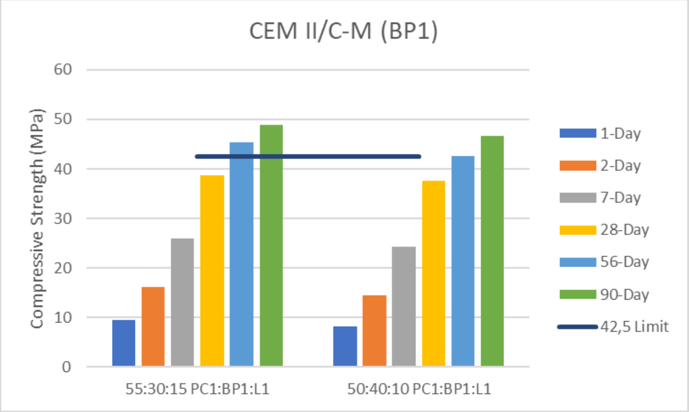

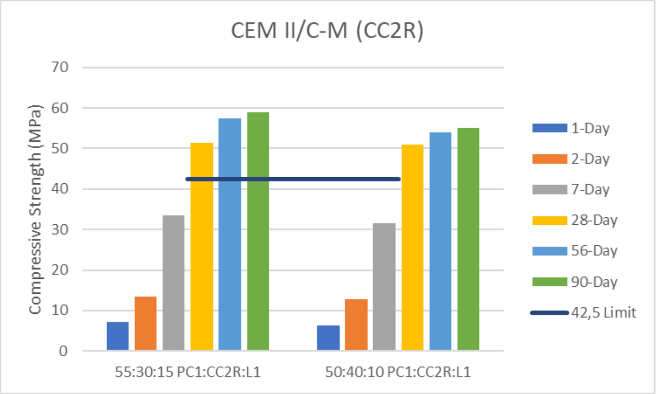

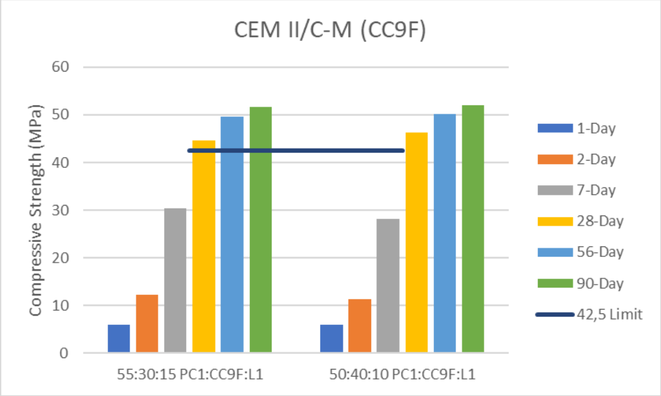

Figure 15: Strength development of CEM II/C-M cements at different clay and limestone levels

Table 16: Difference in strength between 55:30:15 and 50:40:10 CEM II/C-M cements

	% Strength Difference (55:30:15 minus 50:40:10)					
	1-Day	2-Day	7-Day	28-Day	56-Day	90-Day
BP1	14.7	9.9	6.6	2.8	6.2	4.7
CC2R	11.1	5.2	6.0	0.8	6.1	6.6
CC9F	-1.7	8.1	7.3	-3.4	-1.2	-1.0

4.3.3.2 Effect of Calcined Clay Fineness

After flash calcination, clays CC7F and CC9F were ground to achieve a fineness similar to that of the fly ash. The flash calcination process also produces a filter dust, the very fine portion of the clay which is captured in the filters. Under commercial operation, this filter dust is added to the calcined clay. As part of this project, it was retained separately. This provided an opportunity to assess the effect the fineness of the calcined clay has on strength development with three different level of fineness being available, the unground calcined clay, the ground calcined clay and the filter dust.

Table 17 below shows the chemical composition of these three components. As would be expected, only small differences are observed between the unground and ground material. The filter dust is also of similar composition, with the only noteworthy difference in the case of the CC7F where a reduced SiO_2 content is offset by an increase in Al_2O_3, iron oxide Fe_2O_3 and sulfate SO_3.

Table 17: Chemical analysis CC9F and CC7F at different stages of process

Clay	Condition	SiO_2	Al_2O_3	Fe_2O_3	CaO	MgO	MnO	TiO_2	SO_3	Na2O	K_2O	Na2Oeq	Sum
CC9F	Ground	63.17	21.38	8.93	2.08	0.85	0.11	1.23	0.12	0.06	1.11	0.79	99.83
	Pre-Grinding	61.55	22.22	7.46	2.87	0.99	0.12	1.27	0.35	0.09	1.34	0.97	99.23
	Filter Dust	64.06	21.12	8.78	1.97	0.84	0.10	1.23	0.14	0.06	1.11	0.79	100.20
CC7F	Ground	59.90	22.67	7.80	2.29	1.74	0.02	1.19	1.22	0.27	3.14	2.34	100.24
	Pre-Grinding	58.94	22.14	7.77	2.54	1.71	0.03	1.17	1.45	0.25	3.06	2.27	99.05
	Filter Dust	54.71	23.67	9.83	2.68	1.77	0.03	1.30	2.40	0.23	2.85	2.11	99.47

The PSD of the two clays at the three different stages is shown in Figure 16 below together with the PSD of the Source 1 reference cement and the fly ash. This demonstrates the coarseness of the clays prior to grinding, the similarity of the PSD of the two ground clays and of the reference cement and the fly ash, and that the filter dust has a steeper and slightly finer distribution than the ground clays.

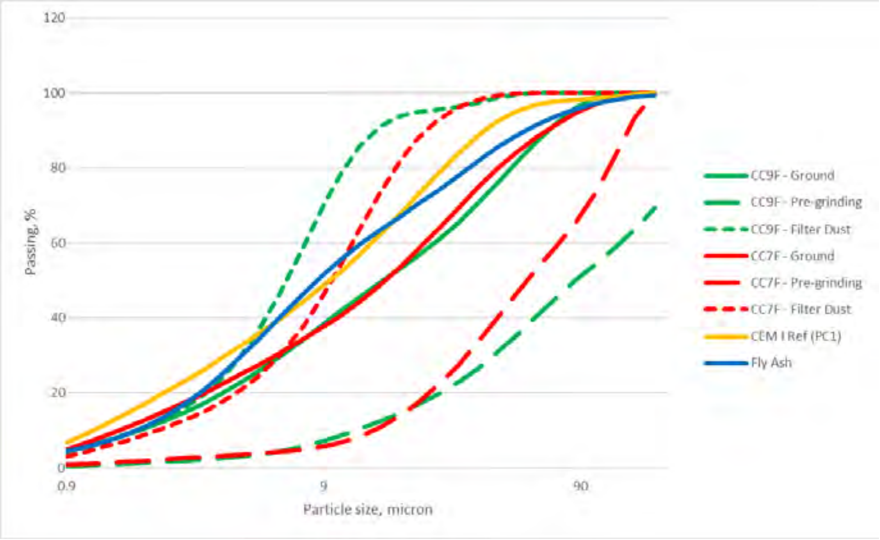

Figure 16: PSD distribution of CC9-F and CC7-F at different stages of process

The activity index (AI) was determined for all three clay processing stages for both CC9F and CC7F using the method described in BS 8615-1, i.e. preparing mixes with 25% calcined clay replacement levels and calculating their relative strength compared to 100% reference cement mixes at 28- and 90-days respectively. The results are summarised in Table 18 below.

Table 18: Activity indices for CC9-F and CC7-F at different fineness levels

Clay	**Condition**	**Activity Index with Reference PC1 (%)**		**Activity Index with Reference PC2 (%)**	
		28-day	**90-day**	**28-day**	**90-day**
CC9F	Ground	94	96	88	88
	Pre-Grinding	78	83	81	81
	Filter Dust	96	96	86	87
CC7F	Ground	99	98	90	92
	Pre-Grinding	82	87	79	80
	Filter Dust	99	98	84	88

The higher values obtained for the activity indices with PC1 compared to PC2 are purely a reflection of the lower strength of PC1 compared to PC2. The requirements of BS 8615-1 are for the 28-day index to be at least 75% and the 90-day index 85%. The results demonstrate that without grinding, the clays do not consistently meet these minimum requirements but that once ground to a fineness similar to that of the CEM I and fly ash, both clays comfortably meet the requirements, also when using the very high strength PC2 as reference. There are no further strength gains from the even finer filter dust compared to the ground clays.

4.3.3.3 Effect of Calcination Process

Figure 17 compares the strength development of CC2R with CC2F and CC9R with CC9F in the 70:30 CEM II/B-Q and the 55:30:15% CEM II/C-M cements. In the case of CC2F and CC2R, the cements have similar strength up to 7-days but slightly higher later strength results following rotary calcination. It should be noted again at this point that additional high kaolinitic material was added to the raw CC2 material prior to rotary calcination in order to achieve the required clay consistency for rotary calcination and that CC2R was ground following calcination but CC2F was not. This therefore excludes a direct comparison. For CC9F and CC9R there is little difference in the strength development between material processed via flash and rotary calcination. These results align with the activity indices reported in Table 10.

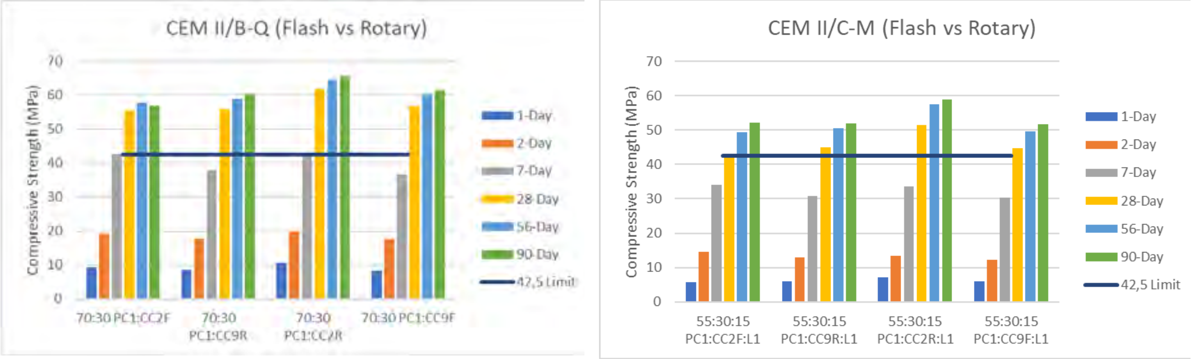
CEM II/B-Q (Flash vs Rotary)

CEM II/C-M (Flash vs Rotary)

Figure 17: Effect of flash versus rotary calcination on strength development of calcined clay cements

4.3.3.4 Effect of Cement and Limestone Sources

Figure 18 and Figure 19 show the effect of different reference cements and different limestone sources used in the cements respectively on strength development.

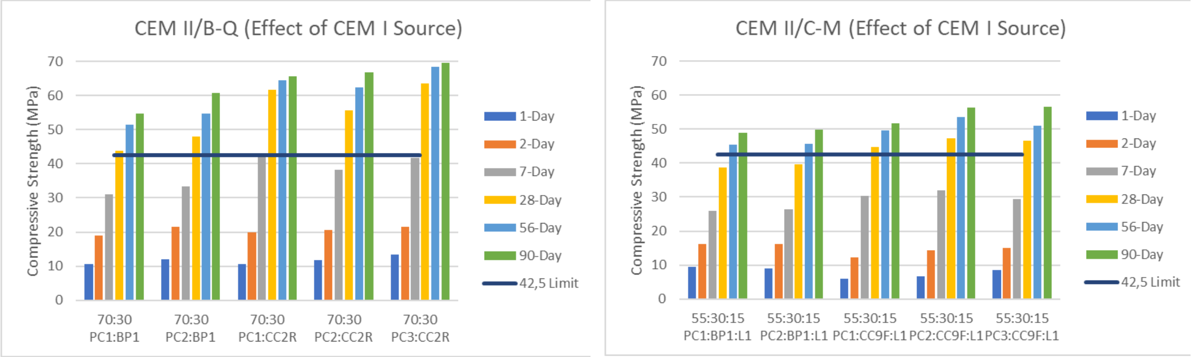
CEM II/B-Q (Effect of CEM I Source)

CEM II/C-M (Effect of CEM I Source)

Figure 18: Effect of reference cement source on strength development of calcined clay cements

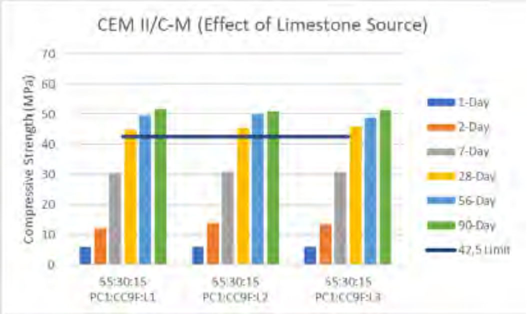
CEM II/C-M (Effect of Limestone Source)

Figure 19: Effect of limestone source on strength development of calcined clay cements

BP1 was tested with PC1 and PC2. The higher strength of PC2 is reflected in the results of the CEM II/B-Q 70:30% whereas in the lower clinker 55:30:15% CEM II/C-M cement, the effect of the cement strength becomes negligible.

All three cement sources were tested with CC2R in the 70:30% CEM II/B-Q cements. In this case, there are unexpected results in that the cement made with PC2 exhibits lower strength at 7, 28 and 56 days compared to the cement made with PC1. With the exception of the 7-day result, the cement made with PC3 exhibits higher strength at all ages than the cements made with PC1 and PC2. This is again surprising as PC2 has higher strength than PC3 except for the 1- and 2-day strength.
All three cement sources were also tested with CC9F in the 55:30:15% CEM II/C-M cements. In this case the results largely reflect strength characteristics of the PC sources, i.e. cements with PC2 give higher results than cements with PC1 and the higher early strength of PC3 is also reflected in the CEM II/C-M results.
The results shown in Figure 19 confirm the expected outcome that the limestone source has no effect on the results.

4.3.3.5 Effect of SO3 Content

The role of sulfate additions to CEM I, usually in the form of gypsum, is to control the hydration of the alumina phase (C3A) to avoid flash setting. It has been reported that the adjustment of the sulfate content in limestone calcined clay cements is key to their hydration not only to prevent flash set but also to avoid sulfate depletion linked to adsorption of SO_4^{2-} onto the positively charted Ca_2^+ layer formed on the surface of calcined clay particles (Maier, Sposito, Beutner, & Thienel, 2022). While Zunino and Scrivener (Zunino & Scrivener, 2019) propose a different mechanism for the acceleration of the early silicate and aluminate clinker reactions in the presence of limestone and calcined clay, they equally highlight the need for sulfate adjustments in limestone calcined clay cements to achieve optimum strength development. Scrivener et al. (2018) attribute the need for additional sulfate to the additional reactive alumina being introduced by the calcined clay and to adjust the timing of the alumina peak. A too early occurance of the alumina peak has been associated with lower late strength (Sharma, Bishnoi, Martirena, & Scrivener, 2021).

In order to study the effect of sulfate content on the strength of calcined clay cements, it was decided to make a not originally planned addition to the cement testing programme. Cement PC1:CC9F at all three blend levels (75:25%, 70:30% and 65:35%) of the CEM II/B-Q and cement PC1:CC9F:L1 at the two different blend levels (55:30:15% and 50:40:10%) of the CEM II/C-M group were chosen for re-sulphurisation. In the latter group cement PC1:CC7F:L1 at the 55:30:15% replacement level was also tested as CC7F had a higher starting SO_3 level than the other clays.

The same gypsum source as used to produce Source 1 CEM I (PC1) was ground in the lab. The SO_3 content was determined (37.9%) and a calculated percentage of gypsum was blended into the cements in order to achieve SO_3 levels of app. 2.5%, 3.0% and 3.5% in the blended cements. The comparison in SO_3 content of the orginal cements and the resulphurised cements, is shown in Table 19 below. It demonstrates that the target SO_3 levels were closely met by the gypsum additions made.

Table 19: SO3 levels of re-sulfated cements

Cement	Target SO_3 (%)	Actual SO_3 (%)
75:25 PC1:CC9F	original cement	2.28
	2.5	2.46
	3.0	2.92
	3.5	3.37
70:30 PC1:CC9F	original cement	2.10
	2.5	2.50
	3.0	2.96
	3.5	3.42
65:35 PC1:CC9F	original cement	1.96
	2.5	2.46
	3.0	2.97
	3.5	3.42
55:30:15 PC1:CC9F:L1	original cement	1.86
	2.5	2.52
	3.0	3.04
	3.5	3.53
55:30:15 PC1:CC7F:L1	original cement	2.25
	3.0	2.94
	3.5	3.47
50:40:10 PC1:CC9F:L1	original cement	1.63
	2.5	2.52
	3.0	3.05
	3.5	3.47

The effect of the increased SO3 levels on the strength development is shown in Figure 20 as the difference in strength between the original cement and the re-sulfated cement.

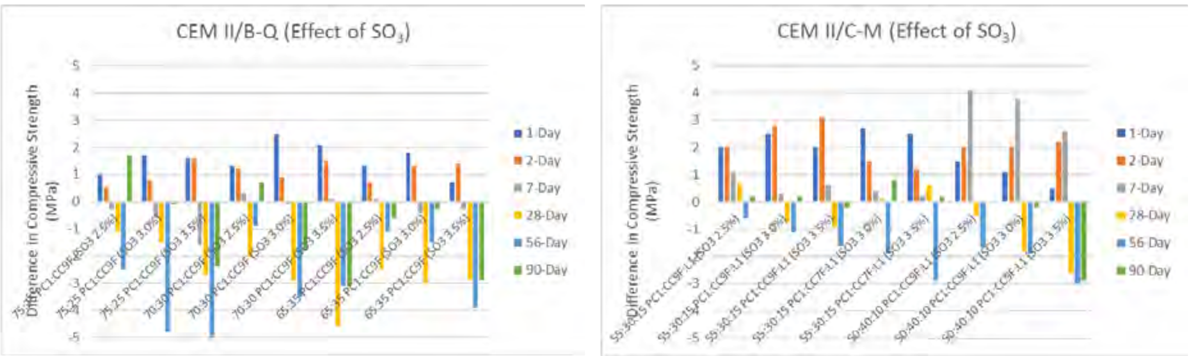

Figure 20: Effect of SO3 additions on strength development

The following main observations can be made from these results:

- In all cases the 1- and 2-day strength increase with the SO3 addition.
- The early strength increase is more pronounced with the CEM II/C-M cements.
- At 7 days, there is no consistent effect of SO3 addition. The significant increase on 7-day strength of the 50:40:10% cement is notable but unexplained.
- At 28-days and beyond, the SO3 addition results in general in a loss in strength which is more pronounced in the CEM II/B-Q cements than the CEM II/C-M cements.
- The early strength gains typically peak at 3.0% SO3 and then drop off at 3.5% SO3.

4.4 Comparison with Results from Other Work Packages

In work package E of the project, UCL have carried out an extensive programme of activity testing of the calcined clays using a modified R3 test procedure and Dundee University have carried out an extensive concrete durability testing programme in work package K. Some of the results from these work packages are analysed in the following together with the results of the cement assessment programme of this report.

4.4.1 Comparison with R3 Results

UCL carried out modified R3 heat of hydration testing to establish the cumulative heat after 140 hrs of hydration. The cumulative heat results from a binary system of a calcined clay to CaOH ratio of 1:1 have been correlated with the 28-day compressive strength results of the 70:30 CEM II/B-Q and the 55:30:15 CEM II/C-M cements of the current work package, Figure 21.

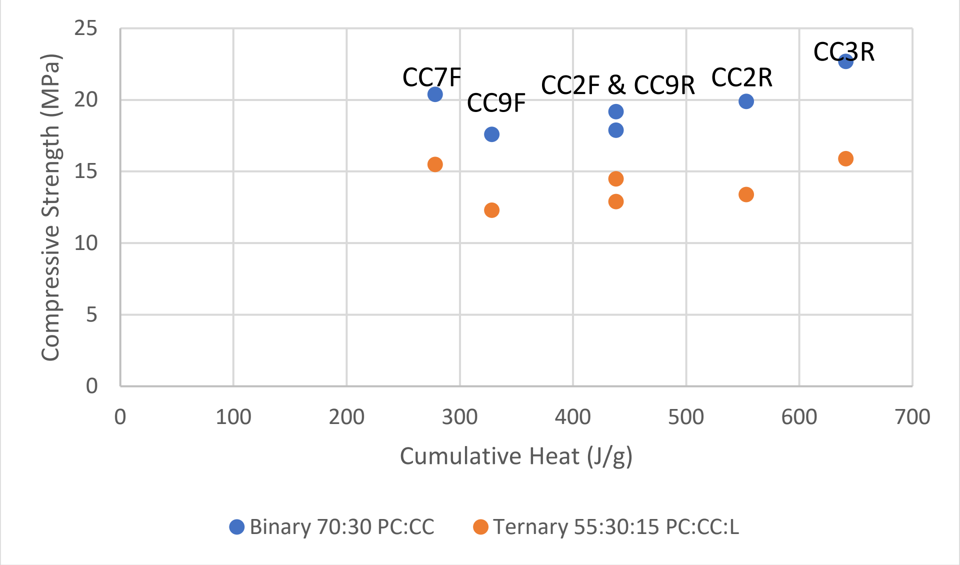

Figure 21: Correlation of modified R3 results with 28-day strength of 70:30 CEM II/B-Q cements

The results for calcined clays 2F, 2R and 3R, the clays with the higher kaolinite content, show the expected trend of increasing strength with increasing cumulative heat. CC7F, CC9F and CC9R, however, do not follow this trend. If assumptions on the reactivity of the calcined clays in cementitious systems were made based on the modified R3 results, this could lead to wrong decisions. Yet to be published data from Heidelberg Materials indicates that the correlations between R3 results and compressive strength for kaolinitic clays and for predominantly illitic clays follow different patterns. Different reactivity classifications based on R3 results may have to be devised for these two different groups of clays.

4.4.2 Comparison with Concrete Compressive Strength Results

The 28-day strength results of the cement testing programme have been correlated with the 28-day concrete strength results of the concretes made with the same cements at the water/cement ratio of 0.5. This correlation is shown in Figure 22.

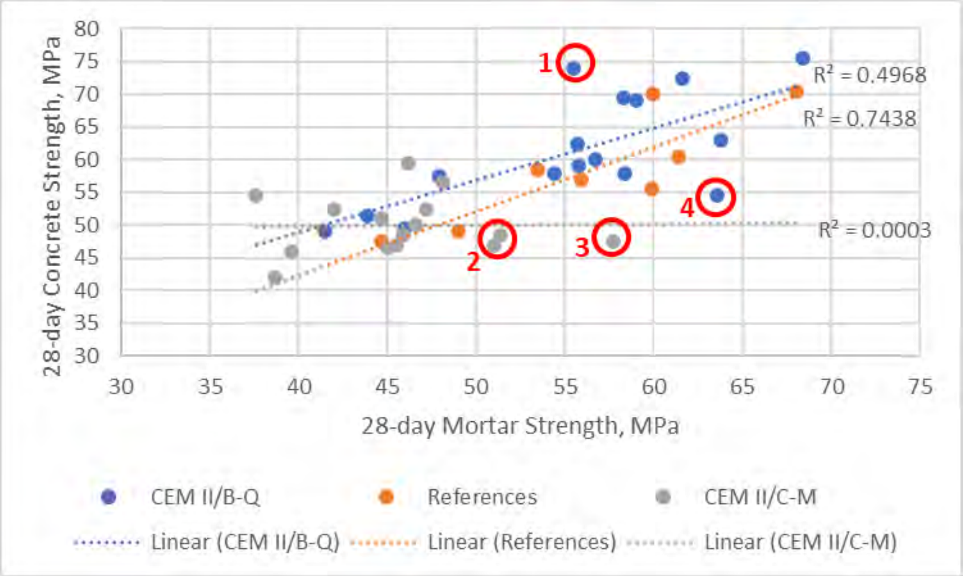

Figure 22: Correlation between cement mortar prism and concrete cube 28-day strength results

Five potential outliers have been identified visually; two close together marked as ‘2’ in the graph above. These outliers all relate to cements made with the higher kaolinitic clays, and four out of the five of those made via the rotary process, as follows:

- Outlier 1: Relates to 70:30% PC1:CC2F
- Outliers 2: Relate to 55:30:15% PC1:CC2R:L1 and 50:40:10% PC1:CC2R:L1
- Outlier 3: Relates to 55:30:15% PC1:CC3R:L1
- Outlier 4: Relates to 70:30% PC3:CC2R

For all of the outliers with the rotary produced clays, the concrete strength is low compared to the cement strength. Only for outlier 1 made with the flash calcined CC2F clay, is the concrete strength high for the given cement strength. The cement strength results were therefore further analysed for outlier 1. In Figure 23 the CEM II/B-Q 70:30% and CEM II/C-M 55:30:15% results are all plotted for all cements made with PC1 and L1. The curve for the 70:30% cement with CC2F which produced the outlier at 28 days is shown with the dotted red line in the left graph. This curve does not show an anomaly. Comparing the graphs for the 70:30% and 55:30:15% cements also shows a very similar strength ranking of the different clays and the CC2F clay rates as second lowest at 28-days in both graphs. This indicates that it is most likely the concrete strength result of outlier 1 that is atypical rather than the cement strength result.

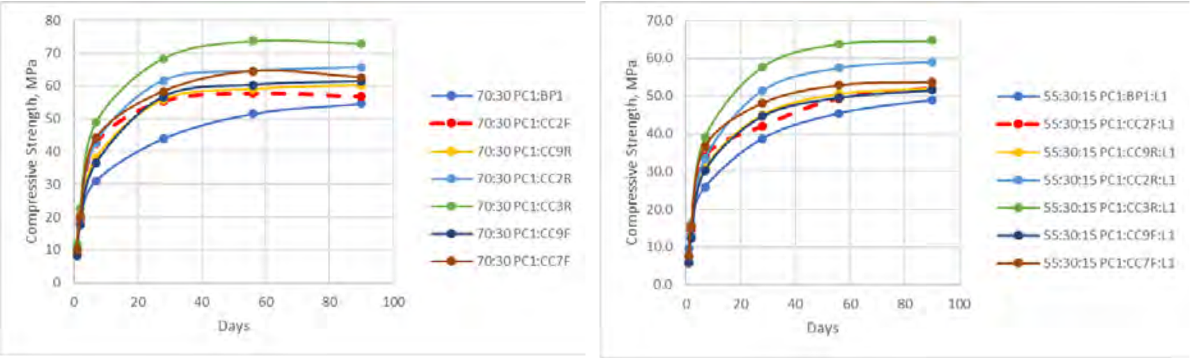

Figure 23: Strength development of 70:30 and 55:30:15 cements with PC1 and L1

4.4.3 *Effect of Superplasticiser on Early Strength*

UCL observed from compressive strength testing carried out on mortars produced with and without admixture, that the early age strength of mortars made with admixture is lower than that of mortars made without admixture whereas the 28-day strength is not affected by the addition of a superplasticising admixture. This has been attributed to the superplasticisers delaying the early hydration.

In order to investigate this effect further, the 1-to-28 day strength ratio of the cement mortar strength and that of the concretes produced by Forterra for the demonstration phase of the project and by the University of Dundee for the durability test programme have been compared in Figure 24 below. The superplasticiser additions in the Forterra mixes ranged from 0.6% for the ternary blend made with BP1 to 1.65% for the binary blend made with CC2F. The dosage during standard production is 0.6%. It should be noted that the Forterra mixes were made with a different CEM I source than the mortar mixes. The superplasticiser dosage used at Dundee for the 0.5 w/c ratio mixes ranged from 0.4% to 1.1%, again the lower dosage being associated with BP1 and the highest dosage with CC2F. The superplasticiser additions for the concretes made at Dundee with the reference cements were ranged from about 0.4% for PC2, PC3, the fly ash and 36% GGBS cement to 0.6% for PC1.

Figure 24: Relationship of 1-to-28 day strength ratio between mortar and concrete mixes

The strength ratios of the mortars compared to those of the concrete mixes from Forterra show that in all cases the ratio is higher for the concretes than the mortars, indicating that the concretes, despite the superplasticiser additions, have a higher relative early strength than the mortars. In the case of the comparison of the mortars with the concrete mixes made at Dundee, the ratios are surprisingly similar in most cases, and there is not consistent trend the in concrete mixes having proportionally a lower early strength.

5. Discussion

5.1Clay composition

The comparison of the mineralogical clay composition estimates in Table 2 and Table 3 has demonstrated how difficult it is to obtain accurate estimates of the mineralogical composition of clays. Rietveld refinements used in conjunction with XRD are commonly used but are accurate only for narrow ranges of known materials. It is therefore important when quantifying clay mineralogies for a wider range of clays to do so using XRD from first principles.

5.2 Reactivity of clays and calcined clay cement strength

The compressive strength results obtained from the clays assessed in this work package demonstrates that high levels of reactivity can also be obtained from clays such as CC7F, CC9F, and CC9R even if the kaolinite content is limited and other 2:1 clay minerals are present instead. The key is to carefully determine the optimum calcination temperature to ensure that dihydroxylation has taken place but not exceeding the temperatures where re-crystallisation would occur.

It is an encouraging outcome of this project to have been able to demonstrate that all four clays, none of which are prime kaolinitic clays, produce cement strengths which exceed those of fly ash cements with the same or similar replacement level (25% and 40%) and even the brick powder meeting the 42,5 N strength class at 25% replacement level.

Contrary to reports from the literature though, where LC3-50 (50% ground clinker, 30% calcined clay, 15% limestone, 5% gypsum) produced 28-day strength similar or higher to that of a CEM I cement as long as the kaolinite content of the clay is greater than 40% (Scrivener et al., 2018), the addition of limestone fines to create LC3 type cements has not proven to have any synergetic effects. In the LC3-type cements produced in this project, the addition of 10% and 15% limestone with 40% and 30% calcined clay respectively, has led to proportional strength losses. While all calcined clay limestone cements except the ones with the brick powder meet the 42,5 N strength class, their 2-day and 28-day strengths are significantly reduced compared to the CEM I strength and also compared to the calcined clay cements without limestone fines. This reduction in strength of the LC3-type cements compared to the 52,5N reference CEM I also applies to the cements made with the CC2 and CC3 clays which contain more than 50% kaolinite.

5.3 Effect of SO_3 content

The additional cement mortar compressive strength testing carried out with the cements re-sulfated to 2.5%, 3.0% and 3.5% SO3, has demonstrated a positive effect on early strength with SO_3 levels increased to 3.0% but also an adverse effect on 28-day strength and beyond. The positive effect on early strength was more pronounced for the CEM II/C-M cements than the CEM II/B-Q cements. As the benefits on early strength are small, sulfate additions are not considered to be a mandatory aspect of calcined clay concrete mix optimisation would benefit the ternary cements more than the binary cements. This finding is of relevance for the UK market, where calcined clays may be sold as an addition rather than in the form of factory blended cement, where at the mixer the clays will be blended with a range of cement sources which will have different SO_3 contents. In general UK CEM I cements tend to have relatively high SO_3 contents compared to continental Europe CEM I cements, probably because of the established practice of blending at the mixer with high levels of GGBS or fly ash.

5.4 Conformity with BS 8615

The one aspect where not all clays conformed with BS 8615-1 was on water demand. However, the water demand is not necessarily related to the reactivity of the clays. Figure 25 indicates only a week correlation between the water demand and activity index results as obtained per BS 8515.

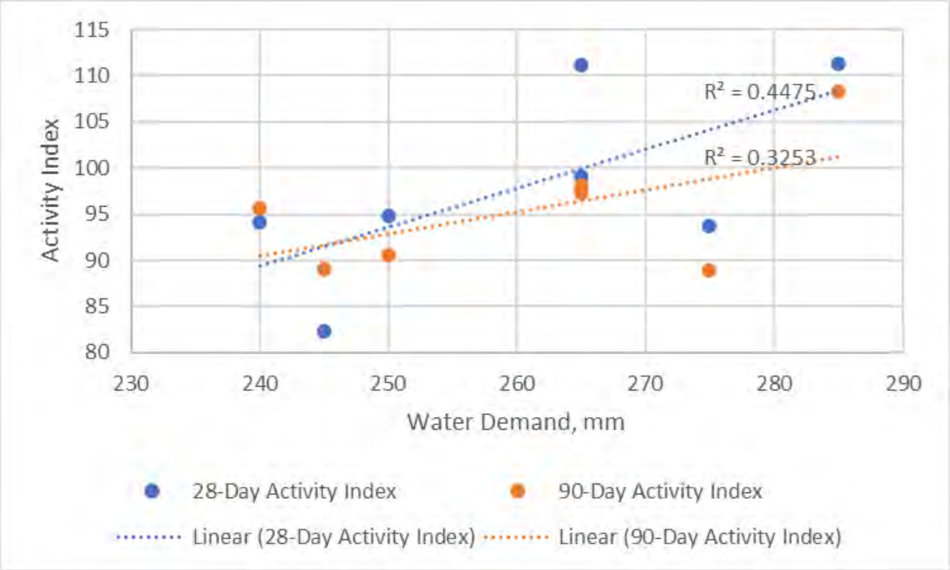

Figure 25: Water demand versus activity index

The lack of a correlation between workability and strength is further demonstrated in Figure 26 where the flow of the cement mortars is plotted against their respective 28-day strength. This implies that admixture dosage aimed at workability of calcined clay cement concretes are likely to require careful adjustments for each individual calcined clay source.

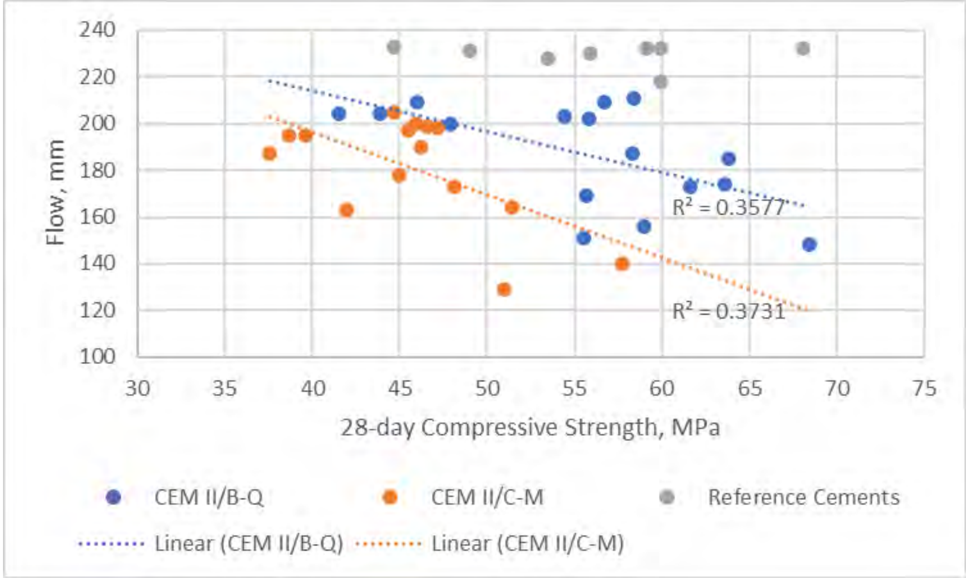

Figure 26: Mortar flow versus 28-day strength

6 Conclusions and Recommendations

The work carried out in work package J of the Re-C3 project has led to the following conclusions:

- There is good agreement in test results between the two laboratories at which the cement assessment programme was carried out.
- Consideration must be given to the methods used for the mineralogical analysis of clays. If not calibrated or interpreted appropriately misleading results can be obtained.
- All clays, with the exception of the high kaolinitic clay after flash calcination, required grinding after calcination to optimise the clay fineness and reactivity.
- Using a reducing atmosphere during flash calcination has resulted, as intended, in a grey-coloured appearance of the calcined clay as opposed to the much more red-coloured clays from the rotary process where no atmosphere control was applied.
- There was no discernible effect of flash versus rotary calcination on compressive strength nor fresh mortar properties.
- The limestone source also had no noticeable influence on compressive strength or fresh mortar properties.
- There was no clear picture of how the CEM I source affects the strength development of the calcined clay cements.
- While SO_3 additions increased the early strength of the calcined clay cements, they reduced the 28-day strength and beyond.
- Early strength improvements with SO_3 additions peaked at a 3% SO_3 content in the cements.
- All waste clay produced respectable strength results, most cements with up to 40% calcined clay content meeting the 42,5N strength class. The clays with lower kaolinite contents also demonstrated good reactivity. Most of the calcined clay cements without limestone additions outperformed the 25% and 40% fly ash reference cements in terms of strength development.
- The R3 test results do not directly correlate with the strength development of the cements.

- Performance against BS 8615-1:
    - Despite the clays being waste or by-products, they all meet, with only one minor exception, the chemical requirements of BS 8615-1.
    - As for the chemical requirements, the clays also all met the physical properties stipulated in BS 8615-1 except for the water requirement. Four calcined clays exceeded the value allowed for water requirement in BS 8615-1.
- Fresh mortar properties:
    - The initial setting times of the calcined clay cements are all significantly higher than the setting time requirements of EN 197-1 and most closely match the setting times of the fly ash reference cements.
    - The calcined clay cements with and without limestone additions have a higher water demand and exhibit a lower mortar flow than any of the reference cements and the water demand is highest and the flow lowest in the higher kaolinitic clays.
    - There is, however, no direct correlation between the water demand and the activity index of the clays or the mortar flow and the 28-day strength of the cements.
    - The mortar flow decreases with an increase in the clay content of the cements, this being more pronounced for the clays with the higher kaolinite content with a higher fineness
    - The calcination process, i.e. flash versus rotary, has no distinct effect on the fresh properties of the clay cement mortars.
- Compressive strength development:
    - The early strength of the CEM II/B-Q cements is comparable to that of the 25% fly ash reference cements, whereas that of the CEM II/C-M cements is closer to that of the 40% fly ash reference cement.
    - With the exception of the brick powder, all CEM II/B-Q cements meet the 2-day and 28-day 42,5N and 52,5L strength requirements of EN 197-1 comfortably.
    - The CEM II/C-M cements meet the 42,5N strength class with a reduced margin at 28-days and borderline 2-day strength levels and with one exception would not meet the 52,5L strength class.
    - Generally, though not consistently so, the cements with the higher kaolinitic clays from Imerys produce the highest strength.
    - The limestone seems to act as a filler rather than contributing to the strength development, also in the cements made with the higher kaolinitic clays.
    - An increase in clay content from 25 to 35% does generally lead to a small reduction in early and later strength. This also applies to CC2R despite its 28-day activity index being >100%.

In order to promote the take up of calcined clays in the UK, the following additional work is recommended.

- Guidelines should be developed on how to determine the mineralogical phases of clays consistently.
- The water requirement limit in BS 8615-1 should be reviewed. Four clays in the programme exceeded the limit but, using appropriate admixtures, satisfactory concrete mixes were produced using these clays.
- The effect of different clinker sources on the strength development of calcined

clay cements warrants further investigation.

- With the R3 test method becoming more prominent for the assessment of the reactivity of SCMs, the correlation between R3 results and the traditional activity indices based on cement mortar tests should be further studied.

Bibliography

Bristish Standards Institution. (2019). BS 8615-1:2019 Specification for pozzolanic materials for use with Portland cement. Part 1: Natural pozzolana and natural calcined pozzolana. London: BSI.

British Standards Institution. (1999). BS EN 1015-3:1999 Methods of test for mortar for masonry - Part 3: Determination of consistence of fresh mortar (by flow table). London: British Standards Institution.

British Standards Institution. (2006). BS EN 15167-1:2006 Ground granulated blast furnace slag for use in concrete, mortar and grout - Part 1: Definitions, specifications and conformity criteria. London: BSI.

British Standards Institution. (2011). BS EN 197-1:2011 Cement Part 1: Composition, specifications and conformity criteria for common cements. London: British Standards Institution.

British Standards Institution. (2012). BS EN 450-1:2012 Fly ash for concrete. Part 1: Definition, specifications and conformity criteria. London: BSI.

British Standards Institution. (2019). BS 8615-2 Specification for pozzolanic materials for use with Portland cement. Part 2: High reactivity naterual calcined pozzolana. London: British Standards Institution.

British Standards Institution. (2021). BS EN 197-5:2021 Cement Part 5: Portland-composite cement CEM II/C-M and Composite cement CEM VI. London: British Standards Institution.

Maier, M., Sposito, R., Beutner, N., & Thienel, K.-H. (2022). Particle characteristics of calcined clays and limestone and their impact on early hydration and sulfate demand of blended cement. *Cement and Concrete Research, 154*, 103736.

Scrivener, K., Martirena, F., Bishnoi, S., & Maity, S. (2018). Calcined clay limestone cements (LC3). *Cement and Concrete Research, 114*, 49-56.

Sharma, M., Bishnoi, S., Martirena, F., & Scrivener, K. (2021). Limestone calcined clay cement and concrete: A state-of-the art review. *Cement and Concrete Research*, 149.

Skrivener, K; Martirena, F; Bishnoi, S; Maity, S. (2018). *Cement and Concrete Research, 114*, 49-56.

Zunino, F., & Scrivener, K. (2019). The influence of the filler effect on the sulfate requirement of blended cements. *Cement and Concrete Research, 126*, 105918.

Annexes

XRF analyses of reference cements

	SiO_2	Al_2O_3	Fe_2O_3	CaO	MgO	MnO	TiO_2	SO_3	Na2O	K_2O	Sum
CEM I Ref (PC1)	20.48	5.25	3.13	65.31	1.29	0.05	0.34	3.06	0.32	0.62	99.85
CEM II/A-LL Ref	19.56	4.85	2.75	67.24	1.37	0.06	0.36	3.02	0.25	0.60	100.05
CEM II/B-V Ref (25% FA)	28.71	8.65	4.24	49.21	1.33	0.07	0.45	2.66	0.48	0.91	96.71
CEM III/A Ref (36% GGBS)	26.03	7.90	2.11	55.28	4.04	0.13	0.42	2.95	0.28	0.60	99.72
CEM III/A Ref (45% GGBS)	27.16	8.61	1.91	53.20	4.69	0.15	0.44	2.89	0.29	0.60	99.95
CEM II/B-V Ref (40% FA)	33.93	10.79	4.98	40.63	1.42	0.07	0.53	2.38	0.64	1.10	96.47
CEM I Ref (PC2)	19.87	5.22	3.49	63.97	0.78	0.08	0.28	2.62	0.05	0.39	96.75
CEM I Ref (PC3)	19.54	4.48	2.86	62.53	1.19	0.07	0.25	3.63	0.27	0.64	99.57

XRD analyses of reference cements

	C3S	C2S	C3A	C4AF	MAC/Filler
CEM I Ref (PC1)	57.74	15.79	9.17	6.96	4.90
CEM II/A-LL Ref	65.70	7.73	10.02	5.46	12.00
CEM II/B-V Ref (25% FA)	54.47	15.94	8.37	7.17	4.34
CEM I Ref (PC2)	55.91	19.80	7.33	10.21	4.36
CEM I Ref (PC3)	54.90	21.70	7.60	7.80	4.50

XRF analyses of blended cements

	SiO_2	Al_2O_3	Fe_2O_3	CaO	MgO	MnO	TiO_2	SO_3	Na2O	K_2O	Sum
75:25 PC1:BP1	28.81	8.21	3.65	50.57	1.36	0.06	0.48	2.98	0.27	1.19	97.58
70:30 PC1:BP1	30.52	8.86	3.78	47.61	1.38	0.06	0.51	2.98	0.29	1.31	97.30
65:35 PC1:BP1	32.08	9.46	3.89	44.91	1.39	0.06	0.54	2.98	0.29	1.42	97.02
70:30 PC2:BP1	30.22	8.93	4.09	48.28	1.05	0.06	0.47	2.71	0.15	1.18	97.14
75:25 PC1:CC2R	29.04	12.77	2.70	47.41	1.03	0.06	0.27	2.23	0.25	1.50	97.26
75:25 PC1:CC9F	30.78	9.10	4.49	48.23	1.15	0.08	0.55	2.28	0.19	0.72	97.57
75:25 PC1:CC9F (2.5% SO3)	30.75	9.02	4.47	48.01	1.15	0.08	0.55	2.46	0.16	0.72	100.01
75:25 PC1:CC9F (3.0% SO3)	30.56	8.93	4.45	47.72	1.19	0.08	0.54	2.92	0.17	0.72	100.01
75:25 PC1:CC9F (3.5% SO3)	30.23	8.86	4.40	47.51	1.22	0.08	0.54	3.37	0.17	0.72	99.89
70:30 PC1:CC2F	30.97	13.40	2.80	44.50	1.01	0.06	0.28	2.09	0.24	1.87	97.22
70:30 PC1:CC9R	32.55	10.26	4.67	44.66	1.19	0.09	0.59	2.12	0.20	0.84	97.17
70:30 PC1:CC2R	30.84	14.40	2.62	44.26	1.00	0.05	0.26	2.09	0.23	1.68	97.43
70:30 PC1:CC3R	30.87	15.09	2.50	44.42	0.99	0.05	0.24	2.09	0.21	1.46	97.92
70:30 PC1:CC9F	32.94	9.82	4.81	45.13	1.11	0.08	0.60	2.10	0.15	0.75	97.49
70:30 PC1:CC9F (2.5% SO3)	32.94	9.82	4.79	45.09	1.15	0.08	0.59	2.50	0.16	0.75	100.40
70:30 PC1:CC9F (3.0% SO3)	32.60	9.70	4.75	45.26	1.20	0.08	0.59	2.96	0.16	0.75	100.46
70:30 PC1:CC9F (3.5% SO3)	32.06	9.52	4.63	44.99	1.21	0.08	0.58	3.42	0.16	0.74	100.08
70:30 PC1:CC7F	32.05	10.00	4.40	45.42	1.39	0.06	0.57	2.46	0.20	1.30	97.85
65:35 PC1:CC2R	32.78	15.95	2.57	41.21	0.95	0.05	0.25	1.91	0.17	1.86	97.70
65:35 PC1:CC9F	34.90	10.50	5.08	42.14	1.10	0.08	0.63	1.96	0.14	0.77	97.30
65:35 PC1:CC9F (2.5% SO3)	34.87	10.55	5.04	41.85	1.14	0.08	0.63	2.46	0.15	0.77	99.96
65:35 PC1:CC9F (3.0% SO3)	34.58	10.47	4.99	41.77	1.17	0.08	0.63	2.97	0.14	0.77	100.05
65:35 PC1:CC9F (3.5% SO3)	34.24	10.36	4.93	41.69	1.21	0.08	0.62	3.42	0.15	0.77	100.05
70:30 PC2:CC2R	30.81	14.47	2.95	44.90	0.67	0.06	0.23	1.82	0.07	1.55	97.53
70:30 PC3:CC2R	29.77	13.68	2.59	44.28	0.94	0.07	0.21	2.38	0.12	1.72	95.76
55:30:15 PC1:BP1:L1	30.10	9.19	3.86	49.98	1.40	0.05	0.54	2.71	0.33	1.42	99.57
50:40:10 PC1:BP1:L1	33.53	10.50	4.21	44.06	1.44	0.05	0.61	2.77	0.38	1.65	99.18
55:30:15 PC2:BP1:L1	29.14	9.19	4.08	51.16	1.09	0.05	0.46	2.47	0.24	1.23	99.11
55:30:15 PC1:CC2F:L1	31.01	14.20	2.65	46.36	0.95	0.05	0.26	1.87	0.27	2.03	99.64
55:30:15 PC1:CC9R:L1	32.43	10.66	4.70	47.26	1.17	0.07	0.59	1.89	0.23	0.85	99.85
55:30:15 PC1:CC2R:L1	30.56	15.36	2.45	46.11	0.91	0.04	0.24	1.83	0.24	1.84	99.58
55:30:15 PC1:CC3R:L1	30.53	15.87	2.29	46.28	0.91	0.04	0.22	1.85	0.22	1.55	99.75
55:30:15 PC1:CC9F:L1	32.84	10.28	4.77	47.11	1.12	0.06	0.64	1.86	0.23	0.75	99.67
55:30:15 PC1:CC9F:L1 (2.5% SO3)	32.76	10.26	4.76	46.66	1.18	0.06	0.59	2.52	0.26	0.75	99.81
55:30:15 PC1:CC9F:L1 (3.0% SO3)	32.44	10.08	4.71	46.96	1.21	0.06	0.59	3.04	0.26	0.76	100.12
55:30:15 PC1:CC9F:L1 (3.5% SO3)	31.84	9.95	4.69	46.83	1.22	0.06	0.57	3.53	0.26	0.79	99.73
55:30:15 PC1:CC7F:L1	31.78	10.50	4.35	47.11	1.34	0.05	0.60	2.25	0.29	1.37	99.63
55:30:15 PC1:CC7F:L1 (3.0% SO3)	30.55	10.07	4.28	45.98	1.41	0.04	0.53	2.94	0.34	1.39	97.52
55:30:15 PC1:CC7F:L1 (3.5% SO3)	31.08	10.31	4.28	47.20	1.46	0.04	0.55	3.47	0.35	1.38	100.12
50:40:10 PC1:CC2R:L1	34.48	18.40	2.42	39.16	0.82	0.04	0.26	1.63	0.25	2.15	99.62
50:40:10 PC1:CC9F:L1	37.83	12.07	5.49	39.66	1.07	0.06	0.74	1.63	0.19	0.83	99.57
50:40:10 PC1:CC9F:L1 (2.5% SO3)	37.11	11.79	5.43	39.93	1.14	0.06	0.68	2.52	0.24	0.85	99.75
50:40:10 PC1:CC9F:L1 (3.0% SO3)	37.00	11.87	5.38	40.02	1.27	0.07	0.68	3.05	0.27	0.83	100.43
50:40:10 PC1:CC9F:L1 (3.5% SO3)	36.38	11.68	5.34	39.53	1.20	0.06	0.65	3.47	0.26	0.84	99.40
55:30:15 PC2:CC9F:L1	32.57	10.43	5.10	47.77	0.82	0.06	0.61	1.61	0.11	0.64	99.71
55:30:15 PC3:CC9F:L1	32.57	9.95	4.87	47.13	1.05	0.07	0.59	2.13	0.17	0.79	99.32
55:30:15 PC1:CC9F:L2	32.74	10.31	4.86	46.93	1.13	0.06	0.64	1.85	0.21	0.75	99.48
55:30:15 PC1:CC9F:L3	32.85	10.36	4.82	46.89	1.08	0.06	0.64	1.82	0.21	0.76	99.48

PSD (% passing at given particle size in micron) of reference materials and blended cements

	0.9	1.1	1.3	1.5	1.8	2.2	2.6	3.1	3.7	4.3	5	6	7.5	9	10.5	12.5	15	18	21	25	30	36	43	51	61	73	87	103	123	147	175
75:25 PC1:BP1	7.00	8.99	10.86	12.64	15.19	18.43	21.50	25.11	29.11	32.76	36.61	41.42	47.36	52.13	56.02	60.26	64.56	68.85	72.58	77.02	81.83	86.54	90.68	93.99	96.64	98.44	99.49	99.91	100	100	100
70:30 PC1:BP1	7.42	9.51	11.47	13.34	16.02	19.43	22.66	26.45	30.64	34.44	38.42	43.35	49.36	54.11	57.96	62.12	66.33	70.55	74.25	78.65	93.39	87.97	91.93	95.00	97.36	98.90	99.72	99.98	100	100	100
65:35 PC1:BP1	7.52	9.63	11.60	13.48	16.18	19.60	22.85	26.66	30.88	34.72	38.74	43.73	49.82	54.62	58.47	62.58	66.65	70.65	74.11	78.21	82.66	87.04	90.93	94.07	96.63	98.41	99.46	99.90	100	100	100
70:30 PC2:BP1	6.74	8.62	10.39	12.10	14.59	17.83	20.99	24.79	29.08	33.07	37.32	42.67	49.32	54.62	58.93	63.58	68.22	72.77	76.66	81.15	85.82	90.15	93.70	96.31	98.18	99.30	99.87	100	100	100	100
75:25 PC1:CC2R	5.54	7.30	9.01	10.70	13.16	16.37	19.48	23.24	27.55	31.61	36.02	41.72	48.96	54.83	59.61	64.67	69.56	74.13	77.88	82.09	86.45	90.53	93.95	96.49	98.34	99.43	99.90	100	100	100	100
75:25 PC1:CC9F	5.73	7.34	8.87	10.35	12.49	15.24	17.88	21.02	24.54	27.80	31.27	35.67	41.23	45.78	49.59	53.83	58.23	62.74	66.75	71.59	76.90	82.22	87.03	91.03	94.42	96.93	98.58	99.51	100	100	100
70:30 PC1:CC2F	4.15	5.40	6.60	7.75	9.42	11.54	13.58	16.03	18.85	21.56	24.59	28.70	34.40	39.59	44.30	49.94	56.14	62.59	68.20	74.58	81.05	86.90	91.64	95.10	97.59	99.08	99.83	100	100	100	100
70:30 PC1:CC9R	5.71	7.45	9.15	10.82	13.28	16.51	19.65	23.42	27.69	31.64	35.87	41.19	47.81	53.07	57.32	61.85	66.33	70.68	74.40	78.79	83.50	88.07	92.02	95.09	97.44	98.94	99.74	99.98	100	100	100
70:30 PC1:CC2R	5.54	7.32	9.05	10.76	13.26	16.52	19.71	23.57	28.02	32.24	36.83	42.75	50.26	56.31	61.16	66.24	71.06	75.48	79.05	83.03	87.13	90.98	94.19	96.61	98.38	99.45	99.90	100	100	100	100
70:30 PC1:CC3R	7.53	10.09	12.59	15.02	18.52	22.92	27.06	31.88	37.18	42.01	47.06	53.29	60.75	66.39	70.64	74.80	78.45	81.59	84.06	86.88	89.93	92.93	95.54	97.53	98.97	99.77	100	100	100	100	100
70:30 PC1:CC9F	5.68	7.28	8.81	10.29	12.44	15.21	17.88	21.05	24.60	27.89	31.39	35.82	41.40	45.96	49.75	53.95	58.29	62.69	66.59	71.28	76.46	81.67	86.45	90.47	93.92	96.55	98.33	99.37	99.89	100	100
70:30 PC1:CC7F	6.01	7.74	9.38	10.95	13.23	16.12	18.88	22.15	25.81	29.20	32.81	37.39	43.16	47.85	51.73	55.99	60.34	64.72	68.58	73.18	78.22	83.23	87.73	91.43	94.50	96.74	98.17	98.95	99.33	99.46	99.55
65:35 PC1:CC2R	5.56	7.36	9.12	10.86	13.41	16.75	20.02	24.01	28.62	33.00	37.78	43.95	51.75	57.98	62.95	68.07	72.83	77.09	80.45	84.14	87.93	91.48	94.48	96.75	98.44	99.46	99.90	100	100	100	100
65:35 PC1:CC9F	5.63	7.23	8.76	10.25	12.40	15.18	17.84	21.01	24.55	27.83	31.32	35.73	41.29	45.84	49.62	53.80	58.10	62.43	66.24	70.80	75.83	80.95	85.73	89.85	93.48	96.30	98.21	99.31	100	99.99	100
70:30 PC2:CC2R	4.99	6.55	8.10	9.64	11.96	15.06	18.17	22.03	26.57	30.94	35.74	41.97	49.91	56.32	61.50	66.94	72.14	76.91	80.75	84.95	89.16	92.94	95.94	98.01	99.31	99.89	100	100	100	100	100
70:30 PC3:CC2R	5.20	6.90	8.57	10.23	12.70	15.96	19.19	23.15	27.74	32.12	36.90	43.09	50.93	57.25	62.31	37.60	72.60	77.16	80.80	84.80	88.84	92.51	95.48	97.58	99.01	99.77	100	100	100	100	100
55:30:15 PC1:BP1:L1	9.25	13.07	16.56	19.73	24.04	29.1	33.46	38.16	42.95	46.98	50.93	55.56	60.91	64.98	68.4	72.48	76.87	81.21	84.65	88.26	91.63	94.4	96.41	97.77	98.75	99.42	99.84	100	100	100	100
50:40:10 PC1:BP1:L1	10.52	14.85	18.76	22.3	27.07	32.57	37.23	42.13	46.98	50.96	54.81	59.31	64.57	68.58	71.82	75.39	79.07	82.91	86.34	90.15	93.51	95.77	96.94	97.53	98.08	98.81	99.58	100	100	100	100
55:30:15 PC2:BP1:L1	8.95	12.61	15.9	18.88	22.9	27.59	31.66	36.1	40.73	44.76	48.86	53.81	59.64	64.03	67.62	71.87	76.63	81.66	85.84	90.18	93.98	96.83	98.64	99.58	99.95	100	100	100	100	100	100
55:30:15 PC1:CC2F:L1	3.56	5.07	6.48	7.79	9.61	11.84	13.86	16.16	18.66	20.92	23.32	26.42	30.54	34.29	37.96	42.94	49.13	56.72	63.64	71.66	79.62	86.49	91.68	95.15	97.45	98.73	99.39	99.75	99.94	100	100
55:30:15 PC1:CC9R:L1	4.58	6.59	8.49	10.3	12.89	16.12	19.12	22.62	26.48	30	33.71	38.36	44.21	49.03	53.25	58.37	64.18	70.37	75.65	81.42	46.91	91.57	95.09	97.45	98.96	99.71	99.97	100	100	100	100
55:30:15 PC1:CC2R:L1	4.6	6.68	8.7	10.65	13.48	17.09	20.49	24.5	28.95	33.03	37.33	42.75	49.6	55.25	60.06	65.63	71.53	77.34	81.91	86.55	90.67	93.96	96.4	98.08	99.22	99.81	100	100	100	100	100
55:30:15 PC1:CC3R:L1	6.07	8.73	11.26	13.66	17.08	21.33	25.28	29.86	34.88	39.43	44.19	50.11	57.45	63.31	68.18	73.68	79.3	84.53	88.36	92	94.99	97.18	98.61	99.45	99.88	100	100	100	100	100	100
55:30:15 PC1:CC9F:L1	4.95	7.09	9.1	11	13.67	16.96	19.97	23.4	27.09	30.38	33.76	37.89	42.93	47.01	50.59	55.01	60.1	65.6	70.34	75.62	80.87	85.68	89.82	93.16	95.95	97.99	99.27	99.87	100	100	100
55:30:15 PC1:CC7F:L1	4.98	7.13	9.14	11.02	13.67	16.91	19.86	23.21	26.81	30	33.28	37.29	42.2	46.15	49.61	53.9	58.88	64.31	69.05	74.39	79.73	84.61	88.79	92.18	95.06	97.23	98.7	99.56	99.95	100	100
50:40:10 PC1:CC2R:L1	4.88	7.4	9.11	11.09	13.92	17.48	20.81	24.7	29.02	32.99	37.21	42.6	49.53	55.31	60.25	65.98	72.03	77.94	82.57	97.27	91.43	94.74	97.12	98.64	99.57	99.95	100	100	100	100	100
50:40:10 PC1:CC9F:L1	4.82	691	8.86	10.71	13.3	16.48	19.38	22.67	26.2	29.33	3253	36.43	41.2	45.07	48.49	52.77	57.8	63.33	68.16	73.61	79.04	84.02	88.31	91.82	94.87	97.23	98.83	99.7	100	100	100
55:30:15 PC2:CC9F:L1	4.05	5.84	7.54	9.16	11.5	14.44	17.2	20.45	24.08	27.41	30.91	35.29	40.74	45.21	49.14	54	29.61	65.7	70.99	76.89	82.63	87.61	91.54	94.44	96.73	98.38	99.45	99.95	100	100	100
55:30:15 PC3:CC9F:L1	5.09	7.26	9.27	11.16	13.8	17.05	20.03	43.46	27.23	30.66	34.25	38.69	44.14	48.51	52.29	56.93	62.27	68.03	72.99	78.48	83.79	88.41	92.07	94.81	96.97	98.53	99.53	99.97	100	100	100
55:30:15 PC1:CC9F:L2	4.79	6.91	8.93	10.85	13.57	16.94	20.01	23.47	27.14	30.35	33.59	37.53	42.4	46.41	49.9	54.12	58.94	64.25	69.01	74.48	79.97	84.93	89.12	92.51	95.41	97.65	99.1	99.82	100	100	100
55:30:15 PC1:CC9F:L3	5.83	8.3	10.57	12.68	15.61	19.13	22.29	25.84	29.61	32.93	36.32	40.42	45.37	49.32	52.81	57.19	62.34	67.94	72.74	78	83.1	87.62	91.35	94.25	96.6	98.3	99.37	99.89	100	100	100
CEM I Ref (PC1)	6.69	9.40	11.83	14.02	16.94	20.33	23.23	26.37	29.63	32.51	35.53	39.37	44.34	48.58	52.35	56.96	62.21	67.83	72.70	78.21	83.71	88.61	92.49	95.18	96.95	97.84	98.22	99	99	100	100
CEM I Ref (PC2)	5.30	6.72	8.07	9.39	11.36	13.98	16.60	19.85	23.63	27.24	31.20	36.34	42.98	48.51	53.17	58.40	63.86	69.41	74.22	79.75	85.41	90.50	94.51	97.26	99.02	99.84	100	100	100	100	100
CEM I Ref (PC3)	5.83	8.24	10.43	12.44	15.19	18.50	21.46	24.84	28.56	31.96	35.61	40.25	46.15	51.04	55.03	60.49	66.38	72.67	78.05	83.93	89.44	93.89	96.96	98.75	99.67	99.98	100	100	100	100	100
CEM II/A-LL Ref (11% L)	6.77	9.63	12.27	14.71	18.08	22.11	25.67	29.61	33.74	37.33	40.97	45.42	50.88	55.32	59.20	63.92	69.29	74.99	79.78	84.93	89.70	93.59	96.36	98.10	99.13	99.58	99.71	100	100	100	100
CEM II/B-V Ref (25% FA)	5.69	7.29	8.84	10.35	12.59	15.53	18.41	21.86	25.77	29.40	33.26	38.13	44.21	49.12	53.16	57.57	62.06	66.56	70.50	75.17	80.22	85.17	89.55	93.07	95.90	97.88	99.08	99.71	99.96	100	100
CEM II/B-V Ref (40% FA)	5.41	6.96	8.48	9.98	12.22	15.19	18.12	21.67	25.71	29.48	33.51	38.62	44.98	50.05	54.15	58.50	62.79	66.96	70.57	74.86	79.58	84.29	88.57	92.10	95.07	97.25	98.67	99.47	99.87	99.99	100
CEM III/A Ref (36% GGBS)	6.56	9.26	11.73	13.96	17.01	20.58	23.69	27.10	30.65	33.75	36.94	40.94	46.04	50.39	54.31	59.11	64.51	70.19	75.03	80.42	85.72	90.36	93.97	96.45	98.07	98.91	99.25	99.41	100	100	100
CEM III/A Ref (45% GGBS)	6.33	8.94	11.32	13.49	16.44	19.92	22.97	26.33	29.85	32.96	36.18	40.23	45.38	49.74	53.66	58.48	63.95	69.76	74.70	80.11	85.36	89.97	93.64	96.25	98.03	98.98	99.38	99.56	100	100	100
FA	4.51	5.86	7.25	8.67	10.9	13.98	17.12	21	25.47	29.64	34.08	39.6	46.29	51.44	55.46	59.59	63.51	67.17	70.25	73.85	77.81	81.8	85.5	88.7	91.57	93.95	95.8	97.17	98.22	98.94	99.41
GGBS	3.97	5.66	7.23	8.69	10.75	13.29	15.65	18.42	21.57	24.54	27.80	32.08	37.76	42.67	47.02	52.25	58.05	64.10	69.21	74.89	80.57	85.78	90.19	93.63	96.37	98.24	99.34	99.85	100.00	100	100
L1	3.26	4.96	6.74	8.58	11.44	15.35	19.30	24.16	29.75	34.88	40.16	46.42	53.54	58.68	62.74	67.35	72.14	76.71	80.15	83.59	86.76	89.61	92.26	94.75	97.12	98.89	99.81	100	100	100	100
L2	4.77	7	9.2	11.37	14.55	18.62	22.47	26.94	31.79	36.03	40.24	45.13	50.62	54.53	57.58	61.01	64.73	68.64	72.07	76.09	80.5	85.14	89.71	93.72	97.03	99.1	99.93	100	100	100	100
L3	8.09	11.51	14.69	17.65	21.78	26.86	31.51	36.76	42.71	47.96	53.34	59.72	66.91	71.97	75.83	80.08	84.44	88.56	91.64	94.57	96.97	98.65	99.6	99.96	100	100	100	100	100	100	100

Compressive strength results (MPa) of CEM II/B-Q, CEM II/C-M and reference cements

Cement	1-Day	2-Day	7-Day	28-Day	56-Day	90-Day
75:25 PC1:BP1	11.4	20.8	34.7	46.0	55.6	59.1
70:30 PC1:BP1	10.6	18.9	31.1	43.9	51.5	54.6
65:35 PC1:BP1	8.9	17.6	28.0	41.5	48.5	55.8
70:30 PC2:BP1	12.1	21.5	33.4	47.9	54.8	60.8
75:25 PC1:CC2R	11.4	21.8	43.3	63.8	65.9	66.2
75:25 PC1:CC9F	9.3	19.4	38.5	58.4	64.5	64.3
70:30 PC1:CC2F	9.3	19.2	42.6	55.5	57.8	56.9
70:30 PC1:CC9R	8.5	17.9	38.1	55.8	59.0	60.2
70:30 PC1:CC2R	10.5	19.9	42.8	61.6	64.5	65.7
70:30 PC1:CC3R	11.9	22.7	48.9	68.4	73.7	72.9
70:30 PC1:CC9F	8.2	17.6	36.5	56.7	60.3	61.4
70:30 PC1:CC7F	10.3	20.4	44.1	58.3	64.5	62.6
65:35 PC1:CC2R	9.6	18.3	41.0	59.0	64.4	65.1
65:35 PC1:CC9F	7.3	15.8	35.6	54.4	57.0	59.9
70:30 PC2:CC2R	11.8	20.5	38.3	55.7	62.4	66.7
70:30 PC3:CC2R	13.5	21.6	41.7	63.6	68.4	69.6
55:30:15 PC1:BP1:L1	9.5	16.1	25.9	38.7	45.4	48.9
50:40:10 PC1:BP1:L1	8.1	14.5	24.2	37.6	42.6	46.6
55:30:15 PC2:BP1:L1	8.9	16.1	26.5	39.6	45.7	49.8
55:30:15 PC1:CC2F:L1	5.7	14.5	34.0	42.0	49.4	52.1
55:30:15 PC1:CC9R:L1	6.0	12.9	30.8	45.0	50.5	51.9
55:30:15 PC1:CC2R:L1	7.2	13.4	33.5	51.4	57.4	59.0
55:30:15 PC1:CC3R:L1	7.7	15.9	39.0	57.7	63.8	64.7
55:30:15 PC1:CC9F:L1	5.9	12.3	30.3	44.7	49.6	51.6
55:30:15 PC1:CC7F:L1	7.7	15.5	36.6	48.1	52.9	53.7
50:40:10 PC1:CC2R:L1	6.4	12.7	31.5	51.0	53.9	55.1
50:40:10 PC1:CC9F:L1	6.0	11.3	28.1	46.2	50.2	52.1
55:30:15 PC2:CC9F:L1	6.6	14.2	32.0	47.2	53.5	56.4
55:30:15 PC3:CC9F:L1	8.6	15.1	29.4	46.6	51.1	56.6
55:30:15 PC1:CC9F:L2	6.0	13.8	31.1	45.5	49.9	50.9
55:30:15 PC1:CC9F:L3	6.0	13.4	30.7	45.9	49.0	51.4
CEM I Ref (PC1)	17.3	29.3	47.2	60.0	65.5	67.0
CEM I Ref (PC2)	19.0	32.5	53.7	68.1	73.4	76.3
CEM I Ref (PC3)	22.7	33.0	47.5	59.9	65.5	69.7
CEM II/A-LL Ref	20.8	33.5	50.0	59.1	62.9	64.0
CEM II/B-V Ref (25% FA)	11.2	20.3	34.5	49.0	58.7	63.5
CEM IV/B(V) Ref (40% FA)	9.0	15.3	26.9	44.7	53.4	57.4
CEM III/A Ref (36% GGBS)	8.0	16.9	35.3	55.9	66.1	68.2
CEM III/A Ref (45% GGBS)	6.8	13.9	32.7	53.5	63.8	66.9

Re-C3: Reclaimed Calcined Clay Cements

Appendix 11 -
Durability of calcined clay concrete

Authors
University of Dundee:
Thomas Hope
Roderick Jones
Moray Newlands
Michael McCarthy

Date 27/03/2024

Contents

Table of Figures

Table of Tables

1. Work Package K

Work Package K of the Re-C3 project evaluated the performance of four UK clays, which were either rotary (R) or flash (F) calcined, in binary and ternary concretes, at various levels (up to 50% cement replacement), and w/c ratios ranging from 0.4 to 0.6. The performance of calcined clay concretes was compared to a selection of reference concretes (CEM I, CEM II and CEM III) to evaluate the comparative performance. The cement combinations evaluated as part of Work Package K are given in Table 1.

Table 1 - Cement combinations and additions used in Work Package K

Mix ID	BS 8500 combination	CEM I	Calcined clay	FBP	FA	GGBS	LS
1a	CEM II/B-Q	85	15	-	-	-	-
1		75	25	-	-	-	-
2a		85	15	-	-	-	-
2		75	25	-	-	-	-
3		75	-	25	-	-	-
4		70	30	-	-	-	-
5		70	30	-	-	-	-
6		70	-	30	-	-	-
7		70	30	-	-	-	-
8		70	30	-	-	-	-
9		70	30	-	-	-	-
10		70	30	-	-	-	-
11		65	35	-	-	-	-
12		65	35	-	-	-	-
13		65	-	35	-	-	-
14		70	30	-	-	-	-
15		70	-	30	-	-	-
16		70	30	-	-	-	-
17	CEM II/C-M(Q-L)	55	30	-	-	-	15
18		55	30	-	-	-	15
19		55	-	30	-	-	15
20		55	30	-	-	-	15
21		55	30	-	-	-	15
22		55	30	-	-	-	15
23		55	30	-	-	-	15
24		50	40	-	-	-	10
25		50	40	-	-	-	10
26		50	-	25	-	25	-
27		55	30	-	-	-	15
28		55	-	30	-	-	15
29		55	30	-	-	-	15
30		55	30	-	-	-	15
31		55	30	-	-	-	15
32	CEM I	100	-	-	-	-	-
33	CEM II/A-L	90	-	-	-	-	10
34	CEM II/B-V	75	-	-	25	-	-
35	CEM III/A	64	-	-	-	36	-
36	CEM III/A	55	-	-	-	45	-
37	CEM IV(B(V)	60	-	-	40	-	-

2. Action K1 – Design of Concrete Mix Proportions

2.1. Scope

The aim of Action K1 was to establish suitable concrete mix proportions at 0.4, 0.5, and 0.6 w/c ratio that would produce acceptable concrete using the calcined clays and brick powder, while achieving a target consistence class of S3 (minimum slump of 100mm).

2.2. Materials

The materials and their properties tested as part of Work Package K are covered in this section. A list of the materials and their nomenclatures are given in the Table 2.

Table 2 - Nomenclature for constituent materials used

Abbreviation	Description	Abbreviation	Description
PC1	Portland Cement 1	CC2F	Clay 2 Flash Calcined
PC2	Portland Cement 2	CC2R	Clay 2 Rotary Calcined
PC3	Portland Cement 3	CC3R	Clay 3 Rotary Calcined
L1	Limestone 1	CC7F	Clay 7 Flash Calcined
L2	Limestone 2	CC9F	Clay 9 Flash Calcined
L3	Limestone 3	CC9R	Clay 9 Rotary Calcined
FA	Category N Fly Ash	FBP	Brick Powder
GGBS	Ground Granulated Blastfurnace Slag		
Admixture	Description		
AD1	Superplasticiser including a viscosity modifier (VMA) for 0.5 and 0.6 w/c ratio concretes		
AD2	Strong superplasticiser including a viscosity modifier (VMA) for 0.4 w/c ratio concretes		
AEA	Commercial air-entraining admixture		
DF	Commercial defoaming agent		

The properties of the six calcined clays (CC) and one brick powder (FBP) tested by the University of Dundee as part of Work Package K are given in the Table 3.
It was noted that when compared with the fly ash used (6.19 m^2/g), most calcined clays had a higher specific surface area (5.28 m^2/g to 21.04 m^2/g), as measured by B.E.T., with only CC2R reporting a lower surface area (5.28 m^2/g), and both CC2F and FBP (7.09 and 6.49 m^2/g respectively) comparable to the fly ash. The rotary calcined clays had lower B.E.T. specific surface areas than the fly ash, however, the source of clay had a greater influence than the calcination method. The specific surface areas of the GGBS (1.93 m^2/g) and the limestone (L) sources (1.88 m^2/g to 2.21 m^2/g) were relatively low in comparison. A general hierarchy could be established, with surface area increasing in the following order:
CC2, FBP, CC3, CC7, CC9.

The particle densities of the calcined clays were greater than that of the fly ash

(2260 kg/m^3) and ranged from 2350 kg/m^3 to 2740 kg/m^3 but were lower than that of GGBS at 2900 kg/m^3.

The fineness, measured by 45µm sieve retention, of the rotary calcined clays was lower than that of the rotary clays, reflecting post calcination particle size reduction, whereas this was not carried out for the flash calcined materials. The fineness of the rotary calcined clays ranged from 1.7 to 7.8%, flash calcined from 11.5 to 30.4%, and FBP of 5.3%. In comparison, the fly ash used had a fineness of 16.3% and the limestones ranged from 3.2 to 8.5%. The d_{50} of the calcined clays and brick powder followed the same behaviour as those of fineness.

The loss-on-ignition values for the calcined clays were low, with all but CC2R (1.3%) under 1.0%. Comparatively, the FBP had a higher LOI of 3.4%, which was greater than the fly ash (2.7%) and GGBS (nil). The bulk oxides composition of the calcined clays and brick dust were tested as part of Work Package K, given for reference in Table 3, but are discussed further in other Work Packages.

Table 3 - Physical and chemical characteristics of calcined clays and brick powder as tested by University of Dundee

Property	CC2F	CC2R	CC3R	CC7F	CC9F	CC9R	FBP
45µm sieve ret., %wt	11.5	3.4	1.7	30.4	29.7	7.8	5.3
Loss-on-Ignition, %wt	0.82	1.32	0.62	0.58	0.50	0.49	3.40
PSD*, d_{10}, µm	8.6	2.9	2.1	3.0	2.6	1.8	0.8
PSD*, $d_{50,}$, µm	23.6	12.8	8.6	25.4	24.9	13.2	3.8
PSD*, $d_{90,}$, µm	51.7	40	21.9	75.1	74.9	39.3	19
Particle density, kg/m^3	2490	2582	2352	2601	2631	2740	2689
SSA, B.E.T., m^2/g	7.09	5.28	10.40	15.36	21.04	14.48	6.49
SiO_2, % wt	53.4	51.7	55.3	54.5	59.1	58.9	50.9
Al_2O_3, % wt	33.1	33.6	37.8	23.3	22.6	24.4	19.4
Fe_2O_3, % wt	2.3	1.8	1.3	7.3	8.6	8.3	6.0
CaO, % wt	0.3	0.1	0.2	2.8	2.9	2.8	10.9
MgO, % wt	0.4	0.4	0.3	1.8	1.0	1.2	1.9
K_2O, % wt	4.6	4.0	3.4	3.0	1.2	1.6	3.0
Na_2O, % wt	0.2	0.2	0.2	0.3	0.1	0.3	0.5
P_2O_5, % wt	0.1	0.1	0.1	0.3	0.1	0.1	0.2
Cl^-, % wt	0.0	0.0	0.0	0.0	0.0	0.0	nd[#]
SO_3, % wt	0.0	0.0	0.0	2.0	0.1	0.6	3.1
MnO, % wt	0.0	0.0	0.0	0.0	0.1	0.1	0.0
TiO_2, % wt	0.2	0.1	0.0	1.2	1.2	1.1	0.9

* Using laser diffraction | [#] No data

The physical and chemical properties of the other cements and fillers are given in Table 4.

Table 4 – Physical and chemical properties of cements and filler as tested by the University of Dundee

Property	PC1	PC2	PC3	FA	GGBS	L1	L2	L3
Fineness, 45µm sieve ret., %	-	-	-	16.3	-	8.5	8.1	3.2
d_{10}, µm	1.8	3.3	2.7	1.6	2.3	2.1	2.2	0.8
d_{50}, µm	13.1	17.2	14.9	13.8	15.6	9.3	13.0	6.3
d_{90}, µm	99.9	43.0	40.1	46.5	50.3	45.1	53.2	25.1
Particle density, kg/m^3	3.16	3.14	3.17	2.26	2.90	2.64	2.71	2.73
SSA, B.E.T., m^2/g	*nd	1.89	2.38	6.19	1.93	1.88	1.98	2.21
Loss-on-Ignition, %	-	-	-	2.7	-	43.4	43.4	43.1
mac, %	4.8	4.2	4.5	-	-	-	-	-
SiO_2	20.1	20.2	19.4	55.6	35.0	0.2	0.9	0.6
Al_2O_3	5.1	5.4	4.6	20.4	12.2	0.1	0.2	0.1
Fe_2O_3	3.0	3.5	3.0	8.1	0.4	0.0	0.1	0.1
CaO	64.0	64.9	63.7	5.9	39.1	70.0	76.2	76.6
MgO	1.3	0.8	1.2	1.7	8.7	0.3	0.9	0.3
K_2O	0.6	0.4	0.7	2.0	0.6	0.0	0.1	0.0h
Na_2O	0.3	0.1	0.2	1.4	0.4	0.0	0.0	0.0
P_2O_5	0.1	*nd	*nd	*nd	*nd	*nd	*nd	*nd
Cl	0.0	*nd	*nd	*nd	*nd	*nd	*nd	*nd
SO_3	3.1	2.6	3.5	1.5	1.2	0.0	0.1	0.0
MnO	0.1	0.1	0.1	0.1	0.3	0.0	0.0	0.0
TiO_2	0.3	0.3	0.3	0.8	0.6	0.0	0.0	0.0

*No data

2.3. Aggregates for concrete

Table 5 shows the physical properties of the aggregate package used in Work Package K. The coarse aggregates were a crushed limestone and the fine aggregates a graded quartz from UK sources conforming to BS EN 12620 (BSI, 2013). The particle size grading of the fine and coarse aggregates, shown as percentage passing various sieve mesh sizes, are given in Figure 1.

Table 5 – Work Package concrete aggregate properties

Property	0/4	4/10	10/20
Oven-dried Density, kg/m^3	2652	2639	2645
Surface dry saturated density (SSD), kg/m^3	2662	2670	2657
Water absorption to SSD, %	0.4	0.5	0.5

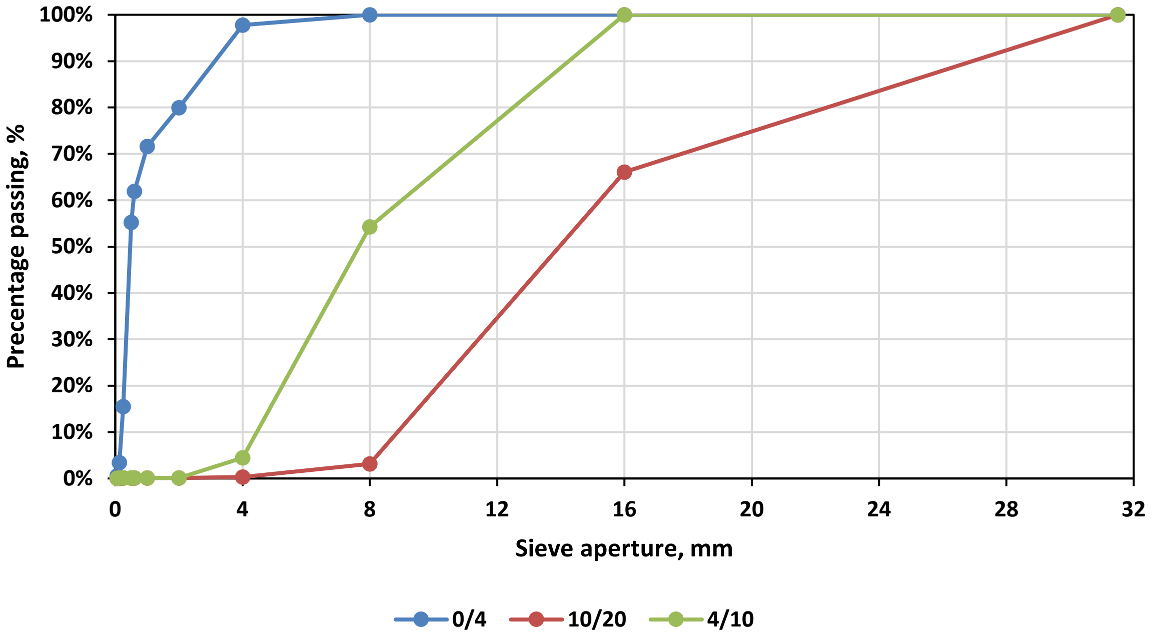

Figure 1 - Work Package K aggregate grading by percentage weight.

2.4. Trial Mixing

The concrete mix proportions developed at the beginning of the project as part of a trial mixing programme are given in Table 6. A fixed water content of 170 kg/m^3 was used, allowing the cement combination content to vary with the water/cement ratio. Mix proportions were established at 0.5 w/c ratio and then further trials made at 0.4 and 0.6 to provide a range. A superplasticising admixture was used to achieve a target consistence class of S3 (minimum slump of 100mm).

Trial mixing the CC9F binary at 30% (CEM II/B-Q), shown in Figure 2, and a CEM I reference identified that there was a lack of cohesiveness in the concrete and calcined clay appeared to be sensitive to the type and dosage of admixture used. The lack of cohesion was resolved by increasing the proportion of fine aggregate and reducing the of 10/20 coarse aggregate fraction, as shown between mixes A and C in Table 6. The cohesiveness of the concretes was also improved by changing the admixture used from a clay specific PCE superplasticising admixture to a PCE containing a viscosity modifying agent (VMA). This admixture (AD1) allowed good cohesiveness in concrete to be achieved using mix design C. Although the inclusion of a VMA increased the superplasticiser demand, the target slump could still be achieved within the manufacturer’s suggested upper dose limit (1.2%) for 0.5 w/c ratio concrete.

Other mix proportions (mix designs D to F) were also explored, by increasing fine aggregates further in mix design D or increasing the 10/20 coarse aggregate fraction in mix designs E and F. However, these did not offer any improvements to mix stability compared to mix design C.

Evaluating CC2R at 0.4 w/c ratio, found that AD1 did not contain a strong enough PCE to allow the target slump to be reached within the admixture dose limits. A second admixture (AD2) was developed for the project, similar to AD1, but with a stronger

PCE component. AD2 allowed the 0.4 w/c ratio CC2R binary concrete to achieve the target slump and was subsequently used for all of the 0.4 w/c ratio binary and ternary concretes.

CC9F-1, 0.30% SP, 65mm slump CC9F-2, 0.36% SP, 90mm slump

CC9F-4, 0.41% SP, collapsed slump CC9F-5, 0.34% SP, 100mm slump

Figure 2 - Trial mixes of CC9F binary, w/c ratio = 0.5, 30% calcined clay in cement

Table 6 - Concrete mixes at 0.5 w/c ratio evaluated during trial mixing

Mix Design Iteration	Water / cement ratio	Free Water, kg/m^3	Total Cementitious, kg/m^3	0/4, kg/m^3	4/10, kg/m^3	10/20, kg/m^3
A	0.50	170	340	765	377	762
B				859	378	672
C				851	405	635
D				916	396	596
E				763	413	732
F				760	374	756

2.5. Final Concrete Mixes

The concrete mixes adopted for the project after trial mixing are given in the Table 7 along with the test combinations evaluated for each.

Table 7 - Summary of concrete mix proportions

w/c ratio	Test combinations	Free water, l/m³	Total Cement (Combination), kg/m³	Aggregates, kg/m³		
				0/4mm	4/10mm	10/20mm
0.40	CEM II/B-Q CEM II/C-M (Q-L) CEM II/B-V	170	425	812	405	588
0.50	CEM I CEM II/A-L CEM II/B-Q CEM II/B-V CEM II/C-M (Q-L) CEM III/A CEM IVB(V)	170	340	851	405	635
0.60	CEM II/B-Q CEM II/C-M (Q-L) CEM II/B-V	170	283	876	405	666
0.55	CEM I CEM II/B-Q CEM II/B-V CEM III/A	170	309	864	405	652

3. Action K2 – Concrete Consistence and Cube Strength

3.1. Scope

The aim of Action K2 was to evaluate the slump and admixture dose required to achieve a target consistence class of S3 (minimum slump of 100mm) for both calcined clay and brick powder binary and ternary concretes. The cube strength development of these concretes was also evaluated. A PC only concrete along with fly ash (25 and 40% replacement), GGBS (36 and 45% replacement), and limestone (10% replacement) binary concretes were also evaluated for comparison with the calcined clays. These concretes are shown with the results of the calcined clays and brick powder where appropriate.

3.2. Results

3.2.1. Concrete slump

The admixture doses and corresponding slump for the binary (CEM II / B-Q) and ternary concretes (CEM II/C-M), at 30% calcined clay replacement in cement and 0.5 w/c ratio, are shown in Figure 3 and Figure 4.

Calcined clay binary and ternary concretes had higher admixture demand (0.46 % to 1.16%) than the fly ash (0.37% and 0.41%) and GGBS (0.35% and 0.52%) concretes. Compared to calcined clay, the FBP concretes had lower admixture requirements (0.35 % to 0.48 %) but were generally higher than those of the FA and GGBS references. Within the calcined clays, no single clay type consistently had the lowest admixture demand, although a general order could be established from lowest to highest, as follows:
CC9F < CC9 < CC3R < CC2R < CC7F < CC2F

It appears that both the source clay and the method of calcination influence the rheology of concrete, but the extent of this could not be established owing to the influence of multiple variables such as particle size, mineralogy, and the specific surface areas of the calcined clays.

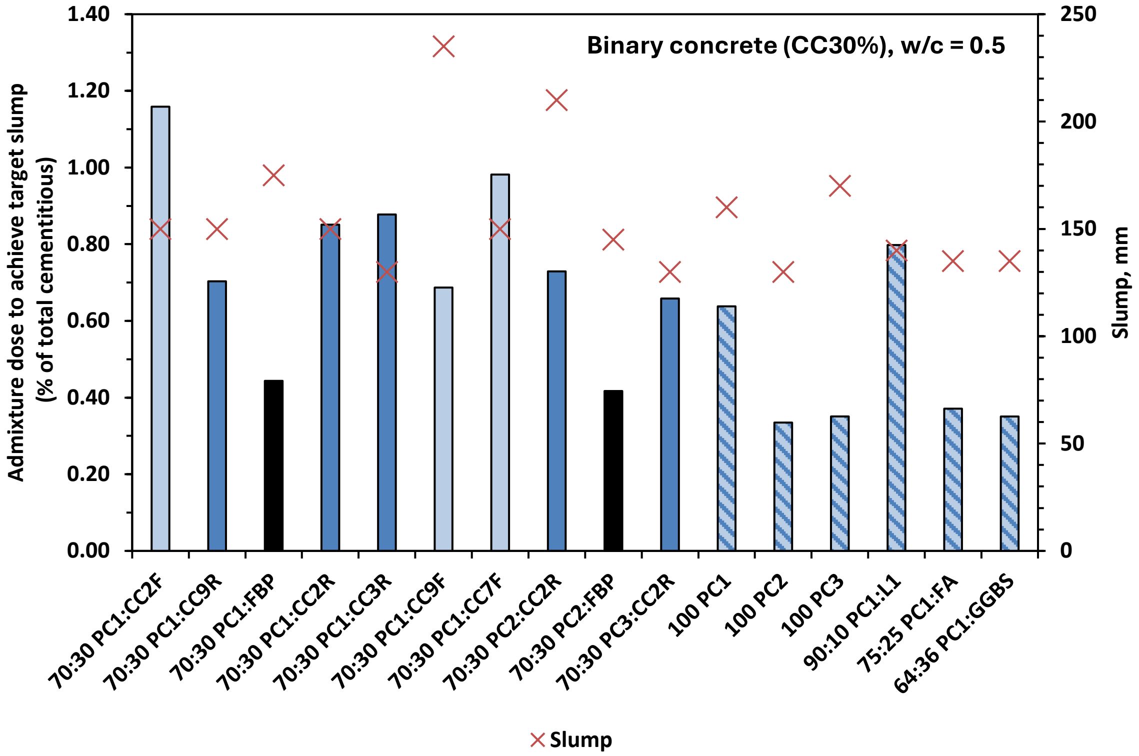

Figure 3 – Admixture dose required to achieve target slump and the corresponding slump achieved for binary concretes at w/c = 0.5

The admixture doses required to achieve the target slump between 0.4, 0.5, and 0.6 w/c ratio for FBP, CC2R, and CC9F are shown in Figure 5 and were generally in line with expectations. Comparing 0.5 and 0.6 w/c ratio concretes shows lower doses of AD1 were required at 0.6 w/c, than at 0.5 w/c ratio in all cases except the CC2R ternary at 0.6 w/c ratio, which may be an erroneous result. The degree of change varied between materials with the largest reduction of 0.22% observed between 0.5 w/c and 0.6 w/c ratios for the CC2R binary, whereas the FBP binary and ternary concretes show negligible change with a decrease between 0.5 and 0.6 w/c ratios of 0.01%. The 0.4 w/c ratio concretes used AD2 containing a stronger PCE, preventing direct comparisons from being made. However, the doses of AD2 required in the 0.4 w/c ratio concretes were comparable to, or greater than, the 0.5 w/c ratio concretes using AD1. The exception to this was CC9F (binary and ternary), which had a lower admixture demand that CC2R, and therefore required less PCE to achieve the target slump.

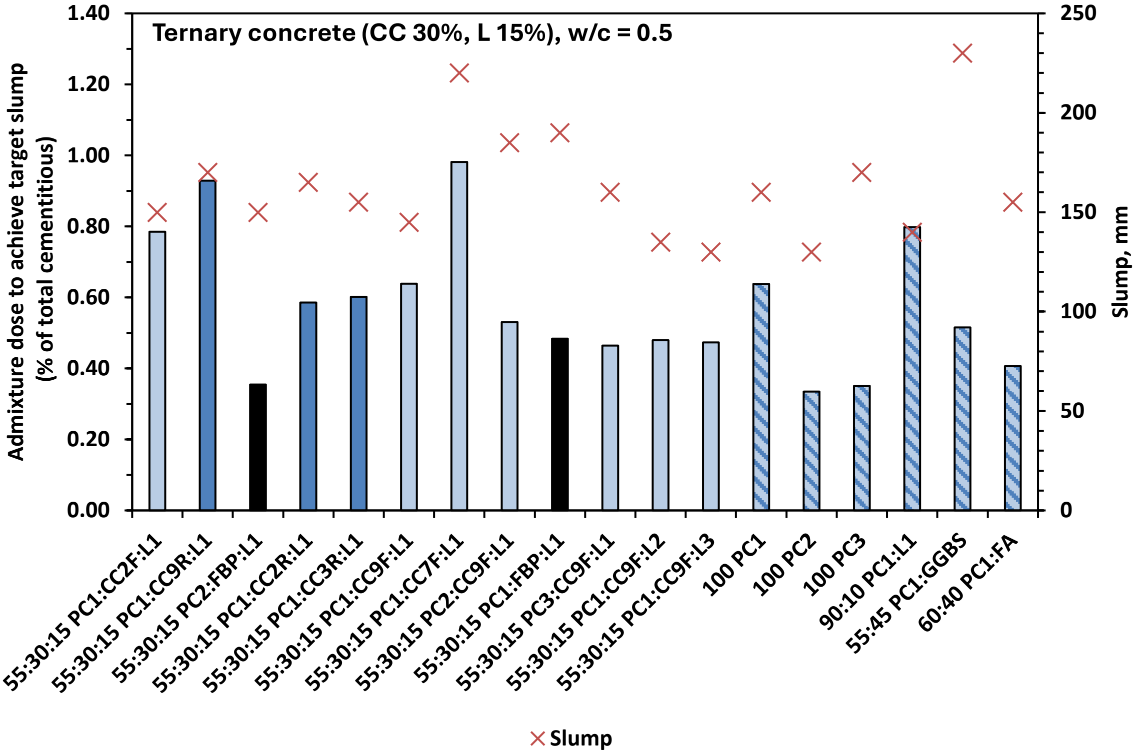

Figure 4 – Admixture dose required to achieve target slump and the corresponding slump achieved for ternary concretes at w/c = 0.5

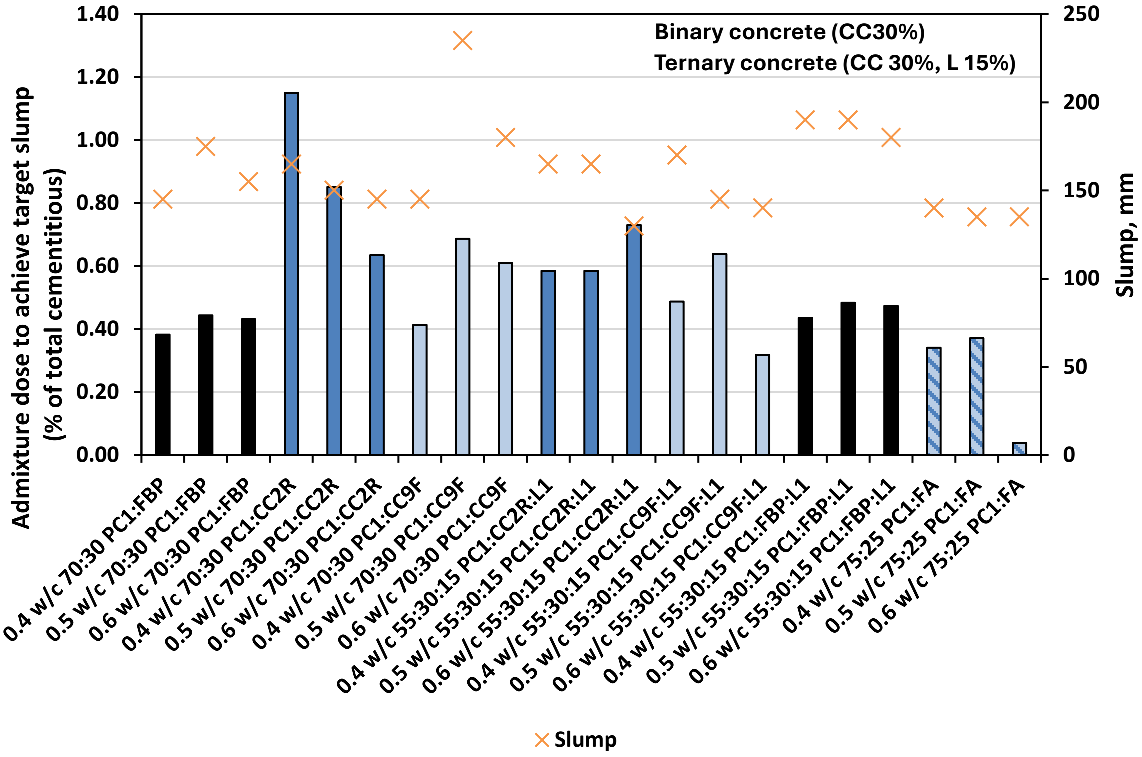

Figure 5 - Admixture dose required to achieve target slump and the corresponding slump achieved for binary and ternary concretes at 0.4, 0.5, and 0.6 w/c ratio

The CC2R, CC9F, or FBP binary concretes could not match the admixture demand of the 0.6 w/c ratio fly ash, as previously observed at 0.5 w/c in Figures 3 and 4.

The admixture doses required to achieve the target slump in CC2R, CC9F, and FBP in binary and ternary concretes at 0.5 w/c ratio with varying calcined clay replacement levels are given in Figures 6 to 8. For both the binary and ternary concretes, increasing the proportion of calcined clay or brick powder increased the admixture dose required to achieve the target slump. This was most evident in CC2R binary concretes where the admixture dose required, increased from 0.54% at 15% CC2R to 0.88% at 35% CC2R.

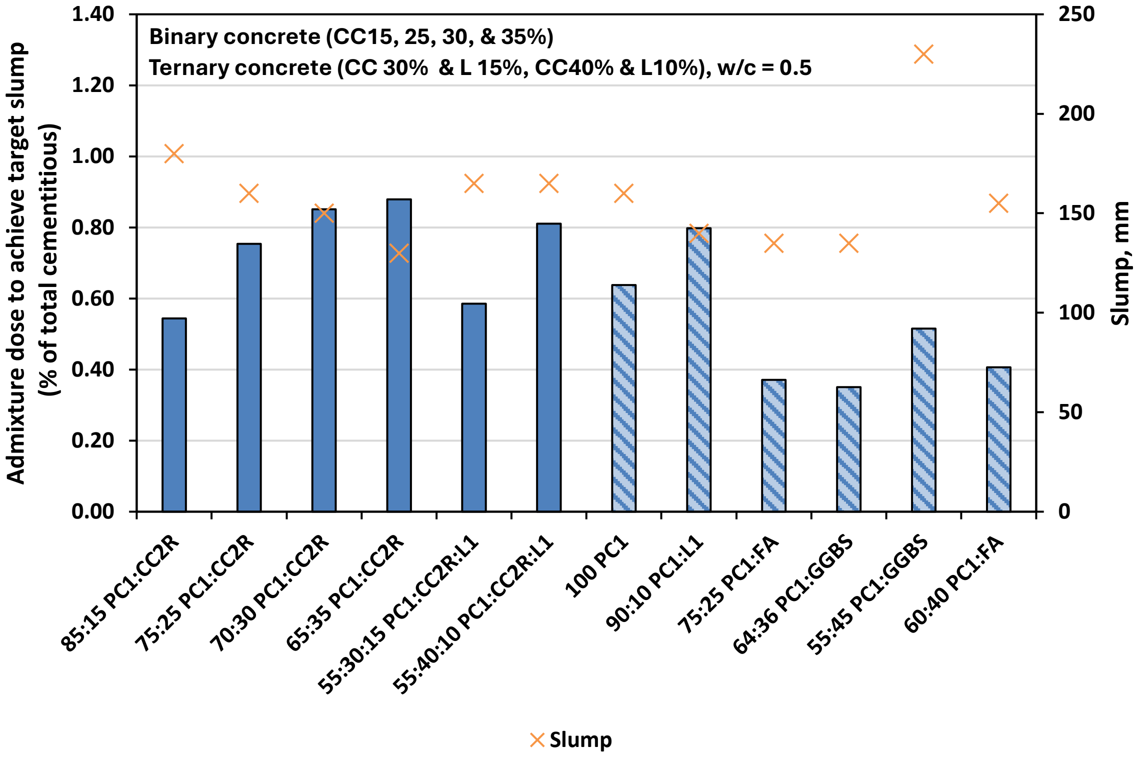

Figure 6 - Admixture dose required to achieve target slump and the corresponding slump achieved for CC2R binary and ternary concretes at varying calcined clay replacement level

It is of note that whilst L1 was primarily used in Work Package K, it appears to have resulted in a higher admixture demand with CC9F in ternary concrete when compared with ternary CC9F concretes using L2 or L3.

Using a suitable admixture within the recommended dosage range of the manufacturer, allowed the calcined clay binary and ternary concretes to achieve the target slump. With further optimisation of the concrete mixes and development of calcined clay specific admixtures, it is likely that higher slump classes could be attained.

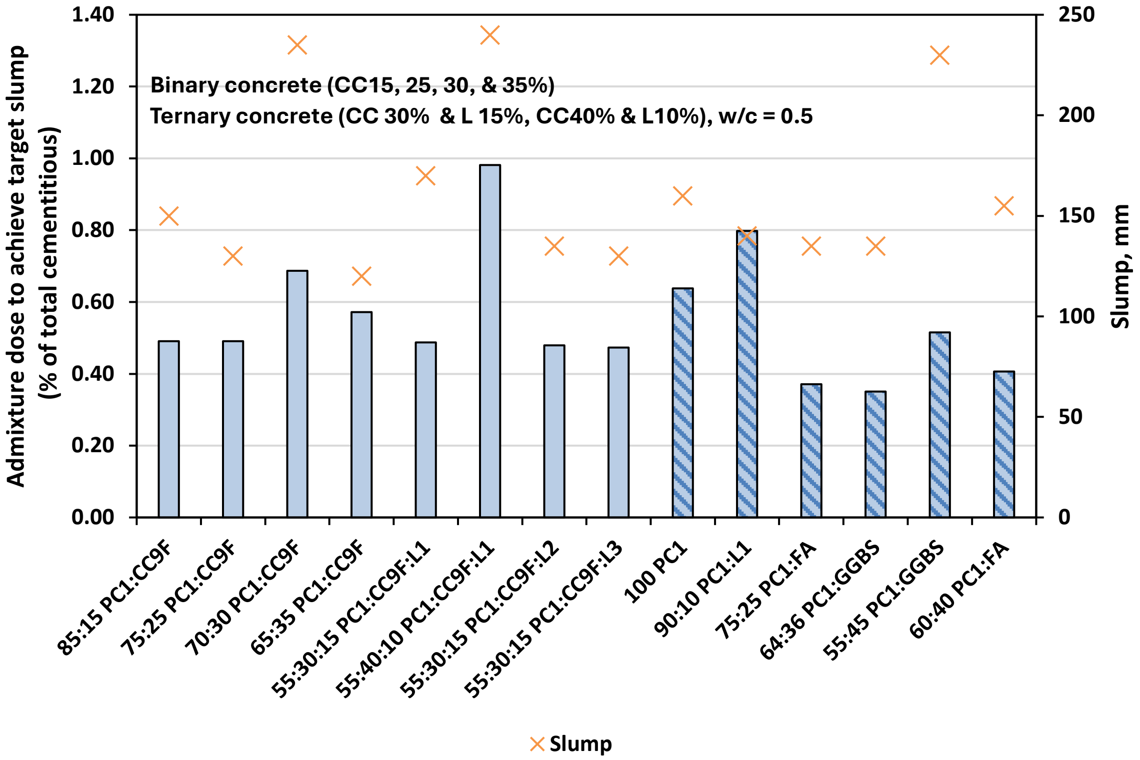

Figure 7 - Admixture dose required to achieve target slump and the corresponding slump achieved for CC9F binary and ternary concretes at varying calcined clay replacement level

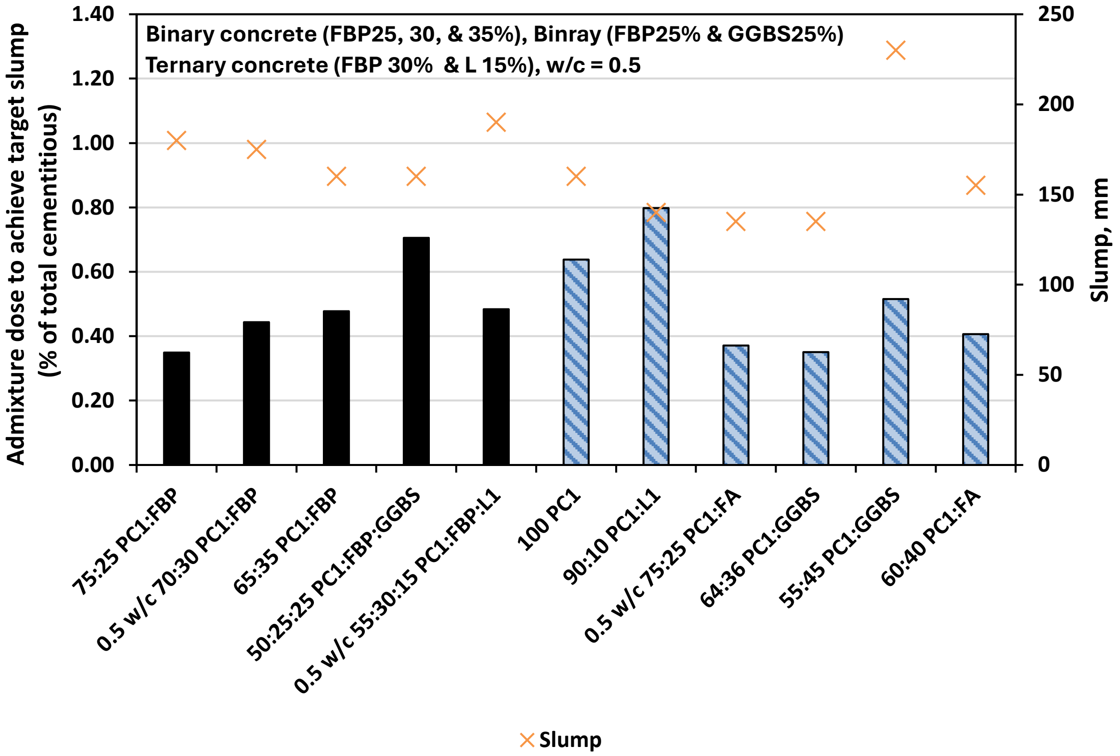

Figure 8 - Admixture dose required to achieve target slump and the corresponding slump achieved for FBP binary and ternary concretes at varying calcined clay replacement level

3.2.2. *Cube strength*

The cube strength development results for the CEM II/B-V binary and CEM II/C-M ternary concretes at an equivalent w/c ratio of 0.5, are given in Figures 9 and 10, which also includes the CEM I, FA, GGBS and L references.

The concrete strength development results show that the calcined clay concretes gained strength rapidly between the ages of 3 days and 14 days, with strength gains reducing thereafter. The 28 days strength of the binary calcined clay concretes (54.5 MPa to 75.5 MPa) exceeded the 28days strength of the 25% FA (49.0 MPa) and were comparable to or greater than that of the 36% GGBS (57.0 MPa). The calcined clays, with the exception of CC9R, had comparable strengths to the 25% FA even at 56 and 180 days (61.0 MPa and 71.0 MPa respectively).

The 28days strength of the ternary calcined clay concretes at a w/c ratio of 0.5 (46.5 MPa to 56.5 MPa), were comparable to or exceeded that of the 40% FA (47.5 MPa) concrete but were lower than that of the 45% GGBS (58.5 MPa). As observed in the binary concrete, at 180 days the 40% fly ash reference was similar to the calcined clay concretes and in many cases exceeded the ternary concretes.

In both binary and ternary concrete, at a w/c ratio of 0.5, FBP gave lower strengths than those with calcined clay at 28 days but continued to gain strength from 28 days to 180 days. Comparatively, the calcined clay concrete strengths did not increase significantly beyond 28 days. Although continuing to gain strength to 180 days, the ultimate strength of the FBP concretes were often lower than or had comparable strength to that of the 25% or 40% FA references in the binary or ternary concretes respectively.

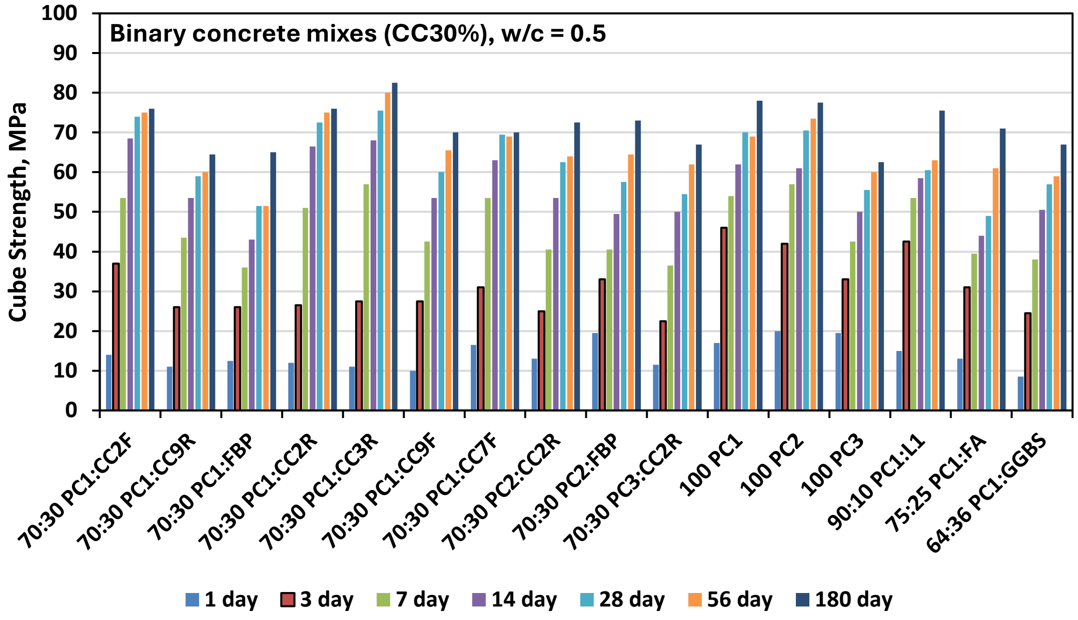

Figure 9 – Concrete strength development of binary calcined clay and reference concretes at w/c = 0.5

The strength results of the calcined clay binary and ternary concretes show that strengths comparable to or greater than the FA, GGBS, and CEM I concretes can be obtained at the same w/c ratio. In ternary concretes, despite the replacement of 15% clinker with limestone giving reductions in strength of 15 % to 37%, when compared to the calcined clay binary concretes, a 28-day strength greater than 45 MPa was consistently attained.

The cube strength development results for the CEM II/B-V binary and CEM II/C-M ternary concretes using CC2R, CC9F, and FBP at w/c ratios of 0.4, 0.5 and 0.6, are given in Figure 11 The same trends observed at 0.5 w/c ratio were also broadly seen at 0.4 and 0.6 w/c ratios. Although the FBP binary and ternary mixes generally had lower cube strengths than calcined clay at all ages at 0.5 w/c ratio, at 0.4 w/c ratio the FBP binary (85.5 MPa) and ternary (79.5 MPa) strengths exceed those of CC9F binary (73.0 MPa) and ternary (66.5 MPa) and the CC2R ternary (66.5 MPa). The highest cube strength of 98.0 MPa was obtained in the CC2R binary at 180 days. When compared to the 25% FA concrete at 0.4 w/c ratio, all binary concretes and that of the FBP ternary exceed the FA 180 days strength of (71.0 MPa) at equal w/c ratio.

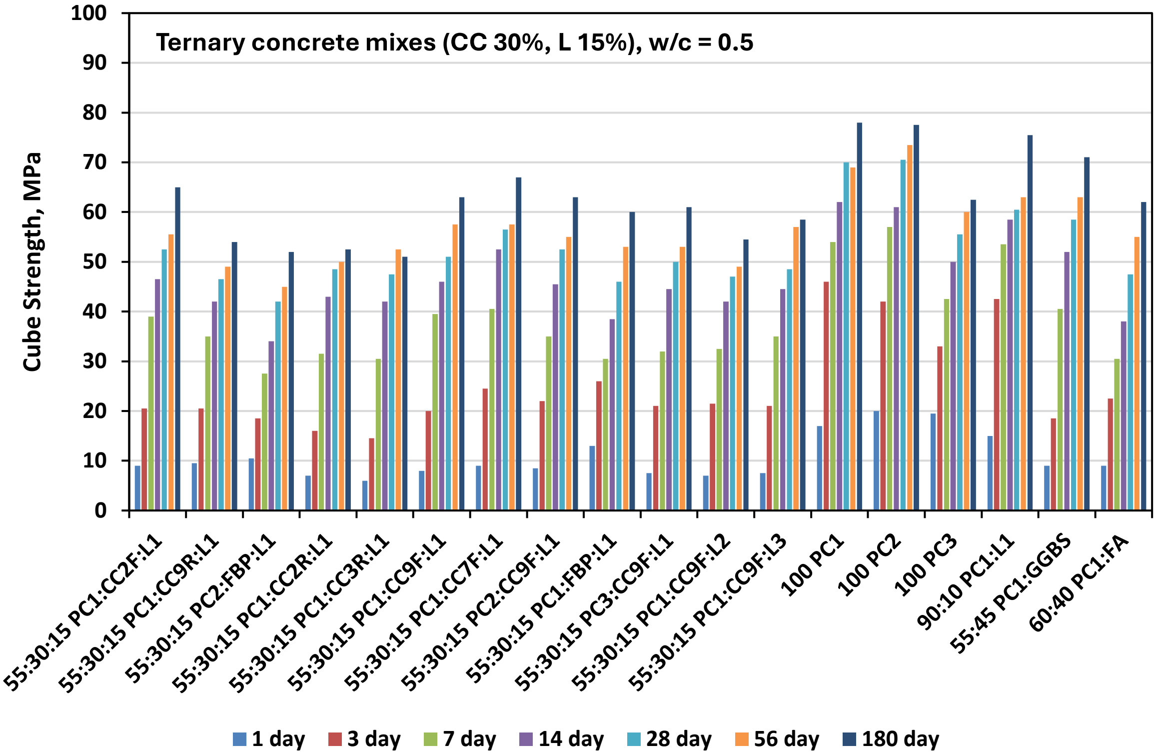

Figure 10 – Concrete strength development of ternary calcined clay and reference concretes at w/c = 0.5

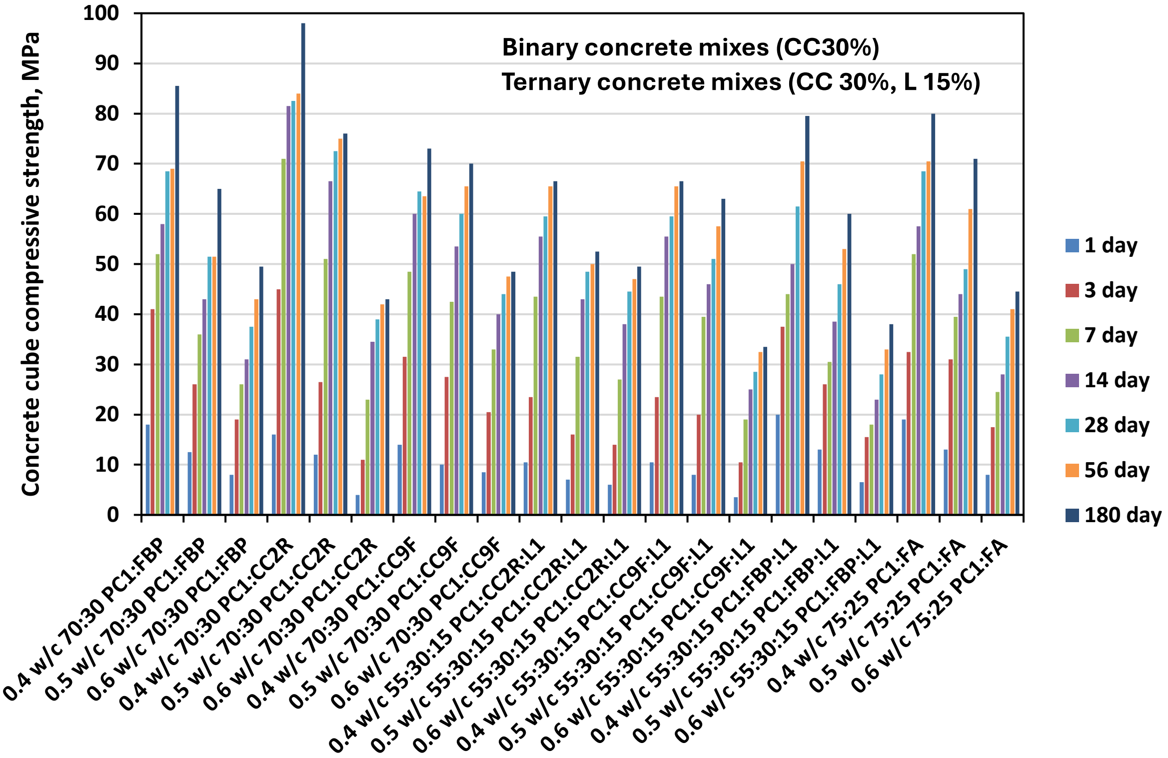

Figure 11 – Concrete strength development of binary and ternary concretes at 0.4, 0.5, and 0.6 w/c ratio

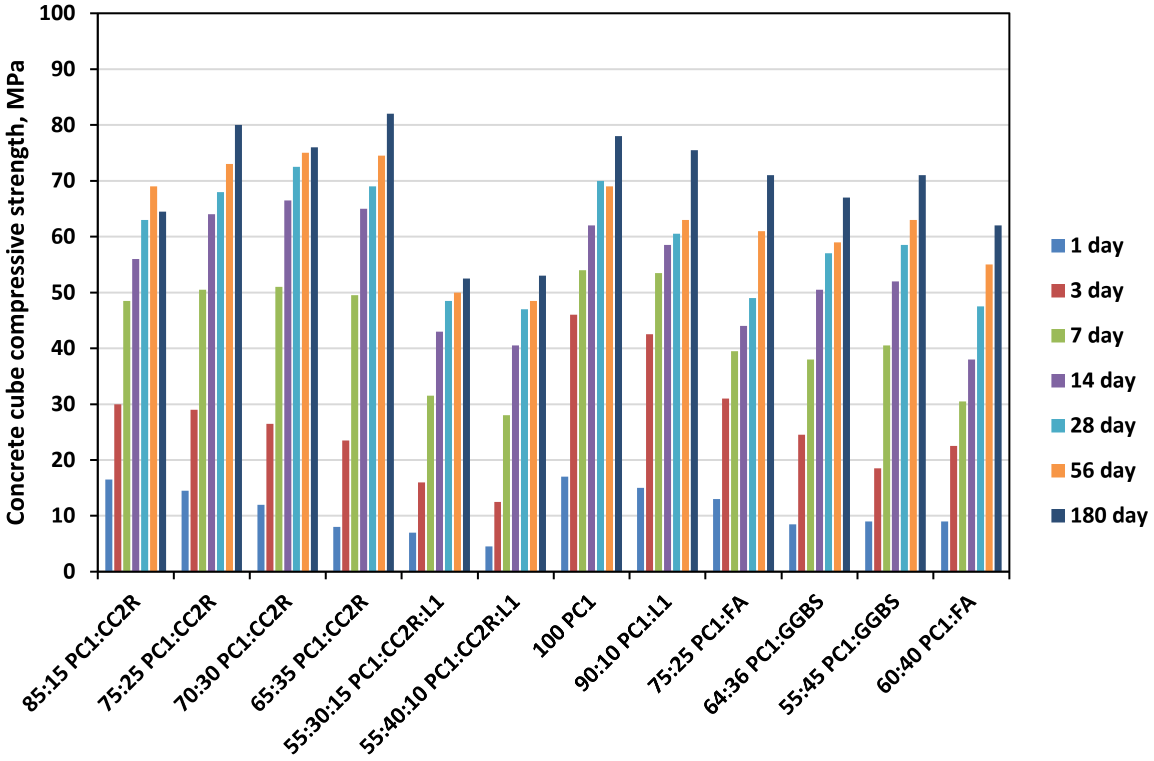

Figure 12 – Concrete strength development of CC2R binary and ternary concretes 0.5 w/c ratio and varying clay replacement levels

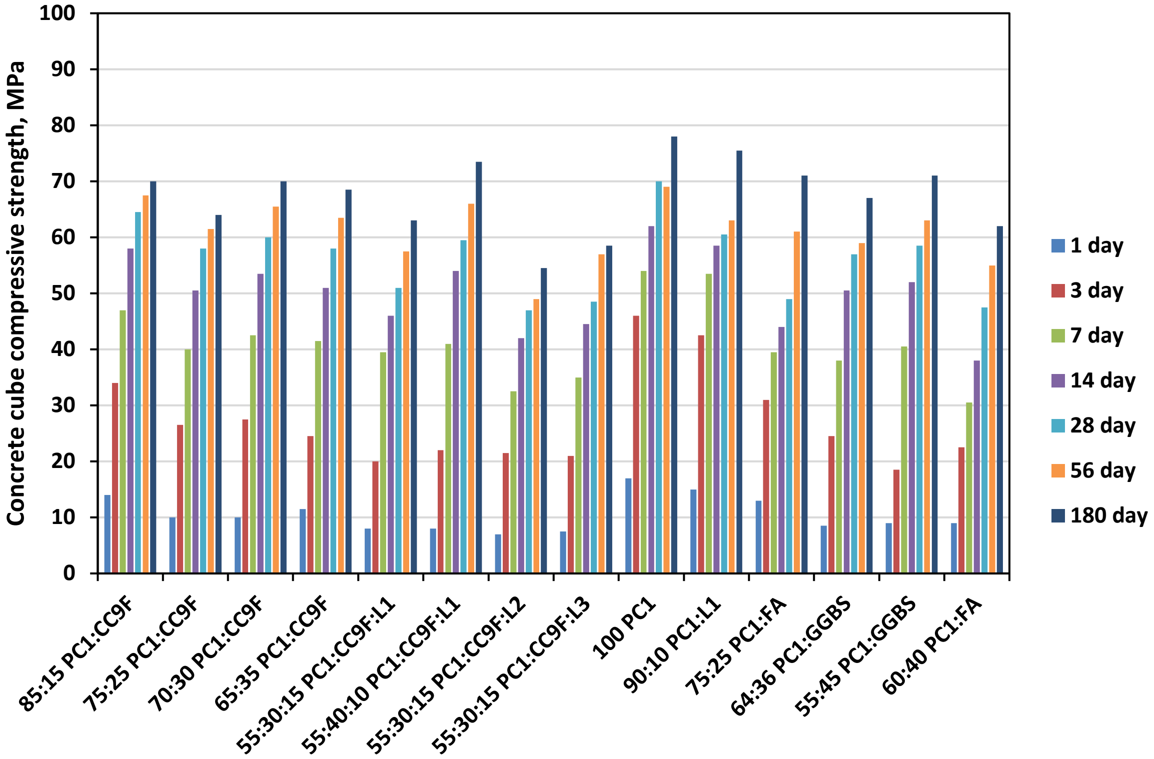

Figure 13 – Concrete strength development of CC9F binary and ternary concretes 0.5 w/c ratio and varying clay replacement levels

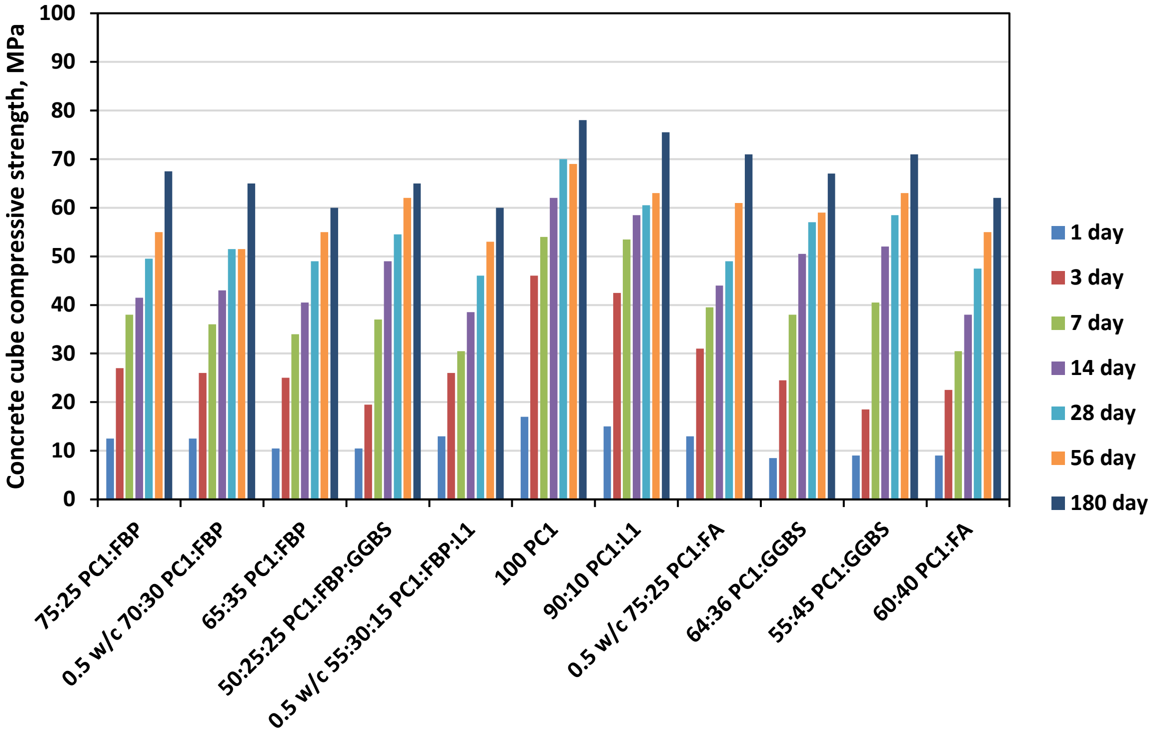

Figure 14 – Concrete strength development of FBP binary and ternary concretes 0.5 w/c ratio and varying clay replacement levels

The effect of varying replacement level of CC2R, CC9F, and FBP in binary and ternary concretes at a w/c ratio of 0.5 are given in Figures 12 to 14 respectively. Generally, a calcined clay combination of 30% was found to be the optimum replacement level in binary concretes (of 15%, 25%, 30%, 35%) and 40% calcined clay and 10% limestone to be optimum for ternary concretes (of 30:15% and 40:10%). It should be noted that the degree of change between these combinations was generally small and all produced good strength results at 28 days of ≥58.0 MPa in binary and ≥47.0 MPa in ternary concrete.

Generally, flash calcined clay gave higher strengths than the same source clay, compared to rotary calcination, although the source clay had a greater influence on strength development than the method of calcination. The concrete strength results indicate the hierarchy for 28days strength development was as follows:
CC2>CC3>CC7>CC9

The strength differences between CC2 and CC3 were relatively small.

4. Action K3 & K4 – Concrete Durability

4.1. Chloride Ingress

4.1.1. Migration

The non-steady state chloride migration coefficients for both the calcined clay and brick powder binary (CEM II/B-Q) and ternary (CEM II/C-M) concretes at 0.5 w/c ratio and 30% calcined clay in cement, plus 15% limestone in the ternary systems, are given in Figures 15 and 16. These were obtained from the BS EN 12390-18 chloride migration test (BSI, 2021).

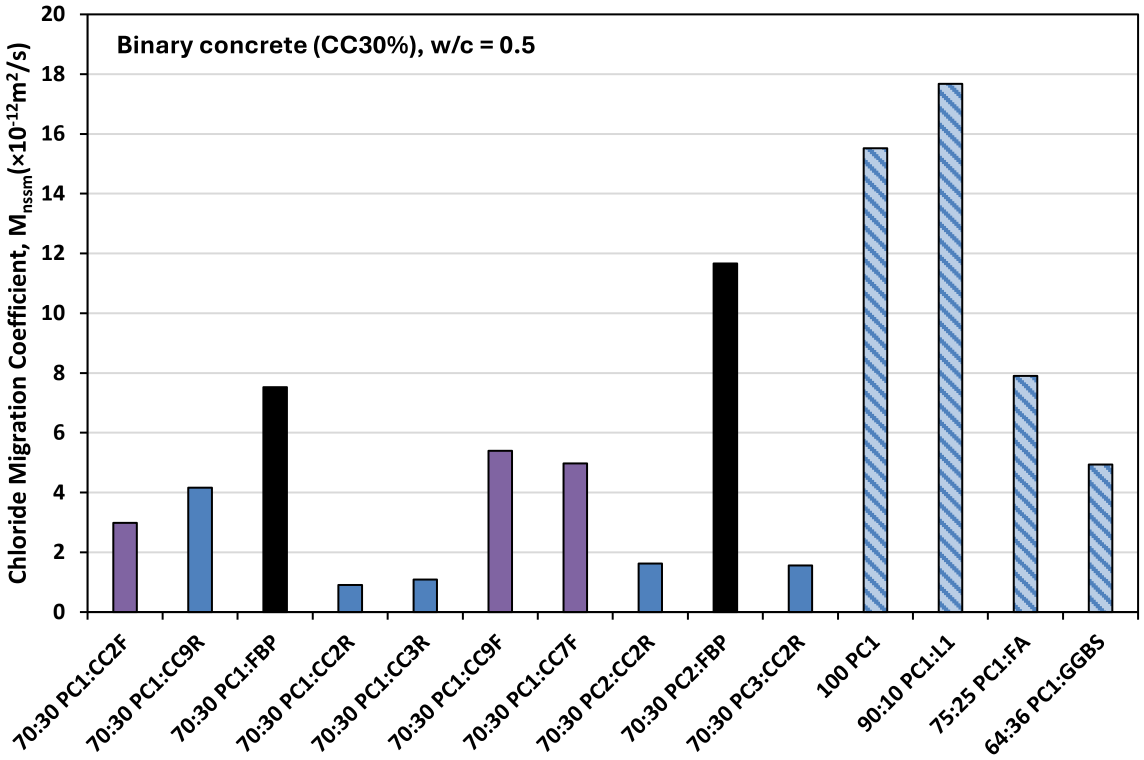

Figure 15 – Non-steady state Chloride Migration Coefficient for binary concretes at w/c = 0.5

The figures show that the inclusion of calcined clay reduces the chloride migration coefficient in both binary and ternary systems. In the binary concretes, calcined clay (0.90 x10^{-12} m^2/s to 5.40 x10^{-12} m^2/s) outperformed the 25% FA concrete (7.90 x10^{-12} m^2/s) and offered better or comparable performance to that with 36% GGBS (4.94 x10^{-12} m^2/s). Similar behaviour was observed in the ternary concretes with all calcined clays (0.64 x10^{-12} m^2/s to 7.38 x10^{-12} m^2/s) giving comparable or better performance than that of the 40% FA (6.77 x10^{-12} m^2/s) concrete. Calcined clays CC2R, CC2F, CC3R, CC9R, and CC9F with PC3 demonstrated better or comparable performance to the 45% GGBS (4.16 x10^{-12} m^2/s) concrete.

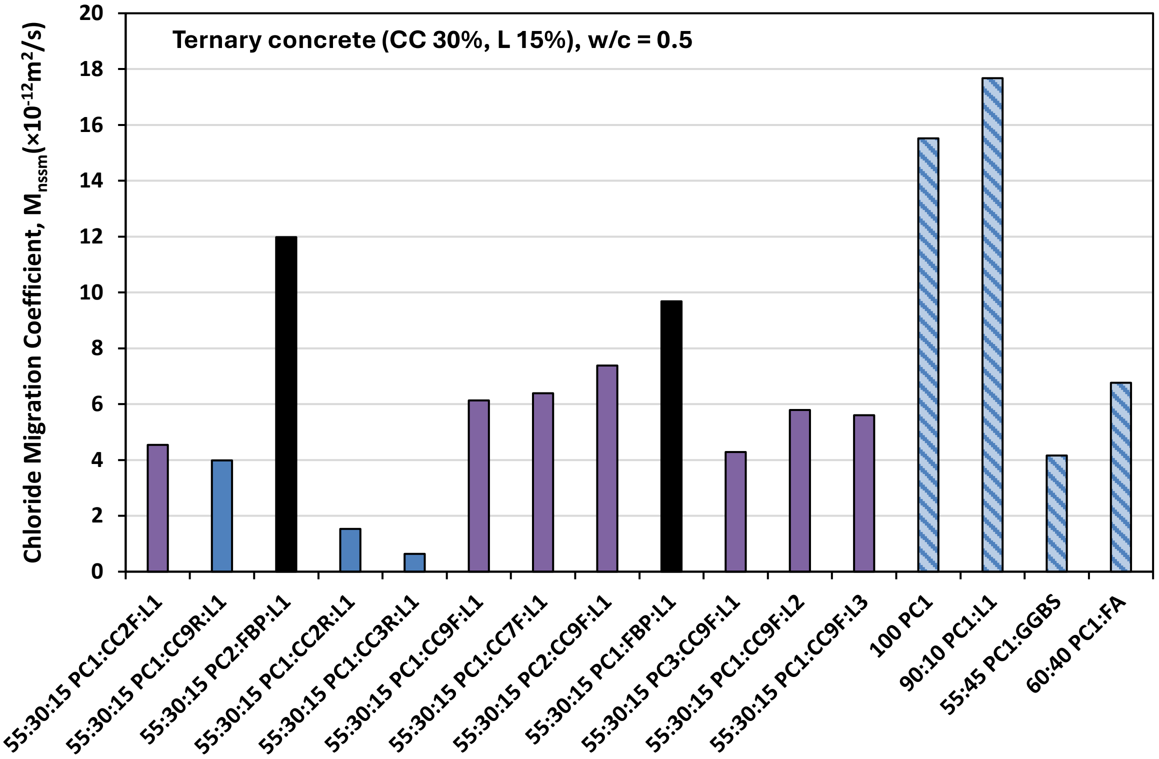

Figure 16 - Non-steady state Chloride Migration Coefficient for ternary concretes at w/c = 0.5

In both binary and ternary concretes the FBP (7.53 x10^{-12} m^2/s to 11.98 x10^{-12} m^2/s) was outperformed by the calcined clay and the FA and GGBS concretes, although it still offered better chloride resistance than those of CEM I (15.52 x10^{-12} m^2/s) and CEM II/A-L (17.68 x10^{-12} m^2/s). The differences in performance between the binary and ternary calcined clay concretes was small, suggesting that the replacement of clinker with limestone has little effect on chloride resistance.

The non-steady state migration coefficients for CC2R, CC9F, and FBP binary and ternary concretes using 30% calcined clay in cement, plus 15% limestone in the ternary systems, at 0.4, 0.5 and 0.6 w/c ratios are shown in Figure 17. The rate of chloride migration increased with w/c ratio, in line with expectations, for all materials evaluated. The degree to which the chloride migration coefficient increased with w/c ratio appeared to reflect the relative chloride migration ranking of the materials (i.e., the concretes with the highest chloride migration coefficients, saw the largest increases between w/c ratios). The greatest increases between w/c ratios were observed in the FBP ternary between 0.5 (9.68 x10^{-12} m^2/s) and 0.6 w/c ratios (17.16 x10^{-12} m^2/s), which also had the highest rates of chloride ingress. In contrast CC2R binary and ternary concretes, which had the lowest rates of chloride ingress, saw very minor increases in chloride migration rate of approximately 0.5 x10^{-12} m^2/s between w/c ratio increments. At 0.6 w/c ratio CC9F binary and ternary mixes gave good chloride performance (<7.0 x10^{-12} m^2/s) and the CC2R binary and ternary concretes gave excellent resistance to chloride ingress of ≤2.0 x10^{-12} m^2/s. Both CC2R and CC9F binary and ternary concretes had lower chloride migration coefficients than the 25% FA at equal w/c ratios. FBP in a binary system marginally outperformed the 25% FA but this was not obtained in the ternary system.

The effects of varying the calcined clay or brick dust content in cement for CC2R, CC9F, and FBP at 0.5 w/c ratio are shown in Figures 18 to 20. Varying the calcined clay proportion in cement did not appear to have any consistent effect on the chloride migration coefficients for the CC2R and CC9F binary concretes at 15, 25, 30, and 35% calcined clay. Increasing the proportion of CC2R in ternary systems from 30% with 15% limestone to 40% with 10% limestone gave a small decrease in chloride migration coefficient.

Increasing the proportion of FBP appeared to improve chloride ingress resistance (11.93 x10^{-12} m^2/s at 25%, 7.53 x10^{-12} m^2/s at 30%, and 6.32 x10^{-12} m^2/s at 35%), although the lowest FBP concrete chloride migration coefficient (0.52 x10^{-12} m^2/s) was observed in the FBP ternary concrete with GGBS (50:25:25 PC1:FBP:GGBS). Changing the limestone source, shown in Figure 19, had little effect on the chloride migration coefficient of CC9F ternary concretes.

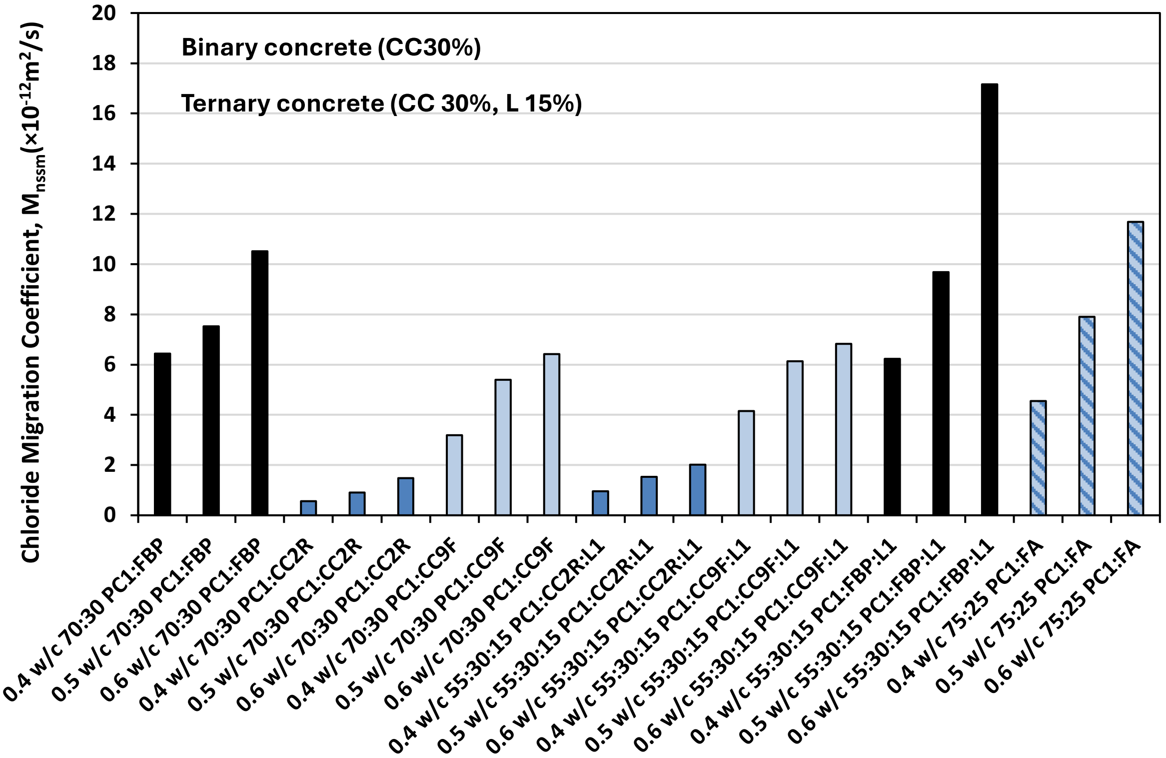

Figure 17 - Non-steady state Chloride Migration Coefficient for binary and ternary concretes at 0.4, 0.5, and 0.6 w/c ratio

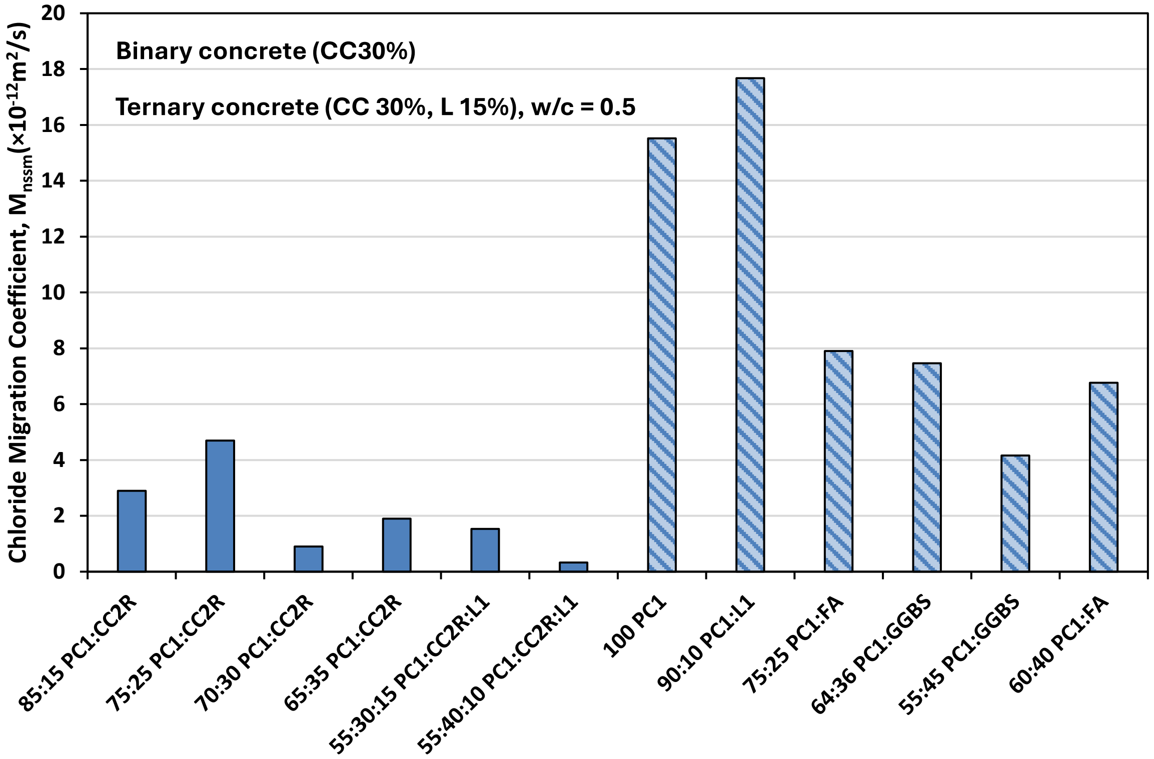

Figure 18 - Non-steady state chloride migration coefficients of binary and ternary concretes with varying proportions of CC2R in cement. W/c ratio = 0.5

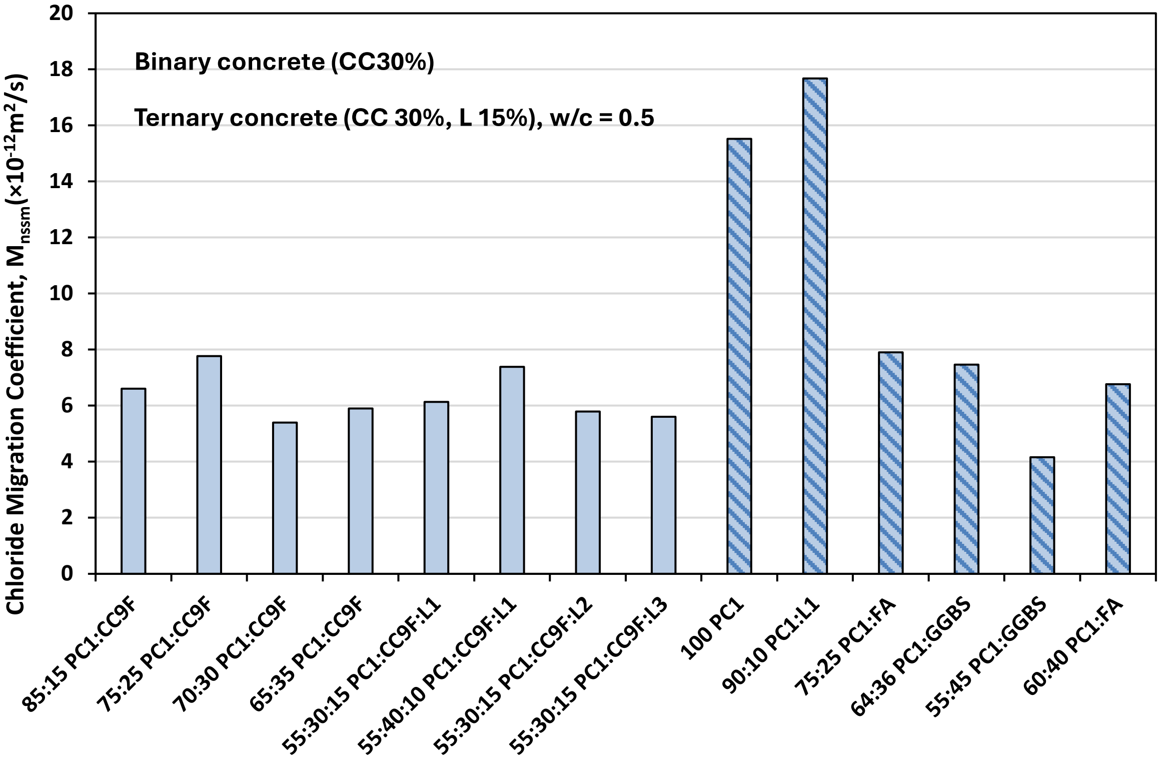

Figure 19 - Non-steady state chloride migration coefficients of binary and ternary concretes with varying proportions of CC9F in cement. W/c ratio = 0.5

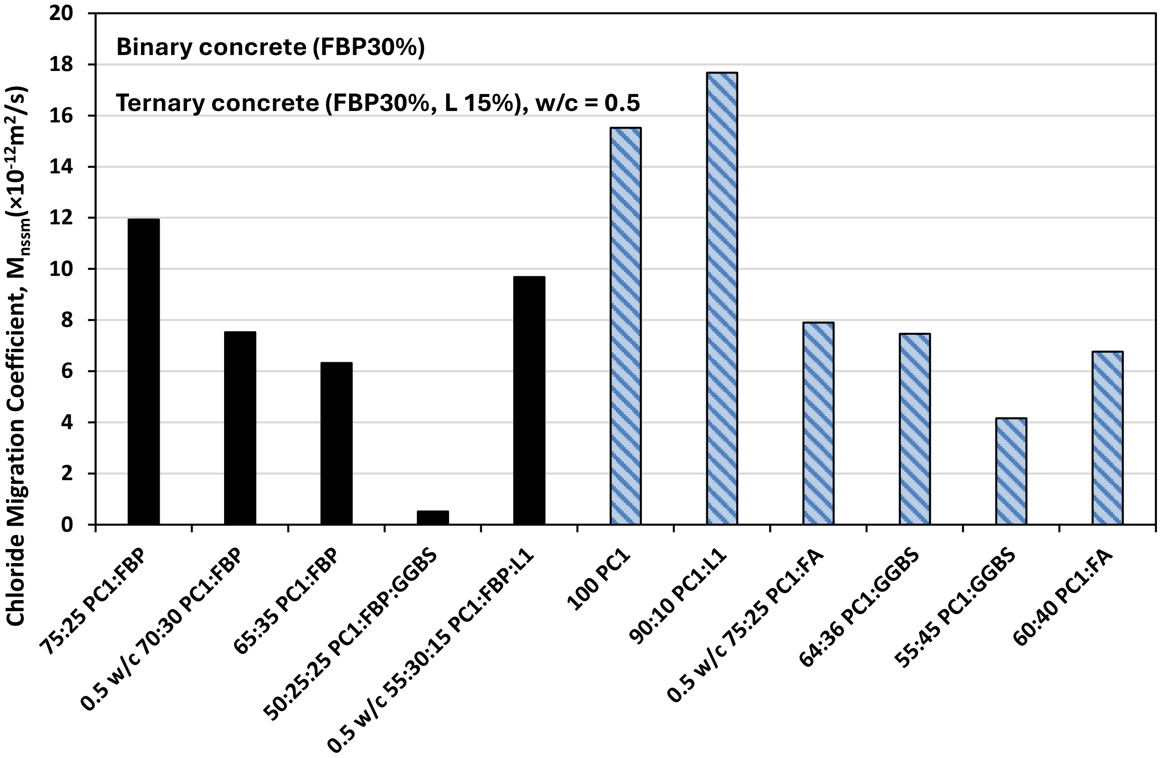

Figure 20 - Non-steady state chloride migration coefficients of binary and ternary concretes with varying proportions of FBP in cement. W/c ratio = 0.5

The relationship between Al_2O_3 content, by XRF, and the chloride migration coefficient of the calcined clay, FBP, and reference concretes is shown in Figure 21.

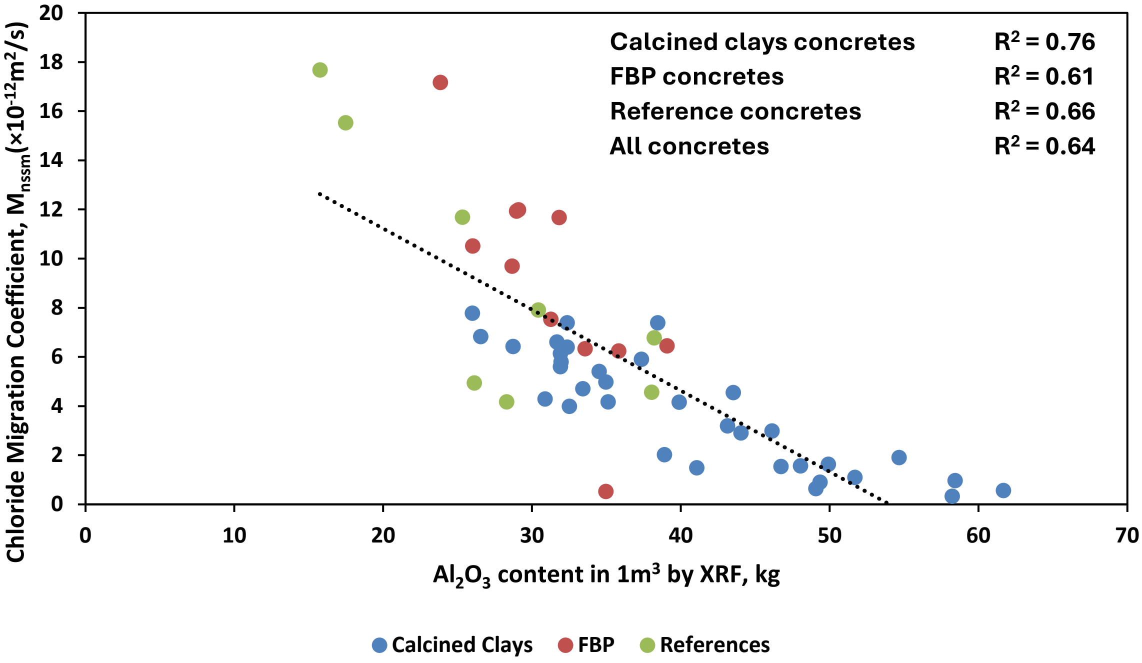

Figure 21 – Influence of aluminium oxide content on non-steady state chloride migration coefficient for all concretes tested

The quantity of Al_2O3 present in concrete appeared to be highly influential on chloride resistance irrespective of the cement materials used. A relationship was identified for all concretes (w/c ratios, replacement levels, and materials) collectively as shown in Figure 21, with a coefficient of determination (R^2) of 0.64. Considering the calcined clays alone gave a higher R^2 of 0.76, indicating a good correlation between Al_2O_3 and chloride resistance of the calcined clay concretes.

All calcined clays gave good resistance to chloride ingress in concrete. Rotary calcination appeared to give the lowest chloride migration coefficients, although the source clay still seemed to be influential with CC2 and CC3 giving the best results. The general hierarchy of chloride performance of the calcined clays and brick powder was as follows:

CC2R/CC3R, CC2F, CC9R, CC7F, CC9F, FBP.

The effect of varying w/c ratio and the level of replacement in cement gave similar chloride resistance performance between replacement levels in both binary and ternary concretes, indicating that the level of calcined clay in cement is less influential than the source of the clay. The results of varying w/c ratio between 0.4, 0.5, and 0.6 at 30% calcined clay replacement are in line with expectations, with lower w/c ratios resulting in a lower chloride migration coefficient, although the performance of CC2R and CC9F at 0.6 w/c ratio was still good.

Using the strength results available at 0.4, 0.5, and 0.6 w/c ratio, interpolation was carried out to estimate the w/c ratios required to achieve 40MPa in FBP, CC2R, and CC9F binary and ternary concretes, as well as that for 25% FA binary. The estimated equal strength performance and the w/c ratios to achieve this for each material are given in Figure 22. These show the same behaviour as observed in the binary and ternary concretes in Figures 15 and 16, and highlight the excellent chloride resistance of CC2 in particular.

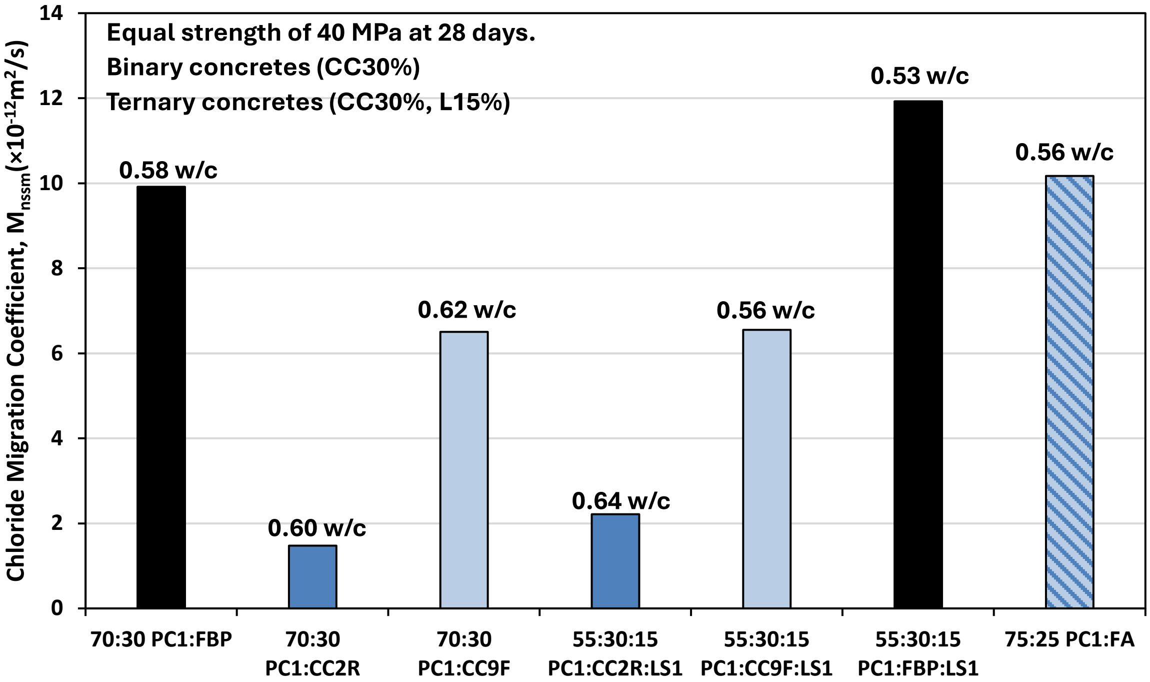

Figure 22 - Non-steady state chloride migration coefficients of binary and ternary concrete at 40 MPa 28 days equal strength

Images of CC2R, CC9F, FBP, and reference concretes after chloride migration testing are available in the Appendix showing chloride ingress depths

.

4.1.2. Diffusion

Chloride diffusion in accordance with BS EN 12390-11 ((BSI, 2015) has been carried out at the University of Dundee on the same materials as the chloride migration testing. A select sample of these is to be profiled and acid digestion carried out to confirm the results observed from chloride migration testing. The results of these will be presented in a later update report.

4.2. Carbonation

4.2.1. Accelerated Carbonation

The rates of carbonation, K_{AC}, for both calcined clay and brick powder binary (CEM II/B-Q) and ternary (CEM II/C-M) concretes at 0.5 w/c ratio and 30% calcined clay in cement are given in Figures 23 and 24. These were derived from the BS EN 12390--12 accelerated carbonation test (BSI, 2020) carried out at 3.0 % CO_2. The rates given are the best fit final rate of carbonation at the end of the test (70 days) per root time (days).

In the binary concretes, the calcined clays and brick powder generally had higher rates of carbonation (0.66 mm/√days to 1.79 mm/√days) than the 25% FA (1.06 mm/√days) and 36% GGBS (1.20 mm/√days), although CC2F and CC7F gave comparable rates. In general, the rotary calcined clays had higher rates of carbonation (1.27 mm/√days to 1.79 mm/√days) than the flash calcined clays (0.66 mm/√days to 1.43 mm/√days), but as previously observed for strength development, the source clay also appears to be more influential. Similar behaviour was observed in the ternary concretes, with the accelerated carbonation rates of the calcined clays and brick powder (2.49 mm/√days to 2.58 mm/√days) exceeding that with 45% GGBS (1.27 mm/√days). CC2F, FBP, CC9R, and CC7F concretes gave lower rates of carbonation than that with40% FA (1.98 mm/√days), whereas these were higher for the CCR, CC3R, and CC9F concretes.

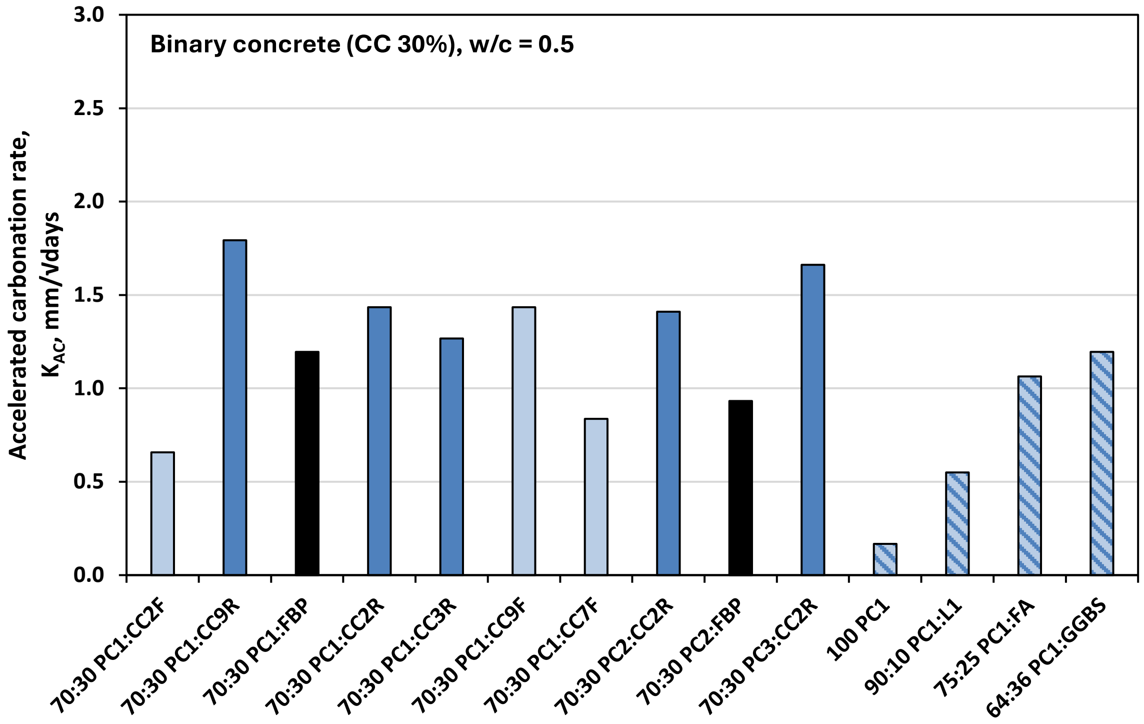

Figure 23 - Rate of accelerated carbonation K_{AC} at 3.0% CO_2 for binary concretes at w/c = 0.5

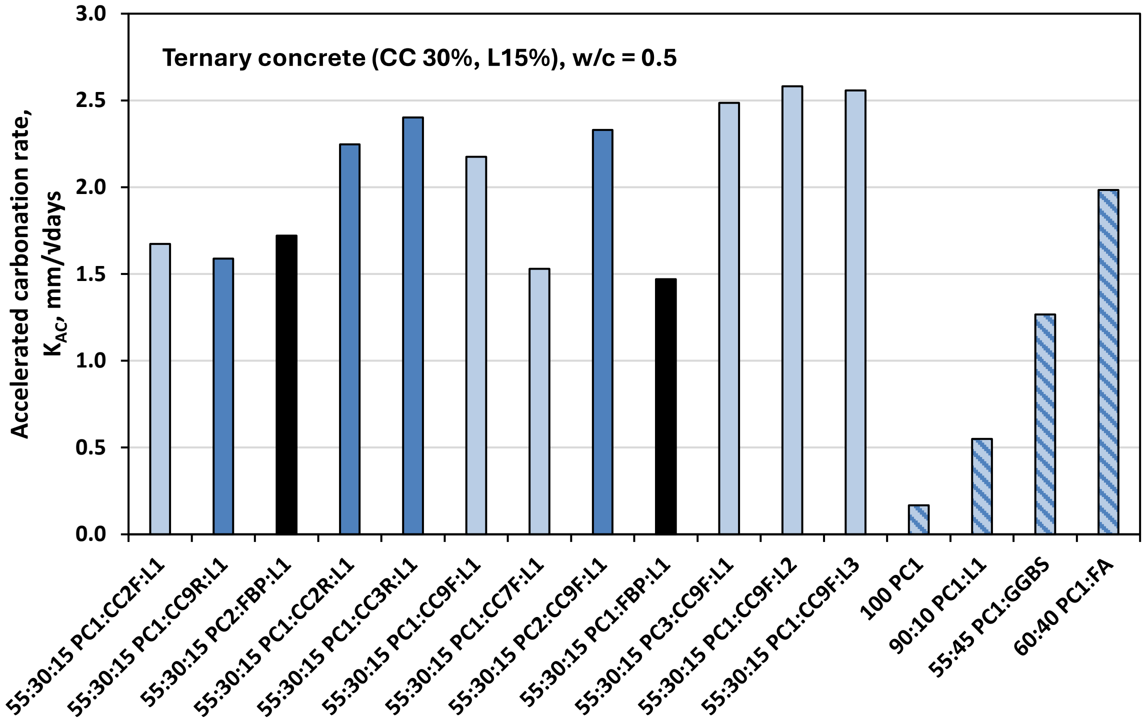

Figure 24- Rate of accelerated carbonation K_{AC} at 3.0% CO_2 for ternary concretes at w/c = 0.5

It should be noted that while the rates of accelerated carbonation were not excessive in the calcined clays, these materials often had higher 28-day strengths (minimum of 54 MPa in binary and 46 MPa in ternary) than the FA and GGBS reference concretes.

Consideration of carbonation performance should be taken into account, when designing lower strength concretes, as the rate of carbonation will increase with reducing concrete strength. This behaviour is shown in Figure 25, comparing the FBP, CC2R, and CC9F in binary and ternary concretes at 0.4, 0.5, and 0.6 w/c ratios against a 25% FA concrete.

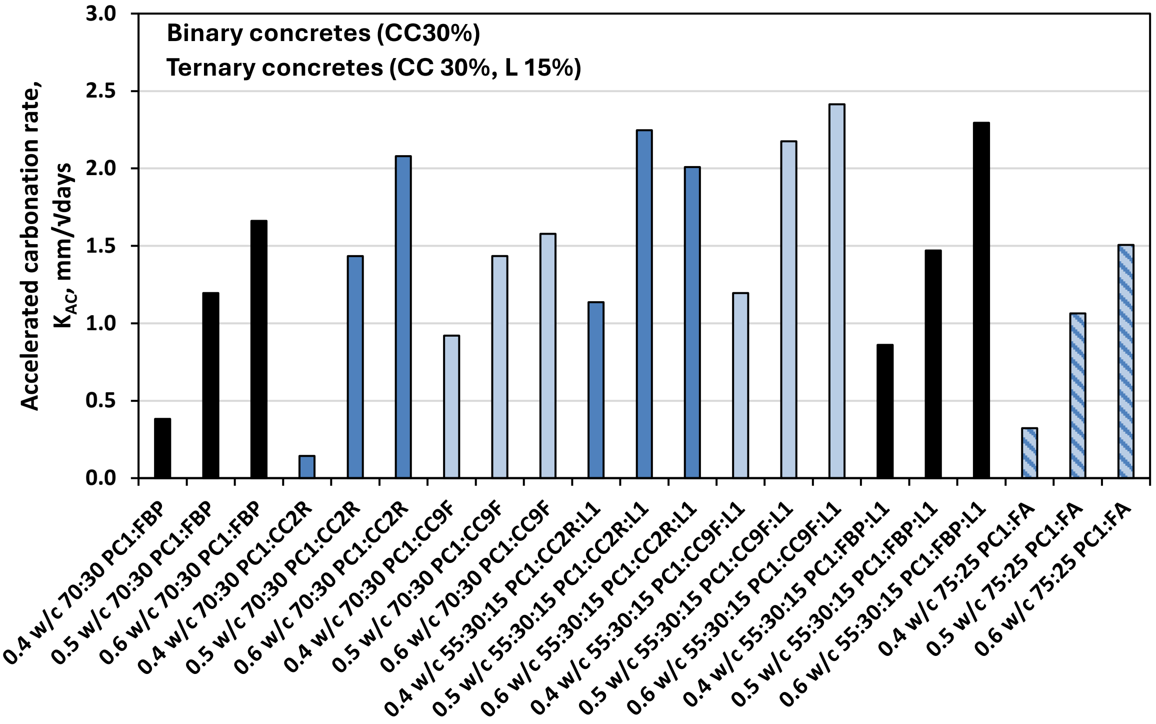

Figure 25- Rate of accelerated carbonation K_{AC} at 3.0% CO_2 for binary and ternary concretes (0.4, 0.5, and 0.6 w/c ratio)

The change in rate of accelerated carbonation of CC2R, CC9F and FBP binary and ternary concretes at 0.5 w/c ratio and varying cement replacement level are given in Figures 26 to 28. Increasing replacement of PC with calcined clay or brick dust led to an increased rate of carbonation due to greater dilution of CaO in the concrete. This effect was most evident in CC9F binary concretes (0.9 mm/√days at 15% to 2.01 mm/√days at 35%) but was lesser in CC2R (1.3 to 1.4 mm/√days) and FBP (0.98 to 1.20 mm/√days) binary concretes. A small increase in rate of carbonation with calcined clay level in cement was also observed in the CC2R ternary concretes between 30% clay and 15% limestone (2.2 mm/√days) and 40% clay and 10% limestone (2.4 mm/√days).

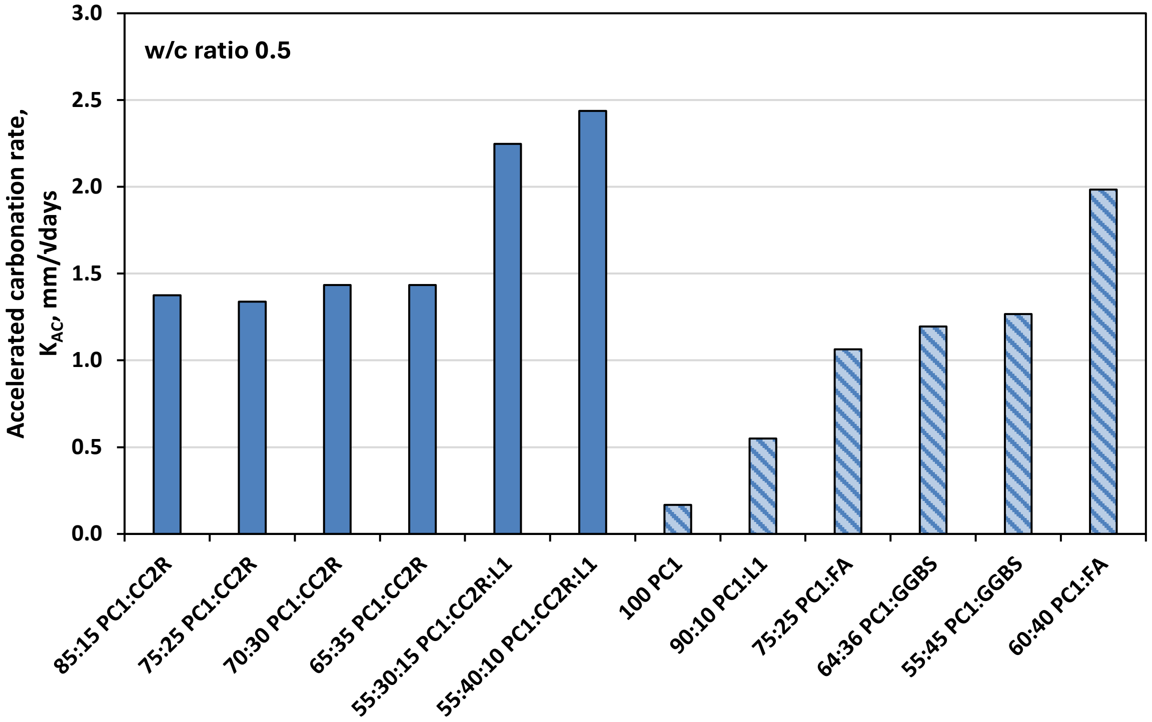

Figure 26 - Rate of accelerated carbonation KAC at 3.0% CO2 for CC2R binary and ternary concretes at w/c = 0.5

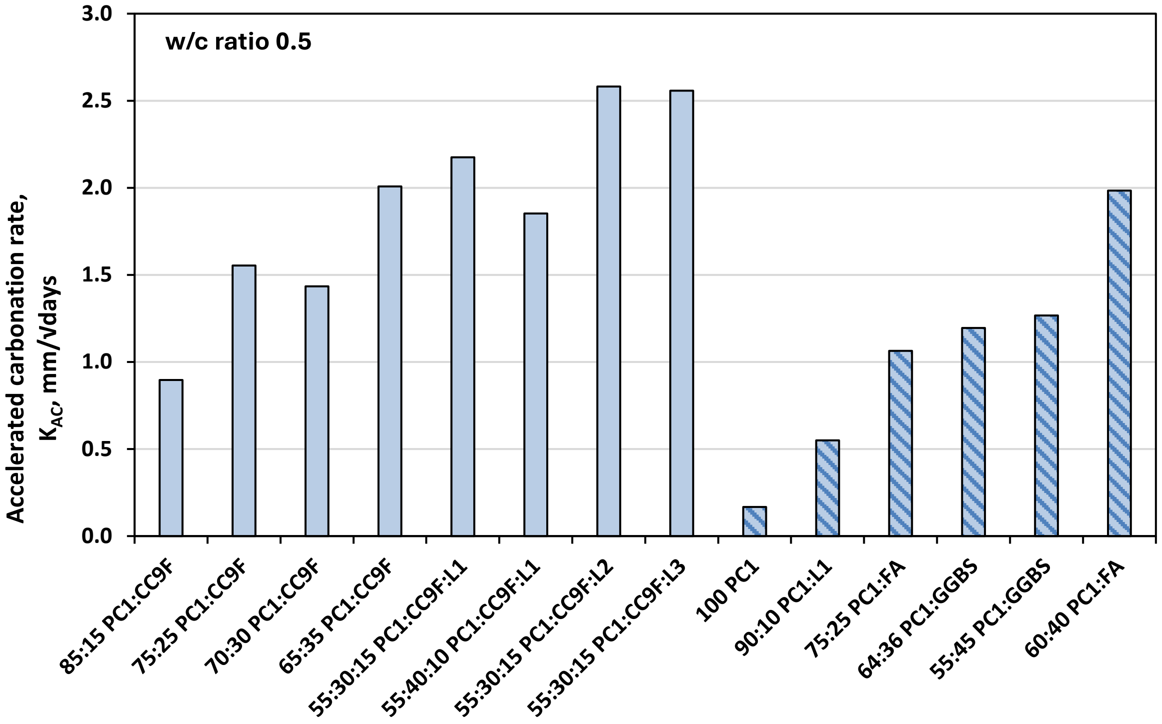

Figure 27 - Rate of accelerated carbonation KAC at 3.0% CO2 for CC2R binary and ternary concretes at w/c = 0.5

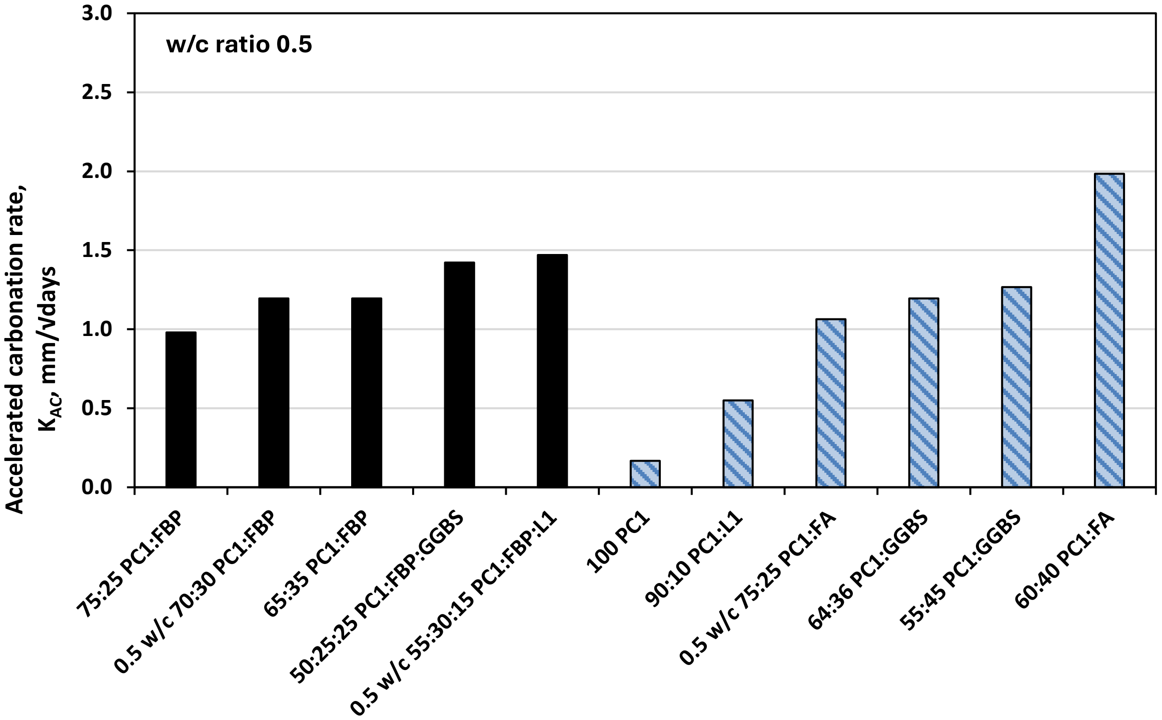

Figure 28 - Rate of accelerated carbonation KAC at 3.0% CO2 for CC2R binary and ternary concretes at w/c = 0.5

The estimated 40 MPa equal strength rates of accelerated carbonation and the corresponding w/c ratios for each concrete combination are given in Figure 29. These show that FBP binary (1.59 mm/√days) and ternary (1.70 mm/√days) concretes and CC9F binary (1.60 mm/√days) concrete have comparable, albeit higher rates of accelerated carbonation at equal strength as the 25% FA (1.37 mm/√days) concrete. In contrast, the CC9F ternary (2.40 mm/√days) and CC2R binary (2.10 mm/√days) and ternary (2.35 mm/√days) concretes had notably higher rates of accelerated carbonation at equal strength. This suggests that replacement of 15% clinker with limestone has a detrimental effect on the rate of carbonation.

The relationship between CaO content and rate of accelerated carbonation for all the calcined clay, FBP, and reference concretes cast is shown in Figure 30. The quantity of CaO was highly influential on the rate of accelerated carbonation in the concretes irrespective of the cementitious materials used. A relationship was identified for all the concretes (w/c ratios, replacement levels, and materials) collectively, with a coefficient of determination (R^2) of 0.70. Considering the calcined clays alone, gave a lower R^2 of 0.55, indicating a general trend between CaO and rate of carbonation for these concretes.

Binary and ternary calcined clay concretes had higher rates of accelerated carbonation than the references, which appears to reflect the reduced CaO content due to higher replacement levels. This should be considered when selecting high clinker replacement concretes for carbonation resistance.

Images of CC2R, CC9F, FBP, and reference concretes after 10 weeks accelerated carbonation testing at 3.0% CO_2 are available in the Appendix showing carbonation ingress depths.

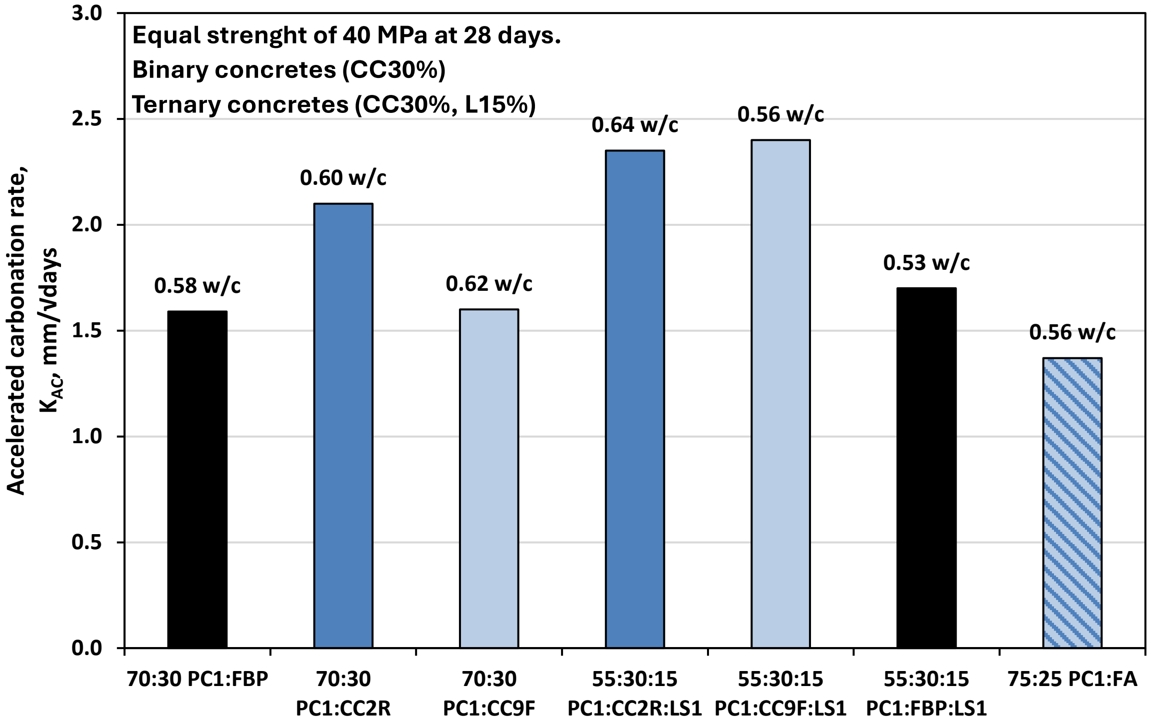

Figure 29 - Rate of accelerated carbonation K_{AC} at 3.0% CO_2 of binary and ternary concrete at 40 MPa 28 days equal strength

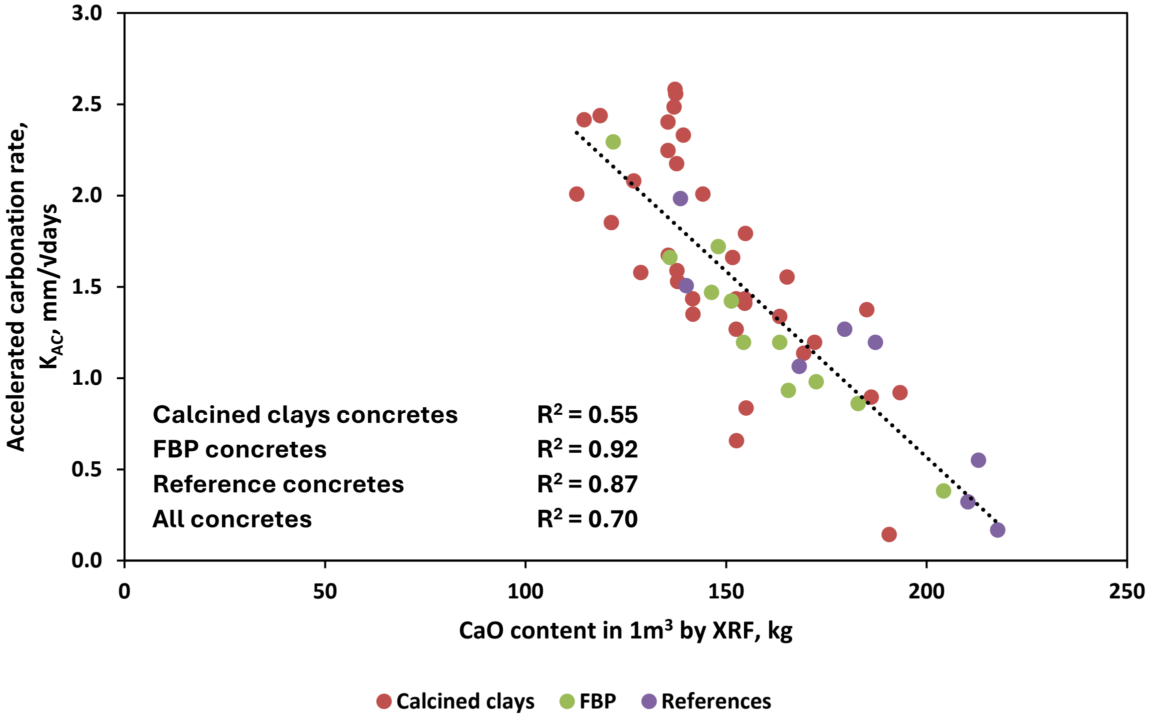

Figure 30 - Rate of accelerated carbonation K_{AC} at 3.0% CO_2 of binary and ternary concrete at 40 MPa 28 days equal strength

4.2.2. Natural (Outdoor Sheltered) Carbonation

The rate of natural carbonation to BS EN 12390-10 (BSI, 2018) was tested at 6 months exposure (outside, sheltered from direct rain), with further testing set to continue beyond the scope of this project. The 6 months natural carbonation depths for the binary (CEM II/B-Q) and ternary (CEM II/C-M) calcined clay concretes are shown in Figures 31 and 32.

In the binary concretes, the natural carbonation depths for calcined clays ranged from 0.2 mm to 1.4 mm. CC9R, CC2R, and CC3R had lower carbonation depths than the 25% FA (0.7mm) and 36% GGBS (0.4 mm) concretes, while these were higher for CC2F, CC9F, and CC7F. Higher depths of carbonation were observed in the ternary concretes with limestone (0.5 mm to 2.5 mm) with only CC9F using PC1 outperforming the 45% GGBS concrete (0.8 mm). CC7F, CC9F using PC2 and PC3, and FBP had comparable depths to the 40% FA concrete (1.3 mm). The carbonation depths of CC2F, CC9R, CC2R, and CC3R exceeded that of the 40% fly ash reference, with carbonation depths of over 2.0 mm after 6 months.

The change of PC appeared to influence the depth of carbonation, with CC2R concretes using PC2 and PC3 having higher carbonation depths (0.7 and 0.9 mm respectively) than CC2R using PC1 (0.2 mm). This behaviour was mirrored in CC9F ternary concretes, with PC2 and PC3 giving higher carbonation depths (1.5 and 1.4 mm respectively) than PC1 (0.5 mm).

The ranking of the calcined clays was also not consistent between binary and ternary concretes, with the rotary outperforming the flash binary concretes, while the opposite was generally true for the ternary concretes.

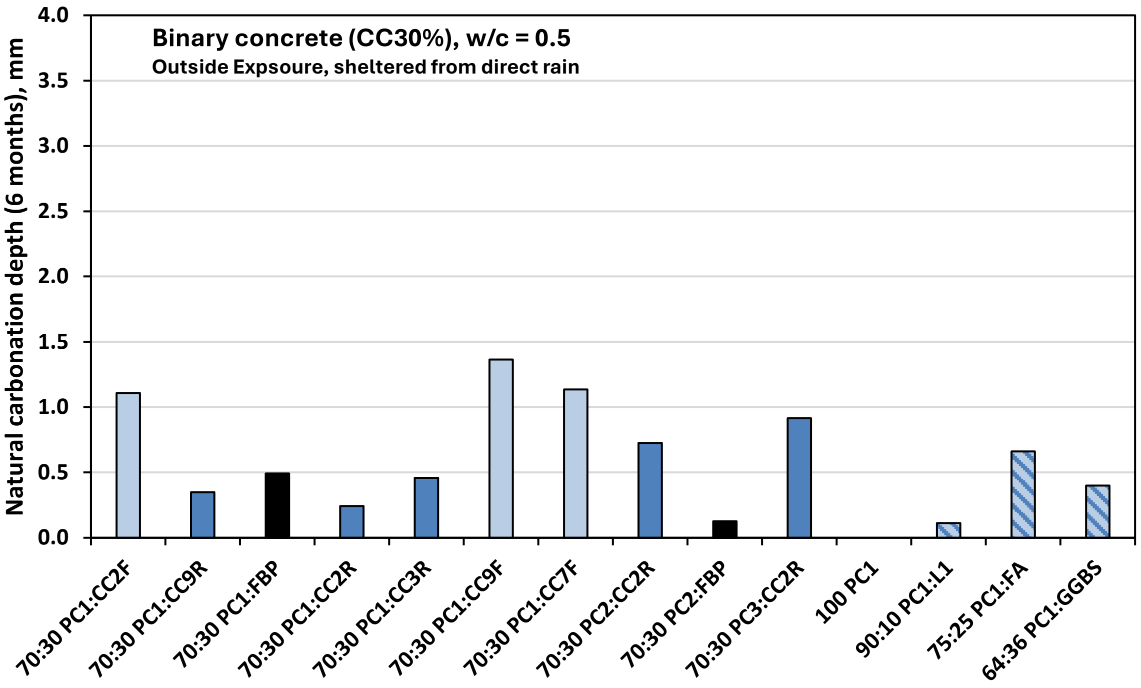

Figure 31 Natural carbonation depths after 6 months exposure for binary concretes at w/c = 0.5

The natural carbonation depths of FBP, CC2R, and CC9F in binary and ternary concretes at 0.4, 0.5, and 0.6 w/c ratios are shown against a 25% FA concrete are shown in Figure 33.

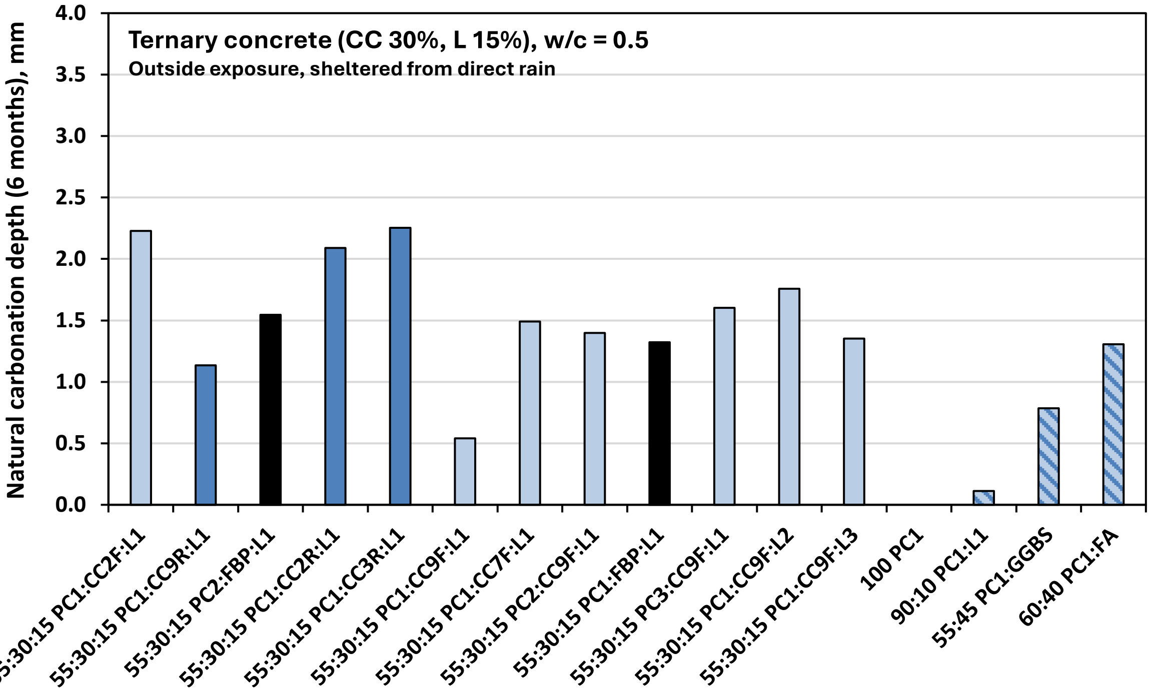

Figure 32 - Natural carbonation depths after 6 months exposure for ternary concretes at w/c = 0.5

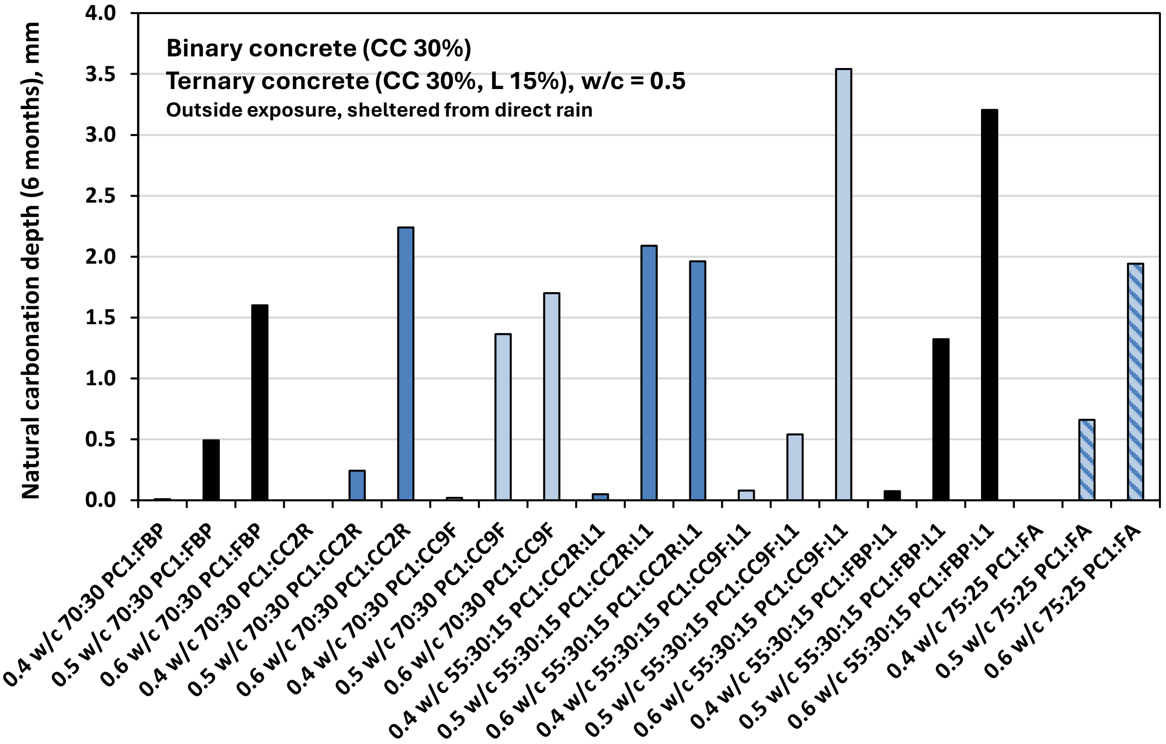

Figure 33 - Natural carbonation depths after 6 months exposure for binary and ternary concretes at w/c = 0.4, 0.5, and 0.6

The natural carbonation depths recorded at 6 months exposure increased with increasing w/c ratio, in line with expectations. Little carbonation (≤1 mm) was observed for the 0.4 w/c ratio concretes, whereas 0.6 w/c ratio concretes had undergone a significant degree of carbonation ranging from 1.6 mm for the FBP binary to 3.5 mm for the CC9F ternary.

The depth of natural carbonation of CC2R, CC9F and FBP binary and ternary concretes at 0.5 w/c ratio and varying cement replacement levels are given in Figures 34 to 36. Increasing replacement of PC with calcined clay or brick dust generally led to an increased carbonation depth due to greater dilution of CaO in concrete, although some variability was observed between calcined clay contents for CC2R concretes due to the comparatively small depths recorded (approx. 0.5 mm).

This effect was most evident in CC9F binary concretes (0.3 mm at 15% to 1.1 mm at 35%) but was less in CC2R (0.3 to 0.6 mm) and FBP (0.2 to 0.5 mm) binary concretes. A small increase in the rate of carbonation with calcined clay level in cement was also observed in the CC2R ternary concretes between 30% clay and 15% limestone (2.1 mm) and 40% clay and 10% limestone (2.6 mm).

The natural carbonation testing of the concretes will continue at the University of Dundee, taking measurements at 1 year and 2 years, the results of which will be presented in an update report in due course.

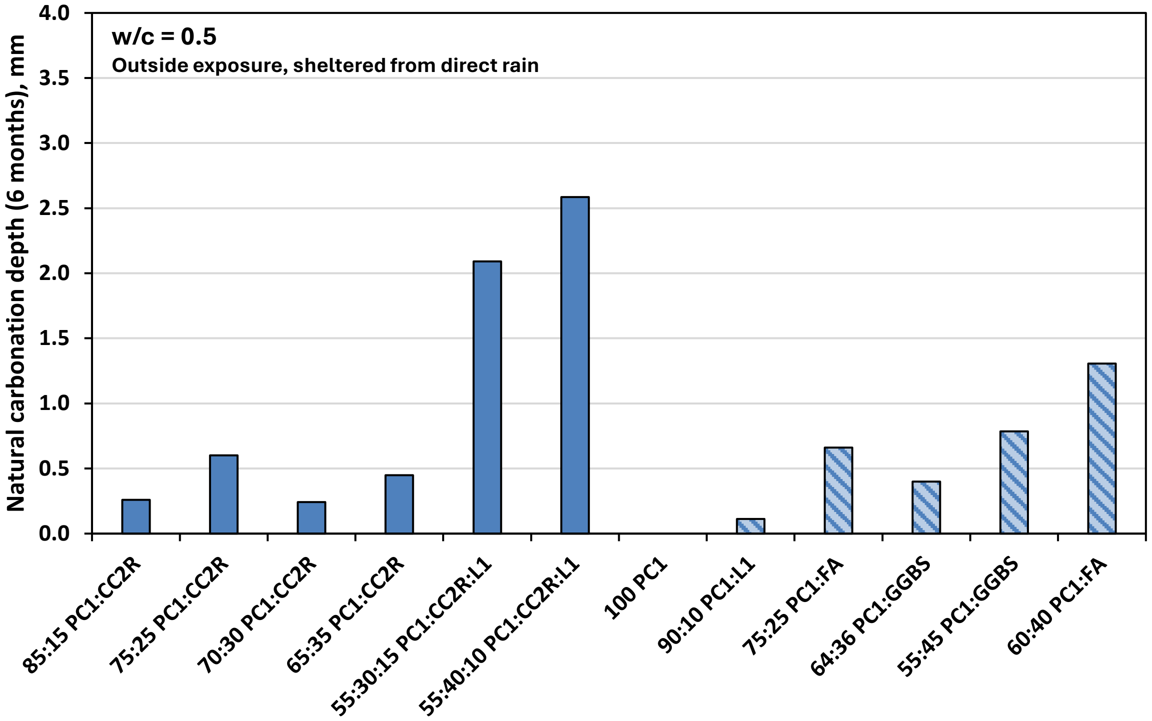

Figure 34 - Natural carbonation depths after 6 months exposure for CC2R binary and ternary concretes at w/c = 0.5

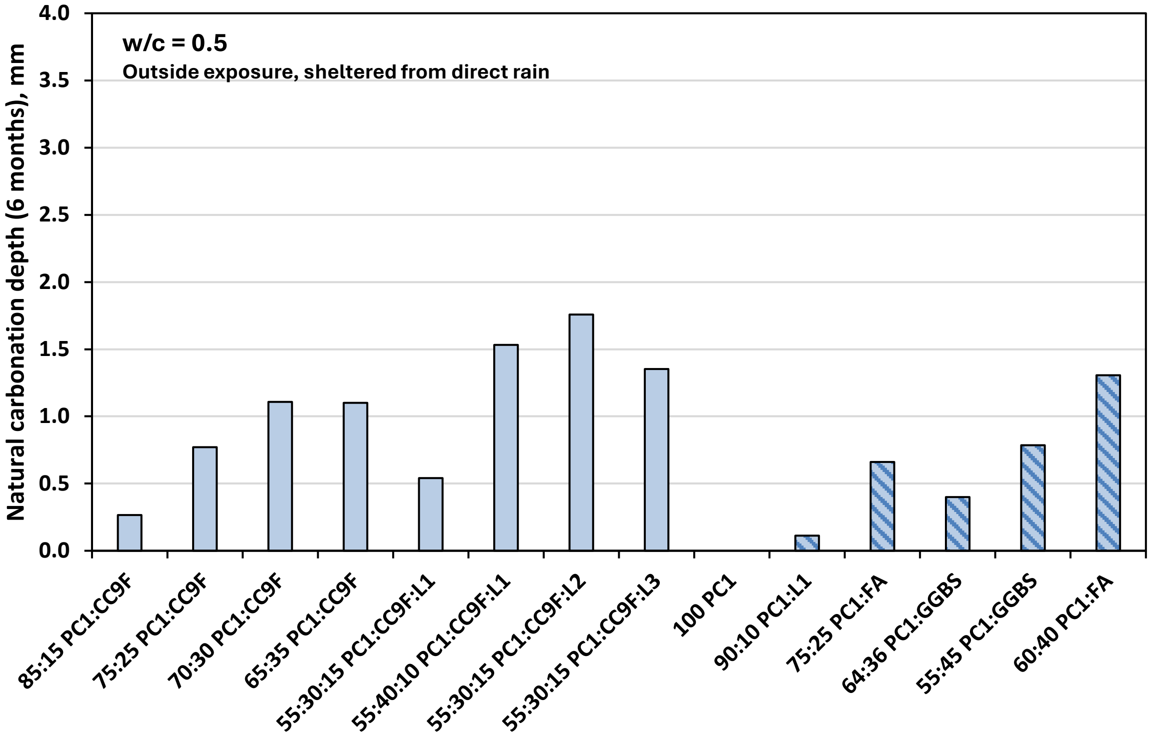

Figure 35 - Natural carbonation depths after 6 months exposure for CC9F binary and ternary concretes at w/c = 0.5

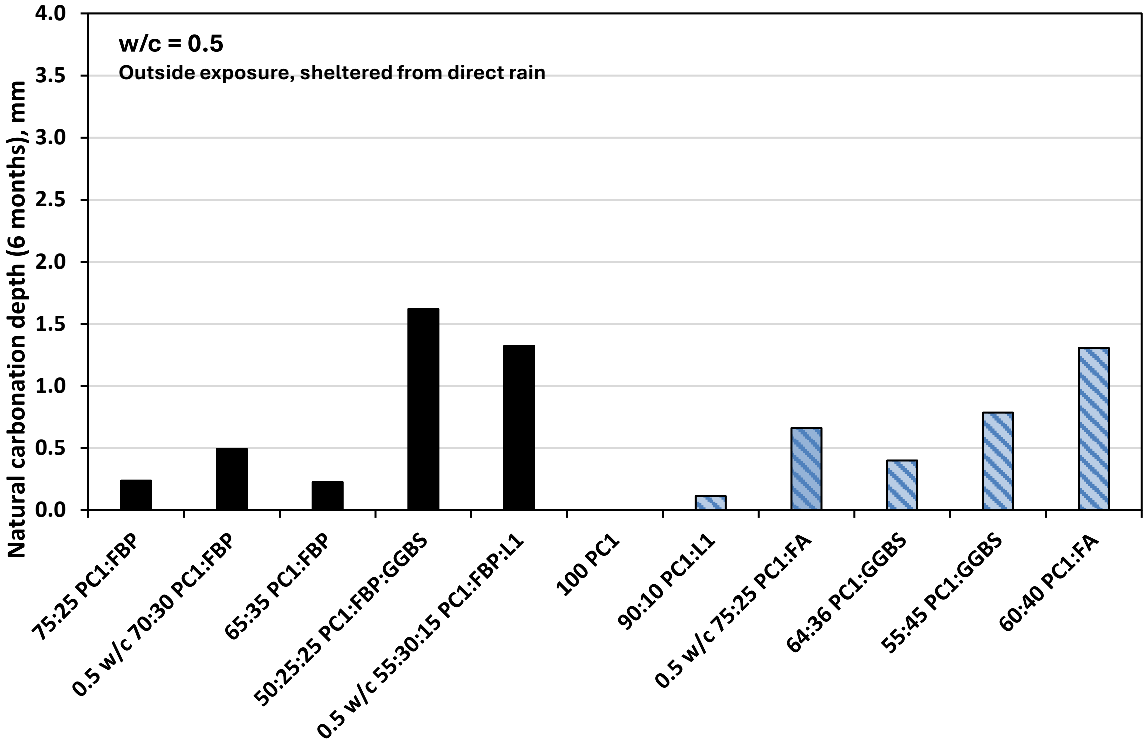

Figure 36 - Natural carbonation depths after 6 months exposure for FBP binary and ternary concretes at w/c = 0.5

The relationship between CaO content and 6 months natural carbonation depth for the calcined clay, FBP, and reference concretes is shown in Figure 37. The quantity of CaO was highly influential on the rate of carbonation in the concretes irrespective of the cementitious materials used. A relationship was identified for all of the concretes (w/c ratios, replacement levels, and materials) collectively, with a coefficient of determination (R^2) of 0.66. Considering the calcined clays alone gave a higher R^2 of 0.68, indicating a relationship between CaO content and carbonation depth.
Binary and ternary calcined clay concretes had higher carbonation depths than the reference concretes, which appears to reflect the reduced CaO content due to higher replacement levels. This agrees with the behaviour observed from the accelerated carbonation testing and should be considered when selecting high clinker replacement concretes for carbonation resistance.

Images of CC2R, CC9F, FBP, and reference concretes after 6 months natural carbonation testing outside, sheltered from direct rain, are available in the Appendix showing carbonation ingress depths.

The estimated 40 MPa equal strength carbonation depths and the corresponding w/c ratios for each concrete combination are given in Figure 38. These show that FBP binary concrete (1.4 mm) had a comparable estimated depth of carbonation ingress as that of 25% FA (1.4 mm). The remaining concretes had higher carbonation depths than the 25% FA, with the highest carbonation depth at 40 MPa equal strength estimated for CC2R binary and ternary at 2.2 mm. With the exception of CC2R binary, the ternary concretes with limestone had higher carbonation depths after 6 months exposure, suggesting that replacement of 15% clinker with limestone leads to increased carbonation.

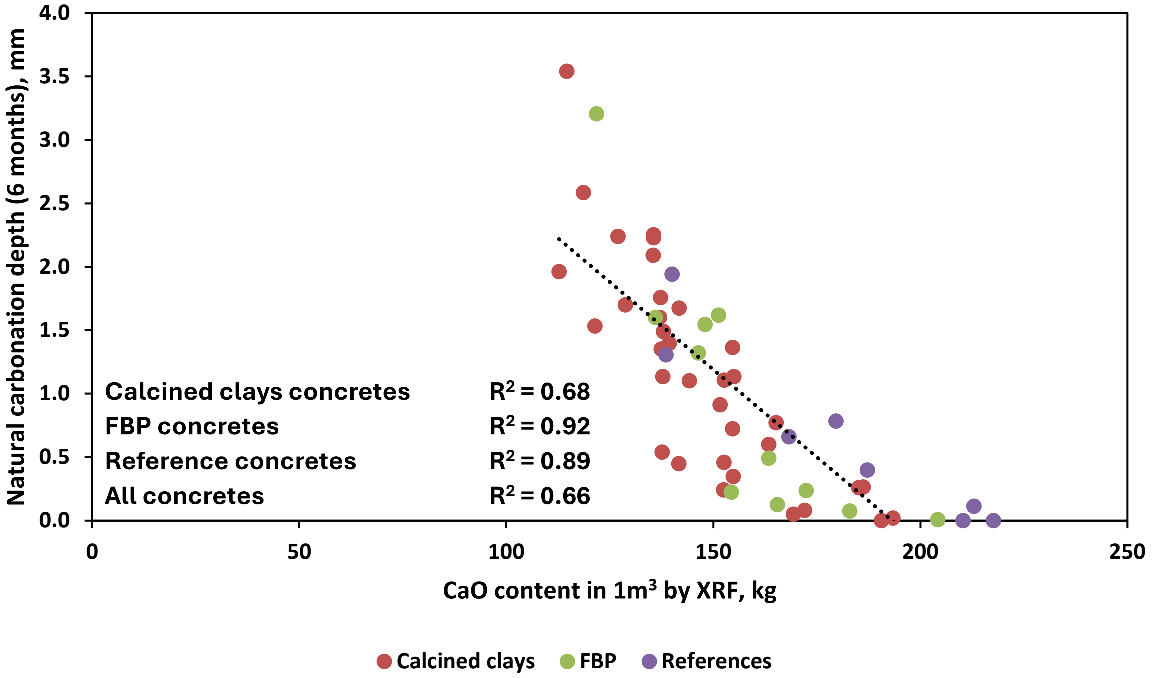

Figure 37 – Natural carbonation depth at 6 months of binary and ternary concrete at 40 MPa 28 days equal strength

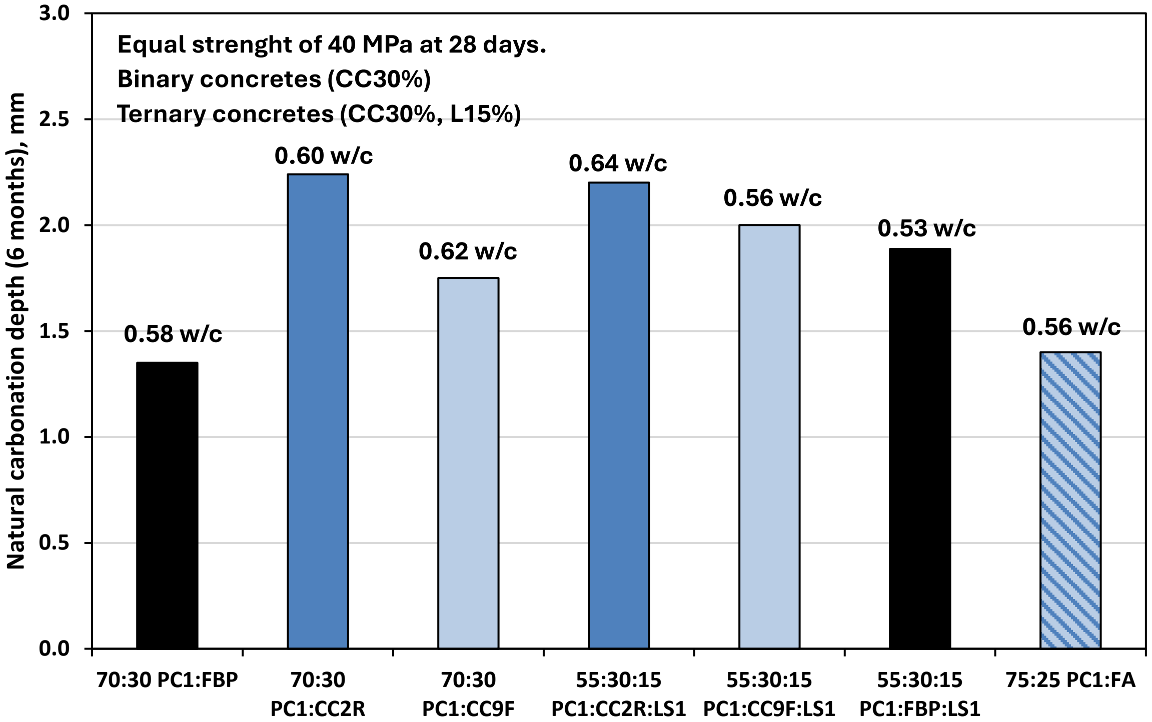

Figure 38 - Natural carbonation depth at 6 months of binary and ternary concrete at 40 MPa 28 days equal strength

4.3. Sulfate Resistance

The BR164 sulfate wear resistance test (BRE, 1992) is currently in progress, using $NaSO_4$ and $MgSO_4$ solutions at 20°C. This is a 1-year test with Figure 39 representing interim results taken at 6 months sulfate exposure of CC2R, CC9F, and FBP binary concretes at 30% replacement of cement and 0.5 w/c ratio, along with 0.5 w/c ratio CEM I, CEM II/B-V 25% FA, and CEM III/A 36% GGBS concretes for reference. The interim results for the ternary concretes of CC2R, CC9F, and FBP with 30% calcined clay and 15% limestone in cement at 0.5 w/c ratio are given in Figure 40 along with CEM II/A-L, CEM IV/B(V) 40% FA, and CEM III/A 45% GGBS concretes.

The most notable surface deterioration of the binary concretes occurred in CC9F in the $MgSO_4$ exposure solution, with minor deterioration observed in the CEM I concrete along the cube edges. Very little deterioration was also observed for CC2R or the FBP concretes in $MgSO_4$, with similar observations for the six concretes after 6 months exposure to the $NaSO_4$ solution.

Figure 39 - Binary calcined clay concretes and references at 0.5 w/c ratio after 6 months exposure (A = $MgSO_4$, B = $NaSO_4$)

The most notable surface deterioration of the ternary concretes occurred in CC9F in the $MgSO_4$ exposure solution, with deterioration also observed in the CEM III/A concrete. Very little deterioration was observed for CC2R or the FBP ternary concretes in $MgSO_4$, with similar observations for the six concretes after 6 months exposure to the $NaSO_4$ solution.

Additional images of CC2R, CC9F, and CEM II/B-V 25% FA concretes at 0.4 and 0.6 w/c ratios are given in the Appendix. These were in line with expectations, with 0.4 w/c ratio concretes showing little deterioration, whereas 0.6 w/c ratio concretes had greater visible deterioration.

Figure 40 – Ternary calcined clay concretes and references at 0.5 w/c ratio after 6 months exposure (A = MgSO4, B = NaSO4)

4.4. Freeze-Thaw Scaling

The PD CEN/TS12390-9 (BSI, 2016) freeze-thaw scaling performance of CC2R and CC9F calcined clay binary concretes at 25% replacement of cement and 0.55 w/c ratio, along with FA, GGBS and CEM I concretes are currently under evaluation. The end of this testing programme falls out of the time scope for this project and will be reported later.

Preparation for the freeze-thaw testing involved determining the AEA dose required to achieve a fresh air content of 4.5 % ± 0.5%. Mixing with the calcined clays was found to entrap air and to negate this a defoamer was used for all air-entrained concretes. With the inclusion of the defoamer, no issues were identified with the concretes and the target air content could be achieved satisfactorily.

4.5. Alkali-Silica Reactivity

The BS 812-123 alkali-silica reactivity concrete prism method (BSI, 1999) is currently in progress and will continue to run beyond the scope of this project and will evaluate CC2R and CC9F at 25% replacement of cement, a high-alkali CEM I and FA, and GGBS references. The results of this testing programme will be reported once complete.

5. Action K5 – Summary Conclusions and Observations

The main conclusions and observations from the concrete study in Work Package K are given below and are based on concretes with equal w/c ratio (and thus do not necessarily have equal standard 28 days strengths):

- The calcined clays generally have higher specific surface areas measured by B.E.T., from 5.28 m^2/g to 21.04 m^2/g than the fly ash, GGBS, and limestones. The calcined clays had higher particle densities, ranging from 2350 kg/m^3 to 2740 kg/m^3 than the fly ash but generally lower than those of the GGBS and limestones.
- This high specific surface area results in calcined clay concrete mixes having increased cohesion and hence water demand, requiring larger doses of admixture than the fly ash, GGBS, and CEM I reference concretes to achieve the target slump. The data indicate that the admixture can be further optimized for the particular clay characteristics.
- Calcined clay binary and ternary concretes were found to react (in terms of increasing compressive strength), from around 3 to 14 days, beyond which only small increases in strength occurred. In contrast, FBP was found to gain strength at a slower rate, but this continued up to 180 days.
- The use of calcined clay resulted in higher 28day concrete strengths compared to the CEM I, fly ash, and GGBS concretes.
- Calcined clays, in particular CC2R and CC3R, demonstrate equal or higher resistance to chloride migration, in both binary and ternary concrete mixes, compared to fly ash or GGBS reference concretes.
- The rates of accelerated carbonation for calcined clay concretes were higher than those of the reference fly ash and GGBS and were more pronounced for the ternary concretes.
- Although the period of exposure was limited, the rotary calcined clays generally had lower or comparable natural carbonation depths to the 25% fly ash in the binary concretes, while those with the flash calcined clays were higher. In the ternary concretes, higher depths of carbonation were observed in the rotary calcined clay concretes, compared to those with flash calcined clay. Both resulted in higher carbonation depths than the 40% fly ash reference.
- Only initial (6 month) data was obtained from tests for sulfate attack by the project completion and visually there was no significant deterioration for binary concretes in $MgSO_4$, or any concretes exposed to $NaSO_4$.
- At the time of project completion, the freeze-thaw scaling tests were still in progress and the test results will be reported at a later stage via professional journals. Similarly, long-term natural carbonation and ASR testing data will be reported as above.
- The results of Work Package K show that although the raw clay characteristics, pre and post-processing methodology and calcination method control reactivity and the behaviour of calcined clays in concrete, all clays tested were highly reactive.

6. References

BRE. (1992). *Sulphate resistance of buried concrete.* Watford: Building Research Establishment Press.

BSI. (1999). BS 812-123: Testing Aggregates - Method for determination of alkali-silica reactivity - concrete prism method. London: British Standards Institution.

BSI. (2013). *BS EN 12620 - Aggregates for concrete.* London: British Standards Institution.

BSI. (2015). BS EN 12390-11: Testing hardened concrete - Determination of the chloride resistance of concrete, unidirectional diffusion. London: British Standards Institution.

BSI. (2016). PD CEN/TS 12390-9: Testing hardened concrete - Freeze-thaw resistance with de-icing salts. Scaling. London: British Standards Institution.

BSI. (2018). BS EN 12390-10: Testing hardened concrete - Determination of the carbonation resistance of concrete at atmospheric levels of carbon dioxide. London: British Standards Institution.

BSI. (2020). BS EN 12390-12: Testing hardened concrete - Determination of the carbonation resistance of concrete. Accelerated carbonation method. London: British Standards Institution.

BSI. (2021). BS EN 12390-18: Testing hardened concrete - Determination of the chloride migration coefficient. London: British Standards Institution.

7. Appendix Images

7.1. Chloride Migration

FBP Binary

70:30 PC1:FBP 0.4 w/c ratio

70:30 PC1:FBP 0.5 w/c ratio

70:30 PC1:FBP 0.6 w/c ratio

CC2R Binary

70:30 PC1:CC2R 0.4 w/c ratio

70:30 PC1:CC2R 0.5 w/c ratio

70:30 PC1:CC2R 0.6 w/c ratio

CC9F Binary

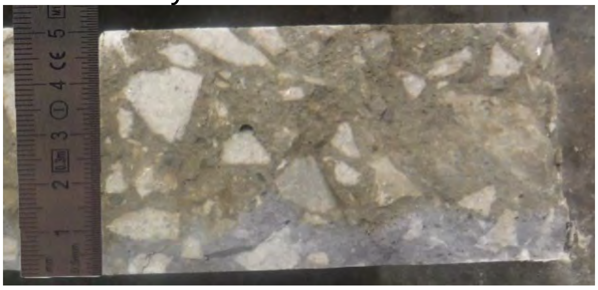

70:30 PC1:CC9F 0.4 w/c ratio

70:30 PC1:CC9F 0.5 w/c ratio

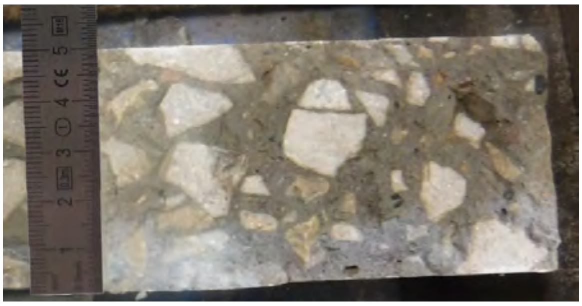

70:30 PC1:CC9F 0.6 w/c ratio

FBP Ternary

55:30:15 PC1:FBP:L1 0.4 w/c ratio

55:30:15 PC1:FBP:L1 0.5 w/c ratio

55:30:15 PC1:FBP:L1 0.6 w/c ratio

CC2R Ternary

55:30:15 PC1:CC2R:L1 0.4 w/c ratio

55:30:15 PC1:CC2R:L1 0.5 w/c ratio

55:30:15 PC1:CC2R:L1 0.6 w/c ratio

CC9F Ternary

55:30:15 PC1:CC9F:L1 0.4 w/c ratio

55:30:15 PC1:CC9F:L1 0.5 w/c ratio

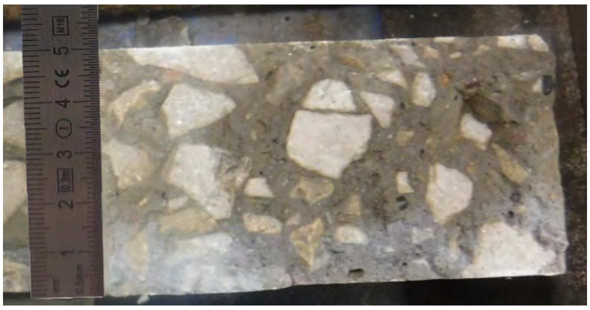

55:30:15 PC1:CC9F:L1 0.6 w/c ratio

Reference concretes

100 PC1 0.5 w/c ratio

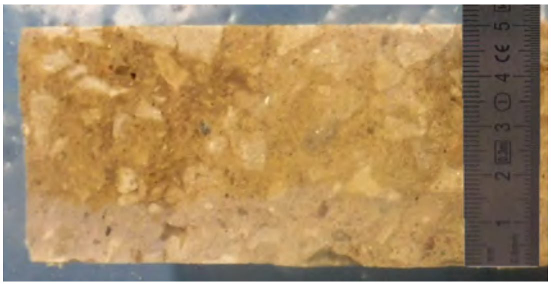

90:10 PC1:L1 0.5 w/c ratio

75:25 PC1:FA 0.4 w/c ratio

75:25 PC1:FA 0.5 w/c ratio

75:25 PC1:FA 0.6 w/c ratio

64:36 PC1:GGBS 0.5 w/c ratio

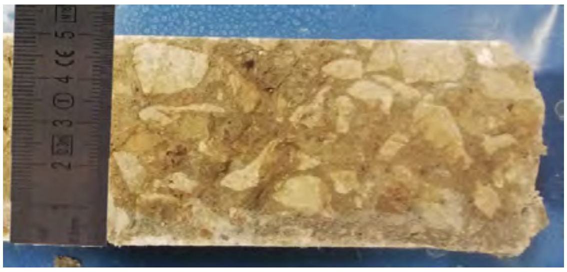

55:45 PC1:GGBS 0.5 w/c ratio

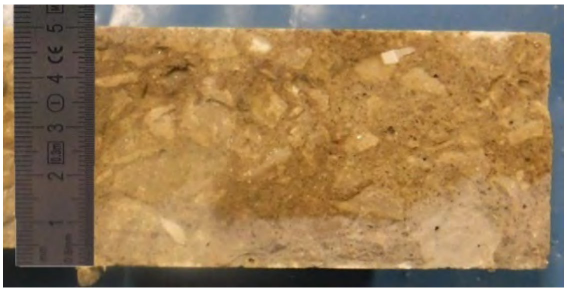

60:40 PC1:FA 0.5 w/c ratio

7.2. Accelerated Carbonation

FBP Binary

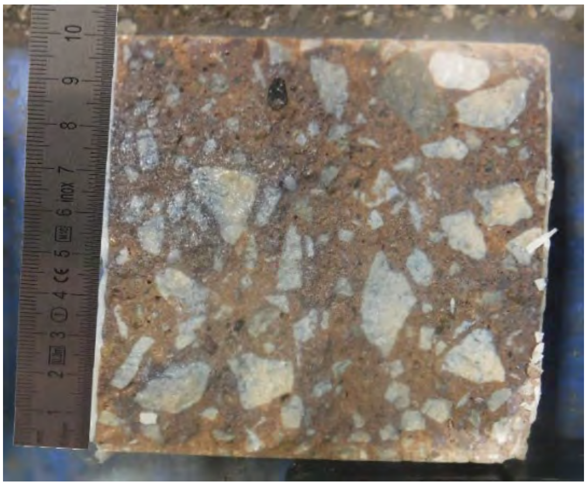

70:30 PC1:FBP 0.4 w/c ratio

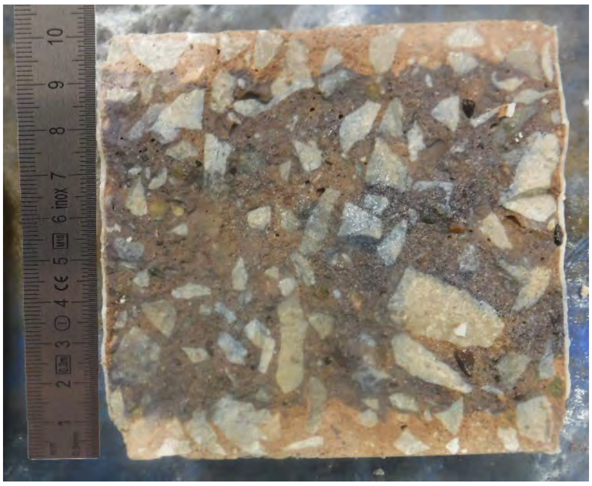

70:30 PC1:FBP 0.5 w/c ratio

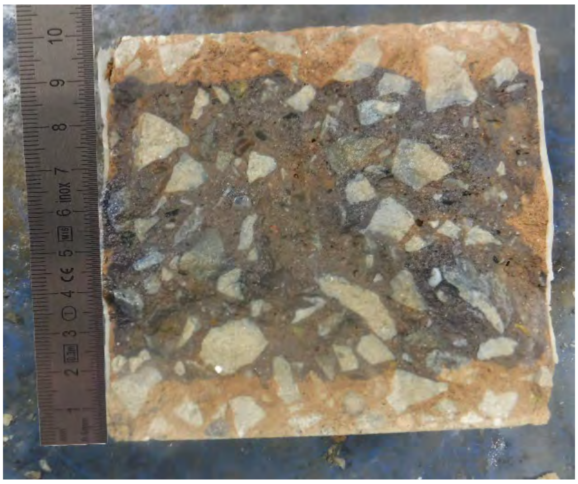

70:30 PC1:FBP 0.6 w/c ratio

CC2R Binary

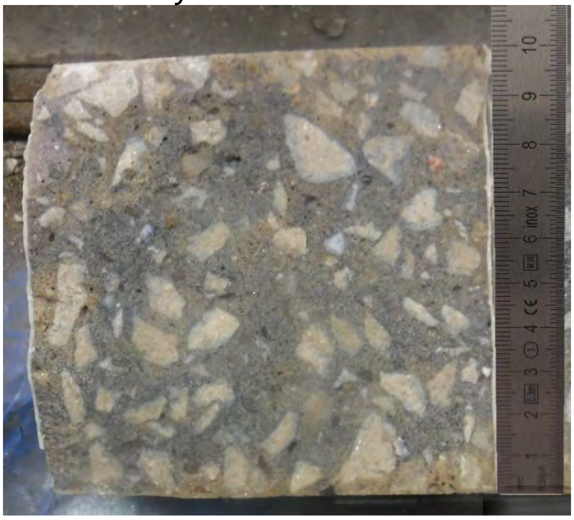

70:30 PC1:CC2R 0.4 w/c ratio

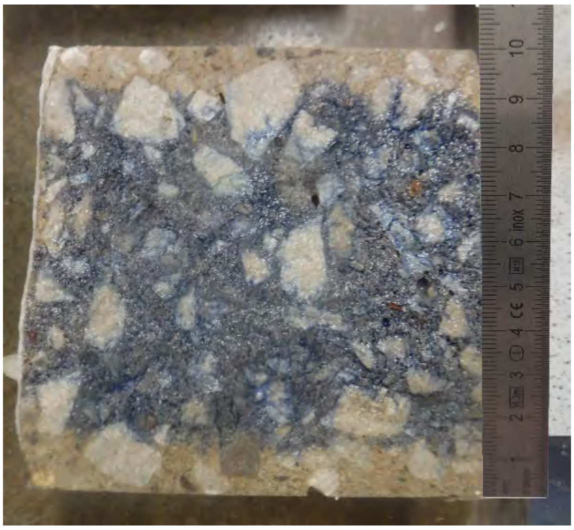

70:30 PC1:CC2R 0.5 w/c ratio

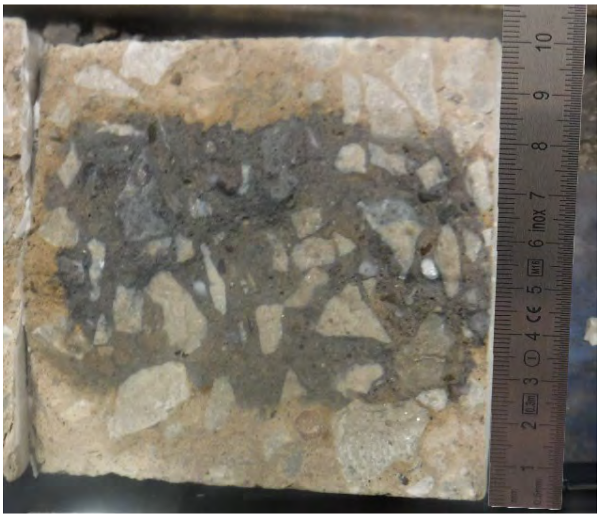

70:30 PC1:CC2R 0.6 w/c ratio

CC9F Binary

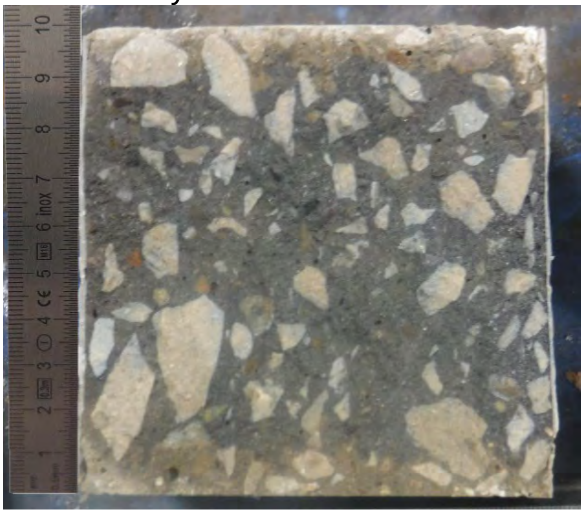

70:30 PC1:CC9F 0.4 w/c ratio

70:30 PC1:CC9F 0.5 w/c ratio

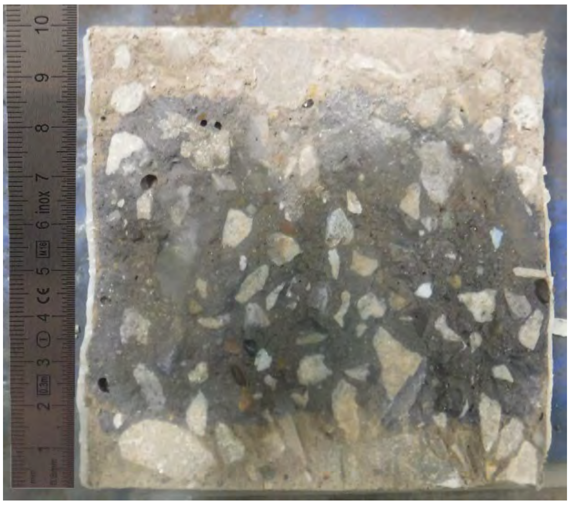

70:30 PC1:CC9F 0.6 w/c ratio

FBP Ternary

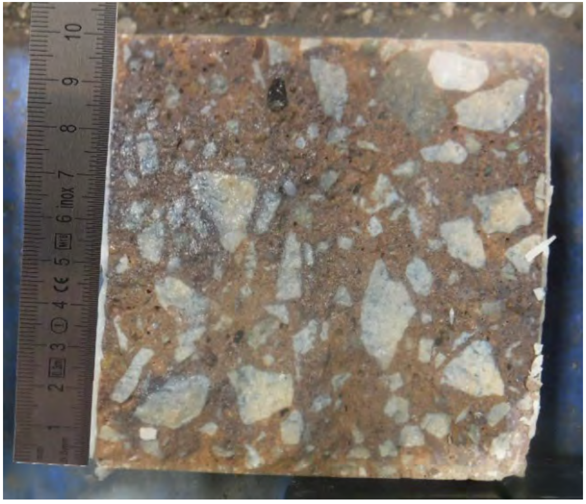

55:30:15 PC1:FBP:L1 0.4 w/c ratio

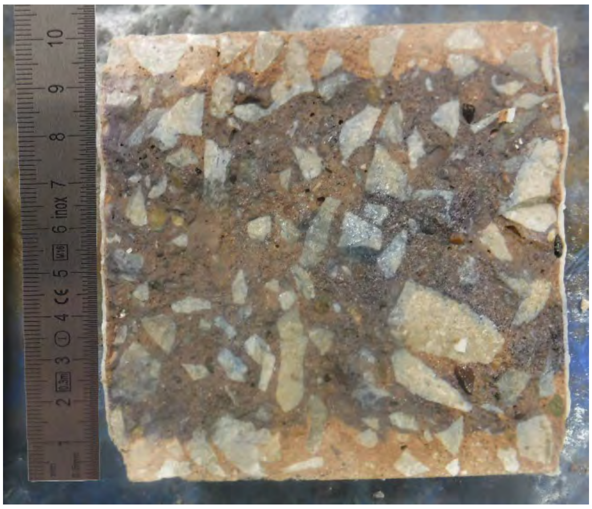

55:30:15 PC1:FBP:L1 0.5 w/c ratio

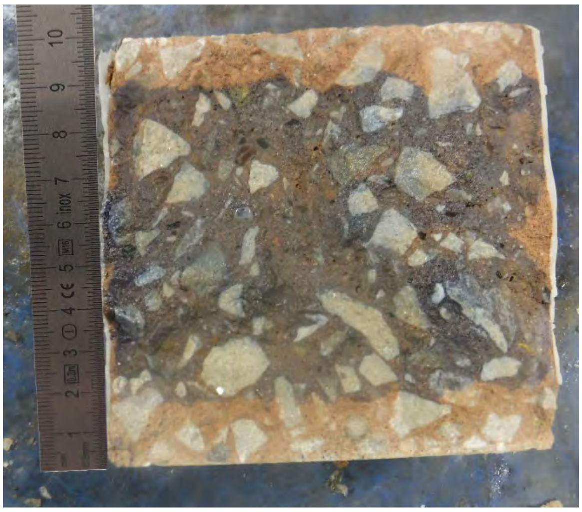

55:30:15 PC1:FBP:L1 0.6 w/c ratio

CC2R Ternary

55:30:15 PC1:CC2R:L1 0.4 w/c ratio

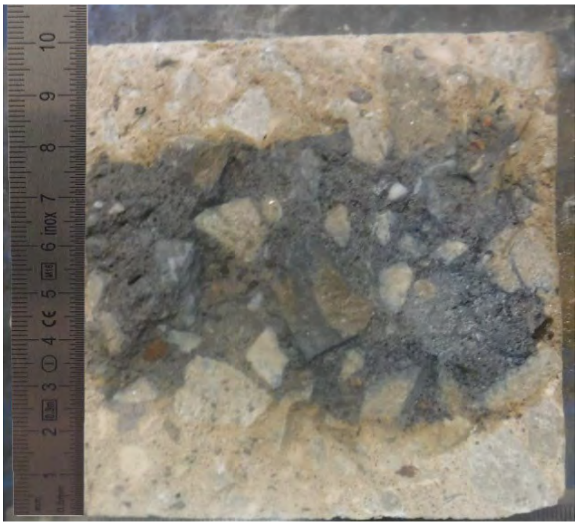

55:30:15 PC1:CC2R:L1 0.5 w/c ratio

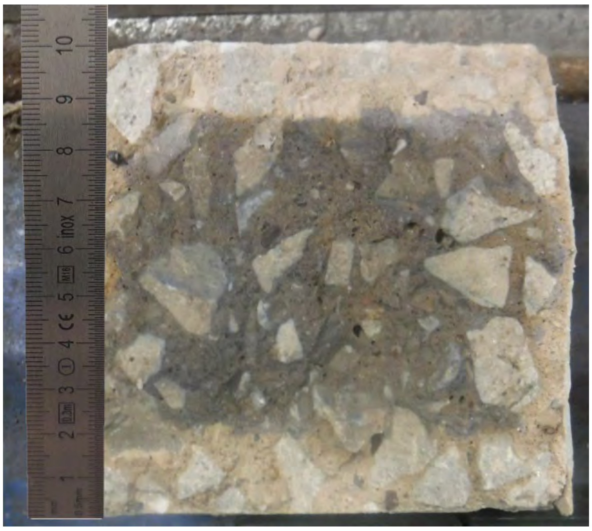

55:30:15 PC1:CC2R:L1 0.6 w/c ratio

CC9F Ternary

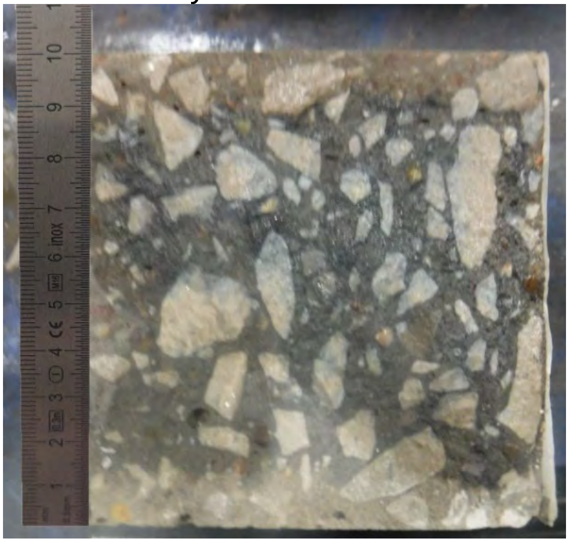

55:30:15 PC1:CC9F:L1 0.4 w/c ratio

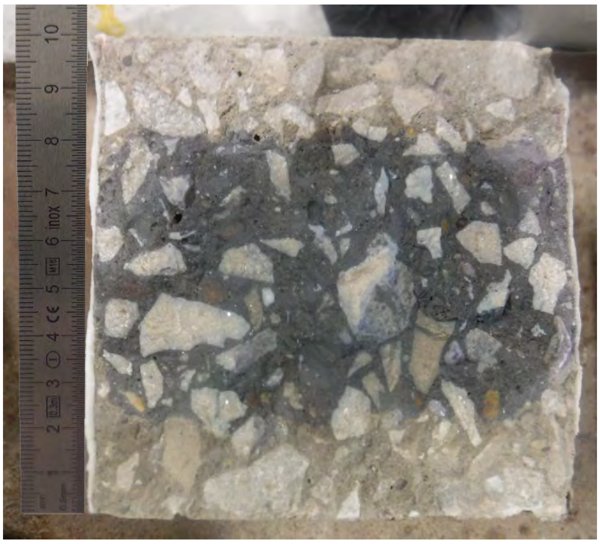

55:30:15 PC1:CC9F:L1 0.5 w/c ratio

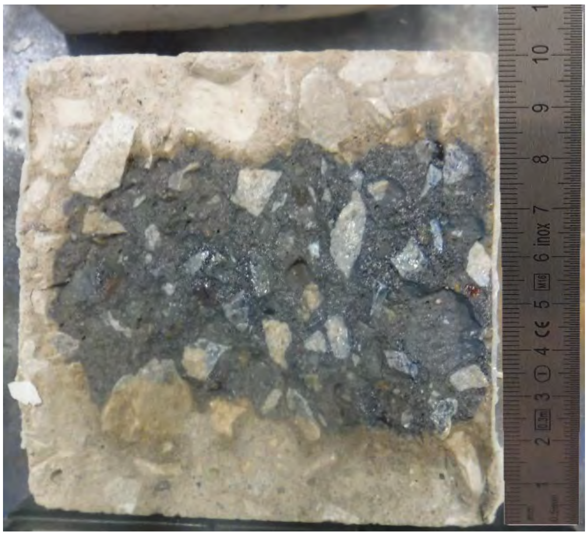

55:30:15 PC1:CC9F:L1 0.6 w/c ratio

Reference concretes

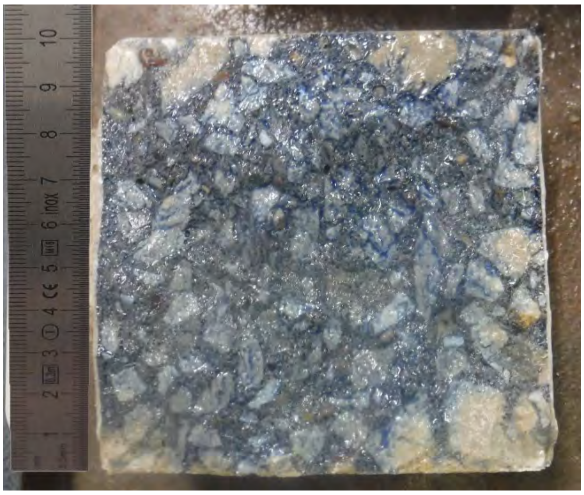

100 PC1 0.5 w/c ratio

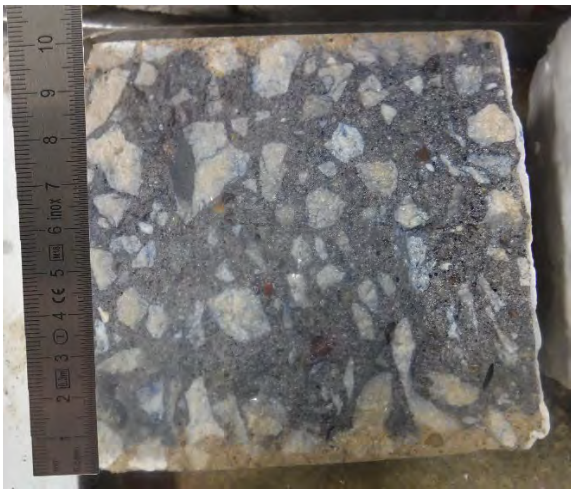

90:10 PC1:L1 0.5 w/c ratio

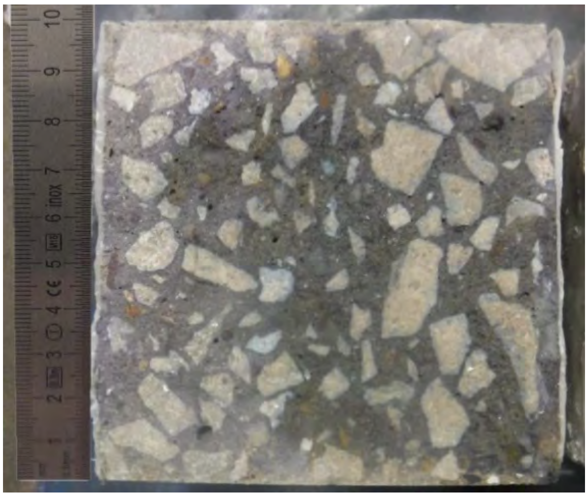

75:25 PC1:FA 0.4 w/c ratio

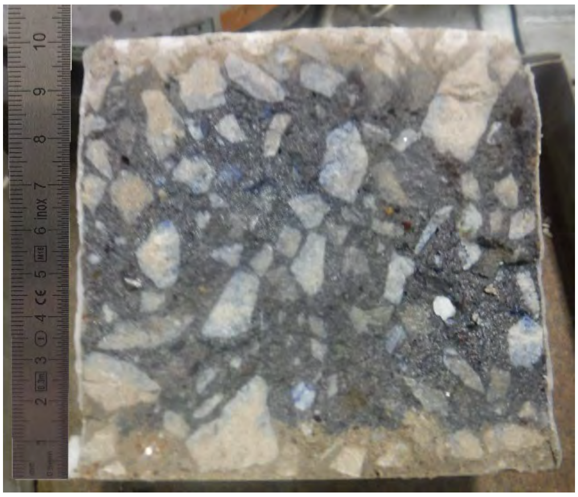

75:25 PC1:FA 0.5 w/c ratio

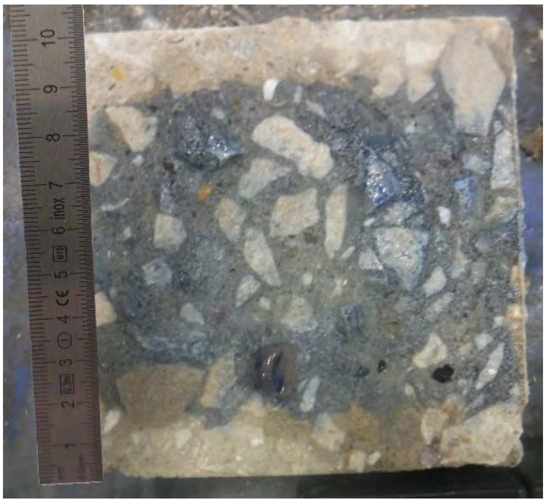

75:25 PC1:FA 0.6 w/c ratio

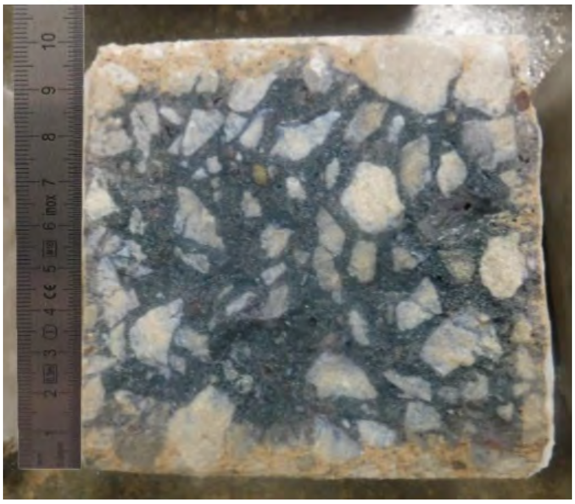

64:36 PC1:GGBS 0.5 w/c ratio

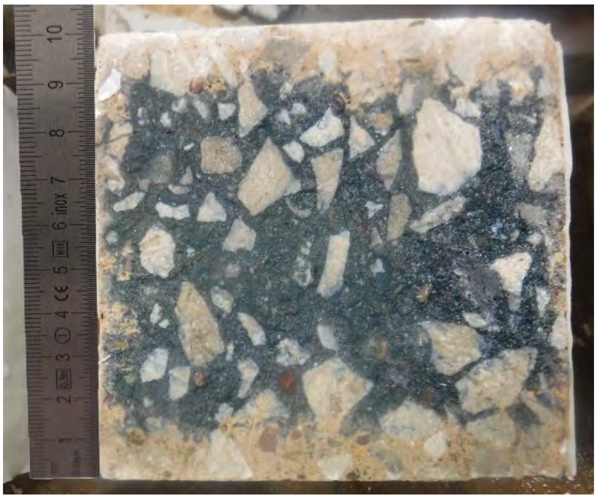

55:45 PC1:GGBS 0.5 w/c ratio

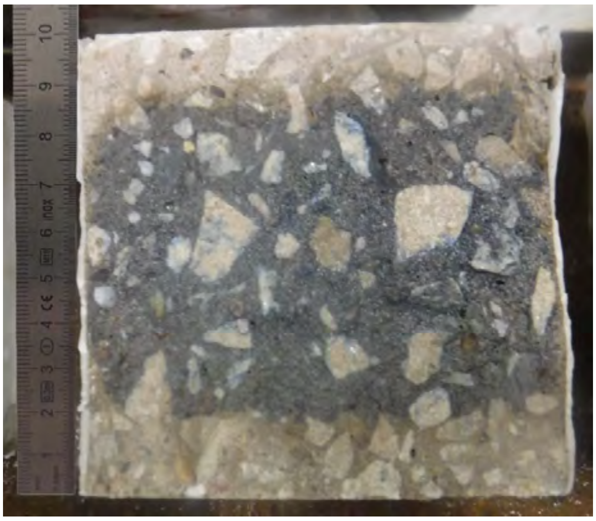

60:40 PC1:FA 0.5 w/c ratio

7.3. Natural Carbonation

FBP Binary

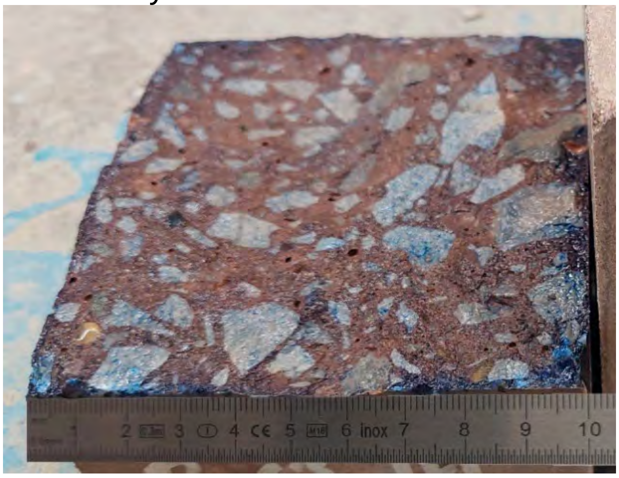

70:30 PC1:FBP 0.4 w/c ratio

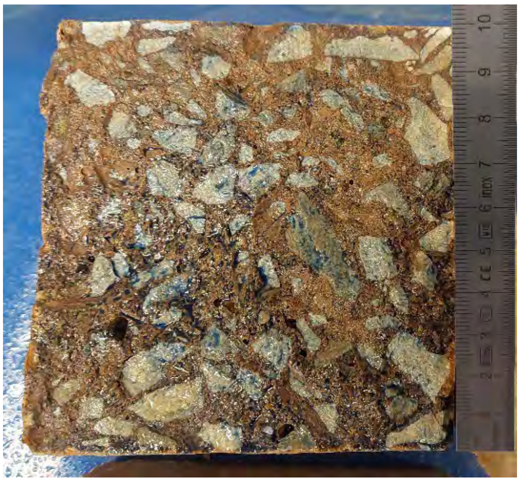

70:30 PC1:FBP 0.5 w/c ratio

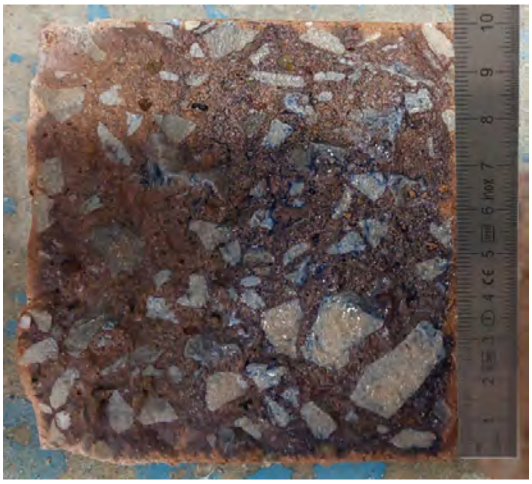

70:30 PC1:FBP 0.6 w/c ratio

CC2R Binary

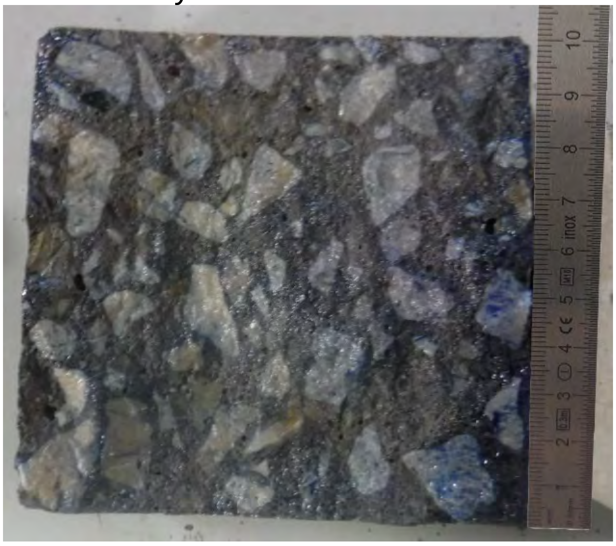

70:30 PC1:CC2R 0.4 w/c ratio

70:30 PC1:CC2R 0.5 w/c ratio

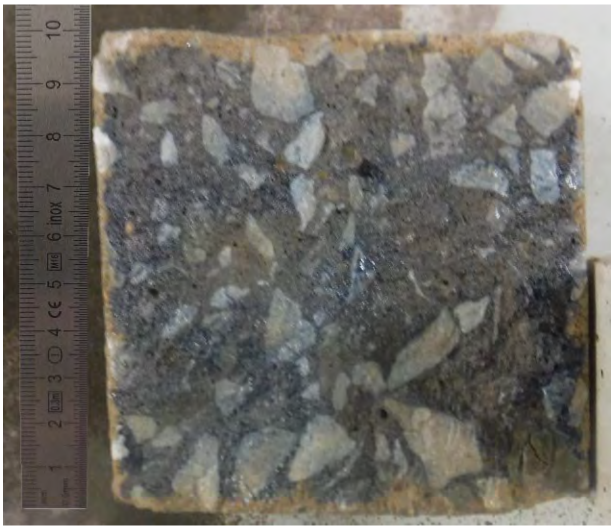

70:30 PC1:FBP 0.6 w/c ratio

CC9F Binary

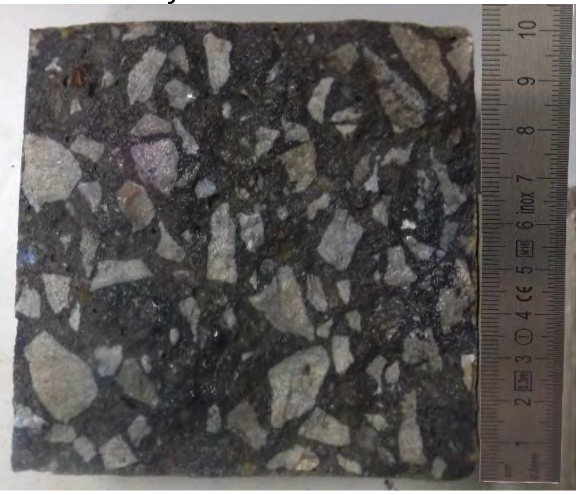

70:30 PC1:CC9F 0.4 w/c ratio

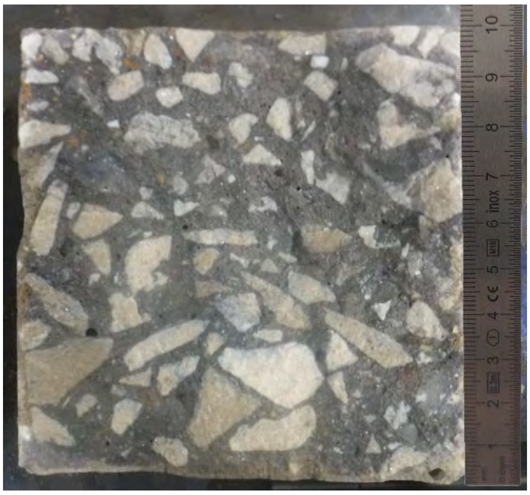

70:30 PC1:CC9F 0.5 w/c ratio

FBP Ternary

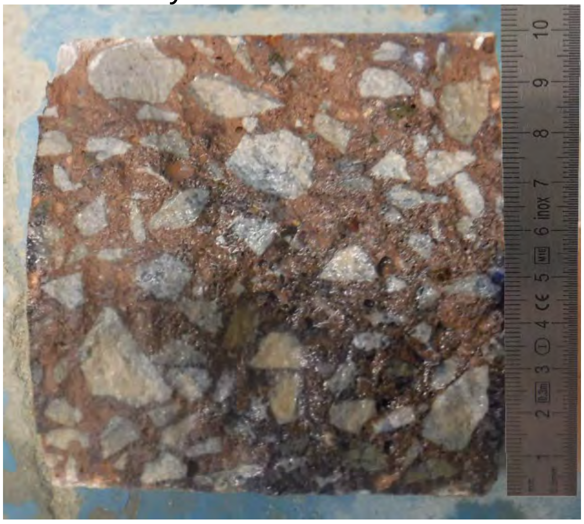

55:30:15 PC1:FBP:L1 0.4 w/c ratio

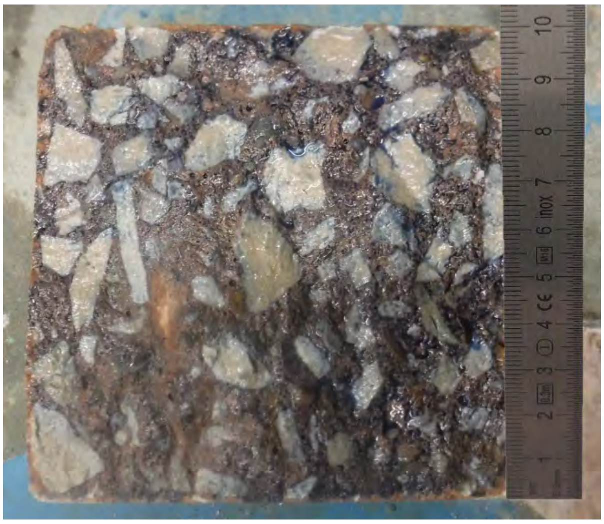

55:30:15 PC1:FBP:L1 0.5 w/c ratio

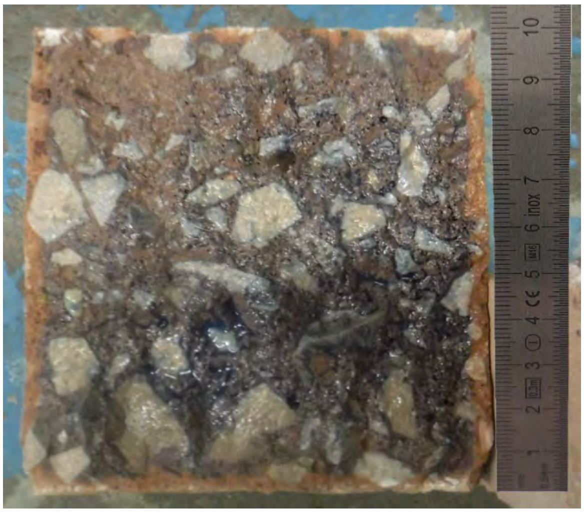

55:30:15 PC1:FBP:L1 0.6 w/c ratio

CC2R Ternary

55:30:15 PC1:CC2R:L1 0.4 w/c ratio

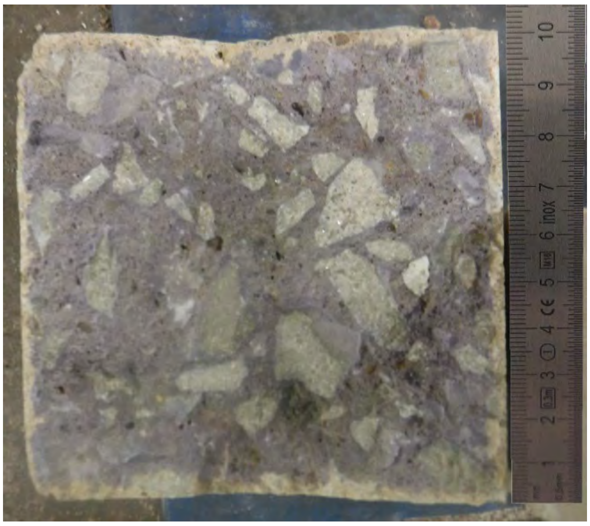

55:30:15 PC1:CC2R:L1 0.5 w/c ratio

55:30:15 PC1:CC2R:L1 0.6 w/c ratio

CC9F Ternary

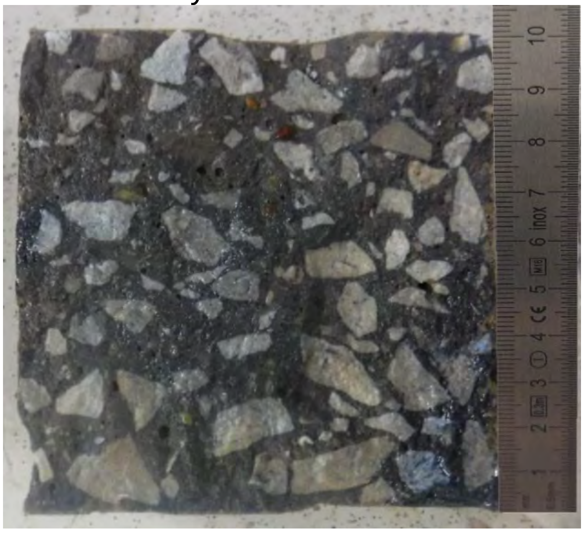

55:30:15 PC1:CC9F:L1 0.4 w/c ratio

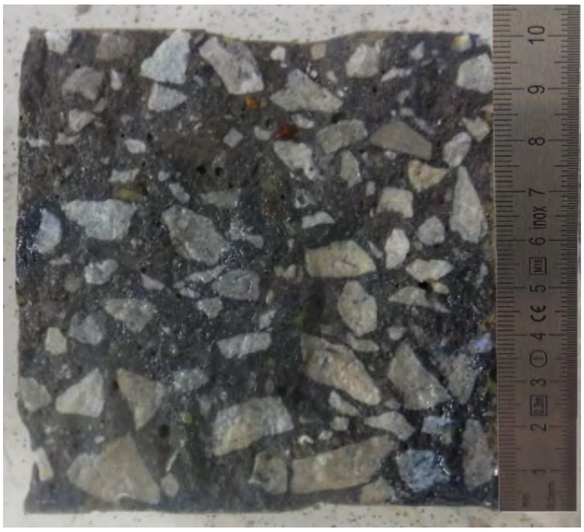

55:30:15 PC1:CC9F:L1 0.5 w/c ratio

55:30:15 PC1:CC9F:L1 0.6 w/c ratio

Reference concretes

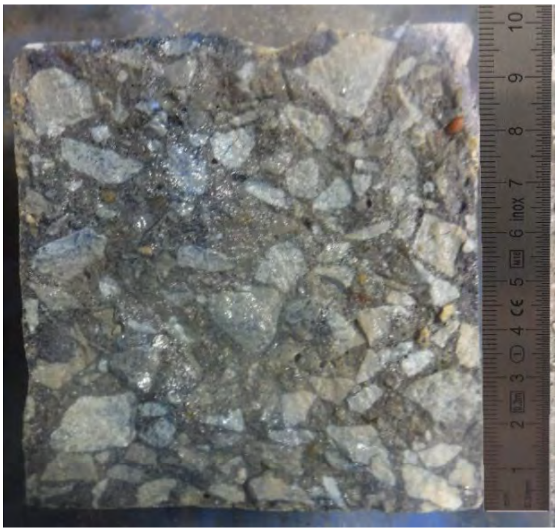

100 PC1 0.5 w/c ratio

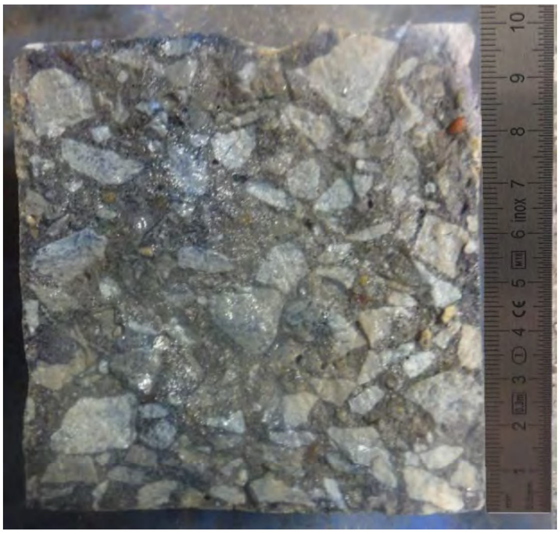

90:10 PC1:L1 0.5 w/c ratio

75:25 PC1:FA 0.4 w/c ratio

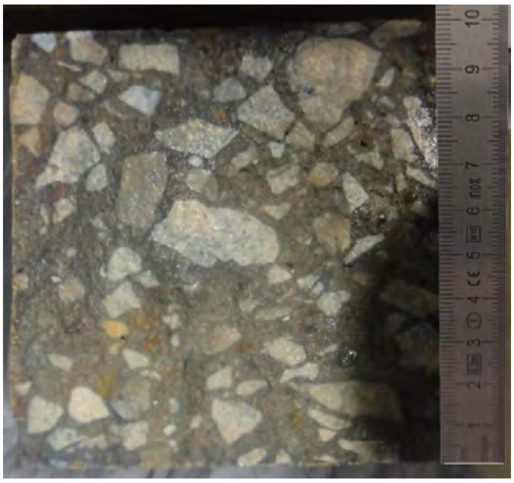

75:25 PC1:FA 0.5 w/c ratio

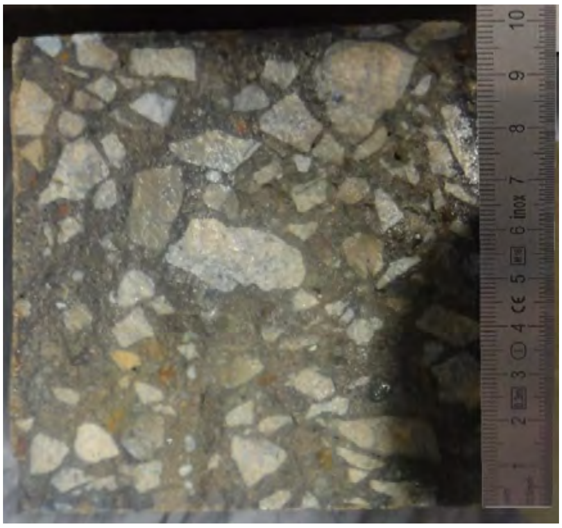

75:25 PC1:FA 0.6 w/c ratio

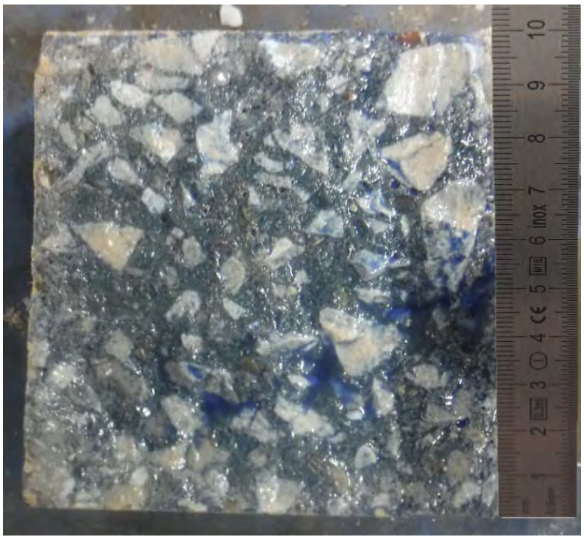

64:36 PC1:GGBS 0.5 w/c ratio

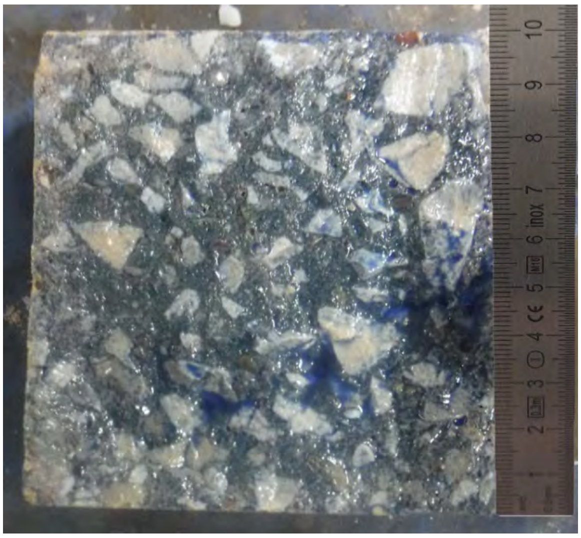

55:45 PC1:GGBS 0.5 w/c ratio

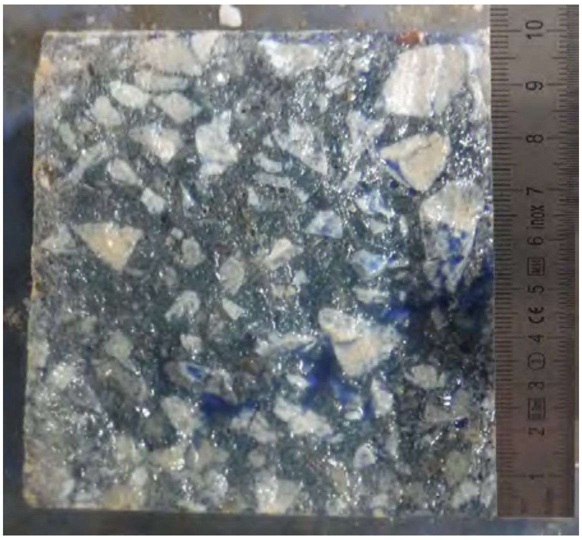

60:40 PC1:FA 0.5 w/c ratio

7.4. Sulfate

FBP Binary

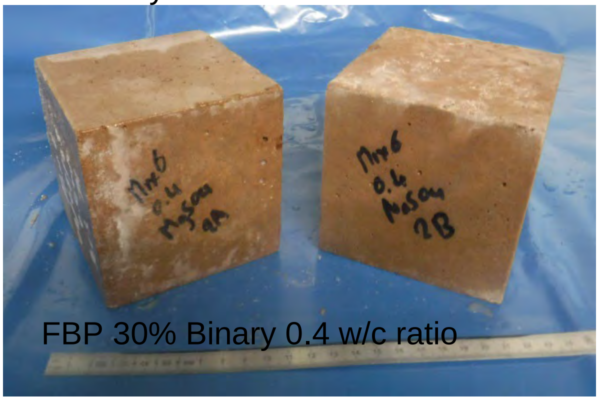

FBP 30% Binary 0.4 w/c ratio

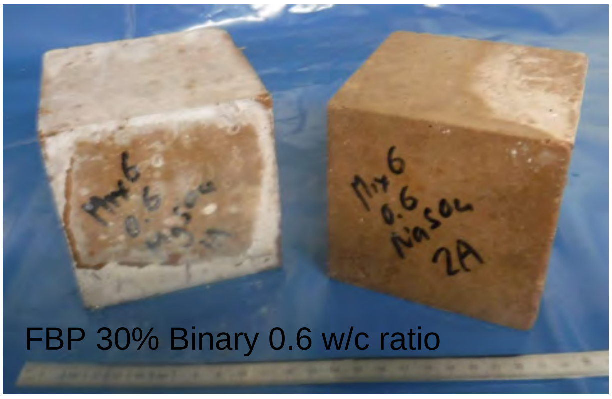

FBP 30% Binary 0.6 w/c ratio

CC2R Binary

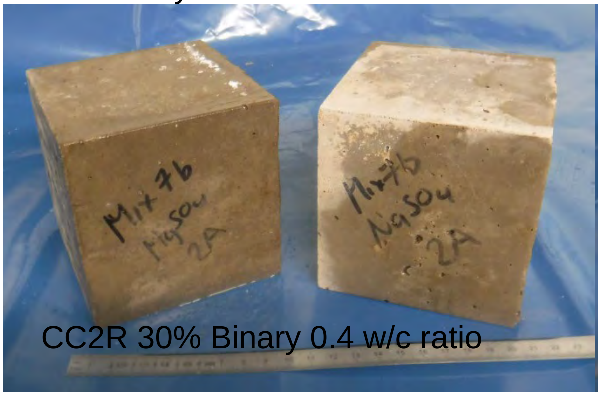

CC2R 30% Binary 0.4 w/c ratio

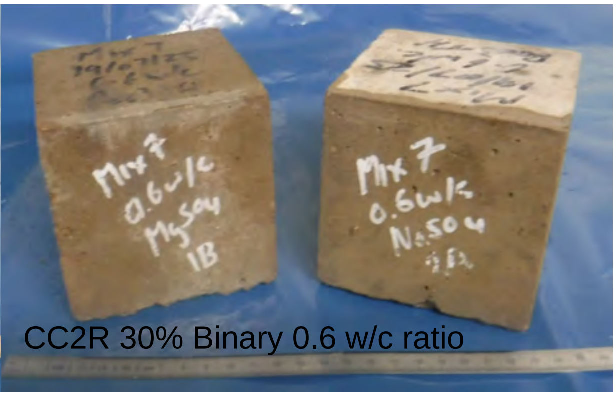

CC2R 30% Binary 0.6 w/c ratio

CC9F Binary

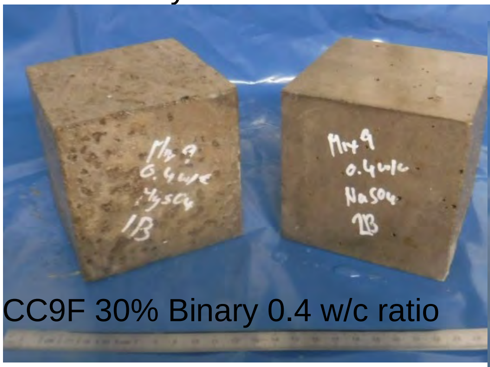

CC9F 30% Binary 0.4 w/c ratio

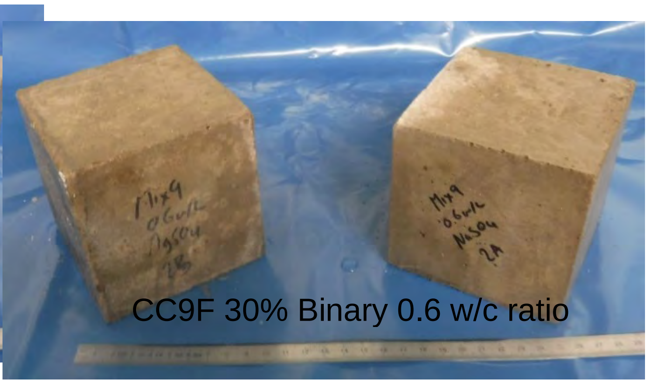

CC9F 30% Binary 0.6 w/c ratio

FBP Ternary

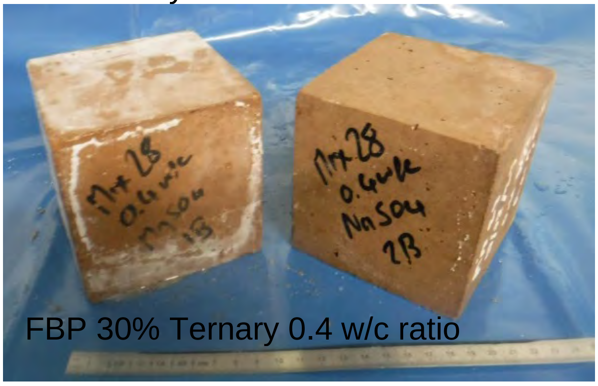

FBP 30% Ternary 0.4 w/c ratio

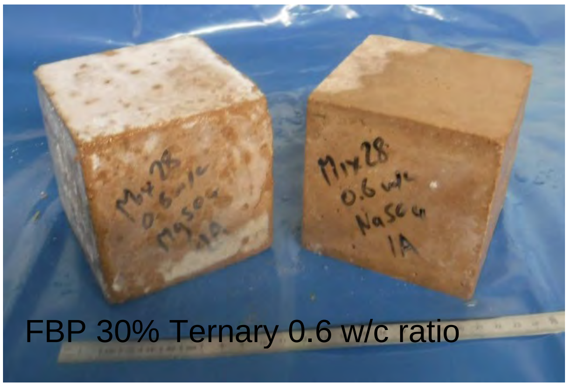

FBP 30% Ternary 0.6 w/c ratio

CC2R Ternary

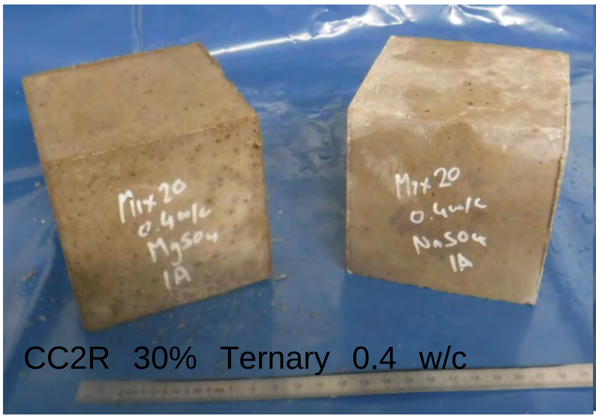

CC2R 30% Ternary 0.4 w/c

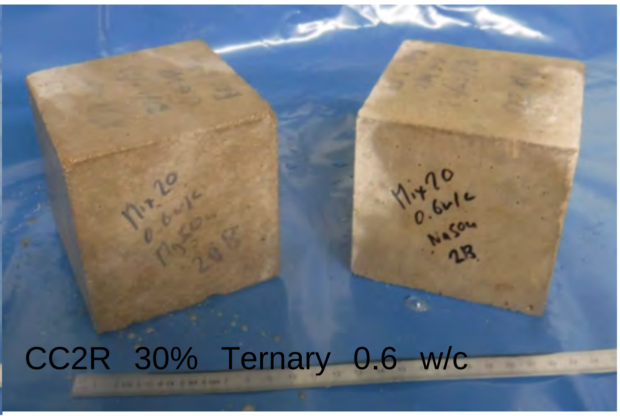

CC2R 30% Ternary 0.6 w/c

CC9F Ternary

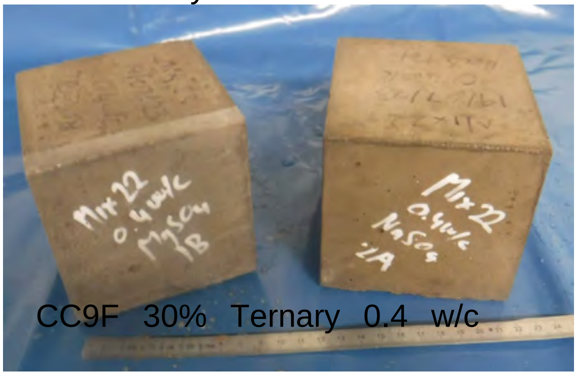

CC9F 30% Ternary 0.4 w/c

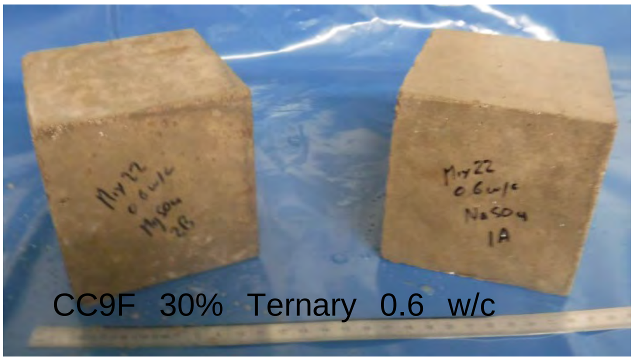

CC9F 30% Ternary 0.6 w/c

Fly Ash Binary

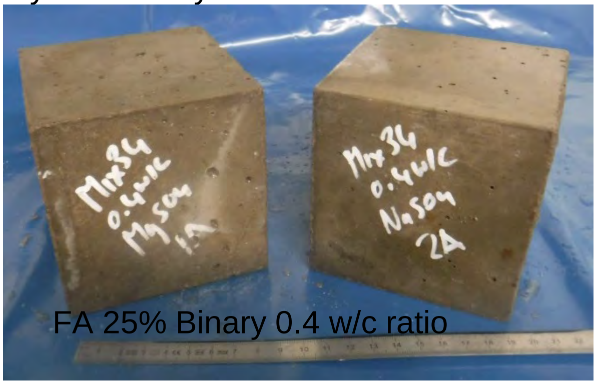

FA 25% Binary 0.4 w/c ratio

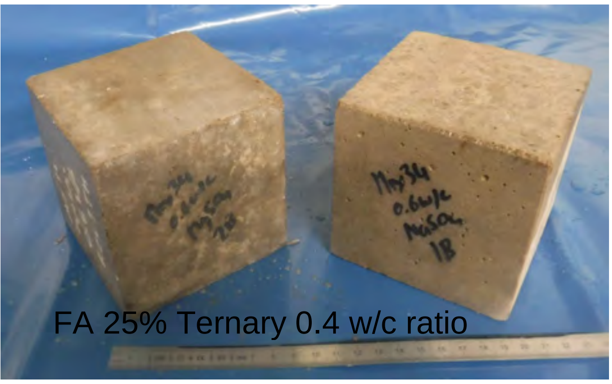

FA 25% Ternary 0.4 w/c ratio

FORTERRA

Re-C3: Reclaimed Calcined Clay Cements

Appendix 12 -
Demonstration project

Precast concrete demonstration of waste derived activated clay cements

Authors
Forterra:
Dr Andrew Smith
Lisa Wachter

1. Date: April 2024

Contents

1. Introduction

In the context of the ReC3 project - **Reclaimed calcined clays,** Forterra did an extended assessment on SCCs (self-compacting concretes). For a precast company, the requirements and focus points differ from the "standard" concrete which is primarily used in ready mix. As precast concrete is mainly about quick and easy pouring and fast turnaround, the principal requirement is a fast strength development/high early strength to strip the parts and free up moulds and space. Also essential, for the easy pouring, is the workability which can either be a very dry slump mix for extruded parts or a very fluid, self-compacting consistency which allows to pour fast. This kind of concrete doesn't require additional compaction energy to be applied.

Work package L focused on self-compacting concrete mixes, as drier mixes were covert in the concrete study (work package K) by University of Dundee.

The preparation work was done with the clay material Forterra contributed to the project, the brick powder. As a starting point some basic trials on cement performance (standard prism testing (BS EN 196-1: Methods of testing cement - Determination of strength., 2016)) were conducted. Followed by workability and compressive strength testing on a chosen production SCC concrete mix, where different cement replacement levels and a variation of admixtures were trialed. This was rounded up by setting trials in which the strength development from 13h to 24h was assessed. Finally, the reference mix design for the demonstration project was set up and workability and compressive strength testing with all the calcined clays from work package I (7 in total) were carried out. Different superplasticisers and their efficiency and performance were assessed.

After specifying mix designs and materials as well as admixture dosages, initial plant trials were performed to rule out any issues in the mixing and pouring process for the demonstration parts.

As a demonstration unit, a L-shaped, retaining wall element was chosen. For each clay, two retaining wall elements were casted in the Somercotes precast plant. The concrete was batched, transported and cast in the same way the usual self-compacting concrete is. Fresh and hardened concrete tests were conducted to confirm the results from the lab trials. The surface of the retaining wall element was examined. In addition, the temperature profile of the cast concrete as well as the ambient temperature profile were recorded and evaluated.

The data collected was compared and analysed, the results will be discussed in the following report.

All compressive strength data for concrete in the following report was sampled and tested on cubes with 100mm dimensions if not stated differently (BS EN 12390 Part 1-4: Testing of hardened concrete., 2009-2021).

2. Materials

An overview of all materials used within this workpackage can be found in table 1.

Table 1: materials overview

Group	Type	Description	Short Code
Cement	Portland cement	CEM I 52.5N	PC4
Secondary Cementitious Materials/Filler	Limestone Powder	Limestone powder	L1
	Calcined Clay	Flash calcined, Source 2, Imerys	CC2F
		Rotary calcined, Source 2, Imerys	CC2R
		Rotary calcined, Source 3, Imerys	CC3R
		Flash calcined, Source 7, Heidelberg Materials UK	CC7F
		Flash calcined, Source 9, Tarmac	CC9F
		Rotary calcined, Source 9, Tarmac	CC9R
	Brick Powder	Milled brick waste	BP1
Aggregates	Sand	0/4mm Quartz Sand	Sand
	Coarse Aggregates	4/10mm Limestone	4/10
Admixtures	Superplasticiser	Superplasticiser for high metakaolin contents	SP1
		Superplasticiser + Viscosity modifying admixture (VMA) Version 1	SP6
		Superplasticiser+ Viscosity modifying admixture (VMA) Version 2	SP7
		Precast Superplasticiser	SP8
		Superplasticiser for clay contaminated aggregates	SP9
		High retention RMC superplasticiser	SP10
		Ready-mix Superplasticiser	SP11
		Superplasticiser Version 3 (no Viscosity modifying admixture (VMA))	SP12
	Accelerator	Set accelerating admixture	AC1
		Hardening accelerating admixture	AC2

3. Brick Powder preparation work

To estimate the performance of the calcined clay in binary C II/B-Q and ternary C II/C-M (Q-L) cements (BS EN 197-1: Cement. Composition, specifications and conformity criteria for common cements, 2011), a prism (160mm*40mm*40mm) study was performed to assess strength development and impact on workability. The standard composition and procedure of (BS EN 196-1: Methods of testing cement - Determination of strength., 2016) was used with the only deviation being the sand used. The w/b ratio was fixed at 0.5, no additional admixture was used in this series.

The reference specimens were made with 100% Portland cement (PC4), further mixes contained 19% limestone (L1) as the production mix is using, as well as 25, 30 and 35% brick powder (BP1). One ternary cement was tested with 43% cement replacement in total, consisting of 30% brick powder and 13% limestone.
Figure 1 shows the compressive strength results as an average of 2 results. Figure 2 shows the flexural strength of the prisms. For each set of specimens 2, 7 and 28 day results were tested.

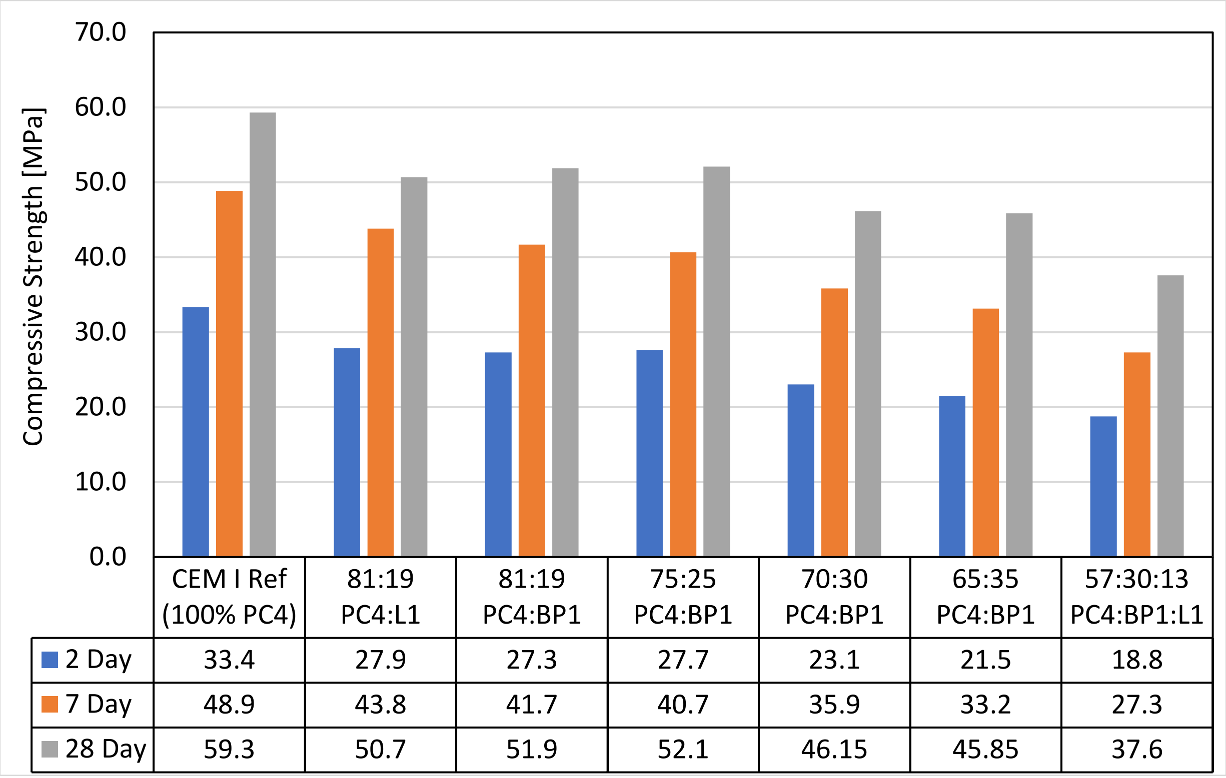

	CEM I Ref (100% PC4)	81:19 PC4:L1	81:19 PC4:BP1	75:25 PC4:BP1	70:30 PC4:BP1	65:35 PC4:BP1	57:30:13 PC4:BP1:L1
■ 2 Day	33.4	27.9	27.3	27.7	23.1	21.5	18.8
■ 7 Day	48.9	43.8	41.7	40.7	35.9	33.2	27.3
■ 28 Day	59.3	50.7	51.9	52.1	46.15	45.85	37.6

Figure 1: Mortar Compressive Strength (BS EN 196-1)

As expected, the compressive strength of the Portland Cement is the highest and it’s developing early strength faster than combinations. The 19% and 25% replacement with brick powder mixes are exceeding the factory reference powder combination in final strength whilst they seem to develop strength slightly slower. Especially early strength is dropping the higher the replacement levels are. All binary cements would be classified in strength class 42.5, as the 2d strength is exceeding 20MPa they would be in the strength class 42.5R (rapid) (BS EN 197-1: Cement. Composition, specifications and conformity criteria for common cements, 2011).

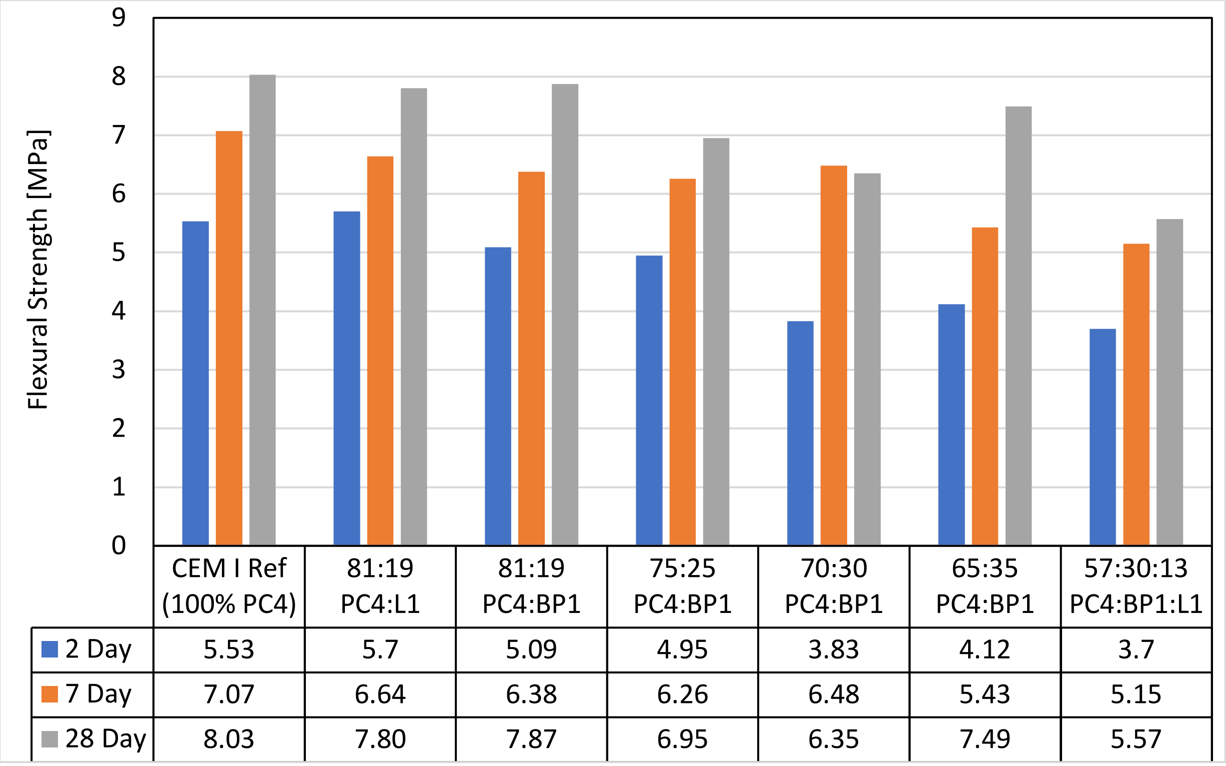

	CEM I Ref (100% PC4)	81:19 PC4:L1	81:19 PC4:BP1	75:25 PC4:BP1	70:30 PC4:BP1	65:35 PC4:BP1	57:30:13 PC4:BP1:L1
■ 2 Day	5.53	5.7	5.09	4.95	3.83	4.12	3.7
■ 7 Day	7.07	6.64	6.38	6.26	6.48	5.43	5.15
■ 28 Day	8.03	7.80	7.87	6.95	6.35	7.49	5.57

Figure 2: Mortar Flexural Strength (BS EN 196-1)

The flexural strength is not completely reflecting the results for compressive strength. Whilst the 28d strength for the first mixes seem to follow a pattern and is going down very slowly as the replacement level increases, it jumps up again for the 35% replacement mix. An explanation for this could be, that only one prism per test age was tested and the flexural strength is impacted by the needling effect of the sand. Thus, this might not fully reflect the actual values.

Workability was tested with the mini flow table (BS EN 1015-3: Methods of test for mortar for masonry. Determination of consistence of fresh mortar (by flow table), 1999). For all mortar mixes the w/b-ratio was kept at 0.5. The results were as expected, the higher the content of brick powder, the stiffer and less flowable are the mortars. Whilst the brick powder is reducing the flow, the limestone addition helps to increase the flow and get a better workability.

4. Self-Compacting-Concrete Development

An extended study was carried out to optimise and assess the performance of the clays in self-compacting concrete. As a base a frequently used production SCC mix from Forterra's bespoke precast plant was chosen. This SCC mix consists of a total of 465kg/m3 CII/A-LL (81% PC4, 19% L1), the grading is composed of 0/4mm Quartz sand and 4/10mm limestone in a ratio of 51/49%. For workability reasons additional limestone powder is added as filler. The performance characteristics of this reference mix were assessed in the R&D lab with the most current materials. The details and test results can be found in Table 2.

Table 2: Characteristic values reference SCC (81% PC4, 19% L1)

	Stripping strength (16h)	28d characteristic strength	Slump class	Cement content	Aggregate size	w/b-ratio
Requirement	15MPa	C50/60	SF3 (760-850 mm)	Min. 380kg	Max. 10mm	Max. 0.45
Actual value	22MPa	64.1MPa	740mm	465kg	10mm	0.41

Taking this mix as a reference and base, different cement replacement levels for the CII/B-Qs were defined as followed: 19% (1/1 replacement of the limestone in the cementitious material of the reference mix), 25%, 30%. All initial work was done with the brick powder (BP1) for availability reasons.

In addition, a ternary cement CII/C-M (Q-L) with the following replacement levels was set up and tested: 55% Portland Cement (PC4), 30% Clay, 15% Limestone (L1).

Table 3: Overview brick powder SCC compositions

Concrete name	% CEM I (PC4)	% Clay (BP1)	% Limestone (L1)	% Fly Ash (FA)	Admixture
CEM II/A-LL (19% L1, SP8)	81		19		SP8
CEM II/A-V (19% FA, SP8)	81			19	SP8
PC4:BP1 81:19 (SP8)	81	19			SP8
PC4:BP1 75:25 (SP8)	75	25			SP8
PC4:BP1 70:30 (SP8)	70	30			SP8
PC4:BP1 81:19 (SP6)	81	19			SP6
PC4:BP1 75:25 (SP6)	75	25			SP6
PC4:BP1 70:30 (SP6)	70	30			SP6
PC4:BP1 81:19 (SP7)	81	19			SP7
PC4:BP1 75:25 (SP7)	75	25			SP7
PC4:BP1 70:30 (SP7)	70	30			SP7
PC4:BP1 81:19 (SP9)	81	19			SP9
PC4:BP1 75:25 (SP9)	75	25			SP9
PC4:BP1 70:30 (SP9)	70	30			SP9
PC4:BP1 81:19 (SP10)	81	19			SP10
PC4:BP1 75:25 (SP10)	75	25			SP10

The focus of the assessment was on workability, where the slump-flow test was conducted (BS EN 12350-8: Testing fresh concrete - Self-compacting concrete. Slump-flow test, 2019), the retention over 30 minutes was measured and a visual inspection conducted to get additional information about tendency of segregation. For precast concretes the focus is more on initial flow and cohesion, but the retention behavior is meaningful as well and can in addition give an indication on early age strength development. The different calcined clays and brick powder were expected to make the concrete “drier” and more sticky, due to the fineness and water absorption. It is well known that aggregates containing clay or clay adhesions are causing problems in the workability performance and control of concrete. Many admixtures were developed in the past to address these issues.

To assess the workability performance different superplasticisers (see table 1) were tested. Each of the superplasticisers is optimised for a slightly different application. From previous trials and the discussions with the admixture supplier, the base characteristics of the used superplasticisers are the following:

- SP6: water reducer for ready mix concrete with a viscosity modifier to improve the rheology.
- SP7: based on the same substance than SP6 with a higher water reduction.

- SP8: high range water reducer for precast, which is optimising high short- and long-term compressive strength.
- SP9: high-range water reducer focused on clay contaminated aggregates.
- SP10: high performance superplasticiser for ready mix concrete for extended slump retention.
-

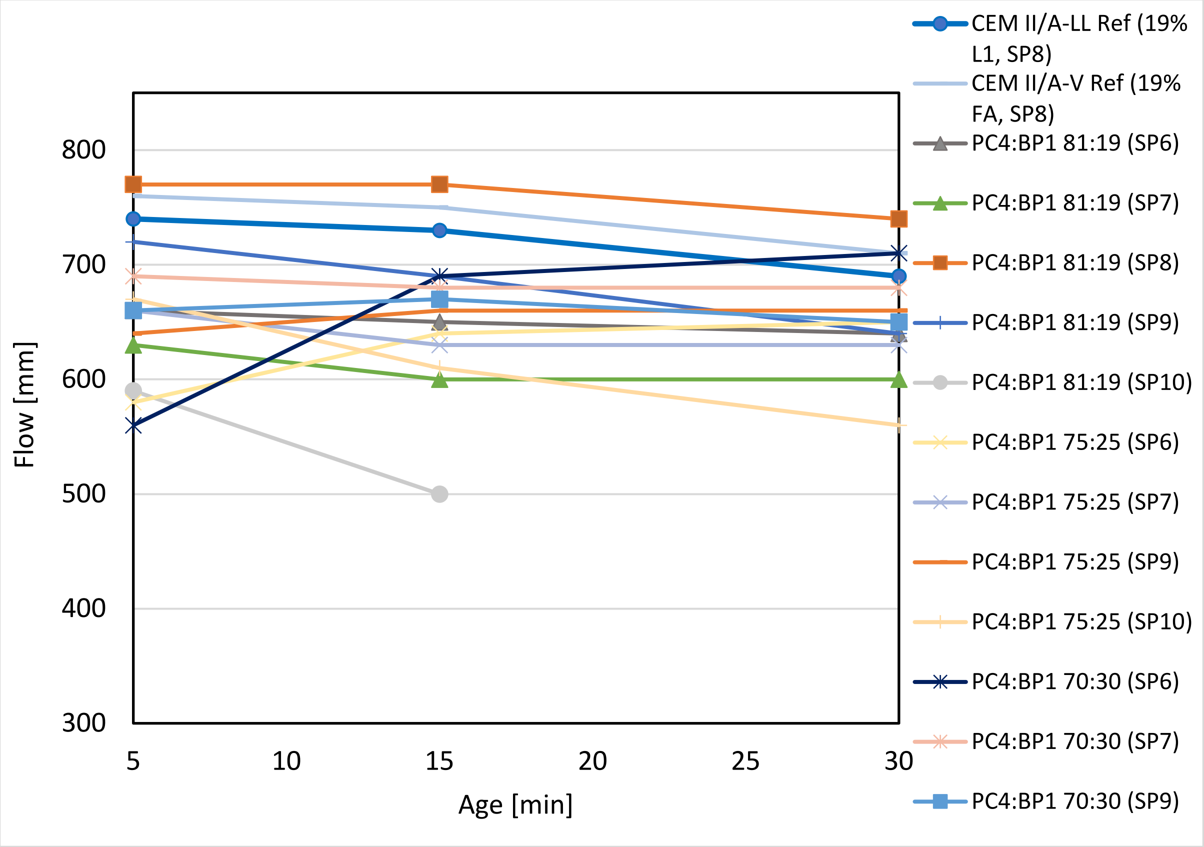

Figure 3: Workability results brick powder SCCs

SP8 is the reference admixture from production. The retention curve of the mix with the 19% cement replacement with brick dust is almost parallel to the reference mix. This means the exchange has nearly no influence on workability performance. As expected, the ready-mix admixture SP6 with the higher retention is changing the behavior of the mix significantly, the flow even increases for the higher replacement levels after 15min. This leads to the conclusion, that the early age strength might be negatively impacted. This is a well-known issue with high dosages of certain admixtures and will show in the next Figure. The adjusted SP7 is giving an almost straight line as a retention curve. The concrete is not losing any flow in the first 30 minutes after mixing. The mixes containing SP9 are behaving similar to the SP6 mixes, the flow is increasing slightly after 15 minutes and stays like this. Unexpected is the behavior with SP10, which is losing flow rapidly despite being developed to extend slump.

The initial flows were the highest with the SP8, which is the precast admixture and a high range water reducer. Thus, some of the other admixtures showed a very good rheology and no segregation appeared despite the high dosages. Aiming for a flow of more than 650mm, the SP6 doesn't seem to be an option. Nevertheless, this wasn't meant to be used for self-compacting concrete and has therefore made a very flowable concrete. Summarising, all tested admixtures were effective with the brick powder. As expected, their efficiency varies, as it would be with concrete with other replacements as well. Some of the admixtures needed a very high dosage to make a flowable concrete, as anticipated when choosing admixtures for a different target concrete.

In addition to workability trials, compressive strength of all the different mixes was tested. For this a total of 6 cubes with the dimensions of 100mm*100mm*100mm were cast and stored in water tanks after demolding until testing after 1d, 7d and 28d (BS EN 12390 Part 1-4: Testing of hardened concrete., 2009-2021).

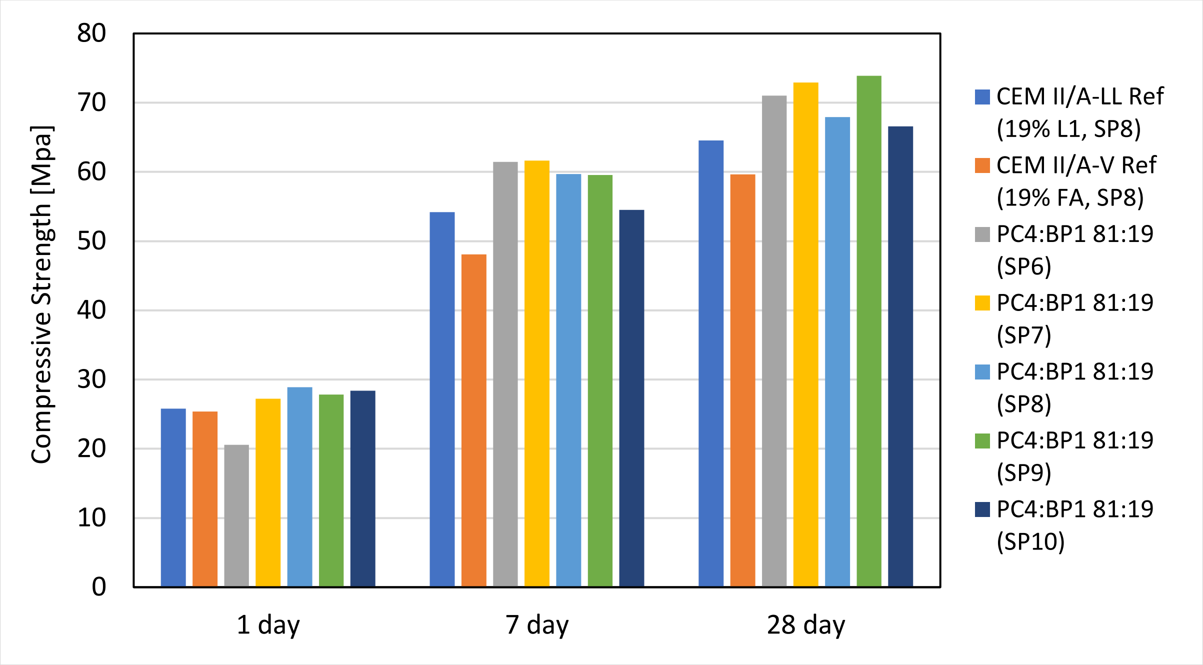

Figure 4: Compressive strength 19% replacement brick powder SCCs

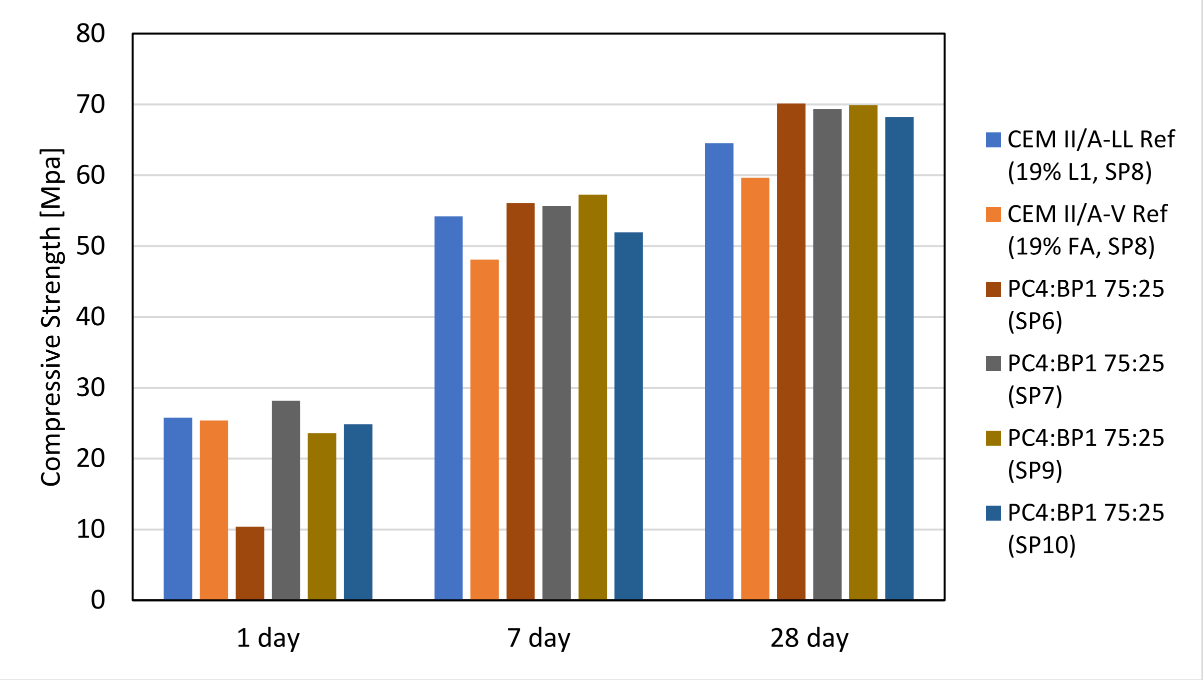

Figure 5: Compressive strength 25% replacement brick powder SCCs

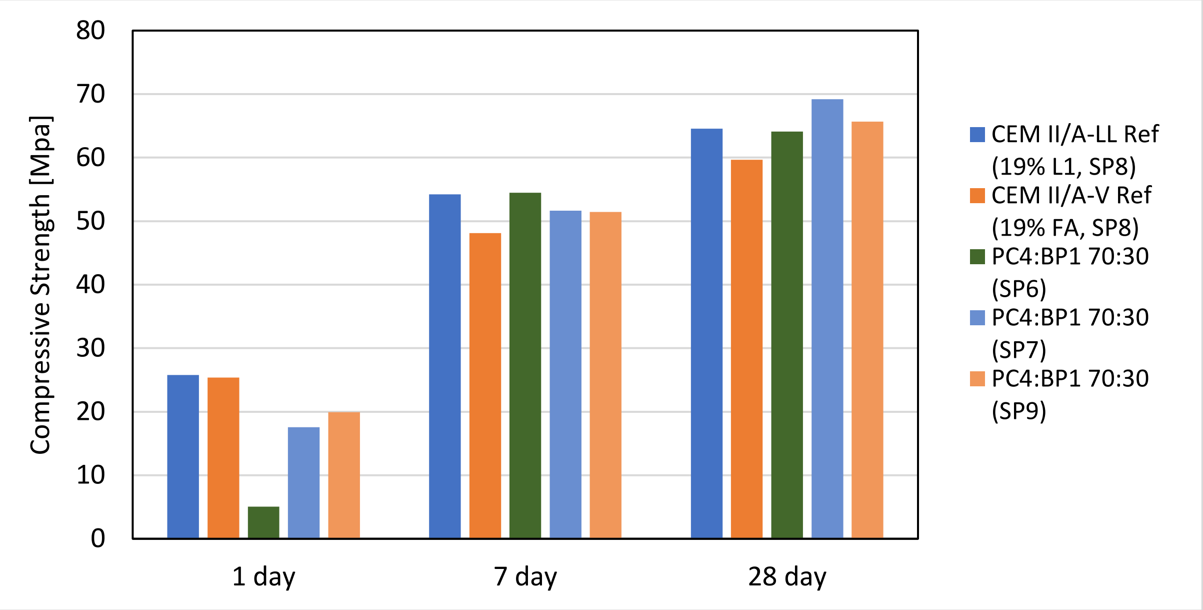

Figure 6: Compressive strength 30% replacement brick powder SCCs

The three Figures above compare the compressive strength data of mixes with the same cementitious replacement levels (Figure 4: 19%, Figure 5: 25%, Figure 6:30%) with different superplasticisers. All Figures have in addition the strength data of the referent cements (CEM II/A-LL with 19% limestone and CEM II/A-V with 19% fly ash) plotted against the brick powder cements. In Figure 4, only the SP6 1 day result is weaker than the reference mixes, all other results exceed the reference compressive strength. Interesting is, that also the mix with SP6 which is low in 1d strength, exceeds the reference mixes in 7d and 28d strength. SP7-SP10 are performing very similar in 1 day strength with compressive strength of 27.25MPa to 28.9MPa, also the 28d and thus final strength of the SP6, SP7 and SP9 are close to each other with results between 71MPa and 73.9MPa.

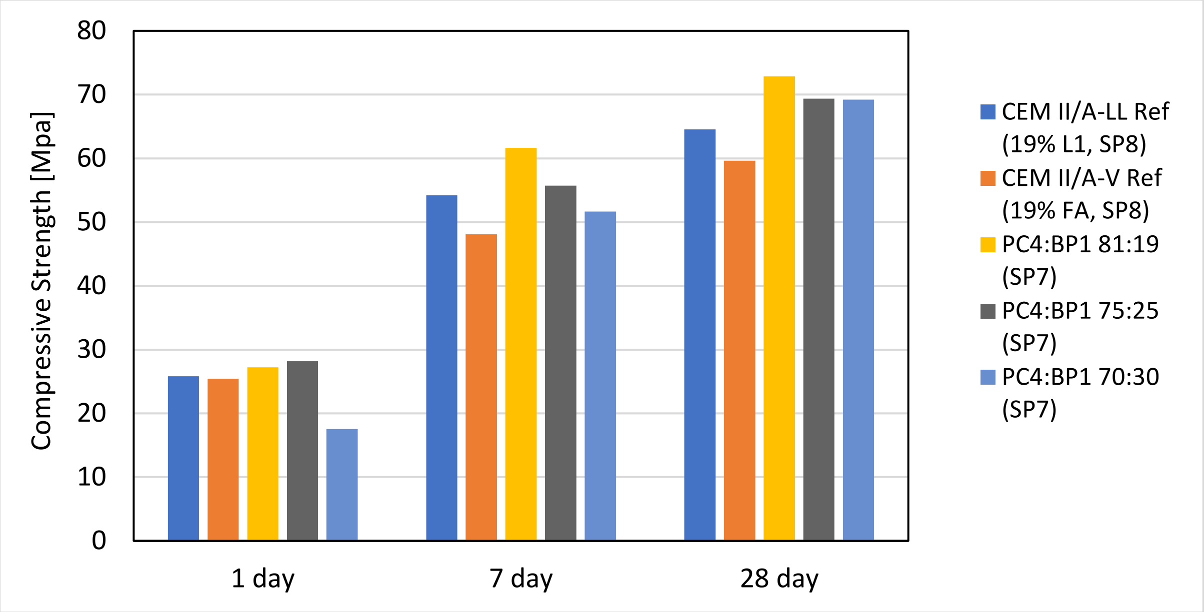

Figure 7: Compressive strength different replacement levels with SP7

As expected, increasing the replacement level is weakening the compressive strength results. This becomes especially apparent in the 1d strength data. Only one of the 25% replacement level mixes (SP7) can keep up with the reference after 1d and none of the 30% replacement mixes does. This is changing with time, after 7days almost all mixes in Figure 5 have caught up with the reference cements and after 28d also the 30% replacement mixes are exceeding the reference compressive strength (Figure 6). This shows the impact of the admixtures on the compressive strength development, especially on the early age strength. Usually, a fast strength development leads to a lack of final strength, this can be observed here as well. SP8 is performing very well in 1d strength, but the mixes with other admixtures are overtaking already before 7d (Figure 4). The opposite can be seen for the mixes with SP6, they are very low in early strength but are catching up end even overtaking most of the other mixes for all replacement levels. SP9 and SP7 seem to perform very similar strength performance wise. Final strength is looking very promising even for the 30% replacement.

When comparing different replacement levels with the same superplasticiser, it is very interesting to see that there is almost no difference in 1d strength for the 19% compared to the 25%. The 19% seems to be stronger in long term. As expected, the 30% replacement mix is the weakest in early strength. After 28d it’s catching up with the 25% mix. All mixes exceed the reference mix.

For the other SPs, this is looking more like a stair and the 19% mix performs best at all ages whilst the 30% mix is slightly weaker for all ages, compare Figure 8.

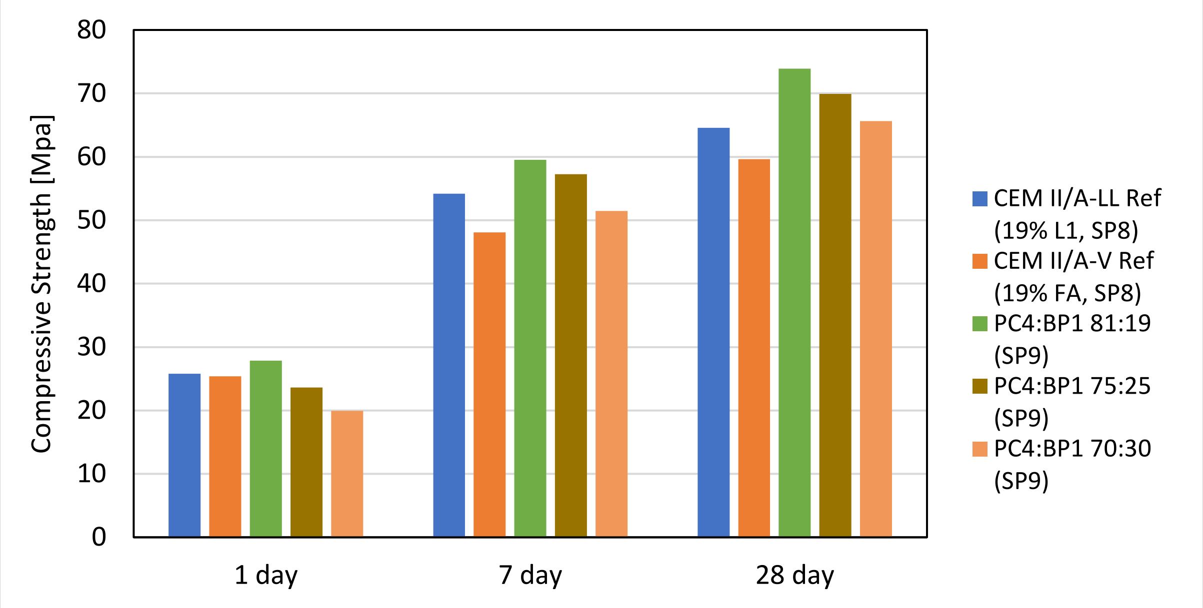

Figure 8: Compressive strength different replacement levels with SP9

For the precast sector in addition to workability and “easy casting” the priority is curing time and early age strength. To assure the turnaround and reduce the space and moulds needed, the demoulding strength must be reached after a certain time. This is individual and depends on things like production size, shift pattern and products. For Forterra’s sites an average stripping strength of 15MPa after 15h is needed. Hence, in addition to the standard test ages (1, 2, 7 and 28d) an early age study was conducted with the brick powder mixes. After consultation with production, an absolute earliest demolding time of 13h was established. Therefore, this was the earliest testing age in the setting trial. To get a meaningful curve the decision for testing ages of 13h, 14h, 16h and 18h was made. In addition, a control cube was made to proof the 28d standard strength is reached.

As accelerating admixtures are used in the precast production frequently, either in cold weather or in very busy periods, the efficiency of accelerator in concrete mixes with CII/B-Q (containing brick powder) was added to this study as well.

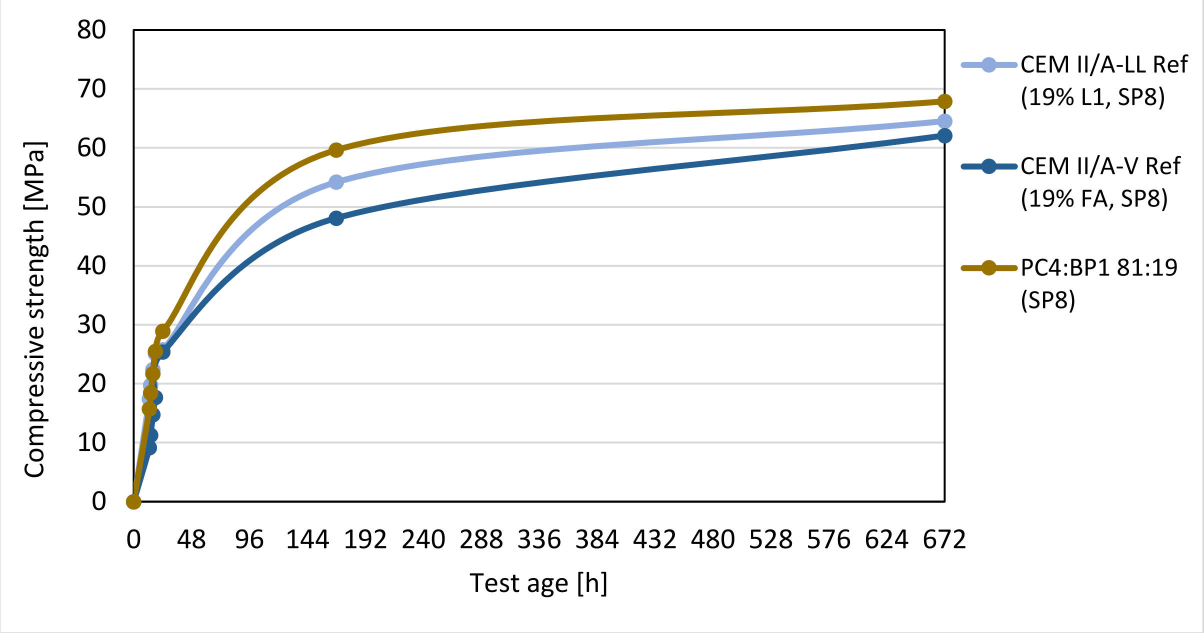

Figure 9: Compressive strength development 13h to 28d

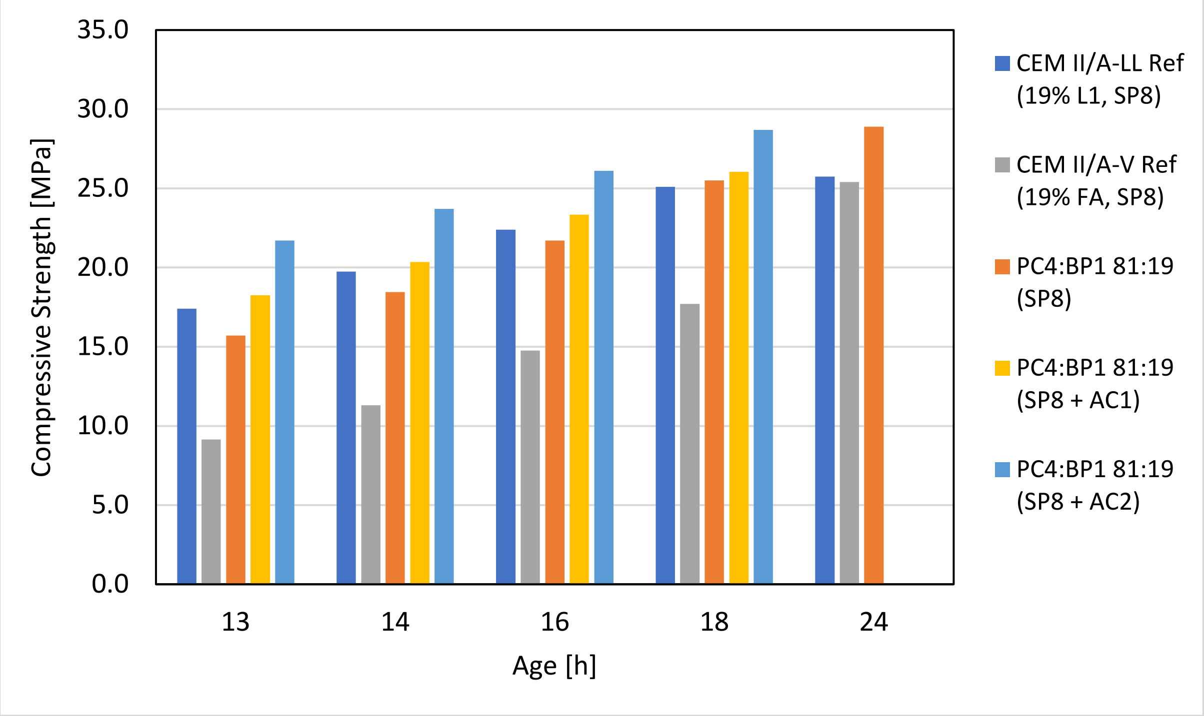

Figure 10: Early Age compressive strength (13-24h) SP8

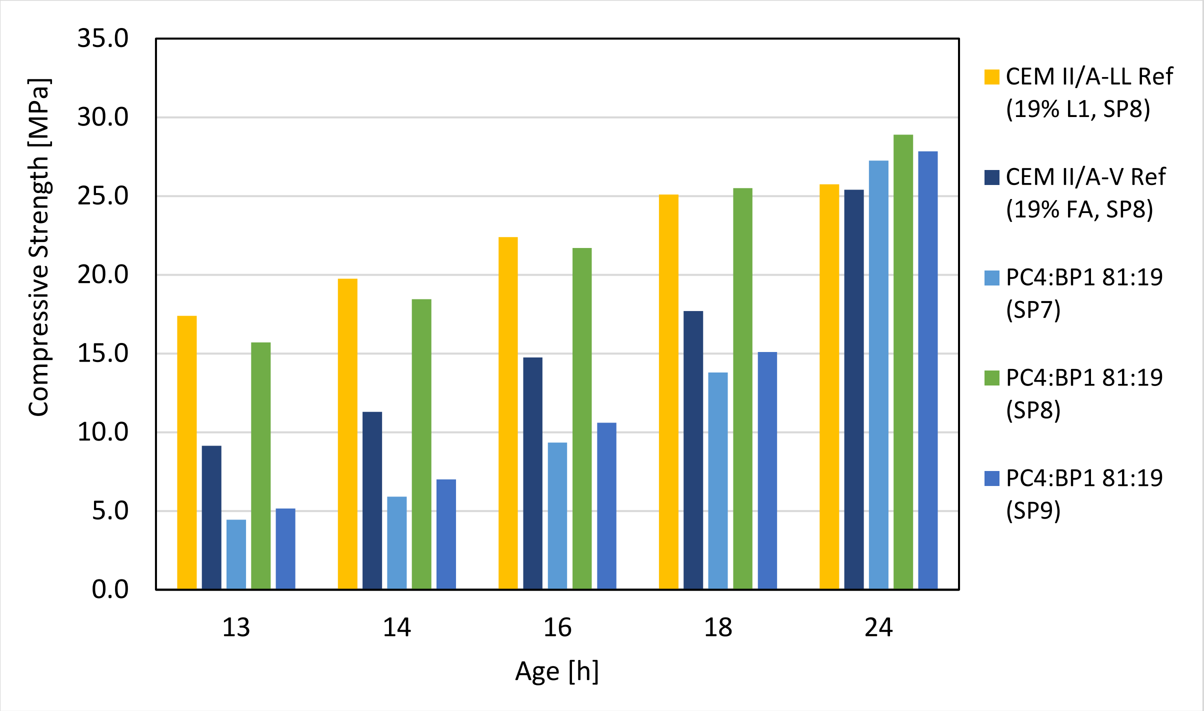

Figure 11: Early Age compressive strength development with different admixtures

Figures 9-11 show the impact of the admixture on compressive strength development. SP8, being an admixture optimized for precast with a focus on high water reduction and fast strength development rather than retention. The results proof it's efficient, the brick powder mix with the SP8 has almost the same early age strength as the reference mix. Figures 9 and 10 show how similar the reference mix and the "81:19 PC4:BP1 (SP8)" mix perform between 16 and 18h, the reference mix is developing strength slightly faster whilst the brick powder mix is overtaking at about 18-20h. A frequently used alternative with fly ash (CEM II/A-V ref) is far behind in early strength, especially in the first 18h. It's catching up with the CEM II/A-LL after 24h. To get more information on the interaction of the brick powder with accelerating admixtures, 2 different accelerator mixes were added to the test series. Figure 9 shows, the accelerators are both effective and would be able to push the 13-16h strengths above the required 15MPa. Especially AC2 is working very well and gives an impressive 13h strength of 22MPa.

Comparing different superplasticisers, it's shown very clearly in Figure 11, most mixes are lacking early strength. This is due to the nature and target group of the admixtures, which are designed for ready mix concrete and more focused on long open times/high retention other than fast strength development. All those mixes are catching up with the reference mix after 24h. This means the admixture study and the early age test series is mandatory for precast, as the 24h result does not give a good enough indication of the actual strength development before 24h.

5. Demonstration project - preparation

After gathering and analyzing all the information from the brick powder trials (see chapter 4), a mix design for the demonstration project was agreed. For sustainability reasons and to get the maximum performance of the calcined clays, a 30% cement replacement was chosen. The cementitious material of the current production mix, 465kg, consisting of 325kg PC4 and 140kg of each clay. All the other materials were kept the same than in the reference mix except for the admixture. Due to the difference in particle size distribution, surface area and chemical composition of the clays differences in water demand were expected. To address those differences, the decision to keep the w/b ratio the same but to vary the admixture type (if needed) and dosage to get to a fit for production SCC.

5.1 Lab trials

All seven clays were tested in this test series. A different behavior and appearance of the concrete with the different clays could be observed. Some of the materials were easy to adjust and adapt in the current mix, whilst the admixture adjustment for some of them needed more testing and options. It was also clearly visible, that some mixes were much stickier and more thixotropic than others. Hence, the measurement of the t500 time was added to the workability trials to make this behavior more visible. Reaching an appropriate flow was possible for all materials with the same admixture, but the flow on it owns didn’t give the full picture of the workability. Measuring t500, which is the time [in seconds] it takes the concrete to reach a flow of 500mm, gave more information about the viscosity and suitability of the mix (BS EN 12350-8: Testing fresh concrete - Self-compacting concrete. Slump-flow test, 2019).

Especially difficult was the CC2F calcined clay material. Even the admixtures develop for high meta kaolinite materials were not effective.

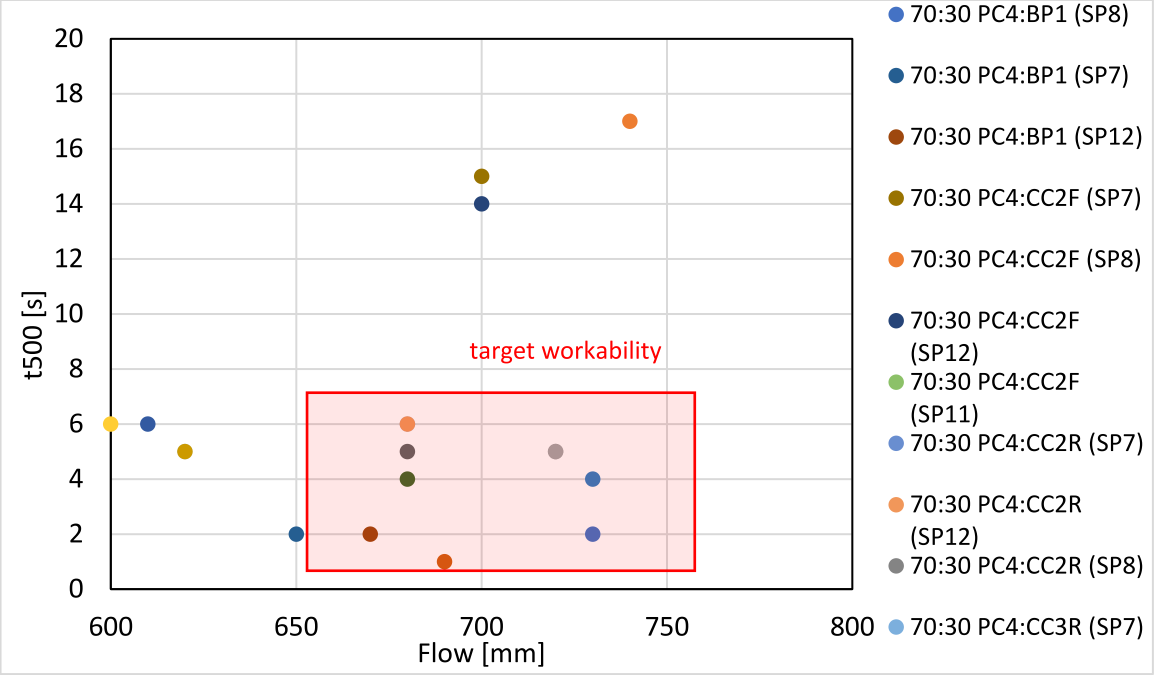

Figure 12: Workability SCCs

Figure 12 shows the flow in mm on the x-axis and the t500 time in seconds on the y-axis. In the trials it was found, that a t500 time of more than 8s meant a very sticky mix, production would be unable to work with. Usually, all SCC mixes used in Forterra's precast plants are specified as SF3, this would mean a minimum flow of 760. Nevertheless, in the workability trials it was found that a flow of about 650mm was the most robust concrete and still fluid enough, to flow in corners and vent itself. Therefore, the target workability was defined as a flow of 650-750mm with a t500 time of 2-8s (red window in Figure). The extended workability trial series resulted in SP8 and SP7 as options for the plant production, both admixtures worked well with all calcined clays. The decision was made to use SP8 for all mixes as this would be the chosen one in a precast factory for the release strength.

As mentioned before CC2F needed a closer look. After many trails it was found that the combination of SP8 with SP11 which was addressing the viscosity issue with this clay gave a mix with a good workability.

Strength data of all lab mixes was gathered and analysed as well as compared to the brick powder and reference mixes from chapter 4.

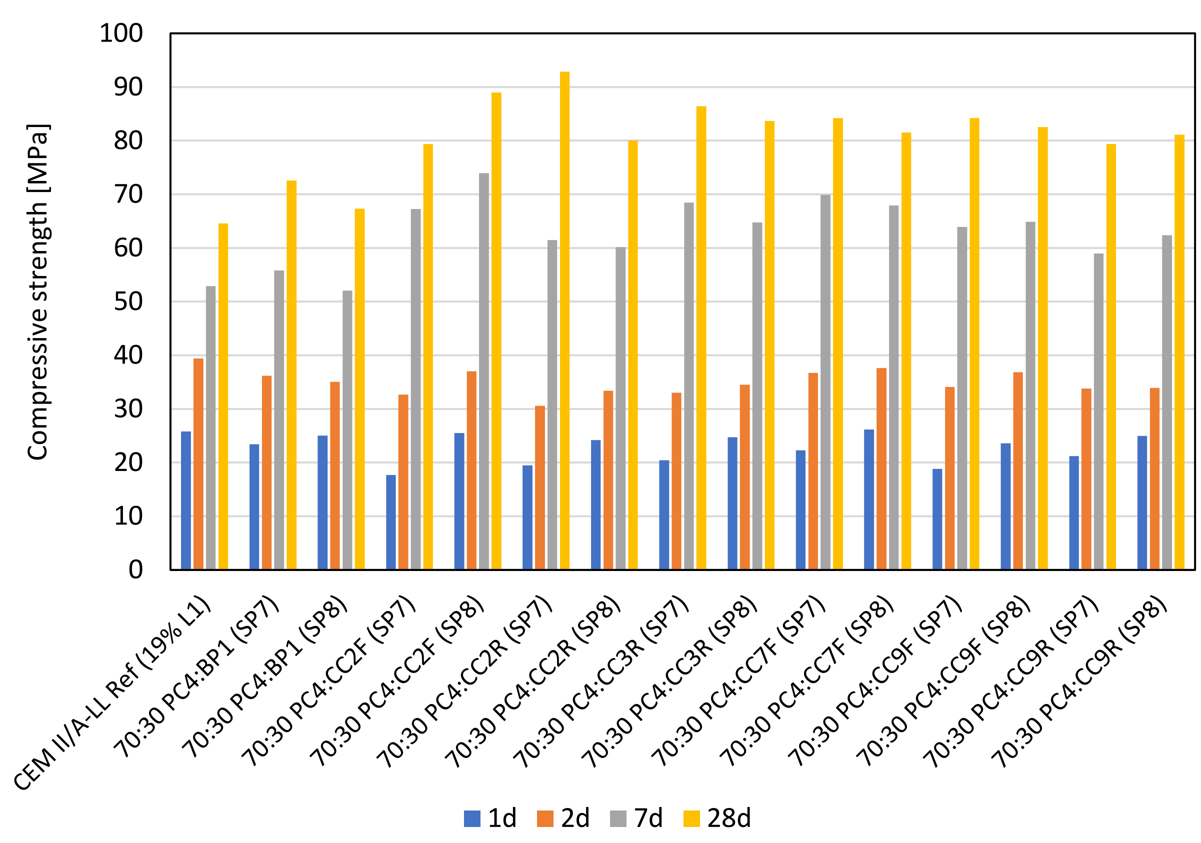

Figure 13: Compressive strength binary SCCs with different admixtures (lab)

For the strength comparison the two most promising admixtures workability wise were chosen, SP7 and SP8 and used with all calcined clays. Comparing the strength data from the calcined clay mixes with the reference Figure 13 shows, that all clay mixes were behind in early strength. The 1d as well as the 2d compressive strength results of the calcined clay mixes are behind the reference mix. Only the mix with 30% CC7F and the SP8 is slightly above the reference 1d strength, but it’s lower in 2d strength. All mixes except the brick powder mix are exceeding the reference 7d strength, all mixes are exceeding the reference final strength of 64.6MPa. By comparing the results of the same calcined clay and replacement level with SP7 to SP8, it shows for all materials, that the SP8 is improving the early strength. 1d and 2d compressive strength is higher for all mixes with SP8 compared to SP7. As expected, for all mixes other than the CC2F mix the 28d strength is slightly higher with the SP7. The admixture has the same impact on all the mixes.

The decision was made to use SP8 for all mixes as this would be the chosen one in a precast factory for the release strength.

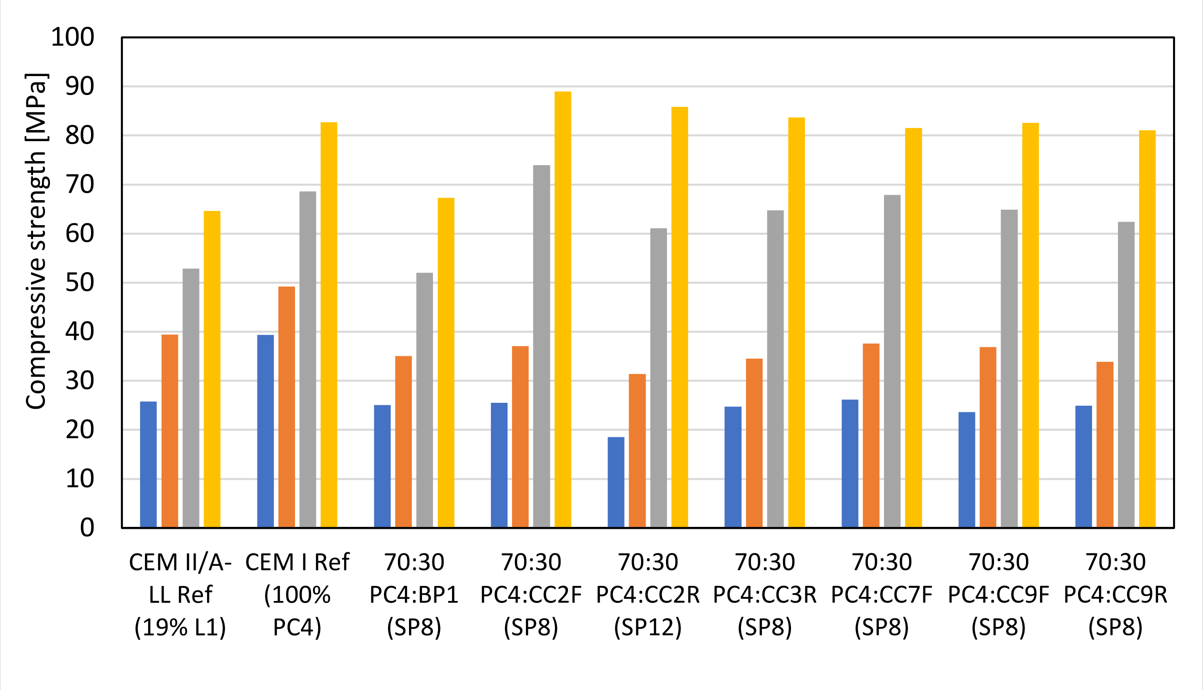

Figure 14: Compressive strength binary SCCs with SP8 (lab)

Taking a closer look at all the mixes with SP8 and adding a pure CEM I (PC4) mix to Figure 14, all 28d results are above 65MPa and would meet the required standard strength. All 7d strengths are above 50MPa, which is a significant strength and shows the strength development isn’t much delayed with the calcined clays. The CC2 mixes outperform in final strength, it’s close to 90MPa with the SP8 and in the previous Figure 13 reached even 93MPa. All calcined clays are exceeding the pure CEMI (PC4) mix in final strength, the brick powder mix doesn’t. The CEM II/A-LL Ref mix is the weakest mix after 28d. No significant difference can be made out in flash and rotary calcination from these results, CC9 is performing about the same for both calcination methods, the rotary calcined CC2 seems to have a slightly slower strength development but the final compressive strength results are very close.

Overall, the above data is looking very promising and showing a strong performance in final strength of calcined clay concretes, but also good early strength performance

compared to other well known SCMs like fly ash and GGBS.
For completion also some ternary mixes were trialed in the lab. For those the decision was made to use the same total cementitious content as before, 465kg per m3 with a total of 55% of Portland cement. This leads to a consistent calcined clay content of 140kg per m3, 255kg PC4 and 70kg limestone powder. All other components remain unchanged.

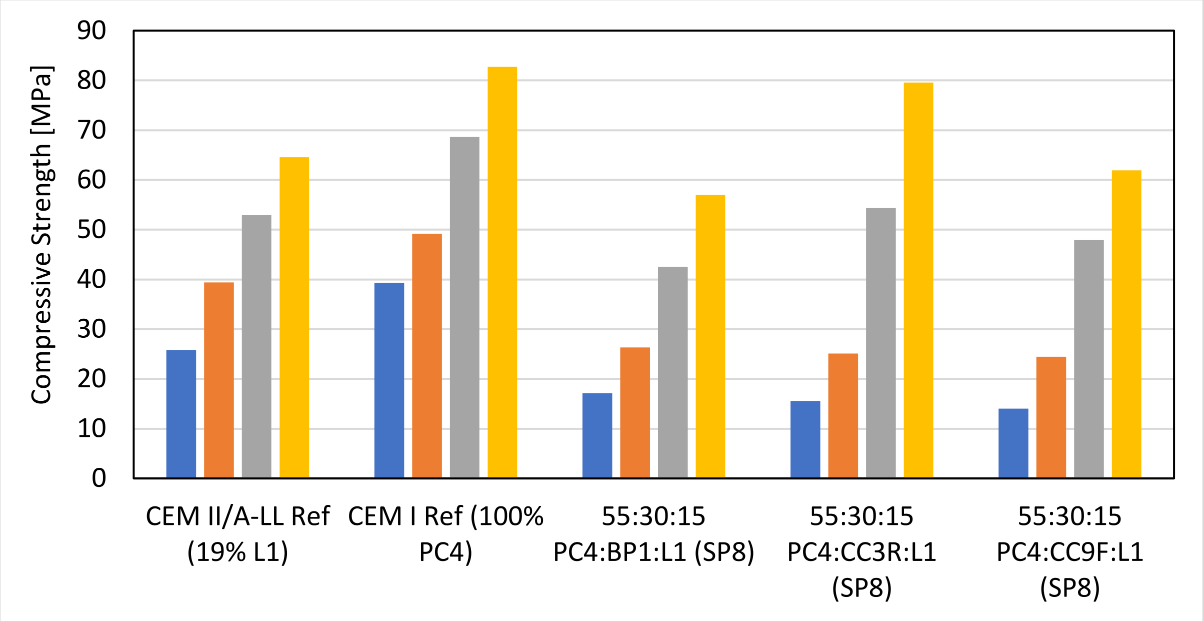

Figure 15: Compressive strength ternary SCCs with SP8 (lab)

The brick powder ternary mix as well as the CC9F ternary mix only reached 14N after 24h, they both reached just below or just above 60N after 28d, what is a strong 28d strength. Workability wise they were easier to adjust and less unstable, the required admixture dosages were lower. It was not unexpected that those would be slower in strength development and therefore not an option for precast yet.

As mentioned in the discussion before, the decision was made to use SP8 for all plant production trials. As the amount of available calcined clay was limited, only one plant trial per clay could be conducted. Therefore, it was essential that the admixture dosage was confirmed. A small mix of all binary and chosen ternaries was mixed in the lab to confirm and determine the plant trial dosages.

Table 4: Demonstration SCC mixes

		Lab trial		Lab trial 2		Demonstration project	
Mix	Admix.	Dosage [%]	Flow [mm]	Dosage [%]	Flow [mm]	Dosage [%]	Flow [mm]
70:30 PC4:CC2F	SP8+SP11	0.55+1.1	740	0.55+1.1	750	0.55+1.1	650
70:30 PC4:CC2R	SP8	0.93	720	1.1	740	1.2	750
70:30 PC4:CC3R	SP8	1.00	620	1.15	740	1.2	750
70:30 PC4:CC7F	SP8	1.09	730	1.15	690	1.2	640
70:30 PC4:CC9F	SP8	0.79	720	0.85	730	0.85	720
70:30 PC4:CC9R	SP8	1.04	690	1.15	750	1.1	500
70:30 PC4:BP1	SP8	0.70	730	0.70	740	0.7	640
55:30:15 PC4:BP1:L1	SP8	0.70	780	0.60	740	0.6	620
55:30:15 PC4:CC3R:L1	SP8	-	-	1.00	700	1	370 *
55:30:15 PC4:CC9F:L1	SP8	0.62	700	0.65	720	0.65	570
* Batching issues							

5.2 Plant and setup

The objective for the demonstration project is to prove the performance and suitability of calcined clays in the precast production. To get as close as possible to daily production, it was agreed to use the standard production facilities and batch plant in the Somercotes bespoke precast plant. As a result of this, some parameters had to be complied with and the schedule of the production must be met.

The batch plant is set up with 4 80t and 2 40t aggregate bins, which are used for 2 different Quartz sands, a 10mm limestone and a 20mm Quartz Gravel (Pic 1.1). The sand bins are equipped with moisture probes and linked to the batch computer. 3 50t powder silos which hold CEM I (PC4), limestone powder (L1) and GGBS for the current production as well as 2 admixture tanks. The mixer is a pan mixer type R1500, manufactured by Rapid International, with a capacity of 1.5m3. The mixer is also equipped with a moisture probe which measures dry and wet moisture contents in % of the mix volume.

Pic 1.1: Plant setup, aggregate bins

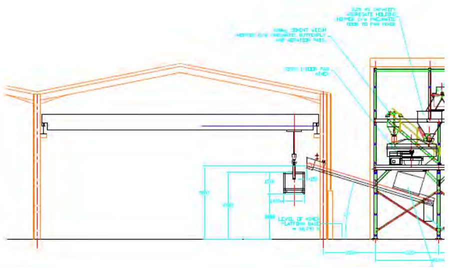

Pic 1.2: Plant setup, discharge area

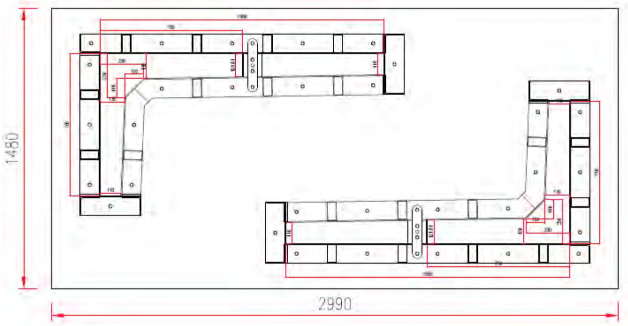

Pic 1.3: Retaining wall moulds, measurements

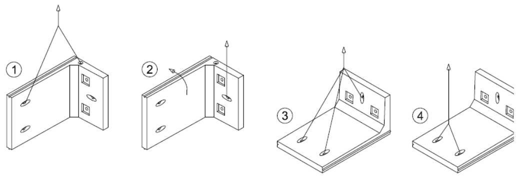

Pic 1.4: Retaining wall elements, lifting and handling fix points

The fabricated element had to meet certain parameters, it had to be the right concrete volume to use the production plant. The pan mixer is only effective from a fill level of 0.6m^3. In addition, it should have a big enough surface to assess the visual properties of the calcined clay concretes and compare them. For the above reasons a retaining wall element was chosen and fabricated by a local company. Measurements and set up is shown in Figure 3. The Forterra design team designed a simple steel cage with lifting and handling fix points (Figure 4).

5.3 Plant trials

In the precast batch plant, the SCCs were mixed in the pan mixer as mentioned above. As there is no spare silo, the calcined clays were manually added directly into the pan mixer. The batched concrete is loaded into a hopper, after a slump-flow test was conducted, it's carried to the moulds by an overhead crane. All seven binary mixes and three ternary mixes were cast from December 2023 to January 2024. An impression of the mixing and casting in pictures can be found below.


Pic 2.1: Pan mixer opened


Pic 2.2: Slump-flow test


Pic 2.3: Moulds prepared


Pic 2.4: Steel cage


Pic 2.5: Casting

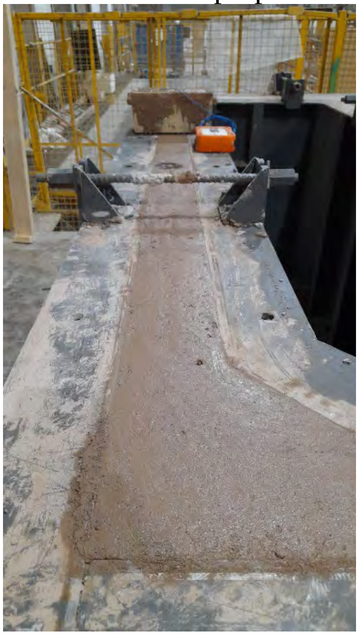
Pic 2.6: Moulds filled

Pic 2.7: Temperature probes

Pic 2.8: Concrete cubes casted

Pic 2.9: Stripped Elements

For all mixes both retaining wall elements were cast as well as 8 cubes (100*100mm) to assess the strength development. The cubes were cast and cured in the lab at 20 °C, after 24h they were stripped and cured in water tanks at 20 °C until they reached the test age. As a big data set of strength results was already created in the lab trials the decision was made to test the cubes after 1d, 7d, 28d and 56d to gain further information on the strength development after 28d.

In addition, 2 release cubes were cast and cured on the shop floor close to the elements. The release cubes were tested after 16-18h and about 24h. In one of the release cubes a temperature probe was applied. This probe is reading the concrete temperature development and allows, if calibrated for the mix design, to draw conclusions on concrete maturity and compressive strength. In case of the demonstration project, it was simply used to measure temperature development in the concrete and ambient temperature in the shop flow to compare.

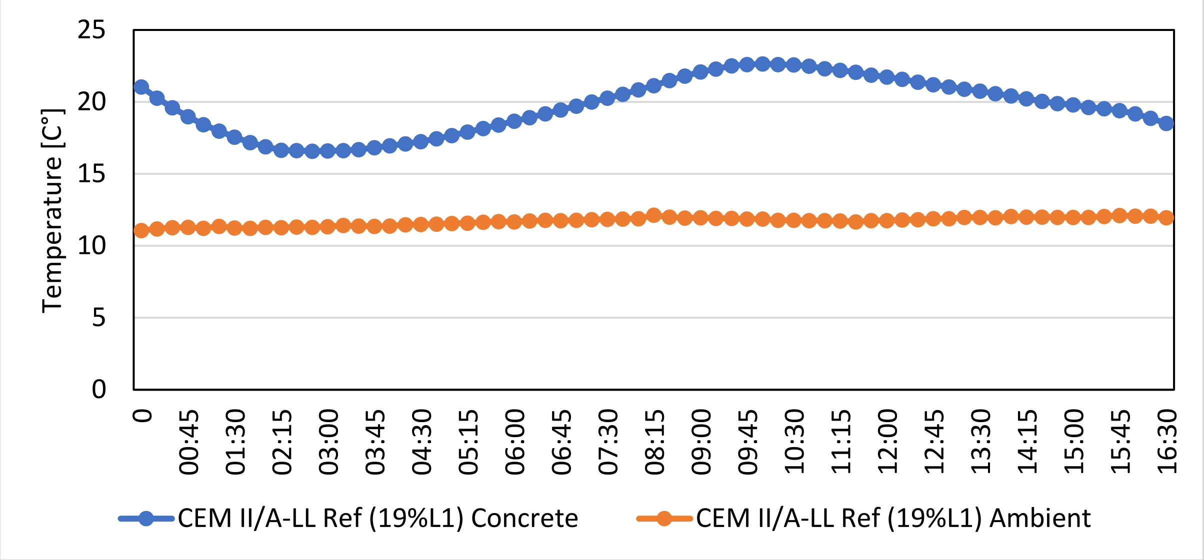

Figure 16: Temperature curve reference mix (CEM II/A-LL)

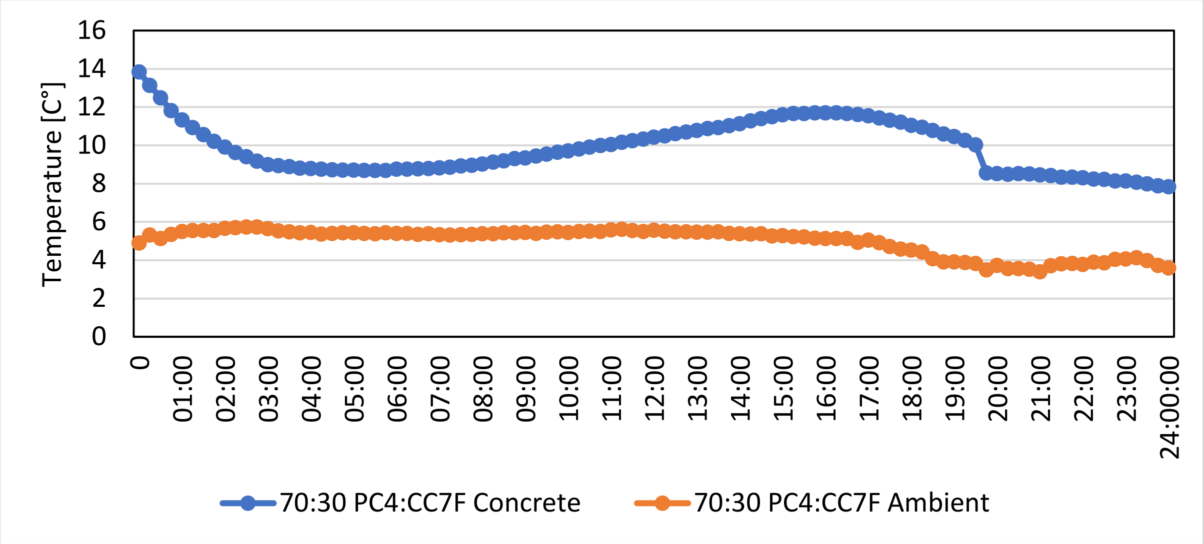

Figure 17: Temperature curve example calcined clay mix (70:30 PC4:CC7F)

Figures 16 and 17 are showing the data gathered from the temperature probes as an example. The blue curves are showing the concrete temperature development in the concrete cubes (100*100mm), the orange curve is showing the ambient temperature in the shop floor at the same time. The reference mix was cast at a very steady ambient temperature of about 10°C, the initial concrete temperature was 21°C. The temperature dropped for the first 3h to about 16.5°C and went up again, this means the hydrarion process begins. The highest temperature was reached after 10h. Compared to this the calcined clay mix (CC7F Figure 17) was cast at only 5 °C and the temperature in the shop floor dropped to 3.5°C in the night. This mix had an initial temperature of 14°C, dropped for the first 5h and went back up again until it reached the high at about 15h. Because of the differences in ambient temperatures and initial concrete temperatures a like for like comparison is not possible. It can only be compared at what point the temperature stops to drop and starts going up as a starting point for hydration. Also the different initial situation must be considered and kept in mind, the numbers can not be compared as factual numbers, more as trends.

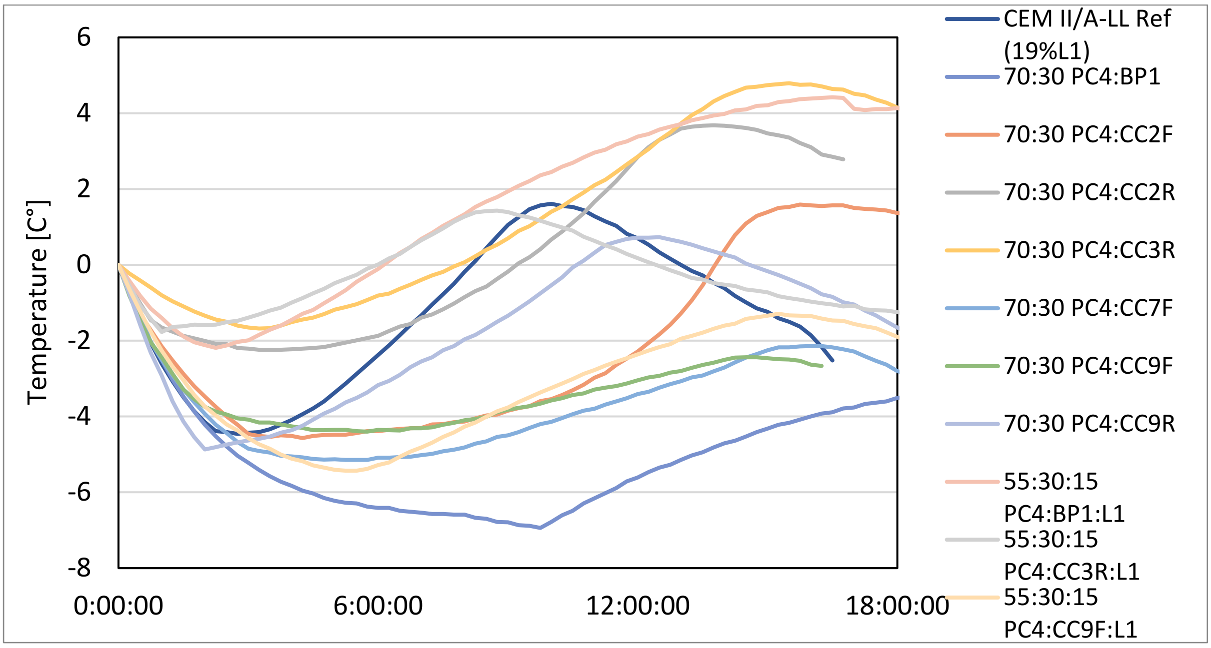

Figure 18: Concrete temperature curves normalised by initial concrete temperature.

As a trend, Figure 18 shows that all the calcined clay mixes have their low after 3-6h whilst the reference mix has its low after 2h. The highest point is reached after 13-17h, the reference mix peaks at 8h. This indicates a slower hydration and thus, lower early age strength. More time could be spent to understand the heat development of the calcined clay concretes better.

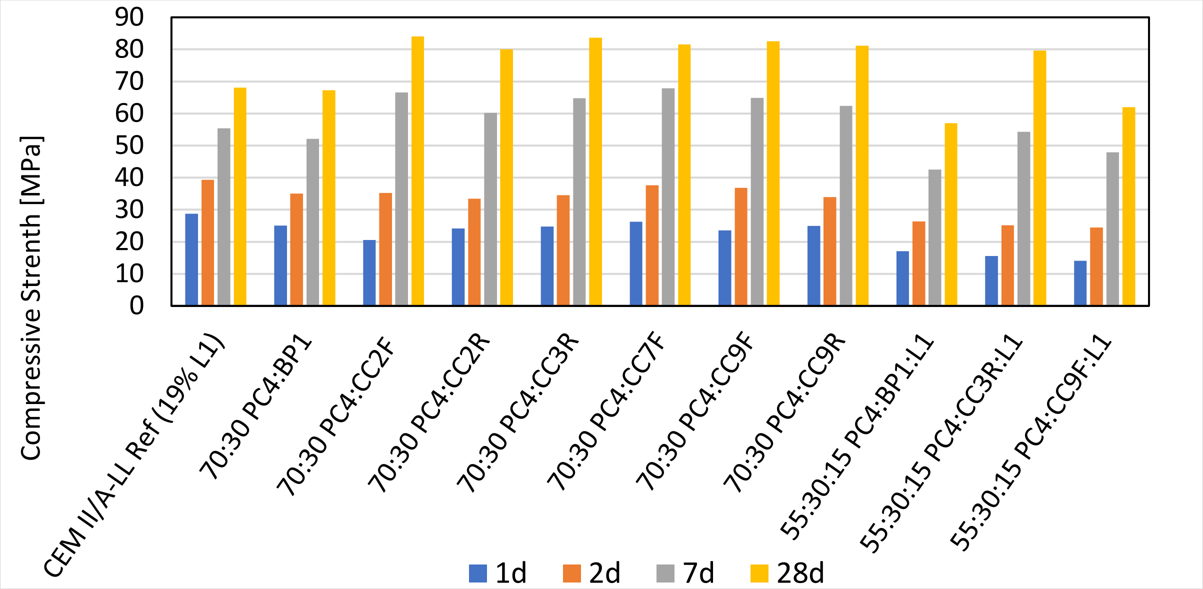

Figure 19: Compressive strength demonstration SCCs, lab mixed.

Figure 19 is combining the data of Figure 13 and 14. It’s a repetition of results discussed before and functions as base for the discussion of Figure 20.

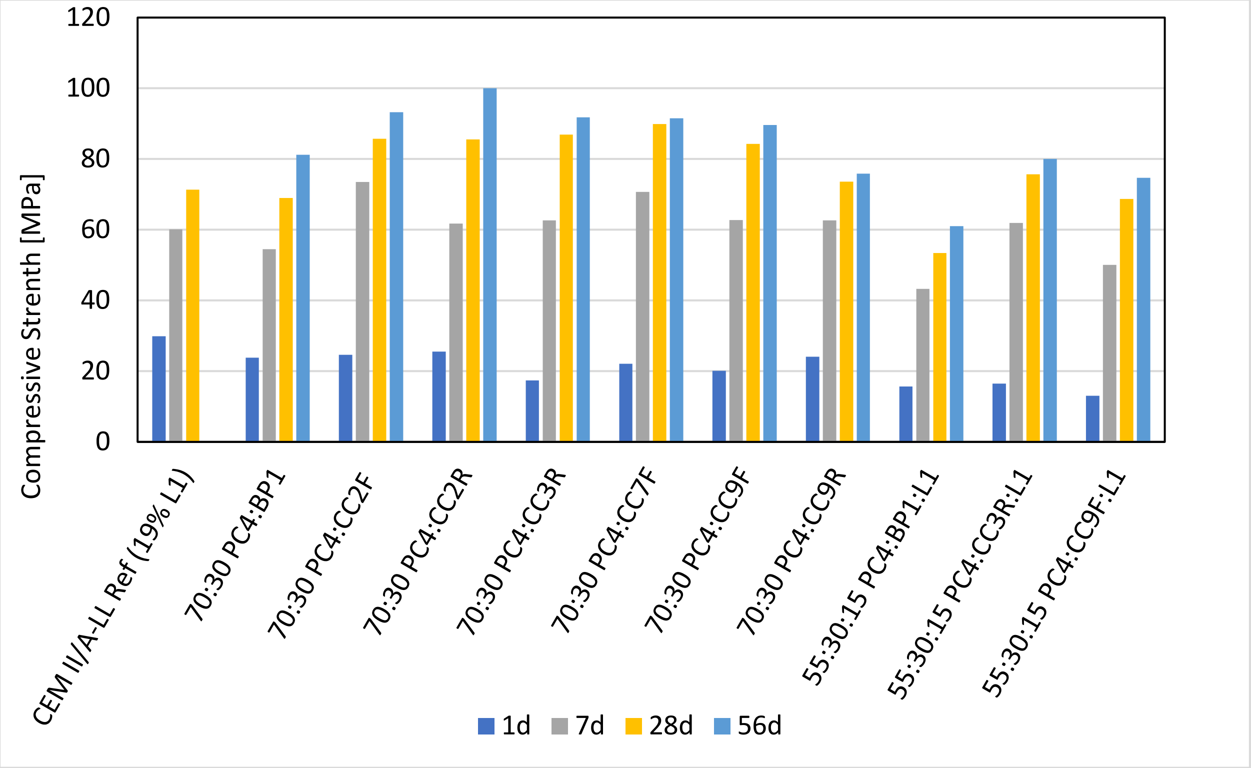

Figure 20: Compressive strength demonstration project

The strength data of the plant trial is proving the data gathered in the lab trials. All 1 day strength are slightly behind compared to the reference mix, whilst all binary mixes except the brick powder mix are catching up after 7 days. Because of the different initial temperatures of all mixes (between 12 and 21 °C) the focus should be on final strength. All binary mixes are exceeding the reference mix (plant batched) in final strength. Except for the brick powder and CC9R, all the binary mixes are about 10MPa higher in 28d strength than the reference mix. More than 85MPa is an impressive compressive strength and not needed for many applications. To get more information about the long-term strength development a 56d result was added on, there is no comparison value for the reference mix. Most of the calcined clay binaries are gaining a bit more strength in between 28 and 56d, about 5-10% (5-8MPa) whilst the CC7F is not adding on strength (only 1.5MPa) and the CC2R records an increase of 15MPa, almost 20%. There is no explanation for this behaviour at this state of the project, the long-term strength would need repeating to exclude any faulty results.

The ternary mixes perform as expected. They are low in 1d strength and improving slightly at 7d. The CC3R and CC9F ternary mixes have high 28d strengths and are similar to (CC9F: 68.7MPa) or exceeding (CC3R: 75.7MPa) the 28d strength of the reference mix. This is with a reduction of the CEM I (PC4) content by 120kg/m^3. All three ternary mixes show ongoing strength increase between 28d and 56d, of between 4 and 7MPa, which equates to 5-9% increase.

In Table 5. the strength data of the binary and ternary mix with the same calcined clays content is compared. This shows that the additional limestone in the ternary mix is totally inert. A 15% reduction of cement leads to about 15% reduction in final strength at both 28d and 56d for CCR3 and CCF9. The reduction in strength for BP1 is though higher, closer to 25% at 28d and 56d.

Table 5: Comparison ternary/binary strength data

	BP1			CC3R			CC9F		
Test age	Binary (70:30)	Ternary (55:30:15)	T/B	Binary (70:30)	Ternary (55:30:15)	T/B	Binary (70:30)	Ternary (55:30:15)	T/B
1d	23.8	15.7	66%	17.4	16.5	95%	20.1	13.0	65%
7d	54.5	43.3	79%	62.6	61.9	99%	62.7	50.1	80%
28d	69.0	53.4	77%	86.9	75.7	87%	84.3	68.7	82%
56d	81.2	61.0	75%	91.8	80.0	87%	89.6	74.7	83%

6. Conclusions

After conducting all the preparation laboratory trials as well as the demonstration plant production of self-compacting concrete with different reclaimed calcined clays, the following additional work on calcined clays is recommended:

- An extended study on suitable admixtures should be conducted to optimise superplasticiser efficiency and dosage rates.
- The long-term strength development (>56d) should be repeated and extended to 90d.
- To get to a precast usable SCM, the impact of temperature on the hydration of CEM II/B-Qs should be assessed. For this a study on strength development with different concrete and ambient temperatures as well as temperature curing would be recommended.
- Additional tests on the hydration temperatures with temperature probes should be conducted in a lab environment.
- For further work an optimsed mix design for the calcined clay SCC should be used, this requires optimising the fines content and adjusting the water content as well as the aggregate distribution (sand/coarse aggregates).
- Develop SCC specific with calcined clay and assess if a total cement reduction would be possible.
- Finally, the following conclusions can be drawn:
- All seven tested reclaimed calcined clay materials have made a cohesive, flowable self-compacting concrete with a high cement replacement level of 30%.
- The strength development for all mixes assessed in the demonstration project is looking promising, especially the final strength is impressively high with up to 100MPa. All binary mixes were exceeding the reference mix.
- Ternary mixes are lacking early strength, which is not surprising. The additional limestone does not seem to contribute to the strength development. Final strength with the CC3R and CC9F is meeting or exceeding the reference mix. Considering the Portland cement reduction of about 30% this is promising for end-users.

- Even the early age strength development is looking promising, only the time between 13 and 18h appears to be weaker. This is not relevant for all businesses.
- Standard admixtures, which are not optimised for metakaolin or clay adhesion, were working well with the calcined clays. It was easy to adapt for production.
- Overall, the calcined clays are a strong alternative for secondary cementitious replacements. No issues or extra effort can be anticipated for the use of calcined clay instead of other SCMs, despite normative rules and availability at this point in time.

7. References

(1999). BS EN 1015-3: Methods of test for mortar for masonry. Determination of consistence of fresh mortar (by flow table). BSI.

(2019). BS EN 12350-8: Testing fresh concrete - Self-compacting concrete. Slump-flow test. BSI.

(2009-2021). BS EN 12390 Part 1-4: Testing of hardened concrete. BSI.

(2016). BS EN 196-1: Methods of testing cement - Determination of strength. BSI.

(2011). BS EN 197-1: Cement. Composition, specifications and conformity criteria for common cements. BSI.